Genetic mutations promoting autonomous B cell proliferation

Sally Jane Mapp

A thesis submitted for the degree of
Doctor of Philosophy
of The Australian National University

Revised and resubmitted August 2013

Statement

This is to certify that

(i) this thesis comprises only my original work towards the PhD except where indicated,

(ii) due acknowledgement has been made in the text to all other material used, and

(iii) this thesis is less than 100,000 words in length

Sally Jane Mapp

Acknowledgements

Firstly I would like to thank my supervisor Chris Goodnow for his guidance throughout my PhD, for challenging me to think laterally and for the superb example he sets as a world-class scientist. I am also indebted to Keisuke Horikawa, Lina Tze and Katrina Randall for their scientific and technical assistance and for encouragement when progress was slow. I would also like to express my gratitude to the Goodnow lab and John Curtin School of Medical research students, post doctoral scholars, research assistants and support staff for their patience, expertise and the friendly and productive working environment they created. I am grateful to the Leukaemia Foundation for their support in funding this research.

I would not have completed my thesis without the support of my husband Steve through his example as a researcher, facilitation of dedicated research time and his kindness and love. My parents have always encouraged my academic and personal pursuits and I am greatly indebted to them. I am extremely fortunate to have a large network of supportive family, friends, scientific colleagues and work colleagues for whom I am extremely grateful.

Abstract

The multi-step nature of neoplastic transformation is relatively well accepted, although the minimum number of genetic perturbations required for the acquisition of a malignant phenotype has not previously been clearly defined.

Using retroviral gene transfer, cells harbouring mutated *Trp53* in conjunction with overexpressed *MYC* have been demonstrated to predispose to B cell lymphoma development in mice. We localised retroviral insertion sites in 24 such lymphomas. Many of these integration sites were similar to those identified in other murine models of malignancy. Oncogenes, proto-oncogenes and B cell regulators were over-represented within these common integration sites.

cDNAs encoding a selection of genes adjacent to the retroviral insertion sites were engineered into separate retroviral expression vectors under the control of the retroviral enhancer and promoter region to determine if they facilitated B cell transformation. Double transduction of *Myb* and *MYC* suggested that the overexpression of *Myb* and *MYC* in *Trp53* mutated cells is sufficient for autonomous B cell growth in vitro.

This novel finding improves understanding of the genetic basis of B cell transformation, and further research based on these findings may provide insights into the pathogenesis and cellular pathways implicated in the development of B cell lymphoma. The recognition that *Myb* and *MYC* were the most notable oncogenes implicated in the induction of B-cell lymphoma increases the need and perhaps opportunity to consider experimental strategies that inhibit *Myb* and/or *MYC* function and thus may offer new therapeutic approaches to treating such malignancies.

Conference Proceedings

Mapp S, Rui L, Tze L, Goodnow C. Analysis of retroviral integration sites in experimentally-induced murine B cell lymphomas. Oral presentation, Haematology Society of Australia and New Zealand Annual Scientific Meeting, Gold Coast, October 2007.

Mapp S, Rui L, Tze L, Goodnow C. Retrovirus induced B cell lymphoma. Oral presentation in the Hot Topics session, New Directions in Leukaemia Research Meeting, Maroochydore, Queensland, March 2008.

Mapp S, Rui L, Horikawa K, Tze L, Goodnow C. Genetic mutations promoting autonomous B cell proliferation. Poster presentation, New Directions in Leukaemia Research Meeting, Maroochydore, Queensland, March 2012.

Table of Contents

Table of Figures

Table of Tables

Abbreviations

Below is the list of recurring abbreviations used. Gene and protein nomenclature follows the International Committee on Standardized Genetic Nomenclature for Mice recommendations (http://www.informatics.jax.org/mgihome/nomen/gene.shtml).

1C10	Hybridoma encoding rat anti-mouse CD40
7-AAD	7-amino-actinomycin-D
ACK	Ammonium- Chloride-Potassium
ACRF	Australian Cancer Research Foundation
AID	Activation-induced cytidine deaminase
ANU	Australian National University
APC	Allophycocyanin
BAFF	B cell-activating factor
BCMA	B cell maturation antigen
BCR	B cell receptor
BL	Burkitt lymphoma
BLIMP	B lymphocyte induced maturation protein
BRF	Biomolecular Research Facility
BSA	Bovine serum albumin
C	Celsius
CD	Cluster of differentiation
cDNA	Complementary deoxyribonucleic acid
CFSE	Carboxyfluorescein succinimidyl ester
CM	Complete medium
DH5α	specific strain of E. coli
DMEM	Dulbecco's Modified Eagle Medium
DMSO	Dimethyl Sulfoxide
DNA	Deoxyribonucleic acid
DOTAP	Cationic lipid N-[1-(2,3-dioleoyloxy)propyl]-N,N,N-trimethylammonium methylsulfate
DsRed	A protein with red fluorescence
dNTP	Deoxyribonucleotide triphosphate

EBV	Epstein-Barr virus
EV	Empty vector
EDTA	Ethylenediaminetetraacetic acid
ENU	N-ethyl-N-nitrosourea
EtOH	Ethanol
EV	Empty vector
FACS	Fluorescence activated cell sorting
FSC/SSC	Forward scatter / side scatter
FW	Fresh Weight
FITC	Fluorescein isothiocyanate
G0	Gap 0. Resting phase of cell cycle
GFP	Green fluorescent protein
huCD4	Tail-less human CD4
H_2O	Water
HBS	HEPES-buffered saline
HEL	Hen Egg Lysozyme
HEPES	4-(2-hydroxyethyl)-1-piperazineethanesulfonic acid
IP	Intra peritoneal
IRES	Internal ribosome entry sequence
IRF4	Interferon regulatory factor 4
KEGG	Kyoto Encyclopaedia of Genes and Genomes
KO	Knock out
LB	Lysogeny broth
LMP1	Latent membrane protein 1
LTR	Long terminal repeat
M	Molar
MALT	Mucosa associated lymphoid tissue
MGI	Mouse Genome Informatics
MHC	Major histocompatibility complex
MiRNA	MicroRNA
MMLV	Moloney Murine Leukaemia Virus
MQ water	Milli-Q water
ml	Millilitres
MSCV	Murine stem cell virus

Mut	Mutant
NEB	New England Biolabs®
NF-κB	Nuclear factor-kB
ng	Nanograms
PBS	Phosphate buffered saline
PE	Phycoerythrin
PerCP	Peridinin chlorophyll protein
PCR	Polymerase chain reaction
Pfx	Platinum® Pfx DNA Polymerase
PIPES	Piperazine-N,N'-bis[2-ethanesulfonic acid]
pMX-DsRed	pMXs-IG vector with a red fluorescent protein replacing GFP
Rag	Recombinase-Activating Gene
RNase	Ribonuclease
Rpm	Revolutions per minute
RPMI	Roswell Park Memorial Institute Medium
RTCGD	Retroviral tagged cancer gene database
S phase	Synthetic phase cell cycle
SOC	Super-optimal broth with added glucose
T75	Flask with growth area of 75cm^2 and 250ml volume
TAE	Tris-Acetate Ethylenediaminetetraacetic acid
TLR	Toll-like receptor
TNF	Tumour necrosis factor
UBC	Ubiquitin conjugating enzyme
UCSC	University of California Santa Cruz
µg	Micrograms
wt	Wild type

1. Introduction

1.1 Preamble

B cell lymphoproliferative disorders are the most common haematological malignancy. Despite much research a common unifying pathogenesis has not been elucidated, limiting targeted drug development.

In more general terms, basic principles such as the number of oncogenic 'hits' that a B cell requires to become neoplastic is still contentious, and the specific pathways that need to be dysregulated in B cells to induce lymphoma remains uncertain. One approach to this problem is to work backwards from malignant lymphomas, identifying the accumulated mutations within them and testing whether these are required for the malignant state by attempting to restore them to normal. This thesis explores the problem from the opposite direction, by starting with cohorts of normal B lymphocytes, introducing defined oncogenic mutations singly and in combination, and tracing their consequences for B cell growth and survival.

1.2 Malignant transformation in general

Dysregulation of the normal homeostatic pathways is required for malignant transformation. The seminal paper published in 2000 by Hanahan and Weinberg [1] (and subsequently updated in 2010 [2]) describes six attributes that a cell must attain before it has a fully malignant phenotype:

1. Self-sufficiency in growth signals
2. Insensitivity to growth-inhibitory (antigrowth) signals
3. Evasion of programmed cell death (apoptosis)
4. Limitless replicative potential
5. Sustained angiogenesis, and
6. Tissue invasion and metastasis.

It is not known how many different genetic mutations are required to confer these attributes, nor how many different combinations might exist to achieve

malignant transformation of a given cell lineage. Recent exome and genome sequencing of human mature B cell lymphomas have revealed that these typically have accumulated 30 or more somatic mutations that alter protein sequence [3-6], but it remains unresolved how many of these are "driver" mutations(conferring a selective growth advantage) as opposed to "passenger" mutations (concepts reviewed by Vogelstein et al [7]).

1.3 Murine models of human lymphoma

B cell neoplasms can be divided broadly into those that express surface immunoglobulin, the mature B cell lymphomas and leukaemias that arise from a diverse number of normal mature B cell counterparts (Table 1), surface immunoglobulin-negative leukaemias that derive from pre-B cells and pro-B cells, and myelomas and plasmacytomas derived from terminally differentiated plasma cells. Many similarities are seen in human and murine mature B cell lymphoma [8,9]. Concordance, however, is not complete, with the differences likely to reflect species-specific idiosyncrasies together with differences in the way the tumours are classified. In both species, classification currently focuses on histopathological parameters. Ideally, mature lymphoma subtypes would be classified by the constellation of oncogenic driver mutations, but as most of these mutations are only just being elucidated this is currently limited to mutations in *MYC* or *BCL2* that were discovered cytogenetically several decades ago.

While spontaneous murine mature B cell lymphoproliferative disorders do occur, the lymphoid malignancies in mice that have been extensively studied in a laboratory setting are usually induced by genetic engineering and somatic mutagenesis with retroviruses or other agents. While this hastens lymphomagenesis and improves consistency, the relevance of such a manipulated system to the very pleomorphic collection of human B cell lymphoma needs to be considered. Mouse models of lymphoma can be used to advance understanding of human disease, but recognition of species-specific differences is important in order not to overstate the significance of findings in murine research.

Better understanding of the molecular drivers of human and mouse B cell malignancy will improve the alignment between experimental animal models and the clinical entitities. This is elegantly illustrated by the evolution of *MYC*-transgenic mouse models for Burkitt lymphoma. The first such animal model was the *Eμ-Myc* transgenic mouse [10], which recapitulates one of the most frequent oncogenic mutations in Burkitt lymphoma [11-13]. However, these animals primarily develop pre-B cell leukaemias and lymphomas, and not the germinal centre-origin malignancies corresponding to Burkitt lymphoma. To better emulate Burkitt lymphomagenesis, Rajewsky and colleagues [14] recently engineered transgenic mice that conditionally expressed a deregulated *Myc* gene only in germinal centre (GC) B cells. When they combined that with a second transgene that conditionally expressed an overactive PI3-kinase in the GC B cells, malignant mature B cell lymphomas arose that shared gene expression profile with Burkitt lymphoma but also acquired somatic mutations in the same Cyclin-D3 gene that has recently been identified by whole transcriptome sequencing of Burkitt lymphoma [5].The latter studies revealed exaggerated PI3K-signalling as a recurring feature of Burkitt lymphoma, reinforcing the congruence between the human disease and the animal model. The goal of this thesis is to define other components that cooperate with *MYC* to drive neoplastic proliferation of mature B cells.

Table 1.1 Common human mature B cell neoplasms

Human mature B cell neoplasm WHO classification [15]	Normal B cell correlate	Corresponding spontaneous murine neoplasm in inbred strains(s) or genetically manipulated murine models(m)
Mantle cell lymphoma	Naïve B cell	Mantle cell lymphoma (blastoid variant) (m)
Follicular lymphoma	Germinal centre B cell	Follicular B cell lymphoma (s) (m)
Burkitt lymphoma	Germinal centre B cell	Classic Burkitt lymphoma (m)
Burkitt-like lymphoma	Germinal centre or post germinal centre B cell	Burkitt-like lymphoma (s)
Diffuse large B cell lymphoma	Germinal centre or post germinal centre B cell	Diffuse large B cell lymphoma (s) (m)
Chronic lymphocytic leukaemia / Small lymphocytic lymphoma	Post germinal centre or naive B cell	Small B-cell lymphoma (s)
Lymphoplasmacytic lymphoma	Post germinal centre B cell	None known
Hairy cell leukaemia	Post germinal centre B cell	None known
Splenic marginal zone lymphoma	Post germinal centre B cell	Splenic marginal zone lymphoma (s) (m)
Plasma cell neoplasms	Plasma cell	Plasmacytoma (s) (m)
Prolymphocytic leukaemia	Unknown	None known
None known	Unknown	B natural killer cell lymphoma (s)

1.4 Mature B cell physiology

An appreciation of the pathways that facilitate normal mature B cell survival and growth and the different stages of B cell differentiation is required before dissection of the abnormalities that precipitate the development of lymphoma can be undertaken.

1.4.1 Survival or Apoptosis

BCR (B cell receptor) and BAFF (B cell-activating factor) pathways: The main pathways that are required for mature B cell survival are those that involve signalling through the B cell receptor and the BAFF pathway [16]. Inducible deletion of the B cell receptor on mature B cells leads to a significant depletion of their numbers [17], which has been demonstrated to be due to a loss of downstream signalling [18]. This cannot be due to loss of antigen specific signalling as all B cells are lost, not just those specific for a certain antigen. The B cell receptor appears to be able to transmit low level signals without receptor cross linking [19], which may be the survival signals required for maintenance of the mature B cell pool. The downstream pathways activated by the B cell receptor are complicated, including many signalling proteins whose mutation result in B cell immunodeficiency disorders, such as Bruton's tyrosine kinase responsible for X-linked agammaglobulinaemia, demonstrating the importance of these pathways in B cell development, survival and function (reviewed by Conley et al) [20]. An important target of these pathways is activation of the phosphoinositide 3-kinases (PI3K), (reviewed in Okkenhaug et al) [21] which result in activation of the serine/threonine kinase AKT/PKB and play an important role in regulating cellular metabolism and growth by activating the mammalian target of rapamycin (mTOR). Rajewsky and colleagues demonstrated that expression of a constitutively activate form of PI3K could prevent loss of B cells when their surface BCR was ablated, whereas activating mutations in other BCR-activated signalling pathways such as NF-κB could not [22].

Genetic deficiency of the tumour necrosis factor-related cytokine, BAFF [23], or one of its receptors, BAFFR [24], causes profound defects in mature B cell survival. BAFF administration promotes survival of mature B cells in vitro [24] and transgenic mice overexpressing BAFF demonstrate increased numbers of mature B cells [25]. The downstream signalling pathways from the BAFF receptor mediating this effect are still not well defined, but are thought to include protein kinase C delta (PKCδ) [26], BCL2 family proteins [27] and both the classical and alternate NF-κB pathways. Mutations in the beta subunit of IkappaB kinase (IKKb) that result in constitutively active NF-kB signalling are sufficient to substitute for BAFFR and promote survival of mature B cells in vivo or in vitro [28]. While this causes larger numbers of mature B cells to accumulate in vivo, the cells remain non-cycling G0 cells. AKT is also activated through BAFF receptor binding [29], although the mechanism of this activation remains to be elucidated.

As with all mammalian cells, the final stages of apoptosis in mature B cells is co-ordinated by two pathways, an intrinsic or mitochondrial pathway regulated by BCL2 and related proteins, and an extrinsic pathway involving members of the tumour necrosis factor family.

BCL2 family: The mitochondrial or intrinsic pathway of apoptosis is triggered by the translocation onto the mitochondrial membrane of pro-apoptotic BCL2 family members, BAX and BAK, causing cytochrome c release into the cytosol and sequentially cell death through a caspase cascade (reviewed by Marsden and Strasser [30]). The BCL2 family of proteins have homologous regions and have either pro apoptotic (eg BAX, BIM, NOXA, PUMA) or anti apoptotic (eg BCL2, BCLXL, MCL1) functions. Deficiency of Bcl2 causes a profound deficiency of mature B cells [31,32] while enforced expression of *Bcl2* promotes accumulation of large numbers of resting mature B cells [33] [34].

Fas: The extrinsic apoptosis pathway is stimulated by tumour necrosis family members such as Fas ligand binding to Fas (CD95) or other 'death receptors' on the cell surface [35]. This precipitates downstream signalling which results in activation of caspase-8 which then activates other downstream caspases, resulting in death of the cell.

Apoptotic pathways are inextricably linked to the B cell activation pathways in order to maintain homeostasis. BAFF stimulation has been demonstrated to reduce B cell apoptosis in vitro and in vivo [36]. Anti-apoptotic members of the BCL2 family, notably *Mcl1*, have been demonstrated to be induced by BAFF stimulation of B cells, while *Bcl2* itself is induced by signals through the canonical NF-κB pathway [37]. *BIM* is pro-apoptotic, and it has been shown [27] that its expression is upregulated by BCR binding, and that this is blocked by BAFF binding, thus inhibiting apoptosis. Some of these interactions between the survival and apoptotic pathways may be mediated by AKT/PKB.

1.4.2 Growth signals for B cell proliferation

Important steps required for mature B cell proliferation can be subdivided into:
-Mitogen binding to B cell surface
-Signal transduction: surface to nuclear cell cycle control mechanisms
-Cell cycle progression

Mitogen binding to B cell surface

Cross linking of the B cell receptor by antigen precipitates recruitment and activation of SYK (spleen tyrosine kinase), a tyrosine kinase, which drives multiple complex signalling pathways, including elevation of intracellular calcium and activation of the ERK MAP kinase pathway and the canonical NF-κB pathway [38]. Replication of mature B cells is classically stimulated by cross linking of the B cell receptor by antigen in association with a co-stimulatory signal such as CD40-CD40 ligand binding provided by T cells. Like BAFF, CD40 binding can activate both the classical and alternate NF-κB pathways, although CD40 ligand signalling, or agonistic antibodies to CD40, are potent mitogens for B cells whereas BAFF alone is not mitogenic although it augments the B cell proliferation stimulated by anti-IgM [39] or CD40 ligand [36].

Thymus independent antigens are a group of antigens that include viral nucleic acids and bacterial lipids and polysaccharides able to stimulate B cells in the absence of helper T cells. This response is mediated by Toll-like receptors (TLR) which are found on most cells, including B cells, with different TLR being stimulated by different microorganism antigens. Toll-like receptors have some

downstream signalling pathways in common such as the NF-κB pathway and mitogen activated protein kinase (MAPK) pathway [40], many of which are similar to the pathways activated by BCR binding, but each receptor subtype also has its own unique features and thus differing patterns of gene expression are seen with activation of different TLR subtypes.

Signal transduction: surface to nuclear cell cycle control mechanisms

NF-κB pathway: Multiple pathways help to transduce the B cell surface binding signal to the nucleus to promote proliferation. One such pathway is the Nuclear factor kappa B (NF-κB) pathway, which is essential for B cell survival and for BCR, CD40 or TLR-induced proliferation, as demonstrated by knock out models [41], and reviewed by Gerondakis et al [42]. The NF-κB family has five homologous members, all of which are transcription factors. They are RELA (also called p65), c-REL, RELB, p105/p50 (also called NF-κB1) and p100/p52 (also called NF-κB2). These factors are only active in the nucleus, where they can regulate gene transcription, but are usually in the cytoplasm bound to inhibitory proteins.

In the classical NF-kB activation pathway signalling through cell surface receptors enables phosphorylation of these inhibitory proteins by the IκB kinase complex, leading to their ubiquitination and degradation and allowing nuclear translocation of NF-κB family members and activation of gene transcription. This pathway can be stimulated in B cells by the BCR, CD40, and TLR4 or TLR9. Genes that have been shown to be transcribed in B cells in response to canonical NF-kB signalling encode key cell cycle proteins (eg Myc [43], Cyclin D1 [44], IRF4 [45]) and anti-apoptotic members of the Bcl2 family (eg $BclX_L$, A1/Bfl1) [46].

The alternative NF-kB activation pathway is activated by ligand binding to members of the TNF receptor superfamily such as the BAFF receptor or CD40. Activation of this pathway results in activation of IKKα which phosphorylates p100/p52, allowing its partial proteolysis, facilitating its translocation into the nucleus. Activation of the alternative pathway in B cells induces the anti-apoptotic Bcl2 family of genes in addition to Pim-2 kinase [46].

B cell cycle progression

This process is promoted by various cyclin dependent kinases at specific stages of the cell cycle, the activity of which are modulated by cyclins and cyclin dependent kinase inhibitors [47]. In B cells, multiple factors influence the activity of these components:

CCND1, CCND2, CCND3: Cyclin D1 is normally only expressed at the G1 phase of the cell cycle and in conjunction with multiple other cyclins and cyclin dependent kinases facilitates the G1/S phase transition by phosphorylating and inactivating the Retinoblastoma tumour suppressor protein. In some cases of Chronic lymphocytic leukemia, *CCND1* is dysregulated by a chromosomal translocation fusing it with the IGH locus [48]. Cyclin D2 is rapidly induced by BCR signalling [49], and high expression of *CCND2* is highly predictive of shorter overall survival in human DLBCL [50]. Cyclin D3 is required for proliferation of germinal centre B cells [51], and recurrent somatic mutations that stabilize the protein are observed in Burkitt lymphoma [5] and its animal model [14].

MYC is a transcriptional amplifier that is essential for B cells to enlarge and enter cell cycle [52]. A detailed discussion of *MYC* is provided below.

***mTOR* and PI3-kinase.** *mTOR* encodes a protein kinase that is the target of the immunosuppressive drug rapamycin, and is an important regulator of cell growth, survival, metabolism and proliferation and modulates protein translation (reviewed by Laplante and Sabatini [53]). mTOR is stimulated by diverse upstream pathways, notably the PI3K/AKT pathway [21]. The precise mechanism of interaction between *mTOR* and *Myc* is unclear, but it has been suggested that activation of *Myc* suppresses *TSC2*, a suppressor of mTOR [54].

TGFβ: Transforming growth factor beta is an anti-proliferative factor for B lymphocytes that blocks cell progression at the G1-S phase transition check point [55]. TGFβ targets include some cyclin dependent kinases, the retinoblastoma protein and *Myc*, the latter possibly through the NF-κB pathway [56].

DNA damage response pathway: This pathway is activated in response to DNA damage, predominantly to double strand breaks. The upstream regulators of this pathway include kinases encoded by *ATM* (Ataxia telangiectasia mutated) and *ATR* (ATM-Rad3-related). They phosphorylate various proteins to facilitate modifications in cell cycle activity and protein repair, including phosphorylation of MDM2 which results in stabilisation of p53 [57]. *TP53* (*Trp53* in mice) encodes the transcription factor p53 which induces inhibitors of cell cycle and promoters of apoptosis, and is discussed in detail in Section 1.6.

1.4.3 Differentiation

Tightly co-ordinated differential gene expression is required at each stage of B cell development to facilitate the development of mature B cells from multipotent stem cells. In brief, the earliest stage of mature (defined as having surface immunoglobulin) B cell development is the naïve B cell. These cells are often CD5 positive and circulate in the blood in addition to being found in primary lymphoid follicles and mantle zones. A small proportion of these cells are subsequently exposed to specific antigen inducing T cell-dependent proliferation and migrate into the centre of a primary follicle where they form a germinal centre. Germinal centre cells express CD10 and BCL6 and commonly undergo somatic hypermutation and class switch recombination. These cells subsequently become plasma cells or post germinal centre memory B cells which are found in blood and lymph nodes and the follicular marginal zones of lymph nodes, spleen and mucosa associated lymphoid tissue. Some of the important genes in this maturation process include:

PAX5 is a member of the PAX family of transcription factor genes. This gene is only expressed within the B cell lineage in the haemopoietic system. Pro-B cells require *PAX5* expression to differentiate into more mature B cells [58]. *PAX5* is also required to maintain the identity of the mature B cell [59]. *PAX5* is not expressed in plasma cells, and it has been demonstrated [60] that Blimp1-induced suppression of *PAX5* is required for plasma cell differentiation.

BCL6 (B cell lymphoma 6) encodes a protein of the same name which is a repressor of transcription. Its expression is required for the formation of

germinal centres [61], and its expression needs to be suppressed for the differentiation of germinal centre B cells into non-dividing memory cells or plasma cells. Its precise role in this process is still being clarified, but it has been shown that it suppresses the DNA damage-sensing machinery, allowing somatic hypermutation and class switch recombination [62].

IRF4 (Interferon regulatory factor 4) (also called MUM1) encodes a transcription factor that is critical throughout much of B cell development. *IRF4* is induced by the NF-κB pathway, and it in turn suppresses *Bcl6* [63]. Teng et al [64] demonstrated that its expression reduces the cell cycle progression of germinal centre B cell-derived Burkitt lymphoma cells. The same group also confirmed that IRF4 represses *Bcl6* expression and induces *BLIMP-1* expression, facilitating plasmacytic differentiation. *IRF4*'s role modifying the expression of genes critical for B cell differentiation suggests that its induction at the later stages of the germinal centre formation helps co-ordinate the termination of this stage of maturation and further B cell differentiation to the plasma cell stage.

BLIMP-1 (B lymphocyte induced maturation protein-1, encoded by the *Prdm1* gene) is a transcriptional repressor, the expression of which induces plasmacytic differentiation through modulation of expression of a large number of genes controlling mature B cell homeostasis and immunoglobulin production including *Pax5*, *Myc*, and *Bcl6* (reviewed in Johnson et al [65]). The expression of *Prdm1* is suppressed by Bcl6 [66].

1.5 Basis for mature B cell lymphoproliferative disorders

1.5.1 Broad Aetiology

Much research has been undertaken into the genetic perturbations that predispose, precipitate and perpetuate B cell lymphomas, usually focussing on genetic factors within the B cell ('cell autonomous'). It must be remembered, however, that non-autonomous genetic factors, such as those influencing the

tumour microenvironment, are likely to also be influential. In addition, although this thesis refers specifically to genetic defects, non genetic defects are clearly important in B cell lymphoma. Such factors include the immune response to the tumour, changes in the cytokine milieu, growth factors, and hormonal changes such as steroid levels. In addition, mesenchymal stem cells are also thought that play an important role (reviewed in [67]). B cell extrinsic factors causing B cell activation also need to be considered. Bacterial infections such as Helicobacter pylori and Chlamydia trachomatis and viruses such as Hepatitis C and HIV have been clearly associated with an increased incidence of lymphoma [68]. Toll-like receptors may be significant in this regard, with repeated stimulation of cell cycling by recurrent viral or bacterial infections facilitating the outgrowth of a malignant clone. Support for this comes particularly from the recent finding that activating mutations in *MYD88*, encoding a critical intracellular mediator of TLR signalling, are found in nearly 100% of Waldenstrom macroglobulinaemia [69] and more than 30% of DLBCL [70].

The increased incidence of B cell lymphoma in patients with autoimmune diseases re-emphasises the importance of immune dysregulation in the aetiology and propagation of B cell lymphoma [71]. Defects in immune surveillance also contribute to the development of malignancy [72], including lymphoma. An example is perforin deficient mice, which have a high incidence of B cell lymphoma (among other lymphoma types), with cell transfer experiments demonstrating that these lymphomas are rapidly destroyed in mice with the same genetic background but with intact perforin genes [73]. Perforin is critical for the cytotoxicity of NK cells and CD8 positive T cells, and is not made by B cells, consistent with a role for NK and T cell surveillance against B cell lymphoma.

Mouse plasmacytoma can be caused by persistent peritoneal irritation in BALB/c mice by intraperitoneal injection of pristine. Most of these tumours overexpress *Myc*, with greater than 80% harbouring a mutation that leads to the juxtaposition of the murine immunoglobulin heavy chain gene on chromosome 12 with the murine *Myc* gene on chromosome 15 [74]. The incidence of plasmacytoma can be further modified by altering gut bacterial flora, or exposure to cholera toxin, and other strains of mice are relatively resistant to

the development of a plasmacytoma in identical conditions [75], all of which suggests that host and environmental factors interact and strongly influence B cell transformation.

In summary, B cell lymphoma is thus likely to be a multifactorial process, and while the following discussion focuses on genetic factors within the B cell, these alone are unlikely to fully explain the pathogenesis of this diverse malignancy.

1.5.2 MicroRNAs

MicroRNAs (miRNAs) were first identified in 1993 [76] although their role in modulation of gene expression was not defined until 2000 [77]. Since then extensive research has helped clarify their role in normal and aberrant human cellular processes. They are short nucleotide sequences which are encoded by the genome and act by reducing translation and altering stability and polyadenylation of target messenger RNA. In the recently released miRBase 19, 2019 unique mature human miRNA sequences are described [78], and it is well known that a single microRNA can modulate the translation of hundreds of mRNAs, and thus their sphere of influence is enormous and they add an important layer to the complex web of gene expression regulation.

MicroRNAs are variably expressed at various stages of B cell development, suggesting a role in differentiation [79]. Zhang et al [80] showed that B cell stage–specific miRNAs are often conserved between B-cell malignancies and the corresponding normal B cell developmental stage from which they are presumed to arise. However, some miRNA expression profiles are perturbed in neoplasia, with the microRNA profile of mature B cell lymphoproliferative disorders varying with the lymphoma subtype (reviewed in [81]), although whether this is a primary or secondary event has not been well defined. Calin et al [82] identified that miRNA genes are frequently located at cancer-associated fragile sites or common breakpoint regions, suggesting that their dysregulation may modulate the initiation of neoplastic transformation.

Deletion of chromosome 13q14 is the most commonly identified genetic mutation in CLL, found in approximately 50% of cases, and associated with

longer time to first treatment. The relevance of this mutation was unclear until it was revealed that this region encoded the miR-16-1/miR-15a cluster [83] which was subsequently demonstrated to negatively regulate BCL2 [84]. miR-155 is very highly expressed in Hodgkin Lymphoma, Primary Mediastinal B cell Lymphoma and Diffuse Large B cell Lymphoma of the Activated B cell subtype. Overexpression of this cluster in the murine B cell compartment (Eμ-mmu-miR155 construct) initially results in a pre-leukaemic pre-B cell proliferation which progresses to a B cell malignancy [85] suggesting that defects in this cluster may be a primary event in lymphomagenesis. Paradoxically, Burkitt lymphoma demonstrates a markedly reduced expression of miR-155 [86].

To date microRNA expression has been shown to have diagnostic and prognostic significance in some B cell lymphoproliferative disorders (reviewed in [81]), with ongoing research into their therapeutic utility. This is a rapidly developing field, and further research is likely to significantly contribute to our understanding of the pathogenesis of B cell lymphoma.

1.5.3 Epigenetic changes

Epigenetic modifications also need to be considered, although there is less definitive literature dissecting their implication in lymphoma. It has been proposed that methylation, particularly of CpG islands associated with gene promoters (the CpG components of which are often methylated in transcriptionally inactive genes), may inhibit gene expression. DNA Methylation patterns are often different in malignant cells compared to their normal counterparts. Pike et al [87] analysed cases of Diffuse Large B cell Lymphoma demonstrating significant CpG island methylation, a frequent association between CpG island methylation and reduced expression of the downstream gene, and differential methylation patterns between subtypes. Mestre-Escorihuela et al [88] demonstrated methylation of putative tumour suppressor genes and corresponding reduced expression levels in many types of lymphoma. In all these studies, however, it remained unclear whether these abnormalities were primary or secondary events in lymphomagenesis. Epigenetic changes also include histone modifications. Morin et al [4] and Pasqualucci et al [89] showed that histone-modifying genes, notably *MLL2* and

EZH2, were frequently mutated in both DLBCL and Follicular Lymphoma suggesting that epigenetic changes have a primary role in tumour initiation or progression.

1.5.4 Causes of somatic mutation in B cell lymphoma

The mutating effect of ionising radiation and chemicals on DNA is well recognised. In addition, spontaneous DNA mutations occur constantly due to defects in DNA synthesis, repair or recombination. Furthermore, recurrent translocations are found in many types of B cell lymphoma such as the t(8;14) in Burkitt lymphoma, t(11;14) in Mantle Cell Lymphoma and t(14;18) in Follicular Lymphoma. These translocations allow juxtaposition of a proto-oncogene with the immunoglobulin heavy chain locus causing overexpression of the former. The recurrent nature of these mutations and their unique occurrence in B cells suggests that the aetiology of these mutations may be relatively B cell specific.

V(D)J recombination occurs as B cells mature, facilitated by recombinase activating genes (RAG). *IGH:BCL2* translocations appear to arise as errors in this process. Somatic hypermutation and class switch recombination are initiated by activation-induced cytidine deaminase (AID) upon antigen and CD40 stimulation of mature B cells. *IGH:MYC* translocations typically arise as errors of class switch recombination. AID deaminates cytosines on the DNA of immunoglobulin genes thereby generating a lesion that results in DNA mutation or breakage. Aberrant somatic hypermutation is thought to contribute to B cell lymphomagenesis. AID has been demonstrated to facilitate initial genetic mutations that predispose a B cell to malignant transformation and subsequent mutations that facilitate tumour evolution (reviewed in Okazaki et al [90]). Aberrant somatic hypermutation and class switch recombination in lymphomagenesis may explain why most B cell lymphomas are derived from germinal centre B cells or their descendants. This may also explain the importance of an intact B cell receptor for lymphomagenesis, as it is cross-linking of the B cell receptor that stimulates the germinal centre reaction.

Insertional mutagenesis by retroviruses strongly promotes lymphomagenesis in mice. This is best illustrated by the acceleration of B cell lymphomas in *Eμ-Myc*

transgenic mice upon infection with Moloney murine leukaemia virus [91,92]. Repeated cycles of MuLV virus production, infection and provirus integration in activated B cells results in copies of the proviral enhancer and promoter being inserted into different cellular genes, where it frequently leads to dysregulated expression of the cellular gene (reviewed by Uren et al [93]). A large database of retroviral insertion sites in lymphoma has been assembled [94], with recurrent integration sites implicated as potential oncogenes.

1.5.5 Mutations in survival/apoptotic pathways and evasion of programmed cell death

BCR: Signalling through the B cell receptor has been demonstrated to be important in the persistence of B cell lymphoma [95], with Refaeli et al demonstrating tumour regression on disruption of B cell receptor signalling. The contribution that B cell receptor signalling is likely to play in lymphomagenesis is further emphasised by the observation that translocations which involve immunoglobulin loci are non-random, being almost always found on the non-productively rearranged locus, leaving the other locus to contribute to the formation of the B cell receptor [96]. The association between infections such as hepatitis C and Helicobacter pylori and lymphoma, and the disease regression that may be seen with treatment of the infection again strengthens the case for the importance of the B cell receptor for lymphomagenesis [97].

CARD11 encodes an intracellular protein essential for BCR-signalling to the canonical NF-kB pathway and induction of B cell proliferation, but not for CD40 or Toll like receptor-mediated signalling of these events. Recently, activating mutations in *CARD11* have been found in approximately 10% of human Diffuse Large B cell Lymphomas [98,99]. Lenz et al [98] also demonstrated that experimental reproduction of such mutations in lymphoma cell lines produced constitutive NF-κB activation. Likewise, shRNA knock-down of *CARD11* inhibits the growth and survival of human Diffuse Large B cell Lymphoma cell lines [100]. These activated *Card11* alleles were sufficient on their own to promote enormous but ultimately self-limiting B cell proliferation when introduced by retroviral gene transfer into antigen-activated normal mature B cells [101].

These observations further suggest that dysregulated BCR signalling to NF-kB is an important element of lymphomagenesis.

BAFF and its family have been demonstrated to be critical for the survival of some B cell lymphoma lines [102]. Human B cell lymphomas express BAFF receptor, and high serum levels of BAFF was found to be an independent prognostic factor for overall survival in treated Diffuse Large B cell Lymphoma [103], although whether this elevation is primary or secondary to transformation remains to be determined.

ATM: Mutations in both copies of the *ATM* gene cause Ataxia telangiectasia, a syndrome which includes neuronal degeneration and a susceptibility to cancer. The malignancies are predominantly lymphoid, being of either B or T cell origin [104]. *ATM* has also been demonstrated to potentiate the induction of lymphoma in the setting of *Myc* overexpression through an impaired apoptotic response [105].

BCL2 family: Apoptotic pathways are commonly disrupted in low growth fraction lymphomas. The t(14;18) typically seen in Follicular Lymphoma in humans, and involves a translocation between *BCL2* and the immunoglobulin heavy chain enhancer. Dysregulation of *BCL2* expression alone is insufficient for a malignant phenotype, as demonstrated by the detection of small numbers of cells in normal individuals with the characteristic t(14;18) [106], and by mouse models showing that *Bcl2* overexpression under the influence of the VavP promoter induces polyclonal B cell expansion initially, followed by follicular lymphoma at greater than 10 months of age [34], the latter presumably requiring further genetic defects. Likewise, *Bcl2* overexpression under the control of the immunoglobulin heavy chain enhancer and promoter does not cause lymphoma, but promotes extensive accumulation of small resting follicular B cells [33].

Fas: Patients with germline *FAS* mutations demonstrate an increased incidence of both B cell and T cell lymphoma (the former including both non-Hodgkin lymphoma and Hodgkin lymphoma) [107]. While the simple explanation for this is that defective apoptosis in B cells facilitates the accumulation of genetic

defects in B cells, altered immune surveillance has also been proposed to be contributory, with the T cell defect produced by *FAS* mutation facilitating the development of the malignancy [107,108].

1.5.6 Mutations in proliferative pathways and self-sufficiency for growth factors

Surface binding factors

BCR: Refaeli et al [95] demonstrated that stimulation of the B cell receptor in *Myc*-overexpressing mice accelerated lymphomagenesis and that the phenotype of the resulting B cell lymphoma was dependent on the activational status of the BCR.

Signal transduction pathways

The **NF-κB pathway** has been demonstrated to be highly significant in many types of B cell lymphoma (reviewed in [109]), consistent with its pivotal role in normal B cell homeostasis and proliferation. The founding member of this transcription factor family, *Rel*, was discovered because a mutated viral derivative, *v-Rel*, is the B cell leukaemia-transforming oncogene carried by the avian reticuloendotheliosis retrovirus [110].

Inhibition of this pathway has been shown to cause regression of cell lines modelling the activated B cell-like subtype of Diffuse Large B cell Lymphoma [100,111]. This subtype of lymphoma has also been demonstrated to commonly harbour mutations in genes that regulate the NF-κB pathway [99], suggesting that dysregulation of this pathway can be a primary pathogenetic event. *A20*, a negative regulator of the pathway, was the most commonly mutated gene in Diffuse Large B cell Lymphoma in the studies performed by Compagna et al [99], and when Kato et al [112] re-expressed this gene in a lymphoma cell line with no functional *A20* alleles, downregulation of the NF-κB pathway resulted in a consequential reduction in cell growth and increased apoptosis.

Other subtypes of B cell lymphoma also commonly harbour mutations in the genes influencing the NF-κB pathway [112,113]. Mucosa-associated lymphoid tissue (MALT) lymphoma is associated with chronic antigenic stimulation, but also demonstrates a number of common genetic mutations. Three of the most common chromosomal translocations seen in MALT lymphoma result in dysregulation of the NF-κB pathway through their interactions with upstream genes including *BCL-10*, *MALT1* and *CARD11* (reviewed in Nakagawa et al [114]).

SYK: Blocking of signalling through Syk, which acts downstream of the B cell receptor as above, has also been shown [115] to precipitate apoptosis is both cell lines and tumour suspensions of Diffuse Large B cell Lymphoma, the responsive cells being demonstrated to have intact BCR signalling prior to the introduction of the inhibitor. In addition, Syk kinase has been found to be constitutively phosphorylated in CLL cells [116], with many cells demonstrating increased apoptosis when exposed to a Syk inhibitor.

Cell cycle factors

MYC is discussed in detail in Section 1.7.

mTOR: *mTOR* has been demonstrated to be overexpressed in several lymphoproliferative disorders (reviewed in [117]). Research has focussed on Mantle cell Lymphoma where the mTOR pathway has been demonstrated in cell lines and patient samples to be activated, with experimental reduction in activation of mTOR inducing cell cycle arrest and apoptosis in Mantle Cell Lymphoma cell lines [118]. Clinical trials have confirmed the efficacy of an mTOR inhibitor [119] in Mantle cell Lymphoma.

The links between Myc and the mTOR pathway were discussed briefly earlier. Early work [120] reported that everolimus, an mTOR inhibitor, reduced lymphomagenesis in *Eμ-myc* mice by up to 90%, despite no effect on the level of *Myc* expression suggesting that much of *Myc*'s activity is mediated through the mTOR pathway.

TGF-β: The role of TGF-β in B cell lymphoma still remains to be clearly defined although it is known to enhance angiogenesis, tumour spread and potentially reducing immune surveillance in solid tumours (reviewed by Elliott et al [121]). Both B cells and T cells produce TGF-β, and this increases with activation [122]. Some B cell malignancies have been shown to have an altered response to TGF-β [123]. These factors may influence the development and progression of B cell lymphoma, but this remains to be clarified.

CCND1 encodes Cyclin D1, dysregulation of which is seen in Mantle Cell Lymphoma in humans, with the classic t(11;14) juxtaposing the immunoglobulin heavy chain enhancer with *CCND1*. A French group also demonstrated that 21% of myeloma patients have translocation t(11;14) using fluorescence in situ hybridisation (FISH) [124], resulting in up regulation of *CCND1*.

1.5.7 Mutations affecting differentiation and its inhibitory effect on growth

Bcl6: Intuitively Bcl6's role in faciliting somatic hypermutation and class switch recombination through suppression of the DNA damage-sensing process may also be permissive for the survival of defective B cells that would otherwise be forced to undergo apoptosis, potentially allowing the development of a malignant clone. Mouse models overexpressing *Bcl6* demonstrate an initial polyclonal proliferation of mature B cells, followed by the outgrowth of a B cell lymphoma resembling human Diffuse Large B cell Lymphoma [125]. *Bcl6* is commonly mutated in human B cell lymphoma, with its overexpression being characteristic of the germinal centre type of Diffuse Large B cell Lymphoma [126].

PAX5 somatic mutations were identified in 32% of paediatric ALL in one study [127]. t(9;14)(p13;q32) was initially reported in approximately 50% of lymphoplasmacytoid lymphomas, and suggested [128] to cause juxtaposition of the *PAX5* gene with IgH regulatory elements, although more recent publications [129,130] have failed to confirm this association.

IRF4: *IRF4* is expressed in a significant proportion of B cell lymphomas [131], although its role, if any, in the pathogenesis is still being defined. Alteration in the IRF4 binding domain of *BCL6* has been noted in a significant proportion of Diffuse Large B cell Lymphoma and Burkitt Lymphoma cell lines [63]. This would result in failure of downregulation of *BCL6*, and may thus facilitate lymphomagenesis. It has also been suggested that IRF4 plays a key role in the transformation of B cells by EBV in vivo and in vitro [132].

BLIMP-1 (the human equivalent being called positive regulatory domain-I binding factor-1 (*PRDIBF1*)) has potential relevance in lymphomagenesis in view of its critical role in B cell maturation. It has been demonstrated that overexpression of *BLIMP-1* hastened apoptosis of a lymphoma cell line [133], but BLIMP-1's role in lymphomagenesis remains to be clarified.

1.6 p53

1.6.1 p53's role as a tumour suppressor gene

TP53 (*Trp53* in mice) is one of the most intensively studied tumour suppressor genes, encoding the protein p53. It is the most frequently mutated gene in human cancers. The first reports of the importance of p53 in cancer were published in 1979 when it was identified in simian virus 40 transformed cell lines and tumours by multiple groups [134-137]. It was initially believed to be an oncogene, and it was almost a decade before it was appreciated [138] that the p53 cDNA clones that had been identified as promoting cellular transformation actually encoded mutant p53, explaining their oncogenic properties. p53 defective mice [139] and humans [140,141] clearly have a cancer-prone phenotype.

The molecular basis for its tumour suppressor function is complex, as p53 is a DNA-binding nuclear protein that activates or represses transcription of numerous target genes. Ablation of individual p53 target genes has been unsuccessful in replicating the tumour-prone p53 knockout phenotype [142] suggesting that its tumour suppressor role may not be due to dysregulation of a

single pathway. PUMA and NOXA are proapoptotic members of the BH3-only Bcl2 family that are strongly induced by p53, and they play key roles in p53 mediated apoptosis [143,144], but neither *Puma* null mice nor *Noxa* null mice are predisposed to cancer, although reduced *Puma* expression cooperates with other oncogenic mutations [145,146]. The potential redundancy between *Puma* and *Noxa* illustrates why mutations in *Trp53* itself are so potent compared to mutations in individual target genes. Liu et al [147] developed a p53 mutant mouse which had lost it apoptosis-promoting function but retained much of its cell cycle arrest capability, and demonstrated that these mice were much less tumour-prone than p53 knockout mice. Brady et al [148] showed that specific mutations of p53 were able to abrogate its role in cell cycle arrest and apoptosis as a response to DNA damage but enabled it to maintain it tumour suppressor and senescence functions, although complete abolition of transcriptional activation function enhanced tumour growth.

1.6.2 p53's role in lymphomagenesis

While p53 mutations are not uncommon in haematological malignancies, the incidence is lower than seen in solid tumours [149]. Within the International Agency for Research on Cancer (IARC) TP53 database (November 2010 release) 19.3% of lymphoid malignancies harboured a mutation in the *TP53* coding sequence [150] with mutations being seen in most exons, most of which were point mutations. *TP53* dysfunction can also occur at an epigenetic, mRNA or protein level (reviewed by Xu-Monette et al [151]). Dysregulation of the p53 pathway, either upstream or downstream from the p53 protein is probably even more common than gene mutation. Overexpression of *MDM2*, a ubiquitin ligase that degrades p53, is frequent in B cell lymphoma [152], and inactivating mutations at the *INK4a/ARF* locus (encoding p14(ARF) a inhibitor of MDM2 and hence an activator of p53) have also been identified in some B cell lymphomas [153]. Mutations in the *ATM* (ataxia telangiectasia mutated) gene (which encodes a p53 activating kinase) have also been reported [154] in CLL and associated with p53 dysfunction. Burkitt lymphoma has a particularly high rate of mutations in *TP53*, *MDM2* and *INK4A* [5,155].

p53 mutations in lymphoproliferative disorders confer a poorer prognosis. *TP53* mutations are more common in high rather than low growth fraction lymphoma [156] and it has thus been suggested that mutated p53 facilitates the progression of low grade lymphomas to high grade variants, or a more aggressive clinical course. Two small studies [157,158] have shown that patients with transformed Follicular Lymphoma commonly acquired p53 mutations in the process of transformation. Malcikova et al [159] showed that some p53 defects in patients with CLL occurred post therapy, but in contrast, Pekova et al [160] were unable to confirm an increased incidence of *TP53* mutations in patients with CLL post chemotherapy.

1.6.3 p53's physiological role

p53 is a transcription factor that transactivates or transrepresses hundreds of target genes including large numbers of microRNAs (reviewed in [151]). More recently it has also been demonstrated to have a cytosolic transcription-independent functions [161]. Its diverse functions include regulation of cell-cycle arrest, DNA repair, apoptosis, senescence, and autophagy in response to various forms of cellular stress, including oncogene activation, DNA damage, and hypoxia. The p53 protein is usually found in low levels in murine cells bound to Mdm2 which facilitates its degradation. Its cellular level and activity is modulated in diverse ways including post-translational modification [162] and altered binding to Mdm2. The function of p53 in the context of cellular stress depends on a multiplicity of factors including the cell type, cell-cycle stage, the nature of the insult and other oncogenic mutations within the cell. While the diverse functions of p53 do not operate in isolation the best defined roles are summarised separately below for clarity.

Apoptosis: p53 facilitates apoptosis in several ways, the best defined being through the intrinsic apoptotic pathway mediated by BCL2 family proteins. Within the nucleus p53 induces expression of pro apoptotic BAX and PUMA [145]. Within the cytoplasm p53 binds to BCL-XL with subsequent PUMA binding releasing p53 to directly activate BAX and induce mitochondrial outer membrane permeabilisation [163] activating a downstream caspase cascade

precipitating apoptosis. p53 can also modulate apoptosis in other ways including via the extrinsic apoptotic pathway (reviewed in [164]).

Cell cycle arrest: p53 causes a reversible cell cycle arrest at the G1 checkpoint predominantly through downstream activation of p21 which subsequently inhibits cyclin-dependent kinases [165,166]. There have also been suggestions that p53 acts at other cell cycle control checkpoints [167,168].

DNA repair: In the setting of genotoxic stress p53 mediates DNA repair mechanisms. p53 has been shown to modulate nucleotide-excision repair, base-excision repair mismatch repair, non-homologous end-joining and homologous recombination [169] in both a transactivation dependent and independent fashion.

Senescence: Senescence is defined as a cell losing its capacity to divide. Oncogene activation or genotoxic stress (such as DNA damage or reduction in telomere length) may precipitate a senescent state. p53 plays a role in senescence which is probably at least partially mediated by p21 [170,171].

Autophagy: This is predominantly a homeostatic process where damaged proteins and organelles are recycled for nutrients, although is enhanced in the context of cellular stress. Recently p53 has been shown to modulate autophagy [172]. In general, nuclear p53 promotes autophagy with downstream pathways including modulation of the damage-regulated autophagy modulator (*DRAM*) gene expression [173] and negative regulation of the mTOR pathway [174]. This process probably promotes cell survival under stressors such as nutrient deprivation or hypoxia. In contrast, cytoplasmic p53 inhibits autophagy [175], the mechanisms of which remain poorly defined, but the consequences of which appear to enhance cell death.

1.7 Myc

MYC overexpression is very common in a diverse range of cancers. Its significance in neoplasia was identified when the oncogenic retrovirus avian

myelocytomatosis virus was found to have a cellular homologue [176]. Subsequent work rapidly confirmed that this gene was activated in many animal and human tumours (reviewed by Nesbit et al [177]). *Myc* dysregulation may occur in many ways including copy number amplifications [178], modulation of transcription or translation and post translational modification. Extensive research has failed to isolate specific *Myc*-mediated dysregulated cellular pathways in oncogenesis but recent publications [179,180] show that rather than targeting specific genes, Myc exponentially amplifies the output of existing transcriptionally active genes.

1.7.1 Myc's role in lymphoma

Early studies identified the *Myc* locus as a common integration site in avian leucocytosis virus induced lymphoma [181]. Later murine experiments [182] subsequently confirmed that sites adjacent to the *Myc* gene were common integration sites in murine leukemia virus-induced lymphoma. Outside of retrovirus-induced cancer, one of the first examples of spontaneous mutation of a cellular proto-oncogene into an oncogene was the recurrent *IgH* translocation first discovered to activate *Myc* expression in mouse plasmacytomas [183] and subsequently confirmed in human Burkitt lymphoma [184,185]. Increased *Myc* expression by translocation of *Myc* adjacent to the immunoglobulin locus was shown experimentally in *Eμ-myc* transgenic mice [10] and by retroviral transduction [186] to expedite lymphoma development, and such models have been very valuable in enhancing understanding of lymphocyte biology and lymphomagenesis.

Myc overexpressing mouse models have demonstrated that *Myc* dysregulation alone is insufficient for cellular transformation, evidenced by the time lag before tumours develop and the clonal nature of the resulting neoplasms [10,187]. *Eμ-myc* transgenic mice almost always develop B cell lymphoma with age, prior to which they have a significant expansion of their B cell compartment, with a predominance of large polyclonal pre-B cells [188]. A frequent somatic mutation in the clonal lymphomas that develop in these mice is inactivation of the *Trp53* pathway, which plays a critical role in preventing Myc-induced transformation [189,190]. These experiments and others in fibroblasts [191-

194] emphasize the potent cooperation between oncogenically activated *Myc*, which promotes growth but also activates p53-mediated cell cycle arrest and apoptosis, and oncogenic inactivation of p53. *Myc* has also been shown [187,195] to contribute to lymphoma viability with some lymphoma regression demonstrated with the withdrawal of *Myc* overexpression.

Pairing of *MYC* and *TP53* mutations is a cardinal feature of human Burkitt Lymphoma. Burkitt Lymphoma was first described in 1958 [196] by Dennis Burkitt as a sarcoma, but subsequently found to be lymphoid in origin and named in his honour. This highly aggressive B cell lymphoma is characterised by *MYC* overexpression. Three subtypes have been identified [15]. Endemic Burkitt lymphoma is the subtype originally described by Burkitt and characteristically occurs in equatorial developing countries such as Africa and Papua New Guinea. This classically affects extranodal sites such as the jaw and facial bones, and is the most common malignancy in children in these regions. Sporadic Burkitt Lymphoma is seen worldwide, characteristically in younger patients, although remains an uncommon lymphoma (1-2% of lymphomas in developed countries). Immunodeficiency-associated Burkitt lymphoma is mainly seen in the context of HIV infection.

Endemic Burkitt Lymphoma is strongly associated with EBV infection, with the majority of tumour cells containing the EBV genome [197]. Sporadic and Immunodeficiency-associated Burkitt Lymphoma is less strongly associated with EBV infection, with approximately 30% and 25-40% respectively of cases having detectable virus. The role of EBV in lymphomagenesis remains unclear and is discussed in more detail in Section 1.9. More recently the role of Plasmodium [198] has been investigated as the distribution of endemic Burkitt Lymphoma mirrors the distribution of endemic malaria. It has been proposed that the role of such infections is stimulation of polyclonal B cell proliferation, potentially enhancing survival of cells acquiring chromosomal translocations (such as those resulting in *MYC* overexpression) and modulating immune responses. The association between HIV infection and Burkitt lymphoma is also likely to be due to more than virus-associated immunosuppression as these lymphomas tend to develop prior to the onset of marked immunosuppression.

Other lymphoma subtypes have been shown to have *MYC* overexpression, albeit in a smaller percentage of cases. Diffuse large B cell lymphoma is associated with *MYC* overexpression in ten percent of cases, conferring a poor prognosis [199]. In plasma cell myeloma *MYC* translocations are seen in 15% of patients [200] (using fluorescence in situ hybridisation) and in this setting the gene is commonly dysregulated by complex chromosomal rearrangements [201].

1.7.2 Myc's physiological role

MYC encodes a transcription factor which influences a broad range of cellular functions. Like p53, its targets are numerous and complex. A screen for MYC binding sites in human cells demonstrated that MYC target sites are found in promoters of approximately 11% of genes [202] with vast numbers of target genes also identified in a B cell model [203]. Myc mediates most of its transcription regulation by dimerisation with Max and subsequent direct binding to the promoter sequence of target genes. Intracellular levels of Myc are tightly regulated at multiple levels. Its transcription is modulated by numerous transcription factors in addition to diverse other regulatory factors which are dependent on DNA configuration (reviewed in [204]). MicroRNAs also modulate the stability and translation of *Myc* mRNA. The Myc protein is short lived and is subject to post translational modification (reviewed by Thomas et al [205]).

Myc-mediated gene repression appears to occur via several different mechanisms including functional interference with transcription activators such as Miz-1 and recruitment of co-repressor proteins [206]. Some of *Myc*'s downstream effects are modulated by microRNAs. The best defined is the miR-17-92 cluster which post translationally represses many target mRNAs including E2F1 activity and several components of the TGF-β signalling pathway [207], thereby promoting proliferation and cell survival [208]. More recently a non transcription-dependent role has also been demonstrated [209].

Myc promotes cell cycle progression through selective activation and repression of cyclins and cyclin dependent kinases [210,211]. B cells with a targeted

deletion of the *Myc* gene are unable to be stimulated to enlarge and proliferate in response to B cell receptor or other mitogenic stimuli [52]. Although counter intuitive, Myc also accelerates apoptosis [191], particularly in the setting of a growth factor deficiency, and in a dose-dependent fashion [192]. This is predominantly mediated by p53 [193,194] although in p53 null pre-B cells Myc-mediated apoptosis is reduced but not entirely abolished [189]. The Bcl2 family of proteins are downstream effectors of Myc-mediated p53 dependent and independent apoptosis [212,213] with Bcl2 being able to rescue cells from Myc-mediated apoptosis [214].

Myc's role in carbohydrate [215] and DNA metabolism and amino acid transport [211] has more recently been recognised.

1.8 Myb

The work subsequently detailed in this thesis identified *c-Myb* as a potent co-operator with oncogenically activated *Myc* and inactivated *Trp53* for inducing growth-factor independent proliferation of mature B cells, and thus its function and role in neoplasia are reviewed here.

Myb was initially discovered as the cellular precursor of the *v-Myb* oncogene (reviewed in [216]). *v-Myb* was identified as a novel sequence homologous to vertebrate mRNAs that had been acquired in two replication defective retroviruses, Avian Myeloblastosis Virus (AMV) and E26 virus, both of which induce myeloid leukaemia in chickens [217-220]. The AMV proviral genome had acquired a spliced cDNA encoding an N- and C-terminally truncated *Myb* sequence, while E26 had acquired a combination of spliced cDNA sequences from two cellular genes, *Ets-1* and *Myb*, with the *Myb* coding sequence truncated at its N- and C-terminus and being oncogenic [221-227].

Myb also emerged as an oncogene in retrovirus-induced mouse myeloid leukaemias and plasmacytoid lymphosarcomas, where recurrent integrations of MuLV resulted in dysregulated expression of *Myb* mRNA and caused aberrant splicing truncating either the N- or C-terminus, in a manner resembling the

dysregulation and truncation characteristic of *v-Myb* in the chicken transforming viruses [228-231].

1.8.1 Myb's role in oncogenesis

Abnormalities in the *MYB* locus or in *MYB* gene expression have been observed in several solid tumours including colon carcinomas [232,233], melanomas [234] and breast cancers [235] (reviewed by Gonda et al [236]), many demonstrating amplification rather than mutation of the gene. *MYB* has also been shown [237] to form one component of a fusion oncogene in adenoid cystic carcinomas of the breast and head and neck in which it is truncated at the C-terminus. *MYB* dysregulation has been identified in cases of T-ALL in infants [238], the mechanism of *MYB* overexpression being through either a juxtaposition of the *MYB* locus with the T-cell receptor locus, or gene duplication. Knock down of *MYB* expression in several *MYB*-overexpressing T-ALL lines precipitates cell differentiation [239], suggesting that the *MYB* defect may be integral to the leukaemia initiation or proliferation, rather than a secondary effect.

1.8.2 Myb's physiological role

MYB encodes a highly conserved 75 kilodalton nuclear protein whose role as a transcription factor has been most intensively studied [216] . It has a DNA binding domain at its amino terminus that binds to targets which have a DNA consensus sequence known as the Myb binding site. It also has a transactivating domain and a negative regulatory domain, the latter at the carboxyl terminus. *Myb* (also called c-myb) belongs to a transcription factor family in humans and mice that also includes A-Myb (*Mybl1*), which is highly expressed in germinal centre B cells, and the ubiquitously expressed B-Myb (*Mybl2*). These three transcription factors have a significant similarity at the protein sequence level with the highest homology in their DNA binding domains [240].

Myb is required for early haemopoiesis [241,242] with the loss of the *Myb* gene being embryonically lethal at day 14.5 due to anaemia as a consequence of a

failure of haemopoietic development. Both early and late myeloid differentiation is dependent on *Myb* expression [243] but in mice with hypomorphic alleles lymphoid maturation is more suppressed than myeloid maturation (reviewed by Greig et al [244]). Early studies in cell lines showed *Myb* overexpression impairs maturation of normal and malignant myeloid cells [245-247]. *Myb* expression is required for maintenance of selected myeloid leukaemia stem cells [248] and overexpression enhances proliferation and inhibits differentiation of haemopoietic (myeloid) stem cells [249-251]. Overall, dysregulated *Myb* modulates both haemopoietic cell growth and differentiation, but the precise mechanism of these actions remains elusive.

Ess et al [252] demonstrated high *Myb* expression during murine development in non-haemopoietic organs such as tooth buds, thyroid, proximal airway epithelium, hair follicles and gastrointestinal crypt epithelium. Interestingly, this group also demonstrated that the last three sites had high Myb levels into adulthood and that loss of Myb was associated with initiation of terminal differentiation, rather than loss of mitotic activity. A recurring pattern is that Myb is particularly active at early stages of cellular differentiation, its level being suppressed with, or its suppression causing, terminal differentiation [216].

1.8.3 Regulation and downstream targets

One of the difficulties in clarifying the role of Myb in normal and malignant cells is that mutations in the gene can substantially change its activity. Lui et al [253] showed that mutations such as N or C-terminal deletions or DNA binding domain mutations conferred a unique set of target genes and activities. *v-Myb* is truncated at both the N-terminus and C-terminus in addition to harbouring point mutations, and is strongly oncogenic. In contrast, full length *c-Myb* has a much weaker growth-promoting effect when overexpressed [250,254]. The precise role of the N-terminus remains to be clarified, but the C-terminus is thought to play an important negative regulatory role with C-terminal truncations increasing transforming capacity in haemopoietic cells [255] in addition to reducing Myb protein degradation [256].

Regulation of *Myb* expression is complex, changing according to the context and cell type. The *Myb* promoter has been characterised (with Myb itself binding to this region and enhancing its own expression) [257], but other mechanisms of transcriptional regulation are potentially more important. A variable block in transcriptional elongation at the level of the first intron was identified in 1988 [258]. Factors regulating this block remain to be well-defined but to date the oestrogen receptor [259] and NF-κB pathway [260] have been shown to have a modulatory activity. Alternative mRNA splicing also occurs to produce a naturally C-terminal truncated protein [261], with the alternative proteins having different transcriptional activities [262]. MicroRNAs control the level of *Myb* mRNA and translation and are discussed in more detail below. Post translational modifications such as phosphorylation [263] and ubiquitination [264] also occur, altering protein activity. MYB also co-operates (via specific MYB domains) with many transcriptional co-activators and co-repressors (reviewed by Oh et al [240]) including Ets family members, p300/Creb binding protein, CCAAT binding protein (c/EBP) family members and the alpha subunit of core binding factor (CBF) in transactivation of target promoters. Mutations in *Myb* which alter these interactions modify Myb's ability to regulate myeloid differentiation and proliferation [265].

MYB's downstream target genes are numerous [216]. Several publications [253,266] have demonstrated that the genes dysregulated by *Myb* overexpression were different in different cell lines. Most research has been performed in myeloid cells. A study by Zhao et al [267] analysed a myeloid stem cell model with inducible *Myb* expression by ChIP-sequencing and gene expression profiling to identify genes whose expression was directly modulated by Myb. This study unexpectedly demonstrated that Myb directly repressed a large number of genes. Myb was seen to activate gene sets associated with myeloid proliferation and self-renewal while repressing genes relating to myeloid differentiation. Genes directly modulated by Myb included those mediating cellular functions such as apoptosis, growth and proliferation, cell cycle and cell signalling. In addition Myb directly modulated the expression of many transcription factors including upregulating *Myc*. Quintana et al [268] looked at Myb binding targets in breast cancer cell lines using ChIP-on-chip assays and found over 10 000 binding sites, although the number of genes that

have been confirmed to be dysregulated by Myb in the same cell lines is much lower [253,269].

1.8.4 Myb's role in B cells

Pro-B cells and pre-B cells express significantly higher levels of *Myb* than more mature B cells [270]. Mutations that decrease Myb activity in B cell progenitors reduce or abolish B cell development, with the most pronounced block in the transition from the pro-B cell stage to the pre-B cell stage [271,272]. The use of tetracycline-regulated *Myb* expression in a *Myb* knockout embryonic stem cell line suggested that the expression of *Myb* needed to be strictly regulated to ensure proper maturation of B lymphocytes [273]. It remains unclear why B cell maturation is so dependent on Myb. Greig and colleagues [274] used hypomorphic alleles to show that Myb was required for cytokine (particularly IL-7) dependent B cell development, but that IL-7 receptor activation alone was unable to replace the role of Myb in B lymphopoiesis. As mentioned above, knockdown of *Myb* expression in T-ALL cell lines promoted differentiation suggesting that it may have a pathogenic role at least in a subset of T-ALL patients. Less is known about the role of Myb in B-cell leukaemia and lymphoma. Waldron et al [275] used a $p190^{BCR/ABL}$-dependent pre-B-cell leukaemia model to show that *Myb* hemizygous B-cells are less leukaemogenic and clonogenic than their normal counterparts. This study did not examine whether the reduction in Myb also promoted B cell differentiation, as the T cell work may suggest.

Myb expression is low in mature B cells, although it increases with B cell activation [276] in association with the G1 to S phase transition. Thomas et al [271] suggested that conditional ablation of *Myb* in mature B cells did not impair proliferation of splenic B cells but instead prevented them from remaining in a quiescent G0 state and enhanced their apoptosis. There is, however, a paucity of publications exploring the role of *Myb* in mature B cells, particularly the consequences of *Myb* overexpression.

The regulation of *Myb* expression in B cells is likely to be complex. Bender et al [277] demonstrated that a block in transcription elongation was underlying the

markedly lower *Myb* mRNA levels in mature versus immature murine B cells. The same group [278] subsequently demonstrated that members of the NF-κB family were likely to modulate this process. *Myb* mRNA also is negatively regulated by miRNA-150 [267,279], the former group confirming that ectopic expression of this microRNA inhibits the pro B to pre B cell maturation step, as is seen with *Myb* inactivation.

1.8.5 Myb's role in lymphomagenesis

The importance of *Myb* in B cell lymphomas is implied through retroviral studies, including work by Kanter et al [280] which demonstrated that B cell lymphomas induced by a modified form of the Avian Leukosis Virus all had retroviral integrations in or near the *Myb* locus. The Retroviral Tagged Cancer Gene Database demonstrates many murine models of B cell lymphoma with insertion sites near the *Myb* locus. The mechanism by which *Myb* enhances lymphomagenesis, however, remains unclear.

Myb is known to regulate and be regulated by several microRNAs as discussed below. Better definition of these interactions and other genes dysregulated simultaneously may be the key to understanding *Myb*'s role in lymphoma. The clear role of miRNA-150 in suppressing *Myb* expression has been mentioned above, but the relationship between this microRNA and B cell lymphoma is not well defined. Zhao [267] demonstrated that microRNA15a was able to reduced *Myb* expression, and that Myb is able to bind to the MiR-15a promoter, creating an autoregulatory feedback loop. This is of particular interest because the region on 13q where MiR-15a is located is commonly deleted in CLL [83,281], suggesting that its dysregulation may be involved in the disease pathogenesis. Vargova et al [282] reported that *Myb* is able to up regulate miR-155 which has been shown to be overexpressed in many B cell lymphoproliferative disorders [283,284] although, interestingly, it is usually downregulated in Burkitt lymphoma [86]. Overall, knowledge regarding the interactions between Myb and microRNAs is fragmented and thus their significance in lymphoma remains to be fully defined.

1.9 EBV and B cell transformation

The development of Burkitt Lymphoma, characterised by the t(8;14) translocation that increases expression of the *MYC* proto-oncogene, appears to be facilitated by Epstein Barr Virus (EBV) infection. Almost all forms of endemic Burkitt Lymphoma contain detectable EBV genome, while a significant proportion (15-85%) of non-endemic (sporadic) Burkitt Lymphoma also has detectable EBV sequences (although the inability to detect the viral components in most lymphomas does not preclude EBV from having a role in their pathogenesis). EBV induces infected cells to express multiple proteins, many of which affect B cell growth. Latent membrane protein 1 (LMP1) has been demonstrated to be important for the transformation of B cells [285] by mimicking CD40 ligand/CD40 signalling [286]. Transgenic mice overexpressing *LMP1* have an increased incidence of B cell lymphoma [287], however this is mainly at an advanced age, and the lymphomas are clonal, confirming that LMP1 alone is insufficient to induce autonomous B cell proliferation.

The way in which EBV facilitates B cell transformation in the presence of t(8;14) remains contentious, but research [288,289] has suggested that EBV-encoded proteins are able to reduce cell apoptosis, allowing unlinking of the cell cycle-promoting capacity of MYC from its apoptosis-promoting effect. The former group suggested that this uncoupling was mediated by Epstein-Barr nuclear antigen 1 (EBNA-1). The latter group demonstrated that latent membrane protein 2A (LMP2A) was able to protect cells overexpressing it in conjunction with *Myc* from apoptosis, and that these mice also developed accelerated lymphoma compared to *Myc* overexpressing mice, which was associated with increased expression of *Bcl-X(L)*. The EBV genome also encodes microRNAs, some of which have been demonstrated to modulate *PUMA*, a member of the anti-apoptotic BCL2 family [290] and a transcriptional target of p53. Similarly, EBV encoded microRNAs have been demonstrated to influence the protein expression of LMP1 and its regulation of the NF-kB pathway [291]. This further broadens the possible mechanisms through which EBV immortalizes B cells.

Alternately, it may be that EBV infection enhances B cell activation and proliferation, allowing cells with mutations (such as t(8;14)) to survive where they otherwise would have undergone apoptosis. It has been suggested that the reduced apoptosis seen in EBV-infected cells is mediated through decreased expression of the proapoptotic Bcl2 family member, *Bim* [292]. p53 is another clear candidate, and it has been demonstrated that the p14ARF-MDM2-p53 pathway is mutated in various ways in most Burkitt Lymphoma-derived cell lines [155]. EBV EBER RNAs are small non coding RNAs that are produced in abundance in EBV infected cells and show evolutionary conservation [293]. They are also postulated to have a role in apoptosis and cellular transformation (reviewed in [293]) but the mechanisms are still unclear.

1.10 Retroviral insertional mutagenesis

1.10.1 Background

Identification of critical proto-oncogenes and tumour suppressor genes involved in tumourigenesis can be undertaken in multiple different ways. Retroviral insertional mutagenesis has been developed to assist in identification of such genes.

Retroviruses are RNA viruses that are reverse transcribed through a DNA intermediate as part of their life cycle. Wild type retroviruses have three critical genes: pol (encoding the enzymes reverse transcriptase and integrase), gag (encoding structural proteins), and env (encoding envelope glycoprotein). The virus binds to cellular surface proteins and is subsequently able to enter the cell to integrate its reverse transcribed DNA provirus into host DNA during mitosis. It then utilises host enzymatic machinery for transcription and translation of its own genes.

By virtue of the fact that retroviruses insert into DNA, they cause genetic mutations in the host (reviewed in Uren et al [93]). The most frequent insertional mutagenic event is a gain-of-function resulting from dysregulated transcription of genes near the provirus insertion site. Strong promoter and

enhancer elements are located in the Long Terminal Repeats (LTRs) at either end of the integrated provirus, and these act both locally and at a distance to increase transcription of neighbouring genes. Occasionally, integration in protein coding exons may result in absence or truncation of the normally transcribed host protein, or create a fusion host/virus protein. Mutations in non-coding regions can induce a plethora of alterations such as modifications of protein stability [294] or transcriptional regulation. Loss-of-function mutations are uncommon [93], however, due to the heterozygous nature of provirus integrations and the need to integrate in much smaller target sites.

Retroviral mutagenesis has been harnessed for research in several ways. Changes in cell characteristics such as alterations in cell proliferation, apoptosis or differentiation may be seen as a consequence of retroviral infection. The retroviral integration site can be identified in such cells, identifying neighbouring genes, the altered expression of which may be contributing to the observed phenotype. Similarly, overexpression of specific genes encoded within the retroviral construct may further impact upon the phenotype observed, and thus genes contributing to dysregulated cell growth may be identified.

The likelihood of retroviral mutagenesis increases with the number of separate proviral integrations. Thus, replication competent retroviruses such as MuLV are potent accelerators of lymphomagenesis in genetically predisposed mice (reviewed in Mikkers et al [295]). Retroviruses have been engineered to improve their utility and safety. Ecotropic retroviruses are unable to infect human cells. Replication defective retroviruses lack the structural genes required for replication and require packaging cells that supply these viral particle components *in trans* such as Phoenix cells developed by the Nolan laboratory at Stanford University. Components within the LTR can be manipulated to alter their activity in particular cell types (for example Mouse Stem Cell Virus LTR resists methylation and inactivation in haemopoietic stem cells), or deletions in the 3' LTR can be introduced to self-inactivate the LTR enhancer/promoter in the integrated provirus (so-called self-inactivating vectors). Specific DNA sequences can be inserted into retroviruses, allowing ectopic expression of genes in the transduced cells, further altering the retroviral oncogenicity. In fact, many important oncogenes including *Src, Myc*

and *Myb* were first recognized because mutant versions are encoded and expressed by naturally arising retroviruses.

The genomic site within which a retrovirus inserts is not sequence-dependent, but neither is it entirely random, with various host and retroviral factors having an impact. This has been sadly but elegantly demonstrated in two retroviral gene delivery trials for X-linked Severe Combined Immunodeficiency. Transfer of the deficient γ chain into autologous CD34 cells utilising a replication-defective retroviral Moloney murine leukemia viral vector resulted in improved T cell counts in most patients, but in 2003 it was reported [296] that 2 of the patients had subsequently developed T cell leukaemia, both having a retroviral integration site in the vicinity of the *LMO2* gene in the leukaemic clone permitting dysregulated expression of this gene. The most recent reports describe 5 patients having developed T cell leukaemia, 4 of whom have demonstrable retroviral insertions within or near the *LMO2* gene [297].

Many studies have reviewed the propensity of retroviruses to insert into preferred sites within the genome (for example the review by Bushman [298]). This is critical because if retroviral mutagenesis is being used to identify oncogenes and their insertion sites are non-random, the pattern of integration may better reflect the predilection of the virus integration machinery for a certain site in the genome, rather than selection for integrations near proto-oncogenes or tumour suppressor genes. It has been demonstrated that variations in the LTR produce different insertion patterns [299,300]. Local structural features such as methylation pattern [301] rather than actual DNA sequence have also been shown to influence the integration pattern of specific retroviruses. Transcriptional activity has been shown to be important for integration site selection by Moloney murine leukemia virus [302]. A large study by Wu et al [303] compared the integration sites of the murine leukemia virus (MLV) with the human immunodeficiency virus-1 (HIV-1) in HeLa cells. They confirmed that MLV selectively integrated near the transcription start site of the more actively transcribed genes, particularly in the region of gene promoters, while HIV-1 preferentially integrated anywhere in the transcribed region but not upstream of the transcriptional start site. These and other studies demonstrate that different

virus/host combinations cause a different spectrum of insertion sites within the mouse genome.

Retroviral insertional mutagenesis contrasts with the more recently developed DNA transposon systems. Commonly used systems include the 'Sleeping Beauty' system, based on the Tc1/mariner superfamily of transposons reconstructed from fossil sequences in 1997 [304] and the moth-derived 'PiggyBac' system. Transposons are synthetic segments of DNA which can stably integrate into DNA within a single cell, although are not able to cross cell membranes, so are not intrinsically infectious. They can be modified to incorporate a gene of interest (although transposition efficiency is inversely correlated with gene length [305] within the Sleeping Beauty system) and can thus be used for genetic transformation and insertional mutagenesis in many vertebrate cells including murine and human.

Several distinct advantages over the retroviral systems are a more random integration site distribution [306,307] , low immunogenicity and reduced cost of mass production, making this system particularly appealing for gene therapy. There are, however, several drawbacks currently limiting their use in research and gene therapy. Transposons require a delivery system such as a plasmid to reach the cell nucleus which is often less efficient than retroviral transduction. Safety issues are always a paramount consideration for gene therapy particularly, and while transposons theoretically have a better safety profile than retroviral vectors due to their more random integration into the genome, their clinical development is at a much earlier phase and thus their safety profile remains to be fully elucidated. There is also less experience in the scientific community with this method of insertional mutagenesis and thus retroviral methods are still currently widely utilised.

1.10.2 Retrovirus insertional mutagenesis screens

Insertional mutagenesis by infecting mice with replication competent retroviruses has proved to be a powerful tool to identify potential tumour associated genes [93]. Such screens commonly identify proto-oncogenes, whose activity is enhanced by the retroviral insertion. Tumour suppressor

genes are less commonly isolated, the retroviral insertion reducing gene expression, but both alleles of a tumour suppressor gene must generally be lost for a significant phenotype, so these are most commonly identified if one copy of the gene is already mutated. However, occasionally haploinsufficiency, with the loss of a single allele of a gene, will be associated with a specific phenotype.

Often these screens are performed by infecting strains of mice that are already predisposed to cancer, as first described in *Eμ-myc* transgenic mice [91,92], facilitating identification of somatically mutated genes that co-operate with the inherited oncogene in the formation of cancer. The lack of expected common sites of integration in such models can help identify genes that work within a common pathway, mutation of both not having a co-operative effect in tumourigenesis.

1.10.3 Methods of integration site identification

Retroviral insertion sites can be identified by amplifying the genomic sequences flanking the retroviral insertion site. Traditionally integration site analysis was performed by Southern blot analysis and genomic library screening. More recent sequencing of the mouse genome and publication in a readily accessible online format has greatly facilitated the identification of the genomic location of each integration site and the surrounding genes.

PCR-based techniques have been developed to amplify a short segment of DNA flanking the integrated provirus. They include Inverse PCR, and the linker-based Vectorette-PCR and Splinkerette PCR, the latter of which is utilised in this thesis. This employs a splinkerette - an adaptor molecule containing a hairpin loop - to ensure that there is no non-specific DNA binding. The principle is illustrated below (Figure 1.1) and the method detailed in the Materials and Methods section.

Newer techniques are constantly being developed including linear amplification-mediated (LAM) PCR [308] in which PCR is initially performed with vector-specific primers, target DNA is isolated, followed by further PCR and

sequencing of amplicons. Nonrestrictive LAM-PCR [309] is a more recent development based on the former but which avoids the use of restriction enzymes and incorporates high throughput sequencing. Clearly the aim of newer methods is to enhance speed and efficiency of integration site analysis, facilitating rapid identification of larger numbers of insertion sites, allowing increased scale and throughput of retrovirus insertional mutagenesis screens.

Figure 1.1 Schematic representation of the splinkerette PCR technique

Sequential steps are illustrated in red.

a) DNA is digested with a restriction enzyme (eg Sau3AI) which results in some fragments containing the retroviral – genomic (bold) DNA junction.

b) An adapter (containing a hairpin loop, to ensure that there is no non-specific DNA binding) binds to the ends of the restriction enzyme-digested DNA.

c) One primer complementary to the retroviral long terminal repeat and another primer containing the same sequence as the non-hairpin strand of the adapter are added. The first round of PCR can thus only amplify the complementary strand to the retroviral LTR.

d) The second primer can now anneal to this product, allowing exponential amplification of the retroviral-genomic DNA junction (and an internal retroviral segment) using primers in both directions.

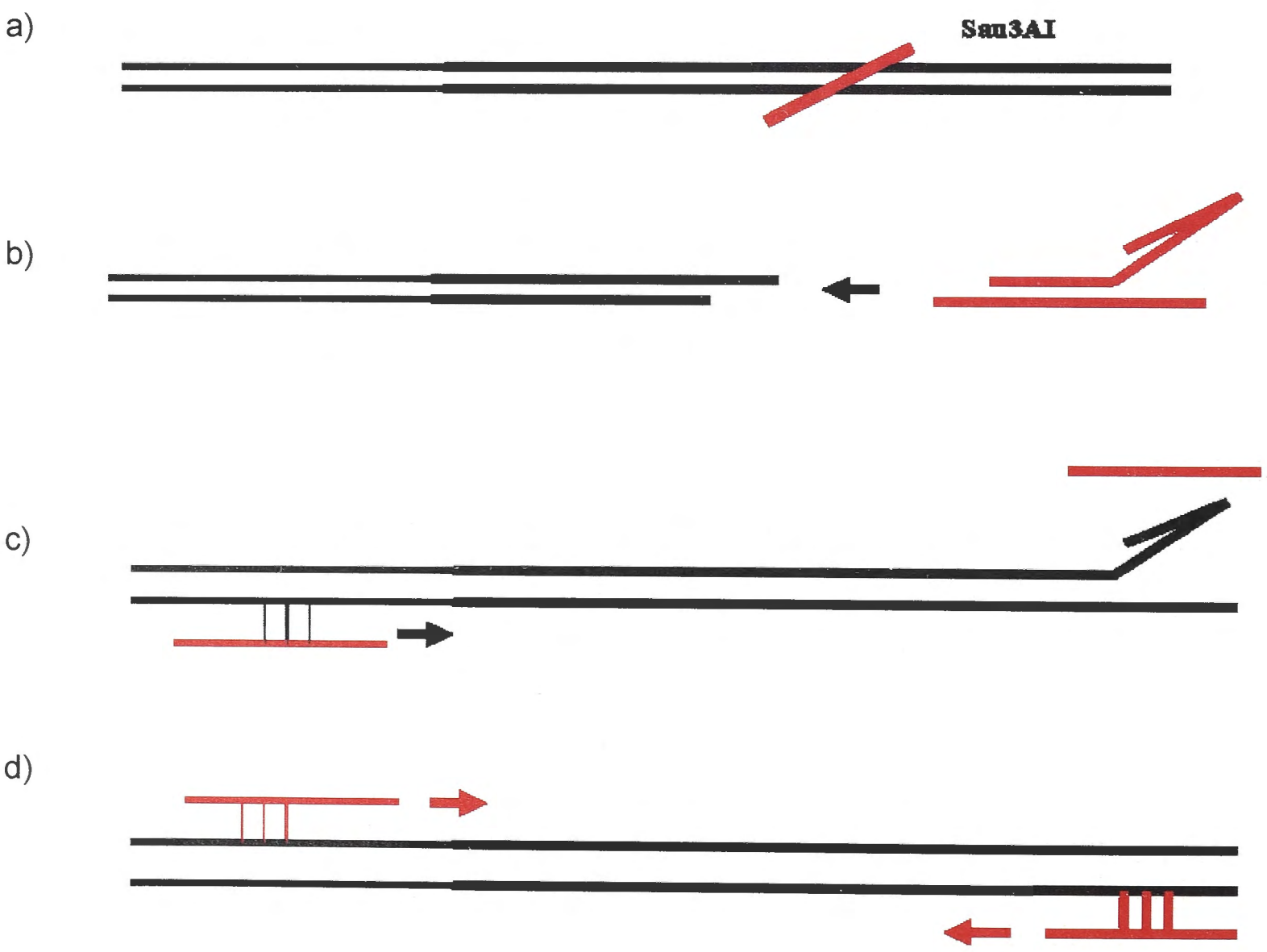

1.10.4 Methods of integration site data analysis

Retroviral insertion, through the retroviral enhancer elements, can modify the activity of genes up to 270kb [310] away. Identifying the important gene whose activity has been modified by the integration and thus altered the cell phenotype is thus difficult when the provirus has integrated in a gene-rich region. By looking at the pattern of integration sites in a large number of retrovirus-induced cancers, clusters of "common insertion sites" (CIS) around a particular gene can help to indicate which gene is likely to be the insertionally activated oncogene. The definition of a common insertion site, however, is difficult as the number that can be found in a particular experiment depends on the size of the "window" defining a common site. If the window is too large, even random patterns of integration will appear to create common integration sites just by chance. If the window is too small, common sites of integration around proto-oncogenes may be missed because of long-range effects of the proviral LTRs. Defining the correct size is further complicated by the propensity for retroviruses to integrate near or in transcriptionally active genes, and the fact that gene density can vary by more than 10-fold across the genome. As common insertion sites give a probability that a gene is significant, this must be followed up by functional experiments to test that overexpression or knock down of the candidate gene does indeed cause the expected phenotype. Corroboration with independent evidence for oncogenic activity in human studies or other animals also helps to redress the statistical uncertainty of interpreting common integration site data.

1.10.5 Retrovirus tagged cancer gene database

A database was developed in Nancy Jenkins and Neal Copeland's laboratory [94] to collate data about retroviral integration sites in mouse models of malignancy in order to facilitate identification of common insertion sites in different tumour models and enable online searching. This is freely available on the internet (http://RTCGD.ncifcrf.gov). As a proof of principle, within the most common 10 insertion sites in this database are the genes *Myc*, *Myb*, *Notch1* and *Pim1*, all of which are well established proto-oncogenes in humans and rodents and known to be frequently mutated in lymphomas by a variety of

means. The beauty of this type of gene discovery is that the data is derived from a whole genome approach, so the results are not skewed due to preconceived ideas about particular genes or pathways.

1.10.6 Retroviral mutagenesis in *Myc* transgenic mice

In order to enhance understanding of the genes that co-operate with *Myc* overexpression in lymphomagenesis, van Lohuizen et al [92] infected *Eμ-myc* mice with Moloney Murine Leukaemia Virus. This process enhanced lymphomagenesis and identified four common insertion sites, *Pim-1, Bmi-1, Pal-1* and *Bla-1*. Haupt et al [91] published a similar study in the same journal issue, identifying common insertion sites at the *Pim-1, Pim-2, Bmi-1* and *Emi-1* loci.

Bmi-1 is a member of the Polycomb group of proteins, which are transcriptional repressors. The action of Bmi-1 in enhancing lymphomagenesis was subsequently shown to be mediated through suppression of *Ink4a* expression [311]. *Ink4a* encodes the tumour suppressors $p19^{ARF}$ and p16, the former stabilising p53, and the latter blocking phosphorylation (inactivation) of the retinoblastoma protein. Thus, one of the actions of the common insertion site locus *Bmi-1* in *Eμ-myc* mice is transcriptional repression of the p53 pathway.

1.10.7 Retroviral mutagenesis in *Trp53* defective mice

Two large studies have performed retroviral mutagenesis in mice that harboured a primary or secondary p53 defect. The first [312] utilised *Cdkn2a* (encoding p19ARF)-defective mice which have increased binding of p53 to Mdm2, and thus reduced p53 activity. These mice also have disruption of the retinoblastoma pathway as this gene also encodes p16INK4a. In total 565 integration sites were isolated, identifying 45 common insertion sites. The most common insertion site in their population of lymphomas and histiocytic sarcomas was in *Myc*. The second paper [313] performed mutagenesis in p19(ARF)-/- mice, p53-/- mice and wild type mice, transducing them with Moloney Murine Leukaemia Virus. The group analysed 510 tumours, predominantly B cell lymphomas and T cell lymphomas, and over 10 000

independent insertion sites and 346 common insertion sites were isolated. *Myc* was the second most common insertion site, with *Myc*-insertion-containing tumours having an over representation of *Nfkbil1/Lta*, *CCnd3*, mmu-mir-106a-363 and *Rasgrp1* mutations.

1.11 Number of required steps for malignant transformation

The minimum number of oncogenic 'hits' required for a neoplasm to develop remains contentious. The question is somewhat artificial, however, as cellular pathways are not active in isolation, and dysregulation of one is likely to have an impact on multiple other pathways. Clearly, the nature of the mutations, in addition to the number, needs to be addressed. In addition this issue has become more complicated recently with the discovery of non-protein-coding genes (microRNAs), the importance of the microenvironment, epigenetic factors, significant inter-individual variation in gene expression, among other factors, which are likely to have a significant impact on lymphomagenesis.

1.11.1 Human studies

Human studies suggest that more than one oncogenic mutation is required for the development of solid tumours. The multistep nature of malignant transformation was demonstrated in colon carcinoma and its precursor lesions by Vogelstein et al [314], suggesting that two lesions are likely to be insufficient for a malignant phenotype. Similarly, the timing and diversity of tumours [140] in patients with germline *TP53* gene mutation (Li-Fraumeni Syndrome) is consistent with further oncogenic events being required for the development of a malignant phenotype. This multi hit hypothesis concurs with the broad spectrum of capabilities that a cell must acquire before becoming fully neoplastic [1], with a single or even two oncogenic mutations being unlikely to provide all these requirements.

Resequencing studies have found that, on average, there are 80 amino acid-changing somatic mutations in human colon or breast cancers, with "mountains" of frequently mutated genes and "hills" of less frequently mutated genes [315]. In view of these and similar studies, some groups have proposed mathematical models of cancer in which tumourigenesis is driven by mutations in many genes, each of which provides only a small growth advantage [316]. A subsequent publication analysing pancreatic cancer [317] reported an average of 67 genetic alterations in a set of 24 pancreatic cancers, the majority of which were point mutations. A recent study [318] sequencing four cases of Chronic lymphocytic leukaemia identified 46 somatic mutations that could potentially affect gene function. These studies, however, cannot determine which genetic mutations are instrumental in tumourigenesis.

Haemopoietic tumours may require fewer mutations than solid tumours. In particular, normal mature B cells are endowed with three of the six malignant cell attributes considered by Hanahan and Weinberg: the capacity to migrate and invade normal tissues; indefinite replication in the process of maintaining life-long immunity; and the ability to promote (lymph)angiogenesis [319]. In addition, as a consequence of *RAG* and *AID* gene-mediated mutations [320], mature B cells may more readily acquire genetic lesions which confer a proliferative advantage.

The BCR-ABL translocation in Chronic Myeloid Leukaemia (CML) appears to be sufficient alone to cause the disease, confirmed by the efficacy of human tyrosine kinase inhibitors targeting this molecular mechanism. Mouse models appear to concur, with Daley et al [321] demonstrating the retrovirus-induced expression of $P210^{bcr/abl}$ could induce a myeloproliferative disorder resembling CML, and Honda et al [322] showed that progeny of transgenic mice with $p210^{bcr/abl}$ expressed under the control of a *tec* promoter also developed a disease resembling CML. However, small numbers of B cells with the BCR-ABL translocation have been isolated in a significant proportion of normal individuals [323,324] suggesting that this translocation may only be sufficient in myeloid precursors or stem cells.

Human studies are enlightening with regards to lymphoid malignancy. Limpens et al [106] demonstrated that over half of a small number of healthy blood donors had t(14;18)(q32;q21) (which juxtaposes the *BCL2* gene with the *IGH* gene) detected by sensitive PCR methods in their peripheral blood lymphocytes, although at an estimated frequency of 1 in 10^5 or less circulating B cells. This is the translocation seen in 80% of human Follicular Lymphoma, resulting in overexpression of *BCL2* and a consequential block in apoptosis. Many of the normal individuals in this study had greater than one t(l4;18)-carrying B-cell clone, and all breakpoints had a structure similar to that seen in Follicular Lymphoma. As the proportion of people identified harbouring this mutation far exceeds the proportion likely to develop Follicular Lymphoma, even over a lifetime, these results suggest that further genetic defects are required for the development of lymphoma. Similarly, Summers et al [325] confirmed that low levels of the t(14;18) are found in a substantial proportion of the normal population.

An interesting publication by Cong et al [326] identified aberrant *BCL2* expression in germinal centre cells in 23 lymph node biopsies, with micro dissection and PCR performed on a smaller number of these cases suggesting that the cells had clonally rearranged immunoglobulin heavy chain genes, labelling this as 'in situ localisation of Follicular Lymphoma. Five of twenty three patients had Follicular Lymphoma at another site, and 3/23 subsequently developed Follicular Lymphoma at relatively short follow up. A small study by Muller [327] demonstrated persistence of clones with t(8;14) (juxtaposition of *MYC* with *IgH*) in 4 HIV positive patients which persisted from 1 to 9 years, with the development of only one t(8;14) negative lymphoma in the follow up period. Similar studies have not been published analysing the incidence of t(8;14) in non-HIV infected normal populations.

In general a single defect selects against further defects in that pathway. This is demonstrated by a review of the Retroviral Tagged Cancer Gene Database [94] which shows that while insertion sites near *Myc* are commonly seen in retrovirus induced B cell lymphomas, if the mouse genotype already results in overexpression of *Myc*, then insertion sites near *Myc* are much less common. Similarly, inactivation of p53 is commonly seen in Burkitt Lymphoma. Lindstrom

et al [155] demonstrated that in Burkitt cell lines with intact p53, other mutations in the p53 pathway are more commonly identified that in those with mutated p53. This concept has been recently disputed. Chanudet et al [328] have demonstrated that some MALT lymphomas have two distinct defects in the NF-κB pathway, one of which involved a tumour suppressor gene. These findings suggest that perhaps there is a threshold of pathway activation beyond which the dysregulation of that pathway facilitates lymphomagenesis. If a single defect is insufficient to cross this threshold then further defects in the same pathway may be complementary.

Viruses such as EBV and HHV8 are thought to be oncogenic in their own right, infecting and transforming cells, as opposed to viruses such as hepatitis C which are associated with an increased risk of lymphoma, but are not directly oncogenic. EBV [289] and HHV8 [329] all produce multiple viral products which affect diverse cellular pathways, so such an infection cannot be truly regarded as a single defect precipitating lymphoma.

1.11.2 Murine research

Some caution is required when extrapolating from murine studies, as murine cells are more readily immortalised than human cells by chemicals or transfection of oncogenes [330], the reason for which is unclear but possibilities include suboptimal DNA repair mechanisms, or variations in telomerase activity [331]. The number and nature of genetic hits required for the development of solid tumours has been addressed to some extent in mouse models. Early seminal studies in rodent fibroblasts indicated that pairs of mutations, such as *Ras* and *Myc* [332] or *Myc* and *Trp53* [194,333] were sufficient to transform them to growth factor-independent proliferation.

With regards to haemopoietic malignancy, overexpression of a single proto-oncogene such as *Bcl2* [33] or *Myc* [334] is insufficient alone to induce lymphoma. Mice constitutively expressing *Myc* and *Bcl2* under the influence of the immunoglobulin heavy chain promoter have increased numbers of pre-B cells and B cells, but these are not initially clonal and do not grow rapidly in cell culture, although these mice subsequently rapidly develop a clonal aggressive

lymphoma [335], suggesting that at least one more oncogenic hit is required for tumour outgrowth. Murine research has, as with human research, demonstrated small populations of apparently benign lymphocytes with characteristic chromosomal translocations. Roschke et al [336] demonstrated small numbers of cells with a translocation between *Myc* and IgA, with the numbers of these cells increasing post immunisation with cholera toxin. Similarly, Ramiro et al [337] have showed that small number of stimulated non malignant B cells in vitro harbour a *Myc-IgH* translocation, numbers of which increased in the setting of *Atm* deficiency or *p53* deficiency

1.12 Nature of pathway dysregulation precipitating B cell malignancy

It has long been postulated that dysregulation of complementary pathways within a single cell is required for the acquisition of a malignant phenotype, such as a proliferative advantage potentiating the effect of an apoptotic defect. Mouse models with a single genetic defect that alone is insufficient to precipitate uncontrolled cell proliferation have been very useful in clarifying the nature of complementary genetic events that enhance the development of malignancy as co-operative spontaneous mutations, or those facilitated by retroviral or chemical mutagenesis, can often be detected in the final tumour.

The genes and pathways commonly dysregulated in human mature B cell lymphoma are discussed below. Specific subtypes of human B cell non Hodgkin lymphoma will be reviewed separately in conjunction with the most relevant mouse models.

Burkitt Lymphoma: This is characterised by *MYC* overexpression and has a unique combination of dysregulated genes [5]. Burkitt Lymphoma cells are BCL6 positive and commonly CD10 positive, their maturation and activation state being similar to that of an actively proliferating germinal centre cell. Schmitz et al identified that mutations in *TCF3* and its negative regulator *ID3* were found in 70% of cases of sporadic Burkitt Lymphoma analysed. TCF3

regulates B cell specific gene transcription during B cell development, but interestingly its knock down was toxic to Burkitt cell lines but not DLBCL cell lines. The group suggested that the dependence on TCF3 signalling related to its role in up regulation of immunoglobulin heavy and light chains which are two components of the B-cell receptor, the mutation disrupting tonic B cell receptor signalling. The B cell receptor is critical for the survival of mature B cells [17,18] with tonic signalling though the PI3K pathway being important in both normal B cells [22] and Burkitt Lymphoma cells [338]. Refaeli et al [95] demonstrated that a mouse model overexpressing *Myc* only developed a Burkitt-like phenotype if the B cell receptor was activated and Sander et al [14] showed that constitutive *Myc* expression and PI3K activity in murine germinal centre B cells produced lymphomas with many features in common with Burkitt Lymphoma. The mir-17-92 cluster of microRNAs promotes Myc-induced lymphoma [339], and antagonises PTEN, a negative regulator of PI3K signalling [340,341]. Genomic amplification resulting in high expression of the miR-17-92 cluster is not uncommon in Burkitt Lymphoma [342,343] and may be an alternative mechanism by which selected cases of Burkitt lymphoma have enhanced PI3K signalling.

Interestingly, the NF-κB pathway does not seem to be particularly active in Burkitt Lymphoma, with NF-κB target genes being expressed at a lower level than seen in DLBCL [344]. Klapproth et al [345] have shown that NF-κB pathway activity appears to promote apoptosis in *Myc*-induced lymphoma. Suppression of the p53 pathway is also very commonly seen in Burkitt Lymphoma. Mutations in the gene expressing p53 have been identified in approximately 30% of Burkitt Lymphoma biopsies and 60-70% of Burkitt Lymphoma cell lines [155]. Mutations in *ARF*, a tumour suppressor gene that binds to and inhibits MDM2, the p53 suppressor, are common in *Eμ-myc* lymphoma [189] and Burkitt cell lines [155]. Wilda et al [346] identified disruption of the ARF-MDM2-p53 apoptotic pathway in 55% of their cases of paediatric sporadic Burkitt Lymphoma. Defects in apoptotic pathways in Burkitt Lymphoma and *Myc* overexpressing murine models are discussed in more detail in Section 1.13.2 below.

Mantle cell lymphoma provides an example of complementary pathway dysregulation in B cell lymphoma. Mantle cell lymphoma is thought to correspond to the naïve B cell but has a characteristic t(11;14) which results in overexpression of *CCND1* encoding cyclin D1 (which promotes cell cycle progression). Studies of human Mantle cell lymphomas frequently demonstrate a wide spectrum of additional genetic mutations, the genes encoded in these regions commonly being involved in cell cycle regulation or the DNA damage response pathway [347]. Interestingly, transgenic mice with a recapitulation of this translocation (Eμ cyclin D1) have a relatively normal B cell compartment, but when crossed with *Eμ N-myc* mice (which themselves have a low lymphoma incidence and long latency period) the progeny rapidly develop B cell lymphoma [348].

Follicular Lymphoma: The maturation and activation state of Follicular Lymphoma cells best corresponds to normal germinal centre B cells. Up to 85% of cases are characterised by the t(14;18)(q32;q21) or a variant translocation which relocates the anti-apoptotic *BCL2* oncogene into an immunoglobulin (*IG*) gene locus, leading to deregulated expression of the BCL2 protein [349]. A subpopulation of the remaining cases demonstrate *BCL2* overexpression, but some morphologically classical cases do not appear to have dysregulated *BCL2* [349]. As discussed in Section 1.11 this classic translocation alone is insufficient in humans to cause lymphoma. Murine models where the *Bcl2* gene is under the control of the immunoglobulin heavy chain locus exhibit prolonged cell survival and an expanded lymphoid compartment [33,350] but do not readily develop lymphoma. In contrast, models where the *Bcl2* gene is placed under the control of the Vav gene regulatory sequences (which results in overexpression of *Bcl2* in multiple haemopoietic lineages rather than just B cells) show delayed development of Follicular Lymphoma [34]. This group confirmed that help from the expanded T cell population was required for lymphomagenesis.

Diffuse large B cell lymphoma (DLBCL): Diffuse large B cell lymphoma cells also have mutated immunoglobulin variable region genes consistent with cells that have been exposed to the germinal centre. Two important subtypes of DLBCL have been identified, Activated B cell-like (ABC) and Germinal centre-

like (GCB), each having a different prognosis, gene expression profile and likely cell of origin. Lenz et al [351] showed that in GCB DLBCL amplification of the mir-17–92 microRNA cluster (often associated with *MYC* overexpression), *REL* amplification and deletion of the tumor suppressor *PTEN* were common, but these events did not commonly occur in ABC DLBCL. Iqbal et al [352] demonstrated that 34% of the GCB subtypes had t(14;18) but no demonstrable change in prognosis compared to the negative GCB subtypes. The genes differentially expressed between the two groups were heterogeneous including genes involved in apoptosis, adhesion/migration, cell cycle progression and regulation and a number of transcription factors. The ABC subtype of DLBCL has been shown by many groups [99,100,112] to be dependent on constitutive activity of the NF-κB pathway which may be driven by *CARD11* mutations [98], *MYD88* mutations [70] or other mutations that facilitate chronic active B cell receptor signalling [353]. In addition, Lenz et al [351] demonstrated that *FOXP1* and *SPIB* (an ETS family transcription factor) were commonly overexpressed and the *INK4a/ARF* tumor suppressor locus was commonly deleted in ABC DLBCL but not GCB DLBCL. Reduced *BLIMP1* expression, often due to biallelic inactivation [354], has also been shown to be specific for the ABC rather than GCB subtypes of DLBCL.

Hairy cell leukaemia is an uncommon mature B cell lymphoproliferative disorder which does not clearly correspond to a specific stage of B cell development. It is of particular interest because recently the BRAF E600V mutation was identified in almost all cases [355,356]. BRAF is a component of the RAS–RAF–MAPK signalling pathway, the V600E mutation resulting in the constitutive activation of BRAF kinase. This pathway relays extracellular signals to the nucleus and is critical for regulation of cellular proliferation, differentiation and survival. This pathway had not been previously demonstrated to be consistently dysregulated in human mature B cell lymphoma. With regards to murine models, Alexander et al [357] demonstrated that transduction of *v-H-ras* or *v-raf* expressing retroviruses into *Eμ-myc* mouse bone marrow resulted in increased numbers of pre-B cell colonies in soft agar within several days which was not seen with either of these genetic mutations alone. These colonies were oligoclonal and grew as tumours in nude mice. In concordance with these findings, Schwartz et al [358]

demonstrated that murine pre-B cells doubly transduced with a *Myc*-encoding retrovirus and a *v-Ha-ras*-encoding retrovirus could grow autonomously in vitro and were tumourigenic in syngeneic mice. The way in which the RAS–RAF–MAPK signalling pathway co-operates with Myc remains unclear. Similarly, co-operating mutations in human Hairy cell leukaemia have not yet been well defined, although the initial publication [355] identifying this genetic defect through whole exome sequencing did not clearly identify any other potentially co-operating genes.

Marginal zone lymphoma: This is postulated to be derived from a post germinal centre memory B cell with three main types depending on the site of origin: splenic, nodal and mucosa associated lymphoid tissue (MALT). MALT lymphoma is thought to commonly be initiated by chronic antigenic stimulation (infective agents or autoantigens). Subsequent genetic events commonly result in dysregulation of the NF-κB pathway (reviewed in [359]).

In conclusion, the various mature B cell lymphoma subtypes correspond to different normal stages of B cell differentiation and thus their constitutively active pathways will vary. The dysregulated pathways and genes that have to date been identified in mature B cell lymphoma vary from subtype to subtype. This is consistent with the nature of the complementary genetic perturbations which facilitate the cell's acquisition of the full complement of capabilities described by Hanahan and Weinburg [1,2] varying according to the B cell's innately active pathways.

1.13 Dysregulation of *Trp53* and *Myc*

1.13.1 Background

Dual *Trp53* and *Myc* dysregulation is commonly seen in both human and murine lymphoproliferative disorders. *Eμ-myc* mutant mice are predisposed to B cell lymphoma, but the dysregulation of *Myc* alone is insufficient to cause lymphoma (reviewed in Section 1.7.1). Analyses of lymphomas developing in such mice demonstrate a high likelihood of mutations in the ARF-Mdm2-p53 pathway

[189]. The same group also demonstrated that *Eμ-myc* mice had a more rapid onset of tumour development in the setting of *Arf* (an activator of p53) deficiency [189]. Similarly, in addition to the classic translocations resulting in overexpression of *MYC* in human Burkitt lymphoma, mutation analysis commonly demonstrates inactivation of the ARF-MDM2-p53 pathway as discussed in Section 1.12 above. In addition, Martins et al [360] showed that restoration of p53 function in *Eμ-myc* lymphomas in vivo resulted in tumour apoptosis and prolonged mouse survival, consistent with the p53 defect being important for tumour maintenance rather than just its initiation.

It has been contentious whether combined dysregulation of both *p53* and *Myc* are alone sufficient to allow neoplastic B cell proliferation. Zindy et al [333] suggested that mouse embryo fibroblasts can be immortalised by a combination of *Myc* overexpression and a p53 pathway defect. Schmitt et al [361] showed that *Eμ–myc* mice rapidly developed lymphomas in the setting of a *Trp53* gene defect, with almost all resulting lymphomas demonstrating deletion of the remaining *p53* allele. Similarly, Jacobs et al [362] demonstrated an oligoclonal or clonal aggressive B cell leukaemia developing rapidly in *Eμ–myc* mice with heterozygosity at the *Ink4a–Arf* locus (encoding the two tumour suppressors p16 and p19Arf, the latter preventing the degradation and inactivation of p53) with 15/15 of their tumours demonstrating loss of their remaining *Ink4a–Arf* locus. These studies have suggested that, in the setting of *Myc* overexpression, homozygous inactivation of *Trp53* was the remaining 'hit' required for a B cell to acquire a neoplastic phenotype. In contrast, it has also been shown that lymphomas that arise in *ARF* null *Myc* overexpressing transgenic mice are clonal [212] consistent with at least three oncogenic hits being required for this subpopulation of cells to grow out. Yu et al [363] refute this. They transduced p53-null bone marrow cells with a *Myc* expressing retrovirus, injecting the resulting cells subcutaneously into syngeneic mice. Analysis of the resulting tumours showed that they were polyclonal, the group concluding that a *Trp53* defect and *Myc* overexpression are sufficient alone to cause tumours. The deficits in this argument are that an additional mutagenic hit is provided in each cell by the very event of retroviral integration, and the lack of confirmation that the resulting cellular outgrowths were neoplastic, with no mention of spread of the tumour beyond the skin.

The frequency with which gain-of-function mutations in *TCF3* and loss of function mutations in its negative regulator *ID3* were identified in the recent publication by Schmitz et al [5] indicate that this mutation occurs in conjunction with *MYC* overexpression and a p53 pathway defect in many Burkitt lymphomas. Sander et al [14] demonstrated cooperation between PI3 kinase pathway activation and *MYC* overexpression for germinal centre lymphomas in mice. Tonic B cell receptor signalling to PI3K, exaggerated by unrestrained TCF3, may thus cooperate with *Myc* overexpression and a p53 pathway mutation in Burkitt lymphoma to drive the highly proliferative phenotype that characterizes this lymphoma subtype.

Evidence that *MYC* activation and *Trp53* inactivation are alone insufficient for B cell transformation has come from research performed by a previous PhD student in the Goodnow Laboratory, Dr Lixin Rui. Dr Lixin isolated mature splenic B cells from mice, activated them in vitro, and transduced them with a replication-defective retroviral vector encoding human *MYC* and either green fluorescent protein (*GFP*) or tail-less human CD4 (*huCD4*). Expression of *GFP* or *huCD4* was from an internal ribosome entry sequence within the same mRNA as *MYC*, and thus identified *MYC*-transduced and expressing B cells in flow cytometric analysis. Upon re-injection of approximately 1 million of these cells into syngeneic mice or lymphopenic *Rag1*-null mice, the GFP positive B cells rapidly disappeared if they co-expressed *MYC*, similar to control cells transduced with empty vector encoding only GFP. Even when the splenic B cells were obtained from mice carrying a homozygous inactivating mutation in *Trp53*, the combination of enforced *MYC* and defective p53 was insufficient to promote spontaneous proliferation upon re-introduction into syngeneic mice or lymphopenic *Rag1*-null mice (Figure 1.2).

However, if recipient mice of *MYC* transduced *Trp53* mutant B cells were tracked for several months, a small percentage of syngeneic recipients and most *Rag1*-null recipients developed an aggressive surface IgM+ GFP+ B cell lymphoma that invaded spleen, lymph nodes, and extra lymphoid sites such as kidney and liver (Table 1.2 and Figure 1.3). No lymphoma developed in recipients of transduced B cells that had a normal *Trp53* gene. Control

experiments were not performed in which non-transduced *Trp53* mutant cells, or mutant cells transduced with an empty GFP expressing vector, were injected into *Rag1*-null recipients. Since all of the lymphomas were GFP positive this implied that *MYC*, expressed from the same bicistronic vector, was contributing to lymphomagenesis, being consistent with the published evidence for cooperation between *MYC* and *Trp53*. It remains possible that the specific DNA mutation conferred through retroviral transduction was actually the event cooperating with the p53 defect in a small number of cells, facilitating outgrowth, with *Myc/GFP* expression merely confirming successful retroviral integration.

Since approximately 1 million *MYC* positive *Trp53* mutant B cells were injected into each recipient mouse, and the majority did not proliferate over the course of 5-10 days as measured by dilution of a cell-division tracking dye, these data indicate that transformation to growth factor self-sufficiency by the *MYC* plus *Trp53* combination was inefficient and occurred in as few as one cell in a million.

Figure 1.2 *MYC* activation and *Trp53* inactivation are insufficient for B cell transformation

Unpublished data from Dr Lixin Rui.

The left panels show flow cytometric analysis of spleen B cells with (A) *Trp53* wildtype or (B)homozygous mutant *Trp53* after in vitro transduction with a bicistronic retroviral vector encoding *MYC* and *huCD4+*. The x-axis measures relative fluorescence with the dye CFSE, which has been incorporated into the cells to measure its dilution during any subsequent cell divisions. Middle and right panels show flow cytometric analysis of spleen cells from *Rag1* null mice 10 days after intravenous injection with the input donor cells on the left. The donor B cells (within gate) were identified by staining with antibodies to the B cell marker B220, and an IgM allotypic marker, IgM^a, that is unique to the donor B cells. The right panels are gated on the donor B cells, showing the *huCD4/MYC*-expressing subset and CFSE fluorescence. Only a small percentage of the donor B cells have divided and diluted out CFSE during the 10 day period, ie shown a left shift and this percentage is not increased in the *MYC/huCD4+* fraction.

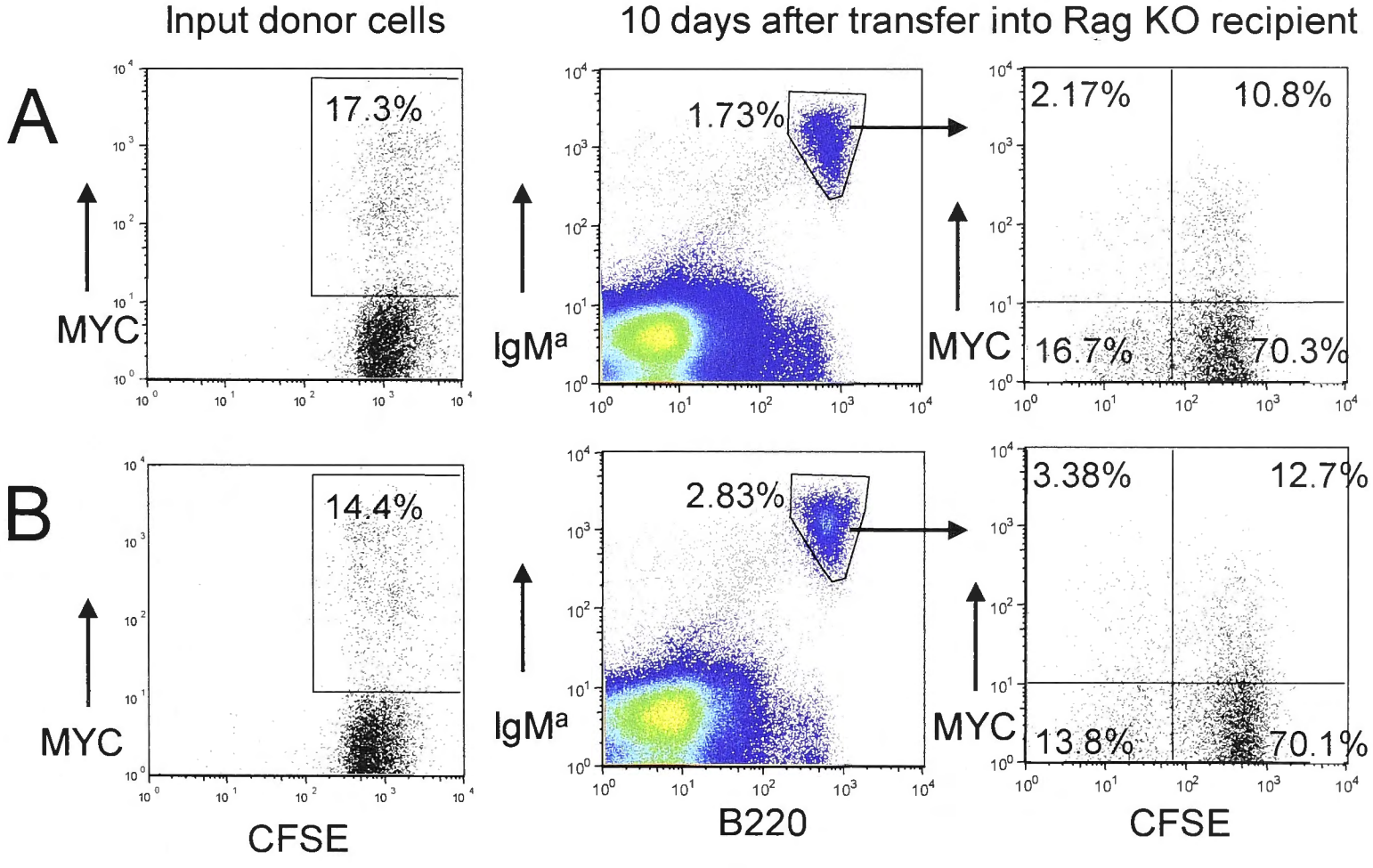

Table 1.2 Tumour incidence in recipients of *MYC*-transduced antigen-specific B cells

Unpublished data from Dr Lixin Rui.

Summary of the occurrence of lymphomas in recipients of *MYC/GFP* transduced (MYC) spleen B cells from C57BL/6 mice carrying either normal *Trp53* (p53wt) or homozygous mutant *Trp53* (p53Bbl) genes. In the final two experiments, the B cells were co-transduced with two retroviral vectors, one encoding *MYC/GFP* and the other encoding the cytokine *BAFF/huCD4* or an empty *huCD4* vector (EV)

Donor cells (million/recipient)	Recipient	Days post transfer	Lymphoma Incidence
p53wt MYC (4)	C57BL/6	30 days	0/4
P53Bbl MYC (4)	C57BL/6	30 days	1/4
p53wt MYC (6)	C57BL/6	35 days	0/6
p53Bbl MYC (6)	C57BL/6	35 days	1/6
p53wt MYC (5)	C57BL/6	45 days	0/10
p53Bbl MYC (5)	C57BL/6	45 days	3/10
p53Bbl MYC (4)	Rag KO	55 days	17/18
p53Bbl MYC (2.5)	C57BL/6	78 days	2/8
p53Bbl MYC (2.5)	Rag KO+T cells	78 days	8/8
p53Bbl MYC+EV (4)	C57BL/6	84 days	1/5
p53Bbl MYC +BAFF(4)	C57BL/6	84 days	5/5
p53Bbl MYC+EV (4)	C57BL/6	65 days	1/4
p53Bbl MYC +BAFF(4)	C57BL/6	65 days	4/4

Figure 1.3 Tumour phenotype in recipients of *MYC*-transduced antigen specific B cells

Unpublished data from Dr Lixin Rui

A) The photograph shows spleens from syngeneic or *Rag1*null mice that received *MYC/GFP*-transduced *Trp53* homozygous mutant spleen B cells 78 days earlier. A spleen from a control mouse that did not receive transferred cells is shown for reference.

B) Representative flow cytometric analysis of enlarged spleens. The top panels show the frequency of IgM+ GFP+ donor B cells (green gate) or IgM+ GFP- donor B cells (red gate). The lower panels show forward scatter of these gated cells (as a measure of relative cell size) and DNA content (*Rag1* null recipient). This reveals a greatly increased population of *MYC/GFP*+ donor cells that are markedly enlarged and contain a large fraction of cells in S, G2 or M phase of the cell cycle.

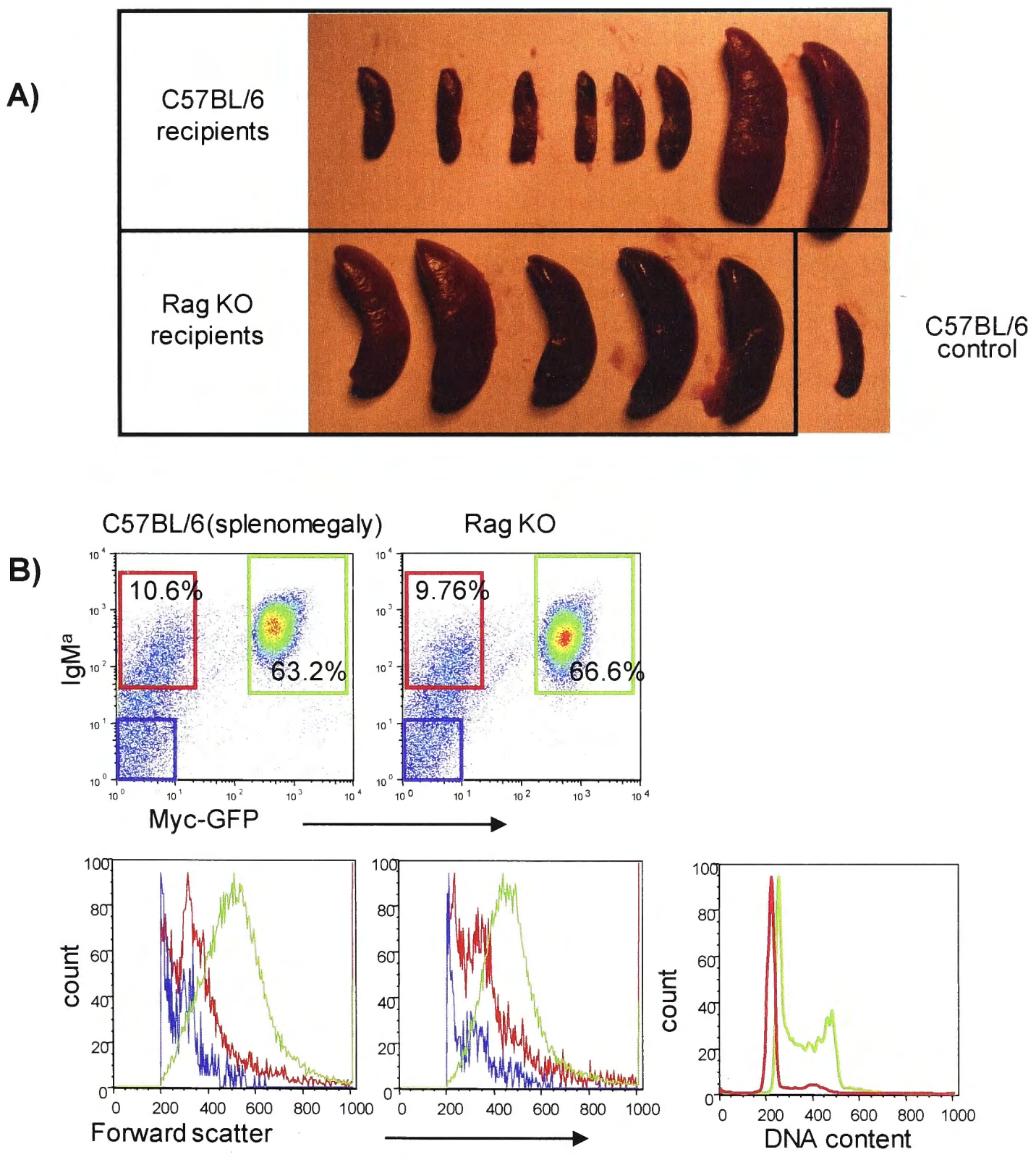

1.13.2 Mechanism of *Myc–Trp53* mutation co-operation

Two distinct mechanisms of p53 activation by Myc have been relatively well defined, although other mechanisms undoubtedly exist. The first is via transcriptional induction of the *ARF* tumour suppressor gene. Bouchard et al [364] demonstrated that *Myc* overexpression induced increased expression of FoxO transcription factors, which were able to bind to and activate the *Ink4a/Arf* locus, thus enhancing p53 expression through Mdm2 suppression. The other mechanism is via the DNA damage response pathway and the activation of *ATM* [365]. MicroRNAs have been demonstrated to mediate large networks of gene interactions, and thus are likely to be implicated in Myc-p53 interactions. Sotilo et al showed that in *Myc* overexpressing B cells miR-34a inhibited p53-dependent apoptosis [366], and Chang et al [367] reported that miR-34a is induced by p53 following DNA damage, promoting apoptosis, which suggests a negative feedback mechanism to modulate apoptosis, but this remains to be confirmed.

The simple hypothesis to explain the interaction between dysregulated p53 and Myc in promoting lymphomagenesis is that loss of p53 abrogates the apoptotic limb of Myc's actions, allowing its proliferative capacity to act unchecked. Two groups [145,146] demonstrated that inhibition of *Puma*, a BCL2 family member that mediates the apoptotic functions of p53, greatly accelerated B cell lymphomagenesis in *Eμ-myc* mice, with the incidence being similar to that seen with p53 inhibition. This suggests that it is a defect in the apoptotic function of p53 rather than its role in cell cycle regulation that is critical in lymphomagenesis, as p53 cell cycle check points did not seems to be compromised. This correlates well with human studies [146] that demonstrated that 12 of 17 Burkitt lymphoma specimens analysed had reduced *PUMA* expression.

However, not all Myc-mediated apoptosis appears to be channelled thorough p53 [212]. *Bim*, a pro-apoptotic member of the BCL2 family, is induced by Myc and can mediate Myc-induced apoptosis, its loss promoting malignancy in *Eμ-Myc* mice [368]. The same group also demonstrated that loss of Bim removes the strong selection pressure for functional inactivation of the p53 apoptotic

pathway that is normally seen during Myc-induced lymphomagenesis. This alone suggests that the loss of Bim either facilitates apoptosis in a p53-independent manner, or that Bim is downstream of p53. Two point mutations (P57S and T58A) in the *MYC* gene found commonly Burkitt Lymphoma [369] have been demonstrated to enhance the gene's transforming ability [370] with this mutant *MYC* being confirmed to have reduced up regulation of *BIM*, without any change in its effect on p53.

The *Myc*-mutant *Trp53* cooperation could potentially extend beyond an apoptosis-specific effect. A *Trp53* mutation would impair cell cycle arrest in the setting of a DNA-toxic insult, and inhibit repair of such a defect. This would facilitate accumulation of genetic mutations, some of which are likely to cooperate with Myc and promote transformation. The relatively new concept of senescence may help explain how mutant *Trp53* facilitates Myc-induced lymphomagenesis in some instances. p53 has been shown to mediate senescence in lymphomas induced by *Myc* overexpression and three different groups [371-373] have demonstrated that promotion of senescence in such lymphomas delays development of overt disease. Overall, it appears that there are multiple mechanisms of *Myc* – *Trp53* mutation cooperation in B cell transformation.

1.14 The current study

The study [313] of retroviral mutagenesis in p53-deficient and *Eμ-myc* mice described above emphasise the potent collaboration between increased *Myc* and inactivation of the p53 pathway in lymphomagenesis. Since the lymphomas had many other integration sites in addition to retrovirally expressed *MYC*, this poses the question of whether these represent collaborating third, fourth, or fifth oncogenic mutations or simply 'passenger integrations'. If they they are collaborating mutations, it is also unknown whether these are specifically necessary for growth factor self-sufficiency, evasion of apoptosis, limitless replication potential, escape from immune surveillance, or other attributes of malignant lymphomas.

Better clarification of the molecular basis of the co-operation between p53 loss and *MYC* overexpression may facilitate comprehension of the precise role of these genes in lymphomagenesis, but would also be directly relevant to the pathogenesis of Burkitt Lymphoma. This B cell lymphoma subtype is characterised by *MYC* overexpression, commonly accompanied by a defect in the p53 pathway, but also carrying many other recurrent mutations such as unrestrained *TCF3* and *CCND3*. A more precise understanding of how Myc, p53 and other mutations co-operate to drive spontaneous proliferation of mature, antigen-activated B cells may facilitate development of targeted therapies for this highly aggressive malignancy.

This thesis addresses these questions by a different approach to retroviral mutagenesis in p53 deficient B cells. The earlier studies cited above employed a replicating retrovirus acting iteratively over many months in an unknown number of precursor cells to create many proviral integration sites per lymphoma. This made it difficult to trace the mechanism of action or efficiency of any individual retroviral insertion. In the approach employed here, a single round of retroviral transduction was performed with a replication-defective retrovirus in a limited number of mature, antigen plus CD40-activated B cells. This finite cohort of B cells with a small number of proviral integrations was then traced for their proliferative self-sufficiency in the absence of antigen or CD40 stimuli in vivo or in vitro. This allowed Myc-p53 cooperating oncogenic mutations to be identified that efficiently promote B cell proliferation in the absence of normal mitogenic stimuli.

In particular, I hypothesised that mature B cells that had previously been activated by antigen and CD40, acquired a constitutively expressed *MYC/GFP* retroviral vector, and carried homozygous inactive *Trp53*, nevertheless still required at least one additional mutation before they could continue proliferating when antigen and CD40 stimuli were withdrawn in vitro or in vivo.

I hypothesised that the clonal B lymphomas that arose from this procedure had acquired a "third oncogenic hit" created by insertional mutagenesis during integration of the *MYC/GFP* proviral vector.

I thus aimed to:

(1) identify the *MYC/GFP* vector insertion sites in a series of these clonal B lymphomas;

(2) identify candidate co-operating oncogenes in the vicinity of these integrations; and

(3) experimentally test whether or not retroviral overexpression of the candidate genes completed a triad with *MYC* and *p53* mutations and became sufficient for B cells to continue proliferating for long periods after antigen and CD40 stimuli were withdrawn.

2. Materials and Methods

2.1 Mice

C57BL/6 mice were bred and housed in the Australian Phenomics Facility at the Australian National University (ANU). All mouse breeding and experiments were performed according to protocols approved by the Australian National University Animal Ethics and Experimentation Committee.

Trp53^{Bblast} mice were identified through ENU mutagenesis [374]. The early onset of tumours in these mice suggested a *Trp53* defect and sequencing of this gene demonstrated a point mutation in the DNA binding domain. The strain is listed as *Trp53*^{Bbl} on the MGI (Mouse Genome Informatics) database with the ID MGI:3611496.

Ig^{HEL} mice produce large numbers of B cells with rearranged immunoglobulin heavy and light chains to have high affinity for Hen Egg Lysozyme (HEL) [375] and thus are able to activated simultaneously by exposure to HEL. The transgenic mouse has an ID MGI:2384162 in the MGI database.

Trp53^{Bblast} mice were bred with *Ig*^{HEL} mice to generate *Ig*^{HEL} *Trp53*$^{Bblast/\ Bblast}$ mice, *Ig*^{HEL} *Trp53*$^{Bblast/\ wt}$ mice Ig^{HEL} *Trp53*$^{wt/wt}$ mice.

*Rag1*KO C57BL/6 recipient mice were used.

Mouse genotyping was performed in the Australian Phenomics Facility, ANU.

2.2 Common recipes

2.2.1 Ammonium- Chloride-Potassium (ACK) lysis solution

The following were combined in MilliQ water:

-0.15M NH_4Cl (FW 53.49) – 8.29 g in 1litre

-10mM $KHCO_3$ (FW 100.12)- 1 g in 1 litre

-0.1mM Na_2EDTA (FW 372.24)-0.0372g in 1 litre

The pH was adjusted to 7.2-7.4 with 1N HCl and the solution filtered.

2.2.2 Fluorescence activated cell sorting (FACS) wash solution

Forty ml of heat inactivated Fetal Calf Serum (final concentration 2%) and 20 ml of 10% sodium azide (final concentration 0.1%) were added to 2 litres of Phosphate buffered saline (PBS) (Media/Wash JCSMR) and stored at 4°C.

2.2.3 Roswell Park Memorial Institute Medium (RPMI) complete medium

RPMI-1640(Gibco®) was supplemented with Penicillin (100 U/ml), Streptomycin (0.1 mg/ml), L-Glutamine (2 mM) (Gibco®), 10mM HEPES (pH 7.0) (Gibco®), 50 µM 2-Mercaptoethanol (2-ME) solution (Gibco®) and 10% heat inactivated Fetal Calf Serum.

2.2.4 Super Optimal Broth (SOB)

Twenty g Bacto Tryptone, 5 g Bacto Yeast Extract, 2 ml 5M NaCl and 1.25 ml 2M KCl were added to Milli-Q H_2O and the volume made up to 990 ml and autoclaved. Ten ml Milli-Q H_2O containing1M $MgSO_4.7H_2O$ and 1M

$MgCl_2.6H_2O$ was also autoclaved. The two solutions were mixed and stored at 4°C.

2.2.5 Transformation buffer (TB)

PIPES (10 mM) 3.0 g, $CaCl_2.2H_2O$ (15 mM) 2.2 g and KCl (250 mM) 18.6 g were added to 950 ml Milli-Q H_2O. The pH was adjusted to 6.7 with KOH. To that solution 10.9 g of 55mM $MnCl_2.4H_2O$ was added. The solution was sterilised by filtration and stored at 4°C.

2.2.6 Lysogeny broth (LB) agar plates

Six g of Bacto Agar was added to 400 ml of L-Broth (John Curtin School of Medical Research (JCSMR) stores) and autoclaved. Once the mixture had cooled below 50°C, 500 µl of 100 mg/ml ampicillin was added (final concentration 100 µg/ml). Eighteen ml of the warm mixture was added to agar plates in a laminar flow hood, and allowed to dry. Plates were then stored at 4°C away from light.

2.3 Retroviral constructs

2.3.1 Background

Murine stem cell virus (MSCV) [376] is an ecotropic retrovirus which is able to infect haemopoietic cells, including stem cells. pMXs is based on the Moloney murine leukaemia virus (MMLV) retroviral vector [377], and is able to infect most murine cell lines. A bicistronic vector is one that encodes two different genes separated by an internal ribosome entry site (IRES), allowing co expression of both genes. The MSCV-human *MYC/GFP* vector was produced by Lixin Rui, using a gift of MSCV-GFP backbone from the Nolan laboratory. A subset of the lymphomas used a modification of the above vector containing an amino acid substitution in *MYC* at Thr58 which abolishes *Bim* induction. The pMXs-Red empty vector was produced by Keisuke Horikawa using the pMXs-IG backbone from the Kitamura [377] laboratory, replacing the GFP sequence with the

DsRed Express 1 sequence (Clontech). These viruses are replication defective, and so while a single cell can be infected by more than one virus, one virus can only infect one cell and cannot produce further copies to infect other cells or the same cell. This means that the number of retroviral infections in each cell, and thus the number of insertion sites cannot change once the viral supernatant is removed from the cell surface. The pBluescript II SK cloning vector (Stratagene) was used for initial cloning. Figure 2.1 demonstrates the three vector maps with relevant restriction enzyme sites.

Figure 2.1 Vector maps

a) pMXs-DsRed

b) MSCV-MYC-GFP

c) pBluescript II SK

BamHI, EcoRI and XhoI are restriction enzyme cleavage sites.

a)

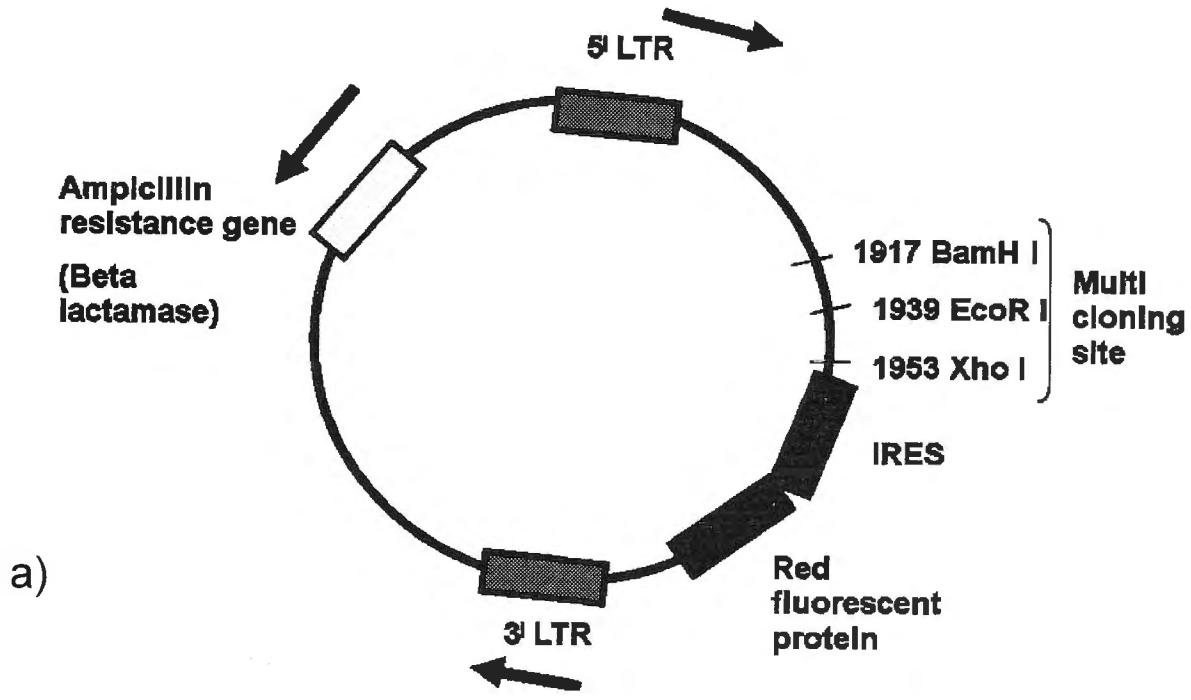

b)

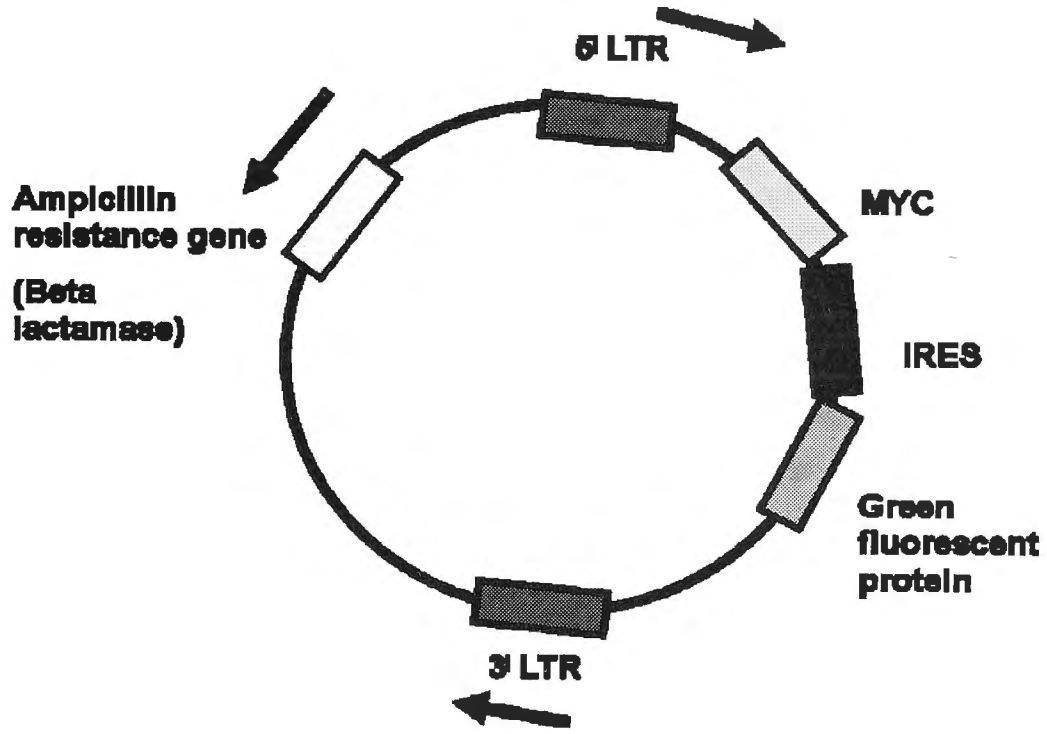

c

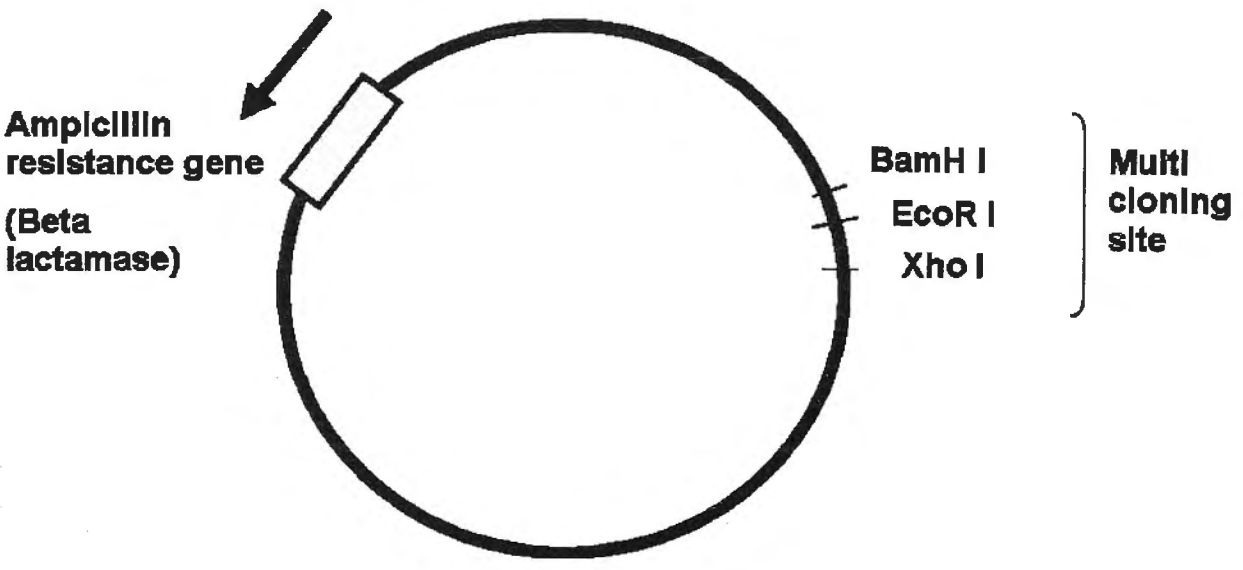

2.3.2 cDNA inserts

The cDNA sequence inserted into the empty vector was obtained by using a 50 µl polymerase chain reaction (PCR) containing 0.5 µl Platinum Pfx (Invitrogen), 5 µl Pfx reaction buffer (10X), 1 µl normal mouse spleen cDNA, 1.5 µl deoxyribonucleotide triphosphates (dNTPs) (10mM), 1 µl $MgSO_4$, 0.75 µl forward primer, 0.75 µl reverse primer, 39.5 µl MilliQ H_2O.

Principles of forward primer design: 2-4 Ts (so that sufficient overhang for enzyme to cut), followed by the restriction enzyme digest site, followed by first 6 bases of the Kozak sequence (GCCACC) followed by the first 24 bases of transcribed sequence from the National Center for Biotechnology Information (NCBI) website (http://www.ncbi.nlm.nih.gov/genbank/).

Principles of reverse primer design: reverse complement of the combination of the last 24 bases of the sequence followed by restriction enzyme cleavage site followed by 2-4Ts. The primer sequences are detailed below with the restriction enzyme sites underlined and the portion of the Kozak sequence prior to the initiation codon in bold.

Myb: (restriction enzymes BamHI (New England Biolabs (NEB)) and XhoI (NEB))
forward:5' TTG GAT CC**G CCA CC**A TGG CCC GGA GAC CCC GAC ACA GC 3'
reverse:5' AAA ACT CGA GTC ACA TGA CCA GAG TTC GAG CTG A 3'

Ikbkb: (restriction enzymes EcoRI (NEB) and XhoI)
forward:5' TGA ATT C**GC CAC C**AT GAG CTG GTC ACC GTC CCT CCC A 3'
reverse:5' AAA ACT CGA GTC AGG CGG TTA CCG TGA AGC TTC T 3'

Laptm5: (restriction enzymes BamHI (NEB) and XhoI)
forward:5' TTT TGG ATC C**GC CAC C**AT GGC CTC CCG TGC AGC GCC GGT C 3'
reverse:5' AAA ACT CGA GTC ACA CTT CTG AGT ATG GGG GTG G 3'

Lmo2: (restriction enzymes EcoRI and XhoI)
forward:5' TTT TGA ATT C**GC CAC C**AT GTC CTC GGC CAT CGA AAG GAA G 3'

reverse:5' AAA ACT CGA GCT AGA TGA TCC CAT TGA TCT TGG T 3'

The PCR cycling conditions were 94°C for 2 minutes, 35 cycles of 94°C for 15 sec, 55°C for 30 sec, 68°C for 1 minute per 1000 bp product, and final extension at 68°C for 10 min. Product was confirmed by running 5 µl of the 50 µl reaction on a 50 µl minigel at 100 volts. The product was then purified using the Qiagen PCR purification kit and eluted with Milli-Q water.

2.3.3 Digest of insert and empty vector

The PCR products were digested in a 30 µl reaction containing 3 µl NEB buffer (10X), 3 µl 10xBSA, 20 µl, 1.5 µl Restriction enzyme1, 1.5 µl Restriction enzyme2. The empty vector was digested in a 50 µl reaction containing 5 µl NEB buffer (10X), 5 µl Bovine serum albumin (BSA) (10X), 3 µl DNA, 33 µl Milli-Q H_2O, 2 µl Restriction enzyme1, 2 µl Restriction enzyme2. Reactions were incubated at 37°C for 2 hours. One µl of alkaline phosphatase (Takara) was added to each of the vector digests after 1.5 hours to prevent vector self-ligation.

2.3.4 Purification and ligation

Digests were run on a 1% Tris-acetate-EDTA (TAE) agarose gel, stained with Ethidium Bromide and subsequently visualised with ultraviolet light. Bands were cut from the gel, purified and eluted in approximately 40 µl elution buffer for vector (Qiagen gel extraction protocol) and in 7-12 µl elution buffer (using the QIAEX II protocol from Qiagen) for the insert. One µl of each specimen was run on a gel to ensure a pure product had been obtained.

Inserts and pBluescript II SK cloning vector were ligated to form the desired ligated plasmid in a 5 µl reaction containing 0.5 µl cloning vector, 1.5 µl insert, 0.5 µl T4DNA Ligase (LigaFast™ Rapid DNA Ligation System, Promega) and 2.5 µl ligation buffer. The reaction mix was incubated at room temperature for 15 minutes.

2.3.5 Transformation

Fifty µl of freshly thawed competent E. coli (DH5α) cells were added to 5 µl ligated plasmid, incubated at 4°C on ice for 10 minutes, heat shocked for 30 seconds at 37°C and returned to ice. LB medium (250 µl) was added to each tube and incubated at 37°C with agitation for 30 minutes. Two hundred µl was then plated over entire surface of ampicillin-containing agar plate and incubated for 14 hours at 37°C. Six clones were selected and grown in a 15 ml round bottom tube for greater than 8 hours in 2 ml LB/Ampicillin (100 µg/ml) at 37°C with agitation. Plasmid DNA was extracted from each clone with Wizard® Plus SV Minipreps DNA Purification Systems (Promega), as per protocol, digesting 5% with appropriate restriction enzymes and running it on a gel to confirm the correct band size for the vector and insert combination. Another portion of the Miniprep DNA from the clones with the correct band pattern was sequenced to ensure that the insert sequence is not mutated using primers in both directions (pBluescript II SK primers for either side of the multicloning sites T3 (ATTAACCCTCACTAAAGGGA) and T7 (TAATACGACTCACTATAGGG)). A 20 µl sequencing reaction was prepared as per Section 2.9.5 below. The sequence was confirmed using Sequencher™ version 4.2 (Gene Codes Corporation).

Plasmids were subsequently digested with restriction enzymes and inserts purified and ligated with the pMXs Dsred vector, as per purification and ligation protocols above. Transformation was performed as above but cultures were grown in 2 litre flasks and the plasmid DNA extracted using Gerard Biotech Hurricane Maxi Prep Protocol, based on the alkaline lysis method. The purity and concentration of the resulting DNA was analysed using the spectrometer and band size was confirmed by gel electrophoresis of the products of restriction enzyme digests.

2.4 Transfection – Calcium Phosphate method

Day 0: Phoenix cells (a gift from the Nolan laboratory, Stanford) were replated in T75 (BD Biosciences) flask aiming for 60% confluence at transfection.

Day 1: Chloroquine (25 µM) was added to cells 5-15 min prior to addition of DNA solution. Thirty µg DNA, (1317 µl minus DNA volume) µl MilliQ H_2O, 183 µl 2M $CaCl_2$, and the solution were vortexed. Fifteen hundred µl 2xHEPES (Sigma) Buffered Saline pH optimised around 7.0 was added and the mixtures were subsequently 'bubbled' for 15 sec. After a 1 minute incubation at room temperature the suspension was quickly and evenly distributed into the medium above the cell monolayer and the plate rocked to evenly distribute particles. This was incubated at 37°C and observed under microscope after 1-2 hours looking for small dark calcium granules. The supernatant was carefully replaced with Dulbecco's Modified Eagle Medium (DMEM) medium (Gibco®) and incubated overnight.

Day 2: The medium was changed to RPMI-CM.

Day 3: The supernatant was pipetted into 15 ml tubes, centrifuged at 1500 rpm for 7 min to pellet cellular debris and frozen at -80°C.

Day 4: Supernatant was removed as per Day 3. The remaining Phoenix cells were then trypsinised and analysed using FACS for *GFP* or *DsRed* expression to confirm vector expression.

2.5 Production of competent cells

Competent cells were made based on Inoue et al's published protocol [378], based on the Hanahan protocol [379]. DH5α cells were thawed, plated on an ampicillin-free LB agar plate and cultured at 37°C overnight. The following morning 10-12 colonies were inoculated into 250 ml SOB medium in a sterile 2 litre flask and grown at room temperature with vigorous shaking until the optical density was between 0.4 and 0.5. The flask was then placed on ice for 10 minutes, spun down and the pellet resuspended in 80 ml ice cold transformation buffer (TB) and incubated on ice for 10 minutes. The pellet was then spun down again and resuspended in 20 ml ice cold TB. Slowly 1.2 ml Dimethyl Sulfoxide (DMSO) was added to the resulting suspension and it was frozen at minus 80°C in 1 ml aliquots.

2.6 Production of anti CD40

1C10 cells were thawed from liquid nitrogen storage and grown in RPMI-CM. At approximately 1 litre of culture fresh media was no longer added as the culture grew with consequential cell lysis. The supernatant was then run on a selective liquid chromatography column and the resulting concentrate of anti CD40 antibody dialysed in sterile PBS. The antibody concentrate was titrated against previous batches by stimulating B cells and assessing CD69 expression at 48 hours.

2.7 Transduction

Day 0: One Ig^{HEL} $Trp53^{Bblast/\,Bblast}$ mouse and one control Ig^{HEL} $Trp53^{wt/wt}$ mouse was injected with 4-6 mg HEL (Sigma®) intraperitoneally. Mice were culled 6-8 hours later by cervical dislocation and the spleen was transported in RPMI complete medium. A single cell suspension was made in a sterile Petri dish using a sterile cell filter and 3 ml syringe barrel, and returned to the same tube. This was centrifuged at 1200 rpm for 7 minutes at room temperature and the supernatant removed. Red cells were lysed with 5 ml ACK lysis buffer for 2

minutes at room temperature, replenished with 10ml RPMI-CM to cease lysis, and centrifuged again at 1200 rpm for 7 minutes at room temperature and the supernatant removed. After RPMI complete media was replenished cells were counted and viability assessed using a haemocytometer and trypan blue, diluted to 2 x 10^6 cells/ml and cultured at 37°C with 5% CO_2 for 24-36 hours with 10 µg/ml of anti-CD40.

Day 1: The viral supernatants were thawed and kept on ice away from light. Cells were suspended at 10^8 cells/ml in RPMI complete medium. The viral supernatant(s) was transferred into 6-well plates (approx 2 ml/plate). DOTAP Liposomal Transfection Reagent (Roche Cat No. 11811177001) (10 µg/ml final concentration) was added to optimise transfection [380]. Three to six million (30-60 µl) cells were then added to each well and this was spin-inoculated at 2500-2800 rpm for 90 minutes at room temperature. Half of the supernatant was removed and replaced with RPMI complete medium and 10 µg/ml of anti-CD40 and cells were cultured for at least 24 hours at 37°C

Day 3: Cells were counted, viability assessed and 10^6 cells from the *Ig*^{HEL} *Trp53*$^{Bblast/\ Bblast}$ mouse spleen and control splenocytes were used for FACS analysis. The remaining cells were washed and either cultured in vitro or divided between 4-5 recipient *Rag1* KO mice, injecting approximately 2 million cells/mouse at 10-20 million cells/ml through the lateral tail vein. For in vitro culture, cells were plated in 6 well plates at 2 x 10^6 cells per ml, each well containing 2 ml of RPMI complete media, and incubated at 37°C with 5% CO_2. Several wells were plated out for each gene combination allowing a whole well of cells to be analysed at each time point without disturbing the other wells. At the predetermined timepoints the contents of each well was harvested by pipetting, resuspended and the concentration of viable cells was counted using a haemocytometer. For flow cytometric analysis of in vitro cultured cells, the cells were washed and transferred to a 96 well plate for staining using the FACS protocol described below. Integration of haemocytometric results (concentration of viable cells) with flow cytometric results (percentage of viable cells expressing specific fluorochromes) enabled calculation of the numbers of cells expressing specific fluorochromes.

2.8 Spleen FACS Protocol

Cells were placed in a round-bottomed 96-well plate (at approx 10^6 cells / 25 µl/well). Ice-cold FACS buffer (100-150 µl) was added and this was centrifuged at 1340 rpm for 4 minutes at 4°C, the supernatant removed and vortexed. The above two steps were repeated. The resulting cells were incubated with a CD16/CD32 monoclonal antibody (to block complexed IgG receptors and thus reduce background staining) and incubated at 4°C for 20 minutes. The specific antibody (at optimal concentrations determined by titration) was then added after a wash step, incubating at 4°C for 30 minutes in the dark. Cells were washed twice with FACS buffer as above, resuspended in 50-100 µl FACS buffer and transferred into cluster tubes. FACS antibodies used are tabulated in Table 2.1.

Data acquisition was on the four channel BD FACS Calibur and analysis was performed with the FlowJo (Tree Star Inc) software. When required for calibration the Immuno-Brite™ Standards Kit (Beckman Coulter 6603473) was used. Graphs were drawn with the GraphPad Prism5 software.

Table 2.1 Antibodies used for immunophenotyping

Antigen	Conjugate	Source
B220	APC	BD Pharmingen
B220	PerCP	BD Pharmingen
CD5	PerCP	BD Pharmingen
CD5	APC	cBioscience
CD16/32	N/A	BD Pharmingen
CD19	APC	BD Pharmingen
CD138	Biotin	BD Pharmingen
IgD	Biotin	BD Pharmingen
IgM	APC	BD Pharmingen
Streptavidin	PerCP	BD Pharmingen
Streptavidin	APC	BD Pharmingen

2.9 Splinkerette PCR

2.9.1 DNA

Genomic DNA was extracted from lymphoma samples using QIAamp DNA mini kit (Qiagen) according to the manufacturer's 'Blood and body fluid' protocol. Genomic DNA (1.5 μg) was digested in a 20 μl total reaction volume containing 2 μl Sau3AI (4000U/ml), 2 μl Sau3A1 buffer (10X), 2 μl BSA (10X) and H_2O. The reaction was incubated at 37°C for 3 hours, followed by a heat inactivation step at 65°C for 20 min.

2.9.2 Primers

HMSpAa: 5' CGA AGA GTA ACC GTT GCT AGG AGA GAC CGT GGC TGA ATG AGA CTG GTG TCG ACA CTA GTG G 3'

HMSpBb-Sau3A1: 5' GAT CCC ACT AGT GTC GAC ACC AGT CTC TAA TTT TTT TTT TCA AAA AAA 3'

AB949NEW: 5' GCT AGC TTG CCA AAC CTA CAG GTG G 3'

HMSp1: 5' CGA AGA GTA ACC GTT GCT AGG AGA GAC C 3'

HM001: 5' GCC AAA CCT ACA GGT GGG GTC TTT 3'

HMSp2: 5' GTG GCT GAA TGA GAC TGG TGT CGA C 3'

2.9.3 Annealing and ligation

The splinkerette primers were annealed in a 20 μl reaction volume containing 7.5 μl of HMSpAa (20 μM), 7.5 μl of HMSpBb-Sau3A1 (20 μM), 2 μl NEB Buffer 2 (10X) and H_2O. Annealing was performed at 95°C for 5 min and followed by a

slow cool down process to room temperature. The ligation reaction was performed overnight at 16°C in a 20 μl total reaction volume containing 7 μl Sau3AI digested genomic DNA, 1 μl annealed splinkerette oligonucleotides, 0.5-1.0 μl T4 DNA ligase (10 U/μl), 2 μl ligation buffer (10X) and H_2O. The ligation reaction was subsequently inactivated at 65°C for 20 min. The ligated samples were purified using QIAquick PCR purification kit (Qiagen) and eluted in 30 μl according to the manufacturer's protocol.

2.9.4 PCR

Ten μl of the purified samples was amplified in a 50 μl PCR reaction volume containing 1 μl long terminal repeat (LTR) specific primer AB949NEW (20 μM), 1 μl splinkerette specific primer HMSp1 (20 μM), 2.5μl dNTPs (10 mM), 3.0 μl $MgCl_2$ (50 mM), 0.5μl Platinum Taq (5 U/μl)(Invitrogen) and 5 μl Platinum Taq buffer (10x). PCR cycling condition were 94°C for 2 min, 94°C for 1 min, 68°C for 30 sec, 72°C for 90 sec, 30 cycles of 94°C for 30 sec, 65°C for 30 sec, 72°C for 2 min, and followed by final extension at 72°C for 10 min. The primary PCR products were diluted 200 fold and 5 μl of the diluted products were used as the template for the secondary PCR reaction. This was performed in a 50 μl reaction volume containing 5 μl diluted primary PCR product, 0.5 μl nested primer HM001 (20 μM), 0.5 μl of nested primer HMSp2 (20 μM), 2.5 μl dNTPs (10 mM), 2.5 μl $MgCl_2$ (50 mM), 0.5 μl Platinum Taq (5 u/μl) and 5 μl of Platinum Taq buffer (10X). The secondary PCR cycling condition were 94°C for 90 sec, 30 cycles of 94°C for 30 sec, 60°C for 30 sec, 72°C for 90 sec, and final extension at 72°C for 7 min. The nested PCR products were resolved by electrophoresis using 2% sodium borate agarose gel. Individual bands were excised from the gel and DNA extracted using the QIAquick Gel Extraction Kit (Qiagen) according to the manufacturer's protocol.

2.9.5 Sequencing reaction

A 20 μl reaction mix was made containing 1 μl Big Dye 3.1, 3.5 μl 5x CSA Buffer (Applied Biosystems), 0.175 μl (3.2 pmol) primer (20 μM), template – less than 50 ng and H_2O. The PCR program was 94°C for 5 min, (96°C for 10

sec, 50°C for 5 sec, 60°C for 4 min) x 30 and finishing with 10°C for 10 minutes. Each sample was run separately with the HM001 primer and HMSp2 primer and results were compared for quality control. The PCR reaction was spun and 50 µl 100% EtOH (final concentration of 70%), 2 µl 3M NaOAc (pH 4.6) and 2 µl EDTA (0.125M) were added to the 20 µl reaction. Tubes were inverted 4 times, incubated at room temperature for 15 min and then centrifuged for 30 min at full speed at room temperature and then centrifuged upside-down on tissue for one min at 180g. Seventy µl 70% EtOH was added to wash, and the specimen was centrifuged 10 min at full speed at room temperature, centrifuged upside-down on tissue for 1 min at 180 g, air dried in the dark for 10 min at room temperature, and submitted for sequencing at -20°C in the dark. Sequencing was performed by the Australian Cancer Research Foundation Biomolecular Resource Facility (ACRF BRF) at the John Curtin School of Medical Research, utilising BigDye Terminator v3.1 Cycle Sequencing Kit according to the manufacturer's protocol.

2.10 RNA isolation and cDNA production

Cells (5-10 × 10^6) were pelleted, lysed in 1ml Trizol® Reagent (Invitrogen) by repetitive pipetting and incubated for 5-10 min at room temperature. The insoluble material was pelleted by centrifugation at 12,000 g for 10 minutes at 2 to 8°C, and the RNA-containing supernatant transferred to a fresh tube. 0.2 ml of chloroform (Sigma) was added and the tubes shaken vigorously for 15 seconds and then incubated at 15 to 30°C for 2 to 3 minutes. The samples were then centrifuged at 12,000 g for 15 minutes at 2 to 8°C, separating the mixture into a lower red, phenol-chloroform phase, an interphase, and a colourless upper aqueous phase containing RNA. The aqueous phase was transferred to a fresh tube containing 0.5 ml of isopropanol and inverted several times to ensure mixing. The samples were incubated at 15 to 30°C for 10 minutes and centrifuged at 12,000 g for 10 minutes at 2 to 8°C. The supernatant was removed and the RNA pellet washed once with 1 ml 75% ethanol. The sample was vortexed until pellet floated and centrifuged at 7,500 g for 5 minutes at 2 to 8°C. The ethanol was removed, and the specimen respun briefly and excess ethanol removed with a pipette. The RNA pellet was

air dried for 1-2 minutes, and dissolved in 20 (for cells) – 50 (spleen) µl RNase-free water and incubated for 10 minutes at 55 to 60°C. RNA was stored in aliquots at -70°C after spectrophotometric concentration and integrity analysis (A260:A280 ratio) (NanaDrop, Thermo Scientific). cDNA was produced utilising the Invitrogen SuperScript™ III First-Strand Synthesis System for RT-PCR (Catalogue no 18080-051). The initial reaction mix contained 1 µl 50 µM oligo(dT)$_{20}$ primers, 5 µg RNA, 1 µl 10mM dNTP mix and was made up to 10 µl with RNase free water. This was incubated for 5 minutes at 65°C and then placed on ice for 1 minute. The cDNA synthesis mix was added to this, which contained 2 µl 10xRT buffer, 4 µl 25mM $MgCl_2$, 2 µl 0.1M DTT, 1 µl RNaseOUT (40 U/µl) and 1µl SuperScript III (200 U/µl). After mixing the reaction was incubated at 50°C for 50 minutes and then 85°C for 5 minutes, and then placed on ice. Finally 1 µl of RNase H was added to each tube it was incubated for 20 minutes at 37°C and stored at -20°C.

2.11 Real time PCR

All primers were purchased from GeneWorks Pty Ltd. Primers were designed with the assistance of the Primer Bank (http://pga.mgh.harvard.edu/primerbank/) [381]. Primers were designed to span exon-exon boundaries in order to avoid amplification of any contaminating DNA, with annealing temperatures of 58-60°C, G+C content of 40-60%, target length of 20 nucleotides and the amplified PCR product was approximately 80-250 base pairs in length.

Primer sequences:

Myb: forward: 5' AGACCCCGACACAGCATCTA 3'
reverse: 5' CAGCAGCCCATCGTAGTCAT 3'

Beta Actin: forward: 5' TGTTACCAACTGGGACGACA 3'
reverse: 5' AAGGAAGGCTGGAAAAGAGC 3'

The Real time PCR reaction master mix contained 2 µl cDNA diluted 1/10, 1 µl forward primer (5 µM), 1 µl reverse primer (5 µM), 5 µl SYBR® Green PCR Master Mix (Applied Biosystems) and 1 µl MillQ water. Amplifications were performed in 384-well optical reaction plates (Applied Biosystems) using the 7900HT Fast Real-Time PCR System (at the ACRF BRF, JCSMR, ANU). The reaction conditions were 50°C for 2 min, 95°C for 10 min, 40 cycles each of: 95°C for 15 sec, 60°C for 1 min. To confirm that a single product was generated (ie no primer dimers) PCR amplicons were analysed by dissociation curves (95°C for 15 sec, 60°C for 1 min, 95°C for 15 sec). Raw data was analysed using SDS 2.2.2 software (Applied Biosystems) with the default fixed fluorescent threshold set at a value of 0.2 and baseline set from cycles 3-15, manually ensuring that these values were appropriate.

The comparative C_T method for relative quantitation of gene expression was used. The CT is the cycle number at which the replicating amplicon associated fluorescence crosses a threshold. To ensure approximately equal target and reference amplification efficiency, standard curves were generated for each primer pair to determine primer efficiencies using serial 4-fold dilutions of cDNA. The slope of the curve generated by the relative amounts of cDNA (log_{10} input; x-axis) versus cycle threshold (C_t) value (y-axis) was used to determine primer efficiency. They were found to be between 0.95 and 1.05 using the formula $E = 10^{-1/slope}-1$ as demonstrated in Figure 2.2. The normalised expression of a gene relative to a selected baseline could thus be estimated, assuming equivalent priming efficiencies for the target and reference genes, using the formula [382]:

$$\text{Comparative expression level} = 2^{-\Delta\Delta Ct}$$

where ΔCT=CT(target)-CT(normaliser) and ΔΔCT=sampleΔCT–referenceΔCT

Figure 2.2 Amplification efficiency of primer pairs

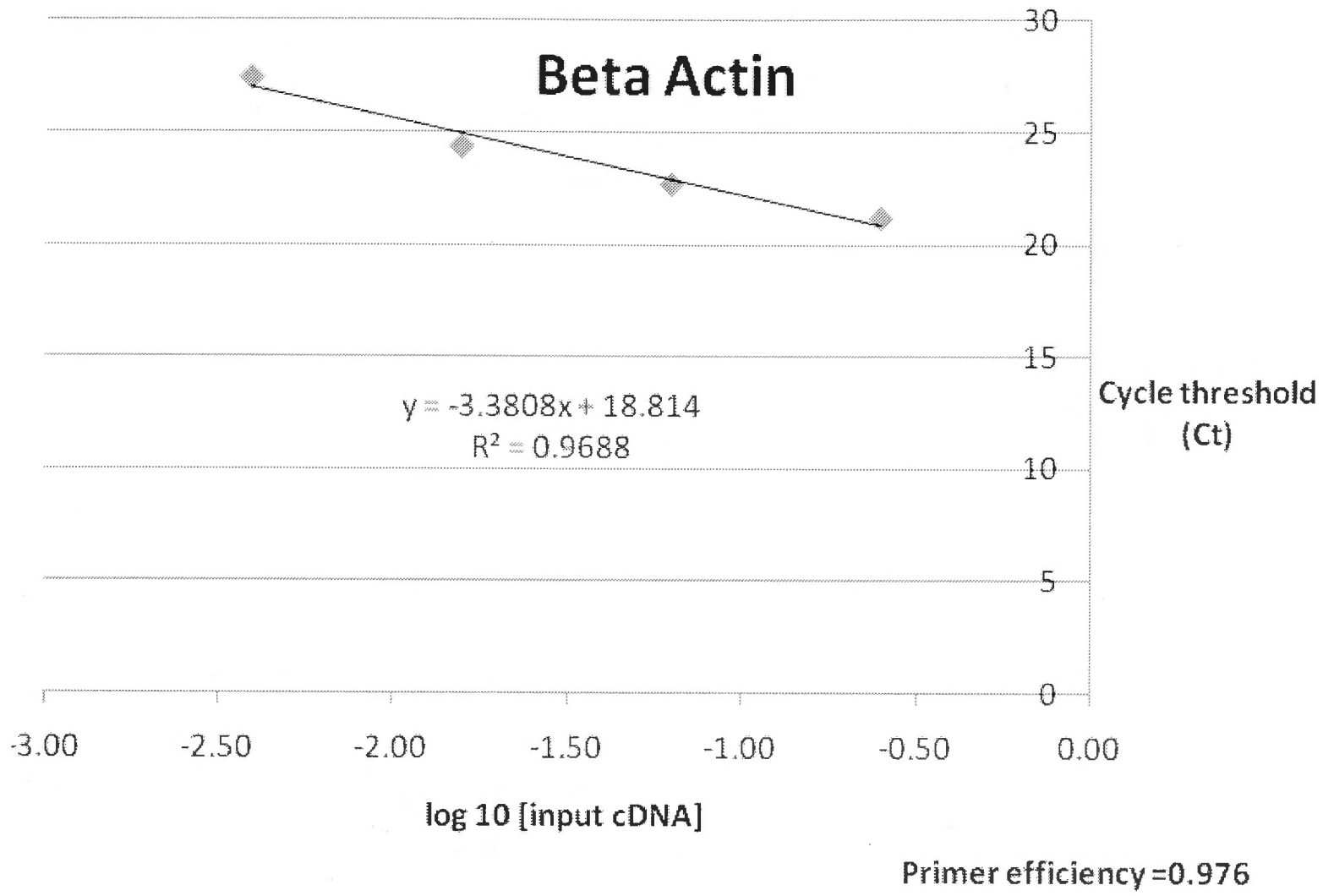

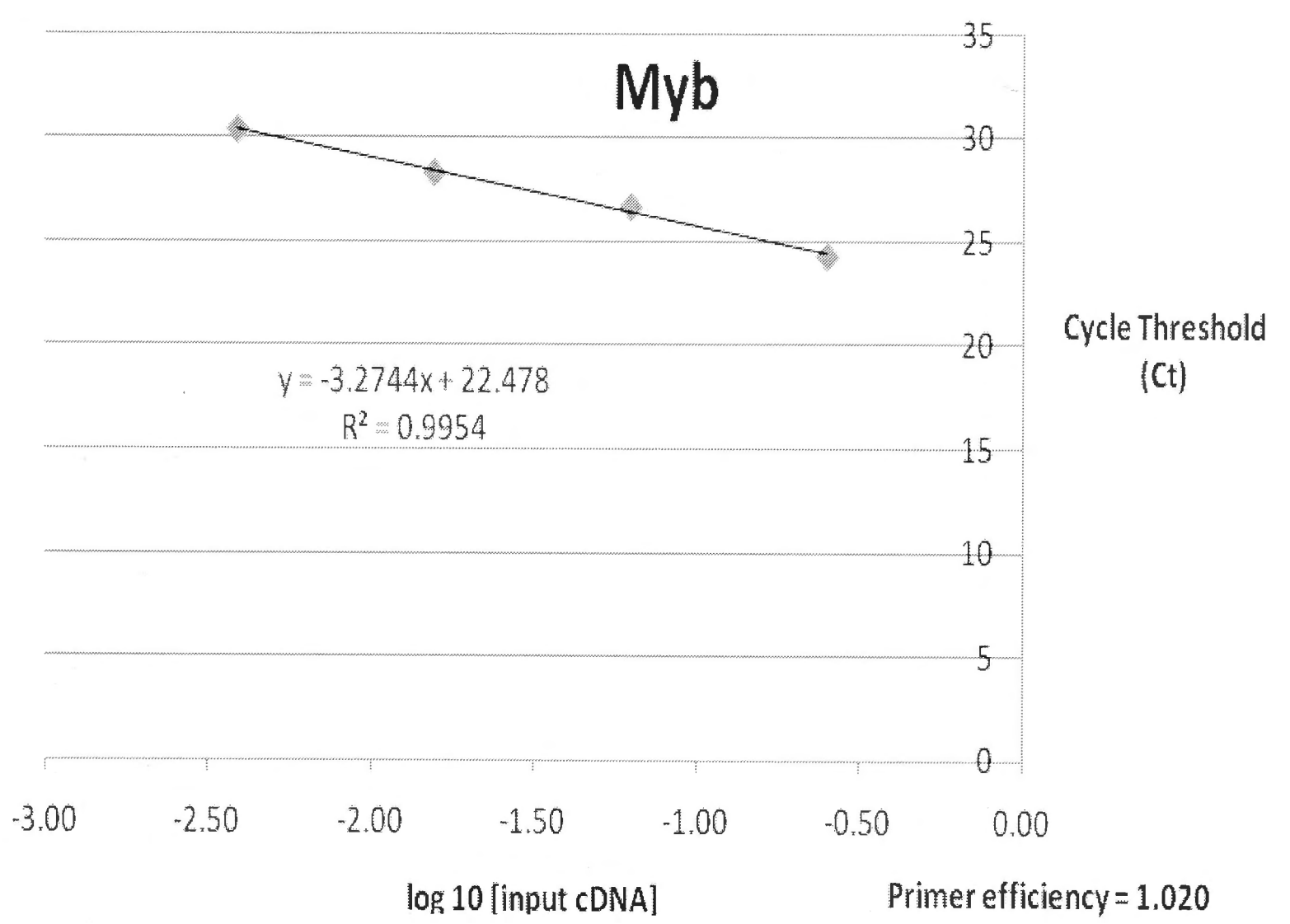

2.12 Microarray

Microarray analyses of oligo-dT primed RNA were performed using the Affymetrix GeneChip®Gene 1.0 ST Array System for Mouse. RNA was isolated (as per Section 2.10) from the following: 1. "**Activated cells**", p53 wild type splenocytes 24 hours after harvest from antigen stimulated mice and culture with anti-CD40 antibody; 2. "***MYC* transduced cells**", *Trp53* mutant anti-CD40 activated B cells flow cytometrically sorted for GFP+ cells 2 days after spinoculation with *GFP/MYC* retrovirus with CD40 still in culture; 3 and 4, "**Outgrowth one and two**", two independent outgrowths of *Myb+MYC* dual transduced B cell lines stably growing in culture for several weeks, each containing approximately 33% viable GFP positive cells. Approximately 5 µg of RNA was used per sample, the concentration ranging from 300-1000 ng/µl. The cell sorting was performed by the Microscopy & Cytometry Resource Facility at JCSMR. Poly-A+ mRNA in each of the RNA samples was converted to cDNA using oligo-dT priming, and then to biotinylated cRNA that was hybridized to Affymetrix GeneChip® 1.0 ST Arrays for mouse and scanned as per the manufacturer's protocol, these steps being performed by staff of the Australian Cancer Research Foundation (ACRF) Biomolecular Resource Facility (BRF) at the John Curtin School of Medical Research using a GeneChip® Fluidics Station 450 and GeneChip® Scanner. Analysis of raw data was also performed at the ACRF BRF using Partek® software to obtain log2(signal intensity) for each gene for each of the four samples and fold changes between samples.

3. **Establishing an efficient model for malignant transformation of a finite cohort of mature B cells.**

3.1 Introduction

All published experimental models of B lymphoid malignancy involve an undefined but extremely large or limitless number of B cells that comprise the target for somatic mutations that eventually lead to a clonal malignancy. For example, the bone marrow produces approximately three million pre-B cells per day [383] so by the age of 12 weeks when a pre-B cell malignancy has evolved in an Eμ-Myc-transgenic mouse, several hundred million pre-B cells will have been subject to dysregulated *Myc* plus an unknown number of other mutations. Similarly, when *Myc*-transgenic mice are infected with the replication-competent retrovirus, Moloney Murine Leukaemia Virus, an unknown number of pre-B and B cells will have been infected and frequently there will have been many rounds of super infection, with current technology capable of identifying an average of approximately 20 [313,384]) integration sites in the malignant clone that finally evolves. While these approaches provide a powerful way to demonstrate cooperation between mutations to produce a malignancy, they do not allow analysis of how many additional mutations were needed for malignant transformation of B cells as it is well established that the majority of retroviral integrations in MMLV-induced tumours are "passenger mutations" and only a few are thought to be "driver mutations". Likewise, a large but unknown number of passenger mutations are likely to have accumulated in spontaneous lymphomas in Eμ-Myc transgenic mice.

This chapter sought to establish in my hands a new experimental strategy to solve this problem, by limiting *MYC* dysregulation to a finite cohort of mature B cells and limiting retroviral insertional mutagenesis to a single round of integration with a replication defective retrovirus. To link these two processes, mature B cells bearing a *Trp53* loss-of-function mutation were transduced in culture with a replication-defective retrovirus expressing *MYC* and *GFP*, and then a small number of these cells were injected into immunodeficient *Rag1*-KO mice to determine if this single round of mutagenesis was sufficient for malignant transformation of mature B cells. The results in this chapter establish the incidence and characteristics of the resulting lymphomas.

3.2 Incidence of lymphomas

As discussed in Section 1.13, lymphomatous outgrowths were seen in a small percentage of C57BL/6 recipient mice injected with *MYC* transduced Ig^{HEL} $Trp53^{Bblast/\ Bblast}$ splenocytes, but such outgrowths were evident in most Rag1KO recipients (Lixin, unpublished data). Ig^{HEL} mice produce large numbers of B cells with rearranged immunoglobulin heavy and light chains with a high affinity for Hen Egg Lysozyme (HEL) [375]. This allows simultaneous physiological activation of B cells by antigen, instead of anti-IgM as a surrogate, and minimizes cell-to-cell variability caused by different antibody specificities and affinities of expressed BCRs. The expression of this uniform, HEL-binding IgM BCR also serves as a unique marker to track mature B cells from the donor, both by allowing staining to detect B cells that bind HEL antigen and because the IgM constant region carries an amino acid polymorphism (a-allotype) that can be detected with anti-IgM^a monoclonal antibody and differs from the IgM^b allotype expressed by C57BL/6 mice.

Twelve intravenous injections of *MYC* transduced Ig^{HEL} $Trp53^{Bblast/\ Bblast}$ splenocytes into Rag1KO mice (see Materials and Methods for details) were performed over three separate experiments (Table 3.1). Despite giving a finite cohort of *MYC* transduced B cells, and noting that the *MYC* retrovirus is not replication competent, in all three experiments an initial cohort of recipient mice was euthanised between day 36 and 38 of cell transfer because the mice were cachectic with prominent abdominal distension. Dissection demonstrated hepatosplenomegaly, often with ascites and lymphadenopathy. The remaining 3 mice in experiment 1 and 4 mice in experiment 2 were not so unwell at the time of euthanasia, with more subtle clinical manifestations such as ruffled fur, mild abdominal distension and lethargy.

As discussed in Section 1.13.1 control experiments in which *Trp53* mutant cells transduced with an empty vector (without *MYC* overexpression) were injected into recipients were not performed, raising the question of whether or not the transduced MYC provirus was necessary for malignant outgrowths. Since only a small percentage of the injected cells were transduced and expressed *GFP*,

yet each malignancy was uniformly GFP positive, this indicates that *MYC/GFP* transduced cells were greatly favoured for malignant transformation, however this bias for GFP expressing cells could result from the activity of *MYC*, the mutagenic effect of proviral integration, or the combination of the two. To resolve this point, it would be valuable in future studies to confirm experimentally the rate at which B cell malignancies evolve in recipients of *Trp53* mutant B cells transduced with empty vector-GFP. If there was an appreciable background rate of *GFP* expressing malignancies with empty vector, this would provide some indication of the extent to which the mutagenic activity of proviral integration can contribute and substitute for *MYC*. Empty vector controls were used for the experiments analysing in vitro transformation of B cells in the following chapter.

Table 3.1 Incidence and timing of lymphoma development after IV injection of *MYC* transduced Ig^{HEL} $Trp53^{Bblast/Bblast}$ splenocytes into *Rag1*KO mice

The number and timing of lymphoma development (splenomegaly macroscopically and a distinct GFP bright population on splenic FACS analyses) in recipients is shown.

Experiment	Total no. B cells transferred	GFP+ B cells transferred	Day post cell transfer	No. of mice euthanised	No. of mice with GFP+ lymphoma
1	2×10^6	1.4×10^5	37	2	2
			42	3	2
2	2×10^6	1.6×10^5	38	1	1
			52	4	3
3	2×10^6	3.6×10^5	36	2	2

3.3 Phenotype of lymphomas

The FACS phenotype of the lymphomatous outgrowths had been previously determined by Dr Lixin Rui in experiments described in Section 1.11.1 above. He demonstrated that they were composed of large GFP positive cells which expressed surface B220, IgD, IgM, CD19, CD45 and CD16/32 but were negative for CD138, Mac-1, CD21, CD23, c-kit, CD25, thy1 and AA4.1. This phenotype is entirely consistent with a mature B cell without any aberrant markers beyond the *GFP* expression. This broad panel of antibodies was not repeated in this work apart from confirmation that the phenotype was that of a mature B cell, a representative example being shown in Figure 3.1. The only aberrant surface marker seen in human Burkitt lymphoma is surface CD10 positivity, the phenotype being otherwise consistent with a mature B cell. CD10 expression in murine germinal centre B cells, or murine models of Burkitt lymphoma is not well described [385] and the murine-specific antibody is not readily available so this was not performed.

The clinical phenotype had been further investigated previously (Lixin, unpublished data) showing that this was an aggressive mature B cell tumour, infiltrating into the liver, kidney and lung (Figure 3.2). The mitotic figures and nucleoli seen in haematoxylin and eosin stained sections suggested rapid cell replication. Peripheral blood was not analysed in any of the experiments.

Figure 3.1 Representative FACS phenotype of lymphomatous spleen

*Rag1*KO mice recipient mice were injected with *MYC* transduced Ig^{HEL} $Trp53^{Bblast/Bblast}$ splenocytes and euthanised 5-8 weeks later. An example of the recipient splenic FACS profile (right column) is compared to normal spleen (left column), both gated on viable (7AAD negative) cells.

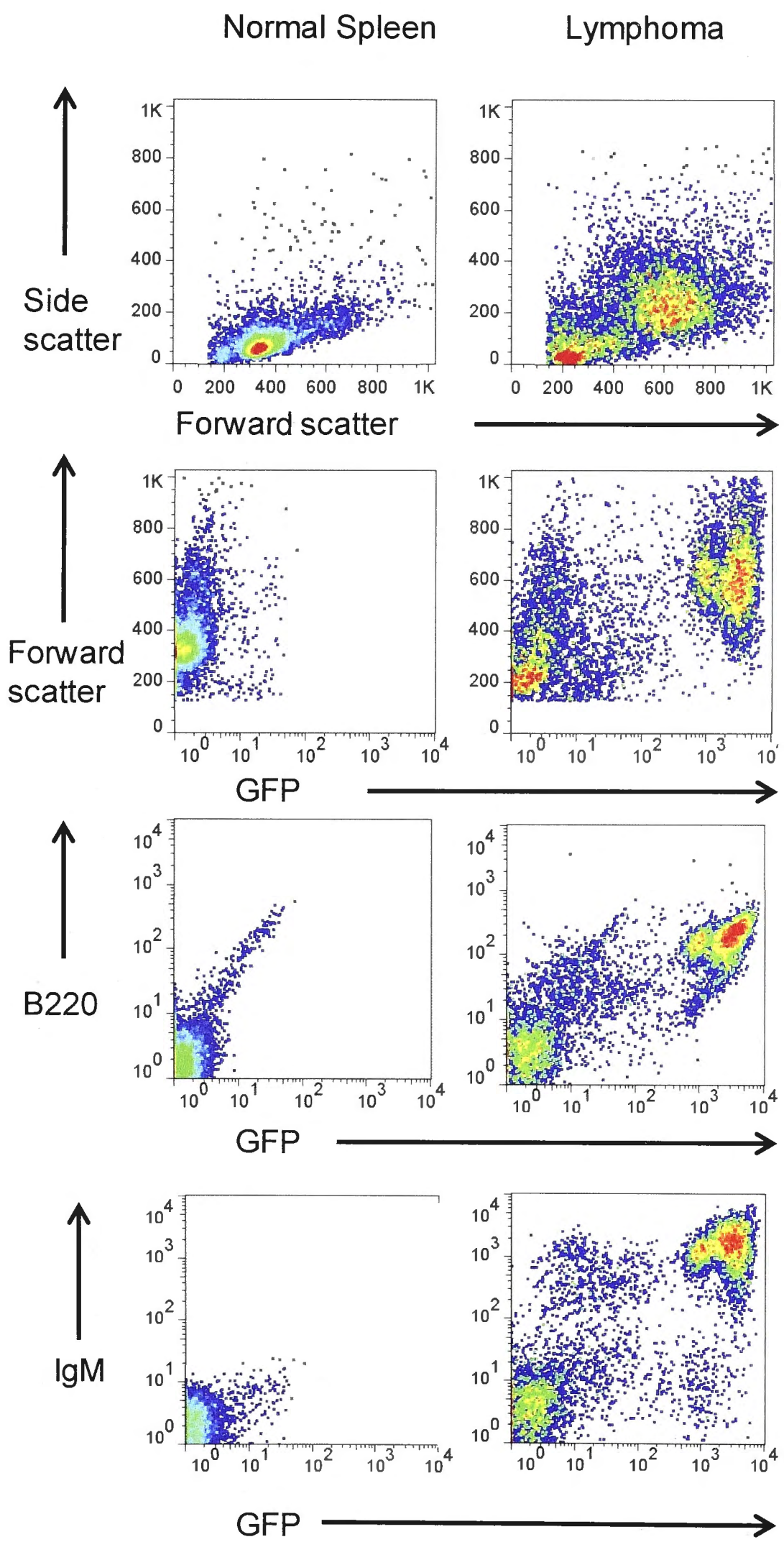

Figure 3.2 Representative haematoxylin & eosin stained paraffin section of a lymphoma

a) Normal murine spleen (x4)
b) Recipient spleen (x4)
c) Recipient spleen (x20)
d) Recipient spleen (x40)

Photographs taken by Sally Mapp of lymphoma samples from earlier unpublished experiments described and illustrated in Section 1.11.1 and performed by Lixin Rui.

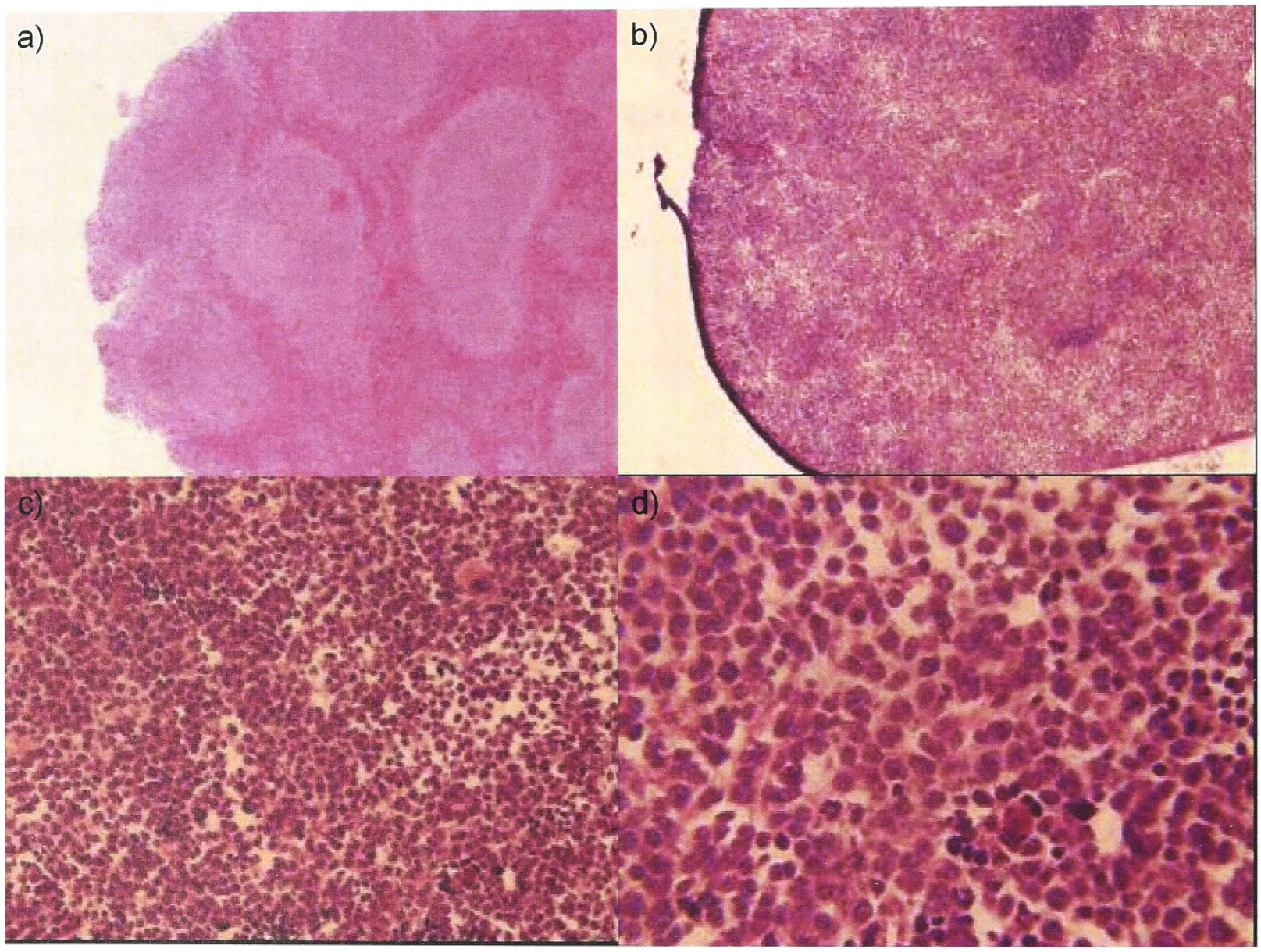

The invasive nature of the lymphomatous growths suggested a neoplastic process, but in the absence of an aberrant FACS phenotype it was important to exclude a polyclonal mature B cell proliferation. Murine B cells mostly express the κ light chain on their surface [386]. Light chain restriction is thus not as useful for determining clonality of murine B cell tumours as it is in human tumours, where the κ to λ ratio is more balanced. In murine experimental models clonality is commonly assessed through analysis of immunoglobulin gene rearrangements to determine if they are all the same (ie cells are clonal) or diverse (ie cells are polyclonal). This was not possible with this experimental system because the Ig^{HEL} cells used already have rearranged immunoglobulin heavy and light chain genes in order to create an immunoglobulin receptor specific for the HEL antigen [375].

Splinkerette PCR amplification of individual proviral integration junction fragments, coupled with cloning of lymphomas in culture by limiting dilution, was thus utilised in order to help determine if cells derived from 'lymphomatous' spleens were monoclonal, oligoclonal or polyclonal (Figure 3.3). This method has many drawbacks [387] but we felt that it could help distinguish an oligoclonal outgrowth from a polyclonal outgrowth. Two unique lymphomas were assessed and results show that the bands obtained by splinkerette PCR (excluding the retroviral vector bands) are the same in most but not all single cell clones, demonstrating that most of the malignant cells were clonally related with identical integration sites. One example was observed of a subclone with one shared and one distinct integration junction fragment (Fig 3-3a). This could either reflect an oligoclonal starting population, or the variant may have undergone a rearrangement of one integration site. These preliminary results indicate that the lymphomas are mono- or oligoclonal rather than polyclonal.

Figure 3.3 Clonality assessment using limiting dilution method

Varying dilutions of a suspension of 'lymphomatous' spleens' cells were plated onto a 96 well plate and the dilution at which approximately 40% of wells demonstrated cell growth was subsequently utilised for clonality assessment. Cell growth theoretically follows a Poisson distribution in this setting, which concludes that the majority of wells with cell growth ("subclones") post incubation will be derived from a single cell [388]. The retroviral integration sites of subclones were thus compared.

a) Gel photo of splinkerette PCR products from four subclones (left) compared to gel photo from original lymphoma number 9 (right)

b) Gel photo of splinkerette PCR products from eight subclones (left) compared to gel photo from original lymphoma number 18 (right)

(The poor resolution of the subclone illustrations is due to the original electronic images being lost).

a)

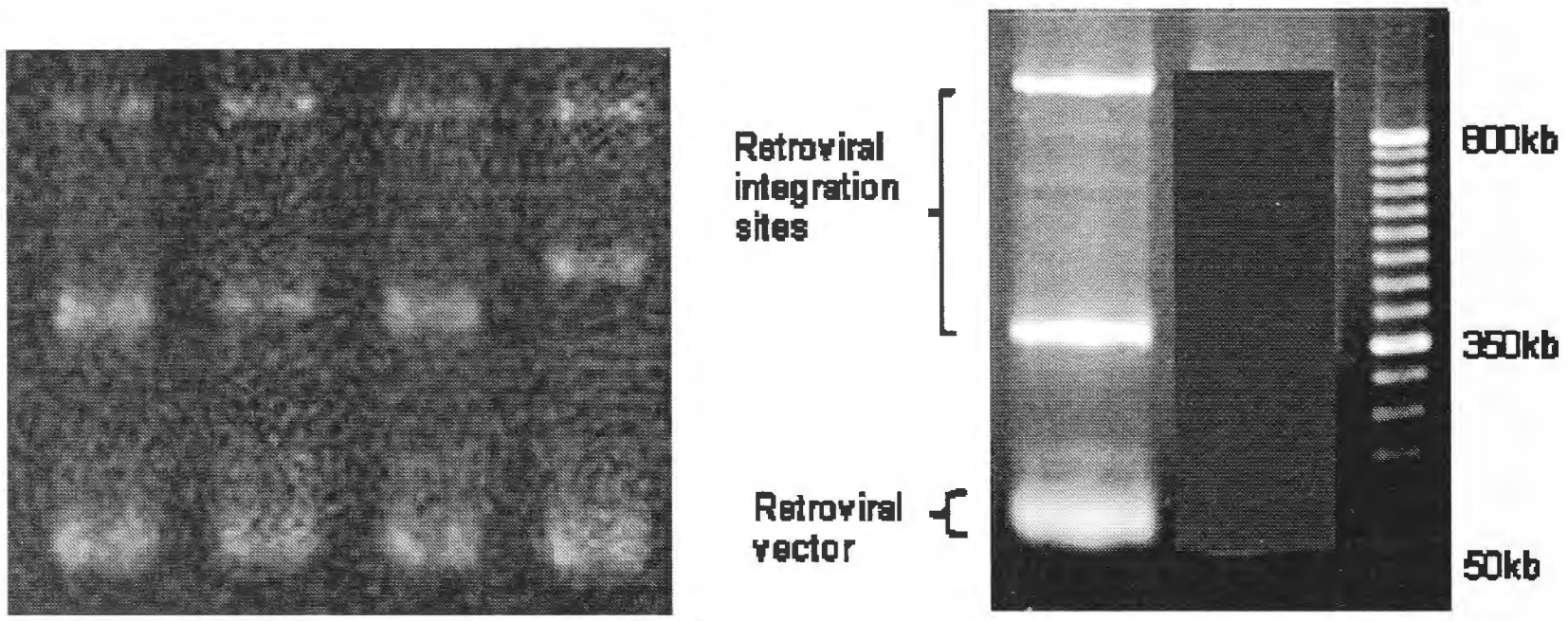

b)

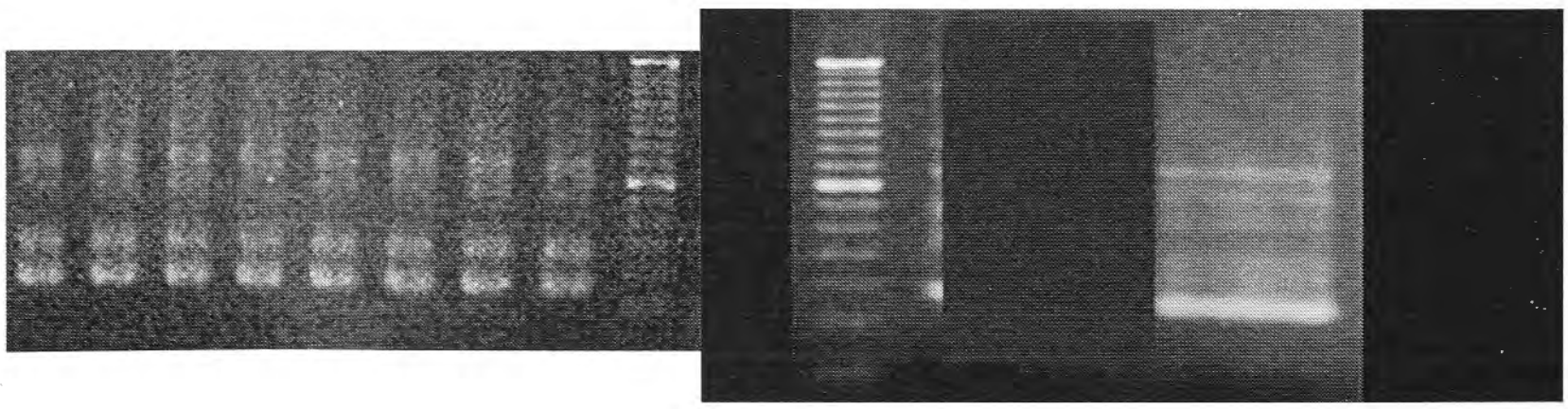

Since each malignant outgrowth expressed GFP at quite high levels, I compared the GFP expression of a malignant outgrowth with the spectrum of GFP expression of the input B cells at the time of transplantation into *Rag1*KO mice and at timepoints after transplantation before the clonal/oligoclonal outgrowths were detectable. Since this required comparison of GFP fluorescence intensity measured days or weeks apart, a standard set of stable calibration beads was added to each sample. These beads fluoresce in the same wavelength range as GFP and hence are measured by the same detector, but the beads can be distinguished by a difference in size using the FSC parameter. As shown in Fig 3-4, most of the GFP+ B cells at the time of transplantation fluoresced with an intensity range near that of the lower intensity calibration bead population (indicated by left hand dashed line). Cells with GFP fluorescence as bright as the high intensity calibration bead population (dashed line on right of each plot) were rare in the injected inoculum, and in the spleen after 11 or 18 days. However, the lymphomatous outgrowth that developed on Day 39 exhibited GFP fluorescence brighter than the high intensity calibration bead. There are two possible explanations for the high GFP fluorescence of the transformed B cells compared to the majority of injected B cells: 1. Cells that express the provirus at high levels are preferentially transformed; or 2. Transformed cells do not express the proviral vector at a higher level, but these growing cells have much more cytoplasmic volume and accumulate much higher total amount of GFP. The latter appears unlikely since there is little correlation between FSC and GFP in the lymphomatous outgrowth, and there are large cells in the transferred inoculum and at earlier time points.

This question was also approached by asking whether the individual lymphomatous outgrowths varied widely in GFP fluorescence or whether there was a narrow band of vector expression that was compatible with transformation. Figure 3.5 compares GFP intensity in three independent lymphomas in different recipients derived from the same pool of injected donor B cells. There was only 2-fold difference in median GFP fluorescence. Again this is consistent with selection for high *MYC/GFP* vector expression, although one cannot rule out a shared metabolic state that results in high GFP accumulation per cell regardless of level of vector expression.

Figure 3.4 Representative FACS analysis of cells at various time points post retroviral transduction

GFP expression of *MYC* transduced Ig^{HEL} $Trp53^{Bblast/\ Bblast}$ splenocytes gated on viable (7AAD negative) cells. Donor mice were euthanized on Day 0, and Day 3 reflects the time of cell transfer into *Rag1*KO recipient mice. Cells at subsequent time points are from recipient spleen, ie 'Day 11" reflects 10 days post initial retroviral transduction and 8 days post injection into recipients. The gates demonstrate the percentage of GFP positive cells, the gate placement being determined using non transduced controls (top row). To control for the variable sensitivity of the flow cytometer, fluorescent calibration beads were used as an internal reference standard in each run (non shaded peaks on histogram), dotted vertical lines showing the same GFP intensity as the calibration beads on the dot plots (the calibration beads not being visualised on the GFP/forward scatter plots).

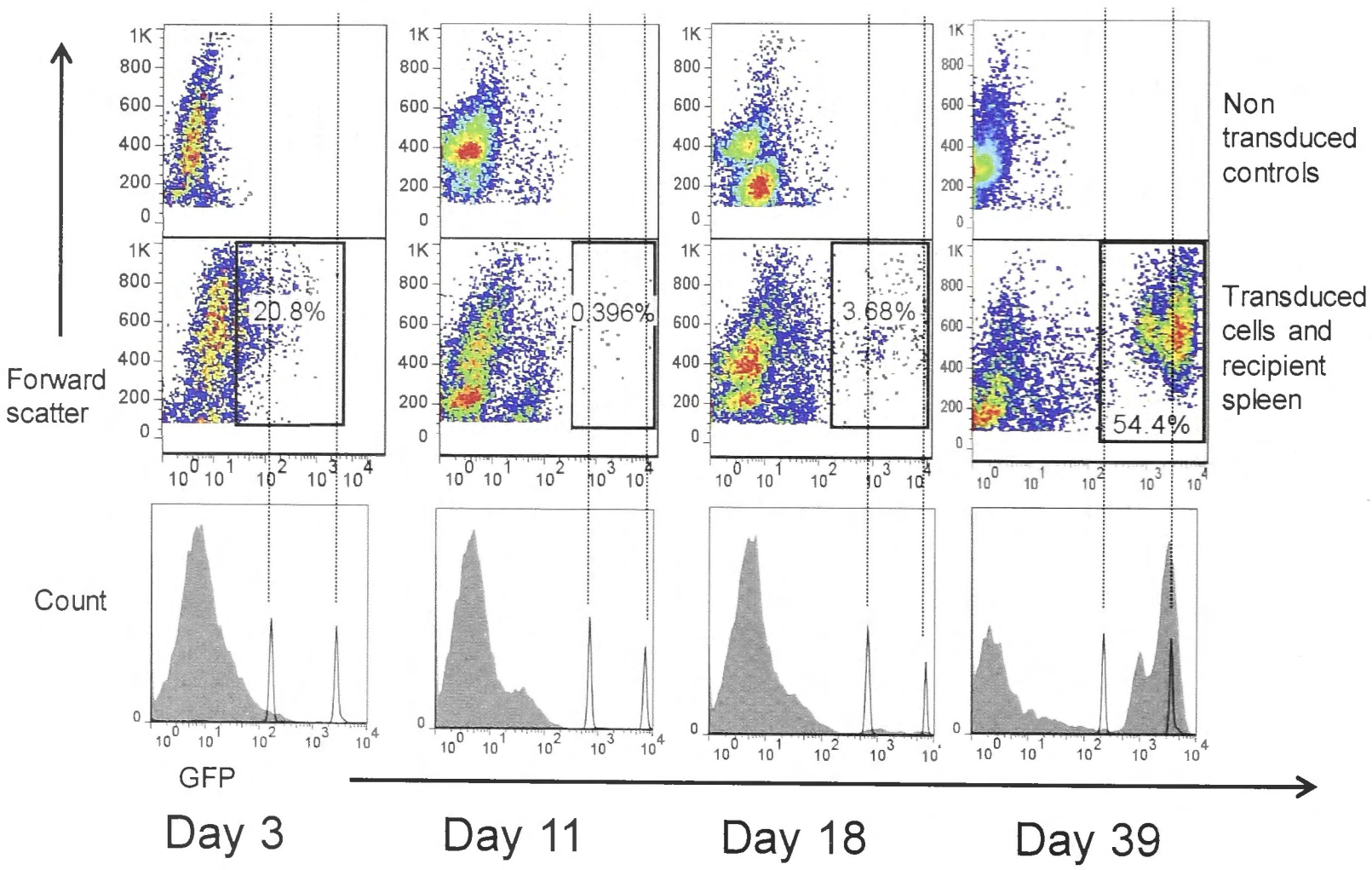

Figure 3.5 Lymphomas demonstrated a spectrum of GFP expression

MYC transduced Ig^{HEL} $Trp53^{Bblast/Bblast}$ splenocytes were injected into four recipient RagKO mice. Fifty two days later three of the mice were unwell, were euthanized and their spleens were analysed by FACS on the same run. Profiles are gated on viable (7AAD negative) B220 positive cells. The GFP intensity of the GFP high cells (which are likely to reflect the lymphoma cells) was thus determined using arbitrary units to facilitate comparison.

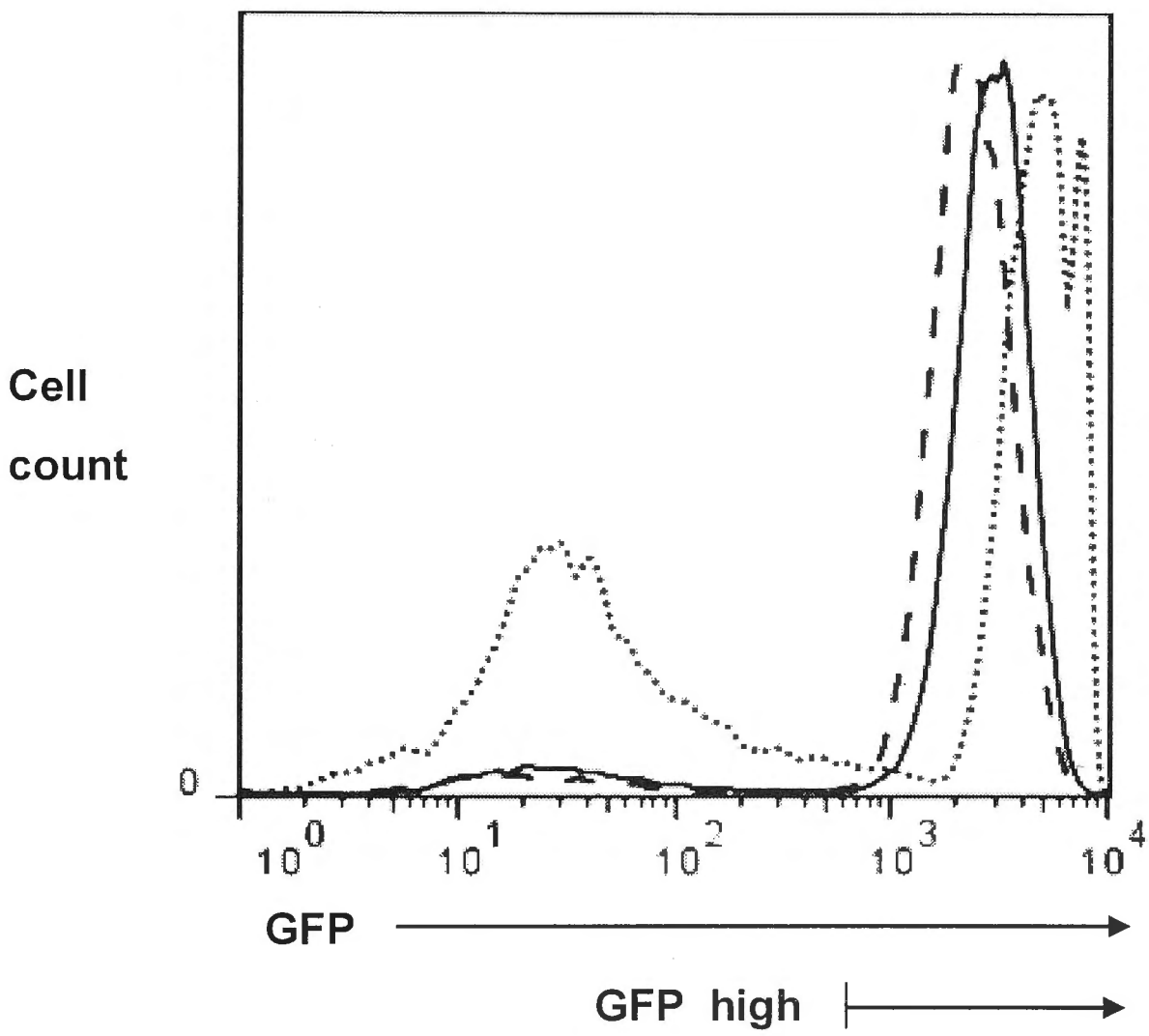

Median GFP intensity of 'GFP high' population

- - - - - 2258 units

——— 2848 units

..... 4744 units

3.4 Discussion

Results in this chapter demonstrate that we have developed a reproducible method of lymphomagenesis. Correlation of this FACS and morphological phenotype with published descriptions of murine and human B cell lymphomas demonstrates similarities to the mouse model of Burkitt lymphoma (BL) developed by Kovalchuk et al [389] which attempted to replicate BL translocation breakpoints by fusing the *MYC* gene derived from a BL-derivative chromosome to elements of the Igκ or Igλ loci. Both models have demonstrated the 'starry sky' pattern in the murine spleen with a diffuse infiltrate of large IgM and CD19 positive B cells punctuated by clearings containing histiocytes. The main difference between our retrovirus-induced lymphomas and those described in this mouse model is that Kovalchuk et al [389] noted predominantly lymphadenopathy rather than splenomegaly, while in our model splenomegaly was prominent. The FACS profile in both models is consistent with a mature B cell phenotype.

Burkitt lymphoma has not been seen to occur spontaneously in mice, and previous attempts to induce lymphoma through overexpression of *Myc* under the control of immunoglobulin promoter regions in mouse models (such as the Eμ-myc model [10]) have consistently resulted in lymphomas with an immature immunophenotype (surface immunoglobulin negative), or with morphological features inconsistent with Burkitt lymphoma. These experimental findings confirm the critical importance of the mode of *Myc* activation in murine lymphoma models.

The presence of the internal ribosomal entry site (IRES) in the retroviral construct in our model means that the *GFP* reporter gene and the *MYC* gene are transcribed together, but two separate protein products are produced. In general the translational efficiency of both genes depends on the derivation of the IRES, the genes within the constructs and intrinsic cellular factors (reviewed by Hennecke et al [390]), and thus the translation of the second gene (GFP in our case) could potentially be modulated by the nature of the first gene,

although the mechanism remains to be defined. Our research assumes that the ratio of *GFP* expression to *MYC* expression is constant (although not 1:1), so that GFP intensity is proportionate to *MYC* expression, although this has not been proven in this system. It must be acknowledged that variations in either *GFP* or *MYC* expression may alter the translation or catabolism of the other protein product, as may the developmental stage or metabolic activity of the cell, so the relationship between these two protein levels may not be as predictable as assumed. MYC has been shown to be modulated by translational control [391,392], altering the direct correlation between mRNA and protein concentration, however the relevance of this to a bicistronic vector remains unclear. Myc protein levels were not assessed in this research (by Western blotting, for example) which would have helped to confirm the assumed relationship between *GFP* expression and MYC levels. This will be performed during further work on this model.

Only small numbers of GFP positive cells were evident in the transferred cells in recipient spleen at Days 11 and 18. By day 39 the GFP positive population had increased significantly in size and GFP intensity. While it is possible that very rare input cells with high GFP expression were not identified through the FACS analysis, it seems more likely that up regulation of *MYC* is part of the transformation process. Kovalchuk's model of Burkitt lymphoma [389] demonstrated a significant difference in *Myc* expression between the transgenic cells and lymphomatous outgrowth, the group coming to the same conclusion.

The next logical question is thus which cells undergo transformation. The clonal or oligoclonal nature of the lymphomas is consistent with a single or small number of cells rapidly proliferating to form the lymphoma. It would seem logical to conclude that the intensity of *MYC* expression in the cell was the defining feature. Variations in tumour phenotype as a consequence of variations in *Myc* expression have been reported by Smith et al [393]. This group monitored the outcome of varying intensity of *Myc* expression under the influence of regulatory elements which allowed it to be expressed in all nucleated haemopoietic cells of all maturity levels. The median survival of the mice was inversely correlated to the *Myc* expression level, and the tumour phenotype also varied according to *Myc* expression, with mice expressing the

highest level of *Myc* developing T cell tumours, and lower expressing ones monocytic/macrophage lineage malignancies. Separate research has shown that a threshold level of Myc is required for maintenance of *Myc*-induced T cell lymphomas [394].

MYC expression would have varied in the input cells depending on the number of retroviral integration sites, the location of the retroviral integration sites and perhaps also the developmental stage or cell cycle stage of the transduced cell. It cannot be assumed that because the lymphoma phenotype in these experiments reflects that of a mature B cell that the initial transforming events occurred within a mature B cell, as it has been demonstrated that progeny of a transformed cell are capable of further maturation [395]. Murine splenic B cells are at varying stages of development [396] and the activated pathways within a particular cell may determine the degree and effect of *MYC* overexpression. The seminal paper describing the Eμ-myc model of lymphomagenesis [10] demonstrated different frequency of lymphoma with different regulatory regions within the constructs. While this may reflect varying degrees of *Myc* expression altering the incidence of lymphoma (as discussed above), it may also be explained by the fact that the different regulatory regions dysregulate *Myc* expression at different stages of B cell maturity or different stages of the cell cycle, which may account for the different tumour incidences.

Although the lymphomatous outgrowth is clearly strongly GFP positive, the GFP intensity varies between tumours from the same input cells harvested on the same day (Figure 3.5). This suggests that there is a spectrum of tolerated *MYC* expression in the final tumour (but does not necessarily imply that the initially transformed cell can tolerate such a breadth of *MYC* expression). Factors which may be influential in determining the GFP intensity of the final tumour include those discussed above regarding the variation in *MYC* expression in a single cell (such as number and site of proviral integration), but spontaneous or retrovirus-induced co-operating mutations also need to be considered in lymphomatous outgrowths that have undergone multiple cycles of replication in a p53 defective state. Cell size may contribute to some degree to these differences as the GFP intensity will be increased in larger cells even if the

concentration of GFP per picolitre of cytoplasm is constant, due to a larger volume of cytoplasm.

Overall this chapter has demonstrated reproducible and rapid formation of aggressive mature B cell lymphomas in Rag1-deficient recipient mice injected with *Trp53* mutant splenocytes with dysregulated *MYC*. The high expression of GFP in these lymphomas relative to input cells suggests selection for rare transduced cells with high *MYC* expression, and hence this alone may be sufficient to explain the clonal or oligoclonal origins of the lymphomatous outgrowths. However it cannot be ruled out that transformation itself results in high GFP expression and may not relate to *MYC* expression at all as no input cells could be identified with the GFP intensity of the malignant lymphoma. The next chapter investigates the additional possibility that the retroviral integration site contributes to the neoplastic growth through insertional activation or inactivation of co-operating cellular genes.

4. Results: Analysis of retroviral integration sites

4.1 Introduction

The results in Chapter 3 provided evidence that only rare cells with high proviral expression underwent lymphomatous transformation, so that this factor alone could theoretically explain the clonal or oligoclonal nature of the transformed B cells. The experiments in this chapter investigated an alternative or additional explanation, namely the integration of the *MYC/GFP* provirus activated cellular proto-oncogenes or inactivated tumour suppressor genes, which co-operated with *MYC* overexpression and p53 loss allowing the cell to escape the normal growth-regulatory mechanisms.

The Retrovirus Tagged Cancer Gene Database [94] demonstrates the critical role that genes adjacent to retroviral integration sites play in retrovirus induced lymphomagenesis. The top ten common integration sites in retrovirus induced lymphoid malignancies in this collation include *Myc*, *Pim1*, *Notch1* and *Ccnd1* which are all clearly validated lymphoid proto-oncogenes [397], in addition to *Myb*, which is a validated proto-oncogene and has recently been demonstrated to be dysregulated in certain subtypes of T-ALL [238]. The experiments described here tested the hypothesis that the retroviral insertion sites in the MYC/GFP+ lymphomas would often be near known or suspected proto-oncogenes or tumour suppressor genes. Insufficient fresh lymphomas were available for gene expression analyses using real time PCR (archived specimens were used for some insertion site analyses) so the relative expression of all important genes near retroviral insertion sites could not be determined.

4.2 Identification of retroviral integration sites

The tumour retroviral integration sites were determined using Splinkerette PCR on DNA extracted from cryopreserved murine splenic lymphomas. The method is detailed in Section 2.9 and illustrated in Figure 1.1, but the basic principle is to cleave lymphoma DNA with a frequent cutting restriction enzyme (*Sau*3AI)

and amplify junction fragments comprising the 5' end of the provirus and several hundred base pairs of flanking host DNA. The size of the junction fragment would vary between integration sites, depending on the distance between the integration site and the first *Sau*3AI site 5' in flanking DNA. Amplification of these junctions employed a reverse primer complementary to the retroviral long terminal repeat, and a forward primer complementary to a synthetic linker that was ligated to the nearest restriction enzyme cleavage site upstream of the proviral integration. The sequence to which the primer binds in the retroviral long terminal repeat was not found in the mouse genome using a University of California Santa Cruz Genome Browser Blat search although the splinkerette PCR protocol was not performed on non transduced cells to confirm a lack of amplification. The PCR products were then separated by gel electrophoresis (Figure 4.1), cut out and sequenced (separately detailed in the Appendix). The sequence of the flanking host DNA was then located in the mouse genome using the UCSC (University of California Santa Cruz) Genome Browser Blat search genome function (July 2007 assembly). RefSeq genes encoding mature mRNA transcripts (ie starting with the 'NM' prefix), both provisional and validated, could thus be collated, initially 10 and subsequently 100 kb either side of the insertion site. Forty six unique integration sites were amenable to being sequenced, representing an average frequency of 1.9 integrants per lymphoma. These results are summarised in Table 4.1, the lymphoma specimen numbers and insertion site labels in this table corresponding to the labels in Figure 4.1.

One limitation in this study was unavoidable amplification of an internal vector fragment from each lymphoma, which will obscure detection of unique junction fragments of similar size. This internal fragment arises because in the vector the 3'LTR is identical to the 5'LTR, providing a second priming site for the reverse primer, and an internal *Sau*3AI site occurs 75 bp 5' to the 3'LTR priming site. It is possible to modify retroviral vectors so that no internal proviral fragments are amplified, however this had not been anticipated. Despite the presence of a consistent 75bp internal fragment, this limitation proved to be minor as it was still possible to identify numerous flanking fragments that were larger than the internal fragment.

Figure 4.1 Agarose gel photographs post splinkerette PCR

Splinkerette PCR was performed on the set of 24 lymphomas to amplify the 5' junction fragment at each retroviral integration site. The PCR products were separated by agarose gel electrophoresis with molecular weight markers. All unique bands visualised under ultraviolet light after staining with ethidium bromide (denoted by lymphoma number and a unique letter) were cut out and sequenced, with the exception of the small internal retroviral fragment (marked "vector"). Unlabelled bands in this figure reflect sequences that could not be identified in the mouse genome, duplicate sequences within the one lymphoma (due to incomplete restriction enzyme cleavage of DNA) or in rare cases contamination from previously amplified fragments in other lymphoma samples.

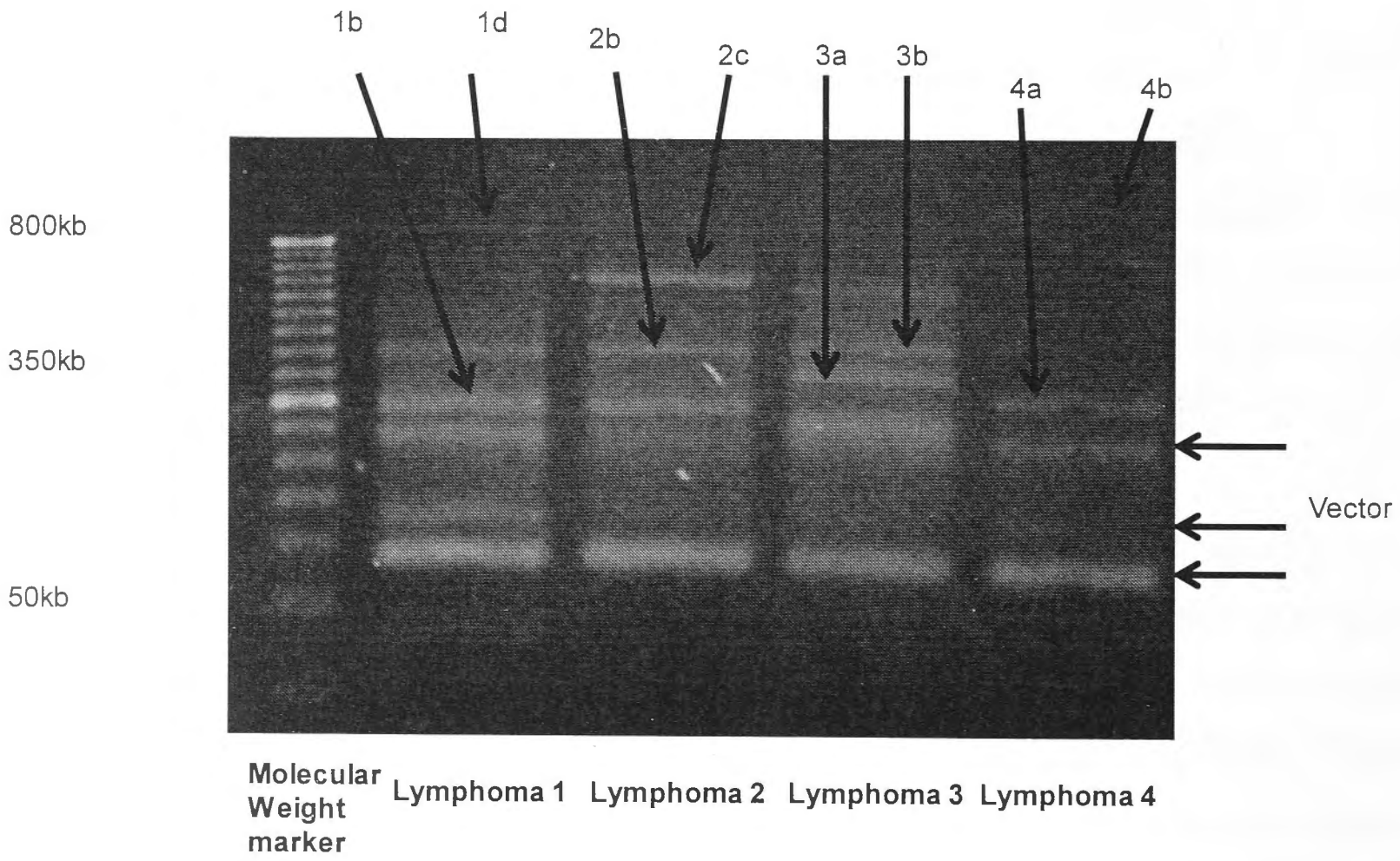

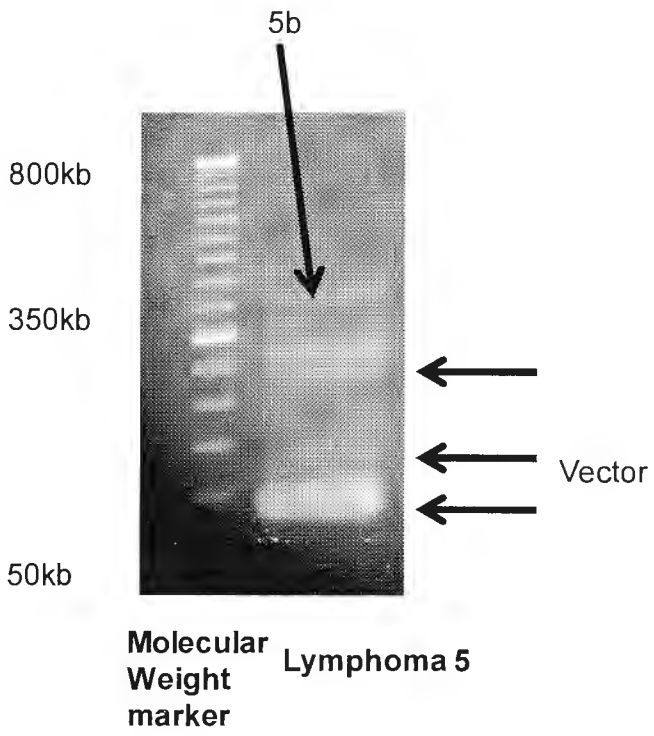
5b
800kb
350kb
50kb
Vector
Molecular Weight marker
Lymphoma 5

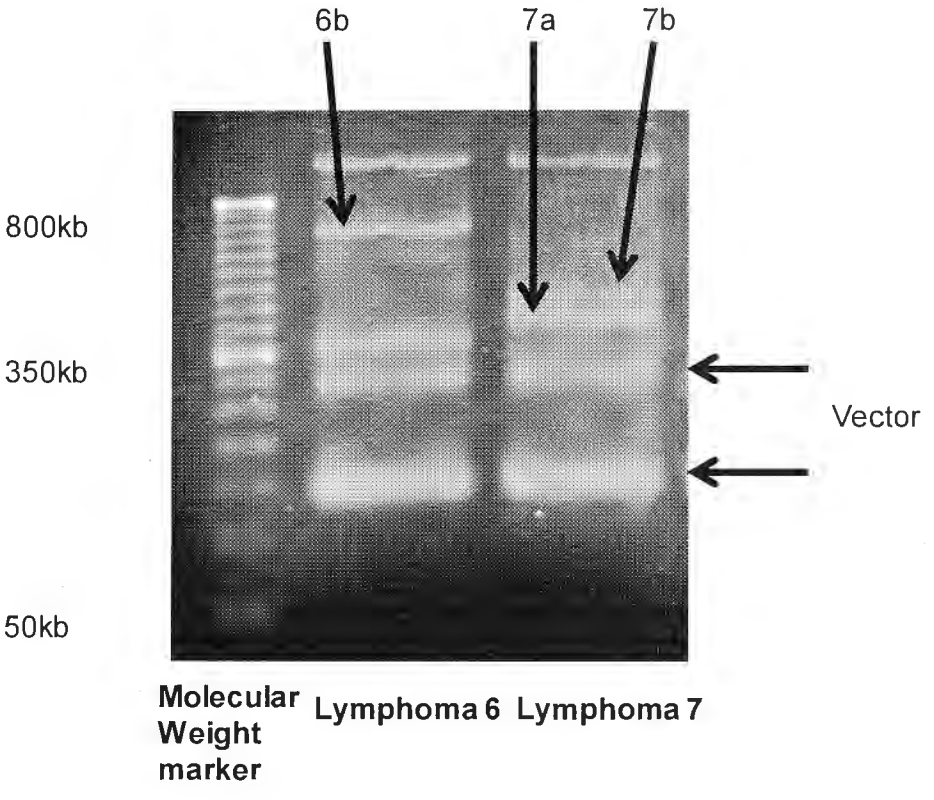
6b
7a
7b
800kb
350kb
50kb
Vector
Molecular Weight marker
Lymphoma 6
Lymphoma 7

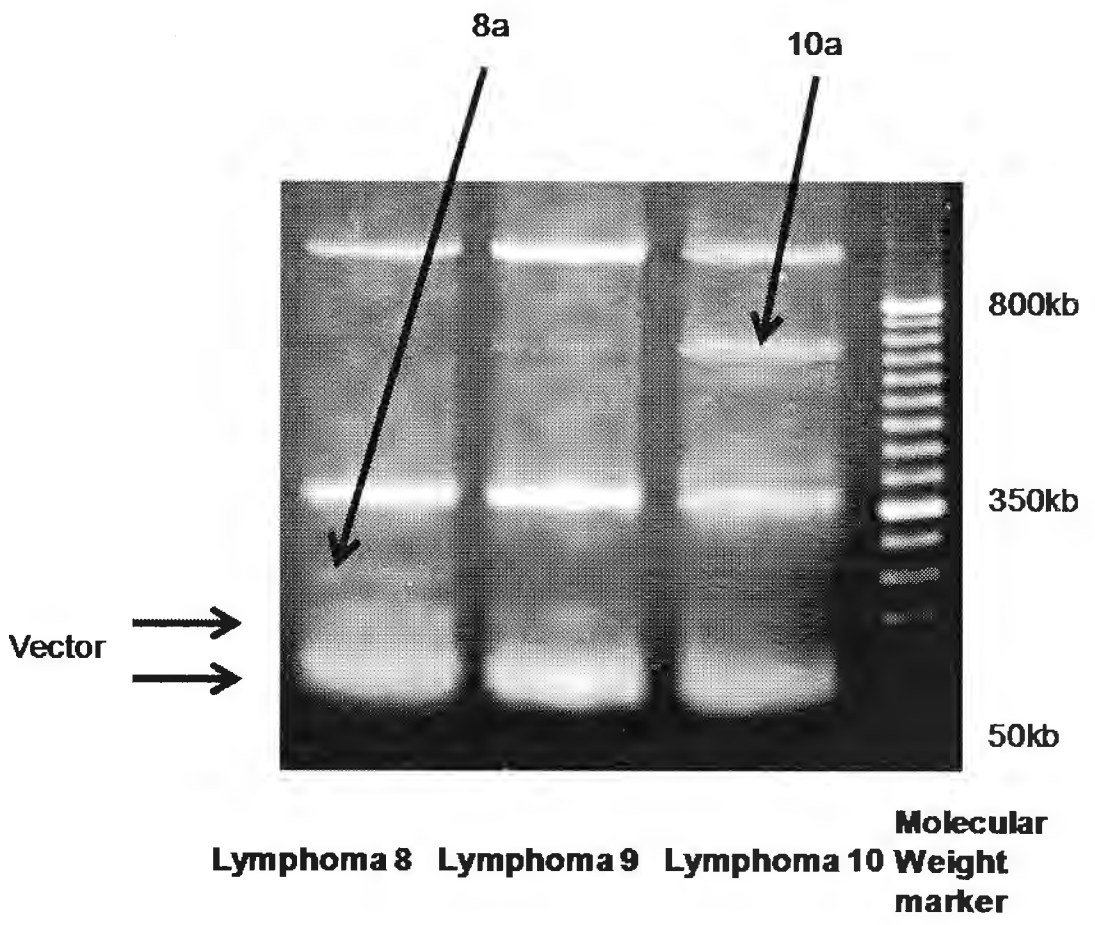
8a
10a
Vector
800kb
350kb
50kb
Lymphoma 8
Lymphoma 9
Lymphoma 10
Molecular Weight marker

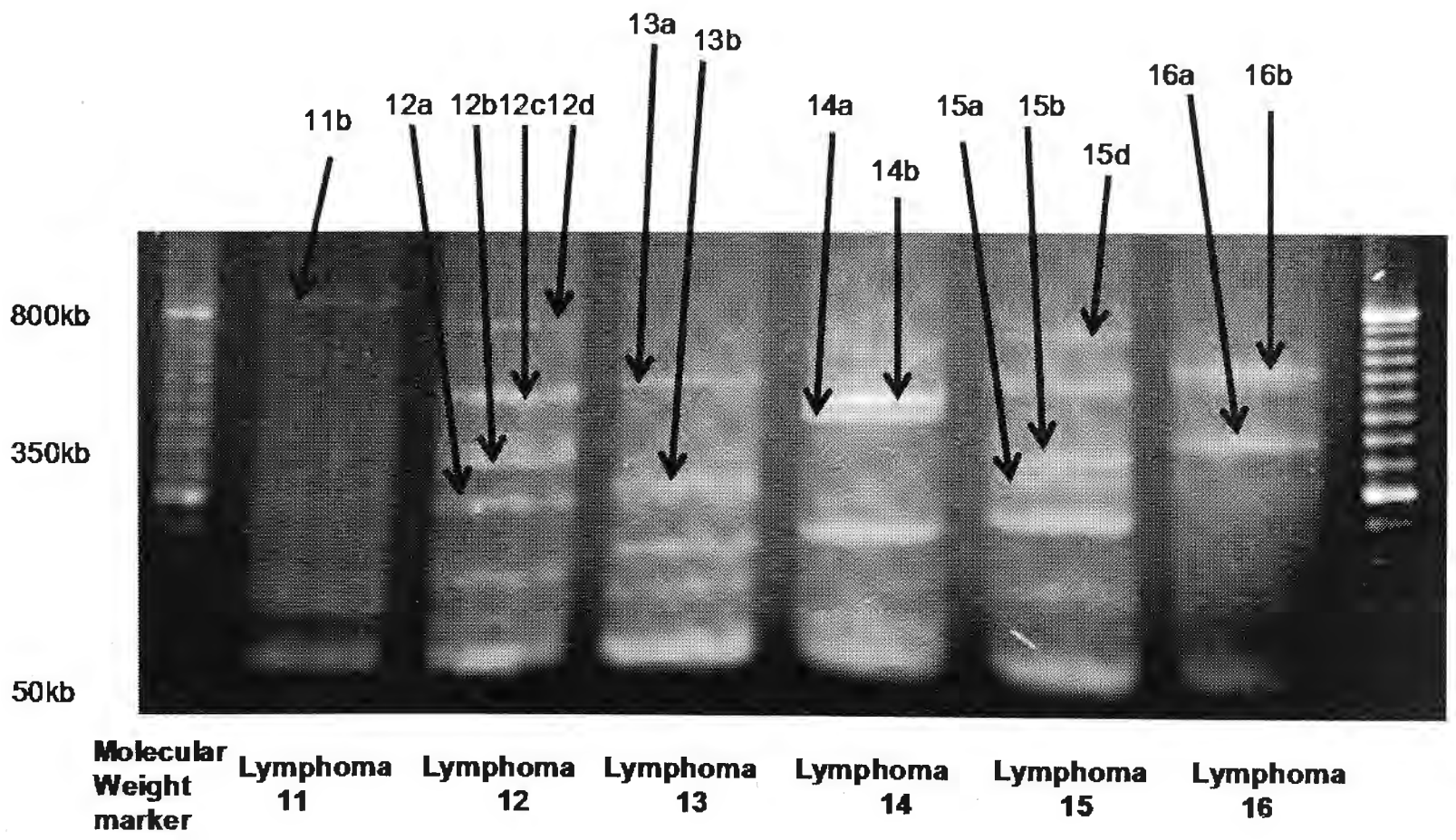
11b
12a
12b
12c
12d
13a
13b
14a
14b
15a
15b
15d
16a
16b
800kb
350kb
50kb
Molecular Weight marker
Lymphoma 11
Lymphoma 12
Lymphoma 13
Lymphoma 14
Lymphoma 15
Lymphoma 16

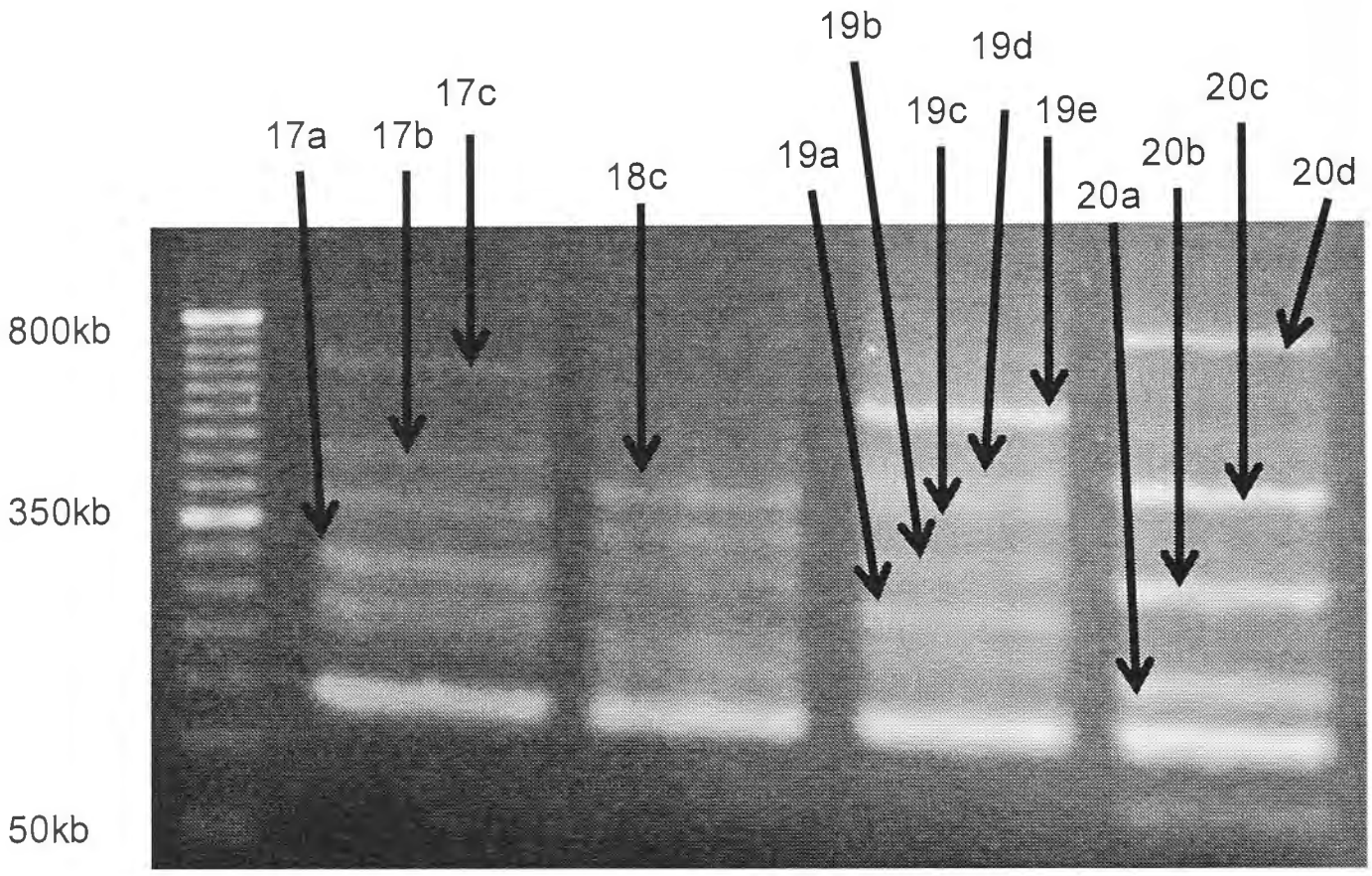
17a
17b
17c
18c
19a
19b
19c
19d
19e
20a
20b
20c
20d
800kb
350kb
50kb
Molecular Weight marker
Lymphoma 17
Lymphoma 18
Lymphoma 19
Lymphoma 20

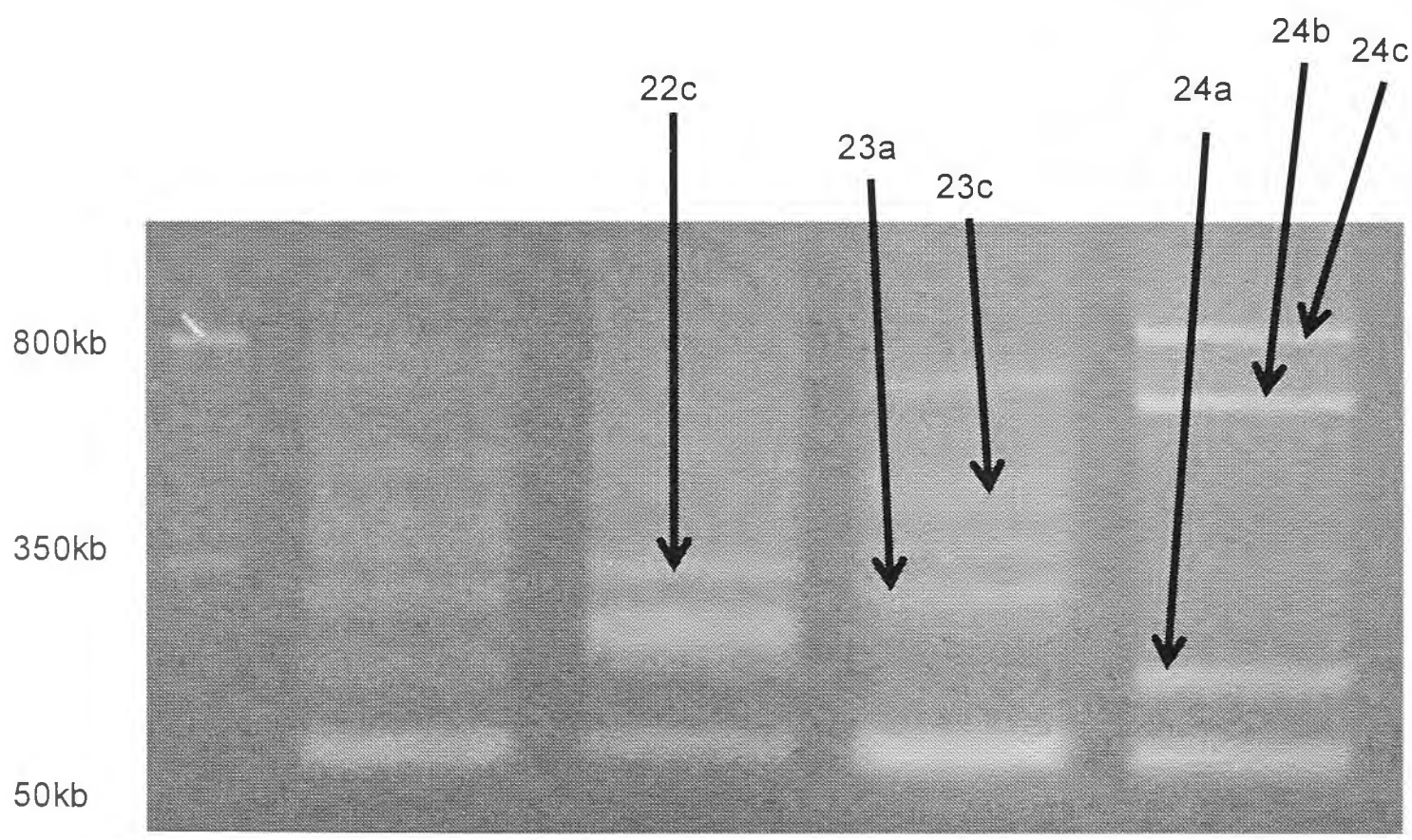
22c
23a
23c
24a
24b
24c
800kb
350kb
50kb
Molecular Weight marker
Lymphoma 21
Lymphoma 22
Lymphoma 23
Lymphoma 24

Table 4.1 Unique integration sites and adjacent genes

The genomic sequence of the 46 unique integration sites identified in the set of 24 lymphomas was located in the mouse genome using the UCSC (University of California Santa Cruz) Genome Browser Blat search genome function (July 2007 assembly). The location of each integration site and adjacent genes are summarised below. The integration site labels correspond to those on the agarose gels in Figure 4.1.

Integration site	Chromosomal location	Intragenic	Nearest gene	Genes within 10kb
1b	chr4:129,560,568-129,560,695		Ptp4a2	
1d	chr8:3,653,584-3,654,293		Retn	Stxbp2,Retn
2b	chr10:80,431,252-80,431,541	Gng7	Gng7	Gng7
2c	chr10:80,874,047-80,874,544	Nfic	Nfic	Nfic
3a	chr4:128,471,215-128,471,553		Zfp362	Zfp362
3b	chr5:36,895,679-36,895,952	Tbc1d14	Tbc1d14	Tbc1d14
4a	chr4:133,179,630-133,179,926	Zdhhc18	Zdhhc18	Zdhhc18
4b	chr4:130,469,507-130,470,144	Laptm5	Laptm5	Laptm5
6b	chr6:50,953,940-50,954,546		Npvf	
7a	chr13:42,196,785-42,197,040	Hivep1	Hivep1	Hivep1
7b	chr9:15,339,454-15,339,837		BC017612	BC017612
8a	chr2:103,735,740-103,735,900		Lmo2	
10a	chr6:50,954,268-50,954,522			
11b	chr19:29,444,583-29,445,081	Cd274	Cd274	Cd274
12a	chr7:88,490,508-88,490,688		Rps17	Rps17,Cpeb1
12b	chr3:88,314,524-88,314,861		Lmna	Lmna
12c	chr16:3885469-3885938		Nat15	Nat15
12d	chr10:20,793,496-20,794,112	Ahi1	Ahi1	Ahi1
13a	chr8:23,823,933-23,824,094		Ikbkb	Ikbkb
13b	chr3:96,357,957-96,358,372		Txnip	Txnip
14a	chr3:129,267,750-129,268,180	Elovl6	Elovl6	Elovl6
14b	chr2:118,553,802-118,554,267	Plcb2	Plcb2	Plcb2
15a	chr10:87,852,957-87,852,997	Gnptab	Gnptab	Gnptab

Integration site	Chromosomal location	Intragenic	Nearest gene	Genes within 10kb
15b	chr4:133,676,096-133,676,170	Ubxd5	Ubxd5	Ubxd5
15d	chr14:32229519-32229730	Sh3bp5	Sh3bp5	Sh3bp5
16a	chr11:8,586,082-8,586,458		Tns3	
16b	chr9:116088308-116088680		Tgfbr2	Tgfbr2
17a	chr11:54,772,810-54,772,858	Tnip1	Tnip1	Tnip1
17b	chr2:167,208,276-167,208,527		B4galt5	
17c	chr3:21,849,100-21,849,374			
18c	chr2:91,805,597-91,805,855	Dgkz	Dgkz	Dgkz
19a	chr3:136,405,342-136,405,516	Ppp3ca	Ppp3ca	Ppp3ca
19b	chr18:78,282,620-78,282,777		Slc14a1	
19c	chr3:95,773,774-95,773,915		Plekho1	
19d	chr12:45,347,928-45,348,274		Pnpla8	
19e	chr5:149,790,016-149,790,534		Katnal1	
20a	chr10:80,448,450-80,448,581	Gng7	Gng7	Gng7
20b	chr3:60,247,139-60,247,376		Mbnl1	
20c	chr17:35,352,001-35,352,390		NF-κB il1	NF-κB il1,Lta
20d	chr3:52,701,066-52,701,441		Cog6	
22c	chr5:66,116,725-66,116,911		Pds5a	
23a	chr11:12,534,246-12,534,393			
23c	chr1:183,142,873-183,143,048		Wdr26	Wdr26
24a	chr4:135,587,257-135,587,343		Tceb3	Tceb3
24b	chr11:62,416,616-62,417,029		Trpv2	Trpv2
24c	chr12:87,027,122-87,027,450	Batf	Batf	Batf

4.3 Analysis of genes within 10kb

From the 46 unique proviral integration sites identified above, the 33 genes within 10kb of the insertion site were initially analysed (results summarised in Table 4.2). Such a narrow window was defined, despite a much wider potential window over which proviral LTRs can dysregulate adjacent genes, in order to provide a stringent test for selection of potential oncogenes near integration sites.

The set of genes was correlated with a peer-reviewed online database of known oncogenes, the Atlas of Genetics and Cytogenetics in Oncology and Haematology (http://AtlasGeneticsOncology.org) [397]. This atlas lists genes relevant to all cancers, not solely B cell lymphoma, and utilises data from human and animal studies, dividing cancer genes into two categories: 'annotated genes' and 'other genes possibly implicated in cancer.'

Two of the genes in the set of 33 closely flanking genes were documented as 'annotated genes' (overall 6.06%). This percentage is not significantly higher than expected by chance: there were 840 annotated cancer genes in the Atlas drawn from a total of approximately 25000 human NCBI RefSeq genes (3.36%), the difference not being statistically significant (two tailed p value 0.39 utilising Chi square test). The remaining 31 closely flanking genes were, however, significantly over-represented in the category of 'other genes possibly implicated in cancer,' with 15 (48%) of them in this category compared to a 7280/25000, or 29% background rate (p=0.017 utilising Chi square test). This provided suggestive evidence for an enrichment of proto-oncogenes near the proviral integration sites, but was by no means convincing.

The closely flanking genes were then reviewed to determine if they represented common insertion sites within the Retroviral Tagged Cancer Gene Database (RTCGD) (http://rtcgd.abcc.ncifcrf.gov) July 2007 build (all tumours, not just lymphoid). This database defines common insertion sites (CIS) as 30kb regions containing 2 insertion sites, 50kb regions with 3 insertion sites or a 100kb region with 4 or additional insertion sites, although definition is somewhat subjective,

with gene orientation and function being taken into account along with the total number of integrations in the database. Seven of the 33 closely flanking genes (21%) were found to be in common insertion sites, an apparently high percentage, although the expected rate by chance alone is unknown because the total number of genes in CISs cannot be quantified in RTCGD.

Table 4.2 Analysis of genes within 10kb of retroviral insertion sites

The 33 genes within 10kb of the retroviral insertion sites were correlated with the Atlas of Genetics and Cytogenetics in Oncology and Haematology [397] and the Retroviral Cancer Gene Database (RTCGD) [94], results of which are summarised below.

Gene	Annotated cancer gene	Possible cancer gene	Common insertion site in RTCGD
Stxbp2	no	no	no
Retn	no	yes	no
Gng7	no	yes	no
Nfic	no	no	yes
Zfp362	no	no	no
Tbc1d14	no	no	no
Zdhhc18	no	no	yes
Laptm5	no	no	yes
Hivep1	no	no	yes
BC017612	no	no	no
Cd274	no	yes	yes
Rps17	no	no	no
Cpeb1	no	yes	no
Lmna	no	yes	no
Nat15	no	no	no
Ahi-1	no	yes	yes
Ikbkb	no	yes	no
Txnip	no	yes	no
Elovl6	no	no	no
Plcb2	yes	N/A	no
Gnptab	no	no	no
Ubxn11	no	yes	no
Sh3bp5	no	no	no
Tgfbr2	no	yes	no
Tnip1	no	yes	no
Dgkz	no	yes	no
Ppp3ca	no	yes	no
Lta	yes	N/A	yes
NF-κB il1	no	yes	no
Wdr26	no	no	no
Tceb3	no	no	no
Trpv2	no	yes	no
Batf	no	no	yes

4.4 Genes and recurrent sites of insertion in cancer within 100kb

The propensity of the genes within 10kb of retroviral integration site to be categorised as a 'possible cancer gene' and to be located in a common insertion site as detailed above suggests that this is a non-random set of genes. These analyses were then extended to the genes within 100kb of the insertion sites. The cut off of 100kb was used as it has been demonstrated that retroviral long terminal repeats can influence of the expression of genes greater than 250 kb away [310], although it remains unclear if this is always the case. The Retroviral Tagged Cancer Gene Database was interrogated for these genes and a brief literature review of gene function was undertaken if one such gene was within a RTCGD common retroviral insertion site as it was a 'gene of interest'.

The figures and tables below detail the key features surrounding each unique integration site. The UCSC Genome Browser Blat search genome function (July 2007 assembly) windows show the insertion site I identified (bold arrow) in the context of RefSeq genes (labelled with gene orientation indicated) and other integration sites in RTCGD (small vertical bars). The only windows illustrated are those where the integration site fell within a RTCGD-defined common integration site. The numbers of integrations within defined regions is enumerated in brackets after the gene name, using the summed incidence of integrations in RTCGD and the sites identified in this work. The lymphoma numbers and insertion site labels correspond to those in Table 4.1 and Figure 4.1.

4.4.1 Lymphoma 1

Table 4.3 Genes near insertion site 1b and genes of interest

Genes within 100kb	Genes of interest
Ptp4a2	No gene of interest

Table 4.4 Genes near insertion site 1d and genes of interest

Genes within 100kb		Genes of interest
Stxbp2	*Trappc5*	No gene of interest
Retn	*Fcer2a*	
Xab2	*Clec4g*	
Pcp2	*Cd209a*	

4.4.2 Lymphoma 2

Table 4.5 Genes near insertion site 2b and genes of interest

Genes within 100kb		Gene of interest
Gng7	*Gadd45b*	***Gng7* (3 integrations in 50kb)**
Tmprss9	*Diras1*	This gene is of interest as another distinct intragenic integration site was identified in a separate experiment. The significance of this gene is considered in the discussion.
Timm13	*Slc39a3*	
Lmnb2	*Sgta*	

Figure 4.2 Blat search results 100kb either side of insertion site 2b locus

The bold arrows show the two intragenic insertion sites in this research in the context of schematically illustrated neighbouring genes. The sites of the other retroviral insertions in the region (from the RTCGD) are illustrated with a vertical line in the row labelled 'retrovirus.'

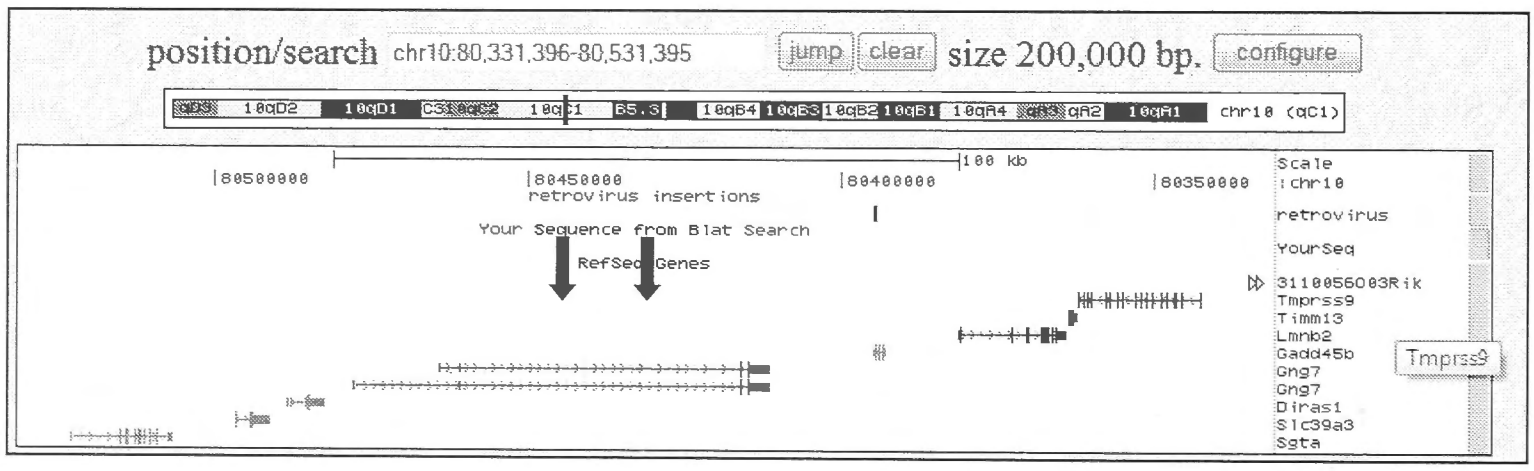

Table 4.6 Genes near insertion site 2c and genes of interest

Genes within 100kb			Gene of interest
Nfic	*Dohh*	*Hmg20b*	***Nfic* (nuclear factor I/C) (5 integrations in 30kb)** Deletion of this gene has been shown to contribute to tooth root defects in mice [398]. No role in neoplasia has been published to date.
Pip5k1c	*Brunol5*	*Gna15*	
Tbxa2r	*Ncln*	*Fzr1*	
Gipc3	*S1pr4*		

Figure 4.3 Blat search results 100kb either side of insertion site 2c locus

The bold arrow shows the intragenic insertion site in this research in the context of schematically illustrated neighbouring genes. The sites of the other retroviral insertions in the region (from the RTCGD) are illustrated with a vertical line in the row labelled 'retrovirus.'

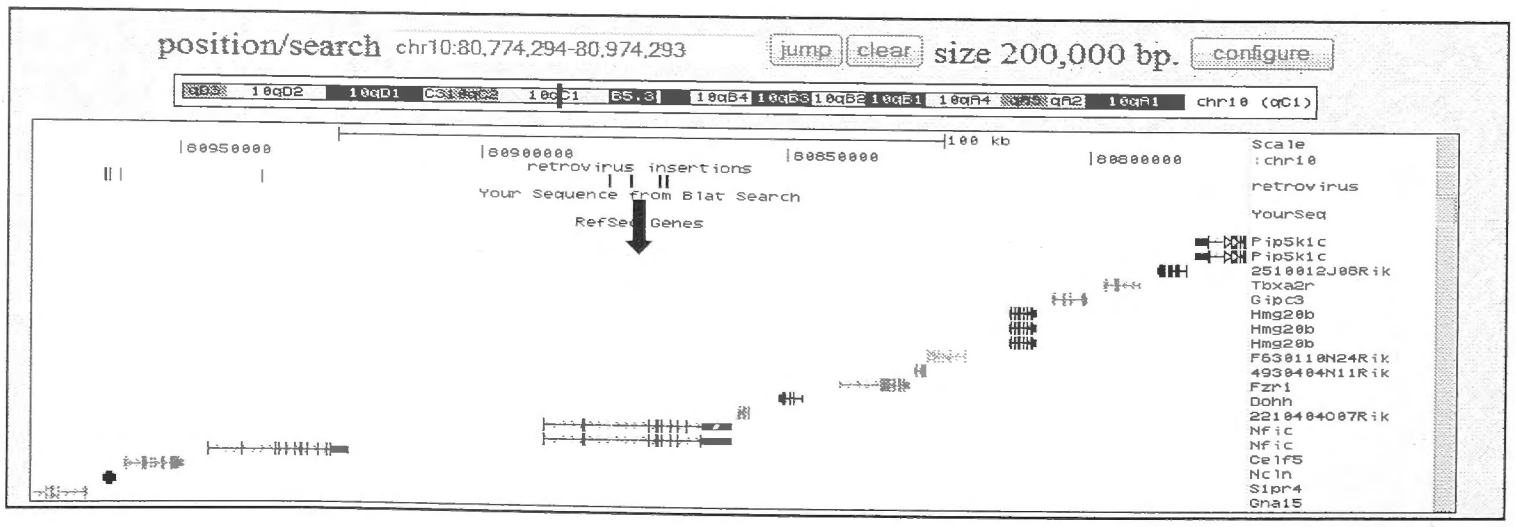

4.4.3 Lymphoma 3

Table 4.7 Genes near insertion site 3a and genes of interest

Genes within 100kb		Genes of interest
Zfp362	*A3galt2*	No gene of interest
Phc2	*Trim62*	

Table 4.8 Genes near insertion site 3b and genes of interest

Genes within 100kb		Genes of interest
Tbc1d14	*Ccdc96*	No gene of interest
Grpel1	*D5Ertd579e*	

4.4.4 Lymphoma 4

Table 4.9 Genes near insertion site 4a and genes of interest

Genes within 100kb	Genes of interest
Zdhhc18	***Zdhhc18*** **(zinc finger, DHHC domain containing 18) (5 integrations in 100kb)**
Nudc	This is a validated protein-coding gene but its function is not well described.
Nr0b2	
Gpatch3	
Gpn2	***Arid1a*** **(AT rich interactive domain 1A (SWI-like)) (5 integrations in 100kb)**
Sfn	Deficiency in embryos causes developmental arrest [399]. Mutations have been identified in ovarian clear cell and endometriod carcinomas, suggesting a role as a tumour suppressor gene [400].
Pigv	
Arid1a	

Figure 4.4 Blat search results 100kb either side of insertion site 4a locus

The bold arrow shows the intragenic insertion site in this research in the context of schematically illustrated neighbouring genes. The sites of the other retroviral insertions in the region (from the RTCGD) are illustrated with a vertical line in the row labelled 'retrovirus.'

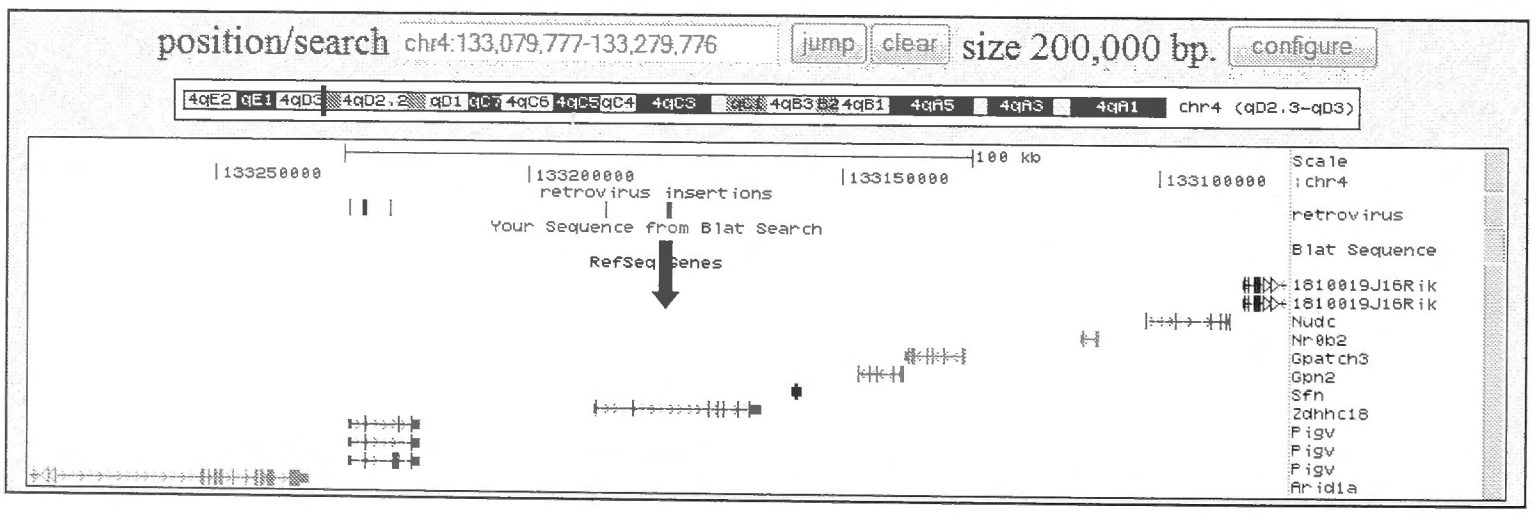

Table 4.10 Genes near insertion site 4b and genes of interest

Genes within 100kb	Genes of interest
Laptm5 *Sdc3* *Matn1*	***Laptm5* (5 insertions in 30kb)** encodes a lysosomal transmembrane protein which appears to have a role in ubiquination [401], but which has not been well characterised. It is initially expressed in embryonal stem cells, and with cell maturation is predominantly expressed in the spleen, thymus, bone marrow and lymph nodes [402]. It was previously called Clast6, E3. It is down regulated on B cell or T cell activation [403] including CD40 ligation and has been shown to be up regulated by retinoic acid in a promyelocyte cell line [404]. During normal B cell maturation *Laptm5* expression is high in the earliest stages, drops during intermediate stages of development, and is again abundantly expressed in mature B cells and B cell lymphomas [405]. Laptm5 enhances degradation of antigen receptors in B and T cells [403,406]. ***Sdc3* (syndecan 3) (5 insertions in 100kb)** deficient mice are characterised by a unique type of muscular dystrophy [407], and polymorphisms have been associated with obesity [408].

Figure 4.5 Blat search results 100kb either side of insertion site 4b locus

The bold arrow shows the intragenic insertion site in this research in the context of schematically illustrated neighbouring genes. The sites of the other retroviral insertions in the region (from the RTCGD) are illustrated with a vertical line in the row labelled 'retrovirus.'

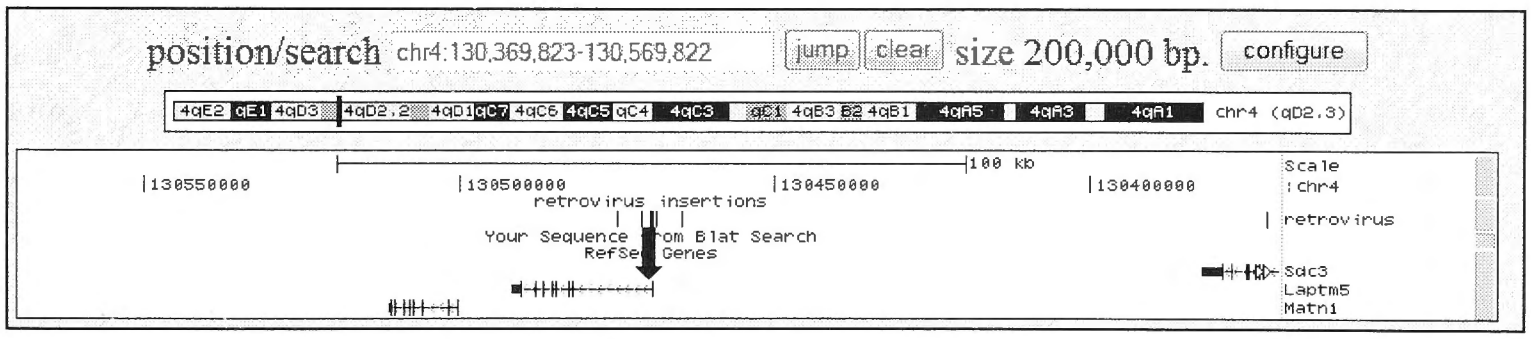

4.4.5 Lymphoma 6

Table 4.11 Genes near insertion site 6b and genes of interest

Genes within 100kb	Genes of interest
Nil	Nil

4.4.6 Lymphoma 7

Table 4.12 Genes near insertion site 7a and genes of interest

Genes within 100kb	Gene of interest
Hivep1	***Hivep1* (human immunodeficiency virus type I enhancer binding protein 1) (2 insertions in 30kb)** There is no published literature linking this gene to malignancy or cell proliferation.

Figure 4.6 Blat search results 100kb either side of insertion site 7a locus

The bold arrow shows the intragenic insertion site in this research in the context of schematically illustrated neighbouring genes. The sites of the other retroviral insertions in the region (from the RTCGD) are illustrated with a vertical line in the row labelled 'retrovirus.'

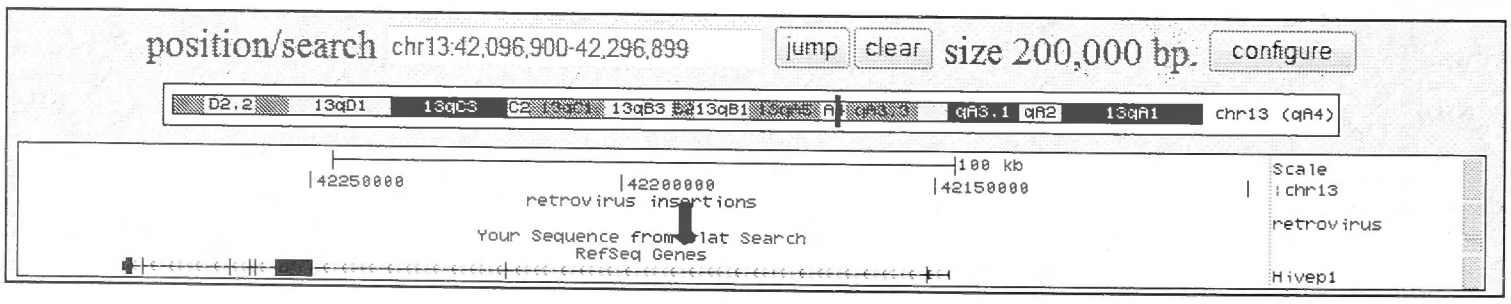

Table 4.13 Genes near insertion site 7b and genes of interest

Genes within 100kb	Genes of interest
BC017612	No gene of interest
Ccdc67	

4.4.7 Lymphoma 8

Table 4.14 Genes near insertion site 8a and genes of interest

Genes within 100kb	Genes of interest
Caprin1 *Lmo2*	***Lmo2* (6 insertions in 100kb)** is widely expressed (particularly in haemopoietic organs) but its precise function is still unclear, although it has been demonstrated to be important in early haemopoiesis [409]. It has two domains and is involved in protein-protein interactions, with LMO2-associated complexes being able to bind DNA and influence gene expression. Enforced expression predisposes to T cell tumours in mice [410]. From a clinical perspective, *LMO2* is dysregulated by nearby integrations of gene-therapy retroviral vectors in multiple cases of T-ALL that developed several years after transplantation of gene-corrected haemopoietic stem cells into children with common gamma chain severe combined immunodeficiency [296]. Breakpoints near the *LMO2* gene have also been demonstrated in spontaneous cases of T cell acute lymphoblastic leukaemias [411]. Expression of *LMO2* is high in germinal centre B cells, and their progeny [412], and its expression in human Diffuse Large B cell Lymphoma has been demonstrated to be associated with prolonged survival [50]. ***Caprin1* (3 insertions in 100kb)** encodes cytoplasmic activation/proliferation-associated protein-1. Knock-down experiments in lymphocyte cell lines have demonstrated that it influences cell division [413]. It has also been shown to be a target of the regulatory miR-16 [414] which has been implicated in the pathogenesis of Chronic lymphocytic leukaemia.

Figure 4.7 Blat search results 100kb either side of insertion site 8a locus

The bold arrow shows the insertion site in this research in the context of schematically illustrated neighbouring genes. The sites of the other retroviral insertions in the region (from the RTCGD) are illustrated with a vertical line in the row labelled 'retrovirus.'

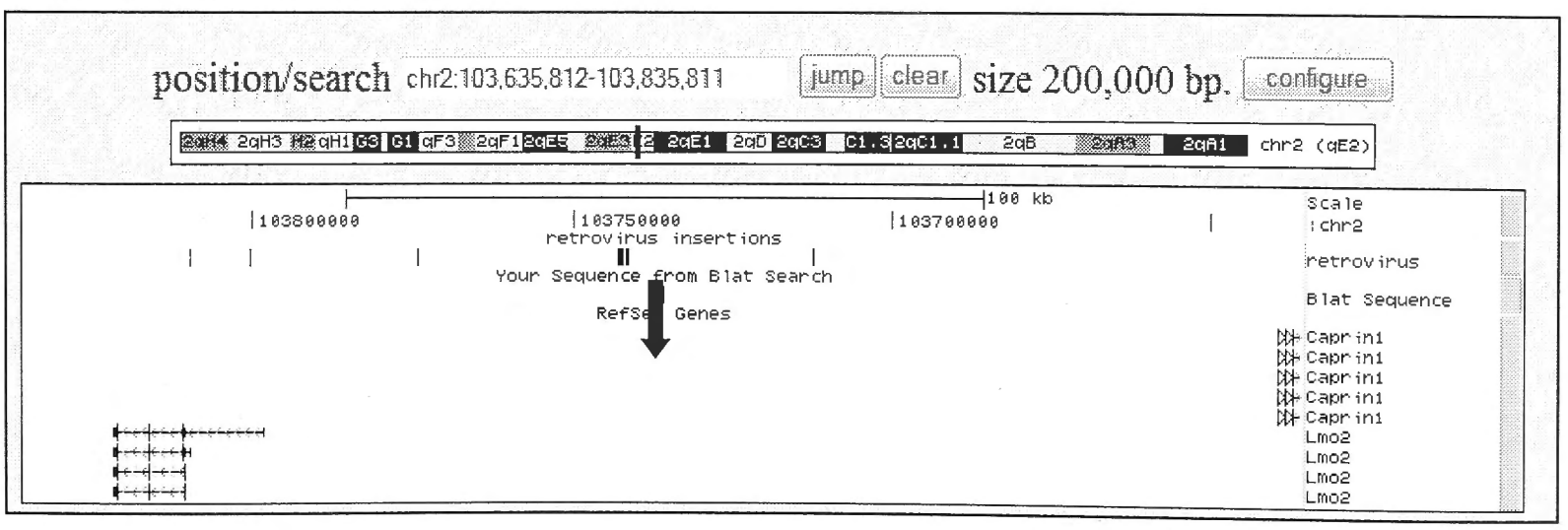

4.4.8 Lymphoma 10

Table 4.15 Genes near insertion site 10a and genes of interest

Genes within 100kb	Genes of interest
Nil	Nil

4.4.9 Lymphoma 11

Table 4.16 Genes near insertion site 11b and genes of interest

Genes within 100kb	Gene of interest
Cd274, *Jak2*, *Insl6*, *Rln1*, *Pdcd1lg2*	***Cd274* (also called PDL1) (3 insertions in 30kb)** is one of the ligands of programmed death-1(PD-1) receptor. This pathway sends inhibitory signals to T cells to modulate their activity in the setting of a chronic antigenic stimulus (reviewed in [415]). The downstream pathways from PD-1 are best characterised in T cells, although this receptor is also expressed on B cells.

Figure 4.8 Blat search results 100kb either side of insertion site 11b locus

The bold arrow shows the intragenic insertion site in this research in the context of schematically illustrated neighbouring genes. The sites of the other retroviral insertions in the region (from the RTCGD) are illustrated with a vertical line in the row labelled 'retrovirus.'

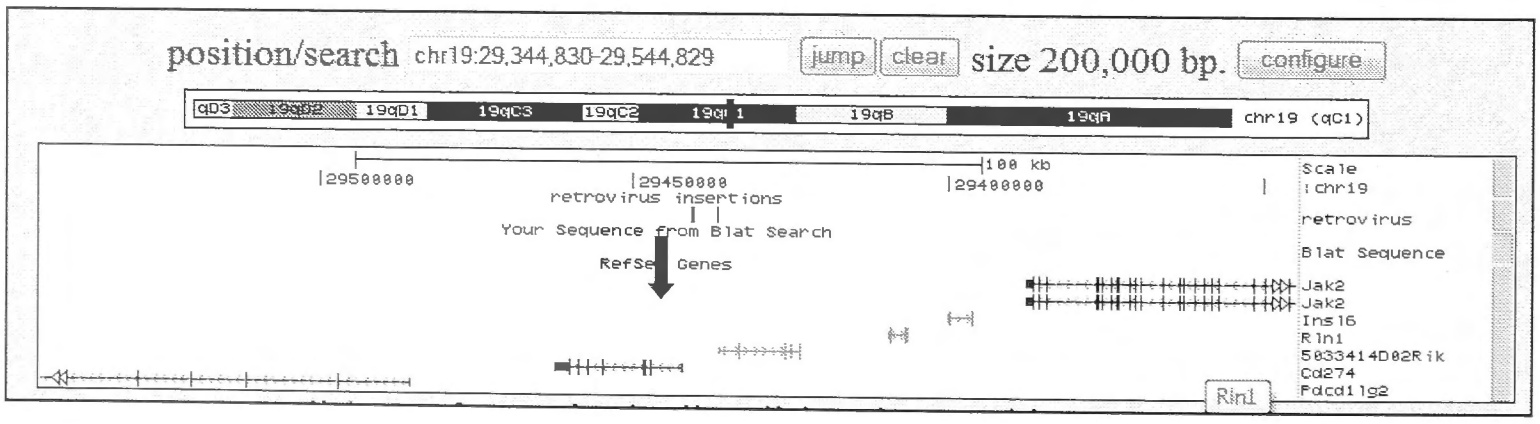

4.4.10 Lymphoma 12

Table 4.17 Genes near insertion site 12a and genes of interest

Genes within 100kb	Genes of interest
Rps17	No gene of interest
Cpeb1	
Pde8a	

Table 4.18 Genes near insertion site 12b and genes of interest

Genes within 100kb		Genes of interest
Lmna	*Rab25*	No gene of interest
Slc25a44	*Robld3*	
Sema4a	*Ubqln4*	
Mex3a	*Ssr2*	

Table 4.19 Genes near insertion site 12c and genes of interest

Genes within 100kb		Genes of interest
Nat15	*Cluap1*	No gene of interest
Olfr15	*Nlrc3*	
Zfp174	*Btbd12*	
Zfp597		

Table 4.20 Genes near insertion site 12d and genes of interest

Genes within 100kb	Gene of interest
Ahi1	***Myb* (63 insertions in 200kb).** This gene is discussed in detail in Section 1.8.
Myb	

Figure 4.9 Blat search results 100kb either side of insertion site 12d locus

The bold arrow shows the intragenic insertion site in *Ahi1* in this research in the context of schematically illustrated neighbouring genes. The sites of the other retroviral insertions in the region (from the RTCGD) are illustrated with a vertical line in the row labelled 'retrovirus.'

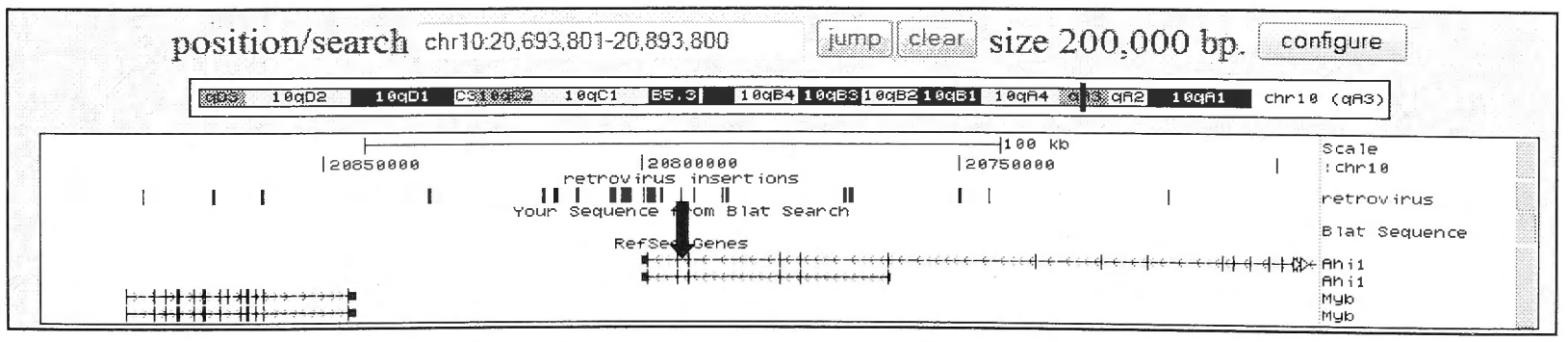

4.4.11 Lymphoma 13

Table 4.21 Genes near insertion site 13a and genes of interest

Genes within 100kb	Gene of interest
Ikbkb *Dkk4* *Polb* *Plat* *Ap3m2*	***Ikbkb,*** despite a lack of retroviral insertions nearby, due to its selective expression in haemopoietic cells, particularly lymphocytes and its known pivotal role in the NF-κB pathway this has been designated as a gene of interest. *Ikbkb* encodes a protein product called inhibitor of kappaB kinase beta (abbreviated as Ikbkb, IKKβ, IKK-B, or IKK2 in scientific literature). Ikbkb forms a part of the IκB kinase complex in conjunction with IKKα and IKKγ (NEMO). The critical nature of this pathway in normal B cell function and differentiation is discussed in Section 1.4.2, and its role in B cell lymphoma is discussed in Section 1.5.6.

Figure 4.10 Blat search results 100kb either side of insertion site 13a locus

The bold arrow shows the insertion site in this research in the context of schematically illustrated neighbouring genes. The sites of the other retroviral insertions in the region (from the RTCGD) are illustrated with a vertical line in the row labelled 'retrovirus.'

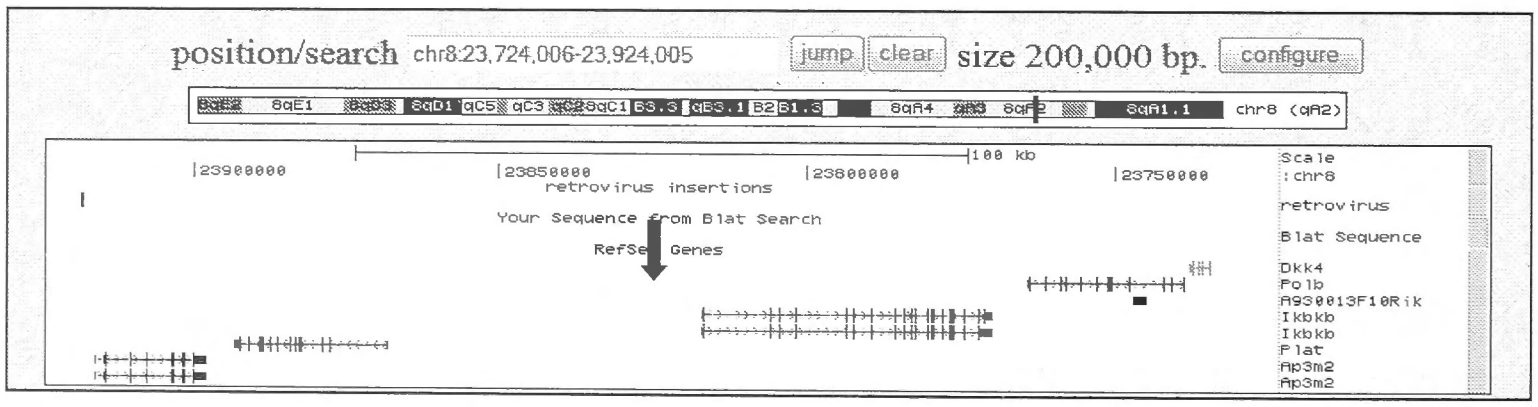

Table 4.22 Genes near insertion site 13b and genes of interest

Genes within 100kb		Genes of interest
Txnip	*Lix1l*	No gene of interest
Hfe2	*Rbm8a*	
Polr3gl	*Pex11b*	
Ankrd34a		

4.4.12 Lymphoma 14

Table 4.23 Genes near insertion site 14a and genes of interest

Genes within 100kb	Genes of interest
Elovl6	No gene of interest

Table 4.24 Genes near insertion site 14b and genes of interest

Genes within 100kb		Genes of interest
Plcb2	*Pak6*	No gene of interest
Gm1337	*Phgr1*	
Bub1b	*Disp2*	

4.4.13 Lymphoma 15

Table 4.25 Genes near insertion site 15a and genes of interest

Genes within 100kb	Genes of interest
Gnptab, Sycp3, Dram1, Chpt1	No gene of interest

Table 4.26 Genes near insertion site 15b and genes of interest

Genes within 100kb	Genes of interest
Ubxn11 Ccdc21 Sh3bgrl3 Aim1l Cd52	***Cd52* (7 insertions in 100kb)** is expressed on the surface of B and T lymphocytes and in the male genital tract. Its role in lymphocytes is poorly defined, although it is a target for the monoclonal antibody alemtuzumab. ***Ubxn11* (also called *Ubxd5*) (7 insertions in 100kb)** encodes Colon Antigen 1 which has been demonstrated to elicit a T cell response in colorectal patients with metastatic disease [416], but the function of this gene remains unclear.

Figure 4.11 Blat search results 100kb either side of insertion site 15b locus

The bold arrow shows the intragenic (in *Ubxn11*) insertion site in this research in the context of schematically illustrated neighbouring genes. The sites of the other retroviral insertions in the region (from the RTCGD) are illustrated with a vertical line in the row labelled 'retrovirus.'

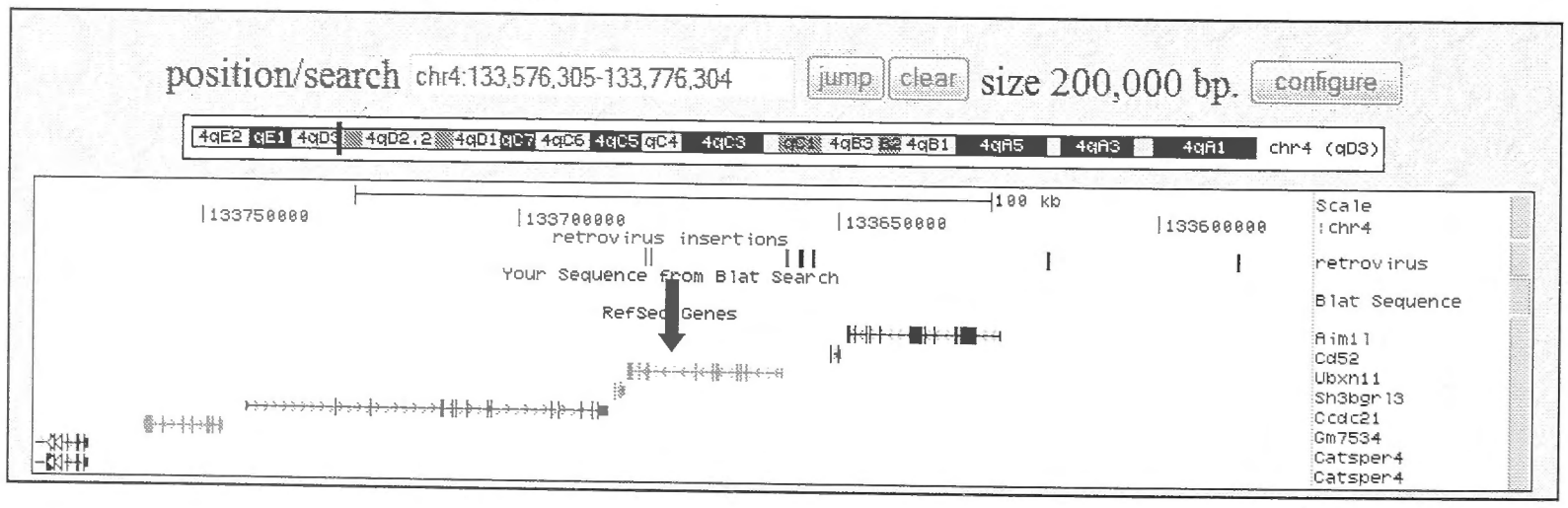

Table 4.27 Genes near insertion site 15d and genes of interest

Genes within 100kb	Genes of interest
Sh3bp5 Capn7 Dnahc1 Mettl6	No gene of interest

4.4.14 Lymphoma 16

Table 4.28 Genes near insertion site 16a and genes of interest

Gene within 100kb	Genes of interest
Tns3	No gene of interest

Table 4.29 Genes near insertion site 16b and genes of interest

Gene within 100kb	Genes of interest
Tgfbr2	No gene of interest

4.4.15 Lymphoma 17

Table 4.30 Genes near insertion site 17a and genes of interest

Genes within 100kb		Genes of interest
Tnip1	*Gpx3*	No gene of interest
Lyrm7	*Anxa6*	
Hint1	*Ccdc69*	

Table 4.31 Genes near insertion site 17b and genes of interest

Genes within 100kb	Genes of interest
B4galt5	No genes of interest
Slc9a8	
Spata2	

Table 4.32 Genes near insertion site 17c and genes of interest

Gene within 100kb	Genes of interest
Nil	No gene of interest

4.4.16 Lymphoma 18

Table 4.33 Genes near insertion site 16b and genes of interest

Gene within 100kb		Genes of interest
Dgkz	*Mdk*	No gene of interest
Ambra1	*Creb3l1*	
Chrm4		

4.4.17 Lymphoma 19

Table 4.34 Genes near insertion site 19a and genes of interest

Gene within 100kb	Genes of interest
Ppp3ca	No gene of interest

Table 4.35 Genes near insertion site 19b and genes of interest

Gene within 100kb			Genes of interest
Siglec15	*Slc14a1*	*Slc14a2*	No gene of interest

Table 4.36 Genes near insertion site 19c and genes of interest

Gene within 100kb		Genes of interest
Mrps21	*Gm129*	No gene of interest
Aph1a	*Car14*	
Anp32e	*Plekho*	
Vps45		

Table 4.37 Genes near insertion site 19d and genes of interest

Gene within 100kb			Genes of interest
Dnajb9	*Pnpla8*	*Nrcam*	No gene of interest

Table 4.38 Genes near insertion site 19e and genes of interest

Gene within 100kb		Genes of interest
Katnal1	*Hmgb1*	No genes of interest

4.4.18 Lymphoma 20

Table 4.39 Genes near insertion site 20a and genes of interest

Gene within 100kb		Gene of interest
Gng7	*Slc39a3*	*Gng7* because another unique integration site has been identified in this gene in this small number of lymphoma samples. The significance of this gene is expanded in thia chapter's discussion.
Tmprss9	*Sgta*	
Timm13	*Thop1*	
Gadd45b	*Creb3l3*	
Diras1	*Lmnb2*	

Figure 4.12 Blat search results 100kb either side of insertion site 20a locus

The bold arrows show the two intragenic insertion sites in this research in the context of schematically illustrated neighbouring genes. The sites of the other retroviral insertions in the region (from the RTCGD) are illustrated with a vertical line in the row labelled 'retrovirus.'

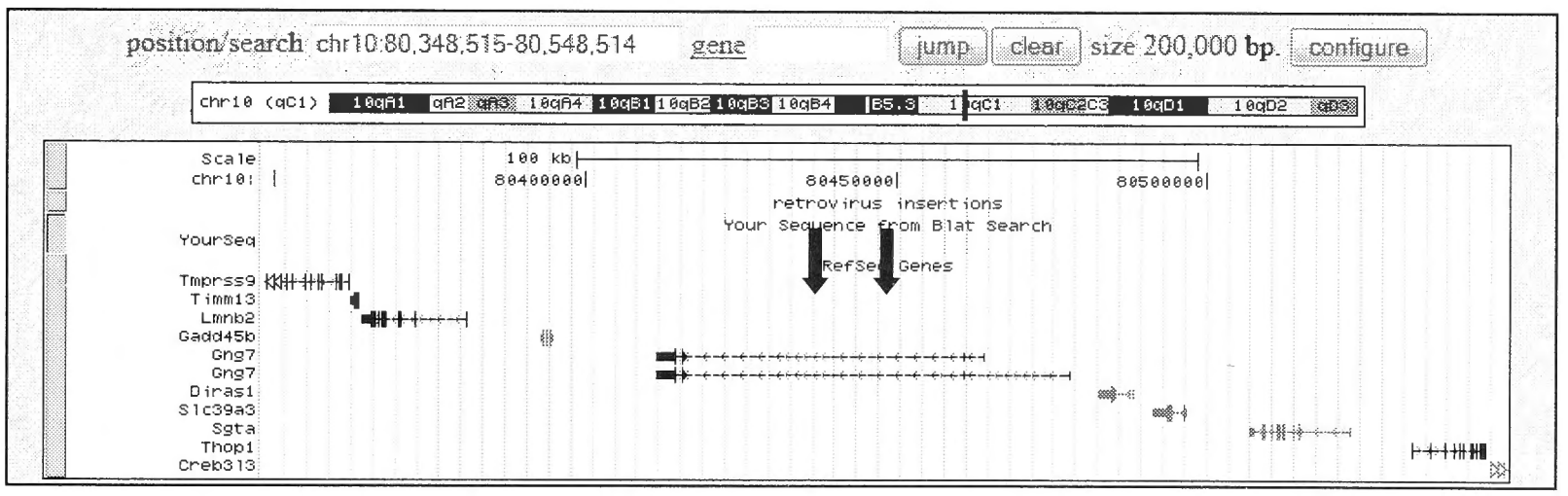

Table 4.40 Genes near insertion site 20b and genes of interest

Gene within 100kb	Genes of interest
Mbnl1	No gene of interest

Table 4.41 Genes near insertion site 20c and genes of interest

Genes within 100kb		Genes of interest
Lta	*H2-D1*	***Lta, Ltb*** and ***Tnf*** **(5 insertions in 100kb).** This integration site is also of interest as it is near (less than 100kb away from some of the genes) the site of the histocompatibility locus genes.
NF-κB il1	*Ly6g5b*	
Bat4	*Csnk2b*	
Bat3	*Gpank1*	***Tnf*** **(**tumour necrosis factor superfamily, member 2) encodes the pro-inflammatory cytokine TNFα which is mainly produced by macrophages, and has a broad spectrum of activities including cellular survival, proliferation and differentiation. TNF can activate a plethora of downstream pathways including the NF-κB pathway, MAPK pathway and death signalling pathways. It frequently acts in concert with other cytokines. *Tnf* single nuclear polymorphisms have been associated with increased risk of lymphoma [417]
Bat2	*Apom*	
Atp6v1g2	*Bag6*	
Bat1a	*Prrc2a*	
Aif1	*Lst1*	
Ltb	*Tnf*	***Lta*** **(**lymphotoxin alpha (TNF superfamily, member 1) gene) produces lymphotoxin b which is also known as TNFβ. It is overexpressed in Burkitt lymphoma cell lines and B lymphoblasts. Lta is produced by lymphocytes and has a role in inflammation, lymphoid organ development, B cell stimulation and inhibition of tumour angiogenesis.
Ddx39b		***Ltb*** **(**lymphotoxin beta (TNF superfamily, member 3) is overexpressed in the above lines and also in T cells and B cells in addition to tonsil, lymph node and thymus (but not bone marrow). It anchors Lta to the cell surface. Ltb is important for early lymphoid organogenesis.

Figure 4.13 Blat search results 100kb either side of insertion site 20c locus

The bold arrow shows the insertion site in this research in the context of schematically illustrated neighbouring genes. The sites of the other retroviral insertions in the region (from the RTCGD) are illustrated with a vertical line in the row labelled 'retrovirus.'

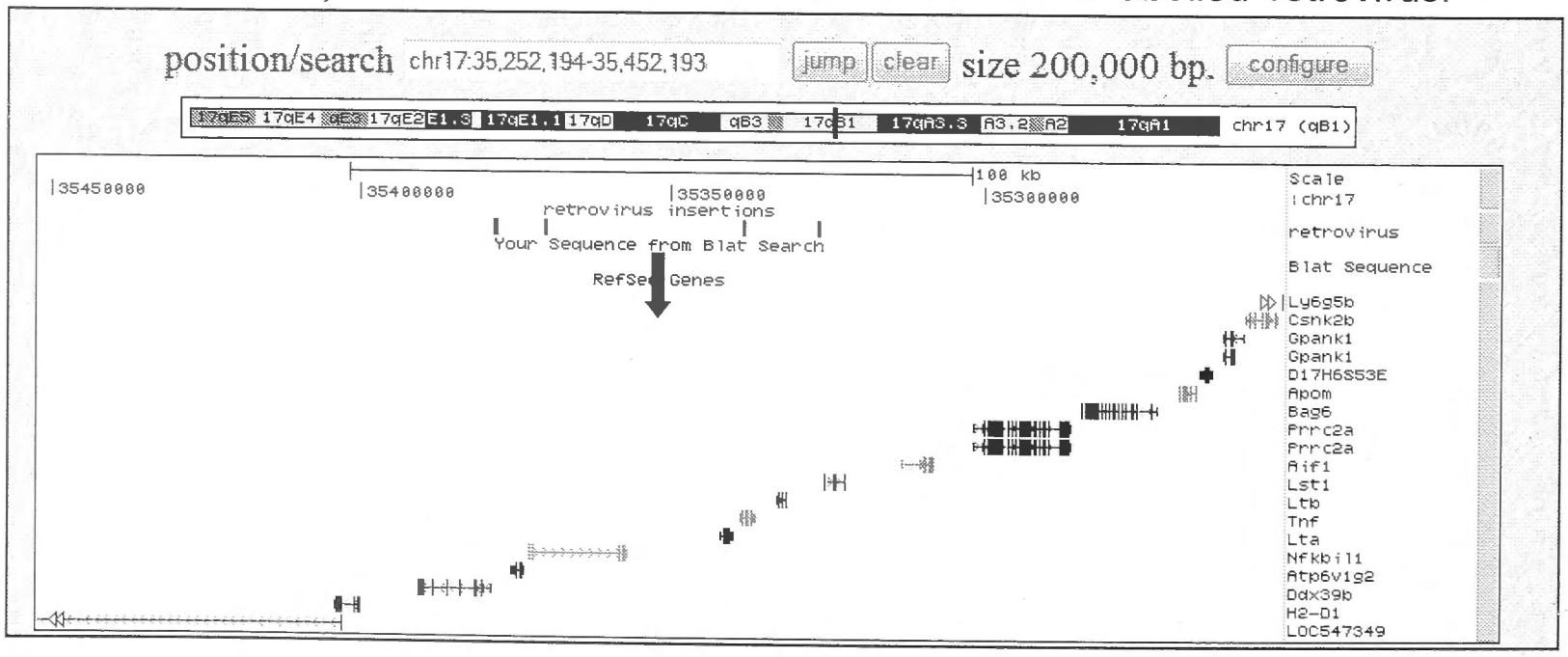

Table 4.42 Genes near insertion site 20d and genes of interest

Gene within 100kb	Genes of interest
Cog6	No gene of interest

4.4.19 Lymphoma 22

Table 4.43 Genes near insertion site 22c and genes of interest

Gene within 100kb	Genes of interest
Pds5a *N4bp2*	No gene of interest

4.4.20 Lymphoma 23

Table 4.44 Genes near insertion site 23a and genes of interest

Gene within 100kb	Genes of interest
nil	No gene of interest

Table 4.45 Genes near insertion site 23c and genes of interest

Gene within 100kb	Genes of interest
Wdr26 *Nvl* *Cnih4*	No gene of interest

4.4.21 Lymphoma 24

Table 4.46 Genes near insertion site 24a and genes of interest

Gene within 100kb	Gene of interest
Tceb3 *Fuca1* *Hmgcl* *Lypla2* *Rpl11* *Gale* *(Id3 just beyond 100kb)*	***Id3* (inhibitor of DNA binding 3) (8 insertions in 50kb)** encodes a dominant negative helix loop helix protein that can bind to members of the basic helix loop helix family of transcription factors, inhibiting their activity [418]. It has been found to function as an E protein antagonist, E protein transcription factors being critical for αβ T cell development. Id3 is also a modulatory factor in γδ T cell development, although the mechanism remains to be well clarified [419]. Interestingly, mice with deleted *Id3* develop an aggressive lymphoma resembling human hepatosplenic γδ T cell lymphoma [420]. More recently its deletion has been demonstrated to impair the production of T regulatory cells and promote the development of TH17 cells [421]. Less has been published regarding its role in B cell maturation and proliferation, although it has been shown to inhibit B cell development [422]. Most importantly, *Id3* inactivating mutations have been discovered to be very frequent in Burkitt lymphoma [5].

Figure 4.14 Blat search results 100kb either side of insertion site 24a locus

The bold arrow shows the insertion site in this research in the context of schematically illustrated neighbouring genes. The sites of the other retroviral insertions in the region (from the RTCGD) are illustrated with a vertical line in the row labelled 'retrovirus.'

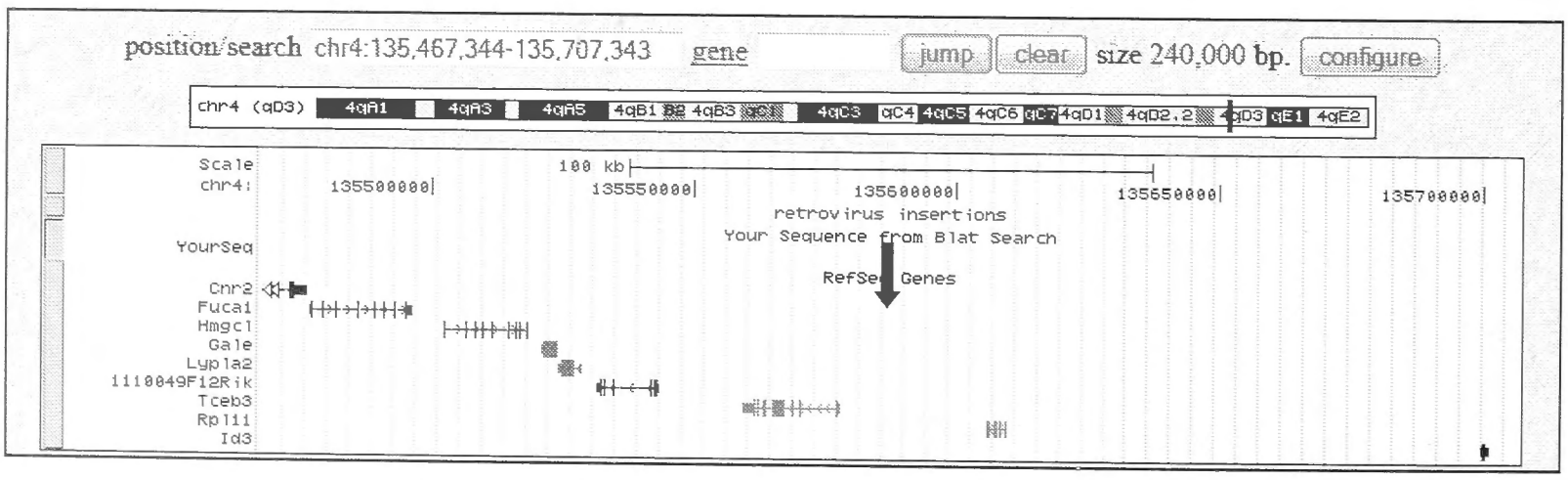

Table 4.47 Genes near insertion site 24b and genes of interest

Gene within 100kb					Genes of interest
Trpv2	*Pigl*	*Cenpv*	*Ubb*	*Mmgt2*	No gene of interest

Table 4.48 Genes near insertion site 24c and genes of interest

Gene within 100kb	Gene of interest
Batf *Jdp2* *Mfsd7c*	***Batf* (4 insertions in 50kb)** encodes basic leucine zipper transcription factor, ATF-like, which is highly expressed in haemopoietic cells. It has increased expression in T helper cells compared to other T cell subsets, with knockout mice demonstrating defective differentiation of IL-17-producing T helper cells [423]. Interestingly, a small study by Lorenzo et al [424] demonstrated that the expression of *Batf* discriminates between normal individuals, those with a history of Burkitt Lymphoma, and the latter who have had a secondary malignancy, however the significance of these findings remains unclear.

Figure 4.15 Blat search results 100kb either side of insertion site 24c locus

The arrow shows the intragenic insertion site in this research in the context of schematically illustrated neighbouring genes. The sites of the other retroviral insertions in the region (from the RTCGD) are illustrated with a vertical line in the row labelled 'retrovirus.'

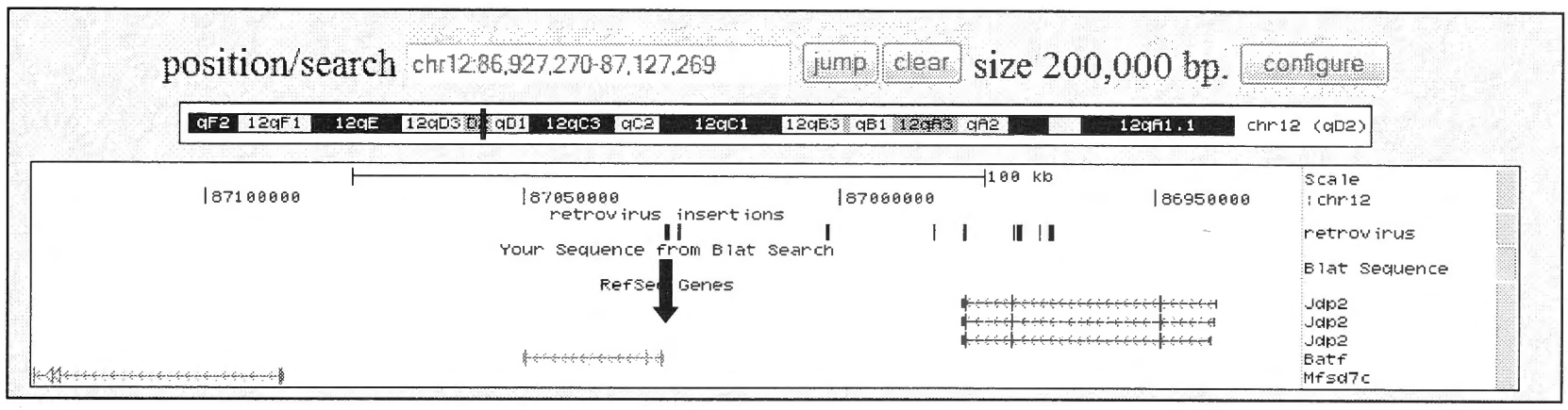

4.4.22 Candidate oncogenes within common retroviral integration sites

Based on the combined incidence of integrations in RTCGD and the sites identified in this work, many of the unique integration sites fulfilled the classification of recurrent sites of integration and the genes in these locations were either known oncogenes or established regulators of B cells (Table 4.49). Among the best known oncogenes at these sites were *Myb* (Section 4.4.10) and *Lmo2* (Section 4.4.7), both of which are well known for being dysregulated by nearby proviral insertions. A number of the genes at these recurrent sites of integration affect the same process or pathway, notably G-protein signalling for chemotaxis, TGFβ signalling (an important anti-proliferative signal in B cells), and NF-κB signalling (a major growth pathway in normal and neoplastic B cells). *Laptm5* is one such gene (Section 4.4.4) shown to negatively regulate antigen receptor expression and signalling in B cells and T cells [403,406]. In addition, one of the integrations was immediately adjacent to *Ikbkb*, encoding a key kinase activating the NF-κB pathway, although recurrent integrations near *Ikbkb* were not found in RTCGD (Section 4.4.11).

Table 4.49 Candidate oncogenes within common integration sites

Many oncogenes, proto-oncogenes and B cell regulators are located within regions fulfilling the definition of a common integration site (using the combined incidence of integrations in RTCGD and the sites identified in this work). Based on our experimental findings, the number of retroviral insertions in the region and the published literature the most important genes within approximately 100kb of our retroviral insertion sites are summarised below.

Candidate oncogene	Retroviral insertions /window	Candidate process	Known functions of candidate oncogene
Myb	63/200kb	Anti-differentiation	Inhibition of differentiation, proliferation, similar to *Lmo2* and *Id3*
Lmo2	6/100kb	Anti-differentiation	Inhibition of differentiation, inhibition of E-box basic helix-loop-helix transcription
Id3	8/50kb; 11/200kb	Anti-differentiation	Inhibition of differentiation, inhibition of E-box basic helix-loop-helix transcription, S-phase induction
Nfic	5/30kb	DNA replication	DNA replication, transcription
Zdhhc18	5/100kb	G proteins & chemotaxis	Palmitoyl transferase, heterotrimeric G protein signalling, ras/rho signalling, proliferation
Gng7	3/50kb	G proteins & chemotaxis	Heterotrimeric G protein signals, chemotaxis, growth
Ltb/Lta	5/100kb	NF-κB signals	Lymphotoxin, autocrine growth factor, NF-κB signalling
Hivep1	2/30kb	NF-κB , TGFβ response	Pim complementation group, NF-κB signalling, TGFβ response
Laptm5	5/30kb	TGFβ response	TGFβ response

4.5 Discussion

The results in this chapter provide suggestive evidence for enrichment of proto-oncogenes or tumour suppressor genes flanking the retroviral integration sites. A higher than expected percentage of nearby flanking genes corresponded to "other genes possibly implicated in cancer" in the Atlas of Genetics and Cytogenetics in Oncology and Haematology. A high fraction of identified integration sites were in recurrent sites of proviral integration in a database of these sites identified in a variety of retrovirus induced lymphomas and other cancers, although it was not possible to determine if the fraction of CIS near the identified insertions was greater than expected by chance. Review of the function of genes flanking these insertion sites identified a number of known proto-oncogenes, a significant proportion of which are known to be dysregulated in haemopoietic malignancies.

These features are consistent with the possibility that the transformed *MYC/GFP*+ *Trp53*-mutant B cells had acquired their neoplastic phenotype as a consequence of their retroviral integration serving as a third mutagenic hit, the retroviral promoter and enhancer elements facilitating dysregulation of adjacent pro-oncogenes, precipitating the development of lymphoma. While the results are consistent with this possibility, they are equally compatible with a null hypothesis that the integration sites play no role in transformation and are selected simply as preferred retroviral integration sites or permissive loci for high *MYC/GFP* proviral expression. In the remainder of this discussion I will consider some of the best candidates for flanking proto-oncogenes that may have been activated by the integrated provirus. In the next chapter, I tested this hypothesis experimentally by deliberately introducing a dysregulated version of the flanking gene as a third mutagenic hit.

The list of potential co-operating genes cannot be neatly categorised into a specific function or cellular pathway. This may be because the integration sites identified only represent a fraction of those present and the majority may represent 'passenger' mutations. It is not possible to ascertain whether retroviral integrations cause gain or loss of function in this model. It has been

assumed that the genes identified were potentially overexpressed due to their proximity to the retroviral promoter or enhancer, but there may be instances where the identified gene is in fact down regulated or even mutated as a consequence of the retroviral integration. The broad association of potential co-operating genes with pathways that have recently been shown to be dysregulated in Burkitt lymphoma (as detailed in Section 1.12) was thus of interest. Candidate oncogenes within common integration sites listed in Table 4.49 and their products have been underlined in the discussion below to emphasize the relationship of the discussion to our research results.

Recent publications [5,14] have highlighted the importance of the PI3K pathway in the pathogenesis of Burkitt Lymphoma. ID3, the negative regulator of TCF3, has been recently reported [5,425,426] to be recurrently mutated in Burkitt lymphoma, enhancing the activity of B cell receptor signalling through the PI3K pathway and promoting cell proliferation. Suppression of the NF-κB pathway has also been recently characterised in Burkitt lymphoma, as discussed in Section 1.12. Despite not being found in a common retroviral integration site in the RTCGD, Ikbkb was of interest due to its key role in the NF-κB pathway. Lta and other tumour necrosis factor-related cytokines stimulate the NF-κB pathway (reviewed in [427]), and both lymphotoxins have been shown to be NF-κB target genes in lymphocytes [428,429].

Myb has been demonstrated to be critical to the development and maintenance of follicular B cells [271], the authors of this research suggesting that this mechanism may be through modulation of B cell receptor signalling. Lauder et al [430] reviewed the role of Myb in T cell activation and survival, finding that PI3K and its effector molecular AKT are activated by the interleukin 2 receptor and that Myb is a downstream effector of this pathway, helping to protect cells from apoptosis. In contrast Watanabe et al [431] found that miRNA-150 (a potent suppressor of Myb) overexpression in NK/T-cell lymphoma cells resulted in reduced levels of phosphorylated AKT. It is tempting to speculate that an analogous link between Myb and the PI3K pathway is found in B cells. Thomas et al [271] showed that Myb-deficient mature B cells have normal proliferation but increased apoptosis with some preliminary data supporting aberrant B cell receptor signalling in these mutant mice.

With regards to the significance of MYB in Burkitt lymphoma, recent findings (Louis Staudt personal communication) confirm that *MYB* is consistently overexpressed in Burkitt lymphoma compared to DLBCL. *MYB* silencing has been shown to reduce proliferation and increase apoptosis in a Burkitt lymphoma cell line [432,433].

Other potentially co-operating genes are difficult to assign to a specific pathway. *Gng7* is such an example, its second intron being a recurrent integration site in two separate experimentally induced lymphomas (Table 4.1). In addition to this, Hummel et al [199] and more recent research (Louis Staudt personal communication) found that it was differentially expressed in Burkitt lymphoma. The full name of this gene is guanine nucleotide binding protein (G protein), gamma 7 and it is one of the twelve known members of the gamma subunit family. These subunits combine with alpha and beta subunits to form heterotrimeric G-proteins which transduce receptor signals across the cell membrane, activating downstream signalling pathways. The only publication regarding this protein in mice [434] reports that knockout mice had behavioural changes associated with altered focal regulation of cerebral adenylyl cyclase activity. Two publications specifically relating to the human gene in the setting of solid tumours demonstrate reduced expression of this protein in pancreatic malignancies [435] compared to normal pancreas and that low *Gng7* expression was associated with poorer survival in oesophageal cancer [436]. An interesting recent publication [437] looked at homozygous deletions in Hodgkin Lymphoma cell lines using array-Comparative Genomic Hybridisation. *Gng7* was one of 7 potential new tumour suppressor genes identified in this publication. The significance of this gene was not further pursued experimentally due to time and resource limitations and the absence of substantial literature to support its role in B cell lymphoma at the time. Its role as a tumour suppressor gene is of particular interest from the literature and as both retroviral insertions were intragenic and may have caused haploinsufficiency, contributing to lymphomagenesis. This could not be pursued with the current research model which focuses on potential proto-oncogenes but models such as those using short hairpin RNA suppression, gene sequencing looking for mutations or promoter methylation pattern differences in

normal and lymphomatous tissue may have been helpful to try to further define this gene's role.

Lmo2 was another gene of interest, but its role in B cell homeostasis and neoplasia remains to be clearly elucidated. It is within a common retroviral insertion site and is reviewed in Section 4.4.7. *LMO2* is known to be overexpressed in germinal centre lymphocytes and germinal centre-type DLBCL but surprisingly its expression is markedly suppressed in Burkitt lymphoma [344,438]. Recent work by Cubedo et al [439] did not implicate MYC or p53 in the LMO2 interactome.

Laptm5 is another gene of interest, although its role in B cell lymphoproliferative disorders is still being defined. Its normal role in B cells is reviewed in Section 4.4.4. There is no literature to date regarding the relationship between this gene and MYC, p53 or Burkitt lymphoma.

There was not an absolute correspondence between the bands sequenced and distinct integration sites identified for several reasons. On some occasions the sequence corresponded to internal vector sequences only (the splinkerette method uses primers that anneal to both of the viral long terminal repeats and a restriction enzyme cleavage site so some of the sequences obtained will be internal viral sequences without crossing the viral-DNA junction), at other times the sequence was not able to be matched with confidence to the murine genome and on other occasions the same sequence was evident from distinct bands within the same lymphoma, presumably due variable restriction enzyme cleavage. The most common reason, however, for this discrepancy was cross-contamination, where that the exact insertion site had been previously identified in a distinct lymphoma. This is most likely to reflect PCR product contamination of DNA despite physical separation of the different stages of the DNA extraction and PCR reactions. Despite this, most samples contain multiple other unique bands, and further analysis was still possible.

Technical issues aside, there are several reasons why results are not definitive. The splinkerette method of identification of retroviral insertion sites is likely to significantly underestimate the number of insertion sites, with more recent

methods commonly identifying approximately 20 retroviral insertion sites per tumour [313,384], while this analysis detected an average of 1.9 unique insertion sites per lymphoma (and this difference will reflect the use here of a single round of transduction with a replication defective vector). It is thus possible that genes dysregulated as a consequence of several retroviral sites within the same B cell may co-operate and facilitate transformation or that key genes have been overlooked. While the identification of common integration sites could suggest selection for integration sites that activate nearby oncogenes or inactivate tumour suppressor genes and thus potentiate neoplasia, the biased propensity for retroviruses to insert into certain niches within the genome could also contribute to this enrichment. In addition, while the analysis using the Atlas of Genetics helped to strengthen the argument, this database accepts contributions from external sources, which are reviewed by the editorial board. The precise definition of these two categories of cancer genes is not listed on the website, nor in the group's publications, and is likely to reflect to some degree the individual interests of contributing authors rather than an objective review of the literature. Most of the data in this database, however, is not from retroviral experiments.

Review of the retroviral insertion sites on the USCS browser does not thoroughly map the sites of microRNA genes. The location of the insertion sites was thus correlated with the genomic location of the known microRNA gene as detailed in the Sanger miRBase microRNA database Release 13.0 March 2009 [440](http://microrna.sanger.ac.uk). One insertion site was located within 100 kb of a known microRNA gene. The insertion site was localised to chromosome 3:88314504-88314699 and MI0008315 mmu-mir-1905 is on the same chromosome at 88340223-88340304, ie approximately 25kb away. This microRNA was identified by He et al [441] by screening non-protein coding RNAs for conservation between mouse and rat and a sequence encoding a hair pin structure, its expression subsequently being confirmed by microarray. In this article, prior to being allocated a name, the predicted miRNA is called Nmir_027. As yet there have been no further publications about this microRNA, so its function remains uncertain.

The concept of the key role of the retroviral insertion site in the transformation process is not necessarily at odds with the hypothesis at the conclusion of Chapter 3 that the intensity of *MYC/GFP* proviral expression was likely to determine if a cell was transformed. Four of the genes that were adjacent to a *MYC/GFP* provirus integration site in the set of lymphomas were selected for further study: *Myb*, *Ikbkb*, *Lmo2* and *Laptm5*. The number of genes was capped due to time and resource limitations. The biological significance of the retroviral insertion site was tested in Chapter 5 by dysregulating these proto-oncogenes under the control of a retroviral LTR in conjunction with *MYC* overexpression to determine if this facilitated B cell transformation.

5. Results: Testing the 'Third Hit' Hypothesis

5.1 Introduction

The experiments in Chapter 3 established an efficient experimental system to induce malignant transformation by a single round of retroviral mutagenesis in a finite number of mature B cells. It was noted that proviral *GFP* expression in the malignant B cells was higher than in the majority of transferred B cells, raising the possibility that malignancy was associated with selection of rare B cells where the proviral GFP and MYC proteins were highly expressed.

The question of selection of B cells in the resulting malignancies was investigated in Chapter 4, where the number and sites of proviral integration in each lymphoma were analysed. These studies revealed that the lymphomas were mono- or oligo-clonal with only a few detectable proviral integration sites. Therefore strong selection for rare clones of B cells appeared to underlie formation of the malignant lymphomas, since more than 100,000 proviral *MYC/GFP*-expressing B cells were transferred into each recipient mouse yet only one or several of these had typically grown out as a lymphoma over the ensuing 5-8 weeks. A substantial proportion of the proviral integration sites in the lymphomas corresponded to sites of recurrent proviral integration in a large database of retrovirus-induced tumours. Among these were proviruses that had integrated near the promoters of lymphoid proto-oncogenes such as *Myb* and *Lmo2* that are well known for being activated by retroviral integrations in other mouse models and in human gene therapy trials. These results raised the possibility that the rare clones of *MYC/GFP* transduced *Trp53*$^{Bbl/Bbl}$ B cells that underwent malignant transformation did so because the strong retroviral enhancer dysregulated the expression of a nearby proto-oncogene, providing a third mutagenic "hit" needed for spontaneous growth of the B cell clone.

The hypothesis tested in this chapter was that dysregulated expression of *Myb, Lmo2, Laptm5* or *Ikbkb*, caused by the strong enhancer/promoter of the retrovirus, would be sufficient to promote growth of mature B cells in concert with *MYC* overexpression and *Trp53* inactivation. To create an experimental setting where a large number of *MYC/GFP* transduced *Trp53*$^{Bbl/Bbl}$ B cells also had retrovirally dysregulated *Myb, Lmo2, Laptm5* or *Ikbkb,* cDNAs (derived from

normal murine spleen) encoding each of these proteins were engineered into a separate retrovirus expression vector based on the pMXs-IG backbone from the Kitamura [377] laboratory but replacing the *GFP* sequence with a *DsRed* sequence (see Figure 2.1 for vector maps). Like the M*YC/GFP* vector, these vectors were also bicistronic and replication defective. Thus, the experimental strategy was to co-transduce mature *Trp53*$^{Bbl/Bbl}$ B cells with the *MYC/GFP* vector and independently integrated vectors encoding *Myb/DsRed*, *Lmo2-DsRed, Laptm5-DsRed* or *Ikbkb-DsRed*. If any of the latter were sufficient to transform mature B cells into spontaneous growth, in concert with *MYC* dysregulation and *Trp53* mutation, then the majority of doubly-transduced B cells should proliferate spontaneously, as opposed to the one singly-transduced B cell in two hundred thousand that grew out in vivo (Chapter 3). The results below show that this appears to be the case for *Myb*, whereas *Lmo2, Laptm5* and *Ikbkb* were an insufficient 'third hit'.

In designing an assay to measure co-operation between mutations in *Trp53*, *MYC* and a third retrovirus-borne gene for B cell growth in the absence of the normal exogenous growth factors, a key consideration was whether to test the effects of the three mutations after adoptive transfer in vivo or immediately following transduction in tissue culture. The advantage of the in vivo assay was that it would employ the conditions that had been used to identify the candidate co-operating third hits. The disadvantage of the in vivo assay was the logistical difficulty of obtaining the large numbers of cells per mouse necessary to track the growth of doubly-transduced cells after transfer, the loss of most of the injected cells shortly after injection, the outgrowth of rare clones of singly MYC-transduced p53-mutant cells over time, and the ethical issues of potentially inducing lymphoma in large numbers of mice when it could be replaced by a tissue culture alternative. Each of these limitations could be overcome by analysing the growth of small numbers of doubly transduced B cells in tissue culture, and hence the latter approach was pursued as a first step. Analysis in vitro would also allow accurate analysis of the effects of the individual and combined mutations to be measured on other growth-factor governed processes that precede cell proliferation or death.

5.2 Measuring single and double-transduced B cells

Splenic B cells were activated into cell cycle by exposure to antigen (HEL) in vivo prior to harvest from the mice (Day 0) and stimulated in culture for 24-36 hours with CD40 antibody. They were subsequently transduced with the various retroviral vectors (Day1). After transduction, the B cells were cultured in RPMI complete medium without additional growth factors. Normal B cells are absolutely dependent for their metabolism and nutrient uptake upon receipt of exogenous growth and survival stimuli through receptors including BCR, CD40, BAFFR or TLR. Absence of these stimuli, by culturing B cells in RPMI without any of these factors, precipitates autophagy, gradual decrease in cell size, and subsequently apoptosis. Flow cytometry was performed when removing anti-CD40 (Day 3), and at various time points after withdrawal of growth stimuli (Figure 5.5, Days 7, 11, 15). A schematic of the experimental approach is shown in Figure 5.1.

Using the two retroviral systems, cells expressing each vector could be independently visualised using FACS. The *GFP* expression vector was detected in the FL1 channel and the *DsRed* expression vector in the FL2 channel of the four channel BD FACS Calibur™ without the addition of further fluorochromes (Figure 5.2). Gate positions were determined by the simultaneous analysis of cultures that were singly transduced or not transduced as negative controls. The labelling of the various gated regions is shown in Figure 5.3.

The percentage of transduced B cells varied according to the cDNA that was introduced upstream of the IRES:DsRed element in the vector (Figure 5.4), with much lower percentage of DsRed positive cells obtained when the vector contained either *Myb* or *Ikbkb* cDNA inserts. With the latter two inserts, it was also observed that the intensity of DsRed fluorescence among DsRed positive B cells was shifted to lower levels closer to the cell autofluorescence background (data not shown). The lengths of the different inserts were: *Myb*

2290 bp, *Ikbkb* 2469 bp, *Laptm5* 2402 bp, *LMO2* 1779 bp, with the DsRed empty vector having no insert. Consequently there appeared to be no direct correlation between the length of the insert and the transduction efficacy of either vector (Figure 5.4). Modifications of the volumes of the retroviral supernatant added prior to spinoculation also failed to significantly alter the transduction efficiency. One possibility is that each cDNA sequence creates a unique secondary structure in the transcribed vector RNA, influencing the efficiency of recognition of the packaging sequence 5' to the cDNA insert and hence the efficiency of packaging vector RNA into retroviral particles. Equally, it is likely that the lower percentage of DsRed+ cells with the *Myb* or *Ikbkb* inserts is due to a larger fraction of transduced cells expressing too little *DsRed* to be detected above the background of cell autofluorescence. The *Myb* or *Ikbkb* inserts may alter the mRNA secondary structure in such a way that the IRES element is less efficiently recognized for translation of the DsRed protein.

Figure 5.1 Timeline representation of the experimental design.

B cells were activated into cycle with antigen and anti-CD40 on Day 0 and spinoculated with bicistronic retroviruses the next day. Two days after spinoculation anti-CD40 was washed off, the cells were analysed by flow cytometry and either injected into recipient mice or continued in culture. Further analysis timepoints are detailed subsequent figures.

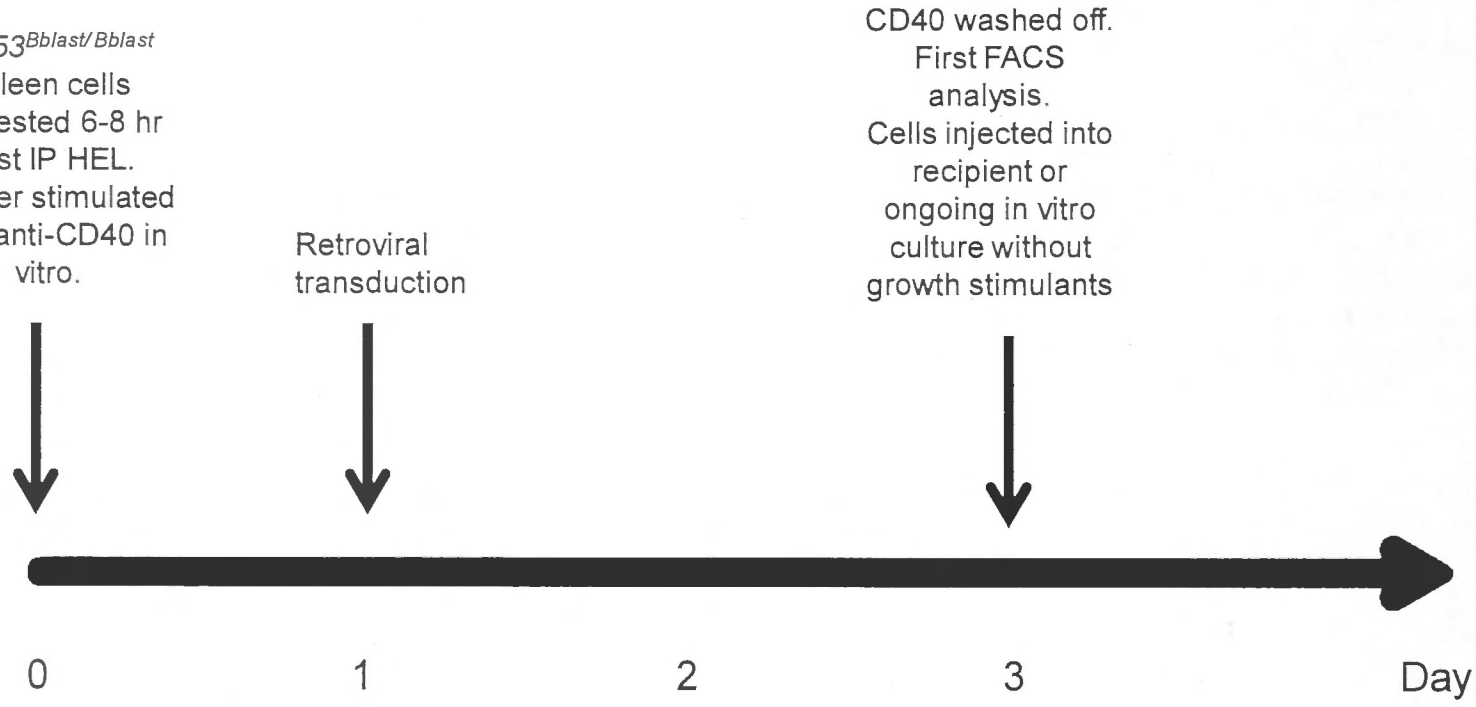

Figure 5.2 Flow cytometric detection of B cells expressing two retroviral vectors

Antigen and anti-CD40-activated B cells were split into four parallel aliquots, and spinoculated with *GFP* or *DsRed* encoding defective ecotropic retroviruses as indicated. Two days after spinoculation the cells in each culture were analysed by flow cytometry without the addition of antibody-coupled fluorochromes but following addition of a DNA dye that is only taken up by dead cells (7AAD). *GFP* expression was detected in the FL1 channel and *DsRed* expression in the FL2 channel of a four channel BD FACS Calibur™. The plots shown were gated on viable cells by excluding 7AAD positive cells. The percentage of viable cells in each gated region is shown.

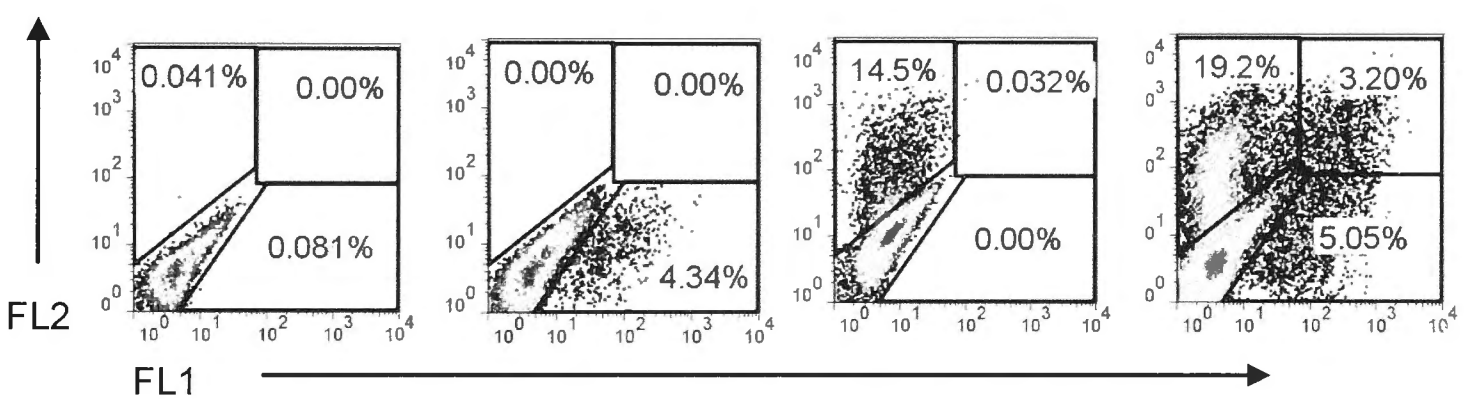

DsRed transduction:	-	-	+	+
GFP transduction:	-	+	-	+

Figure 5.3 Explanation of labels of gated regions

Representative flow cytometric data from doubly spinoculated cells as in Fig 5-2. Labels of each region are shown below for reference.

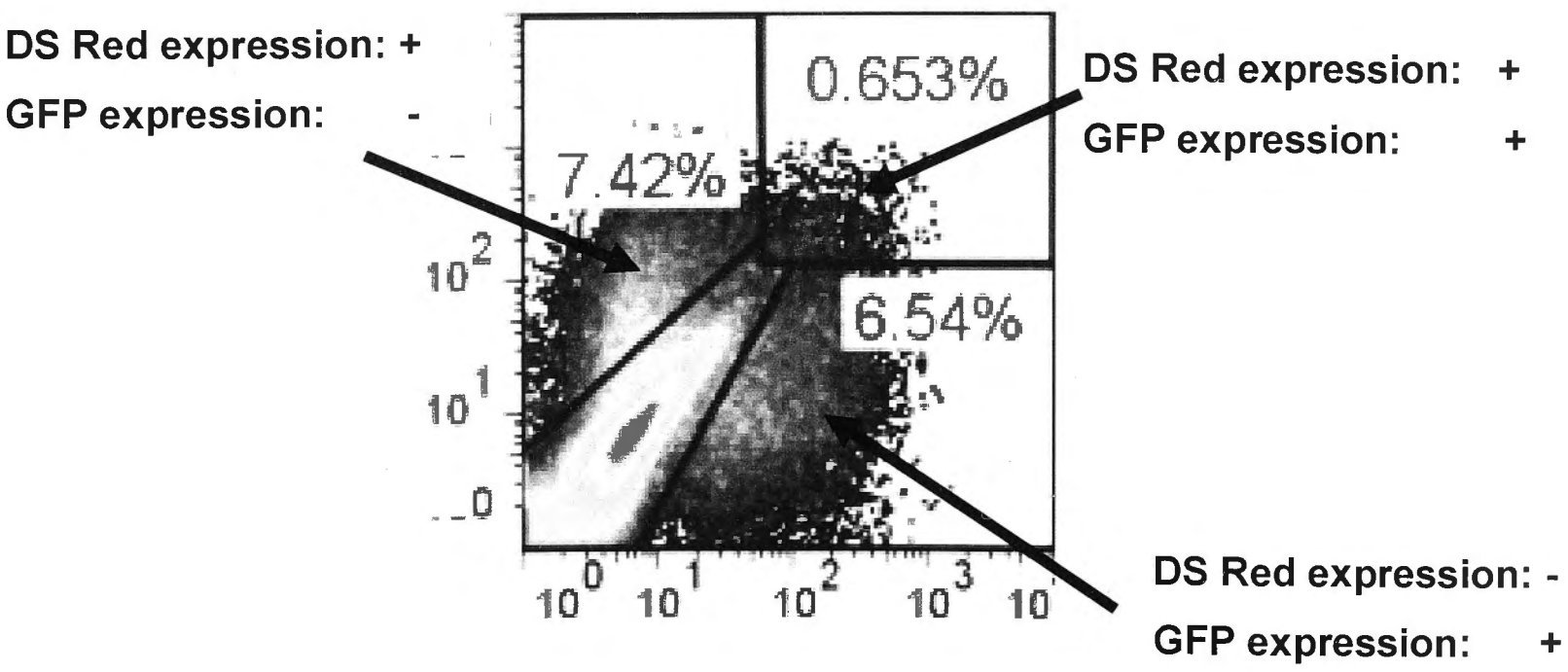

Figure 5.4 Transduction efficiency varied according to retroviral vector

Percentage of viable *Trp53* mutant cells expressing *GFP* from the *MYC/GFP* vector and/or *DsRed* from vectors with the indicated cDNA inserts or empty vector (EV). Gating strategy for single and double positive cells as in Figure 5.2. Data from two different experiments are shown by adjacent bars for each vector, analysed either (a) 2 days after spinoculation, or (b) 6 days after spinoculation. Day 7 data is the mean of triplicate cultures for each vector.

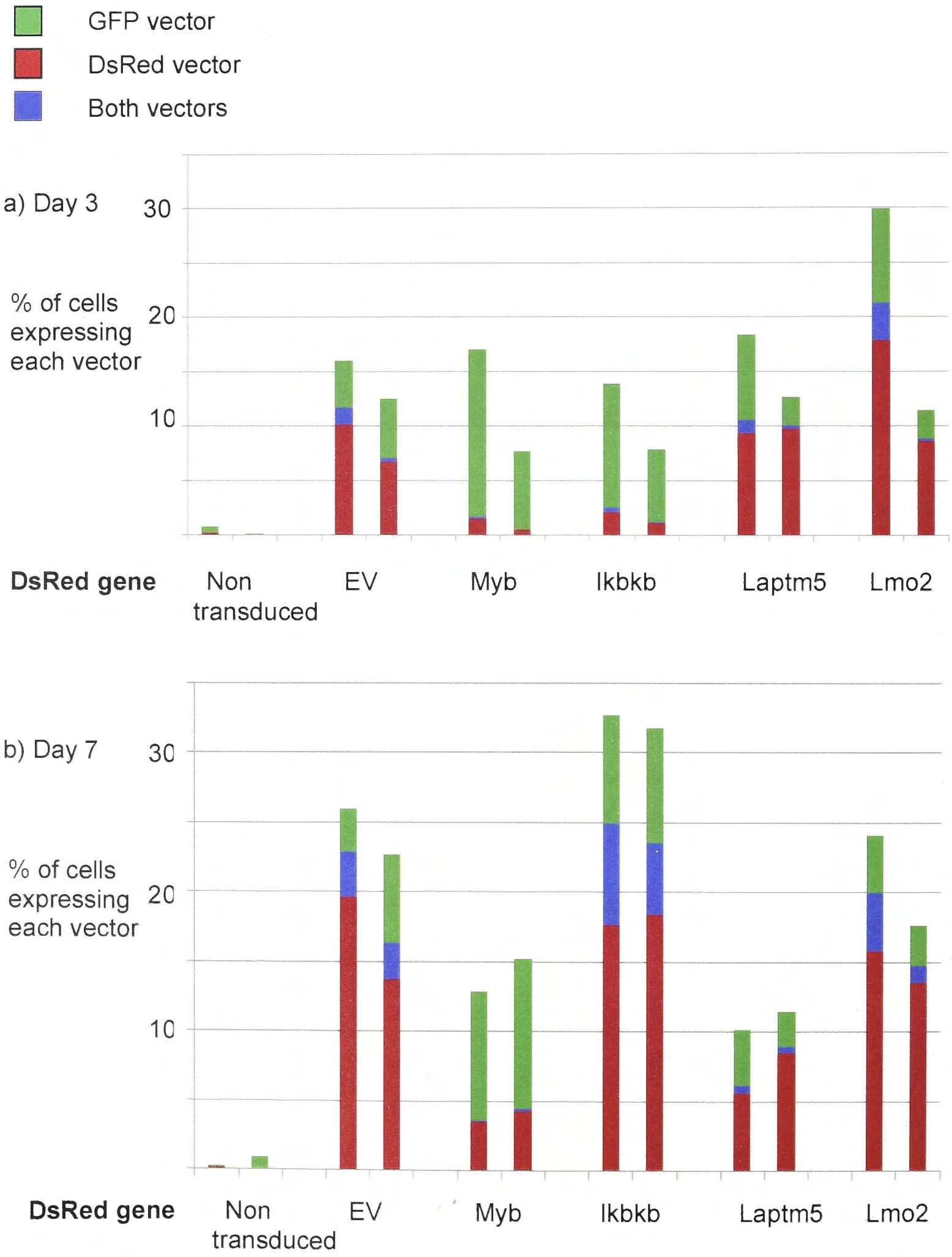

5.3 Effect of single and double transduction on cell size

Cell cycle progression is accompanied by an increase in cell size as a consequence of the synthesis of increased cellular organelles, cytoplasm, and the doubling of chromosomes prior to cell division. Quiescent B cells are mostly in G0 phase of the cell cycle and are thus characteristically smaller than activated cells in G1 phase, which are in turn smaller than B cells with more than 2n DNA content in S, G2 and M phases. These increases in cell size result in corresponding increases on the flow cytometer in the amount of laser light scattered at low angles in the forward direction (Forward Scatter, FSC).

Cell size can also vary with alterations in cellular metabolism, apoptosis and autophagy [442,443] (reviewed by Mason and Rathmell [444]). Of relevance to this study, the apoptotic threshold is reached later if cells constitutively overexpress the Bax-Bak inhibitors Bcl-2 or Bcl-X_L [445,446] so that autophagy is prolonged, resulting in lymphocytes with very small volumes. In contrast, exogenous growth factors like antigen, CD40 stimulation, or enforced *Myc* expression promote glycolysis, ribogenesis and nutrient uptake and cell enlargement [442,447]. By comparing the size of transduced B cells when they were cultured in the absence of exogenous growth factors I sought to detect any anabolic or catabolic effects of Myb, Ikbkb, Lmo2 or Laptm5 alone and combined with MYC. Specifically, I wished to test the hypothesis that these candidate proto-oncogenes would stimulate B cell enlargement either on their own or in *Trp53*-mutant cells doubly transduced with the *MYC/GFP* vector.

On Day 3 most viable cells in each culture had high FSC indicating that they were large cells that had not yet exited cell cycle nor initiated an autophagic decrease in cell volume. After 4 days culture without anti-CD40 (Day 7), the majority of viable cells remaining (most of which have not been transduced with either vector) had greatly decreased FSC. By Day 15 (12 days without anti-CD40) all of the cells were small except cultures containing *Myb* and *MYC* doubly-transduced B cells where a population of intermediate FSC persisted.

Figure 5.5 Representative FSC/SSC plots post dual transduction with various retroviral combinations

p53 mutant splenic B cells were activated into cell cycle by exposure to antigen (HEL) in vivo prior to harvest from mice (Day 0). They were then stimulated in culture for 24-36 hours with anti-CD40 antibody, spinoculated with the indicated vector combinations, and cultured for at least 24 hours with anti-CD40 antibody to allow retroviral integration into dividing B cells. Cells were subsequently washed and either analysed by flow cytometry immediately (Day 3), or incubated in RPMI complete medium without additional growth or survival stimuli for 4 days (analyses on Day 7), 8 days (Day 11) or 12 days (Day15) before flow cytometric analysis. Plots were gated on viable cells (7-AAD negative), but remain open gated with respect to GFP and DsRed fluorescence to include non-transduced and transduced cells.

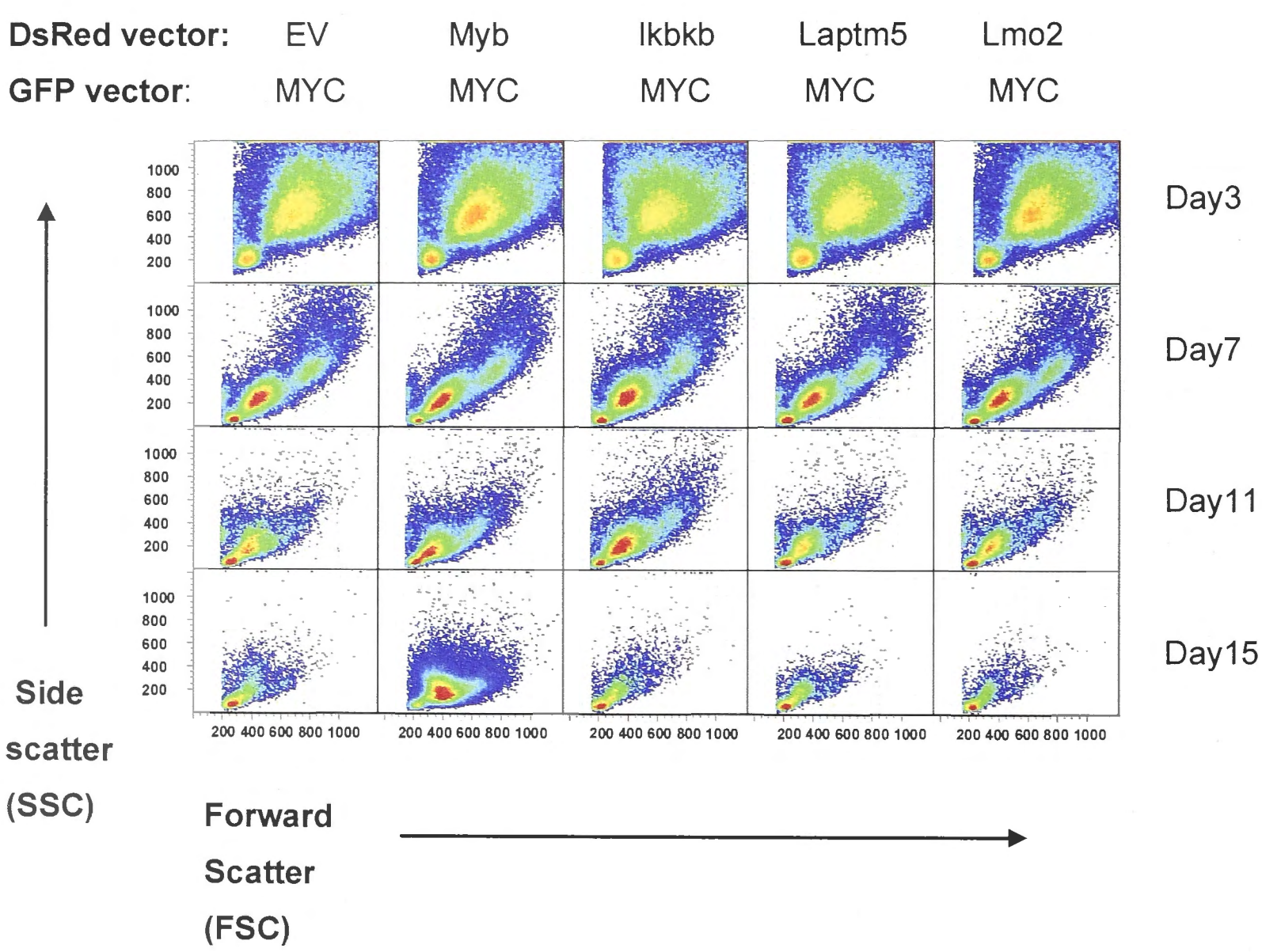

Having established the conditions for single and double transduction of mature B cells and subsequent analysis of cell size without further exogenous growth stimulus, the next analyses focused on comparing the size of cells that were singly or doubly transduced (expressing one or both of the *GFP* and *DsRed* vectors respectively) with each other and with non-transduced cells in the same culture.

5.4 Effect of MYC on cell size

First, the effect of *MYC/GFP* retroviral transduction on cell size was assessed compared to non-transduced cells or cells transduced with a *GFP*/Empty vector (Figure 5-5). When cultures were analysed on Day 3, before removal of anti-CD40, GFP-negative non-transduced cells exhibited fewer large cells than GFP+ cells expressing the *MYC/GFP* vector (Figure 5-6a), but there was no difference in the FSC distribution of GFP+ cells expressing the *MYC/GFP* vector compared to GFP+ cells expressing the *GFP*/Empty vector (Figure 5-6b). The difference between transduced and non-transduced cells in Figure 5-6a can be explained by the absolute requirement for cells to be dividing in order to integrate and express the provirus, which will select for larger, actively dividing cells in the GFP+ subset.

By Day 7, when the B cells had been cultured for 4 days without anti-CD40 or other growth stimuli, GFP+ cells expressing the *MYC/GFP* vector had higher FSC than control GFP+ cells expressing the empty-GFP vector (Figure 5-5b). This is consistent with the known effect of MYC promoting cell metabolism and synthesis of proteins, nucleic acids and lipids, and demonstrates the ability to detect metabolic effects of oncogenes by this assay. FSC was bimodal in all subsets and cultures at this time, which may reflect cells stalled at G1 or G2, heterogeneity of catabolic state within the population, or the larger population could represent cell doublets. The two peaks of cells, small and large, were both shifted to higher FSC in GFP+ cells expressing *MYC/GFP* compared to *GFP*/Empty vector.

Having established an assay that revealed MYC's known metabolic effects, I next analysed the effect of the four different cDNAs expressed in the *DsRed* vector. Initially these effects were assessed when these vectors were expressed alone in *Trp53* wild type cells, and subsequently after dual transduction with the *MYC/GFP* retroviral vector in both *Trp53* wild type and mutant cells.

Figure 5.6 Effect of MYC on size of singly transduced B cells

Representative analysis of FSC as a measure of cell size in *Trp53* wt cells either on Day 3, before culture without anti-CD40, or on Day 7, after culture for 4 days without anti-CD40. Viable 7AAD- cells were gated on GFP single positive or GFP-negative as shown in Figure 5.2 and Figure 5.3.

a) Comparison with non-transduced cells. Black histogram, GFP+ cells expressing *MYC/GFP* vector; grey shaded histogram, GFP-negative non-transduced cells in the same culture.

b) Comparison with empty vector transduced cells. Black histogram, GFP+ cells expressing *MYC/GFP* vector; grey shaded histogram, GFP+ cells expressing GFP/Empty vector.

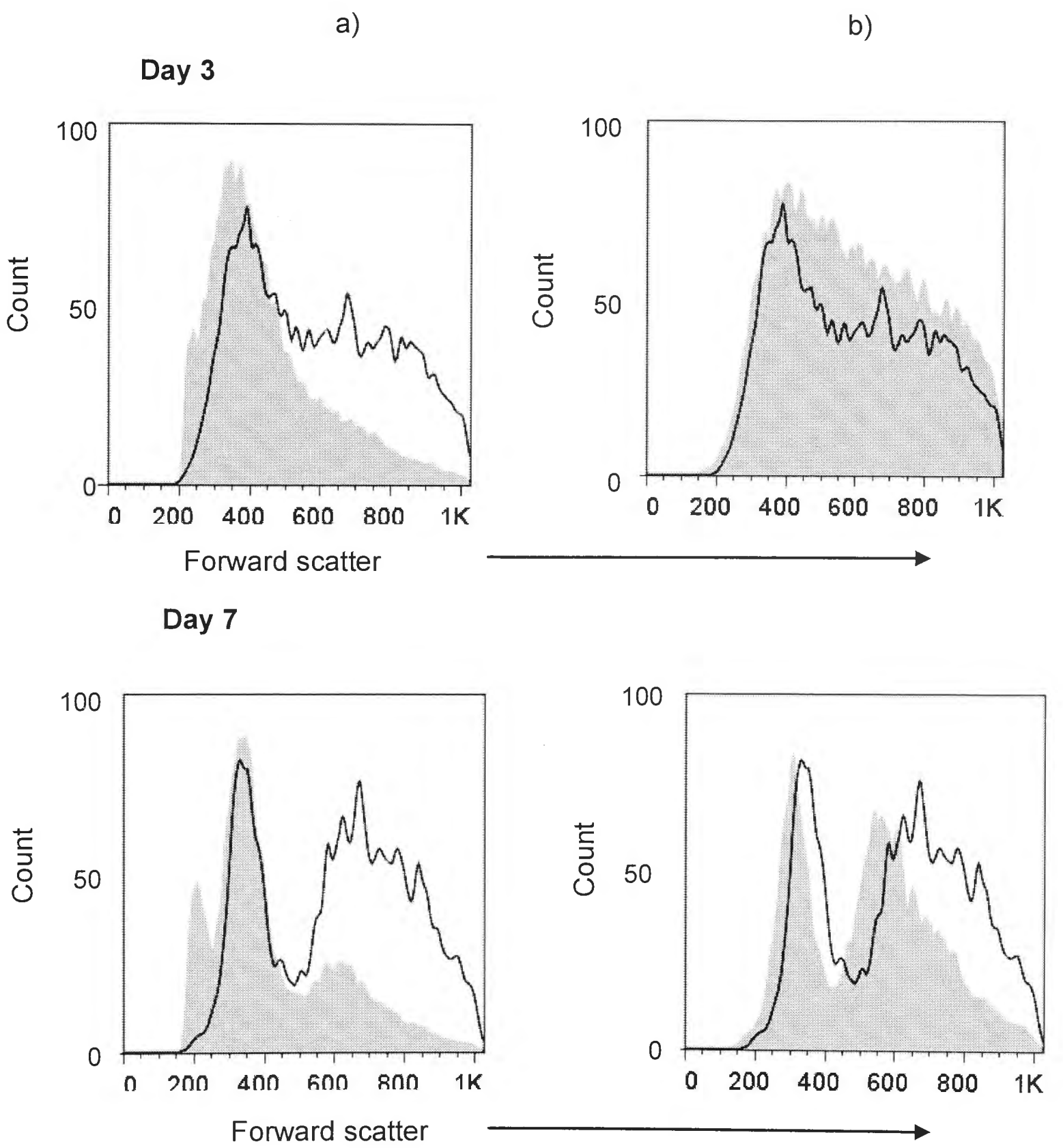

5.5 Effect of Myb on cell size

In *Trp53* wildtype B cells, there was little difference between DsRed+ cells expressing *DsRed/Myb* compared to *DsRed*/Empty vector on Day 3, 24 hours after spinoculation and before removal of anti-CD40 (Figure 5-7b). However, after a further 4 days culture without growth factors (Day 7), cells expressing the *DsRed/Myb* retrovirus were shifted to lower FSC compared to those expressing the *DsRed/EV* retrovirus (Figure 5-7b) or to non-transduced B cells in the same culture (Fig 5-7a). Although FSC was bimodal as noted above, both the large and small peaks of cells were shifted to lower FSC by the *DsRed/Myb* vector. Thus, enforced expression of full-length *Myb* had the opposite effect to *MYC*, as measured by cell size.

Interestingly, the presence of *Myb* in the *DsRed* vector also caused a decrease in FSC on Day 7 in *Trp53* wildtype B cells that were doubly transduced to express both the *DsRed* and *GFP/MYC* vectors (Figure 5-8a), and this also occurred in *Trp53* mutant B cells (Figure 5-8b).

Figure 5.7 Effect of Myb on size of singly transduced B cells

Representative analysis of FSC as a measure of cell size in *Trp53* wt cells either on Day 3, before culture without anti-CD40, or on Day 7, after culture for 4 days without anti-CD40. Viable 7AAD- cells were gated on DsRed single positive or DsRed-negative as shown in Figure 5.2 and Figure 5.3.

a) Comparison with non-transduced cells. Black histogram, DsRed+ cells expressing *DsRed/Myb* vector; grey shaded histogram, DsRed-negative non-transduced cells in the same culture.

b) Comparison with empty vector transduced cells. Black histogram, DsRed+ cells expressing *DsRed/Myb* vector; grey shaded histogram, DsRed+ cells expressing empty vector DsRed vector.

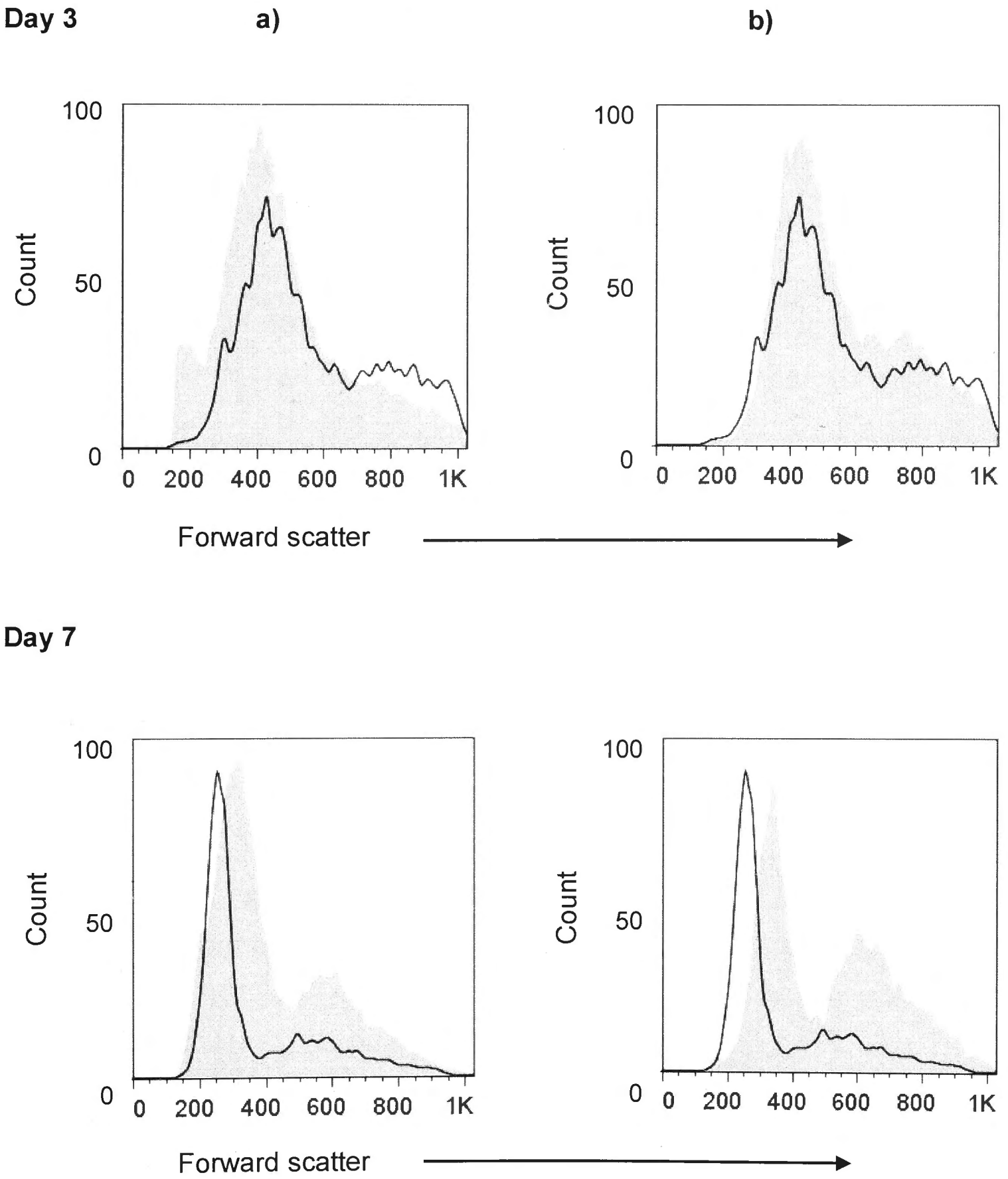

Figure 5.8 Effects of dual *MYC/Myb* overexpression on cell size.
Representative FSC histograms of Trp53 wildtype (a) or Trp53 mutant (b) viable cells gated as in Figure 5.2 on DsRed single positive, GFP single positive, or double positive cells transduced with either *GFP/MYC* and *DsRed/Myb* (purple histograms) or *GFP/MYC* and DsRed/Empty vector (black histograms). Cells were analysed on Day 3, before culture without anti-CD40, or on Day 7, after culture for 4 days without anti-CD40. Day 7 results are shown from triplicate cultures for each vector combination.

a) *Trp53* wt cells

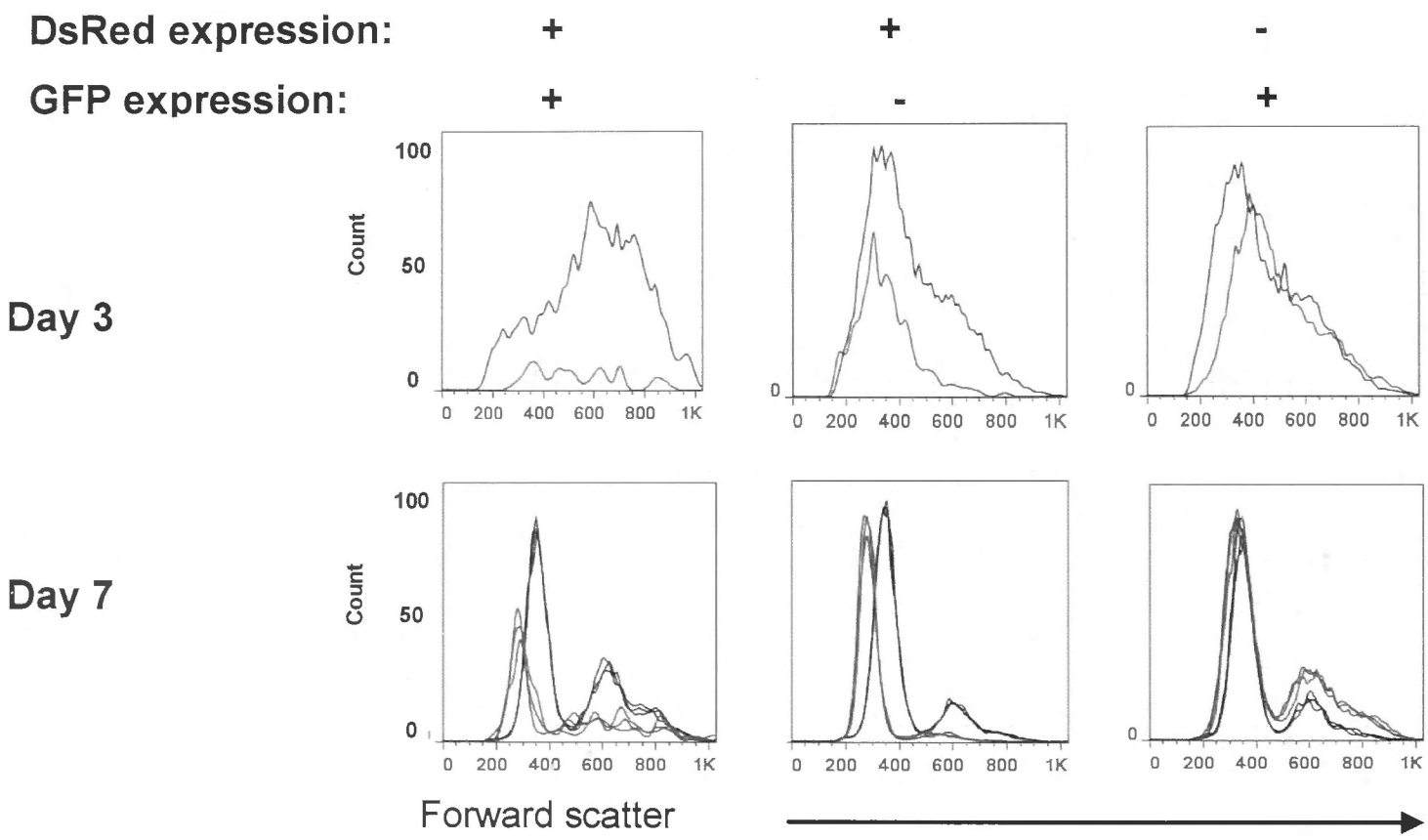

b) *Trp53* mutant cells

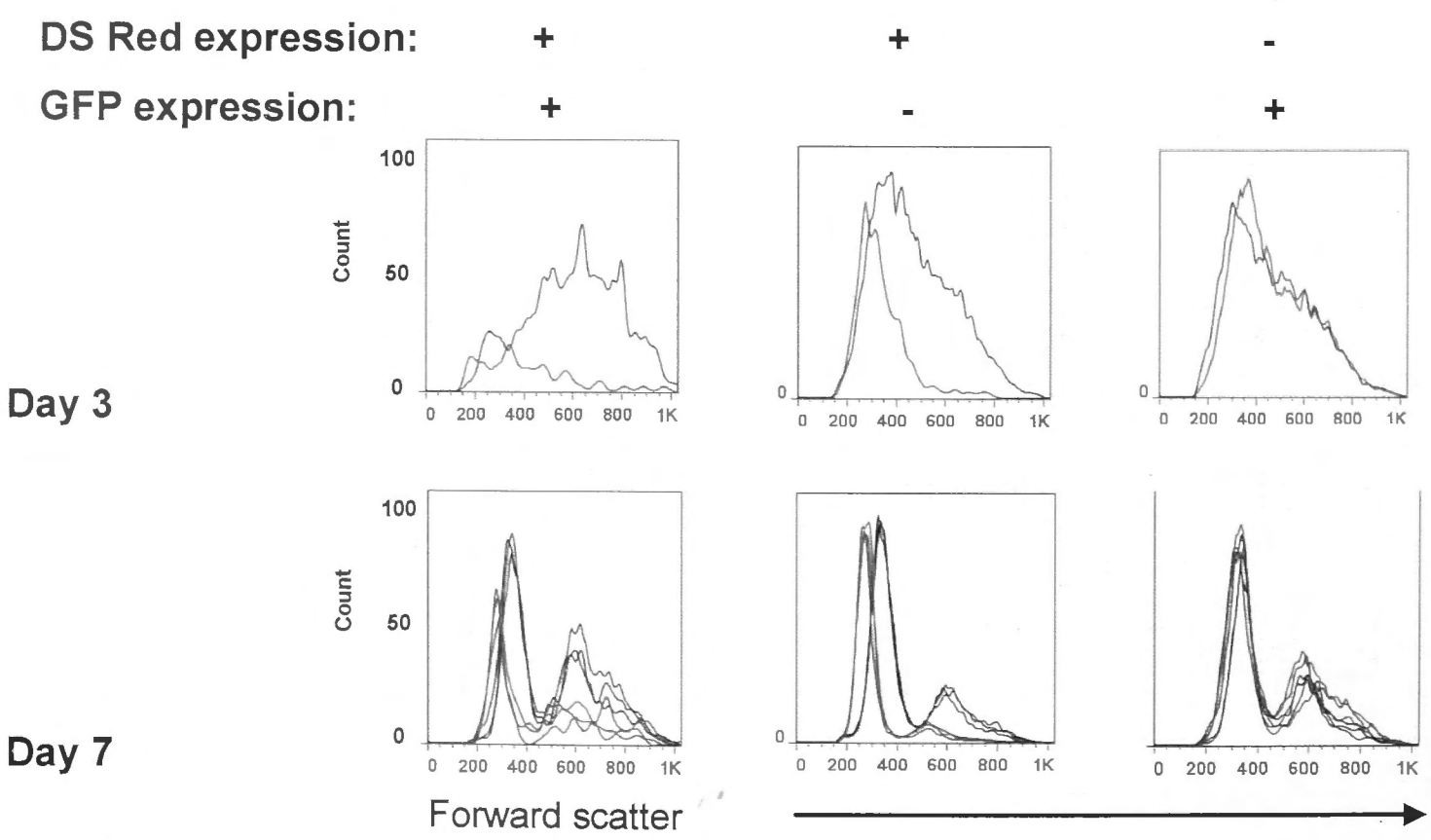

A potential explanation for the reduction in cell size seen in cells transduced with the *Myb*-expressing vector is that *Myb* induced a highly autophagic and low metabolic state that was able to resist apoptosis. This occurs in B cells from *Bcl2* transgenic mice, which even in G0 of cell cycle have a characteristically smaller size and FSC than normal G0 B cells [33]. The t(14;18) classically seen in human Follicular Lymphoma which results in the juxtaposition of *Bcl2* with the immunoglobulin heavy chain promoter locus is similarly associated with an excess of small mature B cells. *Myb* has been demonstrated to positively regulate *Bcl2* expression through its promoter in T cells [448,449] and other MYB family members have been demonstrated to positively regulate *Bcl2* in B cells [450,451], although no publications detail the effect of *Myb* itself in B cells.

To test the possibility that the reduced size of *Myb*-expressing B cells was due to increased expression of *Bcl2*, the transduction experiments were repeated in B cells from a strain of mice with an ENU-induced loss-of-function *Bcl2* mutation to see if the effect was negated. $Bcl2^{dorian}$ mice have a phenotype of premature greying starting as early as weaning age and lymphopenia comparable to that seen in *Bcl2* knock-out mice [31,32], although the homozygous Dorian mice are fertile (on a mixed CBAxB6 background) and do not have terminal polycystic kidney disease (although their kidneys have not been morphologically assessed). The $Bcl2^{dorian}$ allele is a T-C substitution in nucleotide 70 which changes a TCA codon encoding serine to a CCA codon encoding proline. This amino acid substitution (position 24) is near the C terminal end of the conserved BH4 domain of Bcl-2 which is critical for the anti-apoptotic function of the protein [452]. As a consequence of these findings it has been assumed that Dorian mice harbour a hypomorphic allele of *Bcl2*, although this has not been fully characterised.

Splenocytes were harvested from $Bcl2^{dorian}$ homozygous mice and wild-type control (CBAxB6)F_1 mice. $Bcl2^{dorian}$ spleens contained approximately 25% of the number of splenocytes seen in the controls. Both cohorts of splenic B cells were activated with anti CD40 antibody and transduced with the *DsRed/Myb* retrovirus or the *DsRed*/Empty vector retrovirus with results shown in Figure 5.9. As before, DsRed-positive wild-type cells expressing the *Myb/DsRed* vector were shifted to lower FSC by Day 7 compared to cells expressing

DsRed/Empty vector. This shift also occurred in *Bcl2*^{dorian} B cells, and there was no statistical difference in the median FSC between wildtype and *Bcl2*^{dorian} B cells expressing the Myb vector (Fig 5-8b). The effect of Myb on cell size was therefore not negated by a loss-of-function mutation of *Bcl2*.

Figure 5.9 Effect of the *Bcl2*^{dorian} mutation on size of cells transduced with *DsRed/Myb* or *DsRed*/Empty vectors

a) Forward scatter histograms, and b) Median forward scatter six days post retroviral transduction gating on *DsRed* expressing cells. Error bars represent standard deviation. Data is shown in triplicate. p values were calculated using a t test.

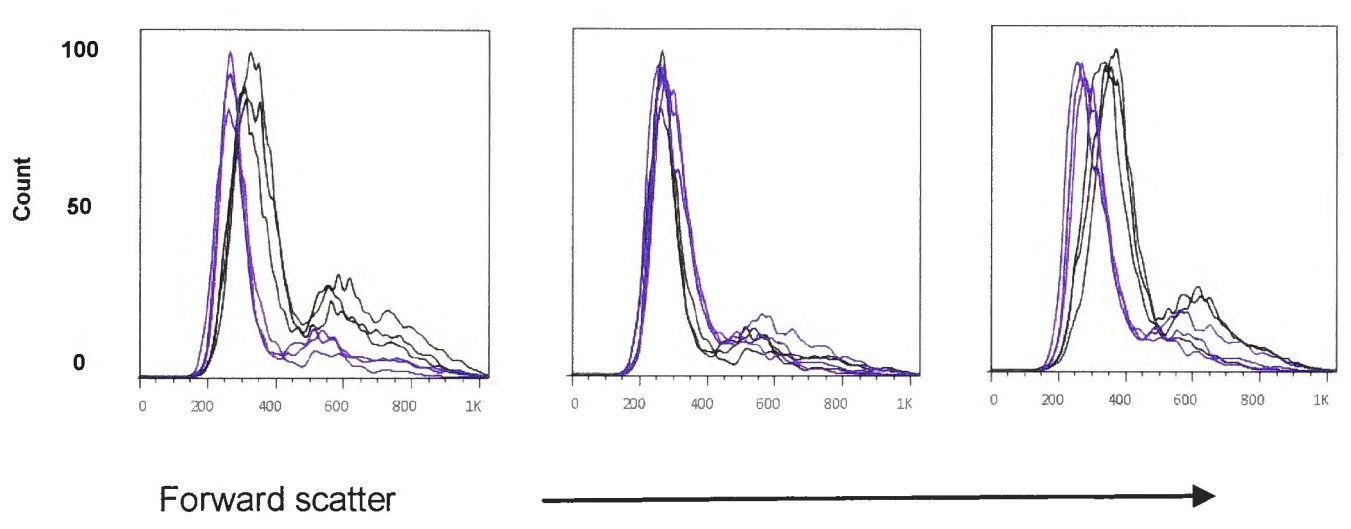

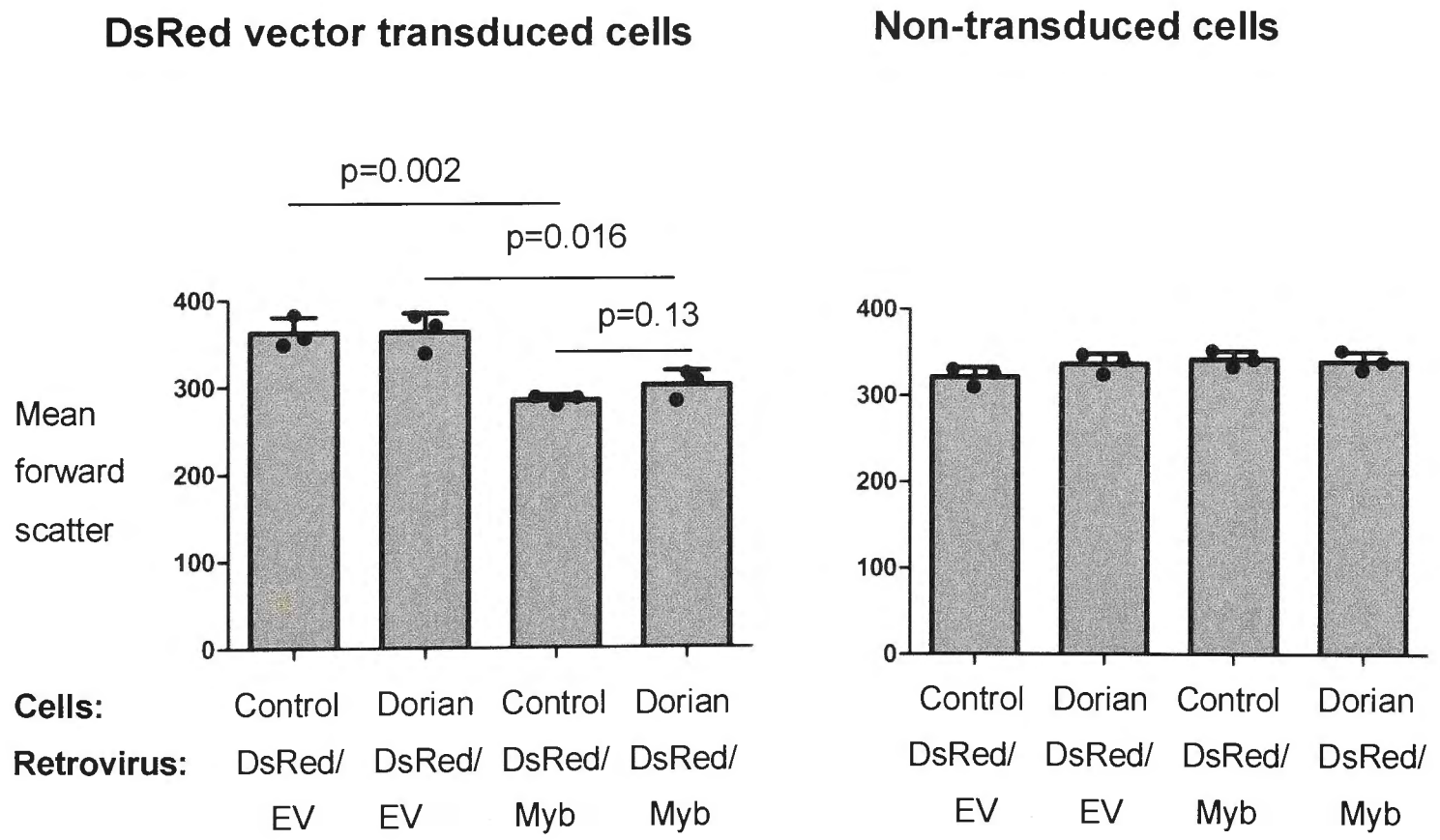

Figure 5.10 Effect of Ikbkb on size of singly transduced B cells

Representative analysis of FSC as a measure of cell size in *Trp53* wt cells either on Day 3, before culture without anti-CD40, or on Day 7, after culture for 4 days without anti-CD40. Viable 7AAD- cells were gated on GFP single positive or DsRed-negative cells as shown in Figure 5.2 and Figure 5.3.

a) Comparison with non-transduced cells. Black histogram, DsRed+ cells expressing *DsRed/Ikbkb* vector; grey shaded histogram, DsRed-negative non-transduced cells in the same culture.

b) Comparison with empty vector transduced cells. Black histogram, DsRed+ cells expressing *DsRed/Ikbkb* vector; grey shaded histogram, DsRed+ cells expressing *DsRed*/Empty vector.

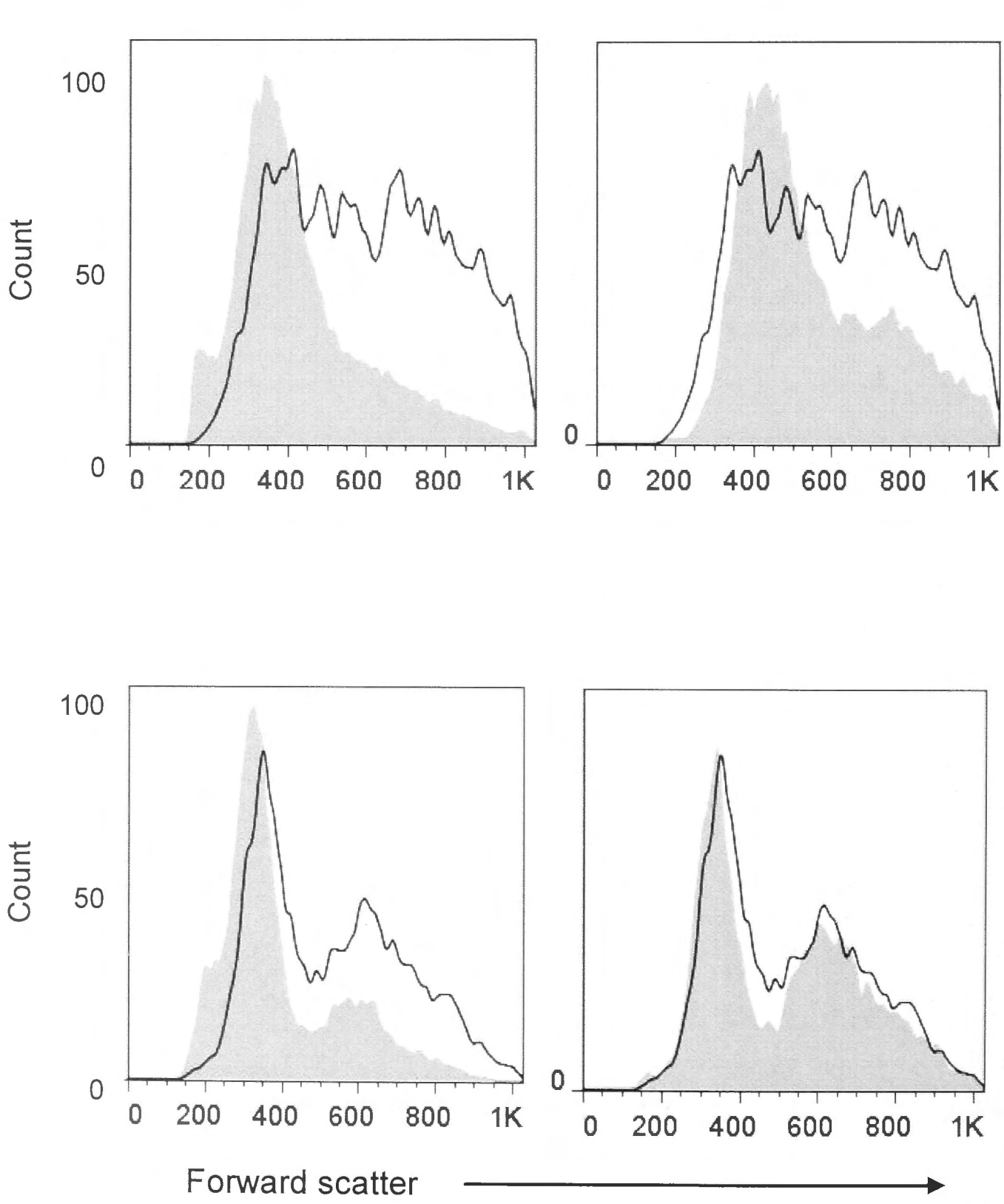

Figure 5.11 Effect of dual *Ikbkb/MYC* overexpression on cell size

Representative FSC histograms of *Trp53* wildtype (a) or *Trp53* mutant (b) viable cells gated as in Figure 5.2 on DsRed single positive, GFP single positive, or double positive cells transduced with either *GFP/MYC* and *DsRed/Ikbkb* (purple histograms) or *GFP/MYC* and *DsRed*/Empty vector (black histograms). Cells were analysed on Day 3, before culture without anti-CD40, or on Day 7, after culture for 4 days without anti-CD40. For Day 7 results are shown from triplicate cultures for each vector combination.

a) *Trp53* wt cells

DS Red expression: + + -

GFP expression: + - +

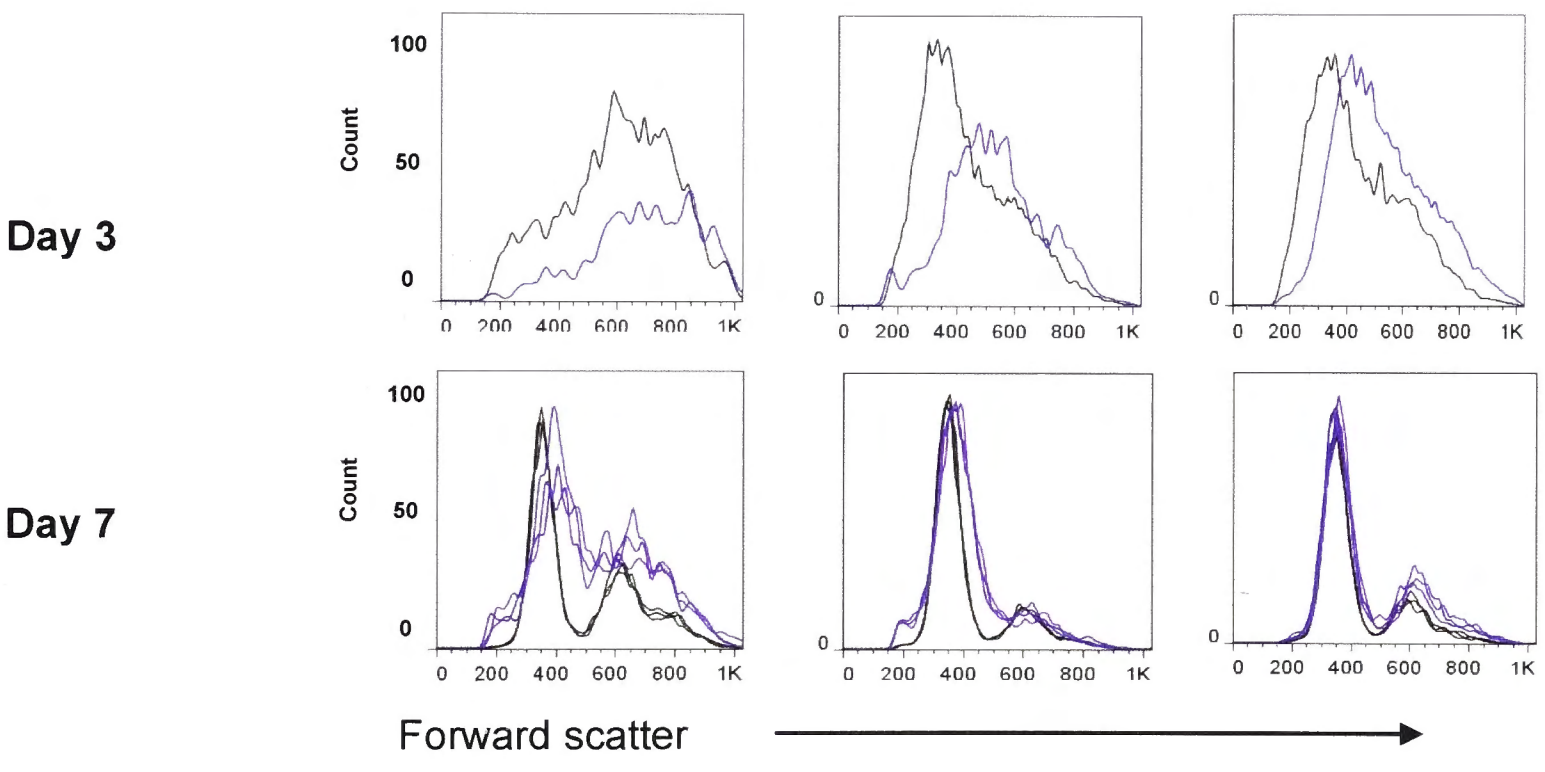

b) *Trp53* mutant cells

DS Red expression: + + -

GFP expression: + - +

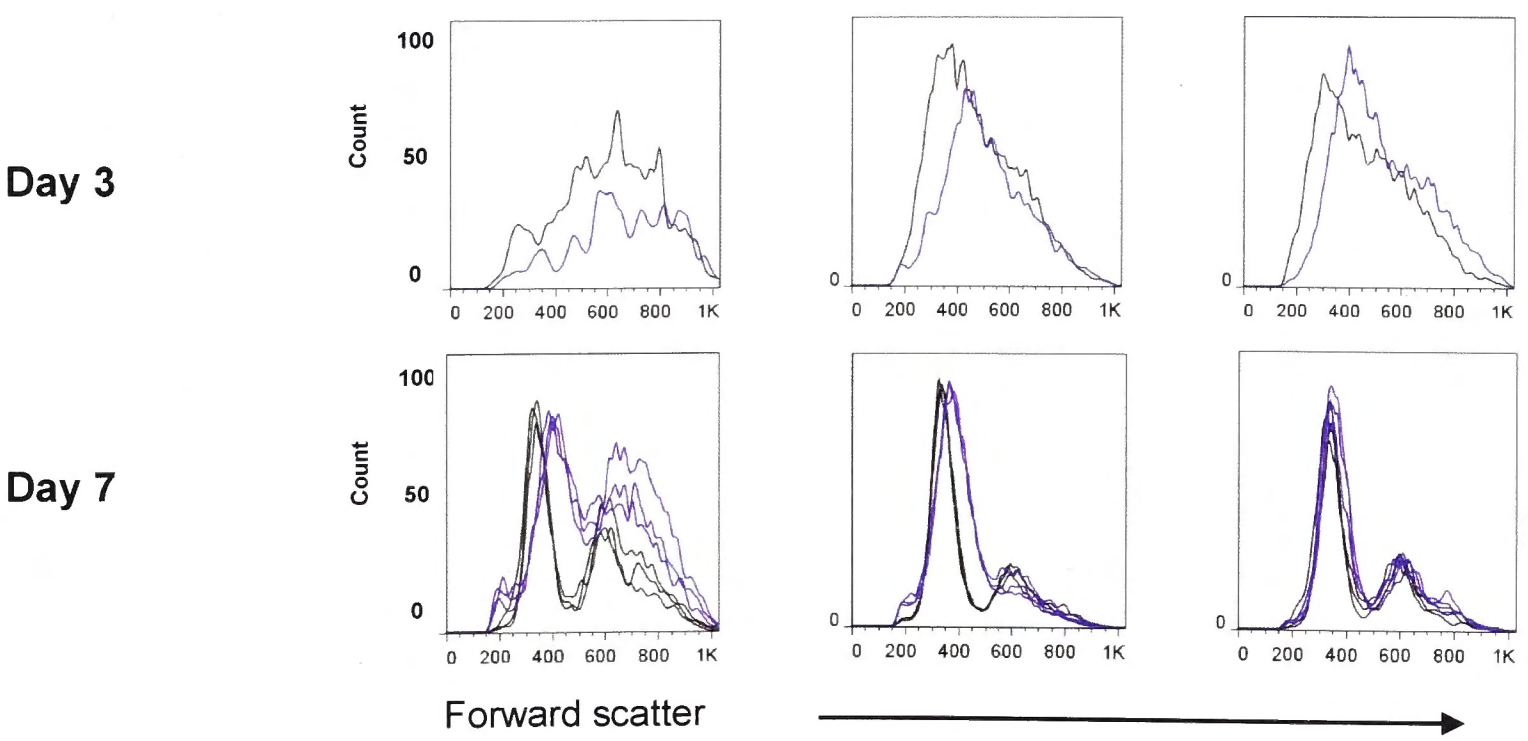

Figure 5.12 Effect of Laptm5 on size of singly transduced B cells

Representative analysis of FSC as a measure of cell size in *Trp53* wt cells either on Day 3, before culture without anti-CD40, or on Day 7, after culture for 4 days without anti-CD40. Viable 7AAD- cells were gated on GFP single positive or DsRed-negative as shown in Figure 5.2 and Figure 5.3.

a) Comparison with non-transduced cells. Black histogram, DsRed+ cells expressing *DsRed/Laptm5* vector; grey shaded histogram, DsRed- negative non-transduced cells in the same culture.

b) Comparison with empty vector transduced cells. Black histogram, DsRed+ cells expressing *DsRed/Laptm5* vector; grey shaded histogram, DsRed+ cells expressing empty vector DsRed vector.

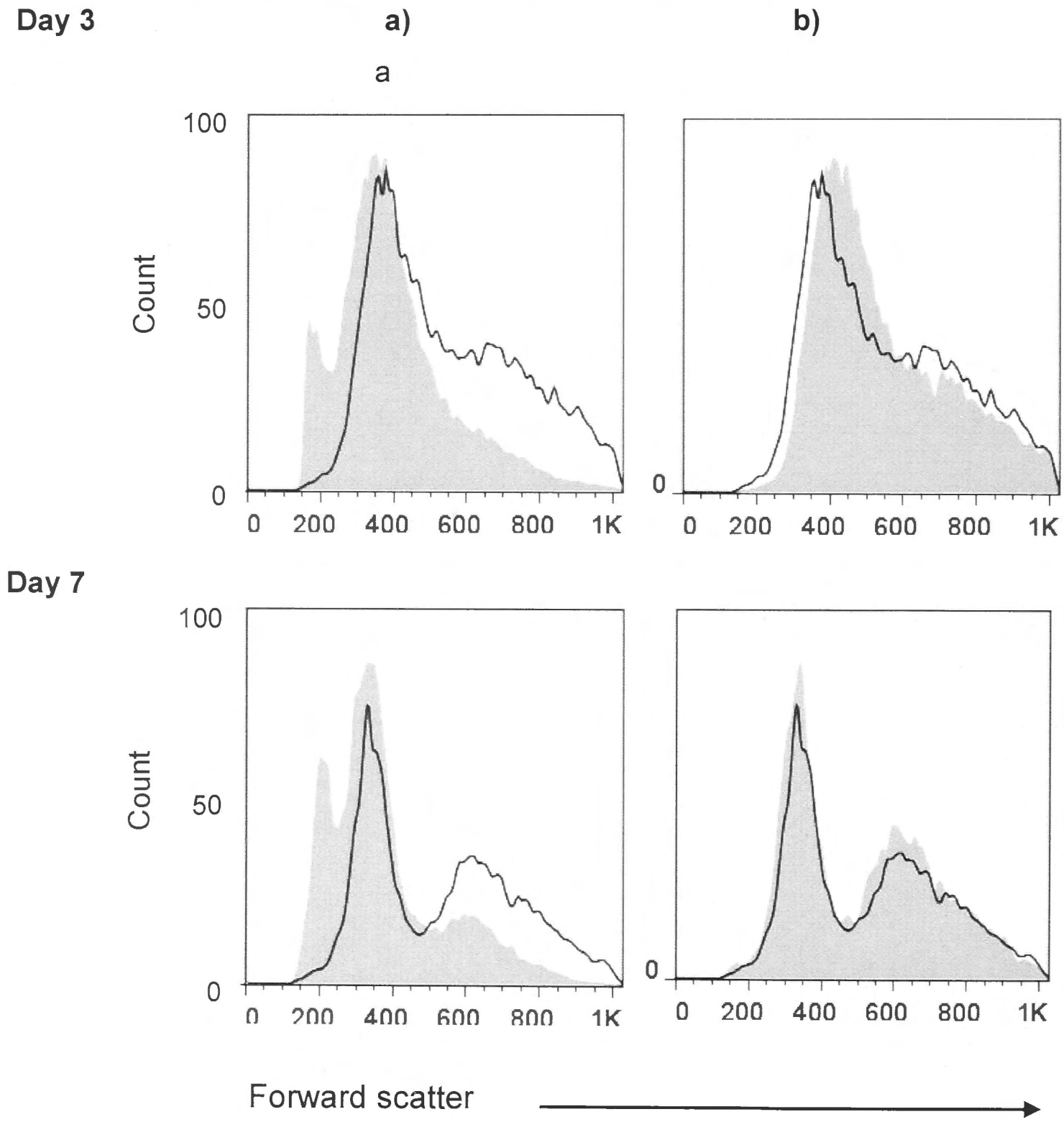

Figure 5.13 Effect of dual *Laptm5/MYC* overexpression on cell size

Representative FSC histograms of *Trp53* wildtype (a) or *Trp53* mutant (b) viable cells gated as in Figure 5.2 on DsRed single positive, GFP single positive, or double positive cells transduced with either *GFP/MYC* and *DsRed/Laptm5* (purple histograms) or *GFP/MYC* and *DsRed*/Empty vector (black histograms). Cells were analysed on Day 3, before culture without anti-CD40, or on Day 7, after culture for 4 days without anti-CD40. For Day 7 results are shown from triplicate cultures for each vector combination.

a)

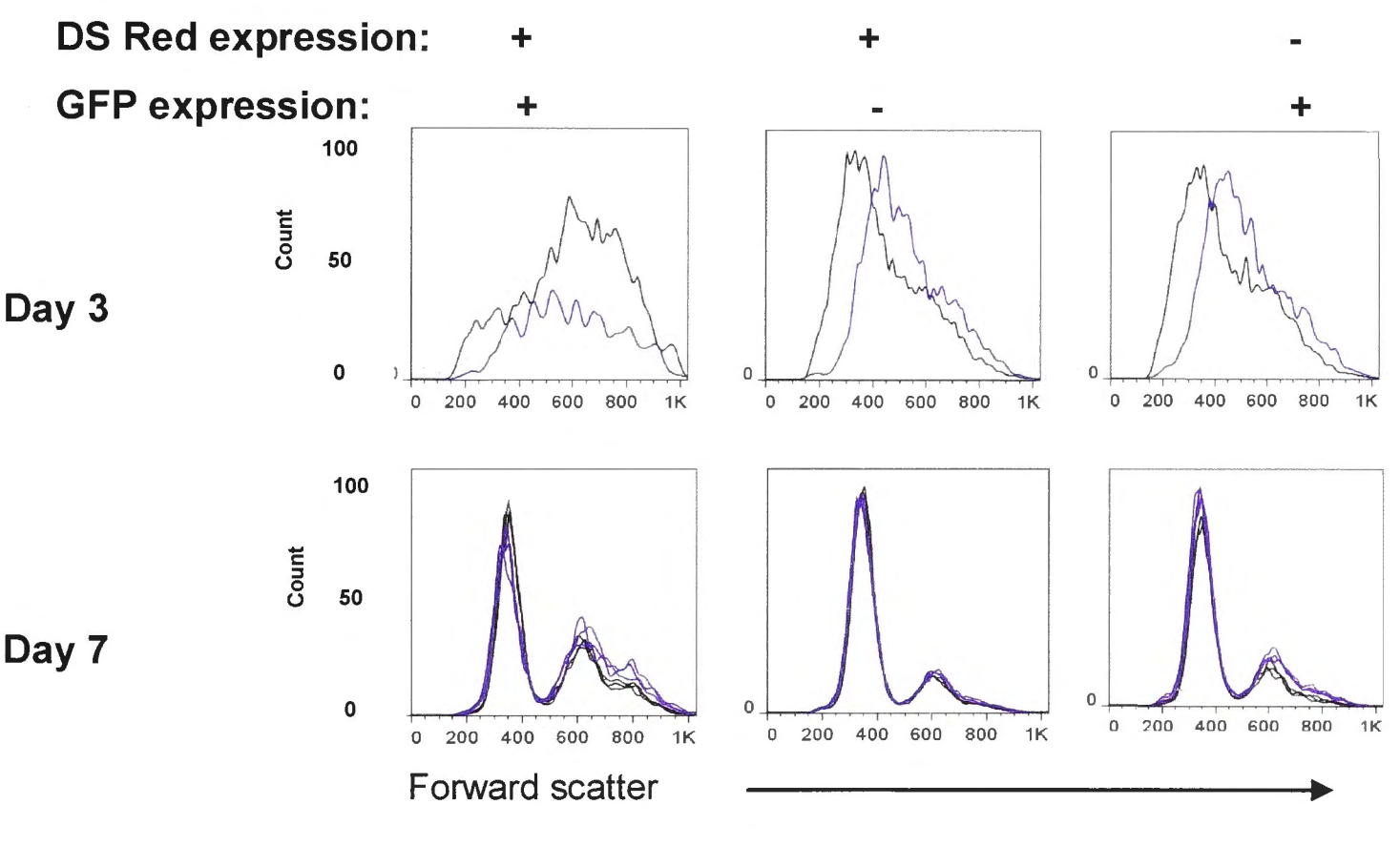

b)

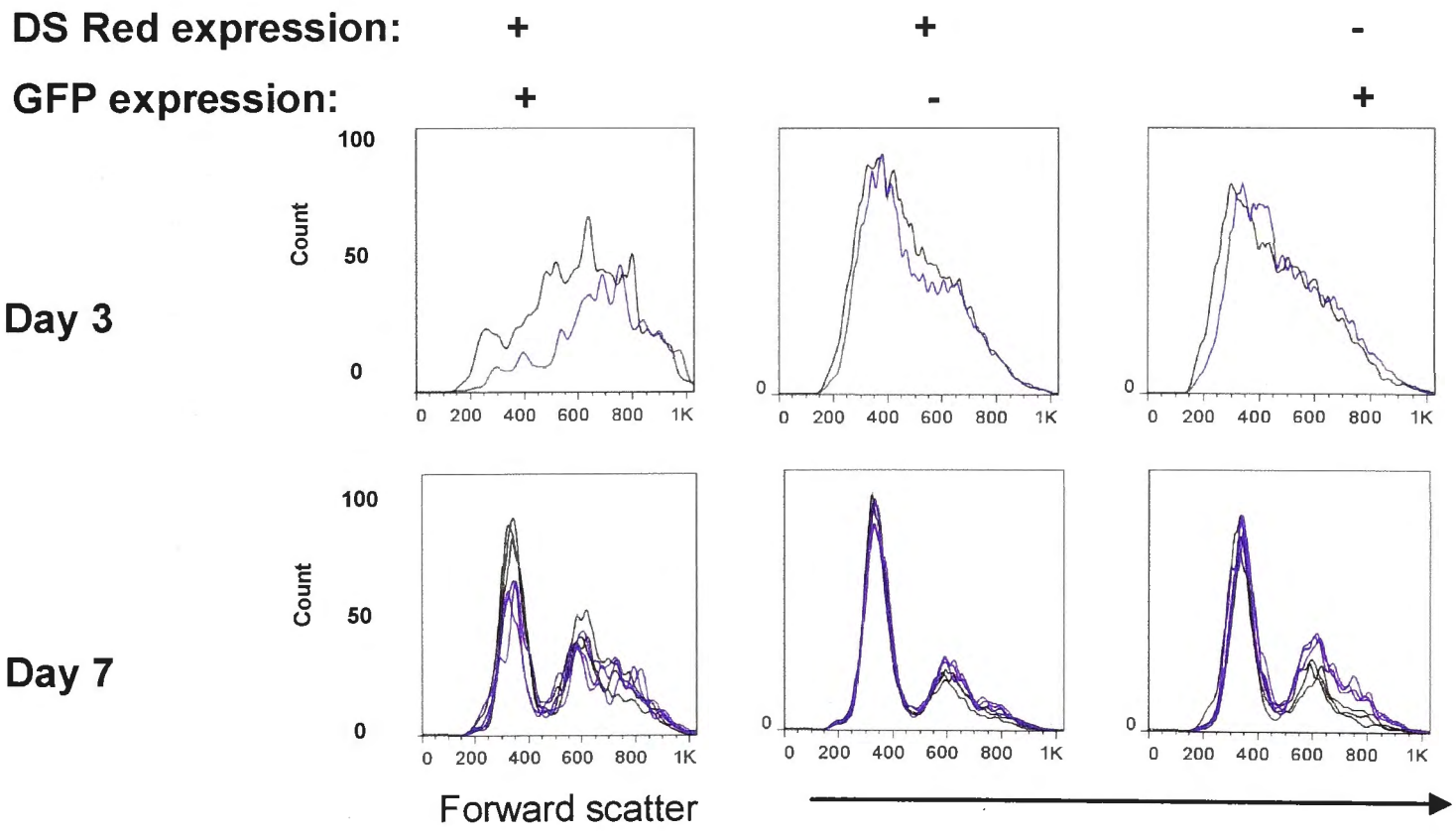

Figure 5.14 Effect of Lmo2 on size

Representative analysis of FSC as a measure of cell size in *Trp53* wt cells either on Day 3, before culture without anti-CD40, or on Day 7, after culture for 4 days without anti-CD40. Viable 7AAD- cells were gated on GFP single positive or DsRed-negative as shown in Figure 5.2 and Figure 5.3.

a) Comparison with non-transduced cells. Black histogram, DsRed+ cells expressing DsRed/Lmo2 vector; grey shaded histogram, DsRed-negative non-transduced cells in the same culture.

b) Comparison with empty vector transduced cells. Black histogram, DsRed+ cells expressing DsRed/Lmo2 vector; grey shaded histogram, DsRed+ cells expressing empty vector DsRed vector.

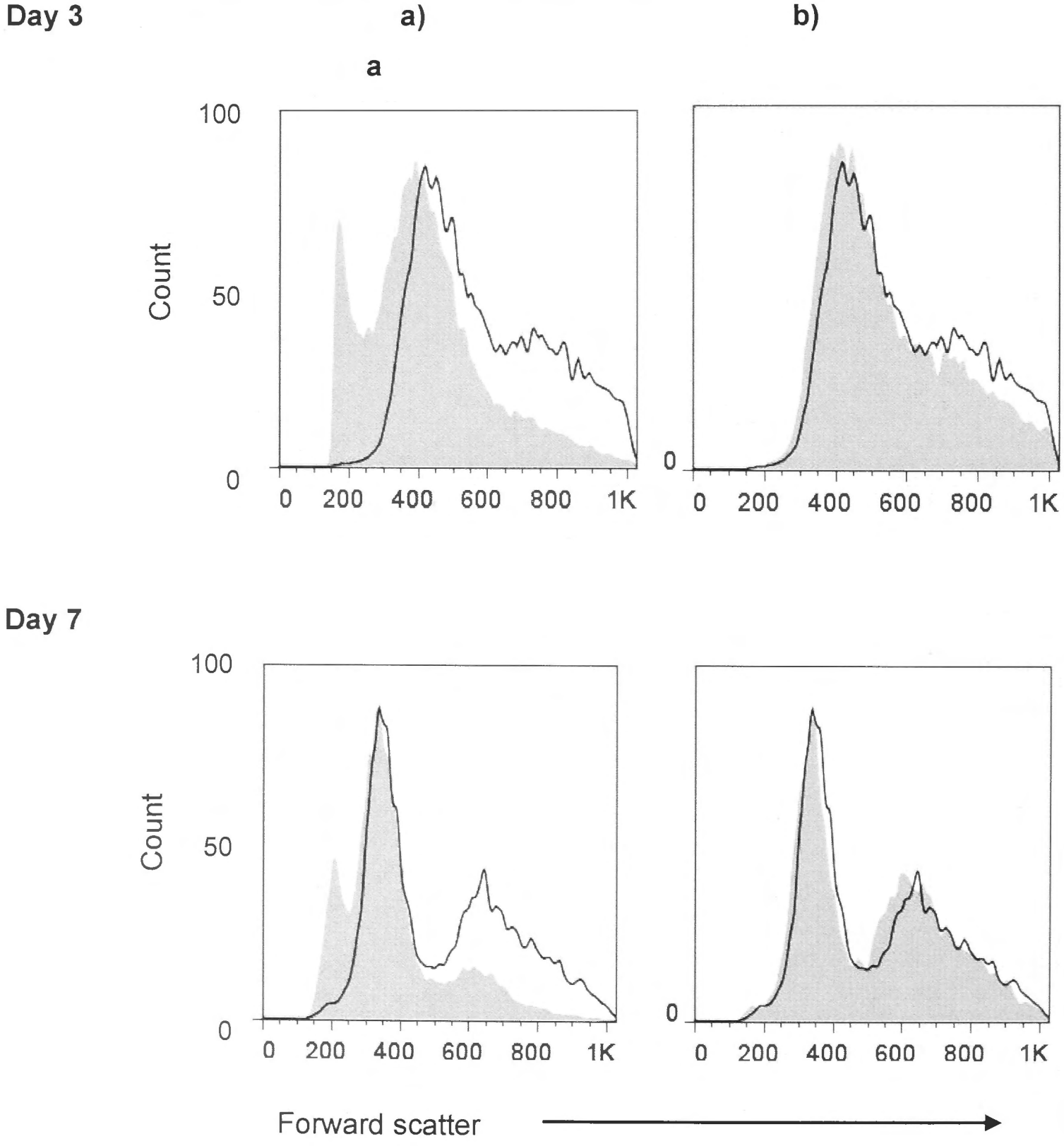

Figure 5.15 Effect of dual *Lmo2/MYC* overexpression on cell size

Representative FSC histograms of *Trp53* wildtype (a) or *Trp53* mutant (b) viable cells gated as in Figure 5.2 on DsRed single positive, GFP single positive, or double positive cells transduced with either *GFP/MYC* and *DsRed/Lmo2* (purple histograms) or *GFP/MYC* and *DsRed*/Empty vector (black histograms). Cells were analysed on Day 3, before culture without anti-CD40, or on Day 7, after culture for 4 days without anti-CD40. For Day 7 results are shown from triplicate cultures for each vector combination.

a)

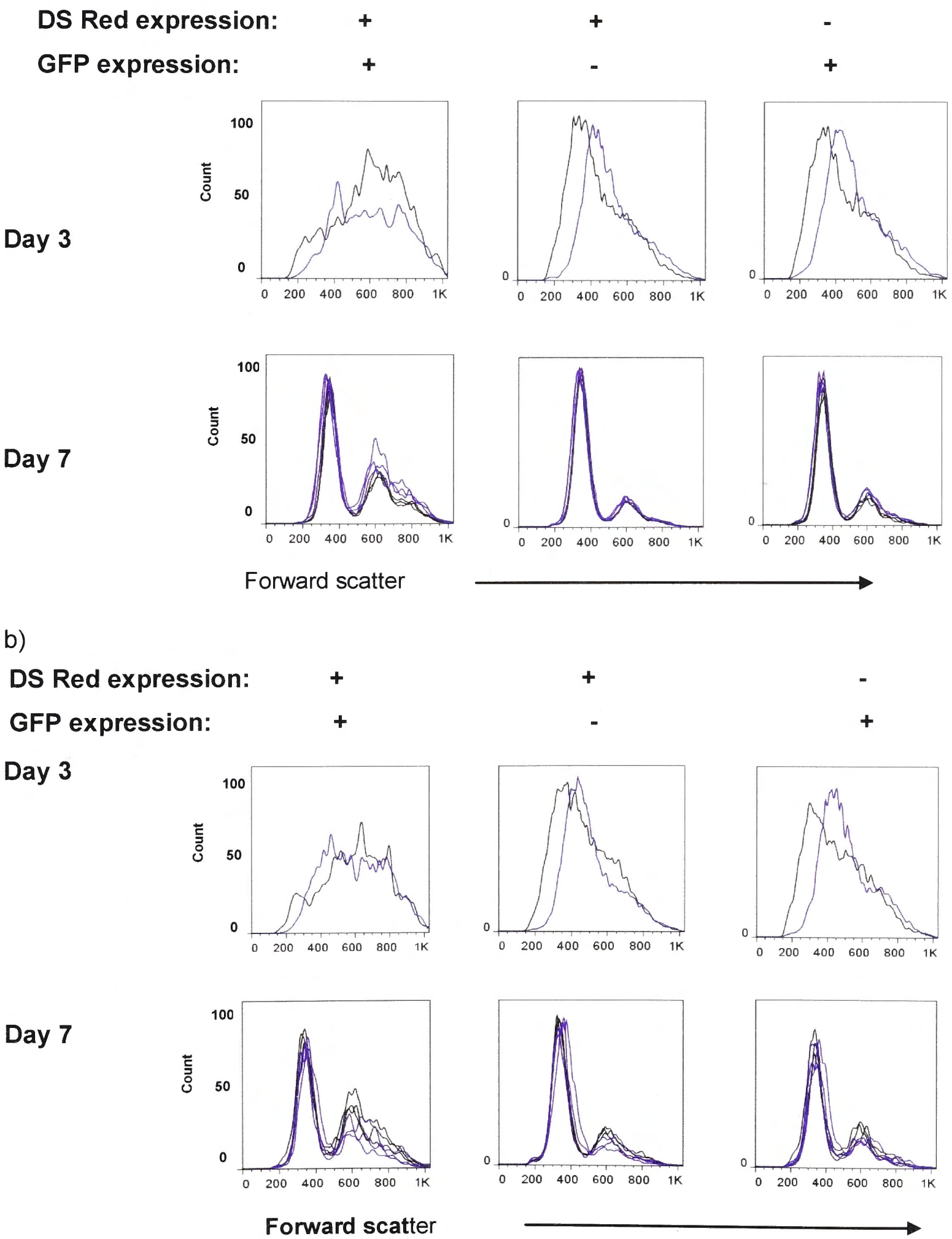

b)

5.5.1 Effect of Ikbkb, Laptm5 or Lmo2 on cell size

The decrease in cell size in B cells expressing the *Myb/DsRed* vector was unique to that vector. Not only was it not observed in *DsRed*/Empty vector transduced B cells (as shown above), but the other cDNA inserts tested in parallel either increased cell size (*Ikbkb*) or had no effect (Laptm5, *Lmo2*).

DsRed/Ikbkb transduction alone into *Trp53* wildtype B cells resulted in a subtle but consistent increase in cell size on Days 3 and 7 compared to cells expressing *DsRed*/Empty Vector (Fig 5-9). In cultures of *Trp53* wt or *Trp53* mutant cells B cells co-transduced with *DsRed* vector and *GFP/MYC* vector, cells expressing the *DsRed/Ikbkb* vector, with or without expression of the *GFP/MYC* vector, were considerably larger than their control counterparts expressing the *DsRed*/Empty Vector on Day 3 and Day 7 (Fig 5-10). The effect was similar in *Trp53* wt and *Trp53* mutant cells, and was statistically significant (Fig 5-16).

Laptm5 and *Lmo2* transduction did not substantially alter cell size either with dual *GFP/MYC* transduction or in *Trp53* wild type or mutant cells. These results are summarised in Figure 5.16 and Figure 5.17.

Figure 5.16 Comparison of cell size post single retroviral transduction

The bar graphs show the mean forward scatter at Day 7 of Trp53 wild type cells that have been singly transduced (on Day 1) with various DsRed vectors (labelled 'transduced gene'). The gating strategy is as for Figures 5.2 and 5.3, gating on cells expressing a *DsRed* vector alone,

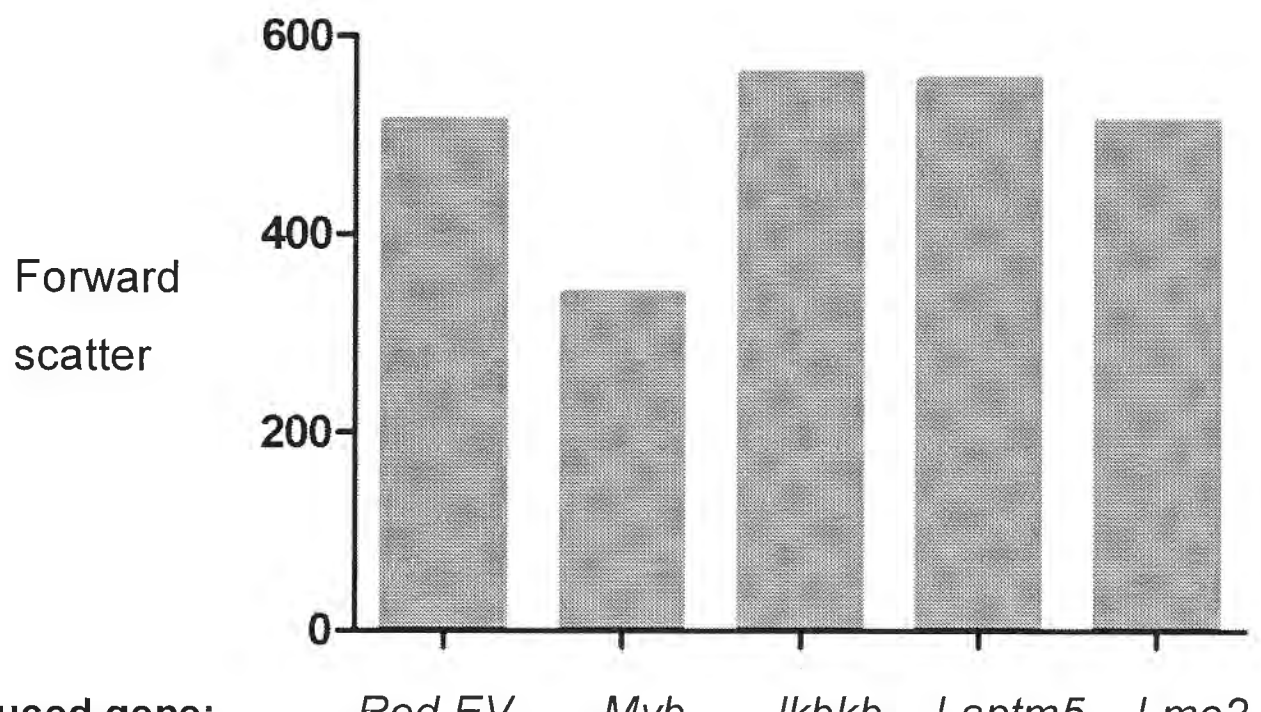

Figure 5.17 Mean forward scatter post dual retroviral transduction

The bar graphs show the mean forward scatter at Day 7 of *Trp53* mutant cells that have been doubly transduced (on Day 1) with various DsRed vectors (labelled 'transduced gene') in addition to the *GFP/MYC* vector. The gating strategy is as for Figures 5.2 and 5.3 with a) showing cells expressing a *DsRed* vector alone, and b) showing cells expressing both the *DsRed* vector and the *GFP/MYC* vector. The experiment was performed in triplicate. The p value was determined using a two-tailed unpaired t test. Error bars reflect standard deviation. The experiment was repeated (in triplicate) and similar results were obtained.

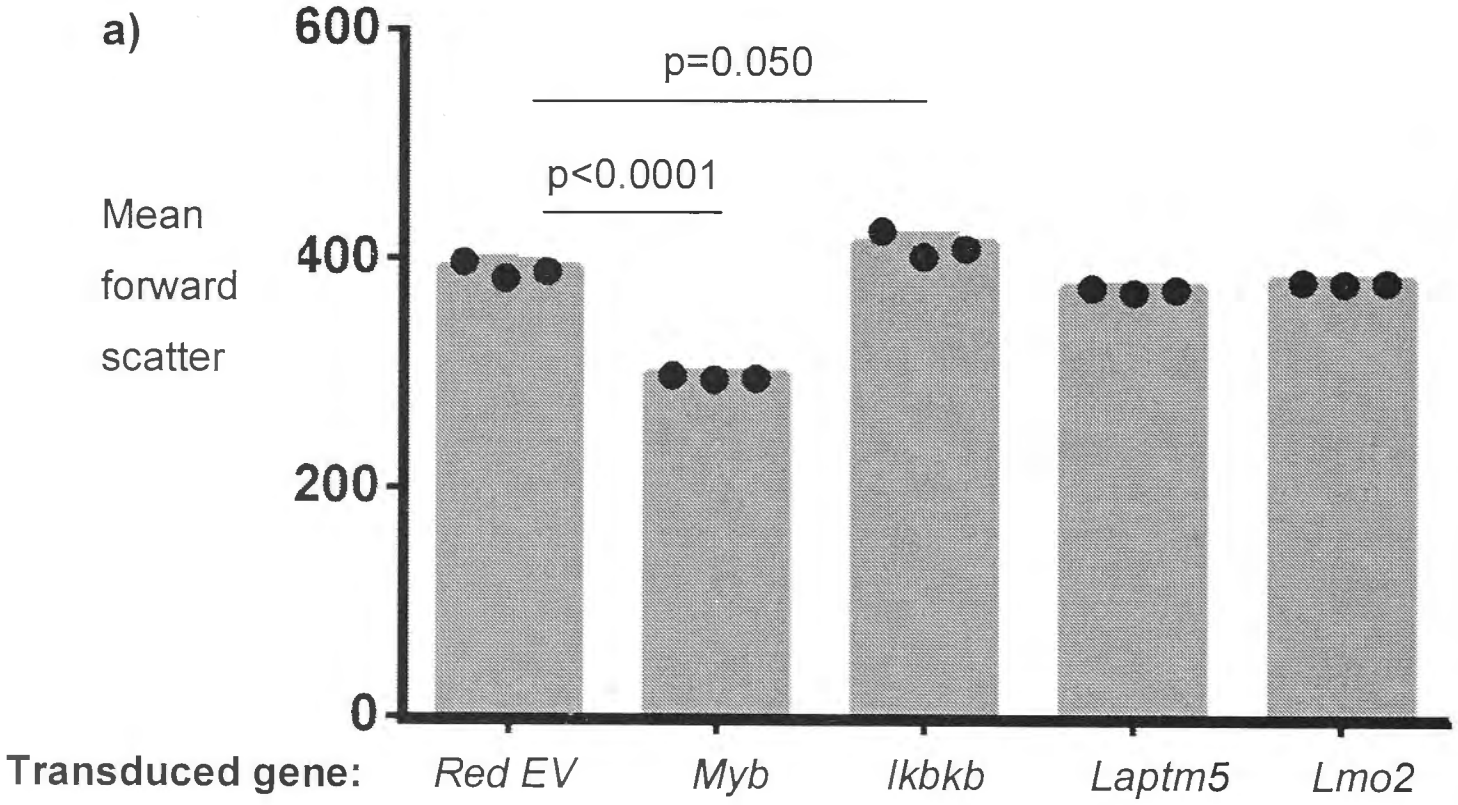

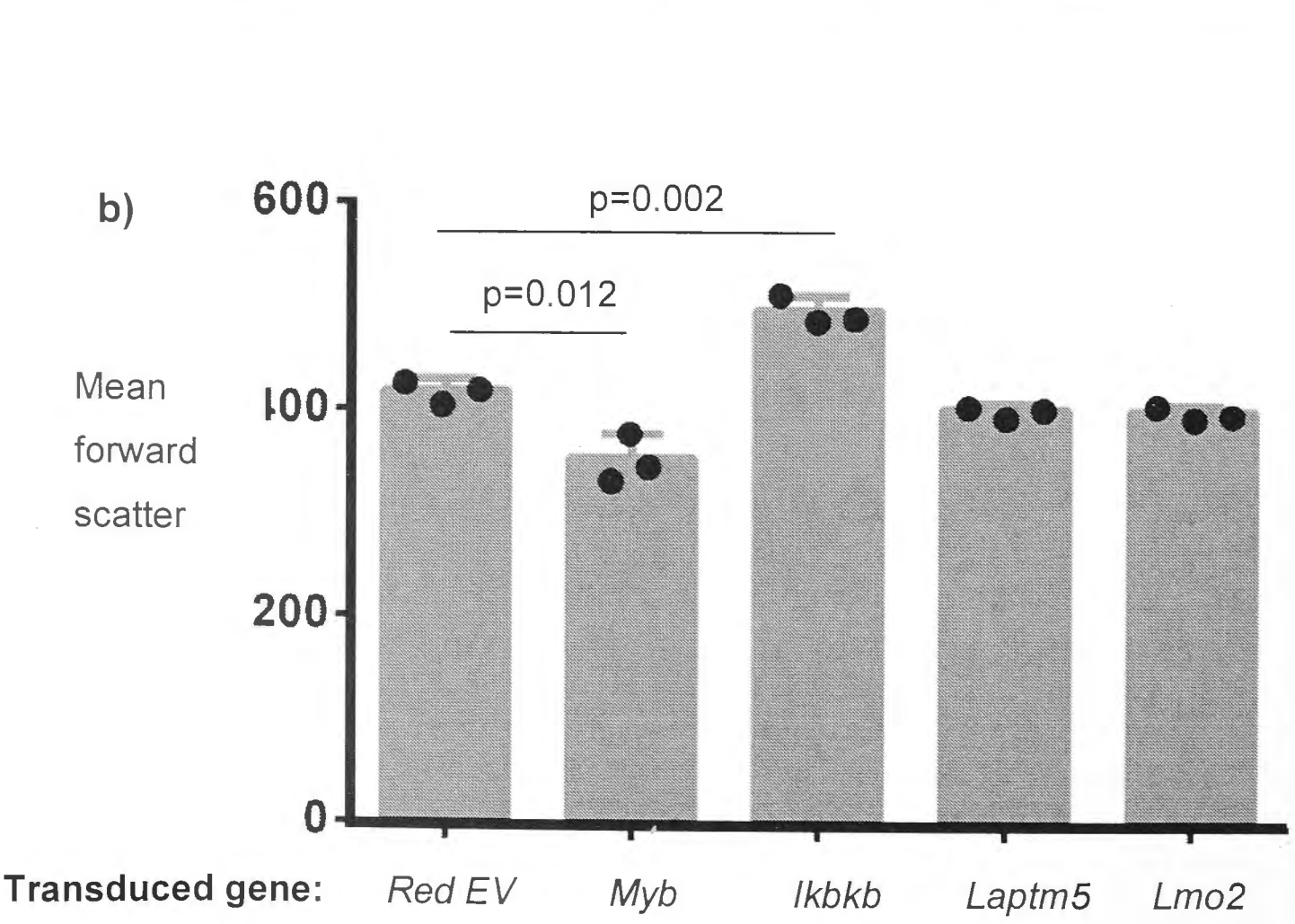

5.6 Effect of single and double transduction on B cell growth in vitro

The experiments above measured effects on B cell size that would integrate changes in the cells' metabolic activity that may or may not result in cell proliferation. To investigate if enforced expression of *Myb, Ikbkb, Laptm5* or *Lmo2* could actually trigger proliferation of mature splenic B cells in the absence of exogenous growth factors, either alone or combined with *MYC* expression and *Trp53* inactivation, cells from *Trp53* mutant and wild type mice were co-transduced with *GFP/MYC* and one of the four DS-Red vectors and then washed to remove anti-CD40 and cultured in medium alone as above (RPMI-1640 medium supplemented with penicillin, streptomycin, L-glutamine, HEPES, 2-mercaptoethanol solution and 10% heat inactivated Fetal Calf Serum and incubated at 37°C with 5% CO_2). In these experiments cultures were harvested at longer times after washing out anti-CD40, and the percentage and number of viable cells expressing *DsRed* or *GFP* or both in each culture was measured by integrating data from the haemocytometer and flow cytometer.

The analyses focus on the *GFP* and *DsRed* expressing cells as expression of these fluorescent proteins implies simultaneous expression of the proto-oncogenes also encoded by these bicistronic vectors. Experiments were duplicated several times. These experimental design features were incorporated to optimise the likelihood that any changes were due to the expression of the proto-oncogene rather the random acquisition of growth enhancing mutations, the chance of the latter being high due to the p53 mutation and DNA mutations produced by retroviral transduction.

In Figure 5.18 parallel cultures of *Trp53* wildtype or mutant B cells were transduced with the different vector combinations, and harvested and analysed before washing out anti-CD40 on Day 3 or after being placed back in culture without anti-CD40 for 4, 8, 12 or 22 days.

On Days 3 and 7 there was little detectable difference in the frequency of cells expressing the different *DsRed* vectors, with the exception that the frequency of *DsRed/Myb* single positive and double positive cells was lower than with the other *DsRed* vectors, and the positive cells had lower DsRed fluorescence as had been noted earlier. By Day 11 there were few viable cells remaining in all the cultures, with the exception of cultures of *Trp53* mutant dual transduced with *DsRed/Myb* and *GFP/MYC* where a distinct population of GFP^{hi} $DsRed^{negative}$ cells was present. This population of GFP^{hi} $DsRed^{negative}$ cells increased in frequency to account for 83% of viable cells on Day 15, and 96% of the cells by day 25. No distinct population of GFP^{hi} $DsRed^{negative}$ cells consistently developed in *Trp53* wildtype cells transduced with the same *Myb* + *MYC* combination, nor did any single or doubly transduced B cells increase in frequency in cultures of *Trp53*-mutant B cells transduced with any of the other vector combinations. Equivalent results were obtained in three independent experiments comparing the different vectors.

I concluded from these experiments that retroviral expression of *Ikbkb, Laptm5* or *Lmo2* was not sufficient to induce B cells to proliferate in the absence of exogenous growth stimuli, even as a "third hit" paired with enforced *MYC* and inactive *Trp53*. By contrast, the *DsRed/Myb* vector triggered spontaneous proliferation of a substantial subset of B cells only when combined with *MYC* and mutant *Trp53*. These observations were pursued in more detail as described below.

Figure 5.18 Representative flow cytometric plots at various time points

Antigen-activated Ig^{HEL} B cells with wild type or inactive p53 were transduced with the indicated vectors and cultured for up to 24 days in RPMI complete medium. Profiles are gated on viable (7AAD negative) cells and show the percentage that are singly positive for GFP or DsRed or double positive. The non transduced and control cells (top panels at each time point) were used to determine gate position and were not in culture for the same duration as the transduced cells.

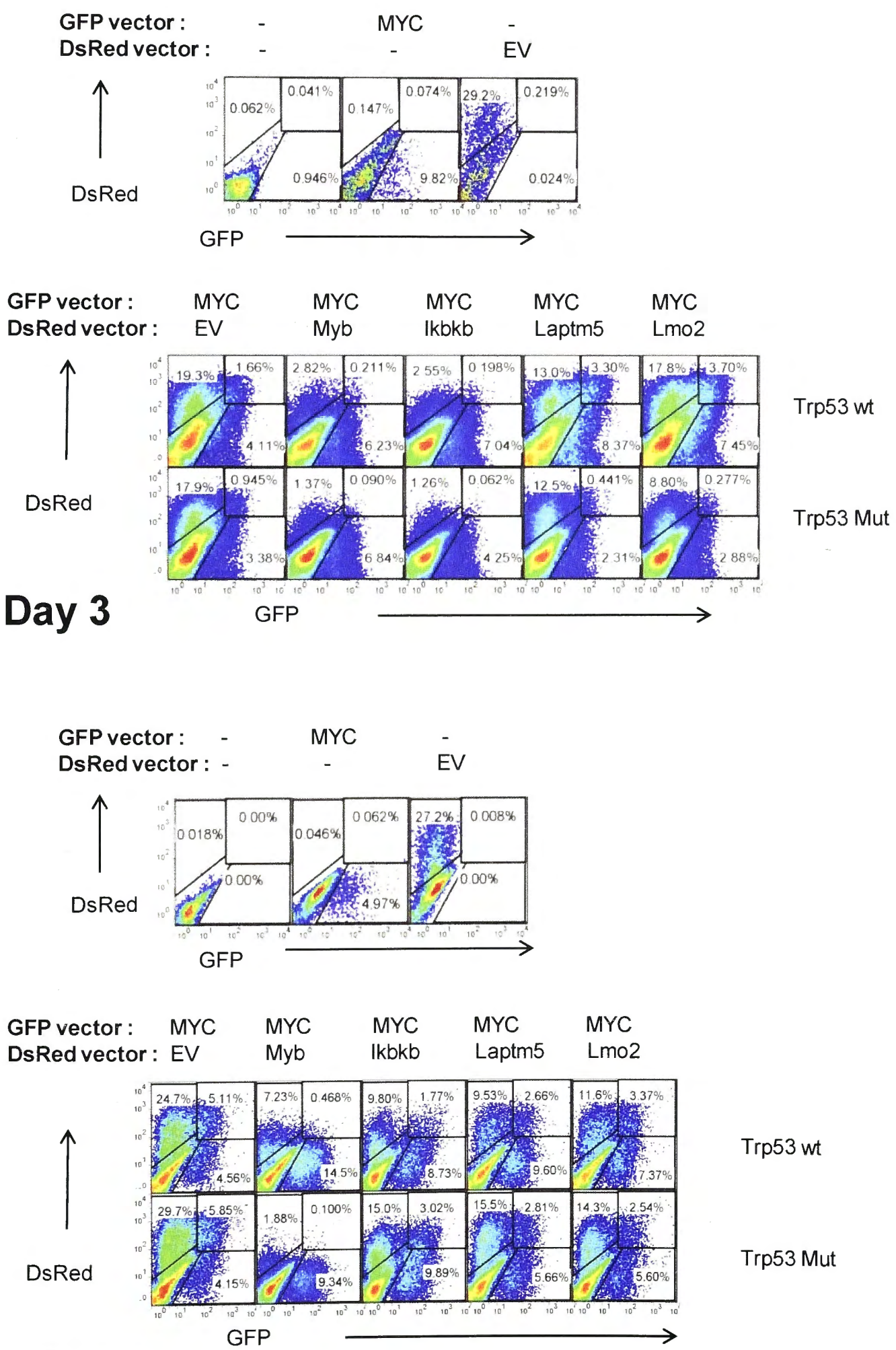

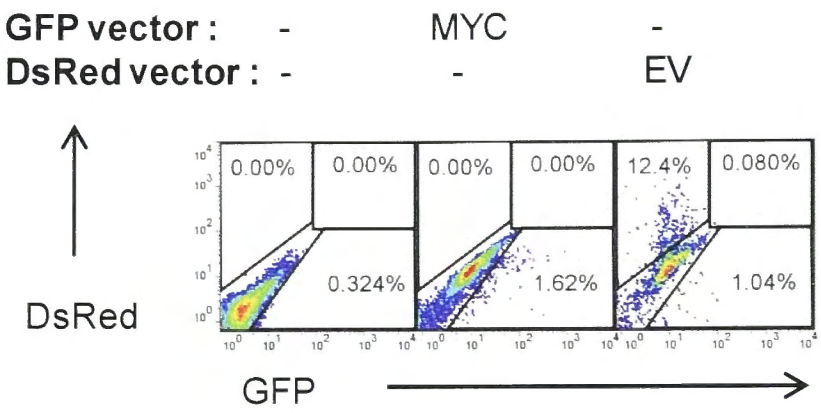
GFP vector : - MYC -
DsRed vector : - - EV
0.00% 0.00% 0.00% 0.00% 12.4% 0.080%
0.324% 1.62% 1.04%
DsRed
GFP

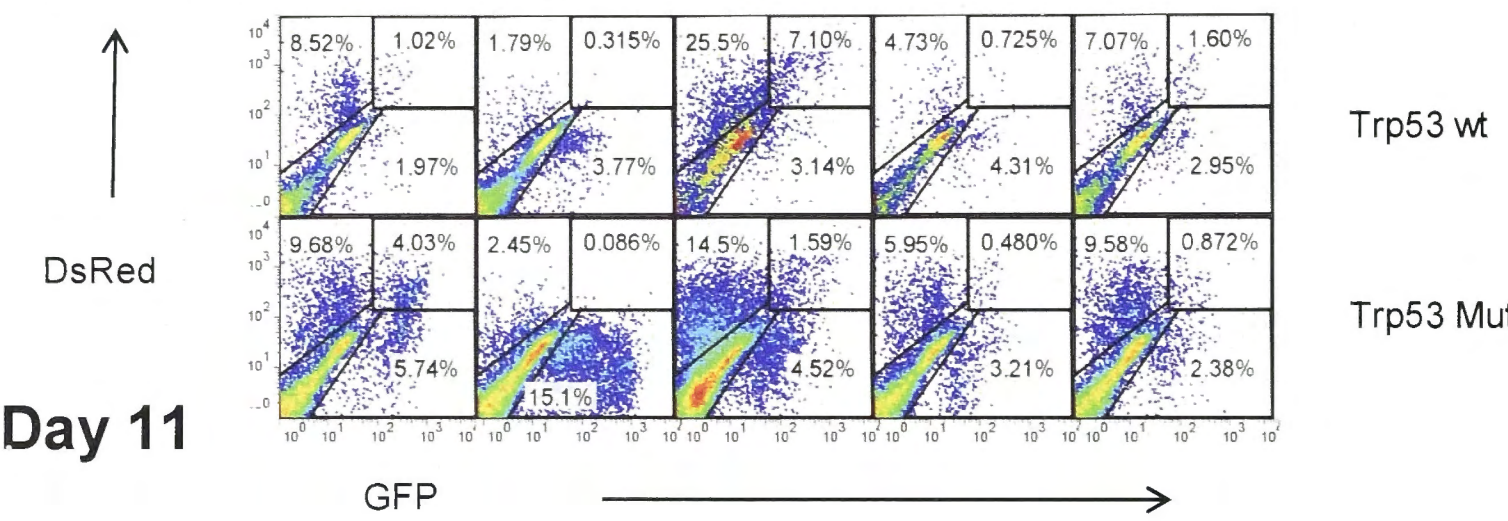
GFP vector : MYC MYC MYC MYC MYC
DsRed vector : EV Myb Ikbkb Laptm5 Lmo2
8.52% 1.02% 1.79% 0.315% 25.5% 7.10% 4.73% 0.725% 7.07% 1.60%
1.97% 3.77% 3.14% 4.31% 2.95%
9.68% 4.03% 2.45% 0.086% 14.5% 1.59% 5.95% 0.480% 9.58% 0.872%
5.74% 15.1% 4.52% 3.21% 2.38%
DsRed
GFP
Trp53 wt
Trp53 Mut
Day 11

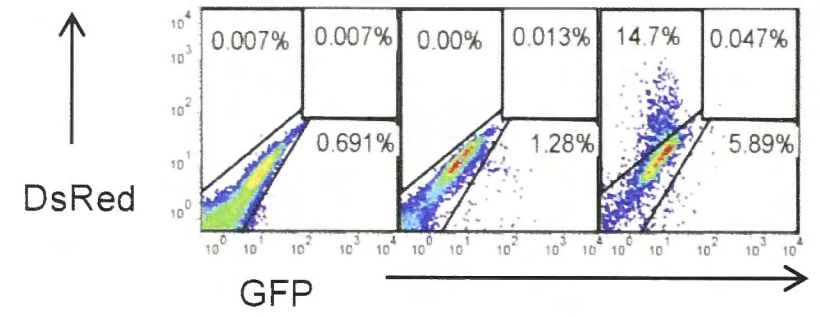
GFP vector : - MYC -
DsRed vector : - - EV
0.007% 0.007% 0.00% 0.013% 14.7% 0.047%
0.691% 1.28% 5.89%
DsRed
GFP

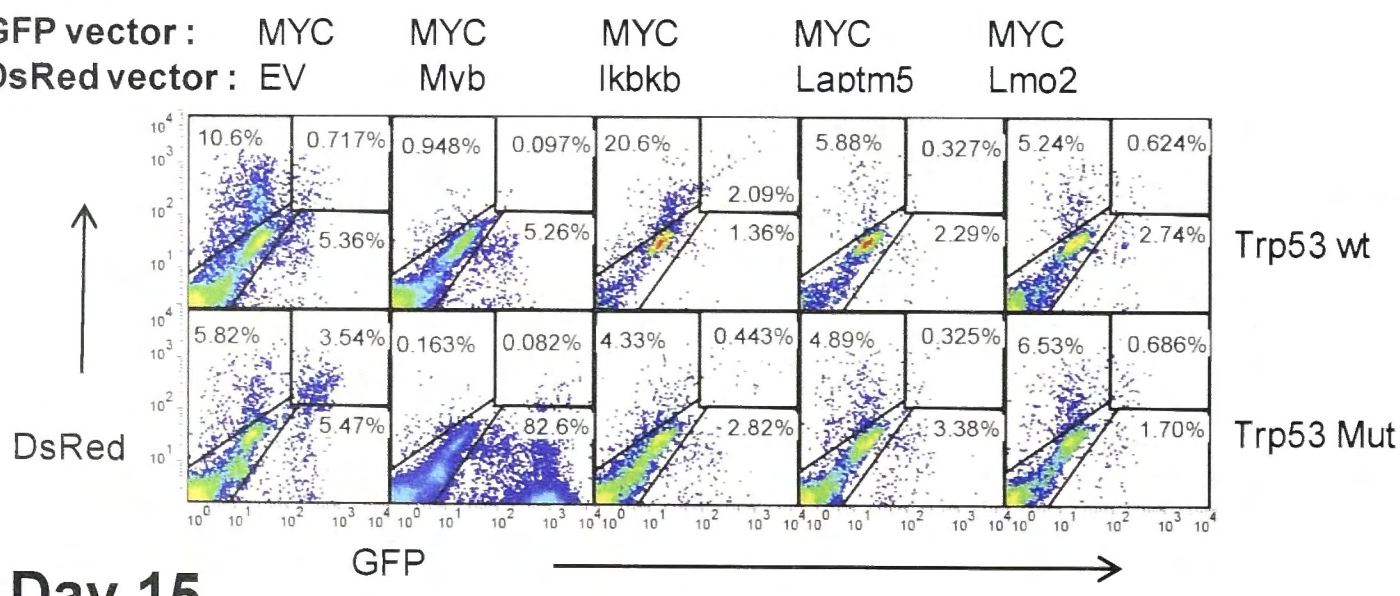
GFP vector : MYC MYC MYC MYC MYC
DsRed vector : EV Myb Ikbkb Laptm5 Lmo2
10.6% 0.717% 0.948% 0.097% 20.6% 5.88% 0.327% 5.24% 0.624%
5.36% 5.26% 2.09% 1.36% 2.29% 2.74%
5.82% 3.54% 0.163% 0.082% 4.33% 0.443% 4.89% 0.325% 6.53% 0.686%
5.47% 82.6% 2.82% 3.38% 1.70%
DsRed
GFP
Trp53 wt
Trp53 Mut
Day 15

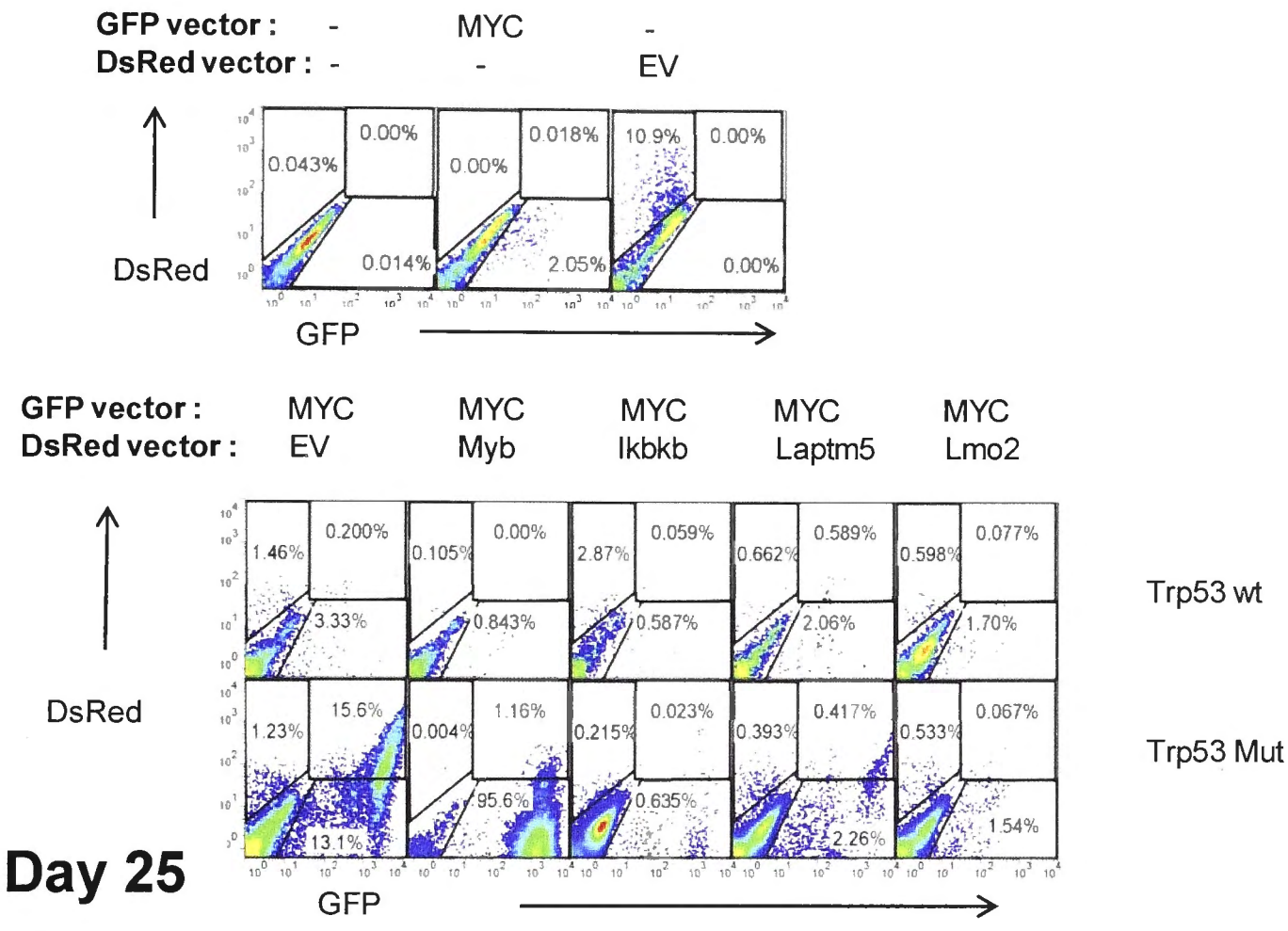
GFP vector : - MYC -
DsRed vector : - - EV
DsRed
0.043%
0.00%
0.014%
0.00%
0.018%
2.05%
10.9%
0.00%
0.00%
GFP
GFP vector : MYC MYC MYC MYC MYC
DsRed vector : EV Myb Ikbkb Laptm5 Lmo2
DsRed
1.46%
0.200%
3.33%
0.105%
0.00%
0.843%
2.87%
0.059%
0.587%
0.662%
0.589%
2.06%
0.598%
0.077%
1.70%
1.23%
15.6%
13.1%
0.004%
1.16%
95.6%
0.215%
0.023%
0.635%
0.393%
0.417%
2.26%
0.533%
0.067%
1.54%
GFP
Trp53 wt
Trp53 Mut
Day 25

5.6.1 Enumerating total number of transduced B cells over time in culture without growth stimulants

To extend the findings above, triplicate cultures with each vector and cell combination were harvested at each timepoint and the numbers of viable cells per ml in each well was counted using a haemocytometer and integrated with the flow cytometric analyses to calculate the total number of cells expressing the different vectors. The results for the *Myb+MYC* combination are shown in Figure 5.19 and Figure 5.20, and for the other vector combinations in Figure 5.21 and Figure 5.22.

As before, a prominent population of GFP^{hi} $DsRed^{negative}$ B cells began to be detectable by Day 11 and accounted for 20-40% of viable cells in cultures transduced with Myb and MYC, but only if the B cells were *Trp53* mutant. GFP^{low} $DsRed^{negative}$ B cells were increased as a percentage in two of three Day 15 cultures of *Trp53* wildtype cells transduced with Myb and MYC (Fig 5-18). However when absolute numbers of GFP+ cells per culture was calculated (Fig 5-20b), these numbers steadily declined over time in control cultures with wildtype *Trp53* or with *DsRed*/Empty Vector in place of *DsRed/Myb*. In contrast, in the Myb+MYC *Trp53* mutant cultures the total number of GFP+ cells stopped declining by Day 11 and began to increase by Day 15. This appeared to result from gradual proliferation of initially rare GFP^{hi} $DsRed^{negative}$ B cells, and this was confirmed and extended as described later.

Analysis of triplicate cultures with the *GFP/MYC* and either *DsRed/Lmo2* or *DsRed/Laptm5* (Figure 5.21 and Figure 5.22) revealed a steady decline in the total number of DsRed- single positive and DsRed+ GFP+ dual positive cells over the timecourse from Day 3 when anti-CD40 was withdrawn, through Days 7, 11 and 15. The progressive loss of single and double-transduced B cells with these vectors paralleled that of single and double-transduced cells with *DsRed*/Empty Vector and *GFP/MYC* (Fig 5-22b and c). This reinforced the conclusion above that enforced expression of *Laptm5* or *Lmo2* was not sufficient to induce B cell proliferation alone or combined with overexpressed *MYC* and mutant *Trp53*.

By contrast, in cultures transduced with the *DsRed/Ikbkb* vector and *GFP/MYC*, there was a 5-10 fold increase in the percentage and absolute number of DsRed- single positive and DsRed+ GFP+ dual positive cells between Day 3, when anti-CD40 was withdrawn, and Day 7 (Figure 5.21 and Figure 5.22b and c). This result, together with the evidence in the preceding section that the *DsRed/Ikbkb* vector caused an increase in cell size, indicates that enforced expression of *Ikbkb* was sufficient to induce B cells to proliferate in the absence of anti-CD40, both on its own and in cells doubly transduced with *GFP/MYC*. However the proliferation did not continue after Day 7, and instead the numbers of DsRed- single positive and DsRed+ GFP+ dual positive cells expressing *Ikbkb* steadily declined on Days 11 and 15 (Figure 5.22b and c). I conclude from this that retroviral expression of *Ikbkb* induces a transient burst of B cell proliferation that is self-limiting after 4 days. As discussed later, this conclusion has been confirmed in independent studies of B cells retrovirally transduced to express a constitutively active *Ikbkb* by another PhD student Yogesh Jeelall [101].

Figure 5.19 Consequences of overexpression of *Myb* and *MYC*

Antigen-activated Ig^{HEL} B cells with wild type or inactive p53 were transduced with the indicated vectors and cultured for up to 12 days in RPMI complete medium. Profiles are gated on viable (7AAD negative) cells and show the percentage that are singly positive for GFP or DsRed or double positive. The non transduced and control cells (top panels at each time point) were used to determine gate position and were not in culture for the same duration as the transduced cells. Data is shown in triplicate after Day 3.

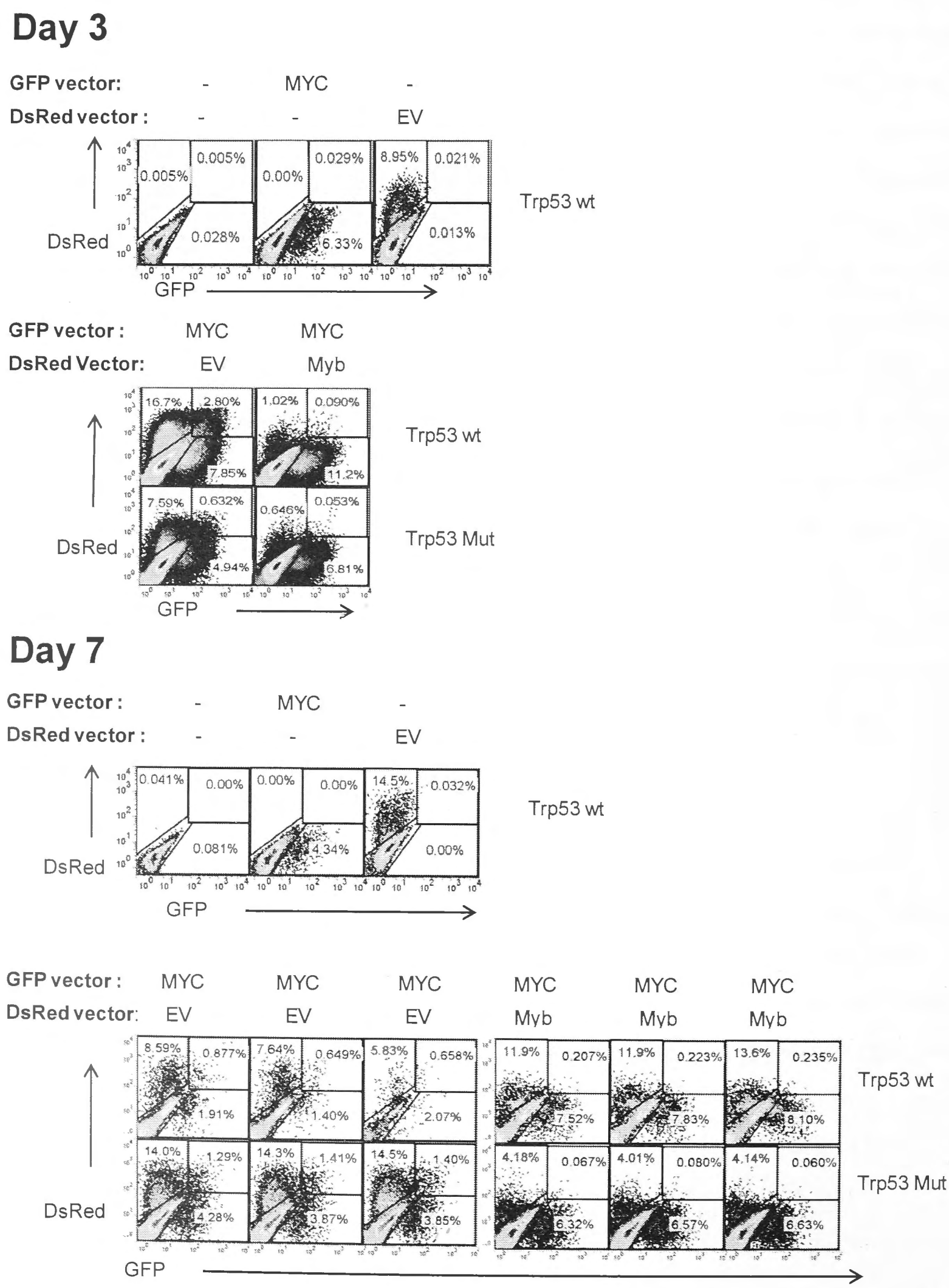

Day 11

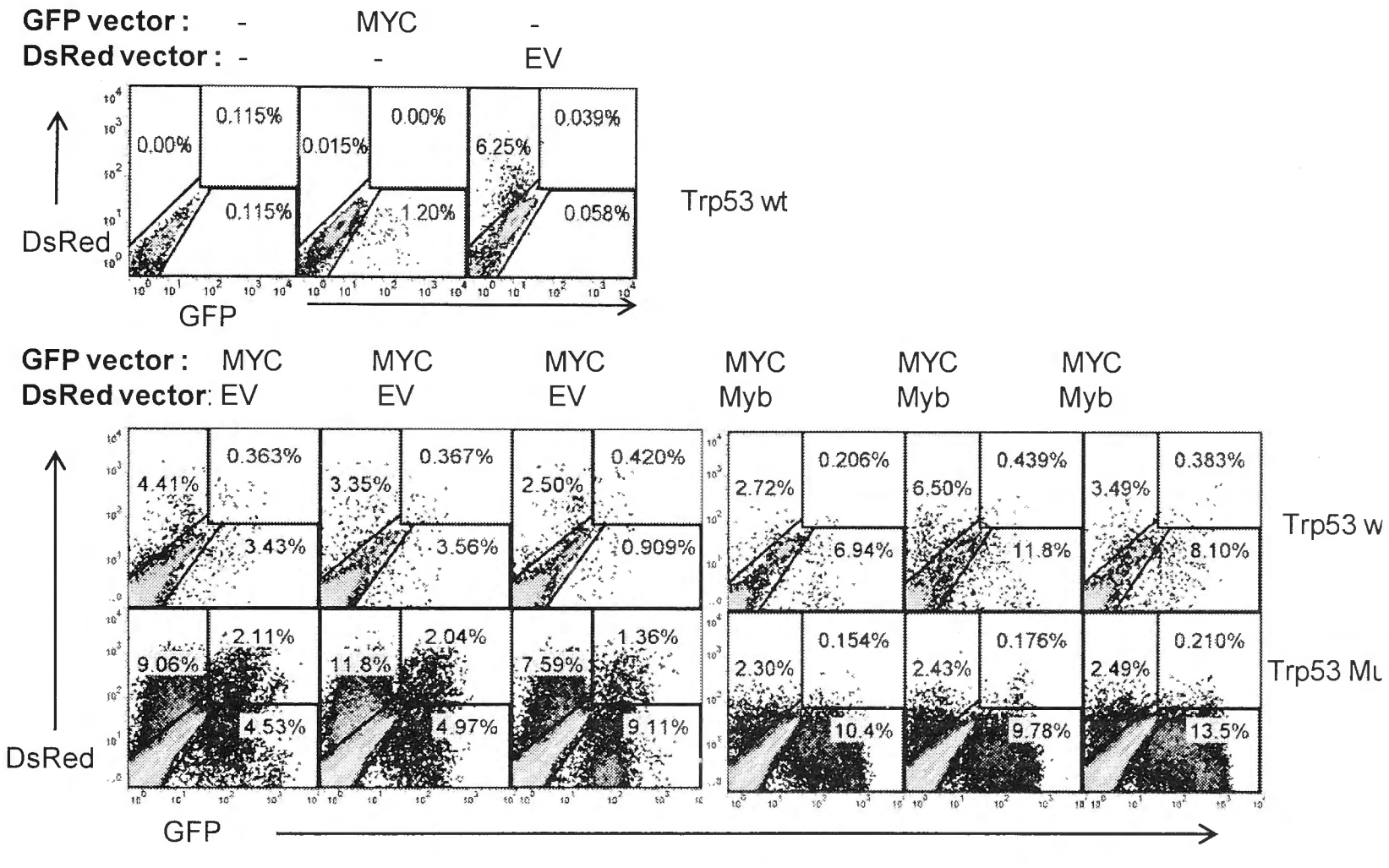
GFP vector : - MYC -
DsRed vector : - - EV
0.00%
0.115%
0.115%
0.015%
0.00%
1.20%
6.25%
0.039%
0.058%
Trp53 wt
DsRed
GFP
GFP vector : MYC MYC MYC MYC MYC MYC
DsRed vector: EV EV EV Myb Myb Myb
4.41%
0.363%
3.43%
3.35%
0.367%
3.56%
2.50%
0.420%
0.909%
2.72%
0.206%
6.94%
6.50%
0.439%
11.8%
3.49%
0.383%
8.10%
9.06%
2.11%
4.53%
11.8%
2.04%
4.97%
7.59%
1.36%
9.11%
2.30%
0.154%
10.4%
2.43%
0.176%
9.78%
2.49%
0.210%
13.5%
Trp53 w
Trp53 Mu
DsRed
GFP

Day 15

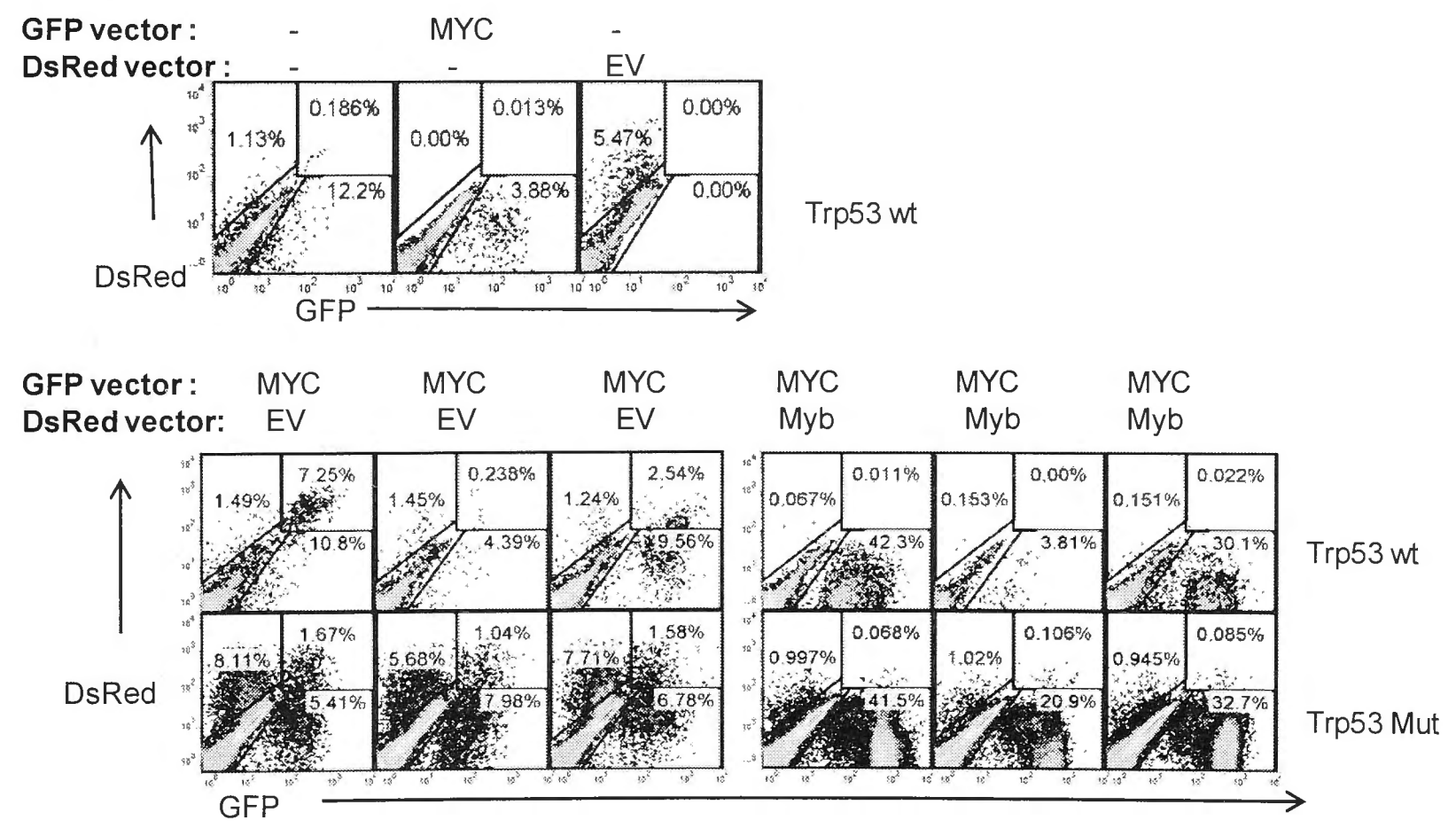
GFP vector : - MYC -
DsRed vector : - - EV
1.13%
0.186%
12.2%
0.00%
0.013%
3.88%
5.47%
0.00%
0.00%
Trp53 wt
DsRed
GFP
GFP vector : MYC MYC MYC MYC MYC MYC
DsRed vector: EV EV EV Myb Myb Myb
1.49%
7.25%
10.8%
1.45%
0.238%
4.39%
1.24%
2.54%
9.56%
0.067%
0.011%
42.3%
0.153%
0.00%
3.81%
0.151%
0.022%
30.1%
8.11%
1.67%
5.41%
5.68%
1.04%
7.98%
7.71%
1.58%
6.78%
0.997%
0.068%
41.5%
1.02%
0.106%
20.9%
0.945%
0.085%
32.7%
Trp53 wt
Trp53 Mut
DsRed
GFP

Figure 5.20 Cell counts with time

Cells described in Figure 5.19 were counted using a haemocytometer (in triplicate) and results were correlated with the FACS results to determine a) the percentage of GFP positive cells of total cells b) the number of GFP positive cells per ml culture medium c) the number of non transduced (not expressing a fluorescent protein) cells per ml in wells with varying dysregulated gene combinations. Error bars reflect standard deviation.

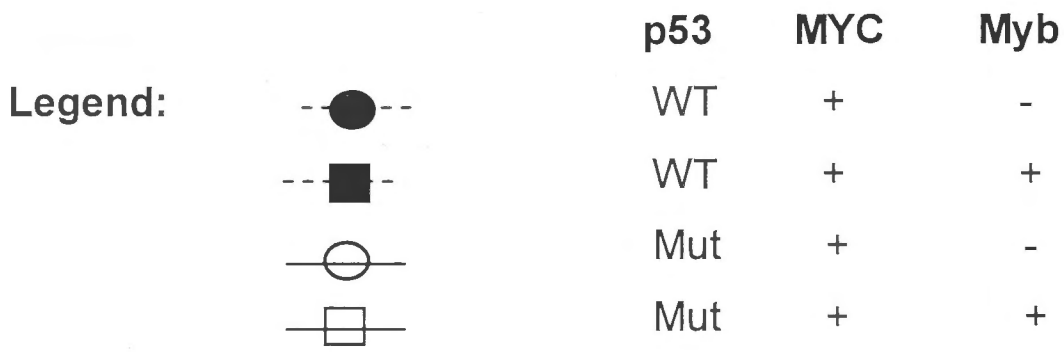

a)

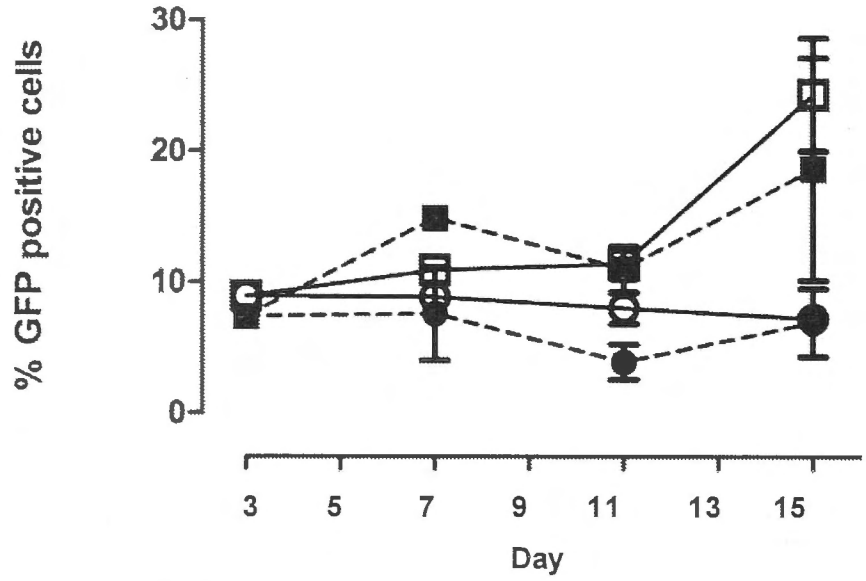

b)

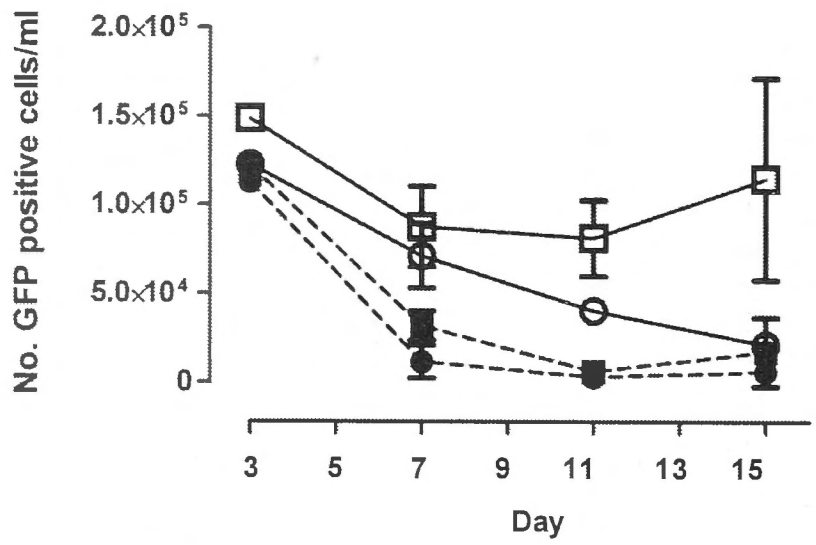

c)

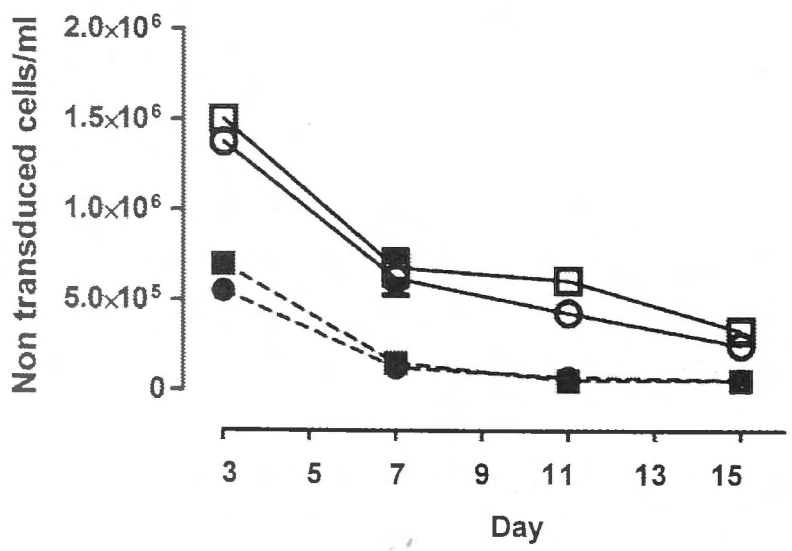

The effect of dysregulation of the *Ikbkb*, *Laptm5* or *Lmo2* in conjunction with *MYC* overexpression were less striking so only the results in p53 defective cells are shown in triplicate in Figure 5.21. Differences in cell counts with time (Figure 5.22) similarly focused on p53 defective cells, attempting to dissect out initial variations in cell proliferation prior to the inevitable cell death seen in these cells when deprived of growth factors.

Figure 5.21 Consequences of overexpression of *Ikbkb*, *Laptm5* or *Lmo2* in conjunction with *MYC* compared to Empty vector (EV)

Antigen-activated Ig^{HEL} B cells with inactive p53 were transduced with the indicated vectors, washed to remove anti-CD40 on Day 3 and cultured for up to 12 days in RPMI complete medium. Profiles are gated on viable (7AAD negative) cells and show the percentage that are singly positive for GFP or DsRed or double positive. The non transduced and control cells (top panels at each time point) were used to determine gate position and were not in culture for the same duration as the transduced cells.

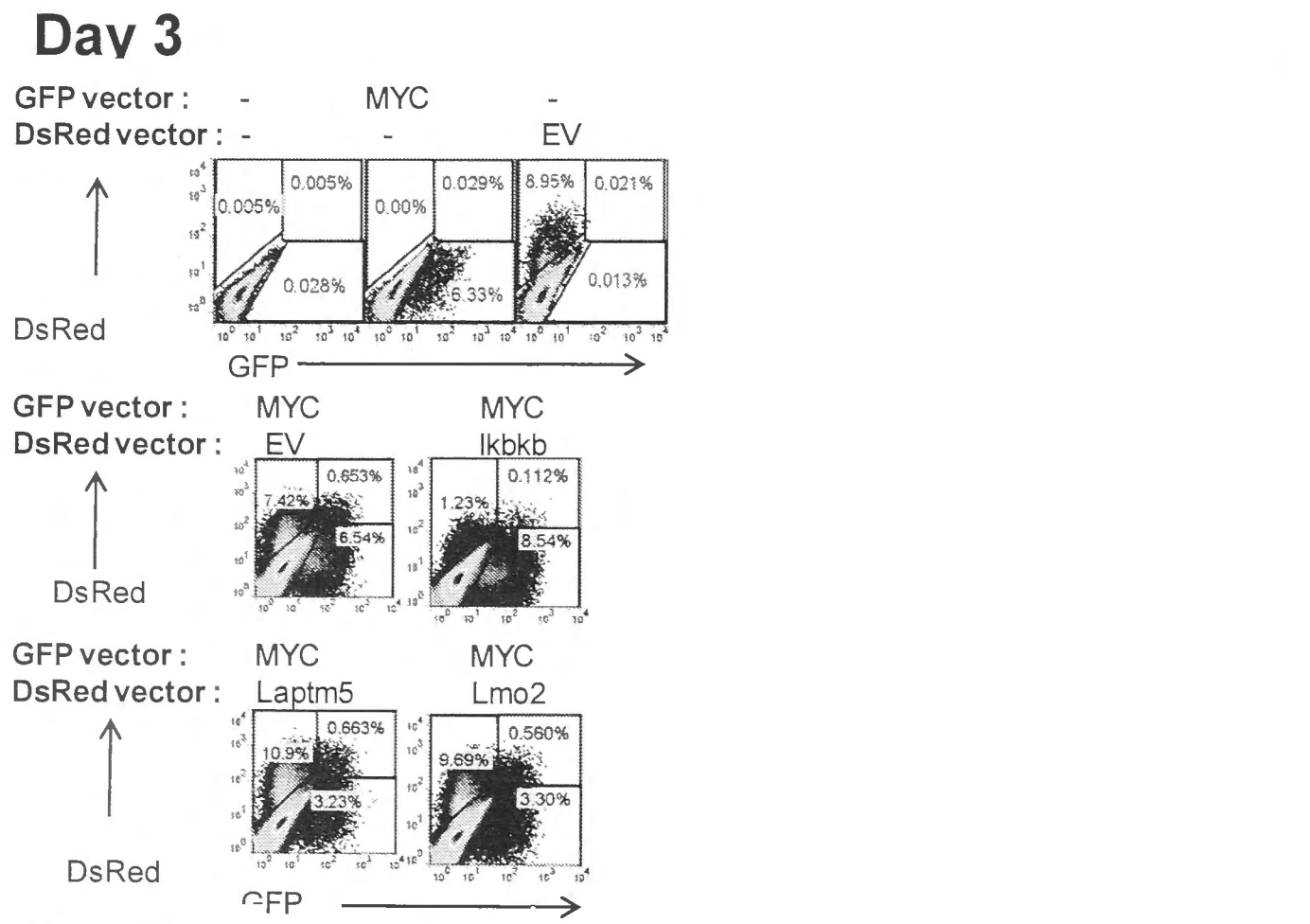

Day 11

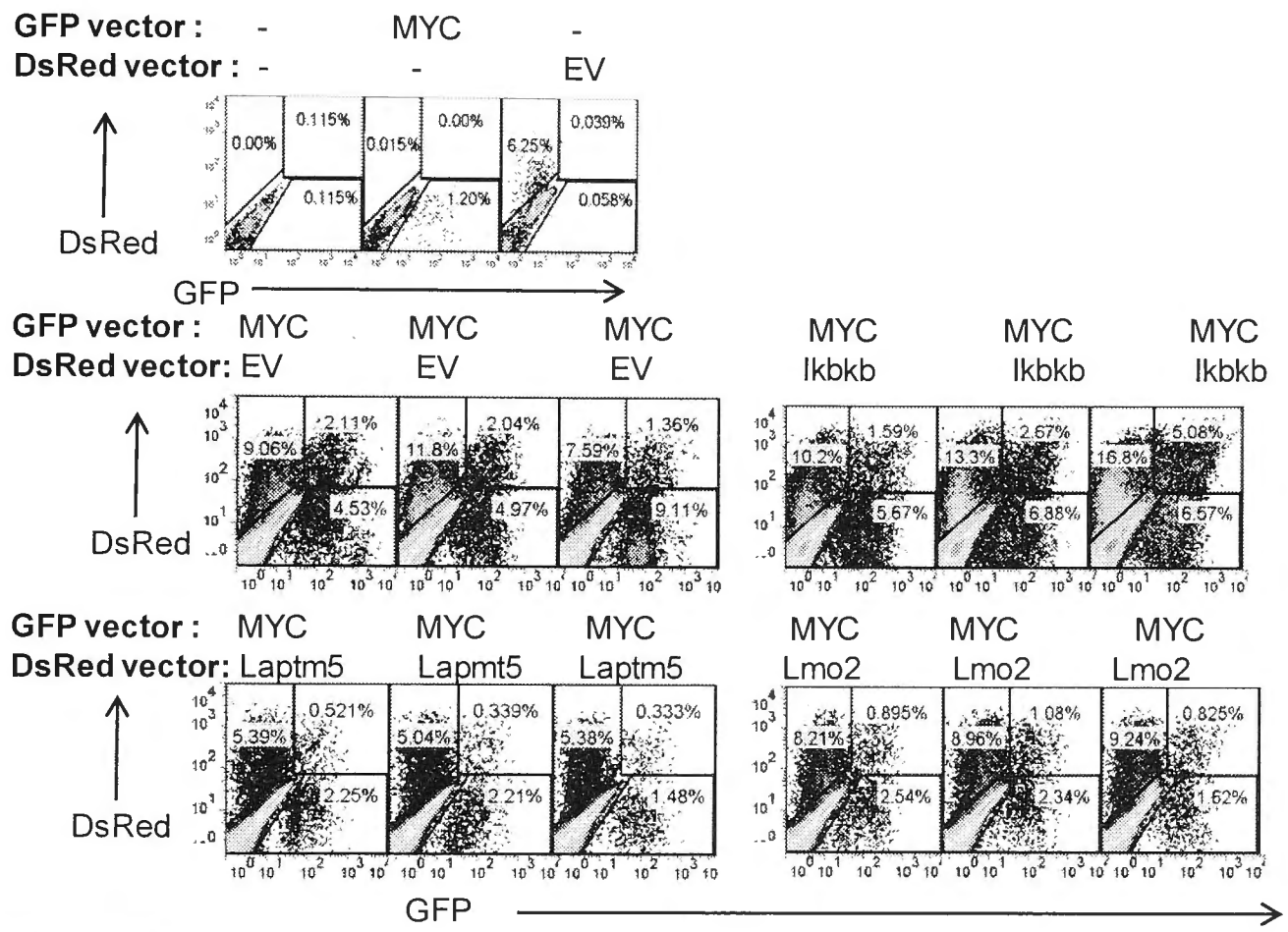
GFP vector : - MYC -
DsRed vector : - - EV
0.00% 0.115% 0.115%
0.015% 0.00% 1.20%
6.25% 0.039% 0.058%
DsRed
GFP
GFP vector : MYC MYC MYC MYC MYC MYC
DsRed vector: EV EV EV Ikbkb Ikbkb Ikbkb
9.06% 2.11% 4.53%
11.8% 2.04% 4.97%
7.59% 1.36% 9.11%
10.2% 1.59% 5.67%
13.3% 2.67% 6.88%
16.8% 5.08% 6.57%
DsRed
GFP vector : MYC MYC MYC MYC MYC MYC
DsRed vector: Laptm5 Lapmt5 Laptm5 Lmo2 Lmo2 Lmo2
5.39% 0.521% 2.25%
5.04% 0.339% 2.21%
5.38% 0.333% 1.48%
8.21% 0.895% 2.54%
8.96% 1.08% 2.34%
9.24% 0.825% 1.62%
DsRed
GFP

Day 15

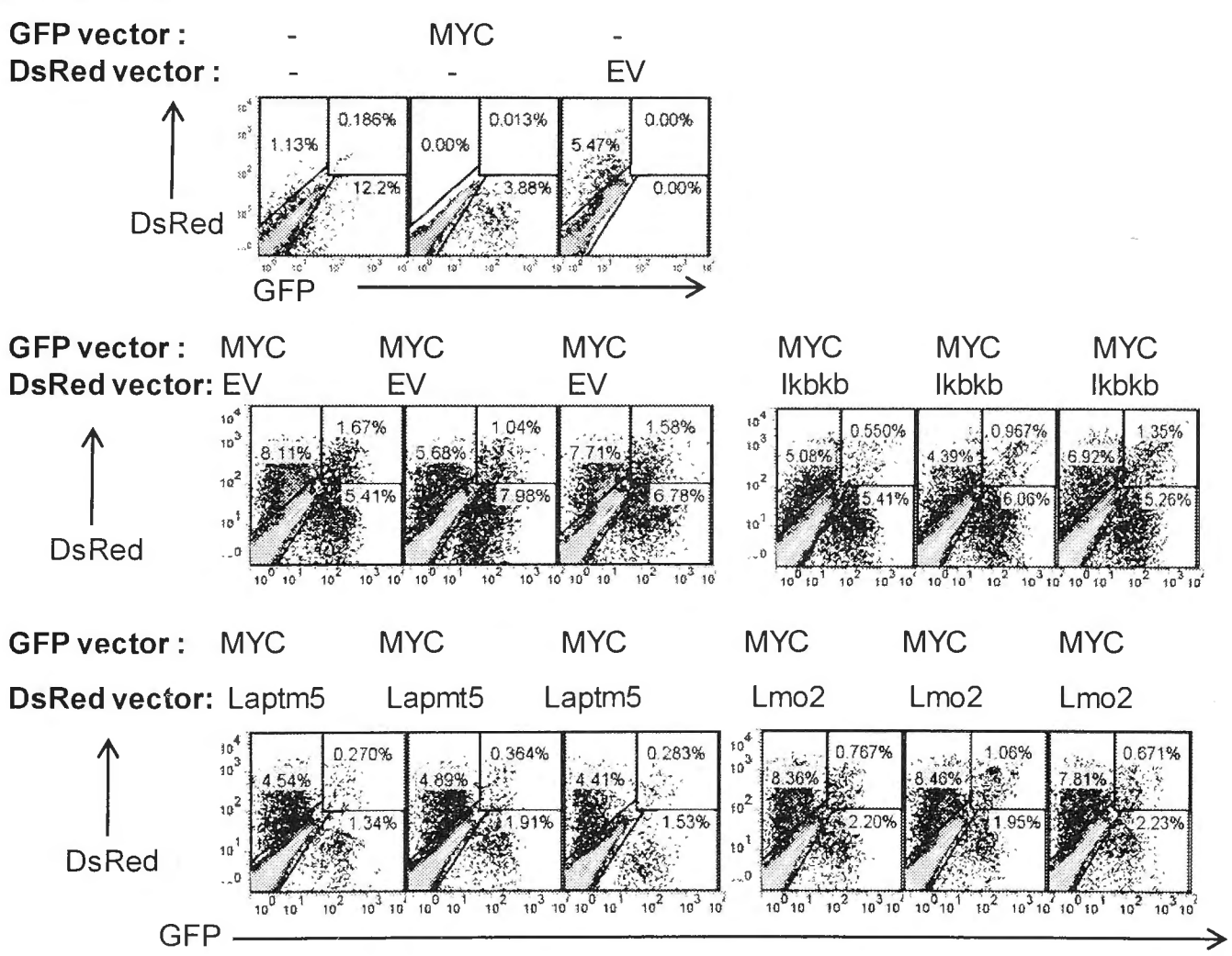
GFP vector : - MYC -
DsRed vector : - - EV
1.13% 0.186% 12.2%
0.00% 0.013% 3.88%
5.47% 0.00% 0.00%
DsRed
GFP
GFP vector : MYC MYC MYC MYC MYC MYC
DsRed vector: EV EV EV Ikbkb Ikbkb Ikbkb
8.11% 1.67% 5.41%
5.68% 1.04% 7.98%
7.71% 1.58% 6.78%
5.08% 0.550% 5.41%
4.39% 0.967% 6.06%
6.92% 1.35% 5.26%
DsRed
GFP vector : MYC MYC MYC MYC MYC MYC
DsRed vector: Laptm5 Lapmt5 Laptm5 Lmo2 Lmo2 Lmo2
4.54% 0.270% 1.34%
4.89% 0.364% 1.91%
4.41% 0.283% 1.53%
8.36% 0.767% 2.20%
8.46% 1.06% 1.95%
7.81% 0.671% 2.23%
DsRed
GFP

Figure 5.22 Cell counts with time

Cells harvested at different times after removal of anti-CD40 from triplicate cultures transduced with the indicated vector combinations, as analysed by flow cytometry in Figure 5.21 , were counted using a haemocytometer (in triplicate) to calculate the mean number per culture and standard deviation of: (a) GFP single positive cells; b) GFP + DsRed dual positive cells; c) DsRed single positive cells; d) GFP + DsRed double negative cells.

a) GFP positive cells
b) Dual positive cells
c) DsRed positive cells
d) Non transduced cells

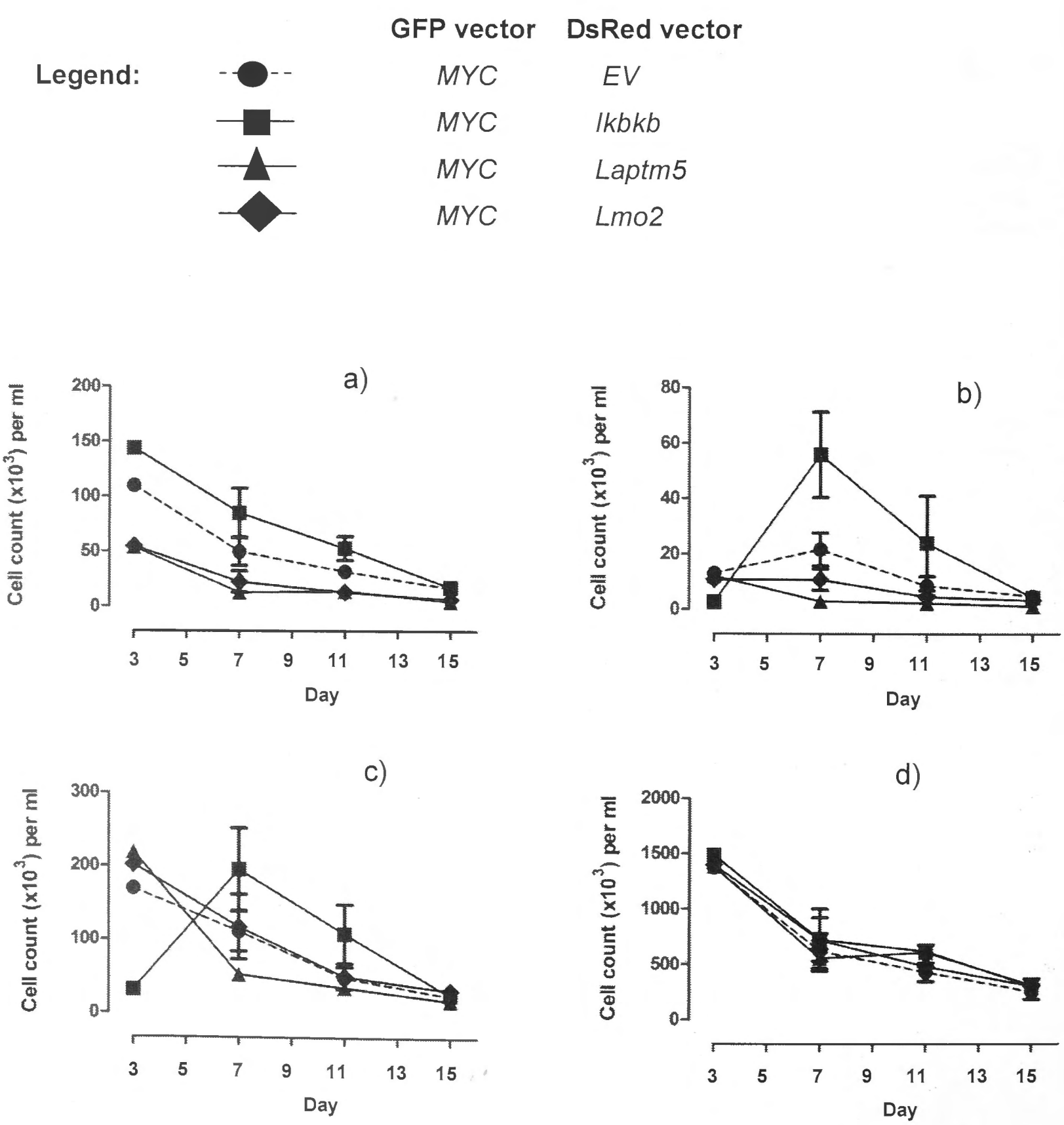

5.6.2 Phenotype of *MYC/Myb* dual transduced B cells

The results above indicated that *Myb* and *Ikbkb* both had the capacity to induce B cell proliferation in cultures lacking B cell mitogens, but the proliferation induced by each had fundamentally different characteristics. The retroviral vector encoding *Ikbkb* was sufficient on its own (without *MYC/GFP*) to induce a transient burst of proliferation of most of the transduced DsRed+ B cells, which peaked 4 days after removing anti-CD40 (Day 7) and then ceased. By contrast, the *DsRed* retroviral vector encoding *Myb* induced sustained proliferation but only by a subset of B cells with an initially rare GFP^{hi} phenotype. Paradoxically, these *DsRed/Myb*-transformed B cells did not express detectable levels of *DsRed* itself. This unusual subset of proliferating B cells were undetectable on Day 7, when the *Ikbkb*-induced proliferation had peaked, and only became frequent in the cultures on Days 11-15. Additional experiments were therefore performed to characterize the proliferating cells in *Myb-MYC* co-transduced $Trp53^{Bbl/Bbl}$ cultures and test if they would continue proliferating for long periods. After 30 days in culture without anti-CD40, the GFP^{hi} $DsRed^{-}$ population continued to increase in frequency and number and when compared to non-transduced B cells that had been activated but then cultured without anti-CD40 for 4 days, the Myb-induced outgrowths displayed moderately increased FSC, equally high levels of cell surface B220 and increased cell surface IgM (Figure 5.23). This analysis identified them as mature B cells. As before, the levels of GFP fluorescence were uniformly high, while there was negligible DsRed fluorescence above the background autofluorescence of activated B cells.

Figure 5.23 Abbreviated phenotype of cells persisting at Day 30

Antigen-activated Ig^{HEL} B cells with mutated p53 were doubly transduced with the *MYC/GFP* and *Myb/DsRed* vectors and cultured for 30 days in RPMI complete medium. The profiles are gated on viable (7AAD negative) cells. The control cells (left column) were viable non transduced splenocytes 7 days post activation of the B cell receptor and 4 days after removal of anti-CD40 from the culture.

The median forward scatter for transduced and non transduced cells is shown with a dashed line (320 units for non transduced, 376 units for *Myb/MYC* transduced).

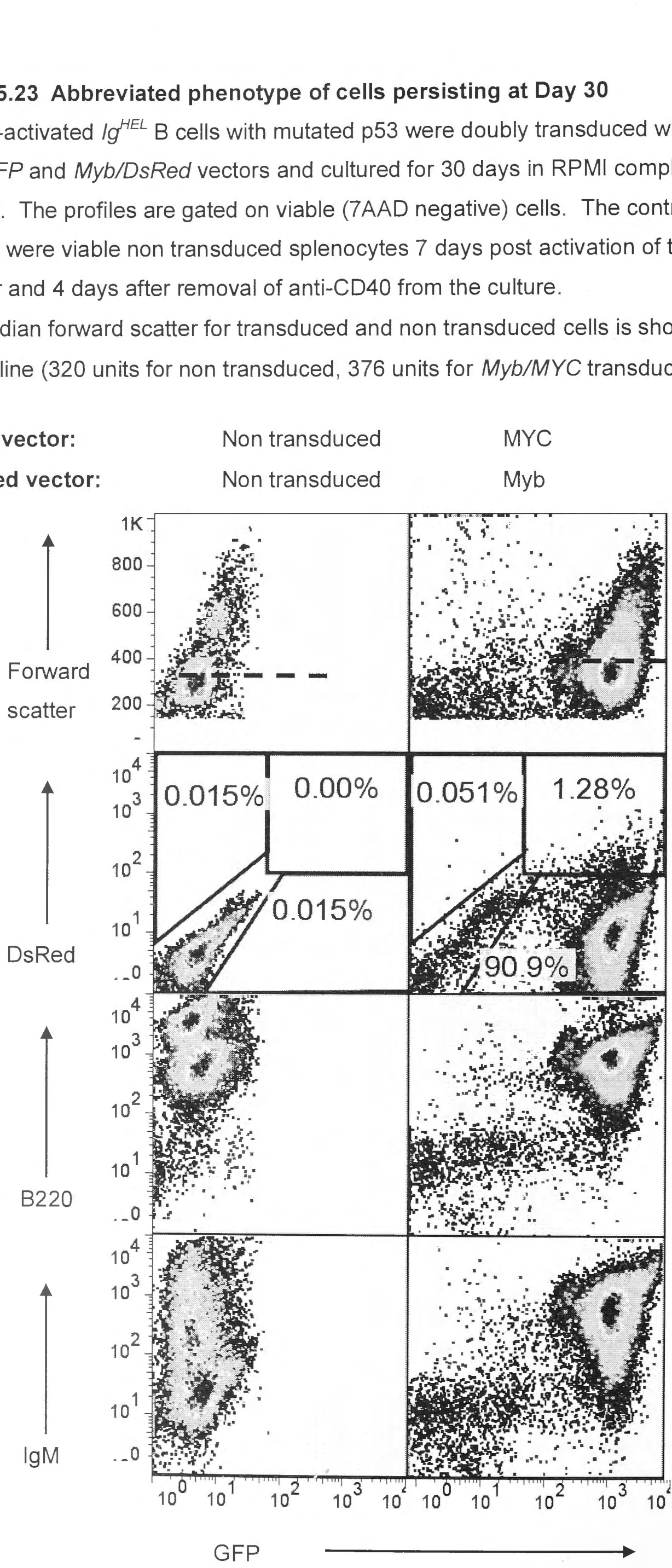

5.6.3 Growth kinetics of *MYC/Myb* dual transduced B cells

Myb/MYC doubly-transduced *Trp53* mutant B cells continued to grow in culture for at least 8-12 weeks without added B cell growth stimulus, provided that the cultures were split intermittently (guided by visible acidity of cultures, on average every 4-8 days) to dilute the cells (approximately 1/10) in fresh media. This confirmed that the combination of the *Myb* and *MYC* vectors and p53 inactivation were sufficient to transform a subset of mature B cells into continuous, mitogen-independent mature B cell lines in culture with high reproducibility. The growth kinetics of these B cell lines (Figure 5.24) after sub-culture revealed that the cell numbers quadrupled in the first 4 days and doubled again by 8 days, implying an initial doubling time of approximately 2 days if there was no loss due to apoptosis. The actual doubling time may be faster, as it is likely that daughter cells are lost due to apoptosis. In the future, it would be useful to obtain more accurate measures of division rate using CFSE labelling and dilution. By comparison, the proliferative rate of well-studied Burkitt cell lines similarly grown in RPMI supplemented with fetal calf serum and penicillin, streptomycin and glutamine is approximately 24 hours [445,453].

As noted previously, very few GFP^{hi} $DsRed^{-}$ cells comparable to the transformed cell lines were present in the first 6 days of culture, but these progressively increased after 10 days, implying that they derived from relatively rare transformed precursors in the initial transduced population. Limiting dilution was used to estimate the frequency of B cells that were transformed into spontaneously proliferating B cell lines in culture. $Trp53^{Bbl/Bbl}$ spleen B cells were dual-transduced with *Myb* and *MYC* vectors as before, and on Day 3 (day 2 post spinoculation) the number of viable B cells and percentage expressing *GFP* or *DsRed* was determined by flow cytometry, and 1000 viable B cells were plated out in each of 9 separate 2ml culture wells. On Day 3 21% of the plated cells were GFP+, so that each culture was seeded with 210 *GFP/MYC* transduced B cells, and 0.08% were DsRed+ GFP+ double positive (but this number may be an underestimate of dual transduced cells if many *DsRed* transduced B cells express too little *DsRed* to detect by flow cytometry).

Twenty days later, each culture was harvested and the cells counted and analysed by flow cytometry (Figure 5.25). In 4 of the 9 cultures, large GFP^{high} cells had increased to more than 20,000 cells per culture, representing 100 times the input number of GFP+ B cells, resulting in populations ranging from 37,475 cells to 80,640 GFP+ cells per culture. Three other wells had much smaller expansions of 1413, 2698, and 4724 large GFP^{high} cells (Figure 5.25).

Based on limiting dilution calculations derived from the Poisson distribution [388], the occurrence of highly proliferating B cells (increased more than 100 fold over starting GFP+ numbers) in 44% of the wells is consistent with the majority of wells with cell growth being derived from a single cell. Thus, a minimum estimate of the frequency of transduced B cells transformed into highly proliferating lines is 1 cell in 210, based on each culture having been seeded with 210 GFP+ cells. This represents very efficient transformation of mature B cells, and is likely to be an underestimate of the transformation efficiency since each culture was seeded with many fewer doubly transduced B cells. The observation that *DsRed* was expressed weakly from the IRES-*DsRed* vector containing *Myb* compared to Empty-IRES-*DsRed* vector (described in Section 5.2 above) means that the measured input frequency of DsRed+ GFP+ cells (0.08%) is likely to underestimate the actual frequency of double-transduced B cells. An upper estimate for the actual number of double-transduced cells at the start of each culture is 50, based on the percentage of cells doubly transduced with the empty DsRed vector, which is more highly expressed. Consequently, a minimum estimate is that one in fifty *Myb-MYC* dual transduced p53 mutant B cells are transformed into a spontaneously growing clone. This represents a very efficient transformation of mature B cells. If these cultures were indeed monoclonal, the formation of 32,768 or 65,536 GFP+ progeny would require 16-17 cell doublings, assuming no loss from cell death. Since these populations were formed in 20 days, it can be inferred that the transformed B cells divided approximately once per day.

In future studies, it would be interesting to repeat this experiment with flow sorted cells selected either for GFP single positive or DsRed & GFP double positivity, to more accurately determine the phenotype of the precursor cells and their transformation efficiency.

Figure 5.24 Growth rate in wells containing proliferating *Myb+MYC* co-transduced *Trp53*$^{Bbl/Bbl}$ cells

Trp53 mutant B cells that had been transduced with *Myb* and *MYC* vectors and maintained for greater than 3 weeks in culture without anti-CD40 by serial passage were subcultured in triplicate into fresh medium on Day 0. The number of cells per ml was counted using a haemocytometer on the indicated days. Data is shown in triplicate with the line joining the mean numbers at each time point.

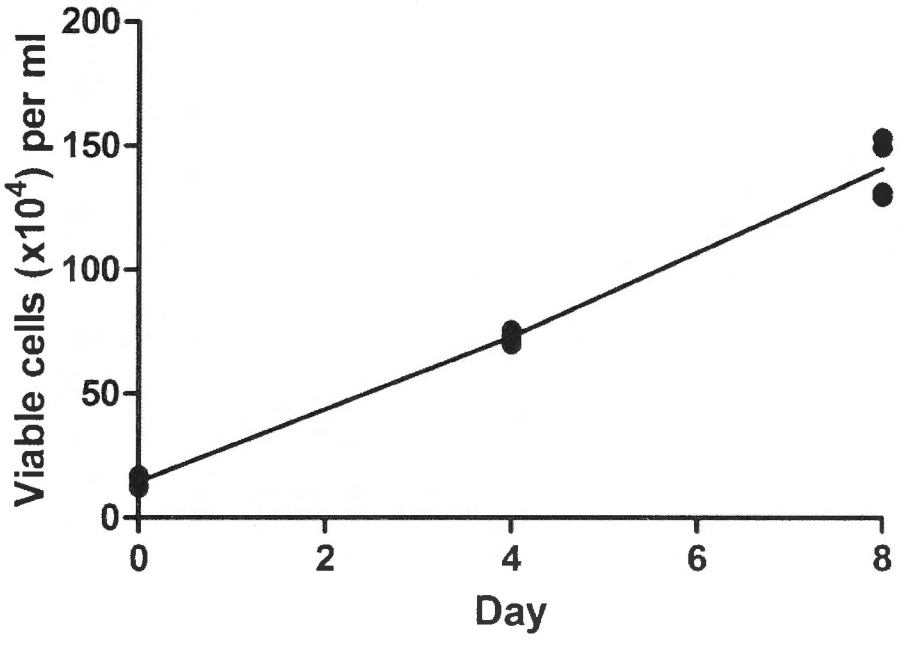

Figure 5.25 Gauging transformation efficiency

Two days post dual retroviral transduction with the *Myb/DsRed* and *MYC/GFP* retroviruses 1000 viable p53 defective B cells were plated out in each of 9 separate 2ml culture wells and incubated at 37°C in RPMI-CM without the addition of exogenous growth factors. Twenty days later the number and percentage of GFP high cells in each of these wells was measured by FACS.

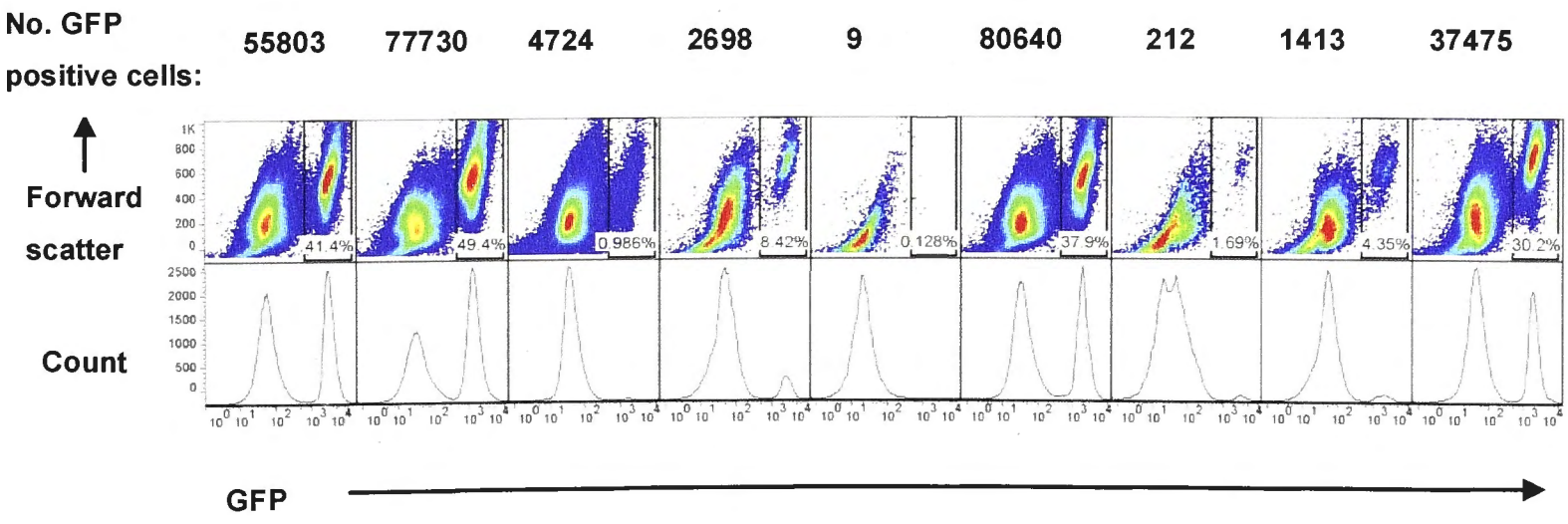

5.6.4 *Myb* Expression in transformed B cells

In contrast to the high expression of the *GFP/MYC* vector in *Myb+MYC* doubly transduced *Trp53* mutant B cell outgrowths, it was remarkable that there was no measurable expression of *DsRed* from the *DsRed/Myb* vector despite the fact that the outgrowths only occurred in wells where the B cells had been transduced with both vectors. As noted earlier, the range of DsRed fluorescence intensity was clearly much lower in *DsRed/Myb* singly-transduced cells than the range exhibited in *DsRed*/Empty vector singly or doubly-transduced B cells (Figure 5.18).

To measure *Myb* mRNA directly, real time PCR with primers complementary to the 5' end of the *Myb* coding sequence was performed on RNA from the spontaneously proliferating *Myb+MYC* dual transduced B cells and from activated B cell controls (Figure 5.26). The calculated relative amount of *Myb* mRNA in the transformed *Myb/MYC* dual transduced cells was much higher than any of the control activated B cell populations. This conclusion was corroborated by independently comparing *Myb* mRNA levels on Affymetrix GeneChip®Gene 1.0 ST Array System for Mouse (Table 5.1). In the microarray analysis, two *Myb+MYC* transduced outgrowths could be best compared to a sample of sorted *GFP/MYC* singly-transduced B cells. These three samples had comparable levels of *PCNA* and *Cyclin A2* mRNA, providing evidence that they were comparably activated into cell cycle. By contrast, the dual-transduced B cells had 15-fold or 32-fold more *Myb* mRNA than the *MYC* singly transduced B cells.

The results above do not resolve whether the large amounts of *Myb* mRNA present in the transformed B cells are derived from the *DsRed/Myb* provirus or from the endogenous *Myb* gene. However since they expressed much higher *Myb* mRNA levels than actively dividing B cells transduced with *MYC* alone, the simplest interpretation of the data is that this *Myb* mRNA derives from the integrated provirus. If this was the case, the proviral mRNA either has lost the IRES-*DsRed* element or that element is not translated into protein. I did not have time to investigate this key issue further, but future studies will need to analyse the sequence and structure of the integrated provirus and its mRNA in

these transformed B cell lines to confirm that the *Myb* mRNA is of proviral origin and test whether or not the IRES-*DsRed* sequence is still present. This could be done by amplification of cDNA using primers that selectively amplify proviral *Myb* mRNA or endogenous cellular *Myb* RNA, taking advantage of the fact that the 5' and 3' untranslated sequences of the proviral and cellular mRNAs differs. The resulting products could be measured both in quantitative PCR and by gel electrophoresis and sequencing.

Figure 5.26 Relative *Myb* expression

Relative *Myb* expression in four different cell types was determined using real time PCR. The dual *MYC/GFP* and *Myb/DsRed* transduced cells had been stably growing in culture for several weeks. Each well contained approximately 33% viable GFP positive cells. The singly transduced cells were not cell sorted, the populations containing between 10 and 30% transduced cells at the time of RNA extraction (Day 3). Activated non transduced cells were activated in vivo and in vitro on Day 0. RNA was extracted 2 days later. Both singly transduced and activated non transduced cells were still in anti-CD40 at the time of RNA extraction. RNA was extracted and cDNA was produced using an oligo (dT) primer-based method. Real time PCR primers annealed to the *Myb* gene at its 5' end and *β Actin* was the reference gene. Non transduced (activated) cells were arbitrarily assigned a relative *Myb* expression value of 1. The experiment was performed in duplicate, the bars reflecting the mean value, the dots the individual values.

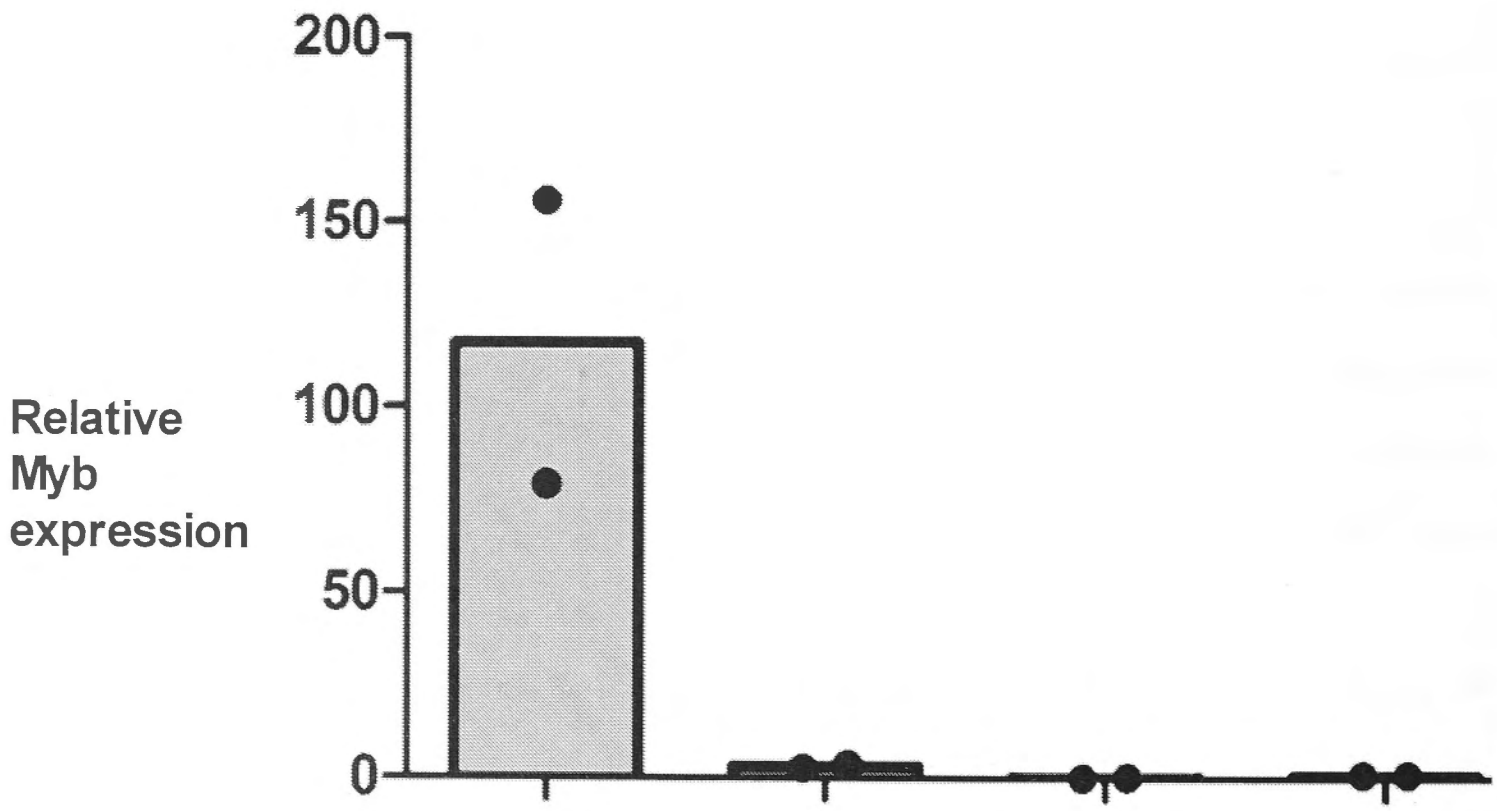

Table 5.1 Relative expression of selected genes using microarray

Microarray analyses of oligo-dT primed RNA were performed using the Affymetrix GeneChip®Gene 1.0 ST Array System for Mouse. Full methodological details are found in Chapter 2. Cytoplasmic RNA was isolated from the following: 1. "**Activated cells**", p53 wild type splenocytes 24 hours after harvest from antigen stimulated mice and culture with anti-CD40 antibody; 2. "***MYC* transduced cells**", *Trp53* mutant anti-CD40 activated B cells flow cytometrically sorted for GFP+ cells 2 days after spinoculation with *GFP/MYC* retrovirus with CD40 still in culture; 3 and 4, "**Outgrowth one and two**", two independent outgrowths of *Myb+MYC* dual transduced B cell lines stably growing in culture for several weeks, each containing approximately 33% viable GFP positive cells. Normalised relative expression of the indicated mRNAs in each sample is shown in arbitrary Affymetrix units

Gene	Activated cells	*MYC* transduced cells	Outgrowth one	Outgrowth two
Myb	461	121	3884	1770
B cell lineage markers				
CD19	2593	3283	856	2505
CD20	7494	8000	195	1518
CD79a	5278	6395	1902	5276
CD79b	4508	6224	1818	4197
Bruton's tyrosine kinase	665	1226	629	1022
Cell cycle genes				
Cyclin D1	91	51	621	1204
Cyclin A2	910	2256	2695	3002
Proliferating cell nuclear antigen	4536	3883	2649	4918

5.6.5 Dysregulated *MYC* and *Myb* must occur in the same B cell for spontaneous proliferation.

As *DsRed* expression was not evident in the spontaneously proliferating B cells yet only the *Myb/DsRed* vector could induce their proliferation, it remained possible that *MYC* singly transduced *Trp53* mutant B cells were reprogrammed to proliferate with the assistance of a secreted factor from *Myb* singly transduced cells in the same culture well. To test this possibility, an experiment was performed where the proliferation of mixtures of *MYC* singly transduced and *Myb* singly transduced spleen B cells was compared with proliferation of identical B cells that had been co-transduced, so that the two proviral vectors would either be restricted to separate B cells in the culture or would co-exist in the same B cell (Figure 5.27). As before proliferating populations of GFP^{hi} large B cells developed by Day 15 in the cultures containing co-transduced B cells. By contrast, in mixed co-cultures of singly-transduced B cells, there were no more GFP^{hi} large B cells than in control cultures transduced with the *MYC* vector alone. This result indicates that co-existence of the *MYC* and *Myb* vectors in the same *Trp53* mutant B cell is required to transform it into spontaneous proliferation. Taken together with the high Myb mRNA observed in the previous section, the simplest explanation for the lack of measurable DsRed in the transformed B cells is that the *Myb/DsRed* proviral mRNA is expressed in these cells but has either lost the IRES or *DsRed* sequence or fails to translate it efficiently.

Figure 5.27 The GFP^{high} outgrowth did not occur in wells containing both *Myb* singly transduced and *MYC* singly transduced *Trp53* mutant cells

Trp53 mutant splenocytes were activated and either singly transduced with *MYC/GFP* or *Myb/DsRed* retroviruses, or co-transduced. After transduction triplicate cultures were established of each of these combinations and, in parallel, triplicate cultures were established comprising a 50:50 mixture of the singly transduced cells (MYB+MYC co-culture). Cells were cultured for 12 days in RPMI complete medium with no added exogenous growth factors. a) Representative FACS plots at Day 15 showing the percentages of GFP^{high} cells in each well. b) Percentage of GFP^{high} cells in each well type at Day 15 and mean value for each group.

a)

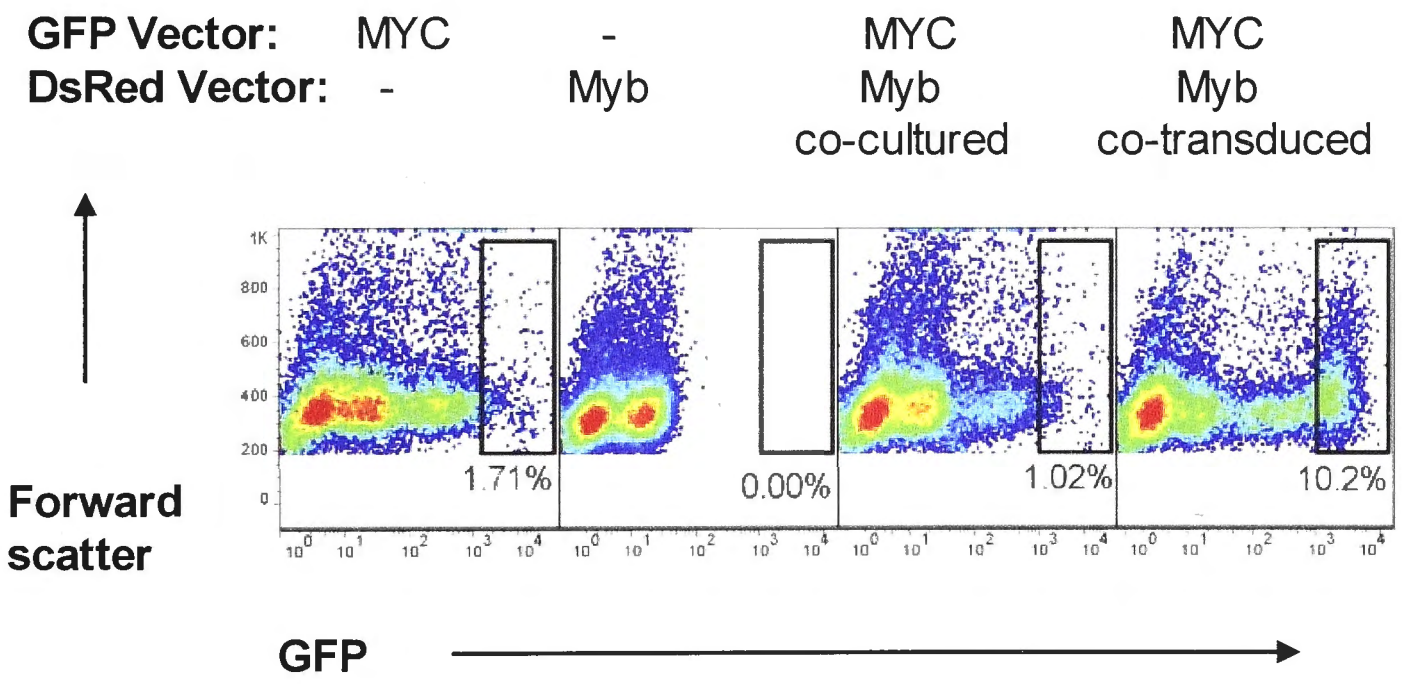

b)

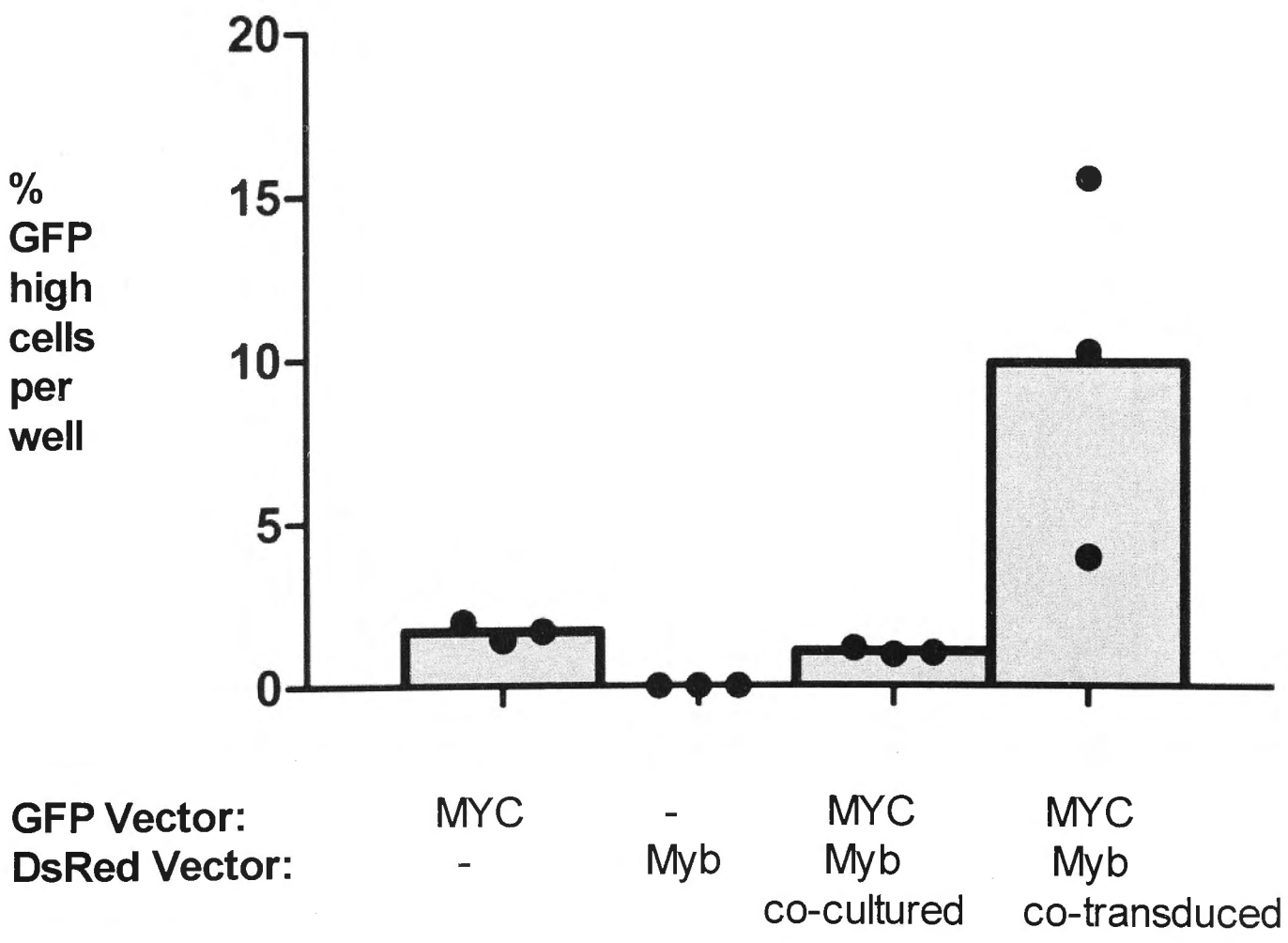

5.7 Growth of *Myb-MYC* dual-transduced *Trp53* mutant B cells in vivo

The experiments above suggest that dysregulated *Myb* may be sufficient as a "third oncogenic hit" for mature B cells with dysregulated *MYC* and defective *Trp53* to proliferate autonomously without the need for growth stimuli such as anti-CD40. I did not have time to extend these studies to determine if the transformed B cell lines, once established in culture, could continue growing as malignant lymphomas in vivo. However, as an initial pilot experiment, a preliminary *in vivo* study was performed to test whether *Myb+MYC* doubly transduced $Trp53^{Bbl/Bbl}$ spleen B cells could generate lymphomas in *Rag1* null mice if they were injected on Day 3 of culture, two days after spinoculation and before any transformed line had grown out in culture. In these initial studies, 200 000 viable cells (representing approximately 30,000 GFP+ cells) were intravenously injected to each of four recipient mice. This is ten-fold lower than the 2-6 million cells *MYC*-singly transduced splenocytes (containing typically 200,000 GFP+ cells) that were injected into each recipient in the studies in Chapter 3. After 46 days two of the four mice were unwell, euthanised, and found to have gross hepatosplenomegaly with large numbers of GFP^{high} mature B cells in their spleen (Figure 5.28). The third mouse died suddenly before it could be examined, and the fourth was euthanized at Day 65, although clinically well, revealing splenomegaly upon necropsy, and a distinct but relatively infrequent GFP high B cell population in the spleen (Figure 5.29). The results of this pilot experiment indicate that it will be valuable to pursue this question systematically in future studies. One line of experiments will need to repeat the pilot design above, transplanting recently transduced B cells but including recipients of single-transduced controls and larger numbers of recipients in each experimental group. Another line of experiments will need to establish multiple independent Myb+MYC transformed B cell lines in culture, and then inject different numbers of these cells into *Rag1* null or wildtype mice.

.

Figure 5.28 Phenotype of spleen cells from a *Rag1* KO recipient mouse displaying malaise 45 days post transfer of *MYC+Myb* doubly-transduced *Trp53*$^{Bbl/Bbl}$ cells

Two hundred thousand Trp53$^{Bbl/Bbl}$ cells two days post *MYC+Myb* dual transduction were intravenously injected into each *Rag1* KO recipient mouse. The recipient mice were regularly checked for signs of illness. After 46 days this mouse appeared unwell with prominent abdominal distension and was thus euthanised. Splenocytes were assessed by FACS and compared to splenocytes from a control C57BL/6 mouse harvested on the same day.

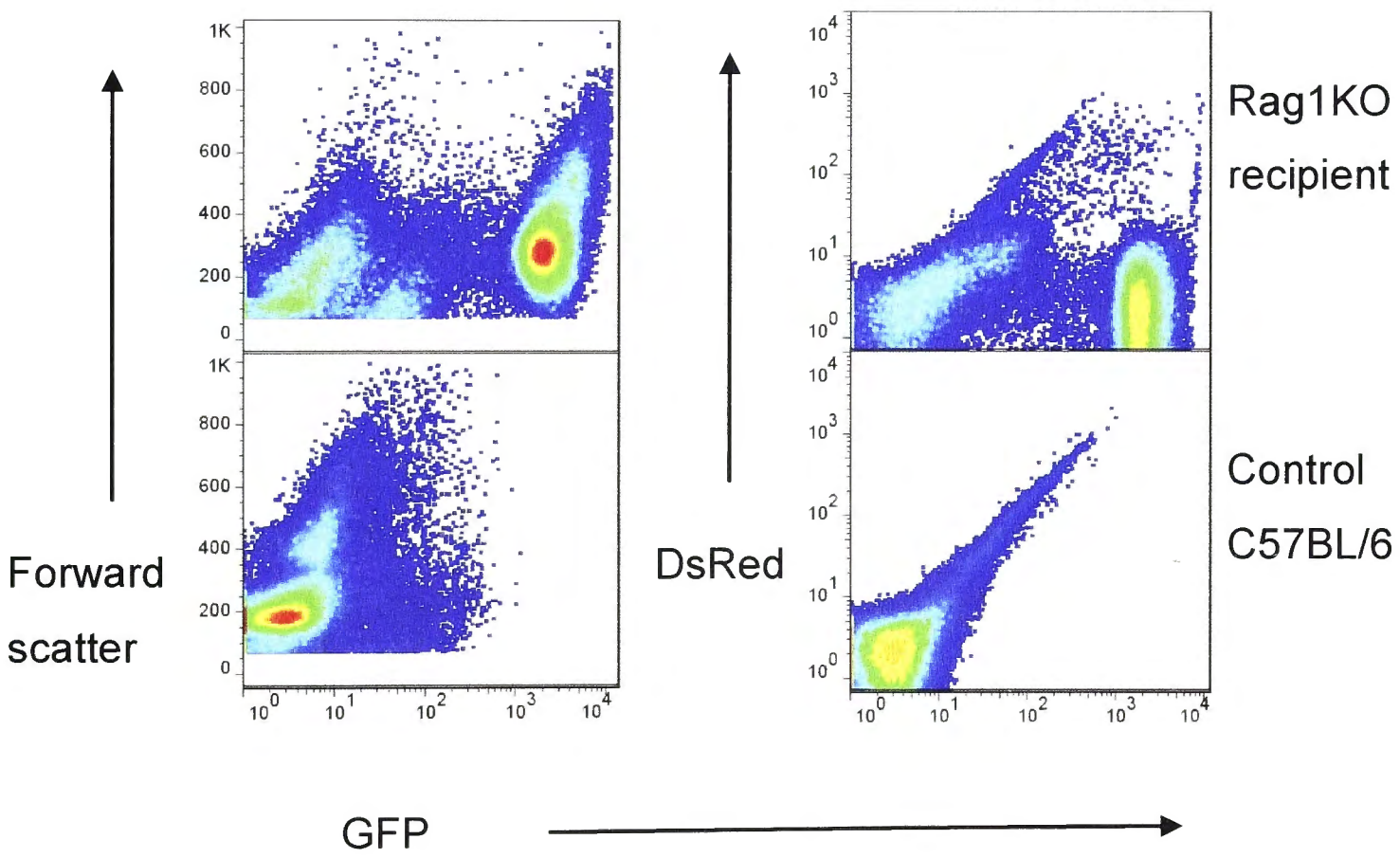

Antibody: B220 CD19 IgD IgM CD5 CD138

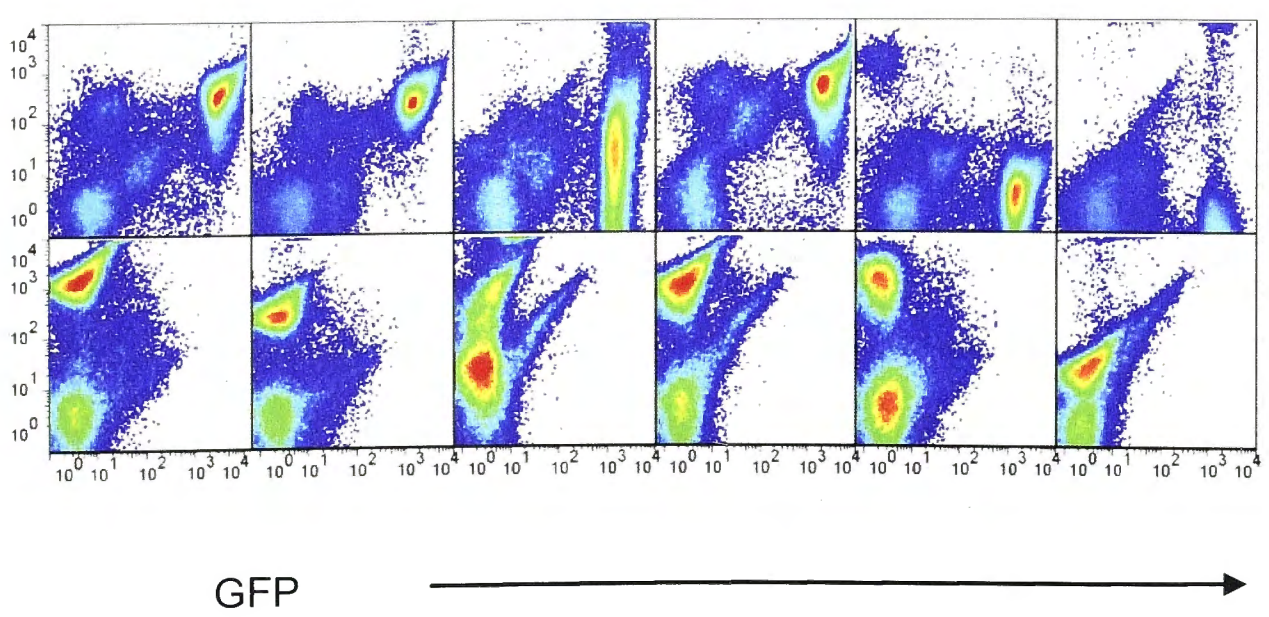

Figure 5.29 Splenic phenotype of a 'healthy' *Rag1*KO recipient mouse 65 days post injection of 200 000 dual transduced *Trp53*$^{Bbl/Bbl}$ cells.

Experimental details are as per Figure 5.28. This recipient did not appear unwell at Day 65 post cell transfer but brief a FACS analysis of splenocytes was performed to detect the expression of the fluorescent proteins.

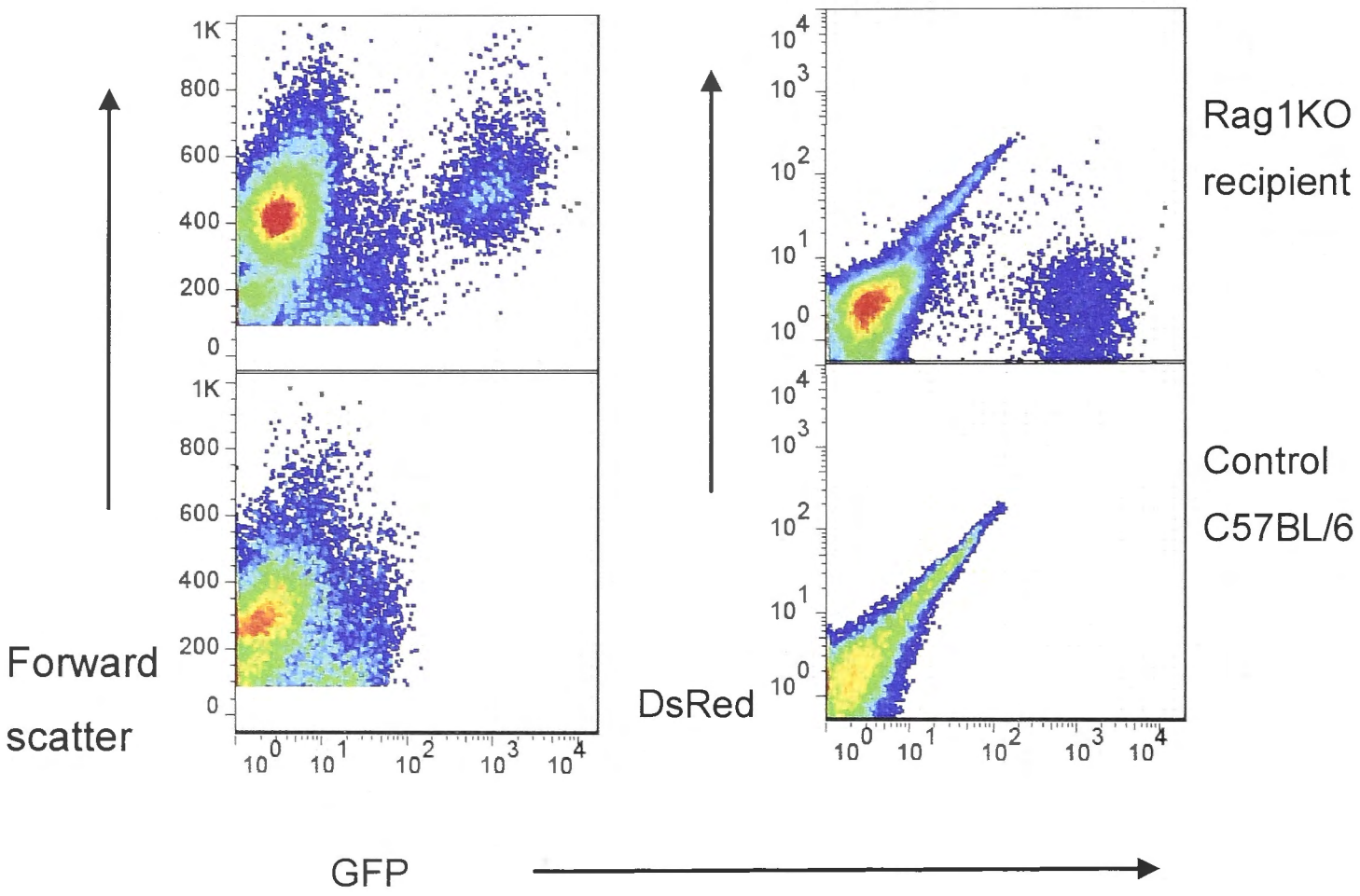

5.8 Discussion

The most striking finding in this chapter was the efficient transformation of activated mature B cells into continuously growing, mitogen-independent B cell lines by co-transduction of p53 mutant cells with a retrovirus expressing *MYC* and a second retrovirus expressing *Myb*, but not when the second retrovirus expressed *DsRed* alone, *Ikbkb, Laptm5* or *Lmo2*. This is informative in addressing the initial research questions of the number of oncogenic 'hits' that a B cell requires to become neoplastic and may help address the specific pathways that need to be dysregulated in B cells to induce neoplasia. The way in which Myb, MYC and p53 may cooperate in oncogenesis is discussed in detail in Chapter 7.

The results clearly reveal a powerful co-operation between dysregulated *Myb*, *MYC* and inactive p53, but a key issue is whether or not one can conclude from these results that these three oncogenic "hits" are alone sufficient to transform mature, activated mouse B cells into continuously growing, mitogen-independent B cell lines. Uncertainty about this conclusion comes from two chief sources. First, the limiting dilution analysis indicates that as few as 1 GFP+ B cell in 210 was transformed into a highly dividing clone. Second, the transformed B cells that grew out after 10 days displayed an unusual phenotype with respect to expression of the GFP and DsRed markers when compared to the majority of B cells present in the first 6 days of culture. Their GFP intensity was much higher than the majority of transduced B cells on Day 3 or Day 7 of culture, and they lacked measurable expression of *DsRed*.

Possible explanations for high GFP in transformed cells: The unusually high GFP expression in the *Myb+MYC* transformed B cells recapitulates the observations in Chapter 3, where very few of the *MYC/GFP* transduced p53-deficient B cells transferred into *Rag1*-deficient hosts had GFP expression as high as the level observed in the rare clones of malignant B cells that spontaneously proliferated in the recipient animals. One simple explanation for the high GFP in the *Myb+MYC* transformed cells is that the three oncogenic hits are sufficient, but only in rare B cells where one or more copies of the *MYC*

provirus have integrated in highly permissive chromosomal loci that support very high *MYC* expression.

Another possibility is that *Myb* increases the transcription or translation of the *MYC/GFP* vector so that cells that start out GFP medium are boosted to become GFP^{high} as Myb "rewires" their transcriptional status in concert with *MYC* overexpression and *Trp53* deficiency. This implies that both the GFP intensity (discussed in Chapter 3) and the retroviral insertion site (discussed in Chapter 4) are critical in the transformation process. Alternatively, the GFP intensity itself may not be critical in determining which cells are transformed and may merely reflect post-transcriptional processes such as increased translation of GFP from the IRES or increased accumulation and stability of the GFP protein due to the stage of differentiation or activity of the B cell, both of which are likely to be important in the transformation process.

These alternative explanations for the selection for high GFP in the transformed B cells could perhaps be resolved using knock-in mice where *MYC* was activated in B cells by Cre-Lox recombination from a single locus (eg Rosa26) to provide uniform expression.

Possible explanations for lack of DsRed in transformed cells: Several possible explanations are apparent. First, I have not formally demonstrated that the *Myb/DsRed* provirus is present in these cells. The possibility remains that the observed Myb overexpression may be a consequence of endogenous rather than retroviral Myb. While the experiments showed that dual retroviral transduction of the same cells was necessary for the outgrowths to develop, it is conceivable that the provirus was lost as part of the transformation process. Future experiments will therefore require Southern blotting or Splinkerette PCR to identify the integrations of the *Myb/DsRed* provirus, and real time PCR experiments with one primer complementary to the 3' end of the Myb gene and the other to the 5' end of the IRES (or 5' primer complementary to LTR and 3' primer complementary to the 5' end of the *Myb* coding region), and thus only retroviral *Myb* would be amplified. Alternatively, an epitope tag could be incorporated in the retroviral construct enabling proviral-derived Myb to be specifically detected by Western blotting. PCR to document the presence of the

MMLV retrovirus in the outgrowth could have also been performed but clearly alone would not exclude possible silencing of the MMLV long terminal repeat. These experiments were planned but time limitations precluded their completion.

Assuming that the *Myb* mRNA was provirally derived, a second explanation for lack of DsRed is that the transformed state was less permissive for translation of the bicistronic pMX *DsRed* vector than the initial transduced cells, or downregulated the transcription of the provirus itself. It has been reported that while pluripotent haemopoietic stem cells can be transduced with the Moloney Murine Leukaemia Virus (MMLV) (the virus upon which the pMX *DsRed* vector is based), expression of this virus reduces with cell division. The viral integration sites are still evident in subsequent generations, but mRNA expression was markedly reduced, associated with and probably due to increased proviral methylation [454]. Other studies, however, have demonstrated persistent retroviral expression many months after transduction of bone marrow cells, with constructs based on the same virus, consistent with sustained expression in a haemopoietic progenitor [455,456]. Expression of this vector at different stages of B cell development has not been thoroughly investigated to our knowledge. In contrast, the Murine Stem Cell Virus (MSCV) vector expressing the *MYC/GFP* mRNA has clearly not been inactivated during transformation, but the different LTR in this vector is reported to be less prone to methylation and inactivation in hemopoietic cell types.

Another possible explanation for the lack of demonstrable *DsRed* expression is that the cellular reprogramming required for the cells to acquire the potential for autonomous growth has resulted in post translational modification or catabolism of the red fluorescent protein. Similarly, post translational modification of Myb in the non physiological conditions of cell culture may prolong its half life, reducing the ongoing need for transcription and translation, and thus uncoupling its protein level from that of DsRed. Another potential explanation for the discrepancy between Myb and DsRed could be microRNA expression or other post transcription modulation which influences the translation of one but not the other open reading frame.

A particularly intriguing possible explanation for high *Myb* mRNA but lack of detectable DsRed protein would be that the proviral mRNA occasional undergoes an internal splicing event in the packaging cell line, so that a minority of the resulting retroviruses carry a variant vector containing the 5' part of the *Myb* coding region, but have deleted the C-terminal negative regulatory domain of *Myb* and the IRES and some or all of the *DsRed* coding regions. Such an event would result in a subset of the transduced B cells expressing a protein resembling v-myb or experimentally truncated c-Myb enhancing its oncogenicity [229,255] (and reviewed by Ramsay and Gonda [216]) but lacking detectable DsRed. This would not have been detected using the real time PCR primers used for quantification of *Myb* expression in Figure 5.26 as these were complementary to the 5' end of the gene. Real time PCR primers could have been designed that annealed to the 3' end of the gene and the relative expression of the two ends of the Myb gene could have been compared. It would also be useful to PCR amplify cDNA from the transformed B cells using a 5' primer at the start of the *Myb* coding region and oligo-dT or different 3' primers corresponding to the IRES, *DsRed* coding region, or 3' LTR of the vector, to detect truncated mRNAs in transformed B cells compared with acutely transduced *Myb/DsRed*+ B cells. Also, one could repeat the dual transduction experiments with variant *Myb/DsRed* vectors where *Myb* was truncated to remove the C-terminal negative regulatory domain. If truncation of *Myb* is indeed a "fourth hit" required for transformation of mature B cells, one would observe efficient continuous proliferation of all of the DsRed/truncated Myb and MYC/GFP dual transduced B cells.

Effect of *Myb* and other genes on cell size and growth: Cell size variations may reflect alterations in cellular pathways, giving a potential insight into downstream pathways influenced by specific gene dysregulation. The mTOR (targets of rapamycin) protein is thought to be a central regulator of cell growth through multiple mechanisms [457]. 4EBP1 and S6K1 are effectors that modulate cell growth, with overexpression of either increasing cell size, expression of both being regulated by mTOR [458]. *Myc* overexpression in B cells has also been shown to increase cell size [459], although a direct downstream link to the mTOR pathway has not been established to date. *Myc* overexpression in Eμ-Myc mice, although selectively increasing the percentage

of less mature B cells, results in increased size (and protein synthesis) of B cells at all maturation phases and all cell cycle stages without an increase in cell cycle progression [460] which the authors conclude is likely to be due to the downstream signalling pathways activated by *Myc* overexpression.

It was initially postulated that the size reduction seen in cells transduced with the *Myb* expressing retrovirus was *Bcl2*-mediated, but Figure 5.9 demonstrated that both Dorian and wild-type cells expressing the *DsRed/Myb* retrovirus had a similar reduction in size, suggesting that the *Bcl2* gene was not a downstream target of *Myb*. An alternate explanation is that *Myb* overexpression may delay activation of the mitochondrial pathway of apoptosis through induction of other anti apoptotic or suppression of pro apoptotic Bcl2 family members. Rathmell et al [445] demonstrated that overexpression of the antiapoptotic homolog of *Bcl2*, *Bcl-X_L* was able to prolong survival at the expense of cell size in a proB cell line deprived of growth factor support. Alternatively, this size reduction may relate to Myb-mediated modulations in cellular metabolism and ribogenesis, a concept that was not further pursued.

Despite review of retroviral insertion sites (Chapter 4) suggesting a possibility of co-operation with MYC, dual overexpression of *Ikbkb*, *Lmo2* or *Laptm5* with *MYC* did not lead consistently to uncontrolled cell growth in our model. A failure to identify other critical factors in the transformation process such as a specific cell cycle stage, maturation stage or cellular environment may explain the difficulty of in vitro validation of the potentially co-operating genes. Experimental investigation of other genes identified near retroviral insertion sites (particularly *Gng7* and *Lta*) may have been more fruitful, but limitations of time and resources necessitated that a finite number of genes were pursued.

While *Ikbkb* did not give the same spectacular results as *Myb* when dual transduced with *MYC* in *Trp53* defective cells, the results suggest it may be a growth enhancer, although insufficient as a third hit for spontaneous proliferation. As demonstrated in Figure 5.22 cells dual transduced with *MYC/Ikbkb* were more abundant than cells transduced with any of the other gene combinations at Day 7. This may either reflect that cells readily express this retroviral construct, or that cells expressing it have an early but non-

sustained growth advantage. The increase in cell size seen in cells transduced with *Ikbkb* in conjunction with *MYC* (Figure 5.11) is another factor suggesting a growth modifying effect. NF-κB pathway activation is not a characteristic of *MYC*-driven Burkitt lymphoma, and its activation has been shown to enhance Fas-mediated apoptosis in a Burkitt lymphoma cell line [345], and thus it may be postulated that in cells overexpressing *Myc* that the NF-κB pathway is suppressed with time to maintain cell viability.

Alternatively, these findings may indicate the need for a fourth hit in addition to the dysregulation of *MYC*, *Trp53* and *Ikbkb* for autonomous cell growth. The other genes within 100kb of the retroviral integration sites near *Ikbkb* were *Dkk4*, *Polb*, *Plat*, and *Ap3m2*. *DKK-4* encodes a protein whose normal role remains unclear, but which is known to inhibit the Wnt/β-catenin signalling pathway and has been noted to be overexpressed in some malignancies [461]. *Polb* encodes DNA polymerase β which is involved in DNA repair and replication. Polymorphisms in *Polb* (and more commonly in other DNA repair genes) have been demonstrated to modify risk for various tumours such as bladder cancer [462] and colorectal cancer [463]. *Plat* (plasminogen activator, tissue) encodes an enzyme that facilitates breakdown of blood clots. It is not known to play a role in cellular proliferation or transformation. *Ap3m2* (adaptor-related protein complex 3, mu 2 subunit) forms part of a protein complex which has a role in intracellular protein trafficking, but a role in cellular proliferations remains to be defined. The genes within 100kb of the other retroviral insertion identified in the same lymphoma were *Txnip*, *Hfe2*, *Polr3gl*, *Ankrd34a*, *Lix1l*, *Rbm8a*, and *Pex11b*. *Txnip* (thioredoxin interacting protein) is not known to have a role in B cell proliferation. The overexpression of Hfe2 precipitates haemochromatosis (iron overload). *Polr3gl* (polymerase (RNA) III (DNA directed) polypeptide G (32kD)-like), *Ankrd34a* (ankyrin repeat domain 34A) and *Lix1l* (Lix1-like) have not been well characterised. *Rbm8a* (RNA binding motif protein 8A) is a nuclear protein that binds to RNA, but has not defined role in neoplasia. *Pex11b* controls with abundance of peroxisomes (organelles within which various metabolic pathways occur) in cells. While none of the above genes are known to cooperate with the NF-κB pathway, this possibility could be tested by overexpressing the four genes in the same B cell and observing consequential cell size and growth.

The transient proliferation and thus cell size increase seen in cells transduced with the *Ikbkb* expressing retroviral vector is consistent with the published literature. Sasaki et al demonstrated that constitutive activation of the canonical NF-κB pathway through Ikbkb kinase overactivity leads to increased numbers of mature B cells (marginal zone cells particularly) through increased cell survival rather than cell cycle progression [28]. In this publication these cells were predominantly resting B cells, although the addition of anti IgM, cross linking the B cell receptor, increased cell proliferation. The process of retroviral transduction requires cell activation, which was performed using intraperitoneal HEL to ligate B cell receptors and supplementary anti CD40 in our model. Jeelall et al [101] confirmed that overactivity of the canonical NF-κB pathway due to constitutively active Ikbkb protein, in conjunction with the complex cascade initiated by CD40 activation and antigen binding, was sufficient to increase B cell proliferation in vitro.

Laptm5 did not substantially alter B cell size in both singly transduced cells and cells co-transduced with the *GFP/MYC* retroviral vector and had not apparent effect on B cell growth. In subsequent studies of *DsRed/Laptm5* vector singly transduced mature splenic B cells, it was shown that the DsRed-positive cells exhibited exaggerated downregulation of surface IgM in response to antigen binding (Helen Richards, Hons thesis, ANU). This result is consistent with recently published work showing that *Laptm5* promotes endosome-lyososome traffic and degradation of antigen receptors in B and T cells [403,406]. While antigen receptor downregulation was not measured in the experiments in this chapter, the subsequent studies establish that the *Laptm5* vector does increase a known activity of *Laptm5*. As the downstream pathways modulated by *Laptm5* remain to be defined, the way in which it modifies B cell size is uncertain, but the principles discussed above remain relevant.

While *Laptm5* dysregulation is implicated as a co-operating "third hit" based on the proviral integration in one of the lymphomas in Chapter 4 and recurrent proviral integrations in lymphoid neoplasms in RTCGD, the lack of an effect of the *Laptm5* vector on B cell growth may indicate that this is not the case because it is in fact a simple 'passenger mutation' in the lymphomas where its promoter is flanked by a proviral integration, or that it is a "driver mutation"

along with *MYC* and *Trp53* defects but only in the context of a "fourth hit". With respect to the latter possibility the other genes within 100kb of this integration site were reviewed. Neither *Sdc3* nor *Matn1* are known to have a role in cellular proliferation. One other proviral integration site was identified in the lymphoma bearing the *Laptm5* integration. Genes within 100kb of this insertion site were *Zdhhc18*, *Nudc*, *Nr0b2*, *Gpatch3*, *Gpn2*, *Sfn*, *Pigv* and *Arid1a*. This second insertion site was within the *Zdhhc18* (zinc finger, DHHC domain containing 18) gene, but the function of this gene is not well described in the literature. *Nudc* (nuclear distribution gene C homolog (Aspergillus)) regulates nuclear movement and has been described as a tumour suppressor gene in prostate cancer through inhibition of cellular proliferation [464]. *Nr0b2* (nuclear receptor subfamily 0, group B, member 2), also known as small heterodimer partner (SHP) encodes a protein that inhibits the activation of some hormone receptors [465]. *Gpatch3* (G patch domain containing 3) and *Gpn2* (GPN-loop GTPase 2) are not well characterised in the literature. *Sfn* (stratifin), also called 14-3-3σ, is thought to be a tumour suppressor gene with a role in differentiation and cell cycle progression [466]. *Pigv* (phosphatidylinositol glycan anchor biosynthesis, class V) has no known role in cellular proliferation. *Arid1a* (AT rich interactive domain 1A (SWI-like)) has been described as a tumour suppressor gene [400] in gynaecological cancer. Overall, none of these genes seem a likely cooperative proto-oncogene with *Laptm5*.

The lack of any effect of *Lmo2* on B cell size or growth may have been a consequence of the retroviral construct being defective, or it may not have facilitated the correct degree of gene overexpression at the required critical time in the cell cycle or cell maturation phase. It would be important in future studies to examine known biochemical or transcriptional targets of *Lmo2* (which to date are not well defined [467]) to confirm that *Lmo2* activity was dysregulated in the transduced B cells. No other unique retroviral insertion sites were identified in this lymphoma specimen using splinkerette PCR, although there are likely to be others detected with more sensitive techniques. The other gene with 100kb of the insertion site near Lmo2 was *Caprin1* (cytoplasmic activation/proliferation-associated protein-1), a cytoplasmic phosphoprotein. Its expression has been shown to correlate with splenic B cell activation status, and knock-down experiments in a lymphocyte cell line have demonstrated that it negatively

influences cell division, although over expression experiments have shown inconsistent results [413] and the implicated pathways remain to be defined. It is possible that overexpression of *Caprin1* co-operates with *Lmo2* overexpression to promote cell growth and proliferation, the cooperative effect being lost when *Lmo2* alone was over expressed in conjunction with *MYC* and a p53 defect in our model.

The IgM+ B220+ GFP^{high} phenotype of the lymphomas developing in recipient mice was comparable to that seen in the in vitro proliferating *MYC/Myb* dual transduced cells. Additional markers were also consistent with a mature B cell phenotype, including positivity for CD19, lower levels of IgD, and CD138 and CD5 negativity. CD138 (syndecan 1) is a relatively specific marker for plasma cells, and although it may be demonstrated on some immature B cells [468] it is not usually expressed on mature B cells. CD5 expression is also uncommon in mature murine B cell neoplasms, being found predominantly in mouse models of Mantle cell lymphoma [9] and Chronic lymphocytic leukaemia [469], although rare reported cases of B cell lymphomas derived from B-1 cells may also express CD5 [470].

Investigation of the growth kinetics of the in vitro outgrowths (Figure 5.25) demonstrated that not all wells seeded with dual *Myb/MYC* transduced cells contained GFP positive cells after 20 days incubation. This suggests that not every doubly transduced p53 deficient B cell is transformed to spontaneous growth, although these results are limited by the lack of quantifiable *DsRed/Myb* expression by flow cytometry. Limiting factors may include the level of proviral expression (which Figure 5.4 demonstrates varies with the retroviral construct), autocrine/paracrine growth factors, acquired deleterious genetic defects, concentration of local substrates such as glucose, lactate, glutamine, cell density, cell cycle stage or maturation stage at transduction. An alternate explanation is that the doubly transduced cells that grow autonomously in culture are carrying a fourth hit. It is possible that prior to harvesting the B cells there has already been some in vivo enrichment for B cells that have accumulated one more somatic mutations that are still insufficient to transform them until the *MYC* and *Myb* vectors are also introduced. Alternatively, spontaneously acquired mutations or those due to non-productive or non-

detected retroviral integrations into the murine DNA may occur in dual transduced cells giving the cells an additional critical growth advantage.

The preliminary in vivo results support the conclusion that dysregulation of *Myb* may be sufficient to provide the third oncogenic hit needed for B cell growth both in culture and in vivo. However, from these data the possibility cannot be excluded that the lymphomas arose independently of the *Myb* vector from *GFP/MYC* singly transduced B cells, since a similar type of lymphoma arose in many *Rag1* knock out recipients that received ten times more cells singly transduced with the *MYC*/GFP retrovirus alone (Chapter 3). Further experiments would ideally use a different model with inducible gene expression or suppression. An example would be a Cre-Lox system, deleting *Trp53* at a specific time point or stage of B cell maturation in an effort to minimise the accumulation of genetic defects prior to the experimental genetic alterations. Inducible gene expression or suppression could be used to examine both the propensity of the cells to develop lymphoma in the setting of dysregulation of specific genes, but could also assess the degree of oncogene addiction of the lymphoma (and thus the potential of specific gene targeting to be of therapeutic utility).

6. Results: Gene expression analyses

6.1 Background

The previous chapter revealed a potent co-operation between retroviral vectors encoding *Myb* and *MYC* in transforming a subset of mature *Trp53*-mutant B cells into continuously growing B cell lines. While flow cytometric profiling showed that the transformed cells continued to express B220 and surface IgM, I wished to determine whether the global gene expression program in these cells resembled activated B cells, germinal centre B cells, or corresponding human lymphoma subsets. To begin addressing this question this chapter describes the findings from a preliminary microarray analysis comparing *Myb+MYC* transformed B cell lines with activated B cells and B cells that had recently been transduced with *MYC* alone. It was performed as a pilot study, with the plan to extend the pilot study and follow up specific genes in a statistically significant number of samples but I did not have time to pursue the follow up studies. Nevertheless, the results of the pilot study are presented here, together with a discussion of key observations.

RNA from two transformed B cell lines ('Outgrowth 1' and 'Outgrowth 2') were used as test samples. Both lines were derived from a pool of *Trp53* mutant B cells dual-transduced with *Myb* and *MYC* at the same time but grown in separate wells for several weeks. Each outgrowth contained approximately 33% viable GFP positive cells. To provide a control sample of dividing, *MYC/GFP*-transduced *Trp53* mutant B cells that was as closely matched to these cell lines except lacking retroviral *Myb* expression, RNA was isolated in parallel from *Trp53* mutant B cells that had been activated with antigen and anti-CD40, transduced with the *MYC/GFP* vector alone, grown in anti-CD40 for two days, and flow cytometrically sorted for GFP+ cells ("*MYC* transduced"). For comparison, RNA was isolated from *Trp53* wildtype splenocytes that had been activated by antigen and cultured for 24 hours with anti-CD40 ("Activated B cells"). The latter would be expected to be less well matched with the transformed B cells because the B cells were only beginning to divide and had normal *MYC* and *Trp53*, but would display a gene expression profile of normal, activated B cells for comparison to the other three samples.

Poly-A+ mRNA in each of the samples was converted to cDNA using oligo-dT priming, and then to biotinylated cRNA that was hybridized to Affymetrix GeneChip® 1.0 ST Arrays for mouse as per the manufacturer's protocol, these steps being performed by the Australian Cancer Research Foundation (ACRF) Biomolecular Resource Facility (BRF) at the John Curtin School of Medical Research. This system focuses on 28 853 well annotated genes with approximately 26 perfect match 25 nucleotide-long exon probes spanning each gene (770 317 distinct probes). Gene sequences were based on NCBI build 36 mouse genome sequence, February 2006 and cover 100% of NM sequences (mature messenger RNA transcripts) in the April 2007 RefSeq (NCBI Reference Sequence) database. Results from these probes were collated using Partek® software by staff at the ACRF BRF.

6.2 Markers of cells in S-G2-M phase of cell cycle

As noted above it was expected that the activated B cell sample would contain fewer B cells in cell cycle than the outgrowths or the *MYC* transduced B cells, and this difference alone would be reflected in substantial differences in gene expression. To test this I compared the expression of 11 murine homologues of a set of human genes that are validated markers of B cell cycle described by Shaffer et al [471] in the two outgrowths and in the *MYC* transduced B cells relative to their expression in the activated B cell sample (Table 6.1). Of the 11 cell cycle genes tested, 10 were increased between 2 and 7 fold in *MYC* transduced B cells and the two outgrowths, compared to the B cells that had simply been activated by anti-CD40 for 24 hours. Taking the set of 10 increased genes as a group, there was no consistent elevation in this gene set in the outgrowths relative to the *MYC* –transduced cells, indicating that the *Myb+MYC* transformed cells appeared relatively well matched to the *MYC*-transduced cells with respect to cell cycle status. The one gene in this set of 11 that was further elevated in both outgrowths relative to the *MYC* transduced cells was *Ccnb1*. While this apparent difference will need confirmation in independent samples, it is notable that *Ccnb1* is a validated target of *Myb* [472].

Table 6.1 Expression of cell cycle genes in outgrowths and MYC transduced cells compared to Activated B Cells

Murine homologues of the human cell cycle gene set described by Shaffer et al [471] were used. RNA was extracted from two *Trp53*^{Bbl} *Myb/MYC* transformed B cell lines (labelled Outgrowth 1 and Outgrowth 2), *Trp53*^{Bbl} antigen-activated B cells 2 days after transduction with *MYC*/GFP vector alone and flow cytometrically sorted for GFP+ cells (labelled *MYC* transduced) and *Trp53*^{wildtype} antigen activated B cells 1 day after activation with cognate antigen and CD40 ligand ("Activated B cells"). The corresponding cRNA was analysed on Affymetrix 1.0 ST Mouse Array chips. Fold changes of the indicated genes in each B cell line compared to activated B cells are shown. Relative gene expression is depicted using the following colour scale:

- >2 fold increase
- -2<fold increase<2
- -2>fold increase

Cell cycle gene	Outgrowth 1	Outgrowth 2	*MYC* transduced
Ccnb1	5.68	6.10	2.92
Bub1	3.52	3.87	2.27
Cenpf	4.53	6.73	5.07
Mad2l1	2.04	1.64	1.58
Top2a	2.74	3.54	1.96
Aurka	4.84	5.80	3.35
Plk1	3.91	5.87	4.14
Birc5	3.35	3.84	2.66
Kif23	2.62	3.69	3.52
Plk4	1.18	1.10	-1.50
Cenpe	2.67	4.59	3.75

6.3 Markers of germinal centre differentiation

MYC dysregulation and *Trp53* inactivation are primarily observed in Burkitt lymphoma, which consistently displays cell surface markers and a gene expression program corresponding to rapidly dividing germinal centre centroblasts [344] - a distinct differentiation state from activated B cells. I therefore asked whether the *Myb+MYC* -transformed *Trp53* mutant B cells had differentiated into germinal centre cells by analysing expression of 22 genes that are strongly upregulated in germinal centre B cells relative to other B cells in the ImmGen database of sorted mouse lymphocyte subsets analysed by Affymetrix microarray profiling (www.Immgen.org). The relative expression of these genes in the *Myb+MYC*-transformed outgrowths was compared to the single *MYC* transduced B cells (Table 6.2). Only one of the 22 genes demonstrated a greater than 2 fold increase in expression in both of the outgrowths (8430410A17Rik), and the most widely used markers of mouse germinal centre differentiation were either decreased (*Aicda, Fas*) or not different (*Gcet, Rgs13, Mybl1*). Comparison of the Activated B cells with the *MYC*-transduced B cells also showed little difference in expression of the set of 22 germinal centre genes, confirming that the *MYC*-transduced *Trp53* mutant B cells themselves had not differentiated into germinal centre B cells. Thus, the two transformed B cell samples did not exhibit evidence of having differentiated into germinal centre cells.

Table 6.2 Expression of germinal centre-specific genes in Myb+MYC transformed B cell lines and Activated B cells relative to MYC-transduced B cells.

Relative expression of 22 genes that are highly expressed selectively in mouse germinal centre B cells in the ImmGen database. Fold changes of the indicated genes in each B cell line compared to Day 3 *MYC*-transduced *Trp53* mutant B cells is shown. Specimens as per Table 6.1. Relative gene expression is depicted using the following colour scale:

>2 fold increase
-2<fold increase<2
-2>fold increase

Germinal centre gene	Activated B	Outgrowth 1	Outgrowth 2
Aicda	7.2008639	-10.777869	-9.3826796
Fas	-2.1406071	-9.7135591	-9.7811222
Ildr1	2.1588455	-2.907945	-3.0314331
Arhgap8	1.58417312	-3.0104935	-1.7411011
Basp1	-1.7848094	-1.2141949	-1.2141949
Ctnnal1	1.13929393	-1.0792282	-1.1250585
Gcet2	-1.2063345	-1.0497167	-1.0497167
Ccrl1	-1.0084783	-1.0352649	-1.0210121
Ehf	1.04074022	1.07177346	-1.0942937
Rgs13	-9.2103118	-1.0210121	1.00695555
Mbd4	2.33752209	-1.5368752	1.55832916
Zdhhc2	-1.7113561	-1.0139595	1.18099266
Stau2	-1.0033118	-1.057018	1.2397077
Phf19	1.44917317	-1.2657566	1.49484925
Efnb1	1.19551315	1.43395525	-1.1407637
Rassf6	-1.2289191	-1.0942937	1.41421356
Mybl1	1.21067363	1.14869835	1.21419488
Gm600	-1.2737128	-1.0497167	3.45814893
H1fx	1.05317122	1.2397077	1.38510947
Dhfr	1.01892651	1.53687518	1.58008262
Gatm	1.82626991	3.48220225	1.85317612
8430410A17Rik	-2.2335987	4.11245531	9.06307108

6.4 NF-κB pathway

As described in Section 1.12 gene expression profiling has revealed that many NF-κB responsive genes show diminished mRNA expression in Burkitt Lymphoma compared to Germinal Centre-type Diffuse Large B cell Lymphoma [344]. The expression of the mouse orthologues of this set of NF-κB regulated genes was compared in the *Myb+MYC* transformed outgrowths with the single *MYC* transduced B cells (Table 6.3). Of the 25 genes in this set nearly half were decreased between 4 and 50-fold in both $Trp53^{Bbl}$ *Myb+MYC* transformed B cell lines compared to *MYC* singly transduced B cells. Two of these genes, *Traf1* and *Nfkb1*, have been shown to both bind and be repressed by Myb [473], and the repression of *Nfkb1* could have a secondary effect on many other NF-κB target genes. By comparison, only 4% of the total probe sets tested (1156 of the 29,221) were decreased 4-fold or more in the outgrowths. Using a Chi square test there is a statistically significant increase in the number of NF-κB target genes with a 4 fold or greater reduction in expression in Outgrowth 1 compared to MYC-transduced Trp53 mutant B cells (two tailed $p<0.0001$). The p value for the same analysis for Outgrowth 2 was similarly significant.

The B cell surface proteins CD21 (*Cr2*), CD23 (*Fcer2*), CD25 (*Il2ra*), Lymphotoxin beta (*Ltb*), EBV-induced receptor 2 (*Ebi2*), and CD95 (*Fas*) are encoded by genes that are well validated to be directly induced by NF-κB [28,42,101]. When mRNA expression of these genes in $Trp53^{Bbl}$ *Myb+MYC* transformed B cell lines was compared to $Trp53^{Bbl}$ *MYC* singly transduced B cells, all six of these genes were decreased (Table 6.4). Recent data from Y Jeelall and J Rayner, current students in Prof Goodnow's laboratory, has begun to validate these gene expression differences by independent approaches. Antigen-activated B cells with wild-type *Trp53* were singly transduced with a *Myb-EGFP* retroviral vector or an empty *EGFP* vector and analysed by flow cytometry to compare CD21, CD23, CD25 and CD95 expression on the surface of GFP+ and GFP- cells (Jeelall, personal communication). Analysis of independent triplicate transduced samples revealed that the expression of each of these proteins was specifically and significantly decreased in *Myb*-transduced B cells compared to non-transduced or empty vector transduced B cells.

Table 6.3 Relative expression of NF-κB responsive genes known to be suppressed in Burkitt lymphoma

Analysed are the mouse orthologues of a set of genes identified by Staudt and colleagues [344] as being NF-kB induced in B cells, and decreased in Burkitt lymphoma compared to GC-type Diffuse Large B cell lymphoma. Fold changes of the indicated genes in each B cell line compared to Day 3 *MYC*-transduced *Trp53* mutant B cells is shown. Specimens as per Table 6.1. Relative gene expression is depicted using the following colour scale:

	>4 fold increase
	-4<fold increase<4
	-4>fold increase

Gene	Outgrowth 1	Outgrowth 2
Ccl22	-51.62507259	-44.01733818
Traf1	-23.91758798	-19.8353232
Ebi3	-11.39240156	-14.92852786
Cd83	-8.397733469	-5.938094283
Cd40	-10.41073484	-2.566851795
Tnf	-4.626752736	-5.775716782
6330500D04Rik (C16Orf32)	-7.160200567	-1.453972517
Lta	-4.198866734	-3.655325801
Nfkb1	-4.658934346	-2.549121255
Nfkb2	-4.25748073	-1.918528239
Tnfaip3	-3.758090997	-1.840375301
Bcl2a1a	1.109569472	-5.42641731
Smarca2	-2.713208655	-1.464085696
Bcl2a1d	1.132883885	-5.13370359
Id2	-2.158456473	-1.705269784
Bcl2a1d	1.140763716	-4.789914818
Nfkbia	-2.143546925	-1.148698355
Cxcl10	-1.494849249	-1.705269784
Cxcl9	-1.172834949	-1.042465761
Birc3	-3.386981249	1.231144413
Gadd45b	-1.569168196	1.028113827
Cd44	1.101905116	-1.214194884
Irf4	1.443929196	1.526259209
Pim1	1.337927555	1.8276629
Dusp2	1.140763716	2.620786808

Table 6.4 Relative expression of NF-kB-induced genes encoding B cell surface proteins

Fold changes of the indicated genes in each B cell line compared to Day 3 *MYC*-transduced *Trp53* mutant B cells is shown. Specimens as per Table 6.1. Relative gene expression is depicted using the following colour scale:

	>4 fold increase
	-4<fold increase<4
	-4>fold increase

Gene	Outgrowth 1	Outgrowth 2
Fcer2a (CD23)	-96.335792	-89.263595
Cr2 (CD21)	-96.335792	-89.263595
Il2ra (CD25)	-3.226567	-3.6553258
Ltb	-46.850742	-14.320401
Ebi2	-19.159659	-17.753112
Fas	-9.7135591	-9.7811222

6.5 Most highly increased genes in *Myb*+*MYC*-transformed B cells

As an additional preliminary analysis of the pilot data, the 25 most increased mRNAs in the transformed B cell lines relative to the MYC-singly transduced B cells were considered (Table 6.5). Notably, the 12th highest was *Myb* (approximately 20-fold increased). Twelve of the remaining 24 genes represent genes that Myb has been shown to bind in Chip or EMSA assays (*Spp1, Acta2, Lyz1, Sox4, Cd93, Gstm1, Plk2, Akap12, Slc40a1, Dab2, Mrc1 and Ccnd1* [474,475]) and a further 4 are known to be induced by Myb or B-Myb (*Fn1, Il7r, Cdkn2a, Uchl1* [274,476-478]). As exemplified by *Cd93* and *Il7r*, the majority of these genes are normally restricted within the B cell lineage to expression in progenitor, pre-B and immature B cells [479].

While these pilot data are preliminary, the high fraction with independent evidence of being Myb-target genes makes it reasonable to pursue these, and other induced genes in the dataset, in follow up studies. A cell surface protein encoded by one of these highly upregulated genes, CD93, has been tested in single *Myb*-transduced B cells in the follow up studies by Y Jeelall noted in the previous section, and was confirmed to be strongly and specifically induced selectively in Myb-transduced B cells within 2 days, without the need for MYC or Trp53 mutations (Y Jeelall personal communication). Notably, the *Cd93* gene contains multiple sites shown to bind Myb [475].

Table 6.5 The 25 most highly increased genes in Myb+MYC transformed Trp53 mutant B cells compared with MYC-transduced Trp53 mutant B cells.

Fold difference in mRNA expression in each sample relative to day 3 *MYC*-transduced *Trp53* mutant B cells. Asterisks mark Myb-target genes defined in the literature. *Myb* itself is noted by the double arrow. Relative gene expression is depicted using the following colour scale:

- >4 fold increase
- -4<fold increase<4
- -4>fold increase

Gene	Activated B cell	Outgrowth 1	Outgrowth 2
Uchl1	1.976954956	18.25221945	16.67945217
Ccnd1 *	-1.790906477	12.21007367	23.58830748
C3ar1	-1.477389265	21.70566924	14.72300241
Cdkn2a	1.096731218	15.88947993	22.94328397
Mrc1 *	-1.060187915	32.44670335	7.568461174
Dab2 *	-1.00453651	27.28431654	13.547925
Slc40a1 *	-1.980438636	39.12448889	2.496661098
Akap12 *	-1.583931561	16.56423878	26.17286587
C1qa	-1.06301356	24.5900029	18.50701094
Plk2	-2.871471017	12.99603834	32
Atp1b1	-5.155527329	14.52030649	30.90996253
Trf	1.22885952	33.59093388	11.87618857
Gstm1	-2.410512649	18.37917368	27.09585
Myb <<	-3.795131828	32	14.52030649
Timp2	-3.215716003	44.01733818	8.75434961
Il7r	-27.40809211	44.94223602	15.34822591
Cd93 *	-3.416573113	37.53071838	24.25146506
C1qc	-1.227446377	41.64293937	22.00866909
Sox4 *	-1.845229164	37.01402188	32.2225776
C1qb	-1.023158746	53.44562684	26.90868529
Lyzs	-22.56054477	51.26847217	31.34144952
Acta2	-1.046200961	58.48521281	30.2738447
Gpnmb	-12.74403298	74.02804377	15.77972327
Fn1	1.234870709	75.58353033	29.85705573
Spp1 *	-1.351264407	58.89200964	50.56264396

6.6 Broader pathway analysis

Given the encouraging results from focussed analysis of specific gene sets above, pathway analysis was subsequently performed on the microarray dataset as a whole. This was undertaken to guide hypothesis generation regarding dysregulated pathways in the cellular outgrowths, and thus guide further research to follow up these preliminary findings. Data were analysed in two different ways, each with their own advantages and disadvantages as discussed below.

6.6.1 Differential gene expression – Method One

The first analysis method was simply identifying genes (for pathway analysis) that were overexpressed or underexpressed at least 2 fold compared to both the *MYC* singly transduced control and the activated B cell control. Only those genes encoding mature messenger RNA transcripts (ie with an 'NM' prefix in the NCBI Reference Sequence database) were considered. I identified 281 genes with increased expression and 262 genes with reduced expression (Table 6.6) from the total of 15 981 genes encoding mRNA on the Affymetrix GeneChip® 1.0 ST Array.

The significance of several of the overexpressed genes has been discussed in Section 6.5. With regards to the underexpressed genes, *Myc* is notable. My experimental system used a bicistronic retrovirus encoding human *MYC* while the microarray probes detect murine *Myc* sequences which are similar but not identical. It is likely that endogenous murine *Myc* expression is suppressed in this experimental system due to the high expression of human *MYC*, the latter not being detectable with the murine-specific probes.

Results from this analysis method (both specific genes and dysregulated pathways) were then compared to a second analysis method (Section 6.6.2) in Section 6.6.3 to determine whether the results obtained were reproducible.

Table 6.6 Genes that had greater than two fold increased (281 genes) or decreased (262 genes) expression in both outgrowths compared to both controls - Method One.

The outgrowths are two *Trp53*^{Bbl} *Myb/MYC*-transformed B cell lines. The controls are *Trp53*^{Bbl} antigen activated B cells 2 days after transduction with *MYC*/GFP vector alone and flow cytometrically sorted for GFP+ cells and *Trp53*^{Bbl} antigen activated B cells 1 day after activation with cognate antigen and CD40 antibody. Partek® software was used to analyse raw data so that differential gene expression between each of the four cell populations could be compared, calculating a fold change for each gene on the array. Only genes that clearly coded for mRNA (RefSeq name starting in NM) were further analysed. The background gene set was all genes coding for mRNA on the chip. Duplicates were removed.

Genes expressed >2x in outgrowths		**Genes expressed <-2x in outgrowths**	
Gene Symbol	**RefSeq**	**Gene Symbol**	**RefSeq**
Atp1b1	NM_009721	*Myc*	NM_010849
Pde2a	NM_001008548	*Hbb-b1*	NM_008220
Myb	NM_010848	*Adm*	NM_009627
Cd93	NM_010740	*Il4i1*	NM_010215
Timp2	NM_011594	*Inpp4b*	NM_001024617
Elovl6	NM_130450	*NF-κB iz*	NM_030612
Gstm1	NM_010358	*Apol7b*	NM_001024848
Slc16a1	NM_009196	*Adora2a*	NM_009630
Mcoln2	NM_026656	*Cd83*	NM_009856
Top1mt	NM_028404	*NF-κB ie*	NM_008690
Tfrc	NM_011638	*Cd69*	NM_001033122
S100a6	NM_011313	*Grap2*	NM_010815
Alpl	NM_007431	*Cflar*	NM_009805
Gclc	NM_010295	*Klrd1*	NM_010654
Ms4a6d	NM_026835	*Ahr*	NM_013464
Dnahc8	NM_013811	*Traf1*	NM_009421
Sox4	NM_009238	*Tspan33*	NM_146173
Rell1	NM_145923	*Slamf1*	NM_013730
Ccnd1	NM_007631	*Cd40*	NM_170701
Trib1	NM_144549	*Cd96*	NM_032465
Galnt7	NM_144731	*Map3k8*	NM_007746
Gfod1	NM_001033399	*Tagap*	NM_145968
Gfi1	NM_010278	*BC065085*	NM_177628
Wdr12	NM_021312	*Ccl22*	NM_009137
Syne2	NM_001005510	*Samsn1*	NM_023380
Acp6	NM_019800	*Il1r2*	NM_010555
Akap12	NM_031185	*Bhlhb2*	NM_011498
Lmo4	NM_010723	*Rel*	NM_009044
Itgam	NM_001082960	*Klf6*	NM_011803
C5ar1	NM_007577	*Plk3*	NM_013807
Tbc1d24	NM_173186	*Icosl*	NM_015790
Mgst1	NM_019946	*Inadl*	NM_172696

Genes expressed >2x in outgrowths		Genes expressed <-2x in outgrowths	
Gene Symbol	**RefSeq**	**Gene Symbol**	**RefSeq**
C3ar1	NM_009779	*Smad7*	NM_001042660
Tirap	NM_054096	*Plscr1*	NM_011636
Mrps18a	NM_026768	*Cd200*	NM_010818
Itgb5	NM_010580	*Tnf*	NM_013693
Serpinb6a	NM_009254	*Sema4a*	NM_013658
Lig4	NM_176953	*Xlr4b*	NM_021365
Apobec1	NM_031159	*Grap*	NM_027817
Thop1	NM_022653	*Plxnc1*	NM_018797
Nuak1	NM_001004363	*Tmem123*	NM_133739
Msr1	NM_031195	*Tlr1*	NM_030682
Klf9	NM_010638	*Cyp2r1*	NM_177382
Ipmk	NM_027184	*Foxj2*	NM_021899
Tmem20	NM_175507	*Pla2g7*	NM_013737
Rragd	NM_027491	*Klf3*	NM_008453
Hmga1	NM_001025427	*Etv6*	NM_007961
Fstl1	NM_008047	*Pdcd1lg2*	NM_021396
Crip1	NM_007763	*Gem*	NM_010276
Zfpm1	NM_009569	*Ccnd2*	NM_009829
Tbxas1	NM_011539	*Syngr2*	NM_009304
Cask	NM_009806	*Tmed8*	NM_001033475
Aoah	NM_012054	*Fnbp1*	NM_001038700
Eps8	NM_007945	*Cd82*	NM_007656
Creg1	NM_011804	*B4galnt1*	NM_008080
Frat1	NM_008043	*C230093N12Rik*	NM_153560
Zeb2	NM_015753	*Sema7a*	NM_011352
Cisd1	NM_134007	*1100001H23Rik*	NM_025806
OTTMUSG00000000971	NM_001081957	*As3mt*	NM_020577
Lima1	NM_023063	*Slfn2*	NM_011408
E2f3	NM_010093	*Epsti1*	NM_029495
Bmpr2	NM_007561	*Fmnl3*	NM_011711
Pmp22	NM_008885	*Dtx3*	NM_030714
Dstn	NM_019771	*Ppp1r16b*	NM_153089
C1qc	NM_007574	*Casp4*	NM_007609
Tada2l	NM_172562	*Skil*	NM_011386
Macrod1	NM_134147	*Tnfrsf18*	NM_009400
Mfge8	NM_008594	*Zfp362*	NM_001081098
Smarca4	NM_011417	*Pacs1*	NM_153129
Anp32e	NM_023210	*St8sia6*	NM_145838
Gpam	NM_008149	*Axud1*	NM_153287
Lrp1	NM_008512	*Chic1*	NM_009767
Dgke	NM_019505	*Btla*	NM_001037719
9130404D14Rik	NM_146119	*Ebi3*	NM_015766
Tmem132e	NM_023438	*Ksr1*	NM_013571
Rabl5	NM_026073	*5730469M10Rik*	NM_027464
Pp11r	NM_008902	*NF-κB 1*	NM_008689
Gdpd1	NM_025638	*P2ry10*	NM_172435
A230097K15Rik	NM_172715	*Slco3a1*	NM_023908
Prelid2	NM_029942	*Atxn7*	NM_139227
Hes1	NM_008235	*EG630499*	NM_001081015

Genes expressed >2x in outgrowths		Genes expressed <-2x in outgrowths	
Gene Symbol	**RefSeq**	**Gene Symbol**	**RefSeq**
Sorcs2	NM_030889	*Scaper*	NM_001081341
Hlx	NM_008250	*Niban*	NM_022018
Arhgap29	NM_172525	*Abhd2*	NM_018811
Prodh	NM_011172	*Plekha5*	NM_144920
Actg2	NM_009610	*Wdr1*	NM_011715
Nr1d1	NM_145434	*Mfhas1*	NM_001081279
Prim2	NM_008922	*Rogdi*	NM_133185
Cpsf2	NM_016856	*Jak1*	NM_146145
Nyx	NM_173415	*Cep63*	NM_001081122
BC002199	NM_145964	*Ifi30*	NM_023065
Atxn2	NM_009125	*Sri*	NM_025618
Man2a2	NM_172903	*H2-Aa*	NM_010378
Mex3a	NM_001029890	*Sorl1*	NM_011436
Nme4	NM_019731	*Sepw1*	NM_009156
Klhdc3	NM_027910	*Mobkl2a*	NM_172457
Sae1	NM_019748	*Jak2*	NM_008413
P4ha1	NM_011030	*Sh3bp5*	NM_011894
Tcfap4	NM_031182	*Bmp2k*	NM_080708
Camk1	NM_133926	*Elk3*	NM_013508
Pls3	NM_145629	*Pacsin1*	NM_011861
Pdia5	NM_028295	*Gimap6*	NM_153175
Lpl	NM_008509	*Runx3*	NM_019732
Ccdc98	NM_172405	*Hmgn3*	NM_026122
Mpi	NM_025837	*Rara*	NM_009024
Xrcc6	NM_010247	*Bcl9l*	NM_030256
Psip1	NM_133948	*Arhgap26*	NM_175164
Myh10	NM_175260	*Mtmr4*	NM_133215
RP23-211P15.2	NM_001099323	*Fcrl1*	NM_178165
Col3a1	NM_009930	*Zdhhc18*	NM_001017968
Fcgr1	NM_010186	*Btg1*	NM_007569
Csf1r	NM_001037859	*Setbp1*	NM_053099
Rab3il1	NM_144538	*Phyh*	NM_010726
Cmtm4	NM_153582	*H2-DMb2*	NM_010388
C1qa	NM_007572	*2310014G06Rik*	NM_001082975
Gsto1	NM_010362	*Vav3*	NM_020505
Slc39a6	NM_139143	*Ifngr2*	NM_008338
Pak1	NM_011035	*Ccdc50*	NM_026202
Pi4k2b	NM_028744	*Prkcb1*	NM_008855
Lgals1	NM_008495	*Tgtp*	NM_011579
Kif24	NM_024241	*Dusp4*	NM_176933
Pkp4	NM_026361	*Tmem62*	NM_175285
Pkd1l3	NM_001039700	*H2-K1*	NM_001001892
Acta2	NM_007392	*Bbs2*	NM_026116
Serinc5	NM_172588	*Gng10*	NM_025277
Nudt4	NM_027722	*Lta*	NM_010735
Rab31	NM_133685	*Tlr9*	NM_031178
5730449L18Rik	NM_025677	*Itgb2*	NM_008404
Frmd4b	NM_145148	*Scotin*	NM_025858
Timp1	NM_001044384	*Cd74*	NM_001042605

Genes expressed >2x in outgrowths		Genes expressed <-2x in outgrowths	
Gene Symbol	**RefSeq**	**Gene Symbol**	**RefSeq**
C1qb	NM_009777	*Slc2a6*	NM_172659
T2bp	NM_145133	*Rhof*	NM_175092
Igf2bp3	NM_023670	*Tmcc3*	NM_172051
Smarcc1	NM_009211	*Bank1*	NM_001033350
Diras2	NM_001024474	*Ddx26b*	NM_172779
Cyb5r1	NM_028057	*Stat4*	NM_011487
Lox	NM_010728	*Trim7*	NM_053166
Cpe	NM_013494	*4432416J03Rik*	NM_030069
Dab2	NM_023118	*Crebl2*	NM_177687
A930008G19Rik	NM_175268	*H2-Q8*	NM_023124
Prkar2b	NM_011158	*Cnn2*	NM_007725
Ppil1	NM_026845	*Hsd11b1*	NM_008288
Tm4sf1	NM_008536	*9130017C17Rik*	NM_027840
Abhd14a	NM_001110271	*St3gal1*	NM_009177
B4galt6	NM_019737	*Ms4a1*	NM_007641
Pcolce	NM_008788	*Ptprc*	NM_011210
Frat2	NM_177603	*Ccdc122*	NM_175369
Gk5	NM_177352	*Mgrn1*	NM_029657
Ryk	NM_013649	*Dexi*	NM_021428
Dcn	NM_007833	*Ctso*	NM_177662
Tspan4	NM_053082	*Ell2*	NM_138953
Wdr34	NM_001008498	*Atp10a*	NM_009728
Cox6a2	NM_009943	*9130227C08Rik*	NM_027143
Ankrd13b	NM_172945	*Gbp1*	NM_010259
Camkv	NM_145621	*Rab27a*	NM_023635
Col1a1	NM_007742	*Ltb*	NM_008518
Gtf3c4	NM_172977	*Irf5*	NM_012057
Mdm1	NM_148922	*Gimap3*	NM_031247
Nudcd2	NM_026023	*Man1a*	NM_008548
Lonrf3	NM_028894	*Lynx1*	NM_011838
Nt5dc2	NM_027289	*Pip4k2a*	NM_008845
Sap30	NM_021788	*Gnpda2*	NM_001038015
Pdpn	NM_010329	*Chd7*	NM_001081417
9430020K01Rik	NM_001081963	*2510002D24Rik*	NM_001033164
Crtap	NM_019922	*Unc119*	NM_011676
Ankrd1	NM_013468	*Ids*	NM_010498
Msh2	NM_008628	*Tmsb4x*	NM_021278
Plod3	NM_011962	*Pglyrp1*	NM_009402
Pomt1	NM_145145	*Ly96*	NM_016923
Parva	NM_020606	*BC026585*	NM_001033284
Mafb	NM_010658	*3830406C13Rik*	NM_146051
Ptplad2	NM_025760	*Pik3ap1*	NM_031376
Sparc	NM_009242	*Mef2c*	NM_025282
BC027057	NM_145976	*Gimap4*	NM_174990
Sdc1	NM_011519	*H2-M3*	NM_013819
Colec12	NM_130449	*Camk2d*	NM_001025439
Srl	NM_175347	*Lrch1*	NM_001033439
Slco4a1	NM_148933	*Phf21a*	NM_001109691
Fbln2	NM_007992	*Slc39a4*	NM_028064

Genes expressed >2x in outgrowths		Genes expressed <-2x in outgrowths	
Gene Symbol	**RefSeq**	**Gene Symbol**	**RefSeq**
Srd5a1	NM_175283	*2010002N04Rik*	NM_134133
Cald1	NM_145575	*Ctsh*	NM_007801
Cdca7	NM_025866	*Ptpn22*	NM_008979
Inppl1	NM_010567	*Gca*	NM_145523
Gfi1b	NM_008114	*Dok1*	NM_010070
Gkap1	NM_019832	*Lrrc61*	NM_177736
Bgn	NM_007542	*Dennd1c*	NM_153551
Tmem41a	NM_025693	*Lilrb3*	NM_011095
Cyr61	NM_010516	*Cd52*	NM_013706
Ypel2	NM_001005341	*Il4ra*	NM_001008700
Thbd	NM_009378	*Dtx4*	NM_172442
Bag2	NM_145392	*Sh3kbp1*	NM_021389
Nsbp1	NM_016710	*Gimap8*	NM_001077410
Cdkn2a	NM_001040654	*Nfatc2*	NM_010899
Adssl1	NM_007421	*Malt1*	NM_172833
Enpep	NM_007934	*Stat1*	NM_009283
Cxcl4	NM_019932	*Hps3*	NM_080634
Insm1	NM_016889	*Vasp*	NM_009499
BC021395	NM_144861	*Cd180*	NM_008533
Gfra1	NM_010279	*5830443L24Rik*	NM_029509
Nfib	NM_008687	*Cnr2*	NM_009924
Sgce	NM_011360	*Csf2rb*	NM_007780
Rnaseh2a	NM_027187	*Capn1*	NM_007600
Ssx2ip	NM_138744	*Ciita*	NM_007575
Akap1	NM_009648	*Rps6ka1*	NM_009097
Steap3	NM_001085409	*Sh3bgrl3*	NM_080559
Cfh	NM_009888	*BC057170*	NM_172777
2310066E14Rik	NM_001081241	*Sema4d*	NM_013660
Eml1	NM_001043335	*Zbtb38*	NM_175537
F11r	NM_172647	*H2-Oa*	NM_008206
Otub2	NM_026580	*Mgst2*	NM_174995
Pgcp	NM_018755	*Serpina3f*	NM_001033335
Alox5ap	NM_009663	*Sh2d2a*	NM_021309
Lgr5	NM_010195	*Pdlim2*	NM_145978
Cks1b	NM_016904	*Ly6a*	NM_010738
Adarb1	NM_001024840	*Gimap5*	NM_175035
Peg10	NM_130877	*Tlr7*	NM_133211
Plod1	NM_011122	*LOC626578*	NM_001039646
Ccdc80	NM_026439	*Iigp1*	NM_021792
Vegfa	NM_001025250	*Itgal*	NM_008400
1700027N10Rik	NM_029338	*Kmo*	NM_133809
Gpr12	NM_001010941	*Atxn1*	NM_009124
B430119L13Rik	NM_177303	*Tcf4*	NM_013685
Ifitm3	NM_025378	*Amigo2*	NM_178114
Mrpl34	NM_053162	*Gbp2*	NM_010260
Bst1	NM_009763	*Ly6c1*	NM_010741
Ckb	NM_021273	*Map3k5*	NM_008580
St3gal5	NM_011375	*Gpr174*	NM_001033251
Col1a2	NM_007743	*1810054D07Rik*	NM_027238

Genes expressed >2x in outgrowths		Genes expressed <-2x in outgrowths	
Gene Symbol	**RefSeq**	**Gene Symbol**	**RefSeq**
Siglec1	NM_011426	*Lbh*	NM_029999
Gstm5	NM_010360	*B630005N14Rik*	NM_175312
Trf	NM_133977	*Car2*	NM_009801
Fn1	NM_010233	*Ms4a4c*	NM_029499
2610002D18Rik	NM_001081099	*BC013672*	NM_001081215
March8	NM_027920	*Gbp3*	NM_018734
Ppm1f	NM_176833	*Capg*	NM_007599
Stambpl1	NM_029682	*Aldoc*	NM_009657
Timp3	NM_011595	*St3gal6*	NM_018784
Ptprs	NM_011218	*H2-T22*	NM_010397
Eef2k	NM_007908	*1300014I06Rik*	NM_025831
Rtkn2	NM_001081346	*Slc46a3*	NM_027872
Tagln	NM_011526	*RP23-45P4.1*	NM_001099328
Hdac5	NM_001077696	*9430067K14Rik*	NM_001039493
Pdxp	NM_020271	*Alcam*	NM_009655
Trem2	NM_031254	*Marveld2*	NM_001038602
Zwilch	NM_026507	*Gbp6*	NM_001083312
Hmgcll1	NM_173731	*Abcg3*	NM_030239
Nedd4	NM_010890	*Syt11*	NM_018804
Msr2	NM_030707	*Slc35d2*	NM_001001321
Cysltr1	NM_021476	*Grm6*	NM_173372
Prkar2a	NM_008924	*Nlrc3*	NM_001081280
Exo1	NM_012012	*Tmem154*	NM_177260
Bcat1	NM_001024468	*A530023O14Rik*	NM_175648
Foxf2	NM_010225	*Lrrk2*	NM_025730
Dck	NM_007832	*4933437F05Rik*	NM_027744
Ltb4dh	NM_025968	*Arhgef3*	NM_027871
Cyp1b1	NM_009994	*Rnase6*	NM_030098
Skp2	NM_145468	*Flt3*	NM_010229
Shcbp1	NM_011369	*Rab30*	NM_029494
Ptgs1	NM_008969	*Gimap7*	NM_146167
Myl4	NM_010858	*A530088I07Rik*	NM_175437
Dusp3	NM_028207	*St14*	NM_011176
Pla2g4a	NM_008869	*Cxcr3*	NM_009910
Pcyox1	NM_025823		
1500011H22Rik	NM_026883		
Rasl10a	NM_145216		
Gas6	NM_019521		
Capn5	NM_007602		
Cdc25b	NM_023117		
Sept10	NM_001024911		
Cenpp	NM_025495		
Hist2h3c2	NM_054045		
Tubb2b	NM_023716		
Ccdc18	NM_028481		
EG639396	NM_001039251		
Ttk	NM_009445		
Chek2	NM_016681		
Sord	NM_146126		

Genes expressed >2x in outgrowths	
Gene Symbol	**RefSeq**
Bcl7a	NM_029850
Vpreb3	NM_009514
Cth	NM_145953
Hist1h2bc	NM_023422

6.6.2 Differential gene expression – Method Two

Analysis of Variance (ANOVA) was the second data analysis method. The initial part of the analysis (Figure 6.1) entailed ensuring that this statistical tool was appropriate for these samples, and identifying excess 'noise' using a Principal Component Analysis and a Sources of Variation graph respectively (Figure 6.1). The Principal Component Analysis (PCA) was used to ensure that the controls were more similar to each other than the test samples and showed that the two outgrowth specimens cluster together while the two controls are less similar to each other (as expected given that the activated B cells had only been activated for 24 hrs and have fewer B cells in cycle), but are also distinct from the outgrowths. 'Sources of Variation' graphs were also created to compare the variation within groups (ie between the two controls or between the two outgrowths), which partly reflects background 'noise' due to subtle differences in array chip manufacture, technique of RNA production, processing date etc, to the variation between groups (ie controls versus outgrowths). Higher variation between groups than within groups suggests that results are more likely to be due to biological variation than error ('noise'). The results from our data suggested that the ANOVA method of analysis was appropriate for this data.

Microarray outputs from 15 981 genes encoding mRNA on the Affymetrix GeneChip® 1.0 ST Array were thus analysed with the assistance of the ACRF BRF using an ANOVA analysis on Partek® software with a view to pathway analysis. Interestingly, *Myb* overexpression and *Myc* suppression did not features in this analysis. Results from this analysis method (both specific genes and dysregulated pathways) were subsequently compared to a first analysis method (Section 6.6.1) in Section 6.6.3 to determine whether the results obtained were reproducible.

Figure 6.1 ANOVA analysis - Validation

a) Principal component analysis. Gene expression data from each cell type has been transformed using Partek® software into three sets of linearly uncorrelated variables called principal components, as shown on separate axes, highlighting similarities and differences between groups.
b) and c) Sources of Variation graph showing mean and median F ratios respectively were generated using Partek® software. The F ratio compares 'between group variation' to 'within group variation,' the higher the value obtained the more likely differences between two groups is due to the factor being tested, and not just the natural variation within a group.

a)

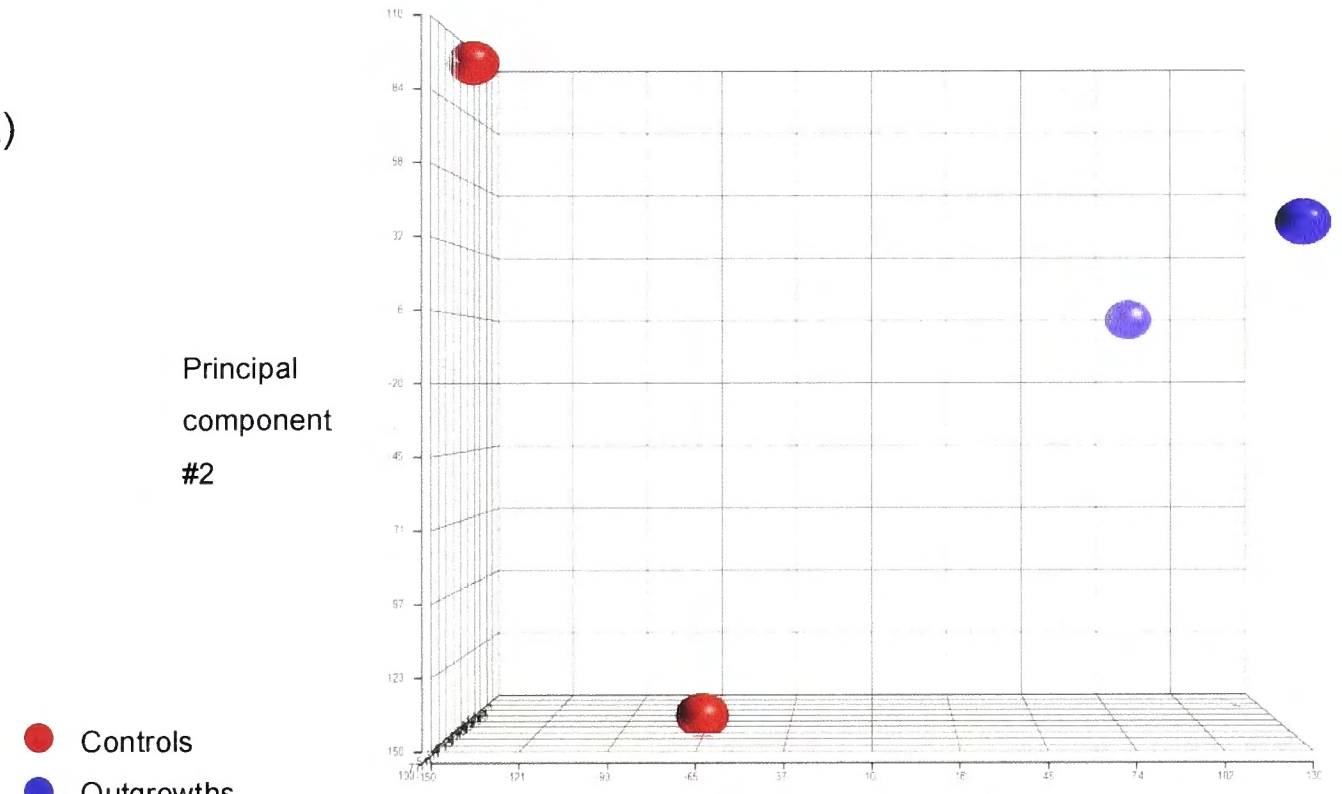

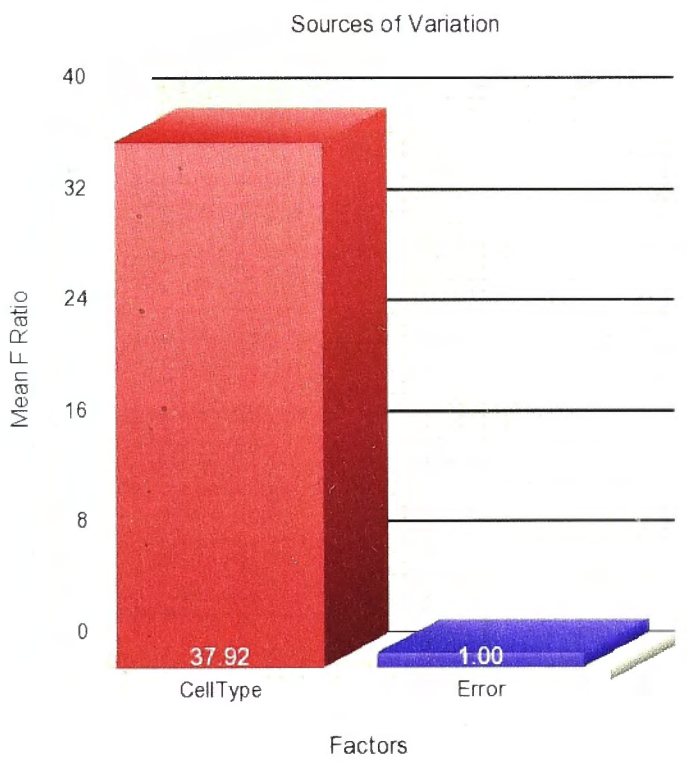

b)

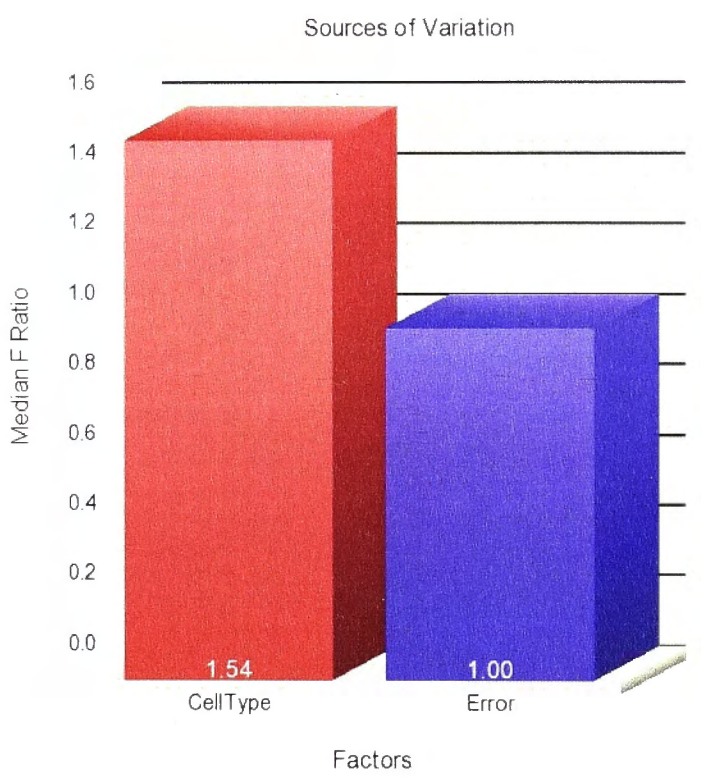

c)

Table 6.7 Genes in outgrowths that had greater than two fold increased (125 genes) or decreased (88 genes) expression than controls – Method Two

The outgrowths are two *Trp53*^{Bbl} *Myb+MYC*-transformed B cell lines. The controls are *Trp53*^{Bbl} antigen activated B cells 2 days after transduction with *MYC*/GFP vector alone and flow cytometrically sorted for GFP+ cells and *Trp53*^{wt} antigen activated B cells 1 day after activation with cognate antigen and CD40 antibody. ANOVA analysis on all 15 981 genes encoding mRNA on the Affymetrix GeneChip® 1.0 ST Array was performed using Partek® software. $p<0.01$

Genes expressed >2x in outgrowths			**Genes expressed <-2x in outgrowths**		
Gene Symbol	**RefSeq**	**Fold change**	**Gene Symbol**	**RefSeq**	**Fold change**
Spp1	NM_009263	33.60	*Gimap4*	NM_174990	-65.66
C1qc	NM_007574	27.36	*Cr2*	NM_007758	-51.27
Sox4	NM_009238	22.85	*Igj*	NM_152839	-37.53
Acta2	NM_007392	22.65	*Stat4*	NM_011487	-31.40
Uchl1	NM_011670	18.05	*Kynu*	NM_027552	-26.05
C1qa	NM_007572	16.43	*Il9r*	NM_001134458	-25.16
Dab2	NM_023118	15.72	*Sema7a*	NM_011352	-22.22
Myl4	NM_010858	14.80	*Dusp4*	NM_176933	-17.89
Nt5dc2	NM_027289	13.60	*Itgal*	NM_008400	-16.95
Fcrls	NM_030707	12.66	*St8sia6*	NM_145838	-15.88
Ehd2	NM_153068	12.44	*Plbd1*	NM_025806	-14.96
Thbd	NM_009378	12.10	*Fas*	NM_007987	-12.73
Igf2bp3	NM_023670	11.47	*Setbp1*	NM_053099	-12.49
Cdkn2a	NM_001040654	10.82	*Ebi3*	NM_015766	-11.96
Timp3	NM_011595	10.27	*Cd80*	NM_009855	-10.21
Cpe	NM_013494	9.59	*As3mt*	NM_020577	-9.56
Otub2	NM_001177841	9.52	*Gimap8*	NM_001077410	-7.43
Enpep	NM_007934	8.69	*Tgtp1*	NM_011579	-6.84
Ryk	NM_013649	8.58	*Gimap6*	NM_153175	-6.46
Sertad4	NM_198247	8.57	*Trim7*	NM_053166	-6.31
Ptprs	NM_011218	6.72	*Pglyrp1*	NM_009402	-6.05
Camkv	NM_145621	6.61	*Cnn2*	NM_007725	-5.88
Bgn	NM_007542	6.47	*Dock10*	NM_175291	-5.63
Eml1	NM_001043335	6.45	*Il4ra*	NM_001008700	-5.59
Arhgap29	NM_172525	6.23	*Hmgn3*	NM_026122	-5.45
Cenpv	NM_028448	5.79	*Bmyc*	NM_023326	-5.35
Lgals1	NM_008495	5.68	*Arap2*	NM_178407	-4.85
Tspan4	NM_053082	5.60	*Man1a*	NM_008548	-4.60
Cfh	NM_009888	5.50	*Ctsw*	NM_009985	-4.43
Pf4	NM_019932	5.28	*Bmp2k*	NM_080708	-4.40
Lgr5	NM_010195	5.15	*Mef2c*	NM_001170537	-4.27
Nfib	NM_00111320	5.11	*H2-gs10*	NM_001143689	-3.99

Genes expressed >2x in outgrowths			Genes expressed <-2x in outgrowths		
Gene Symbol	**RefSeq**	**Fold change**	**Gene Symbol**	**RefSeq**	**Fold change**
	9				
Bmpr2	NM_007561	4.91	*Gca*	NM_145523	-3.93
Mgst1	NM_019946	4.90	*H2-Q8*	NM_023124	-3.77
Car12	NM_178396	4.85	*Jak1*	NM_146145	-3.50
Steap3	NM_001085409	4.81	*H2-Q6*	NM_207648	-3.50
Nyx	NM_173415	4.79	*Arhgap26*	NM_175164	-3.44
B4galt6	NM_019737	4.70	*Rogdi*	NM_133185	-3.38
Gpd1l	NM_175380	4.68	*Pkib*	NM_008863	-3.26
Rcor2	NM_054048	4.45	*Elk3*	NM_013508	-3.16
Dusp3	NM_028207	4.03	*Atp10a*	NM_009728	-3.14
Lrrn4	NM_177303	3.90	*Ccdc50*	NM_026202	-3.13
Hes1	NM_008235	3.88	*Hsd11b1*	NM_008288	-3.09
9430020K01Rik	NM_001081963	3.88	*H2-K1*	NM_001001892	-3.05
Ccbl1	NM_172404	3.86	*Gbp1*	NM_010259	-2.99
Grip1	NM_028736	3.83	*Camk2d*	NM_001025439	-2.98
Akap1	NM_009648	3.80	*3830406C13Rik*	NM_146051	-2.95
Sap30	NM_021788	3.78	*Fxyd5*	NM_008761	-2.87
Hmgcll1	NM_173731	3.61	*Ell2*	NM_138953	-2.82
Frat2	NM_177603	3.59	*Ptprc*	NM_001111316	-2.80
Gsto1	NM_010362	3.56	*Chd7*	NM_001081417	-2.76
Tanc2	NM_181071	3.52	*H2-Q7*	NM_010394	-2.75
Gpr176	NM_201367	3.49	*Acot2*	NM_134188	-2.68
Serinc5	NM_172588	3.45	*Maml2*	NM_001013813	-2.67
Slco4a1	NM_148933	3.42	*Rab27a*	NM_023635	-2.64
Timp1	NM_001044384	3.39	*Tmem62*	NM_175285	-2.61
Arvcf	NM_033474	3.34	*Slc39a4*	NM_028064	-2.60
Lonrf3	NM_028894	3.34	*Ly6k*	NM_029627	-2.57
Pgcp	NM_018755	3.18	*Mbp*	NM_010777	-2.56
Stambpl1	NM_029682	3.16	*Ccdc122*	NM_175369	-2.55
Stc2	NM_011491	3.12	*Pik3ap1*	NM_031376	-2.54
Exo1	NM_012012	3.12	*Lrrc61*	NM_177736	-2.53
Nedd4	NM_010890	3.09	*Mtmr14*	NM_026849	-2.52
Pdxp	NM_020271	2.97	*Fbxl17*	NM_015794	-2.52
Rab31	NM_133685	2.97	*Tmsb4x*	NM_021278	-2.51
Pak1	NM_011035	2.94	*Vav3*	NM_020505	-2.44
Man1c1	NM_207237	2.86	*Gm6377*	NM_001037917	-2.43
Crlf1	NM_018827	2.86	*Tgfbr2*	NM_009371	-2.43
Srd5a1	NM_175283	2.85	*Ifngr2*	NM_008338	-2.42
Plod3	NM_011962	2.82	*Pira11*	NM_011088	-2.39
Lix1l	NM_001163170	2.82	*Vav2*	NM_009500	-2.31
2900026A02Rik	NM_172884	2.81	*Neurl3*	NM_153408	-2.31
Cyb5r1	NM_028057	2.81	*Phf21a*	NM_001109691	-2.29
Pik3r2	NM_008841	2.80	*Runx3*	NM_019732	-2.19

Genes expressed >2x in outgrowths			Genes expressed <-2x in outgrowths		
Gene Symbol	**RefSeq**	**Fold change**	**Gene Symbol**	**RefSeq**	**Fold change**
Kif24	NM_024241	2.76	*Mgrn1*	NM_029657	-2.18
Mrpl34	NM_053162	2.75	*Cr1l*	NM_013499	-2.14
Rcor1	NM_198023	2.73	*Tbxa2r*	NM_009325	-2.12
Nudt4	NM_027722	2.68	*Ccdc50*	NM_001025615	-2.12
Mdm1	NM_001162904	2.68	*H2-D1*	NM_010380	-2.10
Rprd1a	NM_144861	2.63	*Cast*	NM_009817	-2.10
Spire1	NM_194355	2.60	*Tyk2*	NM_018793	-2.08
Xk	NM_023500	2.58	*Crebl2*	NM_177687	-2.08
Nudcd2	NM_026023	2.58	*Dexi*	NM_021428	-2.08
Cpsf2	NM_016856	2.55	*Mtmr4*	NM_133215	-2.07
Tcfap4	NM_031182	2.55	*Ceacam16*	NM_001033419	-2.06
Lamc1	NM_010683	2.50	*2010011I20 Rik*	NM_025912	-2.04
Cd14	NM_009841	2.48	*Ysk4*	NM_011737	-2.04
Capsl	NM_029341	2.47	*Gnpda2*	NM_001038015	-2.03
Cdca7	NM_025866	2.47			
Rsph1	NM_025290	2.45			
Msh2	NM_008628	2.41			
St3gal5	NM_011375	2.41			
Nat8l	NM_001001985	2.40			
Gtf2e2	NM_001167922	2.39			
Tmem41a	NM_025693	2.38			
Zfp422	NM_026057	2.33			
Adam15	NM_001037722	2.32			
Tcf3	NM_001164147	2.31			
Alms1	NM_145223	2.28			
Sirpb1b	NM_001173460	2.28			
Uhrf1bp1	NM_001080769	2.26			
Ppil1	NM_026845	2.25			
Ccl25	NM_009138	2.24			
Meis1	NM_010789	2.24			
Tulp3	NM_011657	2.22			
Rapgefl1	NM_001080925	2.22			
Sae1	NM_019748	2.21			
Mpzl1	NM_001083897	2.21			
Thyn1	NM_144543	2.20			
Zfp358	NM_080461	2.19			
Cdc42bpa	NM_001033285	2.17			
Smarcc1	NM_009211	2.17			

Genes expressed >2x in outgrowths		
Gene Symbol	**RefSeq**	**Fold change**
Rilpl1	NM_021430	2.15
Cxcl14	NM_019568	2.14
Wbp5	NM_011712	2.11
Zranb2	NM_017381	2.09
Fam164a	NM_173181	2.08
Anks1	NM_181413	2.06
Trip13	NM_027182	2.05
Patz1	NM_019574	2.04
Gne	NM_015828	2.03
Chordc1	NM_025844	2.01
Ece2	NM_025462	2.01
Ccdc137	NM_152807	2.01
Hells	NM_008234	2.00

6.6.3 Similarities between groups of differentially expressed genes obtained with different statistical methods

The Venn diagram (Figure 6.2) and table (Table 6.8) below illustrate and detail the common genes identified in the two analysis methods. The modest fraction of similarly differentially expressed genes with the two analysis methods reflects both the small number of samples and controls used in this experiment, and the difficulties and limitations of microarray analyses in general.

On the whole genes shown to be dysregulated in Burkitt lymphoma compared to Diffuse Large B cell Lymphoma [199,344] did not features prominently which is likely to reflect the different control populations in these publications compared to this research and limitations of this pilot microarray analysis, among other factors.

Pathway analysis was performed to review the data in terms of general trends rather than on a gene-by-gene basis.

Figure 6.2 Enumeration of common genes in the two data sets

This figure illustrates the number of genes a) overexpressed and b) underexpressed two fold in the two *Trp53*^{Bbl} *Myb/MYC*-transformed B cell lines compared to controls (*Trp53*^{Bbl} antigen activated B cells 2 days after transduction with *MYC*/GFP vector alone and flow cytometrically sorted for GFP+ cells, and *Trp53*^{wt} antigen activated B cells 1 day after activation with cognate antigen and CD40 antibody) using each microarray analysis method and the number of genes common to both analyses.

a)

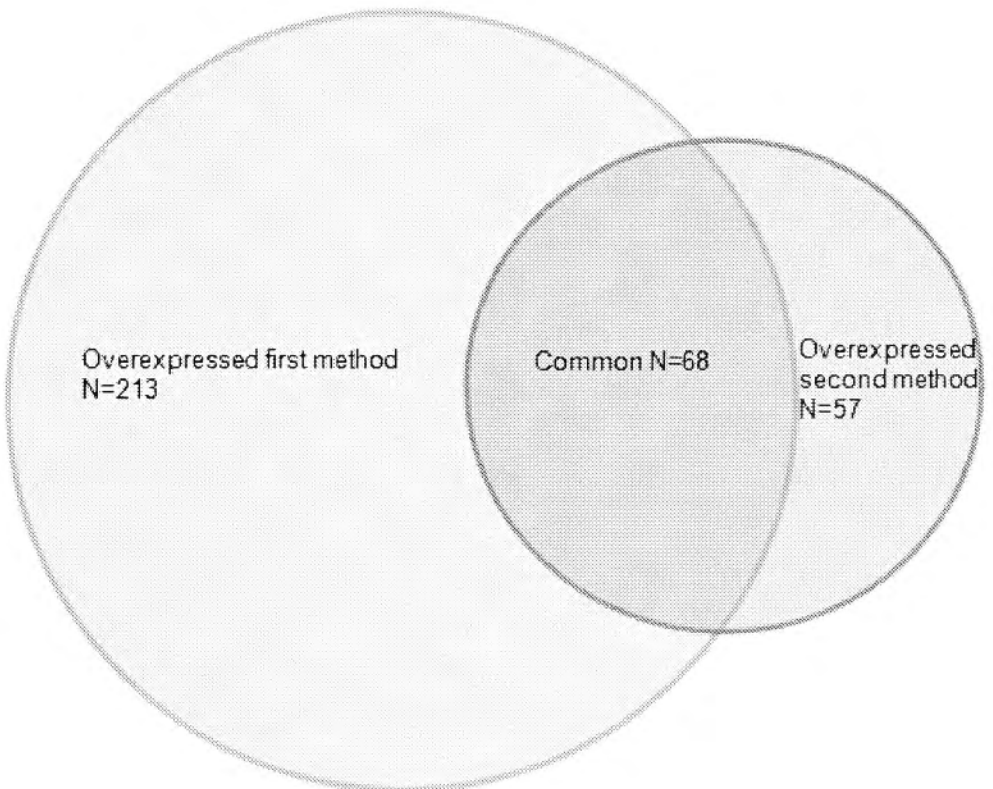

b)

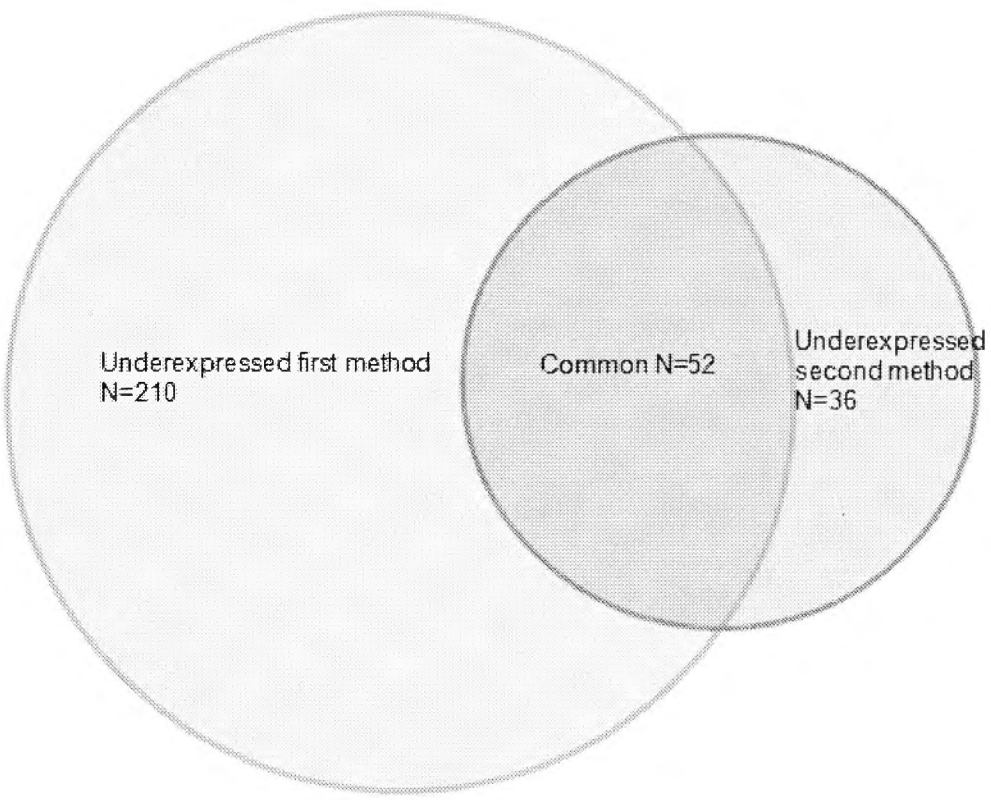

Table 6.8 List of common genes in the two data sets

List of genes overexpressed and underexpressed two fold in outgrowths compared to controls in both microarray analysis methods. The outgrowths are two *Trp53*^{Bbl} *Myb/MYC*-transformed B cell lines. The two controls are *Trp53*^{Bbl} antigen activated B cells 2 days after transduction with *MYC*/GFP vector alone and flow cytometrically sorted for GFP+ cells, and *Trp53*^{wt} antigen activated B cells 1 day after activation with cognate antigen and CD40 antibody.

Genes expressed >2x controls		Genes expressed <-2x controls	
Gene Symbol	**RefSeq**	**Gene Symbol**	**RefSeq**
Sox4	NM_009238	*Sema7a*	NM_011352
Mgst1	NM_019946	*Plbd1*	NM_025806
Bmpr2	NM_007561	*As3mt*	NM_020577
C1qc	NM_007574	*St8sia6*	NM_145838
Hes1	NM_008235	*Ebi3*	NM_015766
Arhgap29	NM_172525	*Rogdi*	NM_133185
Cpsf2	NM_016856	*Jak1*	NM_146145
Nyx	NM_173415	*Bmp2k*	NM_080708
Sae1	NM_019748	*Elk3*	NM_013508
Tcfap4	NM_031182	*Gimap6*	NM_153175
C1qa	NM_007572	*Runx3*	NM_019732
Gsto1	NM_010362	*Hmgn3*	NM_026122
Pak1	NM_011035	*Arhgap26*	NM_175164
Lgals1	NM_008495	*Mtmr4*	NM_133215
Kif24	NM_024241	*Setbp1*	NM_053099
Acta2	NM_007392	*Vav3*	NM_020505
Serinc5	NM_172588	*Ifngr2*	NM_008338
Nudt4	NM_027722	*Ccdc50*	NM_026202
Rab31	NM_133685	*Tgtp1*	NM_011579
Timp1	NM_001044384	*Dusp4*	NM_176933
Igf2bp3	NM_023670	*Tmem62*	NM_175285
Smarcc1	NM_009211	*H2-K1*	NM_001001892
Cyb5r1	NM_028057	*Stat4*	NM_011487
Cpe	NM_013494	*Trim7*	NM_053166
Dab2	NM_023118	*Crebl2*	NM_177687
Ppil1	NM_026845	*H2-Q8*	NM_023124
B4galt6	NM_019737	*Cnn2*	NM_007725
Frat2	NM_177603	*Hsd11b1*	NM_008288
Ryk	NM_013649	*Ccdc122*	NM_175369
Tspan4	NM_053082	*Mgm1*	NM_029657
Camkv	NM_145621	*Dexi*	NM_021428
Nudcd2	NM_026023	*Ell2*	NM_138953
Lonrf3	NM_028894	*Atp10a*	NM_009728
Nt5dc2	NM_027289	*Gbp1*	NM_010259
Sap30	NM_021788	*Rab27a*	NM_023635
9430020K01Rik	NM_001081963	*Man1a*	NM_008548
Msh2	NM_008628	*Gnpda2*	NM_001038015
Plod3	NM_011962	*Chd7*	NM_001081417
Slco4a1	NM_148933	*Tmsb4x*	NM_021278
Srd5a1	NM_175283	*Pglyrp1*	NM_009402
Cdca7	NM_025866	*3830406C13Rik*	NM_146051

Bgn	NM_007542	*Pik3ap1*	NM_031376
Tmem41a	NM_025693	*Gimap4*	NM_174990
Thbd	NM_009378	*Camk2d*	NM_001025439
Cdkn2a	NM_001040654	*Phf21a*	NM_001109691
Enpep	NM_007934	*Slc39a4*	NM_028064
Pf4	NM_019932	*Gca*	NM_145523
Rprd1a	NM_144861	*Lrrc61*	NM_177736
Akap1	NM_009648	*Il4ra*	NM_001008700
Steap3	NM_001085409	*Gimap8*	NM_001077410
Cfh	NM_009888	*Itgal*	NM_008400
Eml1	NM_001043335		
Pgcp	NM_018755		
Lgr5	NM_010195		
Lrrn4	NM_177303		
Mrpl34	NM_053162		
St3gal5	NM_011375		
Stambpl1	NM_029682		
Timp3	NM_011595		
Ptprs	NM_011218		
Pdxp	NM_020271		
Hmgcll1	NM_173731		
Nedd4	NM_010890		
Fcrls	NM_030707		
Exo1	NM_012012		
Myl4	NM_010858		
Dusp3	NM_028207		

6.7 Significantly altered pathways

Functional annotation was performed using the Database for Annotation, Visualization, and Integrated Discovery (DAVID) resource (http://david.abcc.ncifcrf.gov) from National Institute of Allergy and Infectious Diseases (NIAID), NIH [480] version 6.7. Pathway analysis was performed for the two gene sets obtained using the two different methods of microarray analysis (Table 6.9 and Table 6.10) and for the gene set in common to both analysis methods (Table 6.11). These gene sets were individually mapped to cellular pathways defined by the Kyoto Encyclopaedia of Genes and Genomes (KEGG) atlas from Kanehisa Laboratories, Japan [481]. Those pathways in which these differentially expressed genes were over represented compared to the background list of all the mRNAs on the GeneChip® were thus determined.

Less than 50% of the differentially expressed genes were able to be mapped to KEGG atlas pathways, reducing the power of this analysis. In addition, some further information was potentially lost by only analysing mRNA-encoding genes detailed in RefSeq, without including recently discovered but incompletely described genes. Discrepancies in gene labelling between DAVID and the KEGG atlas, including the fact that the KEGG atlas often represents multiple genes of highly related family members as a single gene in their pathways, means that the statistics from this pathway mapping are imprecise.

Several 'pathways' identified in the broader analysis deserve particular mention. It must be recalled that as the KEGG pathways contain genes that both promote and inhibit a given pathway, and the genes mapped to the pathways are either over or under expressed in the data analysis, enrichment of a certain pathway's genes does not necessarily mean that that pathway is more active in that cell population, but rather that it is likely to be differentially regulated.

Natural killer cell mediated cytotoxicity

This 'pathway' has been highlighted, but most of its dysregulated genes are not specific to NK cells, including MHC class I genes and interferon genes which are widely expressed. There are unlikely to be many NK cells in either control

or the autonomously growing cells population, although their numbers were not specifically counted.

Cell adhesion molecules

As illustrated in Figure 6.3 'Cellular adhesion molecules' is not a single pathway, but rather sets of genes involved in different types of intercellular adhesion. Adhesion molecules specific to the immune system were the most common subcategory identified, which will be at least partially due to differences in activation status and numbers of contaminating T cells between the autonomously growing cells and controls. It is possible that this result may also reflect true differences in the requirement for adhesion molecules between control lymphocytes (predominantly B cells) and autonomously growing cells, but this requires further research.

Allograft rejection / Graft versus host disease / Antigen processing and presentation / Viral myocarditis / Type 1 diabetes mellitus / Systemic lupus erythematosus / Autoimmune thyroid disease / Asthma

These pathways have been highlighted predominantly due to the differential expression of major histocompatibility complex (MHC) genes and tumour necrosis factor (TNF) family genes which, as mentioned above, are not specific to these physiological/pathological processes.

Toll-like receptor signalling pathway

As discussed in Section 1.4.2, toll-like receptors are found on many cells and have a role in innate immunity. Their antigens are components of microorganisms and their downstream pathways vary with the receptor subtype but include some pathways in common with downstream signalling from the B cell receptor. It is of interest that this pathway was highlighted, although the significance of this finding is unclear.

Relevance of pathways not significantly over represented

It is also important to consider the pathways that were not found to be enriched in these analyses. KEGG pathways describe a 'B cell receptor signalling pathway', and, as described above, the genes within this pathway were not over represented in our outgrowth. This 'pathway', however, includes, among other

components, the MAPK signalling pathway, NF-κB signalling pathway, and the PI3K signalling pathways. Focussed pathway-specific gene analyses (such as detailed for the NF-κB pathway above) are required to better define these components.

Also of interest, the DAVID analyses do not highlight apoptotic pathways or cell cycle pathway genes in general as being dysregulated in autonomously proliferating cells compared to control populations. This may indicate that altered activity of these pathways is not a feature of this rapidly proliferating population but, as described in this chapter, many factors limit these analyses.

Table 6.9 Pathway analysis from microarray analysis method one

The over and under expressed genes from Table 6.3 were mapped to cellular pathways using the DAVID resource. Over represented pathways, the number and percentage of total genes implicated, fold enrichment and p value are listed below. Only pathways that contained at least five differentially expressed genes were considered. The p value was calculated by the DAVID program and was calculated using a modified Fisher Exact test. Those pathways with $p<0.01$ are shown.

Term	Count	%	p Value	Fold Enrichment
Cell adhesion molecules	18	3.3	0.000012	3.4
Type I diabetes mellitus	10	1.8	0.000062	5.4
Allograft rejection	9	1.7	0.000083	5.9
Graft-versus-host disease	9	1.7	0.000083	5.9
Viral myocarditis	12	2.2	0.000117	4.1
Antigen processing and presentation	12	2.2	0.000137	4.0
Systemic lupus erythematosus	11	2.0	0.000703	3.6
Toll-like receptor signalling pathway	11	2.0	0.003441	3.0
Autoimmune thyroid disease	8	1.5	0.003698	3.9
Hematopoietic cell lineage	10	1.8	0.003848	3.1
Asthma	5	0.9	0.007888	6.0

Figure 6.3 Pathway analysis for microarray analysis method one

The figures below are graphical representations of the location of the dysregulated genes/gene groups listed in Table 6.9 in cellular pathways. The figures are modified from the DAVID website, the under or overexpressed gene in this dataset being highlighted in black boxes. Not all genes in pathways are included in KEGG pathways and some 'gene' names reflect families of genes rather than detailing all the members.

Legend

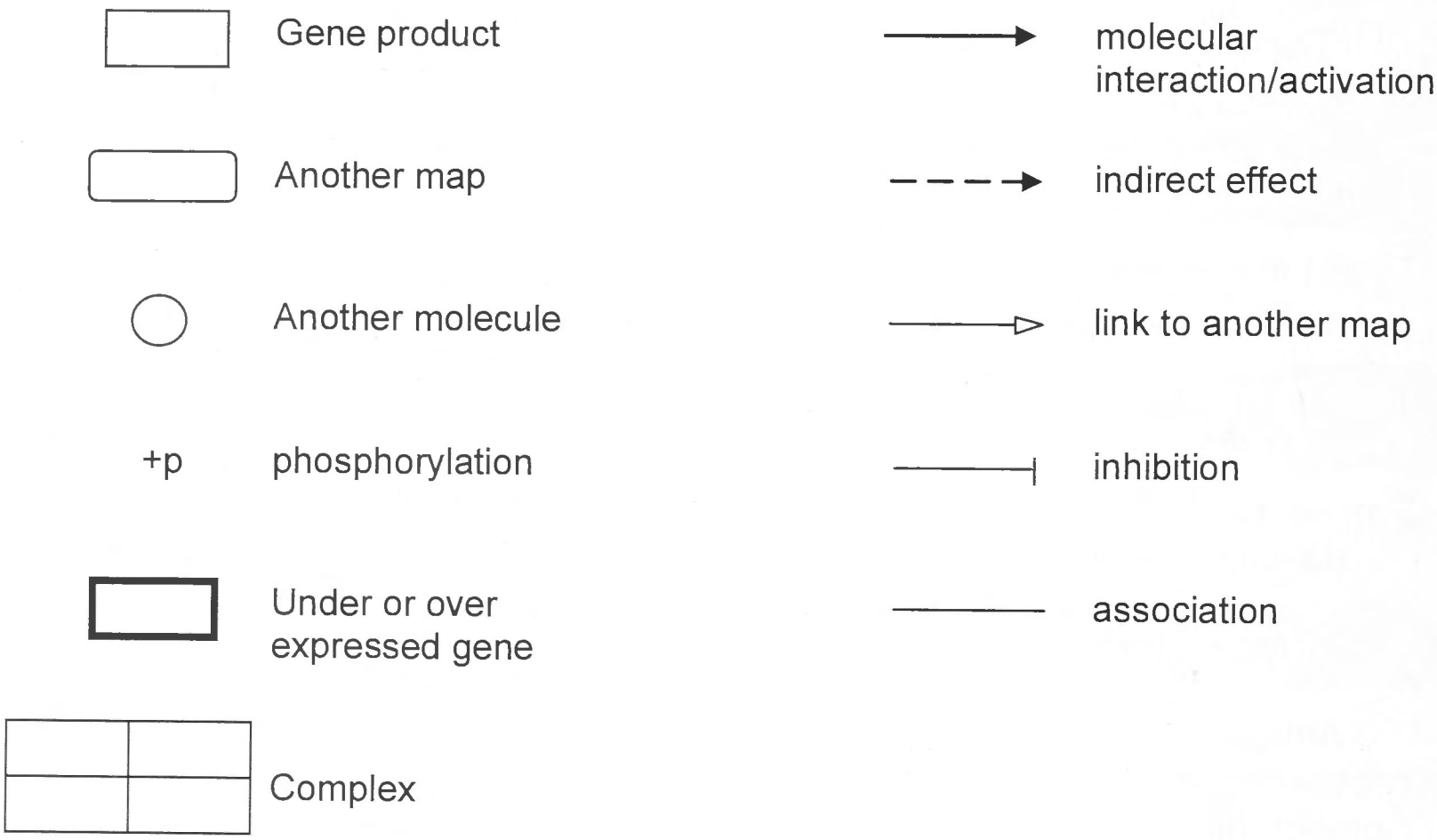

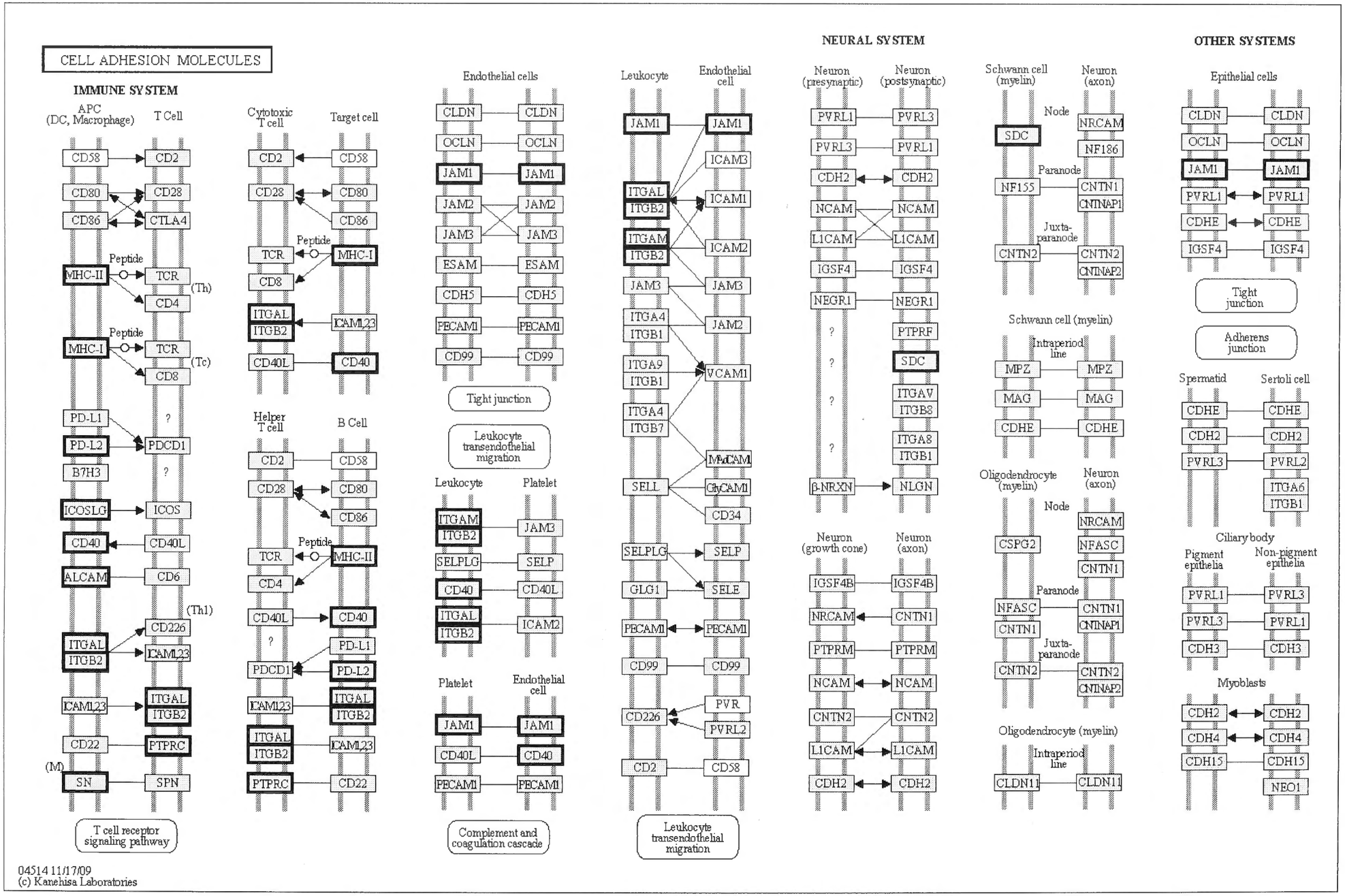
CELL ADHESION MOLECULES
IMMUNE SYSTEM
APC (DC, Macrophage)
T Cell
CD58
CD2
CD80
CD28
CD86
CTLA4
Peptide
MHC-II
TCR
(Th)
CD4
Peptide
MHC-I
TCR
(Tc)
CD8
PD-L1
PD-L2
B7H3
?
PDCD1
?
ICOSLG
ICOS
CD40
CD40L
ALCAM
CD6
(Th1)
CD226
ITGAL
ITGB2
ICAM1,2,3
ICAM1,2,3
ITGAL
ITGB2
CD22
PTPRC
(M)
SN
SPN
T cell receptor signaling pathway
Cytotoxic T cell
Target cell
CD2
CD58
CD28
CD80
CD86
Peptide
TCR
MHC-I
CD8
ITGAL
ITGB2
ICAM1,2,3
CD40L
CD40
Helper T cell
B Cell
CD2
CD58
CD28
CD80
CD86
Peptide
TCR
MHC-II
CD4
CD40L
CD40
?
PD-L1
PDCD1
PD-L2
ICAM1,2,3
ITGAL
ITGB2
ITGAL
ITGB2
ICAM1,2,3
PTPRC
CD22
Endothelial cells
CLDN
CLDN
OCLN
OCLN
JAM1
JAM1
JAM2
JAM2
JAM3
JAM3
ESAM
ESAM
CDH5
CDH5
PECAM1
PECAM1
CD99
CD99
Tight junction
Leukocyte transendothelial migration
Leukocyte
Platelet
ITGAM
ITGB2
JAM3
SELPLG
SELP
CD40
CD40L
ITGAL
ITGB2
ICAM2
Platelet
Endothelial cell
JAM1
JAM1
CD40L
CD40
PECAM1
PECAM1
Complement and coagulation cascade
Leukocyte
Endothelial cell
JAM1
JAM1
ICAM3
ITGAL
ITGB2
ICAM1
ITGAM
ITGB2
ICAM2
JAM3
JAM3
ITGA4
ITGB1
JAM2
ITGA9
ITGB1
VCAM1
ITGA4
ITGB7
MAdCAM1
SELL
GlyCAM1
CD34
SELPLG
SELP
GLG1
SELE
PECAM1
PECAM1
CD99
CD99
CD226
PVR
PVRL2
CD2
CD58
Leukocyte transendothelial migration
NEURAL SYSTEM
Neuron (presynaptic)
Neuron (postsynaptic)
PVRL1
PVRL3
PVRL3
PVRL1
CDH2
CDH2
NCAM
NCAM
L1CAM
L1CAM
IGSF4
IGSF4
NEGR1
NEGR1
?
?
?
?
PTPRF
SDC
ITGAV
ITGB8
ITGA8
ITGB1
β-NRXN
NLGN
Neuron (growth cone)
Neuron (axon)
IGSF4B
IGSF4B
NRCAM
CNTN1
PTPRM
PTPRM
NCAM
NCAM
CNTN2
CNTN2
L1CAM
L1CAM
CDH2
CDH2
Schwann cell (myelin)
Neuron (axon)
Node
SDC
NRCAM
NF186
Paranode
NF155
CNTN1
CNTNAP1
Juxta-paranode
CNTN2
CNTN2
CNTNAP2
Schwann cell (myelin)
Intraperiod line
MPZ
MPZ
MAG
MAG
CDHE
CDHE
Oligodendrocyte (myelin)
Neuron (axon)
Node
CSPG2
NRCAM
NFASC
CNTN1
Paranode
NFASC
CNTN1
CNTN1
CNTNAP1
Juxta-paranode
CNTN2
CNTN2
CNTNAP2
Oligodendrocyte (myelin)
Intraperiod line
CLDN11
CLDN11
OTHER SYSTEMS
Epithelial cells
CLDN
CLDN
OCLN
OCLN
JAM1
JAM1
PVRL1
PVRL1
CDHE
CDHE
IGSF4
IGSF4
Tight junction
Adherens junction
Spermatid
Sertoli cell
CDHE
CDHE
CDH2
CDH2
PVRL3
PVRL2
ITGA6
ITGB1
Ciliary body
Pigment epithelia
Non-pigment epithelia
PVRL1
PVRL3
PVRL3
PVRL1
CDH3
CDH3
Myoblasts
CDH2
CDH2
CDH4
CDH4
CDH15
CDH15
NEO1
04514 11/17/09
(c) Kanehisa Laboratories

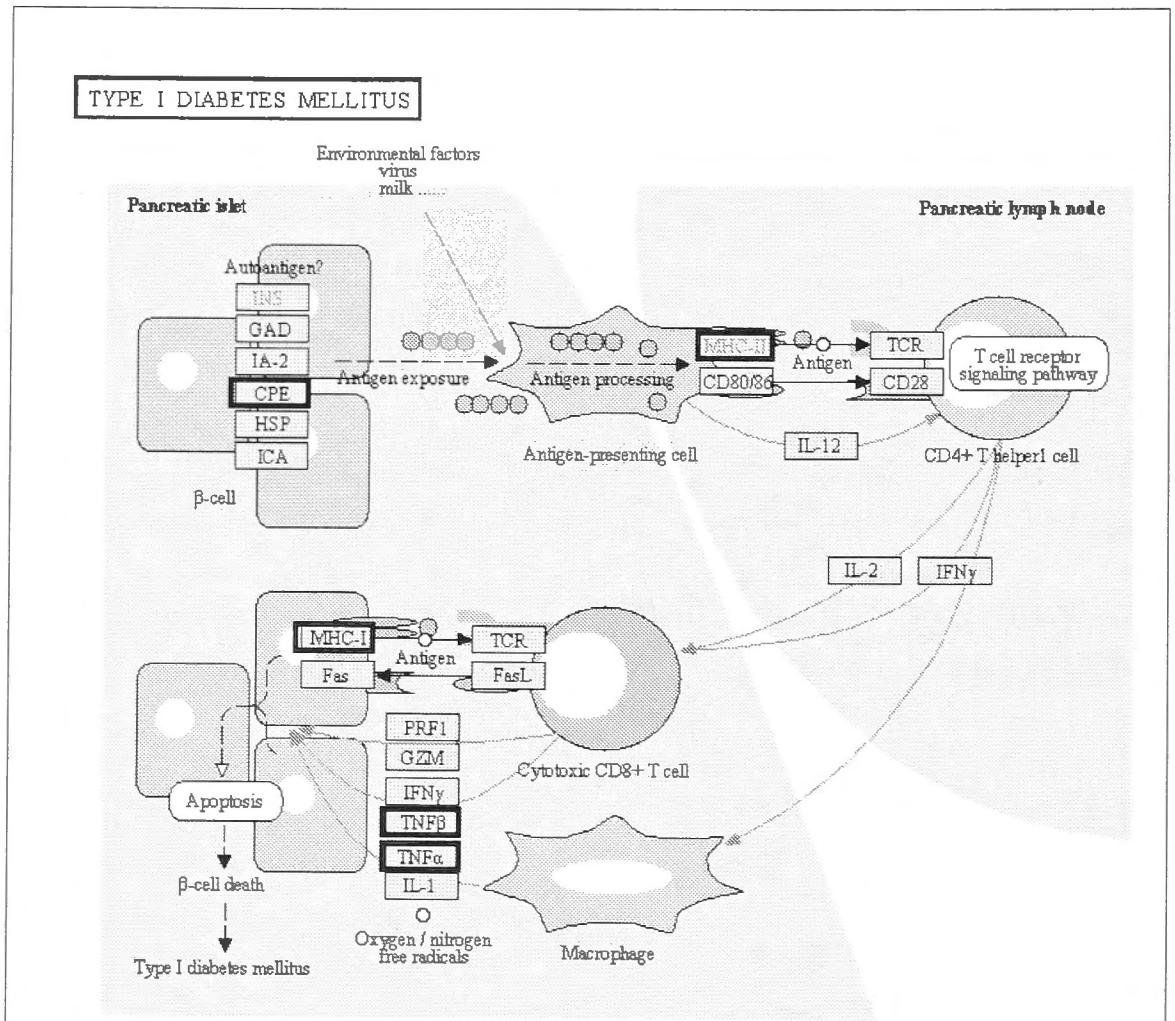
TYPE I DIABETES MELLITUS
Environmental factors
virus
milk .....
Pancreatic islet
Pancreatic lymph node
Autoantigen?
INS
GAD
IA-2
CPE
HSP
ICA
β-cell
Antigen exposure
Antigen processing
MHC-II
CD80/86
Antigen
TCR
CD28
T cell receptor signaling pathway
Antigen-presenting cell
IL-12
CD4+ T helper1 cell
IL-2
IFNγ
MHC-I
Fas
TCR
Antigen
FasL
PRF1
GZM
IFNγ
TNFβ
TNFα
IL-1
Cytotoxic CD8+ T cell
Apoptosis
β-cell death
Type I diabetes mellitus
Oxygen / nitrogen free radicals
Macrophage
04940 5/13/10
(c) Kanehisa Laboratories

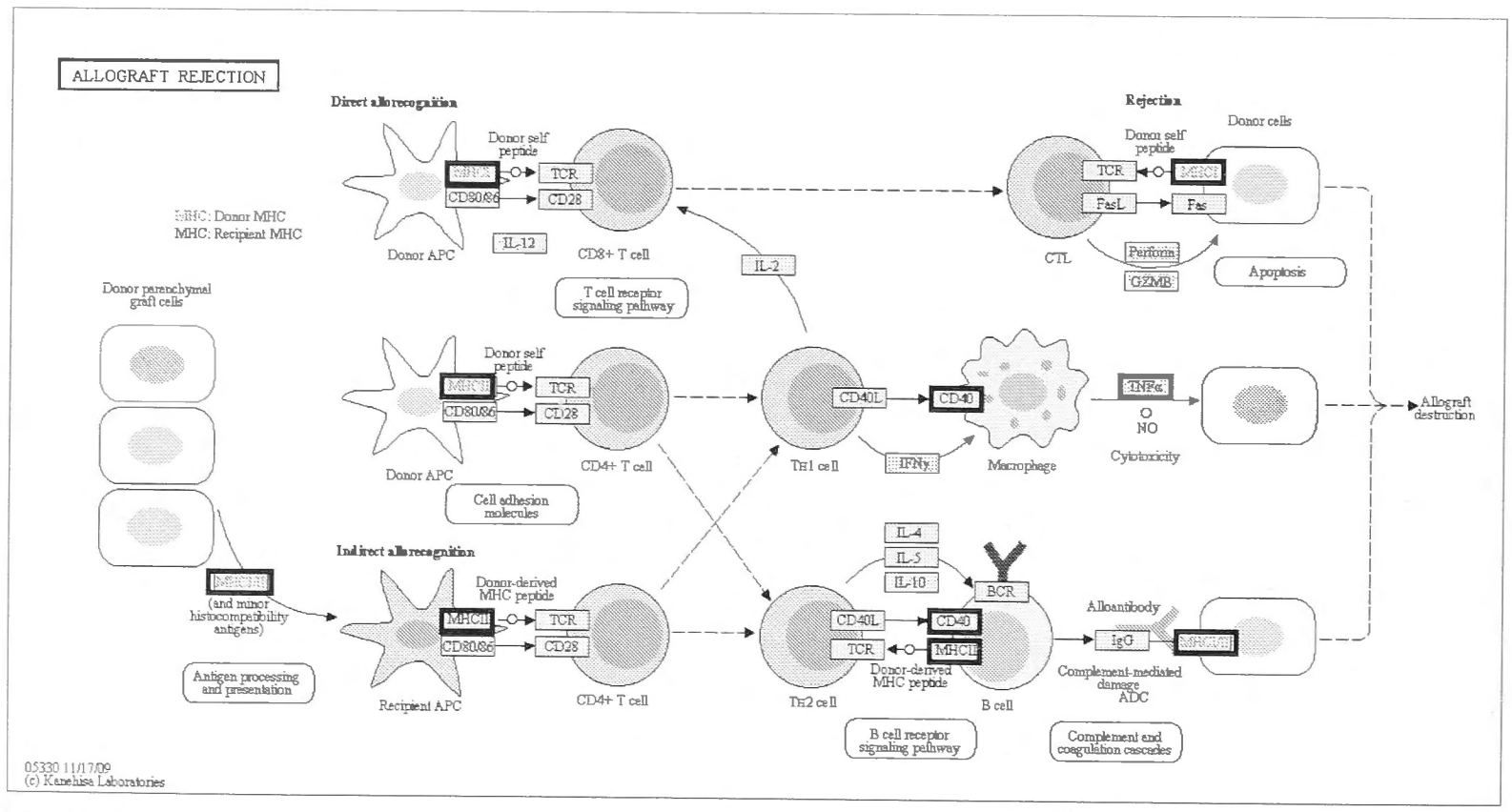
ALLOGRAFT REJECTION
Direct allorecognition
Donor self peptide
MHC-I
TCR
CD80/86
CD28
Donor APC
IL-12
CD8+ T cell
T cell receptor signaling pathway
IL-2
Rejection
Donor cells
Donor self peptide
TCR
FasL
MHC-I
Fas
CTL
Perforin
GZMB
Apoptosis
MHC: Donor MHC
MHC: Recipient MHC
Donor parenchymal graft cells
Donor self peptide
MHC-I
TCR
CD80/86
CD28
Donor APC
CD4+ T cell
Cell adhesion molecules
TH1 cell
CD40L
CD40
IFNγ
Macrophage
TNFα
NO
Cytotoxicity
Allograft destruction
MHC-I
(and minor histocompatibility antigens)
Antigen processing and presentation
Indirect allorecognition
Donor-derived MHC peptide
MHCII
TCR
CD80/86
CD28
Recipient APC
CD4+ T cell
IL-4
IL-5
IL-10
BCR
CD40L
CD40
TCR
MHCII
Donor-derived MHC peptide
TH2 cell
B cell
Alloantibody
IgG
MHC-I
Complement-mediated damage
ADC
B cell receptor signaling pathway
Complement and coagulation cascades
05330 11/17/09
(c) Kanehisa Laboratories

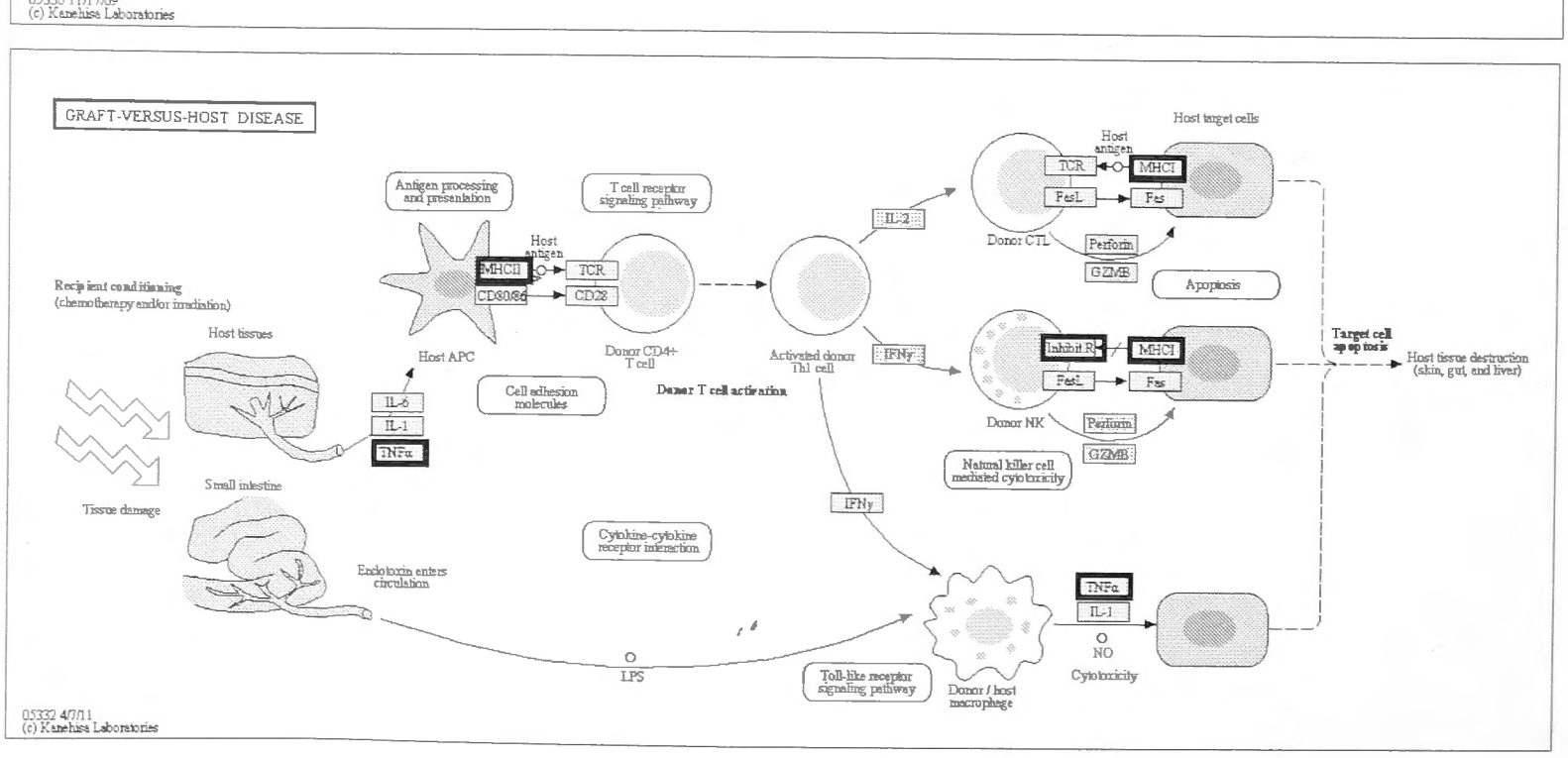
GRAFT-VERSUS-HOST DISEASE
Host target cells
Host antigen
TCR
MHCI
FasL
Fas
Donor CTL
Perforin
GZMB
Apoptosis
Antigen processing and presentation
T cell receptor signaling pathway
Host antigen
MHCII
TCR
CD80/86
CD28
Host APC
Donor CD4+ T cell
Activated donor Th1 cell
IL-2
IFNγ
Recipient conditioning (chemotherapy and/or irradiation)
Host tissues
Cell adhesion molecules
Donor T cell activation
Inhibit R
MHCI
FasL
Fas
Donor NK
Perforin
GZMB
Natural killer cell mediated cytotoxicity
Target cell apoptosis
Host tissue destruction (skin, gut, and liver)
IL-6
IL-1
TNFα
Tissue damage
Small intestine
Cytokine-cytokine receptor interaction
IFNγ
Endotoxin enters circulation
LPS
Toll-like receptor signaling pathway
Donor / host macrophage
TNFα
IL-1
NO
Cytotoxicity
05332 4/7/11
(c) Kanehisa Laboratories

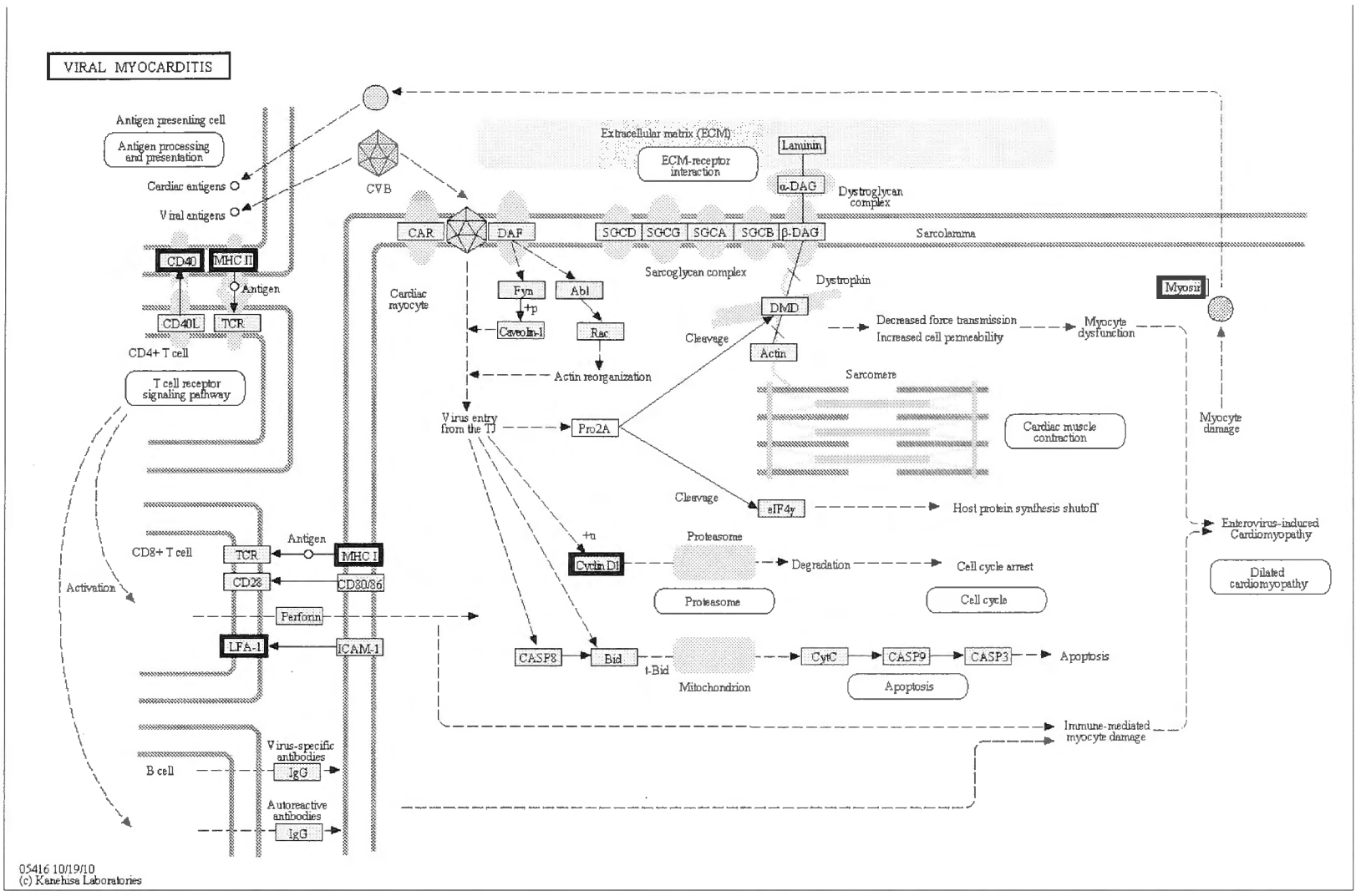
VIRAL MYOCARDITIS
Antigen presenting cell
Antigen processing and presentation
Cardiac antigens
Viral antigens
CVB
Extracellular matrix (ECM)
ECM-receptor interaction
Laminin
α-DAG
Dystroglycan complex
CAR
DAF
SGCD
SGCG
SGCA
SGCB
β-DAG
Sarcolamma
Sarcoglycan complex
Dystrophin
Myosin
CD40
MHC II
Antigen
CD40L
TCR
CD4+ T cell
T cell receptor signaling pathway
Cardiac myocyte
Fyn
Abl
+p
Caveolin-1
Rac
Actin reorganization
Cleavage
DMD
Actin
Decreased force transmission
Increased cell permeability
Myocyte dysfunction
Sarcomere
Cardiac muscle contraction
Myocyte damage
Virus entry from the TJ
Pro2A
Cleavage
eIF4γ
Host protein synthesis shutoff
Enterovirus-induced Cardiomyopathy
Dilated cardiomyopathy
CD8+ T cell
TCR
Antigen
MHC I
CD28
CD80/86
Activation
Perforin
LFA-1
ICAM-1
+u
Cyclin D1
Proteasome
Degradation
Cell cycle arrest
Proteasome
Cell cycle
CASP8
Bid
t-Bid
Mitochondrion
CytC
CASP9
CASP3
Apoptosis
Apoptosis
Immune-mediated myocyte damage
Virus-specific antibodies
B cell
IgG
Autoreactive antibodies
IgG
05416 10/19/10
(c) Kanehisa Laboratories

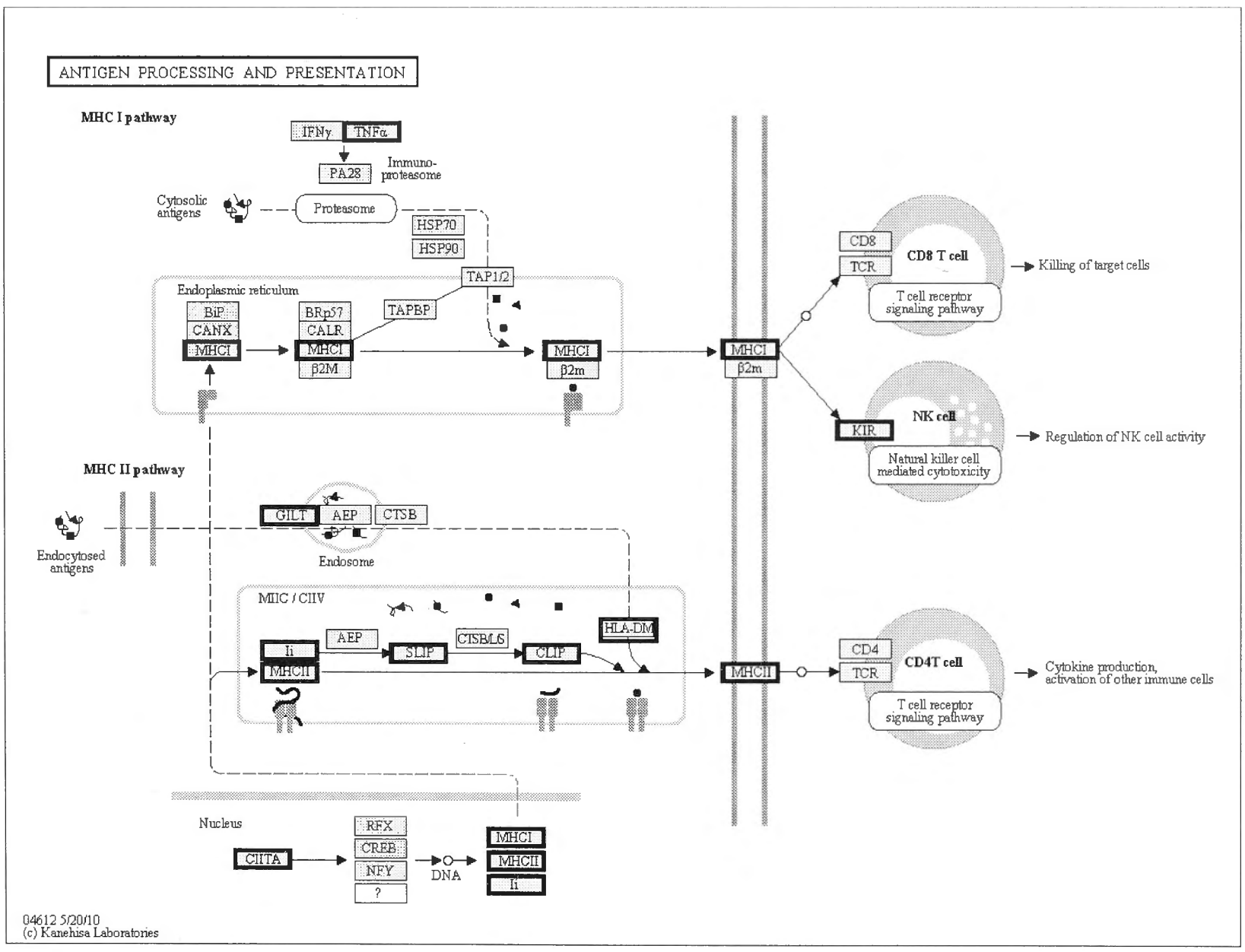
ANTIGEN PROCESSING AND PRESENTATION
MHC I pathway
IFNγ
TNFα
PA28
Immuno-proteasome
Cytosolic antigens
Proteasome
HSP70
HSP90
TAP1/2
Endoplasmic reticulum
BiP
CANX
MHCI
BRp57
CALR
MHCI
β2M
TAPBP
MHCI
β2m
MHCI
β2m
CD8
TCR
CD8 T cell
T cell receptor signaling pathway
Killing of target cells
KIR
NK cell
Natural killer cell mediated cytotoxicity
Regulation of NK cell activity
MHC II pathway
Endocytosed antigens
GILT
AEP
CTSB
Endosome
MIIC / CIIV
Ii
MHCII
AEP
SLIP
CTSB/LS
CLIP
HLA-DM
MHCII
CD4
TCR
CD4T cell
T cell receptor signaling pathway
Cytokine production, activation of other immune cells
Nucleus
CIITA
RFX
CREB
NFY
?
DNA
MHCI
MHCII
Ii
04612 5/20/10
(c) Kanehisa Laboratories

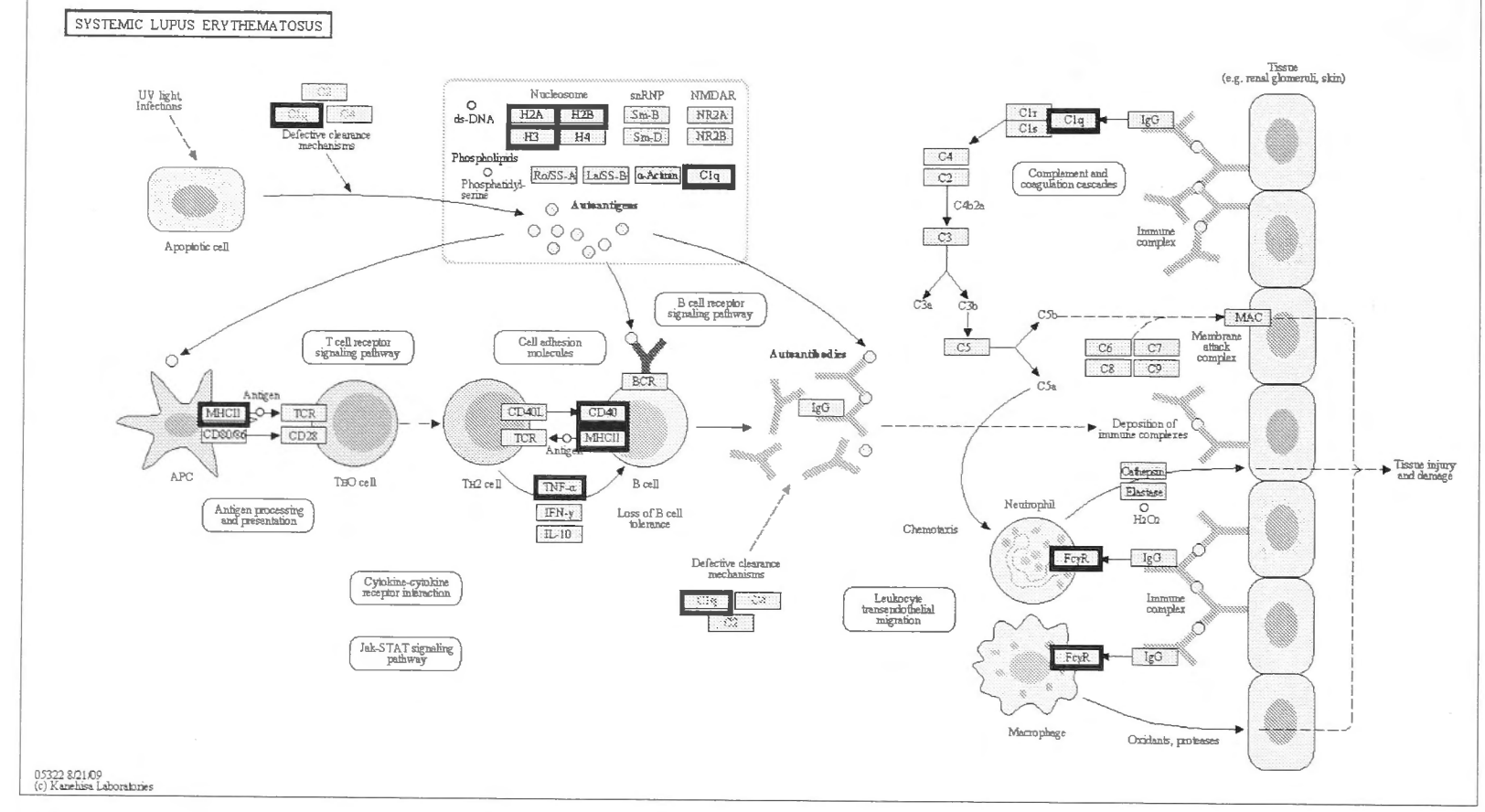
SYSTEMIC LUPUS ERYTHEMATOSUS
UV light, Infections
Defective clearance mechanisms
Apoptotic cell
Nucleosome
ds-DNA
H2A
H2B
H3
H4
snRNP
Sm-B
Sm-D
NMDAR
NR2A
NR2B
Phospholipids
Phosphatidyl-serine
Ro/SS-A
LaSS-B
α-Actinin
C1q
Autoantigens
B cell receptor signaling pathway
T cell receptor signaling pathway
Cell adhesion molecules
Autoantibodies
BCR
IgG
MHCII
TCR
CD80/86
CD28
Antigen
APC
TH0 cell
CD40L
CD40
TH2 cell
B cell
TNF-α
IFN-γ
IL-10
Loss of B cell tolerance
Antigen processing and presentation
Cytokine-cytokine receptor interaction
Jak-STAT signaling pathway
Defective clearance mechanisms
Leukocyte transendothelial migration
Tissue (e.g. renal glomeruli, skin)
C1r
C1s
C1q
C4
C2
C4b2a
C3
C3a
C3b
C5
C5b
C5a
Complement and coagulation cascades
Immune complex
MAC
Membrane attack complex
C6
C7
C8
C9
Deposition of immune complexes
Cathepsin
Elastase
H2O2
Tissue injury and damage
Neutrophil
Chemotaxis
FcγR
Macrophage
Oxidants, proteases
05322 8/21/09
(c) Kanehisa Laboratories

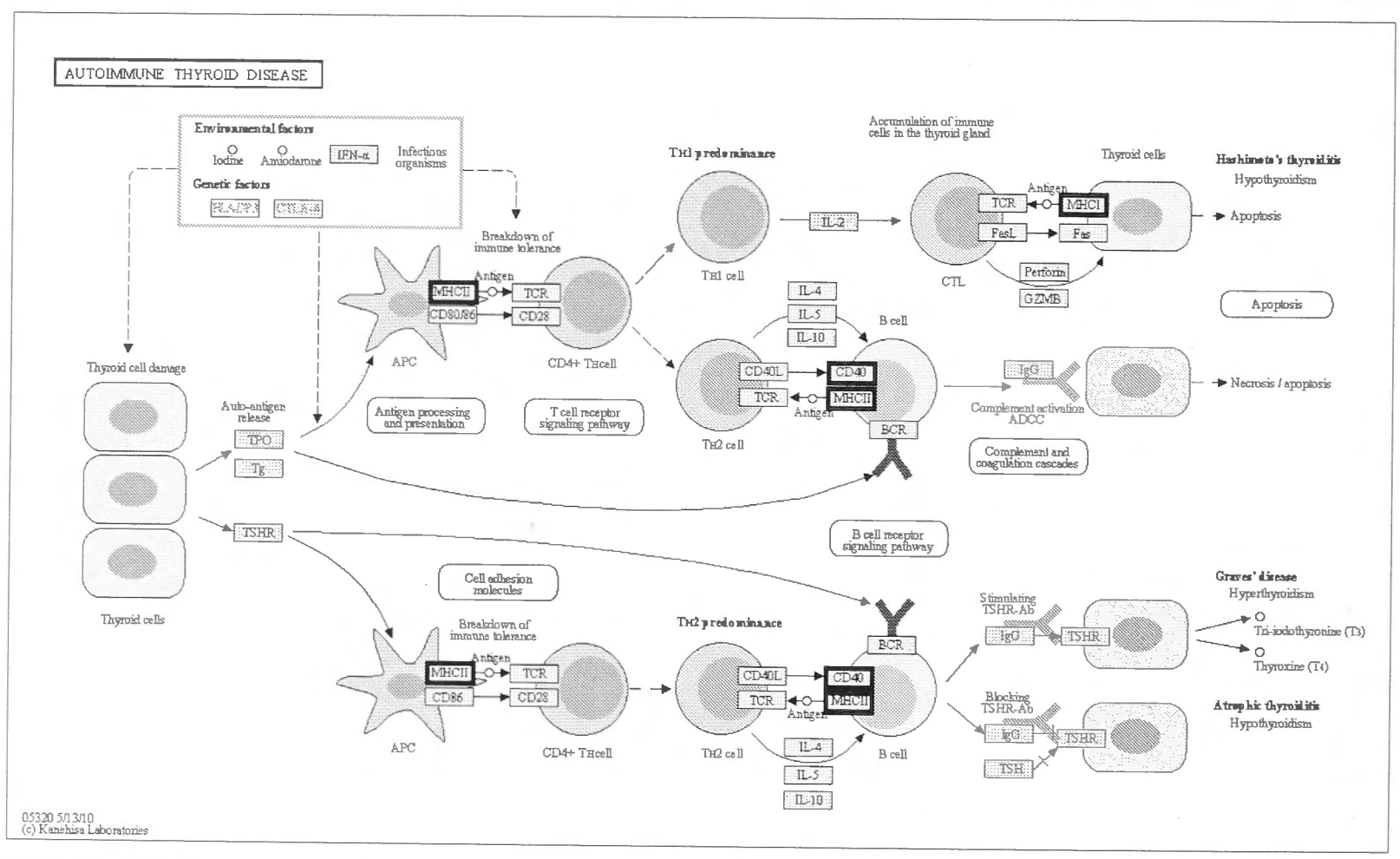
AUTOIMMUNE THYROID DISEASE
Environmental factors
Iodine
Amiodarone
IFN-α
Infectious organisms
Genetic factors
HLA-DR3
CTLA-4
Thyroid cell damage
Thyroid cells
Auto-antigen release
TPO
Tg
TSHR
Breakdown of immune tolerance
Antigen
MHCII
TCR
CD80/86
CD28
APC
CD4+ TH cell
Antigen processing and presentation
T cell receptor signaling pathway
TH1 predominance
TH1 cell
IL-2
Accumulation of immune cells in the thyroid gland
Thyroid cells
TCR
Antigen
MHCI
FasL
Fas
CTL
Perforin
GZMB
Apoptosis
Hashimoto's thyroiditis
Hypothyroidism
IL-4
IL-5
IL-10
B cell
CD40L
CD40
MHCII
TCR
Antigen
BCR
TH2 cell
IgG
Complement activation ADCC
Complement and coagulation cascades
Necrosis / apoptosis
B cell receptor signaling pathway
Cell adhesion molecules
TH2 predominance
Stimulating TSHR-Ab
IgG
TSHR
Graves' disease
Hyperthyroidism
Tri-iodothyronine (T3)
Thyroxine (T4)
Blocking TSHR-Ab
TSH
Atrophic thyroiditis
Hypothyroidism
05320 5/13/10
(c) Kanehisa Laboratories

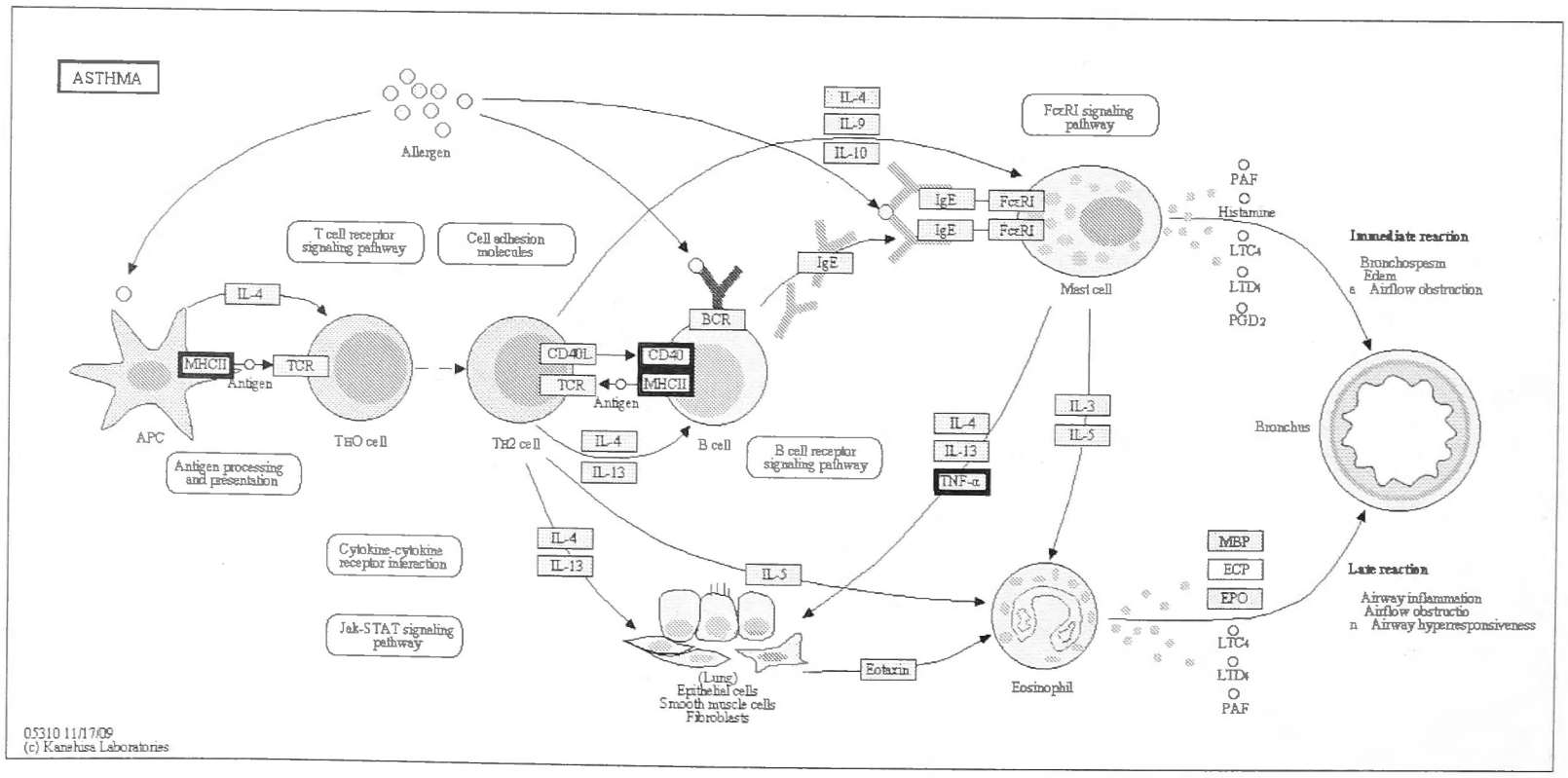
ASTHMA
Allergen
IL-4
IL-9
IL-10
FcεRI signaling pathway
IgE
FcεRI
Mast cell
PAF
Histamine
LTC4
LTD4
PGD2
Immediate reaction
Bronchospasm
Edem
a Airflow obstruction
T cell receptor signaling pathway
Cell adhesion molecules
IL-4
MHCII
TCR
Antigen
APC
TH0 cell
CD40L
CD40
TH2 cell
B cell
BCR
IL-13
TNF-α
IL-3
IL-5
Bronchus
B cell receptor signaling pathway
Antigen processing and presentation
Cytokine-cytokine receptor interaction
Jak-STAT signaling pathway
(Lung) Epithelial cells Smooth muscle cells Fibroblasts
Eotaxin
Eosinophil
MBP
ECP
EPO
LTC4
LTD4
PAF
Late reaction
Airway inflammation
Airflow obstructio
n Airway hyperresponsiveness
05310 11/17/09
(c) Kanehisa Laboratories

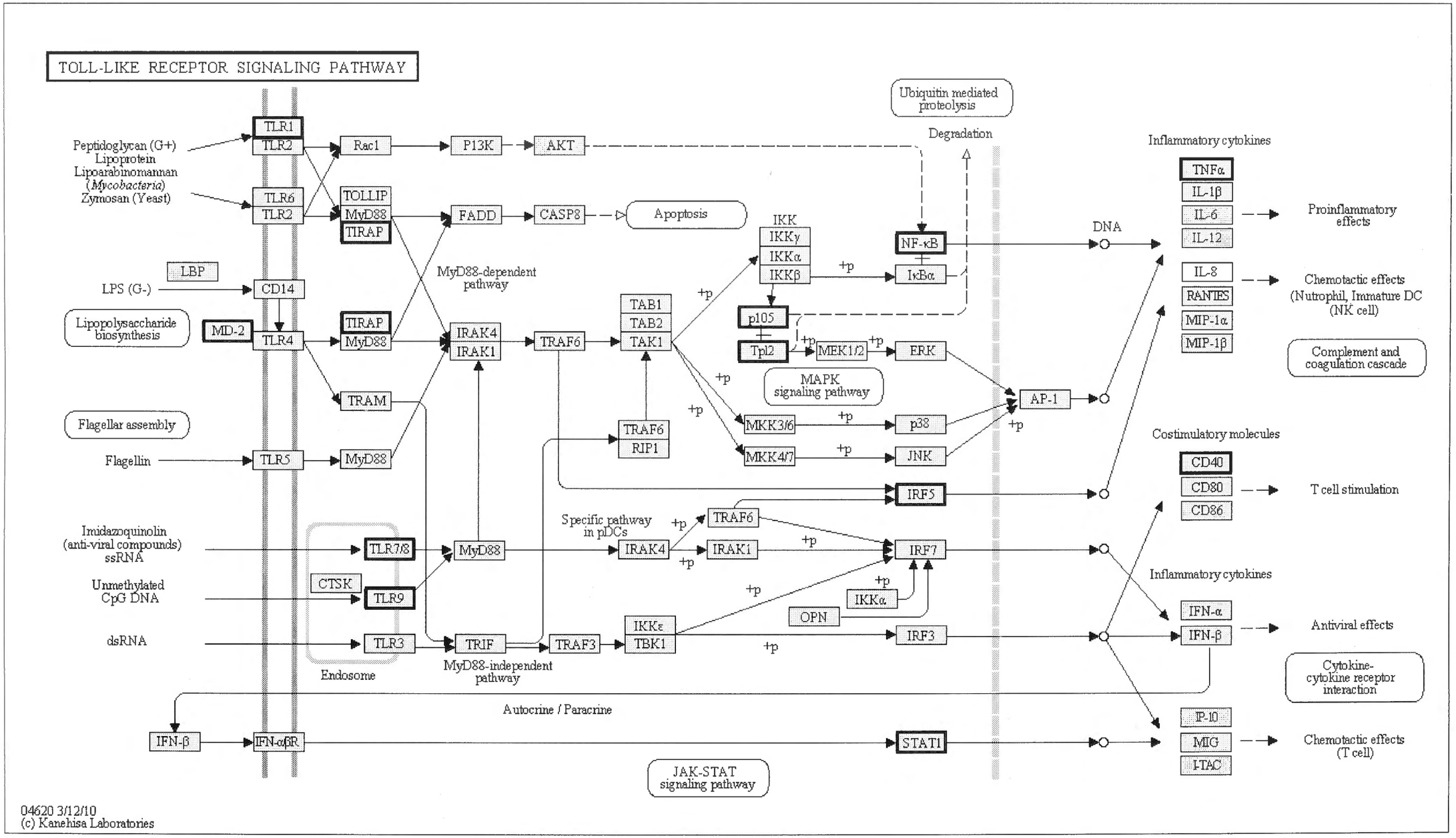
TOLL-LIKE RECEPTOR SIGNALING PATHWAY
Peptidoglycan (G+)
Lipoprotein
Lipoarabinomannan (Mycobacteria)
Zymosan (Yeast)
TLR1
TLR2
TLR6
TLR2
Rac1
P13K
AKT
TOLLIP
MyD88
TIRAP
FADD
CASP8
Apoptosis
Ubiquitin mediated proteolysis
Degradation
LBP
LPS (G-)
CD14
Lipopolysaccharide biosynthesis
MD-2
TLR4
TIRAP
MyD88
MyD88-dependent pathway
IRAK4
IRAK1
TRAF6
TAB1
TAB2
TAK1
IKK
IKKγ
IKKα
IKKβ
+p
NF-κB
IκBα
DNA
p105
Tpl2
MEK1/2
ERK
MAPK signaling pathway
TRAM
Flagellar assembly
Flagellin
TLR5
MyD88
TRAF6
RIP1
MKK3/6
p38
MKK4/7
JNK
AP-1
IRF5
Inflammatory cytokines
TNFα
IL-1β
IL-6
IL-12
Proinflammatory effects
IL-8
RANTES
MIP-1α
MIP-1β
Chemotactic effects (Nutrophil, Immature DC (NK cell)
Complement and coagulation cascade
Costimulatory molecules
CD40
CD80
CD86
T cell stimulation
Imidazoquinolin (anti-viral compounds) ssRNA
Unmethylated CpG DNA
dsRNA
TLR7/8
CTSK
TLR9
TLR3
MyD88
TRIF
TRAF3
Endosome
MyD88-independent pathway
Specific pathway in pDCs
IRAK4
IRAK1
TRAF6
IKKε
TBK1
IKKα
OPN
IRF7
IRF3
Inflammatory cytokines
IFN-α
IFN-β
Antiviral effects
Cytokine-cytokine receptor interaction
Autocrine / Paracrine
IFN-β
IFN-αβR
STAT1
IP-10
MIG
I-TAC
Chemotactic effects (T cell)
JAK-STAT signaling pathway
04620 3/12/10
(c) Kanehisa Laboratories

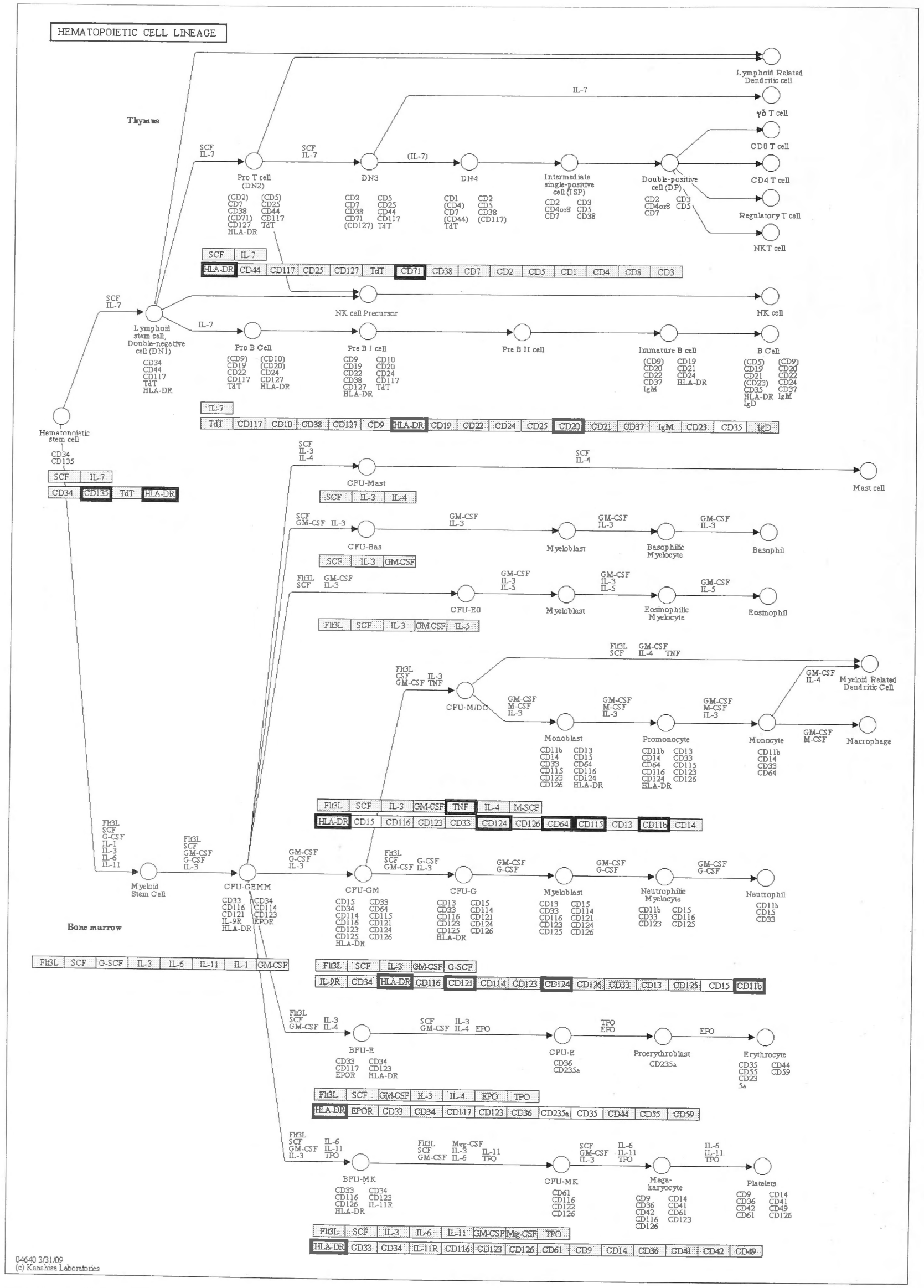
HEMATOPOIETIC CELL LINEAGE
Thymus
Lymphoid Related Dendritic cell
IL-7
γδ T cell
CD8 T cell
CD4 T cell
Regulatory T cell
NKT cell
SCF
IL-7
Pro T cell (DN2)
(CD2) (CD5) CD7 CD25 CD38 CD44 (CD71) CD117 CD127 TdT HLA-DR
SCF IL-7
DN3
CD2 CD5 CD7 CD25 CD38 CD44 CD71 CD117 (CD127) TdT
(IL-7)
DN4
CD1 CD2 (CD4) CD5 CD7 CD38 (CD44) (CD117) TdT
Intermediate single-positive cell (ISP)
CD2 CD3 CD4or8 CD5 CD7 CD38
Double-positive cell (DP)
CD2 CD3 CD4or8 CD5 CD7
SCF IL-7
HLA-DR CD44 CD117 CD25 CD127 TdT CD71 CD38 CD7 CD2 CD5 CD1 CD4 CD8 CD3
NK cell Precursor
NK cell
Lymphoid stem cell, Double-negative cell (DN1)
CD34 CD44 CD117 TdT HLA-DR
IL-7
Pro B Cell
(CD9) (CD10) CD19 (CD20) CD22 CD24 CD117 CD127 TdT HLA-DR
Pre B I cell
CD9 CD10 CD19 CD20 CD22 CD24 CD38 CD117 CD127 TdT HLA-DR
Pre B II cell
Immature B cell
(CD9) CD19 CD20 CD21 CD22 CD24 CD37 HLA-DR IgM
B Cell
(CD5) (CD9) CD19 CD20 CD21 CD22 (CD23) CD24 CD35 CD37 HLA-DR IgM IgD
IL-7
TdT CD117 CD10 CD38 CD127 CD9 HLA-DR CD19 CD22 CD24 CD25 CD20 CD21 CD37 IgM CD23 CD35 IgD
Hematopoietic stem cell
CD34 CD135
SCF IL-7
CD34 CD135 TdT HLA-DR
SCF IL-3 IL-4
CFU-Mast
SCF IL-3 IL-4
SCF IL-4
Mast cell
SCF GM-CSF IL-3
CFU-Bas
SCF IL-3 GM-CSF
GM-CSF IL-3
Myeloblast
GM-CSF IL-3
Basophilic Myelocyte
GM-CSF IL-3
Basophil
Flt3L SCF GM-CSF IL-3
CFU-E0
Flt3L SCF IL-3 GM-CSF IL-5
GM-CSF IL-3 IL-5
Myeloblast
GM-CSF IL-3 IL-5
Eosinophilic Myelocyte
GM-CSF IL-5
Eosinophil
Flt3L SCF GM-CSF IL-4 TNF
Flt3L CSF GM-CSF IL-3 TNF
CFU-M/DC
GM-CSF M-CSF IL-3
Monoblast
CD11b CD13 CD14 CD15 CD33 CD64 CD115 CD116 CD123 CD124 CD126 HLA-DR
GM-CSF M-CSF IL-3
Promonocyte
CD11b CD13 CD14 CD33 CD64 CD115 CD116 CD123 CD124 CD126 HLA-DR
GM-CSF M-CSF IL-3
Monocyte
CD11b CD14 CD33 CD64
GM-CSF IL-4
Myeloid Related Dendritic Cell
GM-CSF M-CSF
Macrophage
Flt3L SCF IL-3 GM-CSF TNF IL-4 M-SCF
HLA-DR CD15 CD116 CD123 CD33 CD124 CD126 CD64 CD115 CD13 CD11b CD14
Flt3L SCF G-CSF IL-3 IL-6 IL-11 IL-1 GM-CSF
Myeloid Stem Cell
Flt3L SCF GM-CSF G-CSF IL-3
CFU-GEMM
CD33 CD34 CD116 CD114 CD121 CD123 IL-9R EPOR HLA-DR
GM-CSF G-CSF IL-3
CFU-GM
CD15 CD33 CD34 CD64 CD114 CD115 CD116 CD121 CD123 CD124 CD125 CD126 HLA-DR
Flt3L SCF G-CSF GM-CSF IL-3
CFU-G
CD13 CD15 CD33 CD114 CD116 CD121 CD123 CD124 CD125 CD126 HLA-DR
GM-CSF G-CSF
Myeloblast
CD13 CD15 CD33 CD114 CD116 CD121 CD123 CD124 CD125 CD126
GM-CSF G-CSF
Neutrophilic Myelocyte
CD11b CD15 CD33 CD116 CD123 CD125
GM-CSF G-CSF
Neutrophil
CD11b CD15 CD33
Bone marrow
Flt3L SCF G-CSF IL-3 IL-6 IL-11 IL-1 GM-CSF
Flt3L SCF IL-3 GM-CSF G-CSF
IL-9R CD34 HLA-DR CD116 CD121 CD114 CD123 CD124 CD126 CD33 CD13 CD125 CD15 CD11b
Flt3L SCF GM-CSF IL-3 IL-4
BFU-E
CD33 CD34 CD117 CD123 EPOR HLA-DR
SCF IL-3 GM-CSF IL-4 EPO
CFU-E
CD36 CD235a
TPO EPO
Proerythroblast
CD235a
EPO
Erythrocyte
CD35 CD44 CD55 CD59 CD235a
Flt3L SCF GM-CSF IL-3 IL-4 EPO TPO
HLA-DR EPOR CD33 CD34 CD117 CD123 CD36 CD235a CD35 CD44 CD55 CD59
Flt3L SCF GM-CSF IL-6 IL-11 IL-3 TPO
BFU-MK
CD33 CD34 CD116 CD123 CD126 IL-11R HLA-DR
Flt3L Meg-CSF SCF IL-3 GM-CSF IL-6 IL-11 TPO
CFU-MK
CD61 CD116 CD122 CD126
SCF GM-CSF IL-6 IL-11 IL-3 TPO
Mega-karyocyte
CD9 CD14 CD36 CD41 CD42 CD61 CD116 CD123 CD126
IL-6 IL-11 TPO
Platelets
CD9 CD14 CD36 CD41 CD42 CD49 CD61 CD126
Flt3L SCF IL-3 IL-6 IL-11 GM-CSF Meg-CSF TPO
HLA-DR CD33 CD34 IL-11R CD116 CD123 CD126 CD61 CD9 CD14 CD36 CD41 CD42 CD49
04640 3/31/09
(c) Kanehisa Laboratories

Table 6.10 Pathway analysis from microarray analysis method two

The over and under expressed genes from Table 6.7 were mapped to cellular pathways using the DAVID resource. The over represented pathways, number and percentage of total genes implicated, fold enrichment and p value are listed below. Only pathways that contained at least five differentially expressed genes were considered. The p value was calculated by the DAVID program and was calculated using a modified Fisher Exact test. Those pathways with $p<0.01$ are shown.

Term	Count	%	p Value	Fold Enrichment
Natural killer cell mediated cytotoxicity	6	2.9	0.0033	5.8
Complement and coagulation cascades	5	2.4	0.0071	6.3

Figure 6.4 Pathway analysis from microarray analysis method two

The figures below are graphical representations of the location of the dysregulated genes/gene groups listed in Table 6.10 in cellular pathways. The figures are modified from the DAVID website, the under or overexpressed gene in this dataset being highlighted in black boxes. Not all genes in pathways are included in KEGG pathways and some 'gene' names reflect families of genes rather than detailing all the members. The legend is detailed in Figure 6.3.

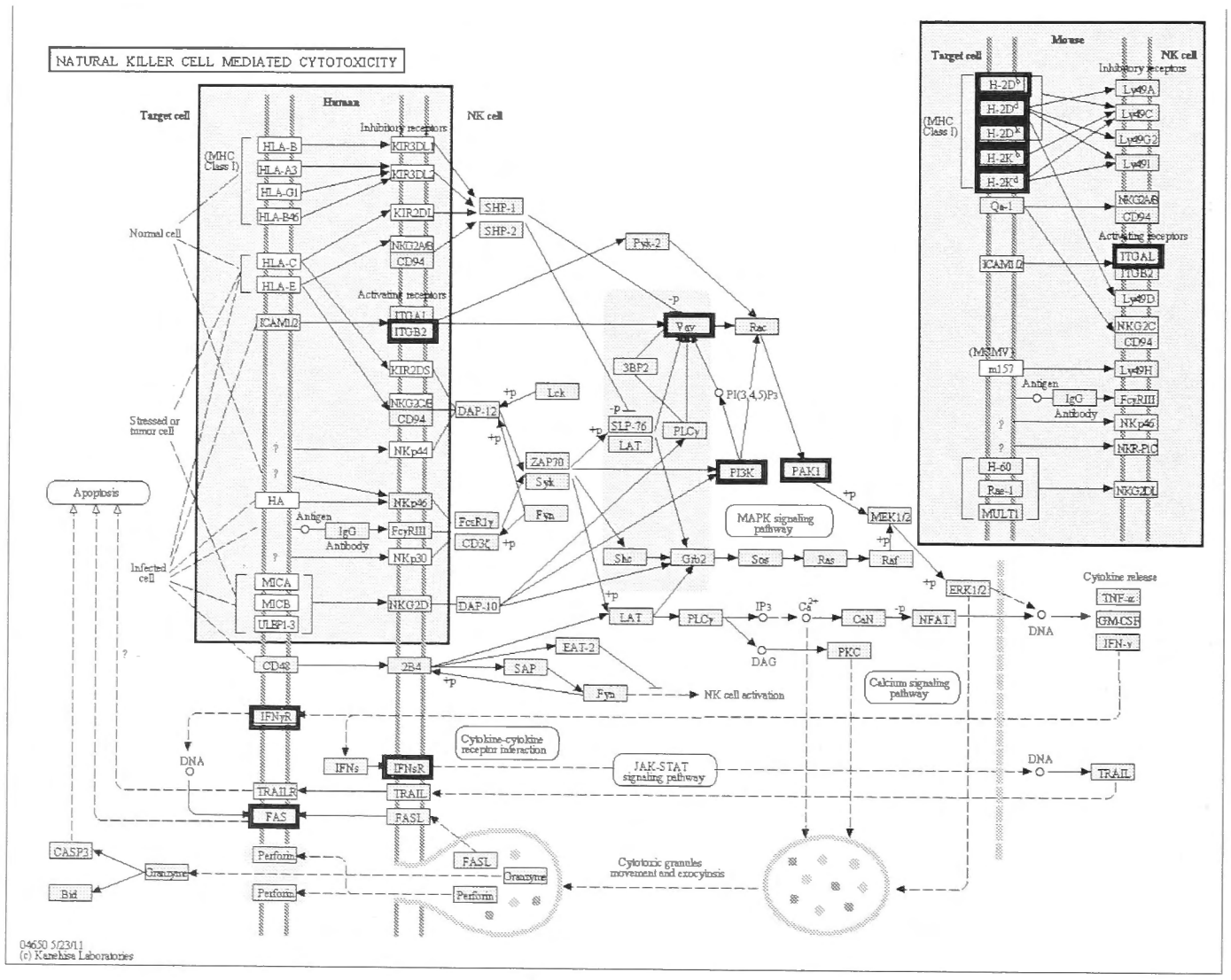

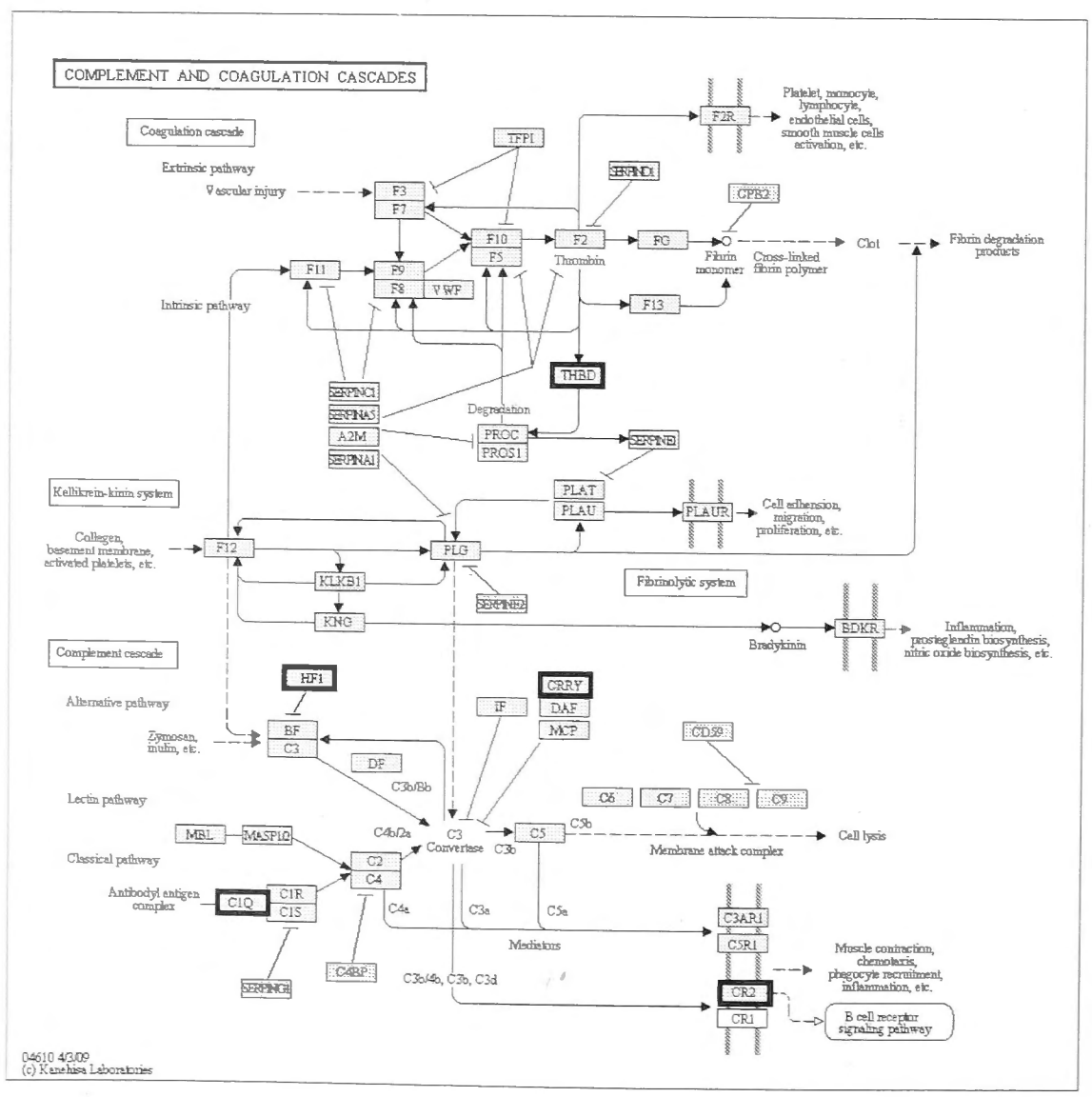

Table 6.11 Pathway analysis for gene set common to both analyses

The over and under expressed genes from Table 6.5 were mapped to cellular pathways using the DAVID resource, the over represented pathway, number and percentage of total genes implicated, fold enrichment and p value are listed below. Only pathways that contained at least five differentially expressed genes were considered. The p value was calculated by the DAVID program and was calculated using a modified Fisher Exact test. The single pathway with $p<0.05$ is shown.

Term	Count	%	p Value	Fold Enrichment
Natural killer cell mediated cytotoxicity	5	4.2	0.016	5.0

6.8 Discussion

The challenge with microarray data analysis is to differentiate the real differences from those that are statistical outliers ('false discovery rate') as a consequence of the large numbers of genes being analysed. Because of the cost of the method, only small numbers of independent samples within each treatment group can be analysed, and the very large number of questions asked (the number of genes measured) weakens any conclusions that can be drawn due to the problem of multiple testing. The studies described above are a preliminary pilot experiment performed to guide further research, which was particularly limited because only two samples of *Myb+MYC* transformed *Trp53* mutant B cells were analysed and compared with a single, well-matched counterpart of *MYC*-transduced *Trp53* mutant B cells. Consequently, no conclusions can be drawn from analysis of single genes, and lists of upregulated or downregulated genes in one sample versus another may have a high fraction of false positives.

The limitations above can be minimized by performing analysis of sets of genes that have been selected based not on the microarray data here but from independent information, as was done for cell cycle genes, germinal centre B cell genes, or NF-kB induced genes inhibited in Burkitt lymphoma. Effectively, these allow comparisons within a single dataset: for example the chi-squared comparison of the fraction of the set of 25 NF-kB induced genes inhibited in Burkitt lymphoma decreased more than 4-fold with the fraction of all the genes on the array decreased more than 4-fold in the same sample. This provided statistical evidence that the high fraction of NF-kB induced genes repressed in each sample of *Myb+MYC* transformed B cells would be unlikely to have been observed by chance. Follow up by a subsequent student confirmed that Myb does indeed suppress expression of cell surface proteins encoded by 4 out of 4 NF-kB induced genes that were repressed in the microarray analysis.

Having recognized the limitations of this microarray analysis, it is notably that among the 25 genes ranked as most highly induced in the *Myb+MYC* transformed B cells relative to *MYC*-singly transduced B cells, two thirds have

been shown to be Myb target genes in independent studies, as discussed in Section 6.5. Moreover, one of these encoding the cell surface protein CD93 has subsequently been tested using independent methods and independent replicate samples, confirming that it is indeed reproducibly and specifically induced by Myb in activated B cells. While this does not mean that all genes in the lists of upregulated or downregulated genes will be validated by independent follow-up, this provides some degree of confidence that the preliminary data in this chapter are a useful starting point for developing hypotheses about how *Myb* cooperates with *MYC* overexpression and *Trp53* defects to transform activated B cells into continuously growing B cell lines.

An ideal control in experiments to determine the effect of over expression of *Myb* in the setting of *MYC* overexpression would be a stable in vitro outgrowth derived from *MYC* singly transduced B cells. Unfortunately most *MYC* singly transduced cells cease dividing and die in culture after several days as illustrated in Figure 1.2, without the development of an autonomously replicating population of cells, so sufficient cell numbers cannot be obtained for a gene expression profiling control. This necessitates using cells that have been recently transduced with a *MYC* overexpressing retrovirus. This difference means that the proliferative rate and extent to which there are contaminating cells (eg T cells) may differ between sample and control cells. The recently transduced control could have been compared to *MYC/Myb* dual transduced cells Day 2 post transduction, but cell sorting would have been limited due to the difficulty identifying the Myb-transduced population. The analysis of cell cycle gene expression was performed in an effort to control for discrepancies in proliferative rate between recently transduced controls and outgrowths that have been proliferating in vitro for several weeks. Such differences may obscure the true results from pathway analyses, potentially increasing the false positive and false negative results.

Microarray profiling of a larger set of independent samples, both transformed cells and *MYC* single transduced controls, would have enhanced this analysis. Clearly the more of each the better, but this needs to be weighed against the expense of multiple microarrays, the difficulty procuring the samples, and the benefit in terms of statistical power while controlling the false discovery rate.

Five outgrowth and 5 control replicates are likely to have given more reliable data while being mindful of resource utilisation. A more statistically robust method would be to limit the number of genes being assessed, focusing on specific pathways, and thus a required sample number could be calculated to optimise the chance of meaningful results.

The advantage of the ANOVA analyses is that in addition to fold changes, p values are able to be obtained because there are duplicates within groups. Ideally the p value should be more stringent than $p<0.01$ as there is likely to be a high false discovery rate due to the number of genes being compared, but the small numbers of samples and controls makes this difficult to achieve in this study. The disadvantage of this analysis in this setting is that the two controls (one activated and *MYC* transduced B cells, and the other activated but not transduced B cells) need to be considered as 'biological replicates'. The initial method of microarray analysis specifically compared these two populations and showed that while there were many genes which were similarly expressed in the two populations, the expression of some genes differed by up to 65 fold.

The analysis of NF-KB pathway target gene expression in the outgrowths revealed reduced expression compared to *MYC* singly transduced controls. As discussed in Section 6.4 this has been observed as one of the primary gene expression signatures differentiating Burkitt lymphoma from Germinal centre-type Diffuse Large B cell Lymphoma [344]. The findings here are interesting because control cells in this analysis were *MYC* overexpressing cells, suggesting that the relative suppression of the NF-κB pathway is not solely due to the MYC overexpression and is potentially induced by Myb. Indeed several of the genes in this set have been confirmed to be suppressed by Myb in activated B cells by FACS of their encoded proteins, in follow-up studies by Y Jeelall. As noted in the results, among this set of downregulated genes is *Nfkb1*, encoding one of the subunits of NF-kB, and *Traf1* encoding one of the activators of NF-kB nuclear translocation. These two genes have been shown in independent studies to both bind and be repressed by Myb [475]. Hence it is reasonable to hypothesise that Myb directly binds to and inhibits transcription of *Nfkb1* and *Traf1*, diminishing expression of many B cell genes that would otherwise be induced by NF-kB.

How might inhibition of NF-kB by Myb relate to the gene expression signature of Burkitt lymphoma? Myb itself was not defined as increased in Burkitt lymphoma in the array analysis of Dave et al [344]. However, as a result of the observations described in this chapter, a collaboration with Dr Staudt's laboratory has revealed in RNA-seq datasets that *Myb* mRNA is indeed highly increased selectively in Burkitt lymphoma, and is indeed a Burkitt signature gene. Collectively, these results support the conclusion that high *Myb* expression contributes to a distinctive signature of low NF-kB induced gene expression both in Myb+MYC p53-mutant transformed non-germinal centre mouse B cells (here) and in MYC+p53-mutant transformed human Burkitt lymphomas. Why *Myb* would be highly expressed in Burkitt lymphoma is unknown.

Given the important role of NF-κB in mature B cell activation, survival and proliferation [42] it is an interesting question whether the suppression of this response by *Myb* is a benefit or a cost to neoplastic growth. Based on the recent finding that constitutively active *Ikbkb* abolishes survival of antigen-activated B cells in vivo [101], limiting NF-κB activity may have a survival advantage for activated B cells through an unresolved pathway. On the other hand, repressing NF-κB would certainly have a cost since *Myc* itself is normally an immediate early NF-κB target gene in antigen-activated B cells [49]. Uncoupling *MYC* expression from NF-κB dependence, either through linking it to a retroviral LTR as done here or by translocation to the *IgH* genes as occurs in Burkitt lymphoma, would allow the transformed B cells to avoid loss of *MYC* when NF-kB was suppressed by *MYB*. It may be that some of the *MYB*-induced genes substitute for other proliferative effects of NF-kB. Thus the co-operation between dysregulated *Myb* and *MYC* and inactive *Trp53* shown here may help explain many of the cardinal features of Burkitt lymphoma.

While several of the dysregulated genes identified in the analysis of the NF-κB pathway were validated by FACS as above, the very preliminary results of the pathway analysis will require confirmation by an independent method (usually real time PCR) prior to further research.

7. Discussion

MYC dysregulation by translocation to the immunoglobulin genes is a hallmark of Burkitt lymphoma, frequently accompanied by inactivation of *Trp53* or its upstream activators. While published literature indicates the pairing of these two defects can be sufficient for neoplastic transformation in fibroblasts, work by a previous PhD student and findings in this thesis demonstrate that these are insufficient for mature activated B cells to proliferate independently from the normal mitogenic signals received through antigen receptors and CD40. This thesis sought to identify what additional "oncogenic hits" are required for neoplastic proliferation of mature B cells.

I focussed on rare clones of activated mature B cells that had been transformed into neoplastic growth in vivo, emerging out of hundreds of thousands that already carried homozygous inactivation of *Trp53* and had been transduced with a replication defective retrovirus encoding a dysregulated *MYC* gene but that did not proliferate. The hypothesis pursued was that retroviral integration served as an additional mutagen by dysregulating expression of adjacent genes that co-operated with dysregulated *MYC* and inactive *Trp53* to complete an oncogenic constellation sufficient for mitogen-independent proliferation of mature B cells.

Analysis of integration sites revealed a high fraction that were frequently targeted in other retrovirus-induced cancers and that had flanking genes possibly associated with cancer, providing suggestive evidence to support the hypothesis. Four flanking genes, *Myb, Lmo2, Ikbkb*, and *Laptm5*, were tested for co-operation with dysregulated *MYC* and inactive *Trp53* by dysregulating their expression as cDNAs in a second, co-transduced retrovirus introduced into activated B cells deprived of normal mitogens. Two of the cDNAs, *Lmo2* and *Laptm5*, had no measurable activity on B cell proliferation in the absence of mitogens. *Ikbkb* induced transient proliferation for several days, with or without *MYC* dysregulation, but then the cells ceased proliferating and died off. However, transduction with a vector carrying the *Myb* cDNA reproducibly transformed at least one activated B cell in several hundred into continuous proliferation in the absence of mitogens, but only in conjunction with retroviral *MYC* dysregulation and *Trp53* inactivation. This result identifies *Myb* as a powerful "third oncogenic hit" cooperating with dysregulated *MYC* and inactive

Trp53 to uncouple mature B cell proliferation from its normal strict dependence on antigen and T cell help. The findings focus attention on Myb in human Burkitt lymphoma, where it has not previously been considered as a co-operating oncogene, and provide additional impetus to pursue the longstanding question of the role of c-Myb (as opposed to v-Myb) as a proto-oncogene.

7.1 *Myb* dysregulation in B cell lymphoma

The work in this thesis confirms that *Myb* is an oncogene in B cell lymphoma, but the way in which it is activated to unleash its full oncogenic capacity and co-operating lesions remains to be defined.

Truncated or mutated myb, exemplified by v-myb, has clear oncogenic activity when it is constitutively expressed, as discussed in Section 1.8. The locus around *Myb* is a frequently isolated retroviral integration site in the Retroviral Tagged Cancer Gene Database, also strongly suggesting that *Myb* is a proto-oncogene. However, most of the retroviral insertion sites in murine lymphoma models in the vicinity of the *Myb* locus are not intragenic, raising the question of whether the integrations increase expression of full length Myb to promote lymphoma or other haemopoietic malignancies. It has proved difficult to demonstrate elevated *Myb* mRNA in malignant cells harbouring retroviral integrations in or near *Myb* [482]. Since Myb is alternatively spliced, an interesting possibility would be that the proviral integrations increase the production of mRNA encoding the alternative spliced Myb product lacking the C-terminal inhibitory domain [228,229,261]. In my studies, *Myb* mRNA was increased 20-30 fold in the double transduced B cells that were transformed into continuous proliferation in culture. However what remains to be determined in future studies is whether this elevated *Myb* mRNA is truly derived from the integrated provirus, and whether it encodes full length or truncated Myb protein.

The question of what form of Myb is produced in the transformed B cells is highlighted by the consistent finding that double transduced cells expressing

both DsRed from the *Myb/DsRed* vector and GFP from the *MYC/GFP* vector were clearly detectable by flow cytometry during the first 6-10 days of culture but showed no evidence of spontaneous proliferation. Their frequency or numbers did not increase over time. In fact B cells measurably expressing both vectors were reproducibly smaller than their counterparts expressing only GFP on Day 7 of culture, implying a suppressive effect of the *Myb/DsRed* vector on B cell growth.

By contrast, the transformed B cells that only became detectable on Day 11 displayed a different phenotype with no measurable expression of *DsRed*. Since the transformed B cells expressed greatly increased Myb mRNA detected by RT-PCR and microarray, it is reasonable to infer that it is provirally-derived although that remains to be demonstrated. If so, there are three possibilities to explain the consistent lack of DsRed fluorescence in the transformed B cells. First, it may reflect a translational difference, for example if the transformation process extinguished activity of the IRES. Second, it may reflect selection for integration sites that express the *Myb*-IRES-*DsRed* mRNA at lower levels, still greatly elevating Myb relative to single *MYC*-transduced counterparts but insufficient to produce detectable DsRed protein. This possibility is reasonable, since the DsRed protein was at lower levels in all cells receiving the *Myb*-IRES-*DsRed* vector compared to empty-IRES-*DsRed* vector. Third, the transformed B cells have been transduced with an altered form of the *Myb*-IRES-*DsRed* vector that has lost some or all of the IRES-*DsRed* segment but retains the *Myb* elements measured by RT-PCR and microarray. For example, occurrence of a cryptic internal RNA splicing event in a small fraction of the vector RNA in the packaging cell line could produce a subset of retroviral particles encoding a truncated Myb protein and no DsRed protein. Given the strong evidence that removal of the Myb C-terminal inhibitory domain is important for oncogenic activity in other cell types [225,229,231], this is an attractive possibility.

To resolve amongst these possibilities, it will be important in future studies to amplify and sequence the *Myb* mRNA in the transformed outgrowths and compare its level of expression and sequence with that in control B cells singly transduced with the *Myb/DsRed* vector or the *MYC/GFP* vector. It would also be valuable to repeat the co-transduction experiments with *Myb/DsRed* vector

encoding a C-terminally truncated Myb protein, to test if DsRed+ GFP+ double expressing cells are now induced to proliferate in the first 6 days of culture.

The consequences of *Myb* overexpression in mature B cells is not well defined as most research has focussed on its role in immature cells. Further research into the feasibility of overexpressing *Myb* in other mature B cell models and the pathways subsequently deregulated may help clarify the oncogenic potential of unmutated *Myb*. The ultimate test would be the in vivo consequences of overexpressing *Myb* under the control of a mature B cell-specific promoter.

7.2 *Myb*, *Myc* and *Trp53* co-operation

7.2.1 Myc and Myb

Several avenues of research have confirmed that *Myc* and *Myb* co-operate in lymphomagenesis. Davies et al [483] demonstrated that transgenic mice constitutively overexpressing *v-myb* in their T cells and subsequently infected with Moloney Murine Leukaemia Virus have reduced latency to T cell lymphoma compared to non-infected controls. Analysis of the retroviral insertion sites demonstrated that in most lymphomas the retrovirus had inserted into the *c-myc* or *N-myc* locus, suggesting co-operation between the *Myb* and *Myc* genes. Similarly Barr et al [484] confirmed that the vicinity of the *Myb* locus was the common insertion site in T cell lymphoma induced by a feline leukaemia virus-*Myc* recombinant retrovirus. Hanlon et al [485] showed that mice expressing both CD2-v*Myb* and CD2-*MYC*-ER transgenes developed T cell lymphoma more rapidly than those expressing a single transgene. Interrogation of the Retroviral Tagged Cancer Gene Database [94] demonstrates that tumour models that have *Myb* as a common insertion site frequently have *Myc* as another common insertion site.

Several publications have demonstrated that *Myb* is able to increase the expression of *Myc* [486], although most of this work is not in B cells. Early work by Evans et al [487] demonstrated that in T-cells transfection of a *Myb*-expressing retrovirus resulted in increased *Myc* expression and that the *Myb*

protein transactivates a portion of the *Myc* gene promoter. Schmidt et al [488] showed that *Myc* is a direct transcriptionally regulated target of Myb in a myeloblastic cell line and proposed that Myc mediates Myb's proliferative effect. Kumar et al [489] confirmed that overexpression of *Myb* resulted in overexpression of *Myc*, however showed that *Myc* overexpression alone was insufficient to explain the Myb-mediated myeloid differentiation block. These observations are less relevant to the co-operation observed here, since MYC transcription in the transformed cells was controlled by the MSCV long terminal repeat.

Indirect mechanisms of Myb-Myc co-operation are also highly likely with dysregulation of one gene modulating the downstream effects of the other. The *Bcl2* family may potentially facilitate such co-operation. As discussed in Section 5.3, *Myb* induces *Bcl2* expression in T cells [448,449] and other MYB family members have been shown to upregulate *Bcl2* in B cells [450,451]. *Myc* induced lymphomagenesis is facilitated by dysregulation of *Bcl2* family members [212,335,490], which could thus potentially be facilitated by *Myb*. Recent publications [179,180] showing that rather than targeting specific genes, Myc exponentially amplifies the output of existing transcriptionally active genes further supports a potential indirect mechanism of cooperation.

A small number of studies have demonstrated that *Myb* and *Myc* expression can result in epigenetic modifications, another potential mechanism of co-operation. *Myb* has been shown [491] to modulate the expression of the histone variant gene *H2A.Z* in T cells, Martinato et al [492] demonstrated that *Myc* has diverse actions on chromatin structure in a B cell line and Knoepfler et al [493] demonstrated that *N-myc* null neurones have different chromatin transcriptional activity to normal neurones. The consequences of epigenetic changes due to *Myb* or *Myc* dysregulation in B cells remain, however, to be well defined.

MicroRNAs are critical components of genetic regulation. miR-150 expression is lower in germinal centre cells than in naive or memory B cells [494] and is markedly suppressed in Burkitt lymphoma cells compared to other B cell Non Hodgkin Lymphomas [342]. miR-150 is a negative regulator of *Myb* and its

experimental overexpression in a *Myc*-mediated lymphoma model results in marked tumour regression [495], potentially as a consequence of *Myb* suppression. Since miR-150 targets sequences in the 3' untranslated region of the *Myb* mRNA [267] that are absent from our proviral vector, this potential mechanism for modulating tumour growth would be bypassed in our lymphoma model, but miR-150 is an example of microRNAs modulating gene interactions.

7.2.2 Myb and Trp53

The interactions between *Myb* overexpression and *Trp53* deficiency are also of importance. p53 induces cell cycle arrest at the G1 checkpoint and consolidates cell cycle arrest at the G2 checkpoint in response to DNA damage. B-myb has been shown [496] to reduce p53 dependent cell cycle arrest at the G1 checkpoint in cell lines. Mannefeld et al [497] have recently described that B-myb promotes recovery from the G2 checkpoint in p53 mutant cells. These actions of the *B-myb* gene may allow ongoing proliferation of defective cells, consolidating the effect of loss of the *Trp53* tumour suppressor gene, but the specific impact of *c-Myb* overexpression remains to be clarified. Dysregulated Myb may relieve cell cycle blocks through its established role in transcriptionally inducing a number of key G1-S phase and G2-M phase mediators including *Ccnb1 [472], Ccne1 [498] and Ccna1 [499]*, although additional experiments would be needed to confirm this.

Myb may also potentially enhance the apoptotic defect in p53 defective cells. As discussed in Chapter 1 the Bcl2 family of proteins are downstream effectors of Myc-mediated p53 dependent and independent apoptosis. *Myb* overexpression in B cells could potentially enhance *Bcl2* expression, broadening the apoptotic defect seen with a p53 defect alone, and thus enhancing the cells' transformation potential.

With regards to the potential impact of p53 on Myb, Takikawa et al [500] demonstrated that p53 negatively regulates *Myb* activity through increased degradation and inhibition of Myb-dependent transactivation in cell lines. This suggests that p53 defective cells may have enhanced Myb-mediated cell proliferation.

7.2.3 Triple *Myb, Myc* and *Trp53* dysregulation

As discussed in Section 1.12 Sander et al [14] demonstrated that activation of the phosphoinositide 3-kinase (PI3K) pathway could cooperate with MYC overexpression in a murine Burkitt Lymphoma model. PI3K is activated by antigen binding to the B cell receptor, is a critical mediator of mature B cell survival [22] and has also been shown to stabilise Myc [501]. Schmitz et al showed that mutations in *TCF3* and its negative regulator *ID3* were found in 70% of cases of sporadic Burkitt lymphoma analysed, and promoted PI3K signalling. The role of Myb in PI3K signalling remains to be well defined as detailed in the discussion of Chapter 4. It could be postulated that Myb is a downstream mediator of the prosurvival signals from the PI3K pathway, or enhances the activity of this signaling pathway. *Myb* mRNA is induced by PI3K-AKT-mTOR signalling in T cells [430] and uncoupling *Myb* induction from its normal sensitivity to rapamycin relieves the inhibitory effect of this drug on HTLV1 replication in T cells [502]. *Myb* overexpression could thus circumvent the necessity for mutations in the PI3K pathway. Other integration sites discussed in Chapter 4 may also contribute to lymphomagenesis through modulation of this pathway, although none clearly fall into the same complementation group as Myb.

The high frequency of p53 pathway mutations and PI3K pathway dysregulation in Burkitt lymphoma confirms that these are not infrequently found together and may cooperate with the *MYC* overexpression that defines this lymphoma. One potential mechanism through which *MYC*, *Myb* and *Trp53* dysregulation all cooperate is through FoxO transcription factors which mediate components of cell survival and proliferation pathways, among other roles. They are inactivated by protein kinase B/Akt (components of the PI3K pathway) - mediated phosphorylation. Bouchard et al [364] showed that disruption of FoxO function dramatically accelerates Myc-driven lymphomagenesis by compromising *Arf* induction and thus p53 function. It could thus be hypothesised that increased PI3K pathway activity (potentially mediated by *Myb* overexpression) enhances the oncogenic function of both *Myc* and *Trp53*, explaining the triple gene co-operative (rather than merely additive) effect.

7.3 Are these three genetic defects sufficient for lymphomagenesis?

The data presented in this thesis indicate that triple *MYC*, *Myb* and *Trp53* dysregulation may complete an oncogenic triad sufficient for mature B cell to proliferate autonomously. However, as discussed in Chapter 5, it is possible that the observed transformation efficiency of less than 100 percent is due to the requirement for additional mutations to accumulate prior to cell transformation. The high efficiency of transformation – at least 1 in 210 MYC/GFP+ cells and 1 in 50 double-transduced cells – rules out the need for the vector to target a specific additional oncogene by insertional mutagenesis because there is not such a great degree of bias to retroviral integration sites. Moreover, the consistency and efficiency of transformation from experiment to experiment makes it very unlikely that the subset of B cells transformed are selected based on carrying a pre-existing fourth mutation elsewhere in their genome. As discussed in Chapter 5 and above, the factor that limits transformation to 1 cell in 50 double transduced B cells may simply be the need for the MYC provirus to integrate in a highly permissive locus, since the outgrowths uniformly displayed much higher GFP than the majority of transduced cells. Alternatively, the remaining factor may be transduction with an internally spliced Myb vector that lacks the C-terminus of Myb, IRES and DsRed coding elements, as discussed above.

Further in vitro studies are needed to confirm and expand upon our findings that *MYC* and *Myb* overexpression in conjunction with a p53 defect co-operate to facilitate B cell proliferation in vitro. Initially the in vitro experimental system described in this thesis could be used to determine the effects of overexpressing other genes of interest such as *Gng7* and *Ltb/Ltb*. Selective overexpression of genes activating the PI3K pathway or suppressing the NF-κB pathway would also be of interest as these pathways are dysregulated in Burkitt lymphoma. Different in vitro techniques could also be used to confirm that our findings are generalisable. These could include the use of a Cre-Lox system to excise *Trp53* at a later time point in an effort to limit the number of random

genetic mutations acquired by cells. Inducible gene systems such as the tetracycline dependent system could also be used to overexpress *Myb* or *MYC* at specific time points. Linking *Myb* or *MYC* overexpression to promoters which are only active in mature B cells may help to confirm the B cell maturation stage which facilitates the genetic co-operation. A robust study of the pathways dysregulated by the triple gene defect would also be of significant interest due to the limitations of our small pilot microarray study as discussed in Chapter 6.

In vivo studies are critical, particularly as this triple gene combination would have been predicted to facilitate cell proliferation in vitro. Initially, the malignant nature of the cellular outgrowth should be confirmed by injecting autonomously proliferating cells with the *MYC/Myb/Trp53* triple gene defect in vitro into syngeneic murine recipients. Further experiments, guided by the success of supplementary in vitro studies, would include selective induction of *MYC* and *Myb* and deletion of *Trp53* in mature B cells in vivo. If the triple gene defect were confirmed to be co-operative, subsequent normalisation of the dysregulated genes in vivo would be of considerable interest to determine if the lymphoma remains addicted to the dysregulated gene(s).

7.4 Application

Assuming that different in vitro and in vivo models are able to confirm that *Myb*, *Myc* and *Trp53* dysregulation facilitates autonomous B cell proliferation, the potential broader application of this finding needs exploration. This research has looked at the dysregulated gene combination that initiates autonomous B cell proliferation, which may not be the same as the dysregulated genes required for maintenance of a mature B cell lymphoma. While the autonomously growing cells in vitro still had overexpression of *MYC* (extrapolated from GFP positivity), *Myb* (confirmed with real time PCR) and defective p53 function (mouse genotype) the scope of this research did not include normalising expression of these genes individually within the autonomously growing cells to determine if they were still necessary for their ongoing viability.

If this triple gene combination were demonstrated to only be critical for the initial transformation rather than maintenance of the lymphoma, targeted therapies based on these results may be of benefit in patients at high risk of developing *MYC* overexpressing B cell lymphoma (particularly Burkitt lymphoma), such as those with HIV or post transplantation. Alternatively, such a therapy may potentially be of use in patients with low grade lymphoma in an effort to prevent a high grade transformation which portends a poorer prognosis.

If it were confirmed that dysregulation of this triple gene combination were critical for persistence of the autonomously proliferating cells in vivo, these results could be used as a basis for the development of targeted treatments. Targeted therapies usually complement rather than replace combination chemotherapy to optimise therapeutic response while minimising toxicity and resistance. Monoclonal antibodies have demonstrated significant therapeutic efficacy in B cell lymphoma. An example of such an approach is the development of rituximab, a monoclonal anti CD20 antibody, which is given in conjunction with chemotherapy and has significantly improved survival [503] in several subtypes of B cell lymphoma. Monoclonal antibodies may be unlabelled where their mechanism of action include antibody-dependent cell lysis and complement dependent cytolysis, or may be conjugated to a toxin or radioisotope in an attempt to optimise local toxicity. Monoclonal antibodies are not the only type of targeted therapy and have the disadvantage of requiring the surface expression of the antigen of interest. Targeted therapies currently in clinical and preclinical studies for B cell lymphoma include those inhibiting the proteasome [504], Bruton's tyrosine kinase [505] and Bcl2 [506].

Based on our research findings it could be proposed that induction of *TP53* expression or suppression of *MYC* or *MYB* expression may be a valid therapeutic goal. Many groups have attempted to increase p53 levels in p53 defective tumours to induce cell cycle arrest and apoptosis. Martins et al [360] used as Eμ-myc model where the p53 status could be modulated. Reinstitution of p53 function precipitated apoptosis and increased survival, but also selected for tumours with mutations further down the p53 pathway. *Mdm2* haploinsufficiency has also been shown to suppress lymphomagenesis in the Eμ-myc model [507]. Nutlins [508] which occupy the p53-binding pocket in

Mdm2, preventing its binding to p53, have showed preclinical potential, however some research groups have demonstrated that increased p53 levels promote ageing [509,510] and Mdm2 helps protect mice from the lethal effects of ionizing radiation [511], tempering enthusiasm for research in this area.

Suppression of *MYC* overexpression is also theoretically a worthwhile target in tumour cells, although its critical role in normal cellular homeostasis necessitates caution in view of the possible off-target ramifications. Soucek et al [512] engineered a mouse model with an inducible dominant-interfering Myc mutant which, when activated, resulted in the regression of early and established lung adenocarcinomas, although accompanied by reversible suppression of normal actively dividing cells. Further murine research by Delmore et al [513] showed that the BET bromodomain inhibitor JQ1 (which selectively downregulates *Myc* and Myc-dependent target genes) has shown efficacy in Myc-dependent myeloma in vitro and in vivo.

Targeting Myb is not a new concept, and the potential therapeutic role of targeting Myb in leukaemia has been reviewed by Pattabiraman and Gonda [514]. Enthusiasm for this approach needs to be tempered with caution due to the key role that Myb plays in normal haemopoiesis. It may, however, be possible to identify a therapeutic window as preliminary experiments have shown [515] that myeloid or lymphoid leukaemia cells have a heightened sensitivity to Myb oligonucleotides compared to normal cells. There has been interest in Myb antisense oligonucleotides for over a decade (reviewed in [516]). More recently Brignole et al [517] refined a technique using anti-disialoganglioside GD_2 liposomal c-myb-selective antisense oligonucleotides, the *Myb* downregulation and reduced cell proliferation only being seen in GD_2 positive neuroblastoma cell lines as targeted. It could be postulated that anti-CD20 liposomal Myb-selective antisense oligonucleotides may have therapeutic efficacy in lymphoma while avoiding the detrimental effects that *Myb* downregulation may have on early haemopoietic precursors. Short interfering RNAs would be another possible mechanism of *Myb* suppression. Zuber et al [518] demonstrated that this approach could knock down *Myb* expression and suppress Acute Myeloid Leukaemia in a MLL-AF9 murine model. Of critical importance, normal granulopoiesis and erythropoiesis were able to be

reconstituted when cells expressing this Myb shRNA were injected into lethally irradiated mice, although lymphopoiesis was adversely affected.

Alternatively, once the critical co-activators specific for Myb's function in B cells are more clearly defined, small molecules or peptides could be designed to block such interactions. The targeting of co-activators in myeloid cells, which may also be applicable to B cells, was reviewed by Pattabiraman and Gonda [514]. As discussed in this article, targeting of upstream or downstream components of Myb pathways also has merit as these are being more clearly defined (reviewed by Ramsay and Gonda [216]).

Any efficacy of such a targeted therapeutic approach would clearly be a gratifying confirmation of the in vitro research presented in this thesis.

7.5 Synthesis

This thesis demonstrates that *Myb* overexpression is able to co-operate with *MYC* overexpression and a *Trp53* defect to induce uncontrolled mature B cell proliferation in vitro. To our knowledge this is the first time that this has been demonstrated. This suggests that three genetic defects may be sufficient to immortalise a B cell, although requires confirmation in other experimental systems. This finding enhances understanding of the genetic basis of B cell transformation, and further research based on these findings may provide insights into the pathogenesis and cellular pathways implicated in the development of B cell lymphoma. In the current era of targeted therapies better defining such pathways is likely to optimise development of new anti-lymphoma therapeutics.

8. Bibliography

1. Hanahan, D. and R.A. Weinberg, *The hallmarks of cancer.* Cell, 2000. **100**(1): p. 57-70.

2. Hanahan, D. and R.A. Weinberg, *Hallmarks of cancer: the next generation.* Cell, 2011. **144**(5): p. 646-74.

3. Pasqualucci, L., V. Trifonov, G. Fabbri, et al., *Analysis of the coding genome of diffuse large B-cell lymphoma.* Nat Genet, 2011. **43**(9): p. 830-7.

4. Morin, R.D., M. Mendez-Lago, A.J. Mungall, et al., *Frequent mutation of histone-modifying genes in non-Hodgkin lymphoma.* Nature, 2011. **476**(7360): p. 298-303.

5. Schmitz, R., R.M. Young, M. Ceribelli, et al., *Burkitt lymphoma pathogenesis and therapeutic targets from structural and functional genomics.* Nature, 2012. **490**(7418): p. 116-20.

6. Lohr, J.G., P. Stojanov, M.S. Lawrence, et al., *Discovery and prioritization of somatic mutations in diffuse large B-cell lymphoma (DLBCL) by whole-exome sequencing.* Proc Natl Acad Sci U S A, 2012. **109**(10): p. 3879-84.

7. Vogelstein, B., N. Papadopoulos, V.E. Velculescu, et al., *Cancer genome landscapes.* Science, 2013. **339**(6127): p. 1546-58.

8. Morse, H.C., 3rd, M.R. Anver, T.N. Fredrickson, et al., *Bethesda proposals for classification of lymphoid neoplasms in mice.* Blood, 2002. **100**(1): p. 246-58.

9. Ford, R.J., L. Shen, Y.C. Lin-Lee, et al., *Development of a murine model for blastoid variant mantle-cell lymphoma.* Blood, 2007. **109**(11): p. 4899-906.

10. Adams, J.M., A.W. Harris, C.A. Pinkert, et al., *The c-myc oncogene driven by immunoglobulin enhancers induces lymphoid malignancy in transgenic mice.* Nature, 1985. **318**(6046): p. 533-8.

11. Leder, P., J. Battey, G. Lenoir, et al., *Translocations among antibody genes in human cancer.* Science, 1983. **222**(4625): p. 765-71.

12. Erikson, J., J. Finan, Y. Tsujimoto, et al., *The chromosome 14 breakpoint in neoplastic B cells with the t(11;14) translocation involves the immunoglobulin heavy chain locus.* Proc Natl Acad Sci U S A, 1984. **81**(13): p. 4144-8.

13. Croce, C.M., J. Erikson, A. ar-Rushdi, et al., *Translocated c-myc oncogene of Burkitt lymphoma is transcribed in plasma cells and repressed in lymphoblastoid cells.* Proc Natl Acad Sci U S A, 1984. **81**(10): p. 3170-4.

14. Sander, S., D.P. Calado, L. Srinivasan, et al., *Synergy between PI3K signaling and MYC in Burkitt lymphomagenesis.* Cancer Cell, 2012. **22**(2): p. 167-79.

15. Swerdlow, S.H.C., E. Harris, N.L. Jaffe, E. S. Pileri, S. A. Stein, H. Thiele, J. Vardiman, J. W., *WHO Classification of Tumours of Haematopoietic and Lymphoid Tissues*. 4 ed2008: IARC Press.

16. Miosge, L.A. and C.C. Goodnow, *Genes, pathways and checkpoints in lymphocyte development and homeostasis.* Immunol Cell Biol, 2005. **83**(4): p. 318-35.

17. Lam, K.P., R. Kuhn, and K. Rajewsky, *In vivo ablation of surface immunoglobulin on mature B cells by inducible gene targeting results in rapid cell death.* Cell, 1997. **90**(6): p. 1073-83.

18. Kraus, M., M.B. Alimzhanov, N. Rajewsky, et al., *Survival of resting mature B lymphocytes depends on BCR signaling via the Igalpha/beta heterodimer.* Cell, 2004. **117**(6): p. 787-800.

19. Wienands, J., O. Larbolette, and M. Reth, *Evidence for a preformed transducer complex organized by the B cell antigen receptor.* Proc Natl Acad Sci U S A, 1996. **93**(15): p. 7865-70.

20. Conley, M.E., A.K. Dobbs, D.M. Farmer, et al., *Primary B cell immunodeficiencies: comparisons and contrasts.* Annu Rev Immunol, 2009. **27**: p. 199-227.

21. Okkenhaug, K. and B. Vanhaesebroeck, *PI3K in lymphocyte development, differentiation and activation.* Nat Rev Immunol, 2003. **3**(4): p. 317-30.

22. Srinivasan, L., Y. Sasaki, D.P. Calado, et al., *PI3 kinase signals BCR-dependent mature B cell survival.* Cell, 2009. **139**(3): p. 573-86.

23. Schiemann, B., J.L. Gommerman, K. Vora, et al., *An essential role for BAFF in the normal development of B cells through a BCMA-independent pathway.* Science, 2001. **293**(5537): p. 2111-4.

24. Thompson, J.S., S.A. Bixler, F. Qian, et al., *BAFF-R, a newly identified TNF receptor that specifically interacts with BAFF.* Science, 2001. **293**(5537): p. 2108-11.

25. Mackay, F., S.A. Woodcock, P. Lawton, et al., *Mice transgenic for BAFF develop lymphocytic disorders along with autoimmune manifestations.* J Exp Med, 1999. **190**(11): p. 1697-710.

26. Mecklenbrauker, I., S.L. Kalled, M. Leitges, et al., *Regulation of B-cell survival by BAFF-dependent PKCdelta-mediated nuclear signalling.* Nature, 2004. **431**(7007): p. 456-61.

27. Craxton, A., K.E. Draves, A. Gruppi, et al., *BAFF regulates B cell survival by downregulating the BH3-only family member Bim via the ERK pathway.* J Exp Med, 2005. **202**(10): p. 1363-74.

28. Sasaki, Y., E. Derudder, E. Hobeika, et al., *Canonical NF-kappaB activity, dispensable for B cell development, replaces BAFF-receptor*

signals and promotes B cell proliferation upon activation. Immunity, 2006. **24**(6): p. 729-39.

29. Otipoby, K.L., Y. Sasaki, M. Schmidt-Supprian, et al., *BAFF activates Akt and Erk through BAFF-R in an IKK1-dependent manner in primary mouse B cells.* Proc Natl Acad Sci U S A, 2008. **105**(34): p. 12435-8.

30. Marsden, V.S. and A. Strasser, *Control of apoptosis in the immune system: Bcl-2, BH3-only proteins and more.* Annu Rev Immunol, 2003. **21**: p. 71-105.

31. Veis, D.J., C.M. Sorenson, J.R. Shutter, et al., *Bcl-2-deficient mice demonstrate fulminant lymphoid apoptosis, polycystic kidneys, and hypopigmented hair.* Cell, 1993. **75**(2): p. 229-40.

32. Nakayama, K., K. Nakayama, I. Negishi, et al., *Targeted disruption of Bcl-2 alpha beta in mice: occurrence of gray hair, polycystic kidney disease, and lymphocytopenia.* Proc Natl Acad Sci U S A, 1994. **91**(9): p. 3700-4.

33. Strasser, A., S. Whittingham, D.L. Vaux, et al., *Enforced BCL2 expression in B-lymphoid cells prolongs antibody responses and elicits autoimmune disease.* Proc Natl Acad Sci U S A, 1991. **88**(19): p. 8661-5.

34. Egle, A., A.W. Harris, M.L. Bath, et al., *VavP-Bcl2 transgenic mice develop follicular lymphoma preceded by germinal center hyperplasia.* Blood, 2004. **103**(6): p. 2276-83.

35. Igney, F.H. and P.H. Krammer, *Death and anti-death: tumour resistance to apoptosis.* Nat Rev Cancer, 2002. **2**(4): p. 277-88.

36. Do, R.K., E. Hatada, H. Lee, et al., *Attenuation of apoptosis underlies B lymphocyte stimulator enhancement of humoral immune response.* J Exp Med, 2000. **192**(7): p. 953-64.

37. Grumont, R.J., I.J. Rourke, and S. Gerondakis, *Rel-dependent induction of A1 transcription is required to protect B cells from antigen receptor ligation-induced apoptosis.* Genes Dev, 1999. **13**(4): p. 400-11.

38. Kurosaki, T., *Genetic analysis of B cell antigen receptor signaling.* Annu Rev Immunol, 1999. **17**: p. 555-92.

39. Schneider, P., F. MacKay, V. Steiner, et al., *BAFF, a novel ligand of the tumor necrosis factor family, stimulates B cell growth.* J Exp Med, 1999. **189**(11): p. 1747-56.

40. Barton, G.M. and R. Medzhitov, *Toll-like receptor signaling pathways.* Science, 2003. **300**(5625): p. 1524-5.

41. Li, Q. and I.M. Verma, *NF-kappaB regulation in the immune system.* Nat Rev Immunol, 2002. **2**(10): p. 725-34.

42. Gerondakis, S. and A. Strasser, *The role of Rel/NF-kappaB transcription factors in B lymphocyte survival.* Semin Immunol, 2003. **15**(3): p. 159-66.

43. Grumont, R.J., A. Strasser, and S. Gerondakis, *B cell growth is controlled by phosphatidylinosotol 3-kinase-dependent induction of Rel/NF-kappaB regulated c-myc transcription.* Mol Cell, 2002. **10**(6): p. 1283-94.

44. Hinz, M., D. Krappmann, A. Eichten, et al., *NF-kappaB function in growth control: regulation of cyclin D1 expression and G0/G1-to-S-phase transition.* Mol Cell Biol, 1999. **19**(4): p. 2690-8.

45. Lossos, I.S., *The endless complexity of lymphocyte differentiation and lymphomagenesis: IRF-4 downregulates BCL6 expression.* Cancer Cell, 2007. **12**(3): p. 189-91.

46. Enzler, T., G. Bonizzi, G.J. Silverman, et al., *Alternative and classical NF-kappa B signaling retain autoreactive B cells in the splenic marginal zone and result in lupus-like disease.* Immunity, 2006. **25**(3): p. 403-15.

47. Nurse, P., *Regulation of the eukaryotic cell cycle.* European journal of cancer, 1997. **33**(7): p. 1002-4.

48. Tsujimoto, Y., J. Yunis, L. Onorato-Showe, et al., *Molecular cloning of the chromosomal breakpoint of B-cell lymphomas and leukemias with the t(11;14) chromosome translocation.* Science, 1984. **224**(4656): p. 1403-6.

49. Glynne, R., S. Akkaraju, J.I. Healy, et al., *How self-tolerance and the immunosuppressive drug FK506 prevent B-cell mitogenesis.* Nature, 2000. **403**(6770): p. 672-6.

50. Lossos, I.S., D.K. Czerwinski, A.A. Alizadeh, et al., *Prediction of survival in diffuse large-B-cell lymphoma based on the expression of six genes.* N Engl J Med, 2004. **350**(18): p. 1828-37.

51. Cato, M.H., S.K. Chintalapati, I.W. Yau, et al., *Cyclin D3 is selectively required for proliferative expansion of germinal center B cells.* Mol Cell Biol, 2011. **31**(1): p. 127-37.

52. de Alboran, I.M., R.C. O'Hagan, F. Gartner, et al., *Analysis of C-MYC function in normal cells via conditional gene-targeted mutation.* Immunity, 2001. **14**(1): p. 45-55.

53. Laplante, M. and D.M. Sabatini, *mTOR signaling in growth control and disease.* Cell, 2012. **149**(2): p. 274-93.

54. Ravitz, M.J., L. Chen, M. Lynch, et al., *c-myc Repression of TSC2 contributes to control of translation initiation and Myc-induced transformation.* Cancer Res, 2007. **67**(23): p. 11209-17.

55. Smeland, E.B., H.K. Blomhoff, H. Holte, et al., *Transforming growth factor type beta (TGF beta) inhibits G1 to S transition, but not activation of human B lymphocytes.* Exp Cell Res, 1987. **171**(1): p. 213-22.

56. Arsura, M., M. Wu, and G.E. Sonenshein, *TGF beta 1 inhibits NF-kappa B/Rel activity inducing apoptosis of B cells: transcriptional activation of I kappa B alpha.* Immunity, 1996. **5**(1): p. 31-40.

57. Cheng, Q., L. Chen, Z. Li, et al., *ATM activates p53 by regulating MDM2 oligomerization and E3 processivity.* Embo J, 2009. **28**(24): p. 3857-67.

58. Nutt, S.L., B. Heavey, A.G. Rolink, et al., *Commitment to the B-lymphoid lineage depends on the transcription factor Pax5.* Nature, 1999. **401**(6753): p. 556-62.

59. Horcher, M., A. Souabni, and M. Busslinger, *Pax5/BSAP maintains the identity of B cells in late B lymphopoiesis.* Immunity, 2001. **14**(6): p. 779-90.

60. Lin, K.I., C. Angelin-Duclos, T.C. Kuo, et al., *Blimp-1-dependent repression of Pax-5 is required for differentiation of B cells to immunoglobulin M-secreting plasma cells.* Mol Cell Biol, 2002. **22**(13): p. 4771-80.

61. Ye, B.H., G. Cattoretti, Q. Shen, et al., *The BCL-6 proto-oncogene controls germinal-centre formation and Th2-type inflammation.* Nat Genet, 1997. **16**(2): p. 161-70.

62. Ranuncolo, S.M., J.M. Polo, J. Dierov, et al., *Bcl-6 mediates the germinal center B cell phenotype and lymphomagenesis through transcriptional repression of the DNA-damage sensor ATR.* Nat Immunol, 2007. **8**(7): p. 705-14.

63. Saito, M., J. Gao, K. Basso, et al., *A signaling pathway mediating downregulation of BCL6 in germinal center B cells is blocked by BCL6 gene alterations in B cell lymphoma.* Cancer Cell, 2007. **12**(3): p. 280-92.

64. Teng, Y., Y. Takahashi, M. Yamada, et al., *IRF4 negatively regulates proliferation of germinal center B cell-derived Burkitt's lymphoma cell lines and induces differentiation toward plasma cells.* Eur J Cell Biol, 2007. **86**(10): p. 581-9.

65. Johnson, K., M. Shapiro-Shelef, C. Tunyaplin, et al., *Regulatory events in early and late B-cell differentiation.* Mol Immunol, 2005. **42**(7): p. 749-61.

66. Tunyaplin, C., A.L. Shaffer, C.D. Angelin-Duclos, et al., *Direct repression of prdm1 by Bcl-6 inhibits plasmacytic differentiation.* J Immunol, 2004. **173**(2): p. 1158-65.

67. Nauta, A.J. and W.E. Fibbe, *Immunomodulatory properties of mesenchymal stromal cells.* Blood, 2007. **110**(10): p. 3499-506.

68. Isaacson, P.G. and M.Q. Du, *MALT lymphoma: from morphology to molecules.* Nature reviews. Cancer, 2004. **4**(8): p. 644-53.

69. Treon, S.P., L. Xu, G. Yang, et al., *MYD88 L265P somatic mutation in Waldenstrom's macroglobulinemia.* N Engl J Med, 2012. **367**(9): p. 826-33.

70. Ngo, V.N., R.M. Young, R. Schmitz, et al., *Oncogenically active MYD88 mutations in human lymphoma.* Nature, 2011. **470**(7332): p. 115-9.

71. Goodnow, C.C., *Multistep pathogenesis of autoimmune disease.* Cell, 2007. **130**(1): p. 25-35.

72. Burnet, F.M., *Immunological surveillance in neoplasia.* Transplant Rev, 1971. **7**: p. 3-25.

73. Smyth, M.J., K.Y. Thia, S.E. Street, et al., *Perforin-mediated cytotoxicity is critical for surveillance of spontaneous lymphoma.* J Exp Med, 2000. **192**(5): p. 755-60.

74. Janz, S., J. Muller, J. Shaughnessy, et al., *Detection of recombinations between c-myc and immunoglobulin switch alpha in murine plasma cell tumors and preneoplastic lesions by polymerase chain reaction.* Proc Natl Acad Sci U S A, 1993. **90**(15): p. 7361-5.

75. Janz, S., *Genetic and environmental cofactors of Myc translocations in plasma cell tumor development in mice.* J Natl Cancer Inst Monogr, 2008(39): p. 37-40.

76. Lee, R.C., R.L. Feinbaum, and V. Ambros, *The C. elegans heterochronic gene lin-4 encodes small RNAs with antisense complementarity to lin-14.* Cell, 1993. **75**(5): p. 843-54.

77. Pasquinelli, A.E., B.J. Reinhart, F. Slack, et al., *Conservation of the sequence and temporal expression of let-7 heterochronic regulatory RNA.* Nature, 2000. **408**(6808): p. 86-9.

78. Kozomara, A. and S. Griffiths-Jones, *miRBase: integrating microRNA annotation and deep-sequencing data.* Nucleic Acids Res, 2011. **39**(Database issue): p. D152-7.

79. Chen, C.Z., L. Li, H.F. Lodish, et al., *MicroRNAs modulate hematopoietic lineage differentiation.* Science, 2004. **303**(5654): p. 83-6.

80. Zhang, J., D.D. Jima, C. Jacobs, et al., *Patterns of microRNA expression characterize stages of human B-cell differentiation.* Blood, 2009. **113**(19): p. 4586-94.

81. Di Lisio, L., N. Martinez, S. Montes-Moreno, et al., *The role of miRNAs in the pathogenesis and diagnosis of B-cell lymphomas.* Blood, 2012. **120**(9): p. 1782-90.

82. Calin, G.A., C. Sevignani, C.D. Dumitru, et al., *Human microRNA genes are frequently located at fragile sites and genomic regions involved in cancers.* Proc Natl Acad Sci U S A, 2004. **101**(9): p. 2999-3004.

83. Calin, G.A., C.D. Dumitru, M. Shimizu, et al., *Frequent deletions and down-regulation of micro- RNA genes miR15 and miR16 at 13q14 in chronic lymphocytic leukemia.* Proc Natl Acad Sci U S A, 2002. **99**(24): p. 15524-9.

84. Cimmino, A., G.A. Calin, M. Fabbri, et al., *miR-15 and miR-16 induce apoptosis by targeting BCL2.* Proc Natl Acad Sci U S A, 2005. **102**(39): p. 13944-9.

85. Costinean, S., N. Zanesi, Y. Pekarsky, et al., *Pre-B cell proliferation and lymphoblastic leukemia/high-grade lymphoma in E(mu)-miR155 transgenic mice.* Proc Natl Acad Sci U S A, 2006. **103**(18): p. 7024-9.

86. Kluiver, J., E. Haralambieva, D. de Jong, et al., *Lack of BIC and microRNA miR-155 expression in primary cases of Burkitt lymphoma.* Genes Chromosomes Cancer, 2006. **45**(2): p. 147-53.

87. Pike, B.L., T.C. Greiner, X. Wang, et al., *DNA methylation profiles in diffuse large B-cell lymphoma and their relationship to gene expression status.* Leukemia, 2008. **22**(5): p. 1035-43.

88. Mestre-Escorihuela, C., F. Rubio-Moscardo, J.A. Richter, et al., *Homozygous deletions localize novel tumor suppressor genes in B-cell lymphomas.* Blood, 2007. **109**(1): p. 271-80.

89. Pasqualucci, L., D. Dominguez-Sola, A. Chiarenza, et al., *Inactivating mutations of acetyltransferase genes in B-cell lymphoma.* Nature, 2011. **471**(7337): p. 189-95.

90. Okazaki, I.M., A. Kotani, and T. Honjo, *Role of AID in tumorigenesis.* Adv Immunol, 2007. **94**: p. 245-73.

91. Haupt, Y., W.S. Alexander, G. Barri, et al., *Novel zinc finger gene implicated as myc collaborator by retrovirally accelerated lymphomagenesis in E mu-myc transgenic mice.* Cell, 1991. **65**(5): p. 753-63.

92. van Lohuizen, M., S. Verbeek, B. Scheijen, et al., *Identification of cooperating oncogenes in E mu-myc transgenic mice by provirus tagging.* Cell, 1991. **65**(5): p. 737-52.

93. Uren, A.G., J. Kool, A. Berns, et al., *Retroviral insertional mutagenesis: past, present and future.* Oncogene, 2005. **24**(52): p. 7656-72.

94. Akagi, K., T. Suzuki, R.M. Stephens, et al., *RTCGD: retroviral tagged cancer gene database.* Nucleic Acids Res, 2004. **32**(Database issue): p. D523-7.

95. Refaeli, Y., R.M. Young, B.C. Turner, et al., *The B cell antigen receptor and overexpression of MYC can cooperate in the genesis of B cell lymphomas.* PLoS Biol, 2008. **6**(6): p. e152.

96. Kuppers, R., *Mechanisms of B-cell lymphoma pathogenesis.* Nat Rev Cancer, 2005. **5**(4): p. 251-62.

97. Wotherspoon, A.C., C. Doglioni, T.C. Diss, et al., *Regression of primary low-grade B-cell gastric lymphoma of mucosa-associated lymphoid tissue type after eradication of Helicobacter pylori.* Lancet, 1993. **342**(8871): p. 575-7.

98. Lenz, G., R.E. Davis, V.N. Ngo, et al., *Oncogenic CARD11 mutations in human diffuse large B cell lymphoma.* Science, 2008. **319**(5870): p. 1676-9.

99. Compagno, M., W.K. Lim, A. Grunn, et al., *Mutations of multiple genes cause deregulation of NF-kappaB in diffuse large B-cell lymphoma.* Nature, 2009. **459**(7247): p. 717-21.

100. Ngo, V.N., R.E. Davis, L. Lamy, et al., *A loss-of-function RNA interference screen for molecular targets in cancer.* Nature, 2006. **441**(7089): p. 106-10.

101. Jeelall, Y.S., J.Q. Wang, H.D. Law, et al., *Human lymphoma mutations reveal CARD11 as the switch between self-antigen-induced B cell death or proliferation and autoantibody production.* J Exp Med, 2012. **209**(11): p. 1907-17.

102. He, B., A. Chadburn, E. Jou, et al., *Lymphoma B cells evade apoptosis through the TNF family members BAFF/BLyS and APRIL.* J Immunol, 2004. **172**(5): p. 3268-79.

103. Kim, S.J., S.J. Lee, I.Y. Choi, et al., *Serum BAFF predicts prognosis better than APRIL in diffuse large B-cell lymphoma patients treated with rituximab plus CHOP chemotherapy.* Eur J Haematol, 2008. **81**(3): p. 177-84.

104. Boultwood, J., *Ataxia telangiectasia gene mutations in leukaemia and lymphoma.* J Clin Pathol, 2001. **54**(7): p. 512-6.

105. Maclean, K.H., M.B. Kastan, and J.L. Cleveland, *Atm deficiency affects both apoptosis and proliferation to augment Myc-induced lymphomagenesis.* Mol Cancer Res, 2007. **5**(7): p. 705-11.

106. Limpens, J., R. Stad, C. Vos, et al., *Lymphoma-associated translocation t(14;18) in blood B cells of normal individuals.* Blood, 1995. **85**(9): p. 2528-36.

107. Straus, S.E., E.S. Jaffe, J.M. Puck, et al., *The development of lymphomas in families with autoimmune lymphoproliferative syndrome with germline Fas mutations and defective lymphocyte apoptosis.* Blood, 2001. **98**(1): p. 194-200.

108. Davidson, W.F., T. Giese, and T.N. Fredrickson, *Spontaneous development of plasmacytoid tumors in mice with defective Fas-Fas ligand interactions.* J Exp Med, 1998. **187**(11): p. 1825-38.

109. Jost, P.J. and J. Ruland, *Aberrant NF-kappaB signaling in lymphoma: mechanisms, consequences, and therapeutic implications.* Blood, 2007. **109**(7): p. 2700-7.

110. Inoue, J., L.D. Kerr, L.J. Ransone, et al., *c-rel activates but v-rel suppresses transcription from kappa B sites.* Proc Natl Acad Sci U S A, 1991. **88**(9): p. 3715-9.

111. Davis, R.E., K.D. Brown, U. Siebenlist, et al., *Constitutive nuclear factor kappaB activity is required for survival of activated B cell-like diffuse large B cell lymphoma cells.* J Exp Med, 2001. **194**(12): p. 1861-74.

112. Kato, M., M. Sanada, I. Kato, et al., *Frequent inactivation of A20 in B-cell lymphomas.* Nature, 2009. **459**(7247): p. 712-6.

113. Honma, K., S. Tsuzuki, M. Nakagawa, et al., *TNFAIP3/A20 functions as a novel tumor suppressor gene in several subtypes of non-Hodgkin lymphomas.* Blood, 2009. **114**(12): p. 2467-75.

114. Nakagawa, M., M. Seto, and Y. Hosokawa, *Molecular pathogenesis of MALT lymphoma: two signaling pathways underlying the antiapoptotic effect of API2-MALT1 fusion protein.* Leukemia, 2006. **20**(6): p. 929-36.

115. Chen, L., S. Monti, P. Juszczynski, et al., *SYK-dependent tonic B-cell receptor signaling is a rational treatment target in diffuse large B-cell lymphoma.* Blood, 2008. **111**(4): p. 2230-7.

116. Gobessi, S., L. Laurenti, P.G. Longo, et al., *Inhibition of constitutive and BCR-induced Syk activation downregulates Mcl-1 and induces apoptosis in chronic lymphocytic leukemia B cells.* Leukemia, 2009. **23**(4): p. 686-97.

117. Drakos, E., G.Z. Rassidakis, and L.J. Medeiros, *Mammalian target of rapamycin (mTOR) pathway signalling in lymphomas.* Expert Rev Mol Med, 2008. **10**: p. e4.

118. Peponi, E., E. Drakos, G. Reyes, et al., *Activation of mammalian target of rapamycin signaling promotes cell cycle progression and protects cells from apoptosis in mantle cell lymphoma.* Am J Pathol, 2006. **169**(6): p. 2171-80.

119. Ansell, S.M., D.J. Inwards, K.M. Rowland, Jr., et al., *Low-dose, single-agent temsirolimus for relapsed mantle cell lymphoma: a phase 2 trial in the North Central Cancer Treatment Group.* Cancer, 2008. **113**(3): p. 508-14.

120. McArthur, G.A., M. Wall, M.J. Bywater, et al., *Targeting mTOR and Ribosome Biogenesis during Myc-Induced Lymphomagenesis*, in *New Insights into Leukaemia Research*2008: Sunshine Coast Australia.

121. Elliott, R.L. and G.C. Blobe, *Role of transforming growth factor Beta in human cancer.* J Clin Oncol, 2005. **23**(9): p. 2078-93.

122. Kehrl, J.H., A.B. Roberts, L.M. Wakefield, et al., *Transforming growth factor beta is an important immunomodulatory protein for human B lymphocytes.* J Immunol, 1986. **137**(12): p. 3855-60.

123. Douglas, R.S., R.J. Capocasale, R.J. Lamb, et al., *Chronic lymphocytic leukemia B cells are resistant to the apoptotic effects of transforming growth factor-beta.* Blood, 1997. **89**(3): p. 941-7.

124. Avet-Loiseau, H., M. Attal, P. Moreau, et al., *Genetic abnormalities and survival in multiple myeloma: the experience of the Intergroupe Francophone du Myelome.* Blood, 2007. **109**(8): p. 3489-95.

125. Cattoretti, G., L. Pasqualucci, G. Ballon, et al., *Deregulated BCL6 expression recapitulates the pathogenesis of human diffuse large B cell lymphomas in mice.* Cancer Cell, 2005. **7**(5): p. 445-55.

126. Alizadeh, A.A., M.B. Eisen, R.E. Davis, et al., *Distinct types of diffuse large B-cell lymphoma identified by gene expression profiling.* Nature, 2000. **403**(6769): p. 503-11.

127. Mullighan, C.G., S. Goorha, I. Radtke, et al., *Genome-wide analysis of genetic alterations in acute lymphoblastic leukaemia.* Nature, 2007. **446**(7137): p. 758-64.

128. Iida, S., P.H. Rao, P. Nallasivam, et al., *The t(9;14)(p13;q32) chromosomal translocation associated with lymphoplasmacytoid lymphoma involves the PAX-5 gene.* Blood, 1996. **88**(11): p. 4110-7.

129. Cook, J.R., N.I. Aguilera, S. Reshmi-Skarja, et al., *Lack of PAX5 rearrangements in lymphoplasmacytic lymphomas: reassessing the reported association with t(9;14).* Hum Pathol, 2004. **35**(4): p. 447-54.

130. George, T.I., J.E. Wrede, C.D. Bangs, et al., *Low-grade B-Cell lymphomas with plasmacytic differentiation lack PAX5 gene rearrangements.* J Mol Diagn, 2005. **7**(3): p. 346-51.

131. Tsuboi, K., S. Iida, H. Inagaki, et al., *MUM1/IRF4 expression as a frequent event in mature lymphoid malignancies.* Leukemia, 2000. **14**(3): p. 449-56.

132. Xu, D., L. Zhao, L. Del Valle, et al., *Interferon regulatory factor 4 is involved in Epstein-Barr virus-mediated transformation of human B lymphocytes.* J Virol, 2008. **82**(13): p. 6251-8.

133. Knodel, M., A.W. Kuss, D. Lindemann, et al., *Reversal of Blimp-1-mediated apoptosis by A1, a member of the Bcl-2 family.* Eur J Immunol, 1999. **29**(9): p. 2988-98.

134. Lane, D.P. and L.V. Crawford, *T antigen is bound to a host protein in SV40-transformed cells.* Nature, 1979. **278**(5701): p. 261-3.

135. Linzer, D.I. and A.J. Levine, *Characterization of a 54K dalton cellular SV40 tumor antigen present in SV40-transformed cells and uninfected embryonal carcinoma cells.* Cell, 1979. **17**(1): p. 43-52.

136. Melero, J.A., D.T. Stitt, W.F. Mangel, et al., *Identification of new polypeptide species (48-55K) immunoprecipitable by antiserum to purified large T antigen and present in SV40-infected and -transformed cells.* Virology, 1979. **93**(2): p. 466-80.

137. Smith, A.E., R. Smith, and E. Paucha, *Characterization of different tumor antigens present in cells transformed by simian virus 40.* Cell, 1979. **18**(2): p. 335-46.

138. Lane, D.P., *Cancer. p53, guardian of the genome.* Nature, 1992. **358**(6381): p. 15-6.

139. Donehower, L.A., M. Harvey, B.L. Slagle, et al., *Mice deficient for p53 are developmentally normal but susceptible to spontaneous tumours.* Nature, 1992. **356**(6366): p. 215-21.

140. Malkin, D., F.P. Li, L.C. Strong, et al., *Germ line p53 mutations in a familial syndrome of breast cancer, sarcomas, and other neoplasms.* Science, 1990. **250**(4985): p. 1233-8.

141. Srivastava, S., Z.Q. Zou, K. Pirollo, et al., *Germ-line transmission of a mutated p53 gene in a cancer-prone family with Li-Fraumeni syndrome.* Nature, 1990. **348**(6303): p. 747-9.

142. Lozano, G. and G.P. Zambetti, *What have animal models taught us about the p53 pathway?* J Pathol, 2005. **205**(2): p. 206-20.

143. Jeffers, J.R., E. Parganas, Y. Lee, et al., *Puma is an essential mediator of p53-dependent and -independent apoptotic pathways.* Cancer Cell, 2003. **4**(4): p. 321-8.

144. Villunger, A., E.M. Michalak, L. Coultas, et al., *p53- and drug-induced apoptotic responses mediated by BH3-only proteins puma and noxa.* Science, 2003. **302**(5647): p. 1036-8.

145. Hemann, M.T., J.T. Zilfou, Z. Zhao, et al., *Suppression of tumorigenesis by the p53 target PUMA.* Proc Natl Acad Sci U S A, 2004. **101**(25): p. 9333-8.

146. Garrison, S.P., J.R. Jeffers, C. Yang, et al., *Selection against PUMA gene expression in Myc-driven B-cell lymphomagenesis.* Mol Cell Biol, 2008. **28**(17): p. 5391-402.

147. Liu, G., J.M. Parant, G. Lang, et al., *Chromosome stability, in the absence of apoptosis, is critical for suppression of tumorigenesis in Trp53 mutant mice.* Nat Genet, 2004. **36**(1): p. 63-8.

148. Brady, C.A., D. Jiang, S.S. Mello, et al., *Distinct p53 transcriptional programs dictate acute DNA-damage responses and tumor suppression.* Cell, 2011. **145**(4): p. 571-83.

149. Peller, S. and V. Rotter, *TP53 in hematological cancer: low incidence of mutations with significant clinical relevance.* Human mutation, 2003. **21**(3): p. 277-84.

150. Petitjean, A., E. Mathe, S. Kato, et al., *Impact of mutant p53 functional properties on TP53 mutation patterns and tumor phenotype: lessons from recent developments in the IARC TP53 database.* Human mutation, 2007. **28**(6): p. 622-9.

151. Xu-Monette, Z.Y., L.J. Medeiros, Y. Li, et al., *Dysfunction of the TP53 tumor suppressor gene in lymphoid malignancies.* Blood, 2012. **119**(16): p. 3668-83.

152. Moller, M.B., Y. Ino, A.M. Gerdes, et al., *Aberrations of the p53 pathway components p53, MDM2 and CDKN2A appear independent in diffuse large B cell lymphoma.* Leukemia : official journal of the Leukemia Society of America, Leukemia Research Fund, U.K, 1999. **13**(3): p. 453-9.

153. Pinyol, M., L. Hernandez, A. Martinez, et al., *INK4a/ARF locus alterations in human non-Hodgkin's lymphomas mainly occur in tumors with wild-type p53 gene.* Am J Pathol, 2000. **156**(6): p. 1987-96.

154. Pettitt, A.R., P.D. Sherrington, G. Stewart, et al., *p53 dysfunction in B-cell chronic lymphocytic leukemia: inactivation of ATM as an alternative to TP53 mutation.* Blood, 2001. **98**(3): p. 814-22.

155. Lindstrom, M.S., U. Klangby, and K.G. Wiman, *p14ARF homozygous deletion or MDM2 overexpression in Burkitt lymphoma lines carrying wild type p53.* Oncogene, 2001. **20**(17): p. 2171-7.

156. Koduru, P.R., K. Raju, V. Vadmal, et al., *Correlation between mutation in P53, p53 expression, cytogenetics, histologic type, and survival in patients with B-cell non-Hodgkin's lymphoma.* Blood, 1997. **90**(10): p. 4078-91.

157. Lo Coco, F., G. Gaidano, D.C. Louie, et al., *p53 mutations are associated with histologic transformation of follicular lymphoma.* Blood, 1993. **82**(8): p. 2289-95.

158. Sander, C.A., T. Yano, H.M. Clark, et al., *p53 mutation is associated with progression in follicular lymphomas.* Blood, 1993. **82**(7): p. 1994-2004.

159. Malcikova, J., J. Smardova, L. Rocnova, et al., *Monoallelic and biallelic inactivation of TP53 gene in chronic lymphocytic leukemia: selection, impact on survival, and response to DNA damage.* Blood, 2009. **114**(26): p. 5307-14.

160. Pekova, S., O. Mazal, R. Cmejla, et al., *A comprehensive study of TP53 mutations in chronic lymphocytic leukemia: Analysis of 1287 diagnostic and 1148 follow-up CLL samples.* Leuk Res, 2011. **35**(7): p. 889-98.

161. Green, D.R. and G. Kroemer, *Cytoplasmic functions of the tumour suppressor p53.* Nature, 2009. **458**(7242): p. 1127-30.

162. Boehme, K.A. and C. Blattner, *Regulation of p53--insights into a complex process.* Critical reviews in biochemistry and molecular biology, 2009. **44**(6): p. 367-92.

163. Chipuk, J.E., L. Bouchier-Hayes, T. Kuwana, et al., *PUMA couples the nuclear and cytoplasmic proapoptotic function of p53.* Science, 2005. **309**(5741): p. 1732-5.

164. Michalak, E., A. Villunger, M. Erlacher, et al., *Death squads enlisted by the tumour suppressor p53.* Biochem Biophys Res Commun, 2005. **331**(3): p. 786-98.

165. Harper, J.W., G.R. Adami, N. Wei, et al., *The p21 Cdk-interacting protein Cip1 is a potent inhibitor of G1 cyclin-dependent kinases.* Cell, 1993. **75**(4): p. 805-16.

166. el-Deiry, W.S., T. Tokino, V.E. Velculescu, et al., *WAF1, a potential mediator of p53 tumor suppression.* Cell, 1993. **75**(4): p. 817-25.

167. Agarwal, M.L., A. Agarwal, W.R. Taylor, et al., *p53 controls both the G2/M and the G1 cell cycle checkpoints and mediates reversible growth arrest in human fibroblasts.* Proc Natl Acad Sci U S A, 1995. **92**(18): p. 8493-7.

168. Giono, L.E. and J.J. Manfredi, *The p53 tumor suppressor participates in multiple cell cycle checkpoints.* J Cell Physiol, 2006. **209**(1): p. 13-20.

169. Sengupta, S. and C.C. Harris, *p53: traffic cop at the crossroads of DNA repair and recombination.* Nature reviews. Molecular cell biology, 2005. **6**(1): p. 44-55.

170. Brown, J.P., W. Wei, and J.M. Sedivy, *Bypass of senescence after disruption of p21CIP1/WAF1 gene in normal diploid human fibroblasts.* Science, 1997. **277**(5327): p. 831-4.

171. Herbig, U., W.A. Jobling, B.P. Chen, et al., *Telomere shortening triggers senescence of human cells through a pathway involving ATM, p53, and p21(CIP1), but not p16(INK4a).* Mol Cell, 2004. **14**(4): p. 501-13.

172. Maiuri, M.C., L. Galluzzi, E. Morselli, et al., *Autophagy regulation by p53.* Curr Opin Cell Biol, 2010. **22**(2): p. 181-5.

173. Crighton, D., S. Wilkinson, J. O'Prey, et al., *DRAM, a p53-induced modulator of autophagy, is critical for apoptosis.* Cell, 2006. **126**(1): p. 121-34.

174. Feng, Z., H. Zhang, A.J. Levine, et al., *The coordinate regulation of the p53 and mTOR pathways in cells.* Proc Natl Acad Sci U S A, 2005. **102**(23): p. 8204-9.

175. Tasdemir, E., M.C. Maiuri, L. Galluzzi, et al., *Regulation of autophagy by cytoplasmic p53.* Nature cell biology, 2008. **10**(6): p. 676-87.

176. Sheiness, D. and J.M. Bishop, *DNA and RNA from uninfected vertebrate cells contain nucleotide sequences related to the putative transforming gene of avian myelocytomatosis virus.* J Virol, 1979. **31**(2): p. 514-21.

177. Nesbit, C.E., J.M. Tersak, and E.V. Prochownik, *MYC oncogenes and human neoplastic disease.* Oncogene, 1999. **18**(19): p. 3004-16.

178. Beroukhim, R., C.H. Mermel, D. Porter, et al., *The landscape of somatic copy-number alteration across human cancers.* Nature, 2010. **463**(7283): p. 899-905.

179. Lin, C.Y., J. Loven, P.B. Rahl, et al., *Transcriptional amplification in tumor cells with elevated c-Myc.* Cell, 2012. **151**(1): p. 56-67.

180. Nie, Z., G. Hu, G. Wei, et al., *c-Myc is a universal amplifier of expressed genes in lymphocytes and embryonic stem cells.* Cell, 2012. **151**(1): p. 68-79.

181. Hayward, W.S., B.G. Neel, and S.M. Astrin, *Activation of a cellular onc gene by promoter insertion in ALV-induced lymphoid leukosis.* Nature, 1981. **290**(5806): p. 475-80.

182. Steffen, D., *Proviruses are adjacent to c-myc in some murine leukemia virus-induced lymphomas.* Proc Natl Acad Sci U S A, 1984. **81**(7): p. 2097-101.

183. Shen-Ong, G.L., E.J. Keath, S.P. Piccoli, et al., *Novel myc oncogene RNA from abortive immunoglobulin-gene recombination in mouse plasmacytomas.* Cell, 1982. **31**(2 Pt 1): p. 443-52.

184. Taub, R., I. Kirsch, C. Morton, et al., *Translocation of the c-myc gene into the immunoglobulin heavy chain locus in human Burkitt lymphoma and murine plasmacytoma cells.* Proc Natl Acad Sci U S A, 1982. **79**(24): p. 7837-41.

185. Dalla-Favera, R., M. Bregni, J. Erikson, et al., *Human c-myc onc gene is located on the region of chromosome 8 that is translocated in Burkitt lymphoma cells.* Proc Natl Acad Sci U S A, 1982. **79**(24): p. 7824-7.

186. Dudley, J.P., J.A. Mertz, L. Rajan, et al., *What retroviruses teach us about the involvement of c-Myc in leukemias and lymphomas.* Leukemia, 2002. **16**(6): p. 1086-98.

187. Felsher, D.W. and J.M. Bishop, *Reversible tumorigenesis by MYC in hematopoietic lineages.* Mol Cell, 1999. **4**(2): p. 199-207.

188. Langdon, W.Y., A.W. Harris, S. Cory, et al., *The c-myc oncogene perturbs B lymphocyte development in E-mu-myc transgenic mice.* Cell, 1986. **47**(1): p. 11-8.

189. Eischen, C.M., J.D. Weber, M.F. Roussel, et al., *Disruption of the ARF-Mdm2-p53 tumor suppressor pathway in Myc-induced lymphomagenesis.* Genes Dev, 1999. **13**(20): p. 2658-69.

190. Hemann, M.T., J.S. Fridman, J.T. Zilfou, et al., *An epi-allelic series of p53 hypomorphs created by stable RNAi produces distinct tumor phenotypes in vivo.* Nat Genet, 2003. **33**(3): p. 396-400.

191. Askew, D.S., R.A. Ashmun, B.C. Simmons, et al., *Constitutive c-myc expression in an IL-3-dependent myeloid cell line suppresses cell cycle arrest and accelerates apoptosis.* Oncogene, 1991. **6**(10): p. 1915-22.

192. Evan, G.I., A.H. Wyllie, C.S. Gilbert, et al., *Induction of apoptosis in fibroblasts by c-myc protein.* Cell, 1992. **69**(1): p. 119-28.

193. Wagner, A.J., J.M. Kokontis, and N. Hay, *Myc-mediated apoptosis requires wild-type p53 in a manner independent of cell cycle arrest and the ability of p53 to induce p21waf1/cip1.* Genes Dev, 1994. **8**(23): p. 2817-30.

194. Hermeking, H. and D. Eick, *Mediation of c-Myc-induced apoptosis by p53.* Science, 1994. **265**(5181): p. 2091-3.

195. Giuriato, S., S. Ryeom, A.C. Fan, et al., *Sustained regression of tumors upon MYC inactivation requires p53 or thrombospondin-1 to reverse the angiogenic switch.* Proc Natl Acad Sci U S A, 2006. **103**(44): p. 16266-71.

196. Burkitt, D., *A sarcoma involving the jaws in African children.* The British journal of surgery, 1958. **46**(197): p. 218-23.

197. zur Hausen, H., H. Schulte-Holthausen, G. Klein, et al., *EBV DNA in biopsies of Burkitt tumours and anaplastic carcinomas of the nasopharynx.* Nature, 1970. **228**(5276): p. 1056-8.

198. Rochford, R., M.J. Cannon, and A.M. Moormann, *Endemic Burkitt's lymphoma: a polymicrobial disease?* Nature reviews. Microbiology, 2005. **3**(2): p. 182-7.

199. Hummel, M., S. Bentink, H. Berger, et al., *A biologic definition of Burkitt's lymphoma from transcriptional and genomic profiling.* N Engl J Med, 2006. **354**(23): p. 2419-30.

200. Avet-Loiseau, H. and R. Bataille, *Detection of nonrandom chromosomal changes in multiple myeloma by comparative genomic hybridization.* Blood, 1998. **92**(8): p. 2997-8.

201. Shou, Y., M.L. Martelli, A. Gabrea, et al., *Diverse karyotypic abnormalities of the c-myc locus associated with c-myc dysregulation and tumor progression in multiple myeloma.* Proc Natl Acad Sci U S A, 2000. **97**(1): p. 228-33.

202. Fernandez, P.C., S.R. Frank, L. Wang, et al., *Genomic targets of the human c-Myc protein.* Genes Dev, 2003. **17**(9): p. 1115-29.

203. Zeller, K.I., X. Zhao, C.W. Lee, et al., *Global mapping of c-Myc binding sites and target gene networks in human B cells.* Proc Natl Acad Sci U S A, 2006. **103**(47): p. 17834-9.

204. Levens, D., *You Don't Muck with MYC.* Genes & cancer, 2010. **1**(6): p. 547-554.

205. Thomas, L.R. and W.P. Tansey, *Proteolytic control of the oncoprotein transcription factor Myc.* Adv Cancer Res, 2011. **110**: p. 77-106.

206. Brenner, C., R. Deplus, C. Didelot, et al., *Myc represses transcription through recruitment of DNA methyltransferase corepressor.* Embo J, 2005. **24**(2): p. 336-46.

207. Dews, M., J.L. Fox, S. Hultine, et al., *The myc-miR-17~92 axis blunts TGF{beta} signaling and production of multiple TGF{beta}-dependent antiangiogenic factors.* Cancer Res, 2010. **70**(20): p. 8233-46.

208. Olive, V., I. Jiang, and L. He, *mir-17-92, a cluster of miRNAs in the midst of the cancer network.* The international journal of biochemistry & cell biology, 2010. **42**(8): p. 1348-54.

209. Cole, M.D. and V.H. Cowling, *Transcription-independent functions of MYC: regulation of translation and DNA replication.* Nature reviews. Molecular cell biology, 2008. **9**(10): p. 810-5.

210. Menssen, A. and H. Hermeking, *Characterization of the c-MYC-regulated transcriptome by SAGE: identification and analysis of c-MYC target genes.* Proc Natl Acad Sci U S A, 2002. **99**(9): p. 6274-9.

211. Dang, C.V., *c-Myc target genes involved in cell growth, apoptosis, and metabolism.* Mol Cell Biol, 1999. **19**(1): p. 1-11.

212. Eischen, C.M., D. Woo, M.F. Roussel, et al., *Apoptosis triggered by Myc-induced suppression of Bcl-X(L) or Bcl-2 is bypassed during lymphomagenesis.* Mol Cell Biol, 2001. **21**(15): p. 5063-70.

213. Maclean, K.H., U.B. Keller, C. Rodriguez-Galindo, et al., *c-Myc augments gamma irradiation-induced apoptosis by suppressing Bcl-XL.* Mol Cell Biol, 2003. **23**(20): p. 7256-70.

214. Bissonnette, R.P., F. Echeverri, A. Mahboubi, et al., *Apoptotic cell death induced by c-myc is inhibited by bcl-2.* Nature, 1992. **359**(6395): p. 552-4.

215. Wang, R., C.P. Dillon, L.Z. Shi, et al., *The transcription factor Myc controls metabolic reprogramming upon T lymphocyte activation.* Immunity, 2011. **35**(6): p. 871-82.

216. Ramsay, R.G. and T.J. Gonda, *MYB function in normal and cancer cells.* Nat Rev Cancer, 2008. **8**(7): p. 523-34.

217. Roussel, M., S. Saule, C. Lagrou, et al., *Three new types of viral oncogene of cellular origin specific for haematopoietic cell transformation.* Nature, 1979. **281**(5731): p. 452-5.

218. Souza, L.M., J.N. Strommer, R.L. Hillyard, et al., *Cellular sequences are present in the presumptive avian myeloblastosis virus genome.* Proc Natl Acad Sci U S A, 1980. **77**(9): p. 5177-81.

219. Klempnauer, K.H., T.J. Gonda, and J.M. Bishop, *Nucleotide sequence of the retroviral leukemia gene v-myb and its cellular progenitor c-myb: the architecture of a transduced oncogene.* Cell, 1982. **31**(2 Pt 1): p. 453-63.

220. Rushlow, K.E., J.A. Lautenberger, T.S. Papas, et al., *Nucleotide sequence of the transforming gene of avian myeloblastosis virus.* Science, 1982. **216**(4553): p. 1421-3.

221. Klempnauer, K.H., G. Ramsay, J.M. Bishop, et al., *The product of the retroviral transforming gene v-myb is a truncated version of the protein encoded by the cellular oncogene c-myb.* Cell, 1983. **33**(2): p. 345-55.

222. Leprince, D., A. Gegonne, J. Coll, et al., *A putative second cell-derived oncogene of the avian leukaemia retrovirus E26.* Nature, 1983. **306**(5941): p. 395-7.

223. Klempnauer, K.H. and J.M. Bishop, *Neoplastic transformation by E26 leukemia virus is mediated by a single protein containing domains of gag and myb genes.* J Virol, 1984. **50**(1): p. 280-3.

224. Rosson, D. and E.P. Reddy, *Nucleotide sequence of chicken c-myb complementary DNA and implications for myb oncogene activation.* Nature, 1986. **319**(6054): p. 604-6.

225. Gerondakis, S. and J.M. Bishop, *Structure of the protein encoded by the chicken proto-oncogene c-myb.* Mol Cell Biol, 1986. **6**(11): p. 3677-84.

226. Metz, T. and T. Graf, *Fusion of the nuclear oncoproteins v-Myb and v-Ets is required for the leukemogenicity of E26 virus.* Cell, 1991. **66**(1): p. 95-105.

227. Wu, Y. and P. Duesberg, *Avian erythroblastosis virus E26: only one (myb) of two cell-derived coding regions is necessary for oncogenicity.* Proc Natl Acad Sci U S A, 1994. **91**(9): p. 4039-43.

228. Shen-Ong, G.L., M. Potter, J.F. Mushinski, et al., *Activation of the c-myb locus by viral insertional mutagenesis in plasmacytoid lymphosarcomas.* Science, 1984. **226**(4678): p. 1077-80.

229. Shen-Ong, G.L., H.C. Morse, 3rd, M. Potter, et al., *Two modes of c-myb activation in virus-induced mouse myeloid tumors.* Mol Cell Biol, 1986. **6**(2): p. 380-92.

230. Weinstein, Y., J.N. Ihle, S. Lavu, et al., *Truncation of the c-myb gene by a retroviral integration in an interleukin 3-dependent myeloid leukemia cell line.* Proc Natl Acad Sci U S A, 1986. **83**(14): p. 5010-4.

231. Rosson, D., D. Dugan, and E.P. Reddy, *Aberrant splicing events that are induced by proviral integration: implications for myb oncogene activation.* Proc Natl Acad Sci U S A, 1987. **84**(10): p. 3171-5.

232. Alitalo, K., R. Winqvist, C.C. Lin, et al., *Aberrant expression of an amplified c-myb oncogene in two cell lines from a colon carcinoma.* Proc Natl Acad Sci U S A, 1984. **81**(14): p. 4534-8.

233. Ramsay, R.G., M.A. Thompson, J.A. Hayman, et al., *Myb expression is higher in malignant human colonic carcinoma and premalignant adenomatous polyps than in normal mucosa.* Cell growth & differentiation : the molecular biology journal of the American Association for Cancer Research, 1992. **3**(10): p. 723-30.

234. Dasgupta, P., A.J. Linnenbach, A.J. Giaccia, et al., *Molecular cloning of the breakpoint region on chromosome 6 in cutaneous malignant melanoma: evidence for deletion in the c-myb locus and translocation of a segment of chromosome 12.* Oncogene, 1989. **4**(10): p. 1201-5.

235. Kauraniemi, P., I. Hedenfalk, K. Persson, et al., *MYB oncogene amplification in hereditary BRCA1 breast cancer.* Cancer Res, 2000. **60**(19): p. 5323-8.

236. Gonda, T.J., P. Leo, and R.G. Ramsay, *Estrogen and MYB in breast cancer: potential for new therapies.* Expert opinion on biological therapy, 2008. **8**(6): p. 713-7.

237. Persson, M., Y. Andren, J. Mark, et al., *Recurrent fusion of MYB and NFIB transcription factor genes in carcinomas of the breast and head and neck.* Proc Natl Acad Sci U S A, 2009. **106**(44): p. 18740-4.

238. Clappier, E., W. Cuccuini, A. Kalota, et al., *The C-MYB locus is involved in chromosomal translocation and genomic duplications in human T-cell acute leukemia (T-ALL), the translocation defining a new T-ALL subtype in very young children.* Blood, 2007. **110**(4): p. 1251-61.

239. Lahortiga, I., K. De Keersmaecker, P. Van Vlierberghe, et al., *Duplication of the MYB oncogene in T cell acute lymphoblastic leukemia.* Nat Genet, 2007. **39**(5): p. 593-5.

240. Oh, I.H. and E.P. Reddy, *The myb gene family in cell growth, differentiation and apoptosis.* Oncogene, 1999. **18**(19): p. 3017-33.

241. Mucenski, M.L., K. McLain, A.B. Kier, et al., *A functional c-myb gene is required for normal murine fetal hepatic hematopoiesis.* Cell, 1991. **65**(4): p. 677-89.

242. Lieu, Y.K. and E.P. Reddy, *Conditional c-myb knockout in adult hematopoietic stem cells leads to loss of self-renewal due to impaired*

proliferation and accelerated differentiation. Proc Natl Acad Sci U S A, 2009. **106**(51): p. 21689-94.

243. Lieu, Y.K. and E.P. Reddy, *Impaired adult myeloid progenitor CMP and GMP cell function in conditional c-myb-knockout mice.* Cell Cycle, 2012. **11**(18): p. 3504-12.

244. Greig, K.T., S. Carotta, and S.L. Nutt, *Critical roles for c-Myb in hematopoietic progenitor cells.* Semin Immunol, 2008. **20**(4): p. 247-56.

245. Beug, H., A. von Kirchbach, G. Doderlein, et al., *Chicken hematopoietic cells transformed by seven strains of defective avian leukemia viruses display three distinct phenotypes of differentiation.* Cell, 1979. **18**(2): p. 375-90.

246. Yanagisawa, H., T. Nagasawa, S. Kuramochi, et al., *Constitutive expression of exogenous c-myb gene causes maturation block in monocyte-macrophage differentiation.* Biochim Biophys Acta, 1991. **1088**(3): p. 380-4.

247. Clarke, M.F., J.F. Kukowska-Latallo, E. Westin, et al., *Constitutive expression of a c-myb cDNA blocks Friend murine erythroleukemia cell differentiation.* Mol Cell Biol, 1988. **8**(2): p. 884-92.

248. Somervaille, T.C., C.J. Matheny, G.J. Spencer, et al., *Hierarchical maintenance of MLL myeloid leukemia stem cells employs a transcriptional program shared with embryonic rather than adult stem cells.* Cell stem cell, 2009. **4**(2): p. 129-40.

249. Pattabiraman, D.R., J. Sun, D.H. Dowhan, et al., *Mutations in multiple domains of c-Myb disrupt interaction with CBP/p300 and abrogate myeloid transforming ability.* Molecular cancer research : MCR, 2009. **7**(9): p. 1477-86.

250. Ferrao, P., E.M. Macmillan, L.K. Ashman, et al., *Enforced expression of full length c-Myb leads to density-dependent transformation of murine haemopoietic cells.* Oncogene, 1995. **11**(8): p. 1631-8.

251. Hogg, A., S. Schirm, H. Nakagoshi, et al., *Inactivation of a c-Myb/estrogen receptor fusion protein in transformed primary cells leads to granulocyte/macrophage differentiation and down regulation of c-kit but not c-myc or cdc2.* Oncogene, 1997. **15**(24): p. 2885-98.

252. Ess, K.C., D.P. Witte, C.P. Bascomb, et al., *Diverse developing mouse lineages exhibit high-level c-Myb expression in immature cells and loss of expression upon differentiation.* Oncogene, 1999. **18**(4): p. 1103-11.

253. Liu, F., W. Lei, J.P. O'Rourke, et al., *Oncogenic mutations cause dramatic, qualitative changes in the transcriptional activity of c-Myb.* Oncogene, 2006. **25**(5): p. 795-805.

254. Fu, S.L. and J.S. Lipsick, *Constitutive expression of full-length c-Myb transforms avian cells characteristic of both the monocytic and*

granulocytic lineages. Cell growth & differentiation : the molecular biology journal of the American Association for Cancer Research, 1997. **8**(1): p. 35-45.

255. Hu, Y.L., R.G. Ramsay, C. Kanei-Ishii, et al., *Transformation by carboxyl-deleted Myb reflects increased transactivating capacity and disruption of a negative regulatory domain.* Oncogene, 1991. **6**(9): p. 1549-53.

256. Bies, J., V. Nazarov, and L. Wolff, *Identification of protein instability determinants in the carboxy-terminal region of c-Myb removed as a result of retroviral integration in murine monocytic leukemias.* J Virol, 1999. **73**(3): p. 2038-44.

257. Nicolaides, N.C., R. Gualdi, C. Casadevall, et al., *Positive autoregulation of c-myb expression via Myb binding sites in the 5' flanking region of the human c-myb gene.* Mol Cell Biol, 1991. **11**(12): p. 6166-76.

258. Watson, R.J., *A transcriptional arrest mechanism involved in controlling constitutive levels of mouse c-myb mRNA.* Oncogene, 1988. **2**(3): p. 267-72.

259. Drabsch, Y., H. Hugo, R. Zhang, et al., *Mechanism of and requirement for estrogen-regulated MYB expression in estrogen-receptor-positive breast cancer cells.* Proc Natl Acad Sci U S A, 2007. **104**(34): p. 13762-7.

260. Suhasini, M. and R.B. Pilz, *Transcriptional elongation of c-myb is regulated by NF-kappaB (p50/RelB).* Oncogene, 1999. **18**(51): p. 7360-9.

261. Shen-Ong, G.L., R.M. Skurla, Jr., J.D. Owens, et al., *Alternative splicing of RNAs transcribed from the human c-myb gene.* Mol Cell Biol, 1990. **10**(6): p. 2715-22.

262. O'Rourke, J.P. and S.A. Ness, *Alternative RNA splicing produces multiple forms of c-Myb with unique transcriptional activities.* Mol Cell Biol, 2008. **28**(6): p. 2091-101.

263. Aziz, N., M.R. Miglarese, R.C. Hendrickson, et al., *Modulation of c-Myb-induced transcription activation by a phosphorylation site near the negative regulatory domain.* Proc Natl Acad Sci U S A, 1995. **92**(14): p. 6429-33.

264. Bies, J. and L. Wolff, *Oncogenic activation of c-Myb by carboxyl-terminal truncation leads to decreased proteolysis by the ubiquitin-26S proteasome pathway.* Oncogene, 1997. **14**(2): p. 203-12.

265. Pattabiraman, D.R., L. Zhao, F. Al-Owaidi, et al., *Insignts into targets of, and mechanisms of transformation by MYB*, in *New Directions in Leukaemia Research*2008: Sunshine Coast, Australia.

266. Lei, W., J.J. Rushton, L.M. Davis, et al., *Positive and negative determinants of target gene specificity in myb transcription factors.* J Biol Chem, 2004. **279**(28): p. 29519-27.

267. Zhao, H., A. Kalota, S. Jin, et al., *The c-myb proto-oncogene and microRNA-15a comprise an active autoregulatory feedback loop in human hematopoietic cells.* Blood, 2009. **113**(3): p. 505-16.

268. Quintana, A.M., F. Liu, J.P. O'Rourke, et al., *Identification and regulation of c-Myb target genes in MCF-7 cells.* BMC cancer, 2011. **11**: p. 30.

269. Rushton, J.J., L.M. Davis, W. Lei, et al., *Distinct changes in gene expression induced by A-Myb, B-Myb and c-Myb proteins.* Oncogene, 2003. **22**(2): p. 308-13.

270. Bender, T.P. and W.M. Kuehl, *Differential expression of the c-myb proto-oncogene marks the pre-B cell/B cell junction in murine B lymphoid tumors.* J Immunol, 1987. **139**(11): p. 3822-7.

271. Thomas, M.D., C.S. Kremer, K.S. Ravichandran, et al., *c-Myb is critical for B cell development and maintenance of follicular B cells.* Immunity, 2005. **23**(3): p. 275-86.

272. Sandberg, M.L., S.E. Sutton, M.T. Pletcher, et al., *c-Myb and p300 regulate hematopoietic stem cell proliferation and differentiation.* Dev Cell, 2005. **8**(2): p. 153-66.

273. Sakamoto, H., G. Dai, K. Tsujino, et al., *Proper levels of c-Myb are discretely defined at distinct steps of hematopoietic cell development.* Blood, 2006. **108**(3): p. 896-903.

274. Greig, K.T., C.A. de Graaf, J.M. Murphy, et al., *Critical roles for c-Myb in lymphoid priming and early B-cell development.* Blood, 2010. **115**(14): p. 2796-805.

275. Waldron, T., M. De Dominici, A.R. Soliera, et al., *c-Myb and its target Bmi1 are required for p190BCR/ABL leukemogenesis in mouse and human cells.* Leukemia, 2012. **26**(4): p. 644-53.

276. Golay, J., G. Cusmano, and M. Introna, *Independent regulation of c-myc, B-myb, and c-myb gene expression by inducers and inhibitors of proliferation in human B lymphocytes.* J Immunol, 1992. **149**(1): p. 300-8.

277. Bender, T.P., C.B. Thompson, and W.M. Kuehl, *Differential expression of c-myb mRNA in murine B lymphomas by a block to transcription elongation.* Science, 1987. **237**(4821): p. 1473-6.

278. Toth, C.R., R.F. Hostutler, A.S. Baldwin, Jr., et al., *Members of the nuclear factor kappa B family transactivate the murine c-myb gene.* J Biol Chem, 1995. **270**(13): p. 7661-71.

279. Xiao, C., D.P. Calado, G. Galler, et al., *MiR-150 controls B cell differentiation by targeting the transcription factor c-Myb.* Cell, 2007. **131**(1): p. 146-59.

280. Kanter, M.R., R.E. Smith, and W.S. Hayward, *Rapid induction of B-cell lymphomas: insertional activation of c-myb by avian leukosis virus.* J Virol, 1988. **62**(4): p. 1423-32.

281. Kerenyi, M.A. and E.W. Mullner, *MYB and miR: a pair well matched.* Blood, 2009. **113**(3): p. 499-500.

282. Vargova, K., N. Curik, P. Burda, et al., *MYB transcriptionally regulates the miR-155 host gene in chronic lymphocytic leukemia.* Blood. **117**(14): p. 3816-25.

283. Eis, P.S., W. Tam, L. Sun, et al., *Accumulation of miR-155 and BIC RNA in human B cell lymphomas.* Proc Natl Acad Sci U S A, 2005. **102**(10): p. 3627-32.

284. Kluiver, J., S. Poppema, D. de Jong, et al., *BIC and miR-155 are highly expressed in Hodgkin, primary mediastinal and diffuse large B cell lymphomas.* J Pathol, 2005. **207**(2): p. 243-9.

285. Kaye, K.M., K.M. Izumi, and E. Kieff, *Epstein-Barr virus latent membrane protein 1 is essential for B-lymphocyte growth transformation.* Proc Natl Acad Sci U S A, 1993. **90**(19): p. 9150-4.

286. Imadome, K., M. Shirakata, N. Shimizu, et al., *CD40 ligand is a critical effector of Epstein-Barr virus in host cell survival and transformation.* Proc Natl Acad Sci U S A, 2003. **100**(13): p. 7836-40.

287. Kulwichit, W., R.H. Edwards, E.M. Davenport, et al., *Expression of the Epstein-Barr virus latent membrane protein 1 induces B cell lymphoma in transgenic mice.* Proc Natl Acad Sci U S A, 1998. **95**(20): p. 11963-8.

288. Kennedy, G., J. Komano, and B. Sugden, *Epstein-Barr virus provides a survival factor to Burkitt's lymphomas.* Proc Natl Acad Sci U S A, 2003. **100**(24): p. 14269-74.

289. Bultema, R., R. Longnecker, and M. Swanson-Mungerson, *Epstein-Barr virus LMP2A accelerates MYC-induced lymphomagenesis.* Oncogene, 2009. **28**(11): p. 1471-6.

290. Choy, E.Y., K.L. Siu, K.H. Kok, et al., *An Epstein-Barr virus-encoded microRNA targets PUMA to promote host cell survival.* J Exp Med, 2008. **205**(11): p. 2551-60.

291. Lo, A.K., K.F. To, K.W. Lo, et al., *Modulation of LMP1 protein expression by EBV-encoded microRNAs.* Proc Natl Acad Sci U S A, 2007. **104**(41): p. 16164-9.

292. Clybouw, C., B. McHichi, S. Mouhamad, et al., *EBV infection of human B lymphocytes leads to down-regulation of Bim expression: relationship to resistance to apoptosis.* J Immunol, 2005. **175**(5): p. 2968-73.

293. Swaminathan, S., *Noncoding RNAs produced by oncogenic human herpesviruses.* J Cell Physiol, 2008. **216**(2): p. 321-6.

294. Shaw, G. and R. Kamen, *A conserved AU sequence from the 3' untranslated region of GM-CSF mRNA mediates selective mRNA degradation.* Cell, 1986. **46**(5): p. 659-67.

295. Mikkers, H. and A. Berns, *Retroviral insertional mutagenesis: tagging cancer pathways.* Adv Cancer Res, 2003. **88**: p. 53-99.

296. Hacein-Bey-Abina, S., C. Von Kalle, M. Schmidt, et al., *LMO2-associated clonal T cell proliferation in two patients after gene therapy for SCID-X1.* Science, 2003. **302**(5644): p. 415-9.

297. Dave, U.P., K. Akagi, R. Tripathi, et al., *Murine leukemias with retroviral insertions at Lmo2 are predictive of the leukemias induced in SCID-X1 patients following retroviral gene therapy.* PLoS Genet, 2009. **5**(5): p. e1000491.

298. Bushman, F.D., *Targeting survival: integration site selection by retroviruses and LTR-retrotransposons.* Cell, 2003. **115**(2): p. 135-8.

299. Johnson, C., P.A. Lobelle-Rich, A. Puetter, et al., *Substitution of feline leukemia virus long terminal repeat sequences into murine leukemia virus alters the pattern of insertional activation and identifies new common insertion sites.* J Virol, 2005. **79**(1): p. 57-66.

300. Nielsen, A.A., A.B. Sorensen, J. Schmidt, et al., *Analysis of wild-type and mutant SL3-3 murine leukemia virus insertions in the c-myc promoter during lymphomagenesis reveals target site hot spots, virus-dependent patterns, and frequent error-prone gap repair.* J Virol, 2005. **79**(1): p. 67-78.

301. Kitamura, Y., Y.M. Lee, and J.M. Coffin, *Nonrandom integration of retroviral DNA in vitro: effect of CpG methylation.* Proc Natl Acad Sci U S A, 1992. **89**(12): p. 5532-6.

302. Scherdin, U., K. Rhodes, and M. Breindl, *Transcriptionally active genome regions are preferred targets for retrovirus integration.* J Virol, 1990. **64**(2): p. 907-12.

303. Wu, X., Y. Li, B. Crise, et al., *Transcription start regions in the human genome are favored targets for MLV integration.* Science, 2003. **300**(5626): p. 1749-51.

304. Ivics, Z., P.B. Hackett, R.H. Plasterk, et al., *Molecular reconstruction of Sleeping Beauty, a Tc1-like transposon from fish, and its transposition in human cells.* Cell, 1997. **91**(4): p. 501-10.

305. Geurts, A.M., Y. Yang, K.J. Clark, et al., *Gene transfer into genomes of human cells by the sleeping beauty transposon system.* Molecular therapy : the journal of the American Society of Gene Therapy, 2003. **8**(1): p. 108-17.

306. Huang, X., H. Guo, S. Tammana, et al., *Gene transfer efficiency and genome-wide integration profiling of Sleeping Beauty, Tol2, and piggyBac transposons in human primary T cells.* Molecular therapy : the journal of the American Society of Gene Therapy, 2010. **18**(10): p. 1803-13.

307. Yant, S.R., X. Wu, Y. Huang, et al., *High-resolution genome-wide mapping of transposon integration in mammals.* Mol Cell Biol, 2005. **25**(6): p. 2085-94.

308. Schmidt, M., K. Schwarzwaelder, C. Bartholomae, et al., *High-resolution insertion-site analysis by linear amplification-mediated PCR (LAM-PCR).* Nature methods, 2007. **4**(12): p. 1051-7.

309. Paruzynski, A., A. Arens, R. Gabriel, et al., *Genome-wide high-throughput integrome analyses by nrLAM-PCR and next-generation sequencing.* Nat Protoc, 2010. **5**(8): p. 1379-95.

310. Lazo, P.A., J.S. Lee, and P.N. Tsichlis, *Long-distance activation of the Myc protooncogene by provirus insertion in Mlvi-1 or Mlvi-4 in rat T-cell lymphomas.* Proc Natl Acad Sci U S A, 1990. **87**(1): p. 170-3.

311. Jacobs, J.J., K. Kieboom, S. Marino, et al., *The oncogene and Polycomb-group gene bmi-1 regulates cell proliferation and senescence through the ink4a locus.* Nature, 1999. **397**(6715): p. 164-8.

312. Lund, A.H., G. Turner, A. Trubetskoy, et al., *Genome-wide retroviral insertional tagging of genes involved in cancer in Cdkn2a-deficient mice.* Nat Genet, 2002. **32**(1): p. 160-5.

313. Uren, A.G., J. Kool, K. Matentzoglu, et al., *Large-scale mutagenesis in p19(ARF)- and p53-deficient mice identifies cancer genes and their collaborative networks.* Cell, 2008. **133**(4): p. 727-41.

314. Vogelstein, B., E.R. Fearon, S.R. Hamilton, et al., *Genetic alterations during colorectal-tumor development.* N Engl J Med, 1988. **319**(9): p. 525-32.

315. Wood, L.D., D.W. Parsons, S. Jones, et al., *The genomic landscapes of human breast and colorectal cancers.* Science, 2007. **318**(5853): p. 1108-13.

316. Beerenwinkel, N., T. Antal, D. Dingli, et al., *Genetic progression and the waiting time to cancer.* PLoS Comput Biol, 2007. **3**(11): p. e225.

317. Jones, S., X. Zhang, D.W. Parsons, et al., *Core signaling pathways in human pancreatic cancers revealed by global genomic analyses.* Science, 2008. **321**(5897): p. 1801-6.

318. Puente, X.S., M. Pinyol, V. Quesada, et al., *Whole-genome sequencing identifies recurrent mutations in chronic lymphocytic leukaemia.* Nature, 2011. **475**(7354): p. 101-5.

319. Angeli, V., F. Ginhoux, J. Llodra, et al., *B cell-driven lymphangiogenesis in inflamed lymph nodes enhances dendritic cell mobilization.* Immunity, 2006. **24**(2): p. 203-15.

320. Robbiani, D.F., S. Bunting, N. Feldhahn, et al., *AID produces DNA double-strand breaks in non-Ig genes and mature B cell lymphomas with reciprocal chromosome translocations.* Mol Cell, 2009. **36**(4): p. 631-41.

321. Daley, G.Q., R.A. Van Etten, and D. Baltimore, *Induction of chronic myelogenous leukemia in mice by the P210bcr/abl gene of the Philadelphia chromosome.* Science, 1990. **247**(4944): p. 824-30.

322. Honda, H., H. Oda, T. Suzuki, et al., *Development of acute lymphoblastic leukemia and myeloproliferative disorder in transgenic mice expressing p210bcr/abl: a novel transgenic model for human Ph1-positive leukemias.* Blood, 1998. **91**(6): p. 2067-75.

323. Biernaux, C., M. Loos, A. Sels, et al., *Detection of major bcr-abl gene expression at a very low level in blood cells of some healthy individuals.* Blood, 1995. **86**(8): p. 3118-22.

324. Bose, S., M. Deininger, J. Gora-Tybor, et al., *The presence of typical and atypical BCR-ABL fusion genes in leukocytes of normal individuals: biologic significance and implications for the assessment of minimal residual disease.* Blood, 1998. **92**(9): p. 3362-7.

325. Summers, K.E., L.K. Goff, A.G. Wilson, et al., *Frequency of the Bcl-2/IgH rearrangement in normal individuals: implications for the monitoring of disease in patients with follicular lymphoma.* J Clin Oncol, 2001. **19**(2): p. 420-4.

326. Cong, P., M. Raffeld, J. Teruya-Feldstein, et al., *In situ localization of follicular lymphoma: description and analysis by laser capture microdissection.* Blood, 2002. **99**(9): p. 3376-82.

327. Muller, J.R., S. Janz, J.J. Goedert, et al., *Persistence of immunoglobulin heavy chain/c-myc recombination-positive lymphocyte clones in the blood of human immunodeficiency virus-infected homosexual men.* Proc Natl Acad Sci U S A, 1995. **92**(14): p. 6577-81.

328. Chanudet, E., H. Ye, J. Ferry, et al., *A20 deletion is associated with copy number gain at the TNFA/B/C locus and occurs preferentially in translocation-negative MALT lymphoma of the ocular adnexa and salivary glands.* J Pathol, 2009. **217**(3): p. 420-30.

329. Du, M.Q., C.M. Bacon, and P.G. Isaacson, *Kaposi sarcoma-associated herpesvirus/human herpesvirus 8 and lymphoproliferative disorders.* J Clin Pathol, 2007. **60**(12): p. 1350-7.

330. Balmain, A. and C.C. Harris, *Carcinogenesis in mouse and human cells: parallels and paradoxes.* Carcinogenesis, 2000. **21**(3): p. 371-7.

331. Greenberg, R.A., R.C. Allsopp, L. Chin, et al., *Expression of mouse telomerase reverse transcriptase during development, differentiation and proliferation.* Oncogene, 1998. **16**(13): p. 1723-30.

332. Land, H., L.F. Parada, and R.A. Weinberg, *Tumorigenic conversion of primary embryo fibroblasts requires at least two cooperating oncogenes.* Nature, 1983. **304**(5927): p. 596-602.

333. Zindy, F., C.M. Eischen, D.H. Randle, et al., *Myc signaling via the ARF tumor suppressor regulates p53-dependent apoptosis and immortalization.* Genes Dev, 1998. **12**(15): p. 2424-33.

334. Harris, A.W., C.A. Pinkert, M. Crawford, et al., *The E mu-myc transgenic mouse. A model for high-incidence spontaneous lymphoma and leukemia of early B cells.* J Exp Med, 1988. **167**(2): p. 353-71.

335. Strasser, A., A.W. Harris, M.L. Bath, et al., *Novel primitive lymphoid tumours induced in transgenic mice by cooperation between myc and bcl-2.* Nature, 1990. **348**(6299): p. 331-3.

336. Roschke, V., E. Kopantzev, M. Dertzbaugh, et al., *Chromosomal translocations deregulating c-myc are associated with normal immune responses.* Oncogene, 1997. **14**(25): p. 3011-6.

337. Ramiro, A.R., M. Jankovic, E. Callen, et al., *Role of genomic instability and p53 in AID-induced c-myc-Igh translocations.* Nature, 2006. **440**(7080): p. 105-9.

338. Spender, L.C. and G.J. Inman, *Phosphoinositide 3-kinase/AKT/mTORC1/2 signaling determines sensitivity of Burkitt's lymphoma cells to BH3 mimetics.* Molecular cancer research : MCR, 2012. **10**(3): p. 347-59.

339. He, L., J.M. Thomson, M.T. Hemann, et al., *A microRNA polycistron as a potential human oncogene.* Nature, 2005. **435**(7043): p. 828-33.

340. Mu, P., Y.C. Han, D. Betel, et al., *Genetic dissection of the miR-17~92 cluster of microRNAs in Myc-induced B-cell lymphomas.* Genes Dev, 2009. **23**(24): p. 2806-11.

341. Olive, V., M.J. Bennett, J.C. Walker, et al., *miR-19 is a key oncogenic component of mir-17-92.* Genes Dev, 2009. **23**(24): p. 2839-49.

342. Robertus, J.L., J. Kluiver, C. Weggemans, et al., *MiRNA profiling in B non-Hodgkin lymphoma: a MYC-related miRNA profile characterizes Burkitt lymphoma.* Br J Haematol, 2010. **149**(6): p. 896-9.

343. Tagawa, H., K. Karube, S. Tsuzuki, et al., *Synergistic action of the microRNA-17 polycistron and Myc in aggressive cancer development.* Cancer science, 2007. **98**(9): p. 1482-90.

344. Dave, S.S., K. Fu, G.W. Wright, et al., *Molecular diagnosis of Burkitt's lymphoma.* N Engl J Med, 2006. **354**(23): p. 2431-42.

345. Klapproth, K., S. Sander, D. Marinkovic, et al., *The IKK2/NF-{kappa}B pathway suppresses MYC-induced lymphomagenesis.* Blood, 2009. **114**(12): p. 2448-58.

346. Wilda, M., J. Bruch, L. Harder, et al., *Inactivation of the ARF-MDM-2-p53 pathway in sporadic Burkitt's lymphoma in children.* Leukemia, 2004. **18**(3): p. 584-8.

347. Jares, P., D. Colomer, and E. Campo, *Genetic and molecular pathogenesis of mantle cell lymphoma: perspectives for new targeted therapeutics.* Nat Rev Cancer, 2007. **7**(10): p. 750-62.

348. Lovec, H., A. Grzeschiczek, M.B. Kowalski, et al., *Cyclin D1/bcl-1 cooperates with myc genes in the generation of B-cell lymphoma in transgenic mice.* Embo J, 1994. **13**(15): p. 3487-95.

349. Horsman, D.E., I. Okamoto, O. Ludkovski, et al., *Follicular lymphoma lacking the t(14;18)(q32;q21): identification of two disease subtypes.* Br J Haematol, 2003. **120**(3): p. 424-33.

350. McDonnell, T.J., N. Deane, F.M. Platt, et al., *bcl-2-immunoglobulin transgenic mice demonstrate extended B cell survival and follicular lymphoproliferation.* Cell, 1989. **57**(1): p. 79-88.

351. Lenz, G., G.W. Wright, N.C. Emre, et al., *Molecular subtypes of diffuse large B-cell lymphoma arise by distinct genetic pathways.* Proc Natl Acad Sci U S A, 2008. **105**(36): p. 13520-5.

352. Iqbal, J., W.G. Sanger, D.E. Horsman, et al., *BCL2 translocation defines a unique tumor subset within the germinal center B-cell-like diffuse large B-cell lymphoma.* Am J Pathol, 2004. **165**(1): p. 159-66.

353. Davis, R.E., V.N. Ngo, G. Lenz, et al., *Chronic active B-cell-receptor signalling in diffuse large B-cell lymphoma.* Nature, 2010. **463**(7277): p. 88-92.

354. Pasqualucci, L., M. Compagno, J. Houldsworth, et al., *Inactivation of the PRDM1/BLIMP1 gene in diffuse large B cell lymphoma.* J Exp Med, 2006. **203**(2): p. 311-7.

355. Tiacci, E., V. Trifonov, G. Schiavoni, et al., *BRAF mutations in hairy-cell leukemia.* N Engl J Med, 2011. **364**(24): p. 2305-15.

356. Blombery, P.A., S.Q. Wong, C.A. Hewitt, et al., *Detection of BRAF mutations in patients with hairy cell leukemia and related lymphoproliferative disorders.* Haematologica, 2012. **97**(5): p. 780-3.

357. Alexander, W.S., J.M. Adams, and S. Cory, *Oncogene cooperation in lymphocyte transformation: malignant conversion of E mu-myc transgenic pre-B cells in vitro is enhanced by v-H-ras or v-raf but not v-abl.* Mol Cell Biol, 1989. **9**(1): p. 67-73.

358. Schwartz, R.C., L.W. Stanton, S.C. Riley, et al., *Synergism of v-myc and v-Ha-ras in the in vitro neoplastic progression of murine lymphoid cells.* Mol Cell Biol, 1986. **6**(9): p. 3221-31.

359. Kuper-Hommel, M.J. and J.H. van Krieken, *Molecular pathogenesis and histologic and clinical features of extranodal marginal zone lymphomas of mucosa-associated lymphoid tissue type.* Leukemia & lymphoma, 2012. **53**(6): p. 1032-45.

360. Martins, C.P., L. Brown-Swigart, and G.I. Evan, *Modeling the therapeutic efficacy of p53 restoration in tumors.* Cell, 2006. **127**(7): p. 1323-34.

361. Schmitt, C.A., M.E. McCurrach, E. de Stanchina, et al., *INK4a/ARF mutations accelerate lymphomagenesis and promote chemoresistance by disabling p53.* Genes Dev, 1999. **13**(20): p. 2670-7.

362. Jacobs, J.J., B. Scheijen, J.W. Voncken, et al., *Bmi-1 collaborates with c-Myc in tumorigenesis by inhibiting c-Myc-induced apoptosis via INK4a/ARF.* Genes Dev, 1999. **13**(20): p. 2678-90.

363. Yu, D. and A. Thomas-Tikhonenko, *A non-transgenic mouse model for B-cell lymphoma: in vivo infection of p53-null bone marrow progenitors by a Myc retrovirus is sufficient for tumorigenesis.* Oncogene, 2002. **21**(12): p. 1922-7.

364. Bouchard, C., S. Lee, V. Paulus-Hock, et al., *FoxO transcription factors suppress Myc-driven lymphomagenesis via direct activation of Arf.* Genes Dev, 2007. **21**(21): p. 2775-87.

365. Shreeram, S., W.K. Hee, O.N. Demidov, et al., *Regulation of ATM/p53-dependent suppression of myc-induced lymphomas by Wip1 phosphatase.* J Exp Med, 2006. **203**(13): p. 2793-9.

366. Sotillo, E., T. Laver, H. Mellert, et al., *Myc overexpression brings out unexpected antiapoptotic effects of miR-34a.* Oncogene, 2011. **30**(22): p. 2587-94.

367. Chang, T.C., E.A. Wentzel, O.A. Kent, et al., *Transactivation of miR-34a by p53 broadly influences gene expression and promotes apoptosis.* Mol Cell, 2007. **26**(5): p. 745-52.

368. Egle, A., A.W. Harris, P. Bouillet, et al., *Bim is a suppressor of Myc-induced mouse B cell leukemia.* Proc Natl Acad Sci U S A, 2004. **101**(16): p. 6164-9.

369. Chang, D.W., G.F. Claassen, S.R. Hann, et al., *The c-Myc transactivation domain is a direct modulator of apoptotic versus proliferative signals.* Mol Cell Biol, 2000. **20**(12): p. 4309-19.

370. Hemann, M.T., A. Bric, J. Teruya-Feldstein, et al., *Evasion of the p53 tumour surveillance network by tumour-derived MYC mutants.* Nature, 2005. **436**(7052): p. 807-11.

371. Wall, M., G. Poortinga, K.L. Stanley, et al., *The mTORC1 Inhibitor Everolimus Prevents and Treats Emu-Myc Lymphoma by Restoring Oncogene-Induced Senescence.* Cancer discovery, 2013. **3**(1): p. 82-95.

372. Reimann, M., S. Lee, C. Loddenkemper, et al., *Tumor stroma-derived TGF-beta limits myc-driven lymphomagenesis via Suv39h1-dependent senescence.* Cancer Cell, 2010. **17**(3): p. 262-72.

373. Campaner, S., M. Doni, P. Hydbring, et al., *Cdk2 suppresses cellular senescence induced by the c-myc oncogene.* Nature cell biology, 2010. **12**(1): p. 54-9; sup pp 1-14.

374. Nelms, K.A. and C.C. Goodnow, *Genome-wide ENU mutagenesis to reveal immune regulators.* Immunity, 2001. **15**(3): p. 409-18.

375. Goodnow, C.C., J. Crosbie, S. Adelstein, et al., *Altered immunoglobulin expression and functional silencing of self-reactive B lymphocytes in transgenic mice.* Nature, 1988. **334**(6184): p. 676-82.

376. Hawley, R.G., A.Z. Fong, B.F. Burns, et al., *Transplantable myeloproliferative disease induced in mice by an interleukin 6 retrovirus.* J Exp Med, 1992. **176**(4): p. 1149-63.

377. Kitamura, T., Y. Koshino, F. Shibata, et al., *Retrovirus-mediated gene transfer and expression cloning: powerful tools in functional genomics.* Exp Hematol, 2003. **31**(11): p. 1007-14.

378. Inoue, H., H. Nojima, and H. Okayama, *High efficiency transformation of Escherichia coli with plasmids.* Gene, 1990. **96**(1): p. 23-8.

379. Hanahan, D., *Studies on transformation of Escherichia coli with plasmids.* J Mol Biol, 1983. **166**(4): p. 557-80.

380. Hodgson, C.P. and F. Solaiman, *Virosomes: cationic liposomes enhance retroviral transduction.* Nature biotechnology, 1996. **14**(3): p. 339-42.

381. Wang, X. and B. Seed, *A PCR primer bank for quantitative gene expression analysis.* Nucleic Acids Res, 2003. **31**(24): p. e154.

382. Pfaffl, M.W., *A new mathematical model for relative quantification in real-time RT-PCR.* Nucleic Acids Res, 2001. **29**(9): p. e45.

383. Johnson, K.M., K. Owen, and P.L. Witte, *Aging and developmental transitions in the B cell lineage.* International immunology, 2002. **14**(11): p. 1313-23.

384. Kool, J., A.G. Uren, C.P. Martins, et al., *Insertional mutagenesis in mice deficient for p15Ink4b, p16Ink4a, p21Cip1, and p27Kip1 reveals cancer gene interactions and correlations with tumor phenotypes.* Cancer Res, 2010. **70**(2): p. 520-31.

385. Kalled, S.L., N. Siva, H. Stein, et al., *The distribution of CD10 (NEP 24.11, CALLA) in humans and mice is similar in non-lymphoid organs but differs within the hematopoietic system: absence on murine T and B lymphoid progenitors.* Eur J Immunol, 1995. **25**(3): p. 677-87.

386. Rolink, A., M. Streb, and F. Melchers, *The kappa/lambda ratio in surface immunoglobulin molecules on B lymphocytes differentiating from DHJH-rearranged murine pre-B cell clones in vitro.* Eur J Immunol, 1991. **21**(11): p. 2895-8.

387. Underwood, P.A. and P.A. Bean, *Hazards of the limiting-dilution method of cloning hybridomas.* Journal of immunological methods, 1988. **107**(1): p. 119-28.

388. Lietzke, R. and K. Unsicker, *A statistical approach to determine monoclonality after limiting cell plating of a hybridoma clone.* Journal of immunological methods, 1985. **76**(2): p. 223-8.

389. Kovalchuk, A.L., C.F. Qi, T.A. Torrey, et al., *Burkitt lymphoma in the mouse.* J Exp Med, 2000. **192**(8): p. 1183-90.

390. Hennecke, M., M. Kwissa, K. Metzger, et al., *Composition and arrangement of genes define the strength of IRES-driven translation in bicistronic mRNAs.* Nucleic Acids Res, 2001. **29**(16): p. 3327-34.

391. Liao, B., Y. Hu, and G. Brewer, *Competitive binding of AUF1 and TIAR to MYC mRNA controls its translation.* Nature structural & molecular biology, 2007. **14**(6): p. 511-8.

392. Wall, M., G. Poortinga, K.M. Hannan, et al., *Translational control of c-MYC by rapamycin promotes terminal myeloid differentiation.* Blood, 2008. **112**(6): p. 2305-17.

393. Smith, D.P., M.L. Bath, D. Metcalf, et al., *MYC levels govern hematopoietic tumor type and latency in transgenic mice.* Blood, 2006. **108**(2): p. 653-61.

394. Shachaf, C.M., A.J. Gentles, S. Elchuri, et al., *Genomic and proteomic analysis reveals a threshold level of MYC required for tumor maintenance.* Cancer Res, 2008. **68**(13): p. 5132-42.

395. Davi, F., C. Gocke, S. Smith, et al., *Lymphocytic progenitor cell origin and clonal evolution of human B-lineage acute lymphoblastic leukemia.* Blood, 1996. **88**(2): p. 609-21.

396. Loder, F., B. Mutschler, R.J. Ray, et al., *B cell development in the spleen takes place in discrete steps and is determined by the quality of B cell receptor-derived signals.* J Exp Med, 1999. **190**(1): p. 75-89.

397. Futreal, P.A., L. Coin, M. Marshall, et al., *A census of human cancer genes.* Nat Rev Cancer, 2004. **4**(3): p. 177-83.

398. Steele-Perkins, G., K.G. Butz, G.E. Lyons, et al., *Essential role for NFI-C/CTF transcription-replication factor in tooth root development.* Mol Cell Biol, 2003. **23**(3): p. 1075-84.

399. Gao, X., P. Tate, P. Hu, et al., *ES cell pluripotency and germ-layer formation require the SWI/SNF chromatin remodeling component BAF250a.* Proc Natl Acad Sci U S A, 2008. **105**(18): p. 6656-61.

400. Wiegand, K.C., S.P. Shah, O.M. Al-Agha, et al., *ARID1A mutations in endometriosis-associated ovarian carcinomas.* N Engl J Med. **363**(16): p. 1532-43.

401. Pak, Y., W.K. Glowacka, M.C. Bruce, et al., *Transport of LAPTM5 to lysosomes requires association with the ubiquitin ligase Nedd4, but not LAPTM5 ubiquitination.* J Cell Biol, 2006. **175**(4): p. 631-45.

402. Adra, C.N., S. Zhu, J.L. Ko, et al., *LAPTM5: a novel lysosomal-associated multispanning membrane protein preferentially expressed in hematopoietic cells.* Genomics, 1996. **35**(2): p. 328-37.

403. Ouchida, R., S. Yamasaki, M. Hikida, et al., *A lysosomal protein negatively regulates surface T cell antigen receptor expression by promoting CD3zeta-chain degradation.* Immunity, 2008. **29**(1): p. 33-43.

404. Scott, L.M., L. Mueller, and S.J. Collins, *E3, a hematopoietic-specific transcript directly regulated by the retinoic acid receptor alpha.* Blood, 1996. **88**(7): p. 2517-30.

405. Seimiya, M., O.W. J, R. Bahar, et al., *Stage-specific expression of Clast6/E3/LAPTM5 during B cell differentiation: elevated expression in human B lymphomas.* Int J Oncol, 2003. **22**(2): p. 301-4.

406. Ouchida, R., T. Kurosaki, and J.Y. Wang, *A role for lysosomal-associated protein transmembrane 5 in the negative regulation of surface B cell receptor levels and B cell activation.* Journal of immunology, 2010. **185**(1): p. 294-301.

407. Cornelison, D.D., S.A. Wilcox-Adelman, P.F. Goetinck, et al., *Essential and separable roles for Syndecan-3 and Syndecan-4 in skeletal muscle development and regeneration.* Genes Dev, 2004. **18**(18): p. 2231-6.

408. Schuring, A.N., F. Lutz, F. Tuttelmann, et al., *Role of syndecan-3 polymorphisms in obesity and female hyperandrogenism.* J Mol Med, 2009. **87**(12): p. 1241-50.

409. Yamada, Y., A.J. Warren, C. Dobson, et al., *The T cell leukemia LIM protein Lmo2 is necessary for adult mouse hematopoiesis.* Proc Natl Acad Sci U S A, 1998. **95**(7): p. 3890-5.

410. Davenport, J., G.A. Neale, and R. Goorha, *Identification of genes potentially involved in LMO2-induced leukemogenesis.* Leukemia, 2000. **14**(11): p. 1986-96.

411. Boehm, T., L. Foroni, Y. Kaneko, et al., *The rhombotin family of cysteine-rich LIM-domain oncogenes: distinct members are involved in T-cell translocations to human chromosomes 11p15 and 11p13.* Proc Natl Acad Sci U S A, 1991. **88**(10): p. 4367-71.

412. Natkunam, Y., S. Zhao, D.Y. Mason, et al., *The oncoprotein LMO2 is expressed in normal germinal-center B cells and in human B-cell lymphomas.* Blood, 2007. **109**(4): p. 1636-42.

413. Wang, B., M.D. David, and J.W. Schrader, *Absence of caprin-1 results in defects in cellular proliferation.* J Immunol, 2005. **175**(7): p. 4274-82.

414. Kaddar, T., J.P. Rouault, W.W. Chien, et al., *Two new miR-16 targets: caprin-1 and HMGA1, proteins implicated in cell proliferation.* Biol Cell, 2009. **101**(9): p. 511-24.

415. Francisco, L.M., P.T. Sage, and A.H. Sharpe, *The PD-1 pathway in tolerance and autoimmunity.* Immunol Rev. **236**: p. 219-42.

416. Maccalli, C., V. Di Cristanziano, V. Fodale, et al., *Induction of both CD8+ and CD4+ T-cell-mediated responses in colorectal cancer patients by colon antigen-1.* Clinical cancer research : an official journal of the American Association for Cancer Research, 2008. **14**(22): p. 7292-303.

417. Rothman, N., C.F. Skibola, S.S. Wang, et al., *Genetic variation in TNF and IL10 and risk of non-Hodgkin lymphoma: a report from the InterLymph Consortium.* Lancet Oncol, 2006. **7**(1): p. 27-38.

418. Norton, J.D., *ID helix-loop-helix proteins in cell growth, differentiation and tumorigenesis.* Journal of cell science, 2000. **113 (Pt 22)**: p. 3897-905.

419. Ueda-Hayakawa, I., J. Mahlios, and Y. Zhuang, *Id3 restricts the developmental potential of gamma delta lineage during thymopoiesis.* Journal of immunology, 2009. **182**(9): p. 5306-16.

420. Li, J., T. Maruyama, P. Zhang, et al., *Mutation of inhibitory helix-loop-helix protein Id3 causes gammadelta T-cell lymphoma in mice.* Blood, 2010. **116**(25): p. 5615-21.

421. Maruyama, T., J. Li, J.P. Vaque, et al., *Control of the differentiation of regulatory T cells and T(H)17 cells by the DNA-binding inhibitor Id3.* Nat Immunol, 2011. **12**(1): p. 86-95.

422. Jaleco, A.C., A.P. Stegmann, M.H. Heemskerk, et al., *Genetic modification of human B-cell development: B-cell development is inhibited by the dominant negative helix loop helix factor Id3.* Blood, 1999. **94**(8): p. 2637-46.

423. Schraml, B.U., K. Hildner, W. Ise, et al., *The AP-1 transcription factor Batf controls T(H)17 differentiation.* Nature, 2009. **460**(7253): p. 405-9.

424. Lorenzo, Y., M. Provencio, L. Lombardia, et al., *Differential genetic and functional markers of second neoplasias in Hodgkin's disease patients.* Clin Cancer Res, 2009. **15**(15): p. 4823-8.

425. Love, C., Z. Sun, D. Jima, et al., *The genetic landscape of mutations in Burkitt lymphoma.* Nat Genet, 2012. **44**(12): p. 1321-5.

426. Richter, J., M. Schlesner, S. Hoffmann, et al., *Recurrent mutation of the ID3 gene in Burkitt lymphoma identified by integrated genome, exome and transcriptome sequencing.* Nat Genet, 2012. **44**(12): p. 1316-20.

427. Schneider, K., K.G. Potter, and C.F. Ware, *Lymphotoxin and LIGHT signaling pathways and target genes.* Immunol Rev, 2004. **202**: p. 49-66.

428. Worm, M.M., A. Tsytsykova, and R.S. Geha, *CD40 ligation and IL-4 use different mechanisms of transcriptional activation of the human lymphotoxin alpha promoter in B cells.* Eur J Immunol, 1998. **28**(3): p. 901-6.

429. Kuprash, D.V., O.A. Osipovich, D.K. Pokholok, et al., *Functional analysis of the lymphotoxin-beta promoter. Sequence requirements for PMA activation.* Journal of immunology, 1996. **156**(7): p. 2465-72.

430. Lauder, A., A. Castellanos, and K. Weston, *c-Myb transcription is activated by protein kinase B (PKB) following interleukin 2 stimulation of Tcells and is required for PKB-mediated protection from apoptosis.* Mol Cell Biol, 2001. **21**(17): p. 5797-805.

431. Watanabe, A., H. Tagawa, J. Yamashita, et al., *The role of microRNA-150 as a tumor suppressor in malignant lymphoma.* Leukemia, 2011. **25**(8): p. 1324-34.

432. Lefebvre, C., P. Rajbhandari, M.J. Alvarez, et al., *A human B-cell interactome identifies MYB and FOXM1 as master regulators of proliferation in germinal centers.* Molecular systems biology, 2010. **6**: p. 377.

433. Joshi, S., A. Wu, D. Verbik, et al., *Oligonucleotides complementary to c-myb messenger RNA inhibit growth and induce apoptosis in human Burkitt lymphoma cells.* Int J Oncol, 1996. **8**(4): p. 815-20.

434. Schwindinger, W.F., K.S. Betz, K.E. Giger, et al., *Loss of G protein gamma 7 alters behavior and reduces striatal alpha(olf) level and cAMP production.* J Biol Chem, 2003. **278**(8): p. 6575-9.

435. Shibata, K., M. Mori, S. Tanaka, et al., *Identification and cloning of human G-protein gamma 7, down-regulated in pancreatic cancer.* Biochem Biophys Res Commun, 1998. **246**(1): p. 205-9.

436. Ohta, M., K. Mimori, Y. Fukuyoshi, et al., *Clinical significance of the reduced expression of G protein gamma 7 (GNG7) in oesophageal cancer.* Br J Cancer, 2008. **98**(2): p. 410-7.

437. Giefing, M., J. Arnemann, J.I. Martin-Subero, et al., *Identification of candidate tumour suppressor gene loci for Hodgkin and Reed-Sternberg cells by characterisation of homozygous deletions in classical Hodgkin lymphoma cell lines.* Br J Haematol, 2008. **142**(6): p. 916-24.

438. Shams, T.M., *High expression of LMO2 in Hodgkin, Burkitt and germinal center diffuse large B cell lymphomas.* Journal of the Egyptian National Cancer Institute, 2011. **23**(4): p. 147-53.

439. Cubedo, E., A.J. Gentles, C. Huang, et al., *Identification of LMO2 transcriptome and interactome in diffuse large B-cell lymphoma.* Blood, 2012. **119**(23): p. 5478-91.

440. Griffiths-Jones, S., *The microRNA Registry.* Nucleic Acids Res, 2004. **32**(Database issue): p. D109-11.

441. He, S., H. Su, C. Liu, et al., *MicroRNA-encoding long non-coding RNAs.* BMC Genomics, 2008. **9**: p. 236.

442. Neufeld, T.P., *Autophagy and cell growth--the yin and yang of nutrient responses.* Journal of cell science, 2012. **125**(Pt 10): p. 2359-68.

443. Altman, B.J. and J.C. Rathmell, *Autophagy: not good OR bad, but good AND bad.* Autophagy, 2009. **5**(4): p. 569-70.

444. Mason, E.F. and J.C. Rathmell, *Cell metabolism: an essential link between cell growth and apoptosis.* Biochim Biophys Acta, 2011. **1813**(4): p. 645-54.

445. Rathmell, J.C., M.G. Vander Heiden, M.H. Harris, et al., *In the absence of extrinsic signals, nutrient utilization by lymphocytes is insufficient to maintain either cell size or viability.* Mol Cell, 2000. **6**(3): p. 683-92.

446. Vander Heiden, M.G. and C.B. Thompson, *Bcl-2 proteins: regulators of apoptosis or of mitochondrial homeostasis?* Nature cell biology, 1999. **1**(8): p. E209-16.

447. Fan, Y., K.G. Dickman, and W.X. Zong, *Akt and c-Myc differentially activate cellular metabolic programs and prime cells to bioenergetic inhibition.* J Biol Chem, 2010. **285**(10): p. 7324-33.

448. Taylor, D., P. Badiani, and K. Weston, *A dominant interfering Myb mutant causes apoptosis in T cells.* Genes Dev, 1996. **10**(21): p. 2732-44.

449. Salomoni, P., D. Perrotti, R. Martinez, et al., *Resistance to apoptosis in CTLL-2 cells constitutively expressing c-Myb is associated with induction of BCL-2 expression and Myb-dependent regulation of bcl-2 promoter activity.* Proc Natl Acad Sci U S A, 1997. **94**(7): p. 3296-301.

450. Heckman, C.A., J.W. Mehew, G.G. Ying, et al., *A-Myb up-regulates Bcl-2 through a Cdx binding site in t(14;18) lymphoma cells.* J Biol Chem, 2000. **275**(9): p. 6499-508.

451. Lang, G., W.M. Gombert, and H.J. Gould, *A transcriptional regulatory element in the coding sequence of the human Bcl-2 gene.* Immunology, 2005. **114**(1): p. 25-36.

452. Hirotani, M., Y. Zhang, N. Fujita, et al., *NH2-terminal BH4 domain of Bcl-2 is functional for heterodimerization with Bax and inhibition of apoptosis.* J Biol Chem, 1999. **274**(29): p. 20415-20.

453. Simonsson, T. and M. Henriksson, *c-myc Suppression in Burkitt's lymphoma cells.* Biochem Biophys Res Commun, 2002. **290**(1): p. 11-5.

454. Challita, P.M. and D.B. Kohn, *Lack of expression from a retroviral vector after transduction of murine hematopoietic stem cells is associated with methylation in vivo.* Proc Natl Acad Sci U S A, 1994. **91**(7): p. 2567-71.

455. Moore, K.A., F.A. Fletcher, D.K. Villalon, et al., *Human adenosine deaminase expression in mice.* Blood, 1990. **75**(10): p. 2085-92.

456. Austin, T.W., S. Salimi, G. Veres, et al., *Long-term multilineage expression in peripheral blood from a Moloney murine leukemia virus vector after serial transplantation of transduced bone marrow cells.* Blood, 2000. **95**(3): p. 829-36.

457. Schmelzle, T. and M.N. Hall, *TOR, a central controller of cell growth.* Cell, 2000. **103**(2): p. 253-62.

458. Fingar, D.C., S. Salama, C. Tsou, et al., *Mammalian cell size is controlled by mTOR and its downstream targets S6K1 and 4EBP1/eIF4E.* Genes Dev, 2002. **16**(12): p. 1472-87.

459. Schuhmacher, M., M.S. Staege, A. Pajic, et al., *Control of cell growth by c-Myc in the absence of cell division.* Current biology : CB, 1999. **9**(21): p. 1255-8.

460. Iritani, B.M. and R.N. Eisenman, *c-Myc enhances protein synthesis and cell size during B lymphocyte development.* Proc Natl Acad Sci U S A, 1999. **96**(23): p. 13180-5.

461. Pendas-Franco, N., O. Aguilera, F. Pereira, et al., *Vitamin D and Wnt/beta-catenin pathway in colon cancer: role and regulation of DICKKOPF genes.* Anticancer Res, 2008. **28**(5A): p. 2613-23.

462. Figueroa, J.D., N. Malats, F.X. Real, et al., *Genetic variation in the base excision repair pathway and bladder cancer risk.* Human genetics, 2007. **121**(2): p. 233-42.

463. Moreno, V., F. Gemignani, S. Landi, et al., *Polymorphisms in genes of nucleotide and base excision repair: risk and prognosis of colorectal cancer.* Clinical cancer research : an official journal of the American Association for Cancer Research, 2006. **12**(7 Pt 1): p. 2101-8.

464. Lin, S.H., M. Nishino, W. Luo, et al., *Inhibition of prostate tumor growth by overexpression of NudC, a microtubule motor-associated protein.* Oncogene, 2004. **23**(14): p. 2499-506.

465. Seol, W., H.S. Choi, and D.D. Moore, *An orphan nuclear hormone receptor that lacks a DNA binding domain and heterodimerizes with other receptors.* Science, 1996. **272**(5266): p. 1336-9.

466. Hermeking, H., *The 14-3-3 cancer connection.* Nature reviews. Cancer, 2003. **3**(12): p. 931-43.

467. Wadman, I.A., H. Osada, G.G. Grutz, et al., *The LIM-only protein Lmo2 is a bridging molecule assembling an erythroid, DNA-binding complex which includes the TAL1, E47, GATA-1 and Ldb1/NLI proteins.* Embo J, 1997. **16**(11): p. 3145-57.

468. Sanderson, R.D., P. Lalor, and M. Bernfield, *B lymphocytes express and lose syndecan at specific stages of differentiation.* Cell Regul, 1989. **1**(1): p. 27-35.

469. Bichi, R., S.A. Shinton, E.S. Martin, et al., *Human chronic lymphocytic leukemia modeled in mouse by targeted TCL1 expression.* Proc Natl Acad Sci U S A, 2002. **99**(10): p. 6955-60.

470. Koganei, S., M. Ito, K. Yamamoto, et al., *B-1a cell origin of the murine B lymphoma line BCL1 characterized by surface markers and bacterial reactivity of its surface IgM.* Immunol Lett, 2005. **98**(2): p. 232-44.

471. Shaffer, A.L., A. Rosenwald, E.M. Hurt, et al., *Signatures of the immune response.* Immunity, 2001. **15**(3): p. 375-85.

472. Nakata, Y., S. Shetzline, C. Sakashita, et al., *c-Myb contributes to G2/M cell cycle transition in human hematopoietic cells by direct regulation of cyclin B1 expression.* Mol Cell Biol, 2007. **27**(6): p. 2048-58.

473. Zhao, L., E.A. Glazov, D.R. Pattabiraman, et al., *Integrated genome-wide chromatin occupancy and expression analyses identify key myeloid pro-differentiation transcription factors repressed by Myb.* Nucleic acids research, 2011. **39**(11): p. 4664-79.

474. Buck, M., D.J. Kim, K. Houglum, et al., *c-Myb modulates transcription of the alpha-smooth muscle actin gene in activated hepatic stellate cells.* American journal of physiology. Gastrointestinal and liver physiology, 2000. **278**(2): p. G321-8.

475. Zhao, L., E.A. Glazov, D.R. Pattabiraman, et al., *Integrated genome-wide chromatin occupancy and expression analyses identify key myeloid pro-differentiation transcription factors repressed by Myb.* Nucleic Acids Res, 2011. **39**(11): p. 4664-79.

476. Huang, Y., J. Wu, R. Li, et al., *B-MYB delays cell aging by repressing p16 (INK4alpha) transcription.* Cellular and molecular life sciences : CMLS, 2011. **68**(5): p. 893-901.

477. Long, E.M., M.A. Long, M. Tsirigotis, et al., *Stimulation of the murine Uchl1 gene promoter by the B-Myb transcription factor.* Lung cancer, 2003. **42**(1): p. 9-21.

478. Tanno, B., F. Sesti, V. Cesi, et al., *Expression of Slug is regulated by c-Myb and is required for invasion and bone marrow homing of cancer cells of different origin.* J Biol Chem, 2010. **285**(38): p. 29434-45.

479. Heng, T.S. and M.W. Painter, *The Immunological Genome Project: networks of gene expression in immune cells.* Nat Immunol, 2008. **9**(10): p. 1091-4.

480. Huang da, W., B.T. Sherman, and R.A. Lempicki, *Systematic and integrative analysis of large gene lists using DAVID bioinformatics resources.* Nat Protoc, 2009. **4**(1): p. 44-57.

481. Kanehisa, M. and S. Goto, *KEGG: kyoto encyclopedia of genes and genomes.* Nucleic Acids Res, 2000. **28**(1): p. 27-30.

482. Jiang, X., L. Villeneuve, C. Turmel, et al., *The Myb and Ahi-1 genes are physically very closely linked on mouse chromosome 10.* Mamm Genome, 1994. **5**(3): p. 142-8.

483. Davies, J., P. Badiani, and K. Weston, *Cooperation of Myb and Myc proteins in T cell lymphomagenesis.* Oncogene, 1999. **18**(24): p. 3643-7.

484. Barr, N.I., M. Stewart, C. Tsatsanis, et al., *The fit-1 common integration locus in human and mouse is closely linked to MYB.* Mamm Genome, 1999. **10**(6): p. 556-9.

485. Hanlon, L., N.I. Barr, K. Blyth, et al., *Long-range effects of retroviral insertion on c-myb: overexpression may be obscured by silencing during tumor growth in vitro.* J Virol, 2003. **77**(2): p. 1059-68.

486. Cogswell, J.P., P.C. Cogswell, W.M. Kuehl, et al., *Mechanism of c-myc regulation by c-Myb in different cell lineages.* Mol Cell Biol, 1993. **13**(5): p. 2858-69.

487. Evans, J.L., T.L. Moore, W.M. Kuehl, et al., *Functional analysis of c-Myb protein in T-lymphocytic cell lines shows that it trans-activates the c-myc promoter.* Mol Cell Biol, 1990. **10**(11): p. 5747-52.

488. Schmidt, M., V. Nazarov, L. Stevens, et al., *Regulation of the resident chromosomal copy of c-myc by c-Myb is involved in myeloid leukemogenesis.* Mol Cell Biol, 2000. **20**(6): p. 1970-81.

489. Kumar, A., C.M. Lee, and E.P. Reddy, *c-Myc is essential but not sufficient for c-Myb-mediated block of granulocytic differentiation.* J Biol Chem, 2003. **278**(13): p. 11480-8.

490. Kelly, P.N., J.M. Adam, and A. Strasser. *The role of endogenous anti-apoptotic Bcl-2 family proteins in lympohoma development.* in *New Directions in Leukaemia Research*. 2008. Sunshine Coast Australia.

491. Hooper, J., D. Maurice, M.J. Argent-Katwala, et al., *Myb proteins regulate expression of histone variant H2A.Z during thymocyte development.* Immunology, 2008. **123**(2): p. 282-9.

492. Martinato, F., M. Cesaroni, B. Amati, et al., *Analysis of Myc-induced histone modifications on target chromatin.* PLoS One, 2008. **3**(11): p. e3650.

493. Knoepfler, P.S., X.Y. Zhang, P.F. Cheng, et al., *Myc influences global chromatin structure.* Embo J, 2006. **25**(12): p. 2723-34.

494. Tan, L.P., M. Wang, J.L. Robertus, et al., *miRNA profiling of B-cell subsets: specific miRNA profile for germinal center B cells with variation between centroblasts and centrocytes.* Laboratory investigation; a journal of technical methods and pathology, 2009. **89**(6): p. 708-16.

495. Chang, T.C., D. Yu, Y.S. Lee, et al., *Widespread microRNA repression by Myc contributes to tumorigenesis.* Nat Genet, 2008. **40**(1): p. 43-50.

496. Lin, D., M. Fiscella, P.M. O'Connor, et al., *Constitutive expression of B-myb can bypass p53-induced Waf1/Cip1-mediated G1 arrest.* Proc Natl Acad Sci U S A, 1994. **91**(21): p. 10079-83.

497. Mannefeld, M., E. Klassen, and S. Gaubatz, *B-MYB is required for recovery from the DNA damage-induced G2 checkpoint in p53 mutant cells.* Cancer Res, 2009. **69**(9): p. 4073-80.

498. Malaterre, J., M. Carpinelli, M. Ernst, et al., *c-Myb is required for progenitor cell homeostasis in colonic crypts.* Proc Natl Acad Sci U S A, 2007. **104**(10): p. 3829-34.

499. Muller, C., R. Yang, G. Idos, et al., *c-myb transactivates the human cyclin A1 promoter and induces cyclin A1 gene expression.* Blood, 1999. **94**(12): p. 4255-62.

500. Tanikawa, J., T. Nomura, E.M. Macmillan, et al., *p53 suppresses c-Myb-induced trans-activation and transformation by recruiting the corepressor mSin3A.* J Biol Chem, 2004. **279**(53): p. 55393-400.

501. Kumar, A., M. Marques, and A.C. Carrera, *Phosphoinositide 3-kinase activation in late G1 is required for c-Myc stabilization and S phase entry.* Mol Cell Biol, 2006. **26**(23): p. 9116-25.

502. Rose, N.J. and A.M. Lever, *Rapamycin-induced inhibition of HTLV-I LTR activity is rescued by c-Myb.* Retrovirology, 2007. **4**: p. 24.

503. Coiffier, B., E. Lepage, J. Briere, et al., *CHOP chemotherapy plus rituximab compared with CHOP alone in elderly patients with diffuse large-B-cell lymphoma.* N Engl J Med, 2002. **346**(4): p. 235-42.

504. Dunleavy, K., S. Pittaluga, M.S. Czuczman, et al., *Differential efficacy of bortezomib plus chemotherapy within molecular subtypes of diffuse large B-cell lymphoma.* Blood, 2009. **113**(24): p. 6069-76.

505. Fowler N, S.M., Smith B, *The Btk inhibitor, PCI-32765, induces durable responses with minimal toxicity in patients with Relapsed/Refractory B-Cell malignancies: results From a Phase I Study* in *American Society of Hematology*2010, Blood Journal. p. Abstract 964.

506. Wilson, W.H., O.A. O'Connor, M.S. Czuczman, et al., *Navitoclax, a targeted high-affinity inhibitor of BCL-2, in lymphoid malignancies: a phase 1 dose-escalation study of safety, pharmacokinetics, pharmacodynamics, and antitumour activity.* Lancet Oncol, 2010. **11**(12): p. 1149-59.

507. Alt, J.R., T.C. Greiner, J.L. Cleveland, et al., *Mdm2 haplo-insufficiency profoundly inhibits Myc-induced lymphomagenesis.* Embo J, 2003. **22**(6): p. 1442-50.

508. Tovar, C., J. Rosinski, Z. Filipovic, et al., *Small-molecule MDM2 antagonists reveal aberrant p53 signaling in cancer: implications for therapy.* Proc Natl Acad Sci U S A, 2006. **103**(6): p. 1888-93.

509. Tyner, S.D., S. Venkatachalam, J. Choi, et al., *p53 mutant mice that display early ageing-associated phenotypes.* Nature, 2002. **415**(6867): p. 45-53.

510. Maier, B., W. Gluba, B. Bernier, et al., *Modulation of mammalian life span by the short isoform of p53.* Genes Dev, 2004. **18**(3): p. 306-19.

511. Mendrysa, S.M., M.K. McElwee, J. Michalowski, et al., *mdm2 Is critical for inhibition of p53 during lymphopoiesis and the response to ionizing irradiation.* Mol Cell Biol, 2003. **23**(2): p. 462-72.

512. Soucek, L., J. Whitfield, C.P. Martins, et al., *Modelling Myc inhibition as a cancer therapy.* Nature, 2008. **455**(7213): p. 679-83.

513. Delmore, J.E., G.C. Issa, M.E. Lemieux, et al., *BET bromodomain inhibition as a therapeutic strategy to target c-Myc.* Cell, 2011. **146**(6): p. 904-17.

514. Pattabiraman, D.R. and T.J. Gonda, *Role and potential for therapeutic targeting of MYB in leukemia.* Leukemia : official journal of the Leukemia Society of America, Leukemia Research Fund, U.K, 2013. **27**(2): p. 269-77.

515. Calabretta, B., R.B. Sims, M. Valtieri, et al., *Normal and leukemic hematopoietic cells manifest differential sensitivity to inhibitory effects of c-myb antisense oligodeoxynucleotides: an in vitro study relevant to bone marrow purging.* Proc Natl Acad Sci U S A, 1991. **88**(6): p. 2351-5.

516. Gewirtz, A.M., *Myb targeted therapeutics for the treatment of human malignancies.* Oncogene, 1999. **18**(19): p. 3056-62.

517. Brignole, C., D. Marimpietri, G. Pagnan, et al., *Neuroblastoma targeting by c-myb-selective antisense oligonucleotides entrapped in anti-GD2 immunoliposome: immune cell-mediated anti-tumor activities.* Cancer letters, 2005. **228**(1-2): p. 181-6.

518. Zuber, J., A.R. Rappaport, W. Luo, et al., *An integrated approach to dissecting oncogene addiction implicates a Myb-coordinated self-*

renewal program as essential for leukemia maintenance. Genes Dev, 2011. **25**(15): p. 1628-40.

9. Appendix

Below are the read outs obtained after the gel bands post splinkerette PCR were sequenced using the BigDye Terminator v3.1 Cycle Sequencing Kit. Only those which were well correlated with the mouse genome using the USCS (University of California Santa Cruz) Genome Browser BLAT search function (July 2007 assembly) are included below (ie sequences amplifying only internal retroviral DNA are not shown). The primer used to obtain the sequence is also listed, as on some occasions one primer did not result in a productive readout, although often both primers gave very similar results, as indicated. The sequence corresponding to the murine genome is underlined.

9.1.1 Lymphoma 1

Specimen 1b

HMSp2 primer

GGTAGCATTATTATATAAGTTTATCTTGGATCTTGCCAGAGTTCTGTTTCTG
GTAGATGGGGTATTGTGTTTTGACTCTCTCACCTTTTTTAGAATCAGAGACTT
ACTTTGACACATTTGATATGAGAGACTGGGACTCAGACAGAGATAGAGAGA
TAGCAAGTGAGTGTGCTTGAGAGAGACAGAGAGACAGAGAGACAGAGACA
GACAGAAATACACACACTCTCACACACACACACACACACACACACACAGAG
AGAGTATAAAGTGTGTTGTGTGCTCTCTCTTGTGTTTTTTGAAACCCCCCCT
GTGTGTTTTTGAC

Specimen 1d

HM001 (same localisation with HMSp2 primer)

ACTCCGTGGGTTTTTGTGACACGGGGTCTGTCATAGCCTCTCTCAACTGTT
ATCAAAATGATAGGAACCCGGGATGATATGTACAATGTGGTTCAACAGTAG
AACTCTTGTTGGCTTACTCTCCCCCCTGACACCCCTCTGTCCATGATGCCT
CATTTGGACAAAAGTGGCTAGGACCACTTGGAAGCTGTTGCTATCTTCCCC
AGAAATGAAGCTTCTGACTGGCTGTGTGTTCAATGATAACTTGTTGCCCTG
GTGACAAGGTTGCTATGACAGATATTTCTGTCAATCAAAGGAGAATTCTTG
ATGCTGTCTGGTAATTGGAGTTTCTGTTGAAAAGTGTTGGATTCTCCTGCT
GTATGCACATGTAGAGAGTGGGTAACCACAGAACAGGAGGCCCATGTTAA
CTTACTTAACTGGCTGGAAACATGTCAACTGTCTGCGTTTTGAACTGGCTG
AATGCACACAGACAGTAATACATACAAAAGACAAAGGAAAGTTATGGAAAT
ATTATCATAAAATCATTACCATCCCCCACCTTTGTGCTAGGAATGGAACTTA

GGGTCCTTATAGGCTAGGGAGTGTTCTATCTCTGAGATATACCCCTAGTCT
CACCCGGCTCCTGTGTGCGGCGCATGTGGAATCTAGAGATTAACATTGTA
CATCTTCCCTTAATCGCTTTTCACTTTCTTTTTTTCTTTTTTTGAGAAAAGGAT
TCTCTAAG

9.1.2 Lymphoma 2

Specimen 2b

HMSp2 (same localisation with HM001 primer)

ATGGTGCCTCTTCAGTACCCGAGGACACATCCCAAGACCCTGAGCAATAA
TGAAAAAGAAAACAGAGCCAGACATTATAACCATCACTAAGAGACACAAAG
TTTGCTACAATTGTAACAAAATTACCACATCACCACCAAGGAGCATTCAGC
ACAGAAGGTCCTGCCTACCATTCCCTCACTCAGGAAGCTGAGGCAGTAGG
ATGGCCACCAGCTTGAAACCAGCCTGGGCTGCAAAGTAAAGCTATCCTAC
TGGAGAAAAGCGGGCAGGCAAAAGAGAAAAAGGGGGAGTCAAAGCCGTG
TTGGCCGCGGGTGTTAAGGGGACCTACTGA

Specimen 2c

HM001 (same localisation as HMSp2 primer)

AAGGTGATACAGAGCTGAGTAATCCCCTTGGGGCCCCTAGGCTCGGCCAC
CAGCCAGAGCACGGGCCACGGCGGAGGTTGGGTGGGGTTGTCGGTGGC
CAGGAGGACCCCTGGGAGGACTTGGCCAGCAAAATGAGTTGGCTCTGGC
CCAGGCCTGCTGGATCTGGAAAGCACCAGCCAGATGGGGAGTTCCTCCC
CTTCTCTGCATACCCAGGGCTCCCCGCGTGTCTGCTGTGTCCATCTGTTTG
GCCCCACTTTTATTTATGCAACAGTGGATTGGCGGGAGTTTTAAGCACTGT
CAAGTGCTCTTCCTGAAGGCACACAGCACAGCCAGGCTGATGTTAGCTTC
TGTGGGTGGGTCAAGGGTGACCGTTTGTGTCACTATCTGCCTGTGCCGTC
TTCAGGAAAGGCCACCTCCAGTCCAGCCGTCACGCTGTGTCTCCTGCAGA
TTTGCTGGGAAGAAATCCACGATTAGGAACCCCGTGGCATTTGGTTGTGG
GTTCCTGGGACAAGGCGTCAGA

9.1.3 Lymphoma 3

Specimen 3a

HMSp2 (same localisation with HM001 primer)

CGATTCATGAAGCACTCGTACTCTTTGTAGGCTCTCTGAGAGGCTGCACCT
CCCAGGCACCACACCTGTGCATTGCTTGCCCACAGCCCTTTGCAGACACG
GTTCCCGCTACCCGAATGCCTGCCCCAGCCTTCTGGTTGAGTCCCACTCA
CTCTCTGAGACACCAGGCAGGCCTCCTTGGTTCACCTTTCCAGGCTAGGC
CAGCATCTCCGCAGCTTATTCCCTTACTTGGAAGTTGAGCAAAAGACTTGC
CCAAGGTCACACATTCAGTGAGGTGGAATCAGGATTAGAACAAGAGCCTG
CTGTTTCCTGGTGGGAGGGAAGTGCTCAAGGCCAGACTGCTGGAGAGGC
TAGAGTGTGAAAGACCCCACCTGTAGGTTTGGCAAAAA

Specimen 3b

HM001 (same localisation with HMSp2 primer)

AATCCTTAATCTCTGGAGATCTGCCTTGCTTGCCTCTTGAGTCCATGCTCC
ACCACCCTGTCGTCCCAATTGAGTATCCAGGTTTTAAACTGGGTGACCTAA
GGAAACTCCACTACAATATCAAGGGGATCAAGTTACCTCATATCAAAACCT
CCGCCACAATGAGAAAGCCCCGGCTCTGGCTGTCCCCAGTTACCCAGTTA
GAGAGGCTTAACTGCCACTCACCTGTCCATGAGCAGAACCAAAGGGGAAG
CCGCCATGATTCTACTGTGACCACACAGTCCTCAGGGACCATCCACAGTT
GCTCTGAATCTCCTGGTGCCTCATACCTGGCAAGCCACAGTGTCAAGGCC
ACA

9.1.4 Lymphoma 4

Specimen 4a

HMSp2 (same localisation with HM001 primer)

ACTGGTTTGATTAAAGCAGCAGTGGAATATCTGATGGTACAAAGAGATAGC
CCACTCCAAGGTACTCACCCAGGCCCAGGTATACTCACAGGACAGACACT
GCCCTCTGTGGTGACCTGTGATGCTCACGGCCAGTGTGTGACTGCCTGTG
CCTGGCTGACCCATGGGCCCCTTCCAGGTCAGGCTGCCTCCTTTCTTCCT
TCCCAGGCAGGCTCAGGACCTTGCCAACCAGGCTGCCCTCCTTTCTCCCC
TCAGCTGTGTTTCTCTGGGCTCAGTTTTGCCTTTCACCCTCTTAAGCTTGG
GAGTTTGAGAGATTGATTACC

Specimen 4b

HMSp2 primer

GCCCAAAGCACCACTATCGAGGCTATAGAGGTTCTGGGTCATGTGATACT
GCACATCAAAGGCTGATTTTGGAGGAGGGGGGTTGGATTGCGCCCGGTAA
CTTCCCGACCCAACTGTTTTGTGTGCTGCCTGGTGCCACACCTTTCTGTGG
CCTTAAACTGATGTCATCCAGATCTGCGCACCGTCCTACTTATTTACGTTG
ATTTTGAAGAACCTCTTCCGAGACCTAGAAATCTGTTTCCCTCGGGTTCTG
TCTGATGCACTGATCCCTATAAATGTTTGGGACTCAAATACCTAACTGTGG
CCAGGGACATGGGGTGAGGGGTAAATCCCAAAAGAAGCAAACCGAGCCT
CCAATTTTAGGCCATTCCCCATGGACACCCATAGCCCAGGTCACTAGTAAT
GTACCTGGGGTCACACTGTGACAATGACTCCCACTGTGACATGCTGGCTG
CCCCCCACCACCCCCGACCCATTCCCCAGCCACAAAGCTTAACCCATCCT
TGAAGGGAGAAGGTGACAGCTTGACTGAGCTGCTGCTGAGAGGAAGCAG
TCGCTGGTTCCCAGTGAGAAGTCCAAAGGTAAACCCCCTTCCTCATTTCTG
AAAGCTTCCTCCCCCCCTACACCCCGGCCTGTGTGGAGCTAGGTCTCCTG
CAACTATCACAACCTGCACTCCTCCCTTTTGCCAGCCTGCCTTTCTCTTTG
CACAGCCACAAACCAAAAGGGCACTATTCTGTTCATCTCACAAGTAACTAC
TAAGGCCAGGATAACTCCGGGCTTGTACCGGGCC

9.1.5 Lymphoma 6

Specimen 6b

HMSp2. Same localisation with HM001 primer

GGCCAGCAGCAAATGGCTGGAGGAGAACAGAGGGACAGATACCTTCTAA
GAGTAAAGTTCAAAGTTGAAGGAAAGATGGACACTAGTCTATTTTCTAAATT
GAAGTTGCCATCTGATAATTAAACGTTTACCCTTCCTTCTGCCTTCAGCCTC
TTTTTACATATCTGGATTTGCACAAAGGAGCTCTGGCATTGCTGAGCCGTG
CTCTGGGCAGTGAAGTGGGCAGAAGAGAGATGCTGCCAACCTGGGGAAA
TTCAGACTACCCAATCAGAGATAAGGGGCAAAGAACCTTTGTCACTGTTGT
CCCTTGCATTTCCCTTCTCACAAATTCATTCAGCAAGTCATGGTGACTCCAT
CTATGTCTTCAGACGCTGGCTCAACACAAAAGCTAGAATAAAGATAACATG
TCTTCATTTATGAAGTAATTCTGATATAATATCTCGAACCACTGTCTTTCATA
TTAGGTTAATTGTTCCTAGCACAAAAGCCCTGAAATAATACCCAACTCTCTC
ATGGAGCTGTTCTTTGTTTGATAACAGTGAACAAAAGCTCAGGCAACACTG
AAAATGTTTTACTGACCTTCTAAGTCAAGGTCATGTAGCACGAGAGTAACC
CTTGAAAGACCCCACCTGTAGGTTAGGCAA

9.1.6 Lymphoma 7

Specimen 7a

HM001 primer. Same localisation with HMSp2 primer

ATCGCCAGCCCCTTGTGATGAGGCTGACATTTATTTGAATTACACACTTCT
GCCAGTTGCATATGCCGAAAGTTGTCCTACACGCATAGCACAAGCATACC
GGAAGCTCTACCCTGTCAGCCACGCAACGACCGCAGTGTGGCCTGTCATT
CACTATCGCAGCAGCGGCCACCTCATGGAGCTGAAGGGAACTGCCCAGC
ATGCCCAGCCTGTTGTGCACACAGACTGTCCAACTCCTACCCAAGGGCTC
GATTTCCAGAACTTAATCCTCAGAAACAAGGTACTCGTTCAGATACTGTCTT
CCATGCTAGATTATAAGGGCAAGGACTAGATCCCACTAGTGTCGACACCA
GTCTCATTCAGCCACAA

Specimen 7b

HMSp2 primer. Same localisation with HM001 primer

TTGGATTATATAATGAGAGTGTCTCATAGGTCAGGTGGGTAATTTTCTTAGA
AACTGAAGTTTGCGTTGTACTTTCCTGTGCATTATTCATTTCTTCCTCACAG
CTGCTCTGCATGGCGCCTGGCCTTACTTAACAAGAACAGACAGCACACCC
AGAGAAATTACTGGCATGGCAGGGTCTCAGCCCTATCCCACTAGTTCCGG
GGACAGTGGCCCTGCCTACCATTGGCCTCTTACACCTTCAATTATTCCATT
GTAAACTAGGGATAAAAATACTCGGTAGGGCGCTGTCTTCACTCACAGGG
AATGTGATCTGGACACCAGCCTCCCTGAGGCTGCTAACTTTCTGGTGAATG
GAGAAAAGGGCTTCCTGAGAAAGTGACCCTGAAGCAGATTCTGGAAGAAG
GTAAGGAATTGAAAGACCCCACCTGTAGGTTTGGCA

9.1.7 Lymphoma 8

Specimen 8a

HM001 Primer. Same localisation with HMSp2 primer.

CAATCCCCCCTTTTTTGTTTCCACACACACACACACATTAAATATATAAACT
ACGAGTTTAAAATAGACCAGCCGATAGTGATCCCACCTGGTCAAATTCTCC
CTGTTTCCCCCACGCTGTCAGCTGCCACACTTCACCATACAGGGCCTCCC
CAAATCTCCAGGGGTCATGCACCTTGATCCCACTAGTGTCGACACCAGTCT
CATTCAGCCACAAA

9.1.8 Lymphoma 10

Specimen 10a

HM001 primer. Same localisation with HMSp2 primer.

GGCTCCCCCCCCCCCCTGCTACTTAACTTGACTTACAAGGTCAGCAGAACAT
TTGCAGAGTTGCCTGAGCTCCCTGATCACTGTTATCAAACAAAGAACAGCT
CCATGAGAGAGTTGGGTATTATTTCAGGGCTTTTGTGCTAGGAACAATTAA
CCTATTATGAAAGACAGTGGTTCGAGATATTATATCAGAATTACTTCATAAC
TGAAAACATGTTATCTTTATTCTAGCTTTTGTGTTGAGCCAGCGTCTGAAGA
CATAAATGGAGTCACCATGACTTG

9.1.9 Lymphoma 11

Specimen 11b

HMSp2 primer. Same localisation as HM001 primer.

GATGACTTGTTATTTTTTGAGTGCATCACTCAGCTGTCGAGCTGCTAATTAAT
GAGATAGAAATGATTTTTTTTTCTTCTTCTAAGAAGCGGGGGAATGAAACAC
CCCCCCTGTAAGTTTGGCACTTGTTTGTACTTTATTTACTCGGAAAGATACA
TTGAGGACCCATGATGTAGGTTTTTTTTCTTCATTTTTTTTGTGGGTATGTCC
AATTTTCAAATGAGTGAATAATCATTTTACTTATTAGGAAAAATAAATCATTA
CACCTATCGAATTTCTTGTGAGGGACCCTGAAACGGAGCTCAGACGTTGT
CACTGAGGTAGAGTGACCATTTCAGTTTATTTTTATGGTTGGATATTGTTGG
TGTTGTTATAAAAACGAATGTAGGCACATTACACACATTCTCCTCTATTGAC
CGTTTGGTAATATTGGCTAACATATTTATTTGGTTGCCAAAGCTTGCTTGGG
ACGAAGGAAAGCTGTTACTGATGTGATGAAATAGAGGCCCGAAATGCTGC
CAAGACCCTGCCCTGCCGCCTTCCCCCCCTCCCGCCCCCCGCCCCGCCC
CAAGGTGACAAACACTGATATGGCCTACAGCACCACTCAGTGCCAATTTTG
AGAAACGGTGACCACTCTCAACATGTCTGTCAATAGTTTCTGTTCAGCCAT
TTTCCTCTACC

9.1.10 Lymphoma 12

Specimen 12a

HM001 primer. Same localisation as HMSp2 primer.

CCCCCCCCTTTTTTTCTGTAAACTAAATAAAAACTTTTATATTATCAGGGTAC
TAGGCTAATTGCGGAGGGCCTCTAGTGTTCTGGGGTCTCACCACACCTCT
CCTATAGTGCCTTTTCTTCTCATCCCAGCACAGTATTCCATTCGAGCTGCT
CTTAAATGTCTGAGCACAATTACTTTTCTCAGCTAGGTTTGAGCTAAACAAG
AAGGGCTAACCTCGAGTGCTTAAATCAGTGGCTGGCTCACAGAGAGGTCT
CAAACACTTTTACCAACAAATTAGGATCCCACTAGTGTCGACACCAGTCTC
ATTCAGCCACAA

Specimen 12b

HM001 primer. Same localisation as HMSp2 primer.

TCCCCCTTTTGGGAGCTTAATCTGATGGTTTTTTAGCTCATGGCCAGCCTG
GTCTACAGTTCCAGGACAGCCAGGGCTATACAGACAAAACTGAAAAGTAG
AATTAAATAAATACAACGTGGAGCACACCCTCTAATCCAGCGCTCCCCAGG
TCGAGGCCAGCCTGGACTAGTTAAACAGTGAGTCTATCTCAAAAAACAAAC
AAACAAAAAAACCAGACAGACAGACAACCAAAGCCTGGTATGGTGGCACA
TTCCAGCAGTTCGGAGGCTGAGGGAGTAAGGAAAAACTGAAGTTGAAGGC
TGTACACAGCCCCATGTCCAGATGAAATCATCTTGGATTACATGTGTGAGA
TCCCACTAGTGTCGACACCAGTCTCATTCAGCCACAA

Specimen 12c

HM001 primer. Same localisation with HMSp2 primer.

AACGAACGGGTTGGAGACTTAATGTTACTGTCTTGAGCTTTGTACTACTTC
GGGACGATGGCCCTTCGGCATCCTCGGGTTTTTAAACACATTGAACTAACT
CGCAGTTCACTGGTGTGTGCATCTCTCTCTGTGTGTACTTATATGCTGTTTT
TGTCCCAGACCTTCCTCTTCCTGACATTTCGGCTGGTAACAAGGTCACAGG
CCTTCTAAAACTCTCCTCCATGTCACATGGTTTTGTGGACTCAAGTCTTTGC
ATAGATGATTTCGGGAGTAACATGACTTTGCCTGCTGGGTCACACAAGCCA
GCAGACAAGCCAAGACTAATTCAGGGATTTTATGTTTCTAGTACTTTGAAAA
AGGAAAAGCTCTTTGGCAACTTCCTTAATTAGCACTCCAGACACCACAGGA
GCCACAGAGTTAGGCTGTGAGTCTCTTCTTTCAAGACCAAAGGGTGACAA
GAATGACCCAAAAGCACATGGCTCTGGGACTTGGCAGAGTTAAGAGATCC
CACTAGTGTCGACACCAGTCTCATTCAGACACAA

Specimen 12d

HM001 primer. Same localisation with HMSp2 primer.

TTTTACGGTTTGTCTGGAGCTAGACATATCTTTTATTTTATCTCAGACTTGC
ACAGTTCGGAATGCCGAGAGTGAGCCCACTAAAGTCCAAACACTTCTCATT
CAGCCTTTTACTCGGTGGCACCATTCTATCTGGCTATACAGTATGAACGTG
TTCGCCCTCCCTTAAAGTCCCTCTGTTCGGATGCTCCCGAGAGAGCCGGA
GATTGACCCCCGTGCGCATGTGAAGTGTGGGCACGCTCTACCCTTCCTCC
ATCCTCTACAGCTCTGTTCAGGATGGTCCTGACTTCCACACATACTCTAGG
GAAAAAACCAGGCCTTACTTCCTGGGGTCCTCTCTTCATGTTTCTGTATTC
ATTTCCCTAACATATAACATTGTGCTACAACAAACCACAGTGTTTCCATTGC
ACTTTCTGTTGCCTTCTGCATTTGCTGTGTGAAGGCTCACTTAAGAACCTCT
TCCTTTTTCTGTCGTTAGGAAAAATCCTGTAACAATATGTTTGCCATCTGTA
TTGATAAAACTTTCAGGCATTCCGAATGCATCTAAATGTTTTTCAGAAACAG
GCAGAATTTGTTTAGTTCGTGTCCCTTCACAGGATGTGGCTAGGATGGAGC
AGCTGTCTCGCACTCCTCTGGATAATCCCACATGTAGCTCTGTCCAGTGGT
TTCCTCAGACCCTCCCACCTGTCGTCTGTGTCCATCCCATCCCTTCCCTAG
ATCCCACTAGTGTCGACACCAGTCTCATTCAGCCACA

9.1.11 Lymphoma 13

Specimen 13a

HMSp2 primer.

CATGACGTGCTAGCATCTGGTGGTTTAGCTGCCCACCAATTTTTGTATCCA
AGTCGGAGGTTAAGGCACCTGATCTCCTAGAACTCTGTGAGACCCCCTGC
AACGCAAGGACATTCTGCATTGCCCAGCCCTTTGCAATGATTCGTATACAA
TCTCTCTAGATGTCACCCCCCTACGAGGTTTTGAGTGTCTCGGAGCCAATA
CATGCTACTTTAGTCCCCTGGAGTCGACGCTGCCTACAACTCTGCTTCCTG
TTCACTAATTCTTCATTGCATTCAGCCTTGGACCCTTGAATTCCCATAATGG
CCTATTGAAAAACCCCACCTGTAGGTTTGGCAA

Specimen13b

HM001 primer. Same localisation with HMSp2 primer.

TCCCCCCCATTTCTGGGATCTATCTAACATCTTTTATTTTATCTATTACTTGT
ACAGCTCGTCCATGCCGAGAGTGATCCCACGAGTGTCGGCTGGAGTCTCA
TTCTGCCTCCCCGCATTTACCCAGTGGCTCCCAGATGGGCACCGTGCTTT

GCCCGAGGTCACAGGTTTCTGTAAGTACATCCAGAACTTCATCCTAGGCCT
ACCTGTTCTGTGCCAGGCAAGCAGGTGACTCACTCTTGTAACTCCAGTACT
GGGAGAGTAAGGCAGAGGAGAGCCACCACTCCAGGACTAGCCTGGGCTA
TGTCGTGAGACATTTAATATTATTTACAAAGGAATGATATACAGATGGAGAA
TGAAAAGCAAAGAAGAGGCCCAATGGGCTGGAGAGGCAGCTCCGTGGTT
AGGAGAAATTGTTGTTGCAGAGGACCCAGGTTTGGTTTTCCAGCACCCAC
GTGGAGGTTCCATACTTCCTCAGGCACCAGGCACAGATGTGAGCCTTGCC
TCTCGGTGCTTTGACTTGTACCTTGTTTGATCCCACTAGTGTCGACACCAG
TCTCATTCAGCCACAG

9.1.12 Lymphoma 14

Specimen 14a

HM001 primer. Same localisation with HMSp2 primer.

CCCCCTTCTGACTGTATTTTGCTACTGTTATGAGCTATAAGGTAAATATGTG
ATATGCAGGAGATCTGATATGTGACACCTCCGCCCCCAAAGGGGTCATGA
CCCACACAGTCAAGAACCACTGCTCTAAGGAAAAATCAAACCACCACCAAC
AAACAACCATTGTATATCCATTTTGAACACCAACTACCTCAAAGAATCAGAG
TTCCTGGGGCAGAGAGCAAAGTCCAGAGAGCACTACACATGCTGAAACAG
ATGAAATACTTCGTTTCATCATACTAAGTAAATTTGTTGCACACATGGGAAA
TAGGAATCAATTACTTCTAAAGTTGAGAGTGTATTGGAGAAATGATTTTTTT
TACAGGAACAGGAAGAAGAAGATACACTTAAATGGTAACTAAGTGTGTAGT
TACTTTATACTAAATAAAAAGATCCCACTAGTGTCGACACCAGTCTCATTCA
GCCACAA

Specimen 14b

HM001 primer. Same localisation with HMSp2 primer.

AACTCCCCGGCAGCAGTGTACACCACCCTCACCCCAGACTTGTTTATCTAG
ATAGACTGTTGTGACGGACTCATAGGCGCCTGGGTGCTGGGAAGACATAA
ACCAACCCTCCATTCTGCAAAGCTCCCAAGCAGCCCAGCCCCCACCGTCC
CGGGGGCTGGGGATTTGAGGGGGGGGAGGCGAACCCTACTCACATCGTC
CCACTTGATGAAGCGCTCCCCTTGGCTCAGATATGCCTTCACGTTAGGGG
GCAATAGAACAGGGTTGAGCAAAGACATGATGTCAAGTGTCCCTCTTTGGA
GAGGTTGGGCAAACCTCTCCAGGGGACAGGAGAAGAGAAGGAAGAAGGG
TGAACAGGAGAGGAAGCTTAGGCTAGGCTCACATGGCACCCGCCCAGTAC

TGGTCCGGAAGTCGGGTGCTCTTATAGCCTGCGGGGTGGCAGTAGCTGG
ATGCAGGACTCAGAGCTTCAGGCCAGGGCCCAGTTGATCCCACTAGTGTC
GACACCAGTCTCATTCAGCCACAAA

9.1.13 Lymphoma 15

Specimen 15a

HM001 primer. Same location with HMSp2 primer.

GCCCCGGGTCCCCTGGAGATATATAAAATCTTTTATTTTATCTCTGTACTTG
TACAGCTCGTCTTGCCTAGAGTGATCCCACGAGGGTCAACACCGGCCCGG
ATACTGACTTCCTGTCTTTAACAAATTGGACTTCTCGCCTCTACTCCGGAC
GCATGGGGGCGGGTATCACCGGCCCCACAGGTGGGGTTGCTGGGGCCTA
TATCGCCGACATCACCGATGGGGAGGATCCCACTAGCGTCTACACCAGTC
TCATTCAGCCACAAGAACGGGAAGTTAAGTTTTATCTCCTGAGCAAGCTAG
ATCCCAGTAGGGGCGACGCCAGTCTCATTCAGCCACAA

Specimen 15b

HMSp2 primer. Same localisation with HM001 primer.

TGCATCACGCGACTTCTAGGTGGGGCGAGCGGGAGACCAAGGCCATAAA
TAAAAAACTTGGTTTGATCGCCTGAGGTACCCTGGAGCCAAGTAAGTTGG
GACAAACTACGGCAGCCACCCTCTGAGCTTCGGGGCTGCTCTTGTCCACC
TTTTACATAAGAGGAAGTTACGACTCGGAAGCTTAGAAGCTTGTCCCAGCC
TACAGAGCTCACAAGCAGCAGCCCTGGCTGTGTGGCCTTGCAGGGCCAA
GAAAGAGTCAAGGAGAAAGGTCAGGCCAGCACTTGGGAGGGGGAGGAAG
GAAAGTCAAGAGTTCAAGGTTCATCCTCACAGTGTGGGCTACCTGTCTTAA
AACTGAAAGACCCCACCTGTAGGTTTGGCAA

Specimen 15d

HM001 primer.

ATCGCTTTTTTCTGGAGATTATAGATCTTTTATTTTATCTCTTTACTTGTACAG
CTCGTCTTGCCGAGAGTGATCCCACTAGTCGTCAACACCCCCCTCATTCC
GCCACTTCACGTCTTTAACAAATTGGACTATTCACCTCTACGCCGGACGCA
TCGTGCTCGGCATCTCCGGCGCCACAGGTGCGGTTGCTGGGGCCTATAT
CGCCGACCTCACCGATGGGGAAGATCCCCCTAGTGTCTACCCCAGTCTCA
TTCAGCCACCTACAGAGTCTGCTGGAAAAACGATTACCTGGAACCTGGCG

AGCCACACAGGCTGCATTATCTCAAAGTCAGCTGTTCACTTTTCTACACGT
GTGTTATTTTGCCTGTATTGTGGTAGGGACAGAGCCTAGGGCCTCTCACTT
ACAGGCAAGTGTTCTAACCACTGAGCAACCCCTCCATCCCTTAGTGTTATT
CCTTCTTGCTTGCTTGGCT

9.1.14 Lymphoma 16

Specimen 16a

HMSp2 primer. Same localisation with HM001 primer.

GTTCTGCGATTTGATAGCGACGTCCGGCTGACTTATACCCATTATTCTTGT
CACATGCTCCTGATATTAGGCCAGGTTCCTTAACTGTTCCTGTCCCTGTCA
ACTACCAGGGGTAATGAGGCTGTTTTGGCAATTGCCTGTAGCCCAAACTCA
CCAGCTTCCAGGCTGGATTGTTTAACCCACCTCTTCCCTAGCCCTCTCAGG
CAGCCTCATGGGCTAGTTGGAACCTGCATCTCCAGTGACCCTCTGTAGGT
GACTGGGGTGAGTCAGAACTTCAAGGCTCCCTCCAGTACAGAGCACAAGC
CACTGGCTGTTAGTCTCTTTTCTGTTACTGAAACTGCAAGCCACAAATGGA
CCAATGTATAACAAAACGGCTTATTCAGTTTATATTCTAAATGAAAGACCCC
ACCTGTAGGTTTGGCAA

Specimen 16b

HMSp2 primer.

TAGTTGATTTTGATCCAGACTCGCGTCAGGGCGACATGATGCTGTGATAAA
AATGTAGATTGACACTGGTGGCGCCCCCCTTGCACCCCATGCTTGGACTT
AGCCACGTGTGCGGGTTTGTTGTTCACACAGCTGCCGTCTTTGAGTGCGA
GGGTGTGTGAGGGTGTGTGTGAAAACCCTGCCTCCCCCCGTGGGTGGTC
TGAAACTTACCTTGGGGGCTGACTTAGAGAGACACCGAGCCACAGGGTCT
GTTTGCCTCCTTCCTCCCCTAGAGCTACAAATCCAAAGTGGTGCCTACAGG
CCGGTCTTCTTTCCTGTGGCGTGTGGGCTCATCTCGGGCTTTCCTGCTTG
CAAGGCAAATACTTCATCATAGATGGTCTTTGCTATTTTGTGGGTTCCTTTT
TTTCTATCATTTATCCCCGCCCCCATTTTTACCCCCTATCAGTAAGATAAAA
GAGAGGGGAATGTATGACTCTAATTTCTTCCTTCTTTTTTTCTTCTTTGTTTG
TAACTGGTTTTTGCTACTTTGCATTTTATTTTTCCCACCCTTCCCCTCCCCC
ACTAAAAGACCACCCCTTAATGTTGGACAT

9.1.15 Lymphoma 17

Specimen 17a

HM001 primer.

CCCCCGGCGGGAAGGGGCTTATTTAATTCTTTATTTTATCTCTTAGTTGTAC
TGGTCGTCCAAGCCGATAGTGATCCCACCTGTGTCACTTCCTGACCAATTT
TGTCCCAGTGGTATTCTAAGTTCTGTGTCCTGTTCGCTGGTGAGATGTGGG
GATACGATGCCTACTAGCCTGGCTTGCCTCTGTATGATCTTCTGAAATCAG
CCATCATCCTGATCCCGGTAACGTTGACCCCAGTCTCGTACAGCCACA

Specimen 17b

HM001 primer. Same localisation with HMSp2 primer.

CGAATCACTTTTTTAAGGGGAATAAATAAGATCTTTTATTTTATCTCGTTCTT
GTCCTGCTCGCCCGAGCCGATTAGCTCCATAGAGACATAGATCAATAGATA
GATAGATACATAGGCCTAAGTCCCGTCCCTTCGCTTATTGTTGTGTGACCC
CTCAAGCTGGAGCTGAAACTCTAACTTTTGAAGCATGCCCTTCCCACCCCC
TGTCCATTAACATTTAAGGTTAAAGTGGCAGCAAGGATGGCTGTGAATTCT
ACCTAAGAGTAGGGGAGGGGGAGCAAAATAAAGGGCTGCTCTCTCCTTCC
AGAGCACAGCCTCCCTCTCCTCAAACCTGGGGAAGGAGGACTTCTCATTC
TTCCCAAAGACCCGGGAGCTGAGAAAGTAGAAGGCCGTGTGTCTGTCTAG
GGATCCCACTAGTGTCGACACCAGTCTCATTCAGCCACA

Specimen 17c

HM001 primer.

GCCATGGGAGGGGGGGGGGAAAGGAAGAGCGAATTCTGATATGTCATATTT
CGGACAGGTCGCCCATGCCAAGAGTGTTTCGAATCATTTTCATACACCCCC
CCCACACACAAAGCCAACCACACACACACACGCTGTTAGGGGTAATCGAA
GAGTTTTACAAAACCTTACATTATTTACACCCTTTTTGGCTAAGATTTTTTGA
AAATTAACCTCCACTAATGCAGCTACACCAGGAAAAGCCTGGGCCTTAGAA
TTGTCCTCAGTAAAGAATAGAGAACAGGGTGGCCTTGAGGGACAGGGTTT
TTTGGAAGATGAAATGGGTTATTTGAAAAAGAAGCTAATCTTTTGCTTGCCT
CT

9.1.16 Lymphoma 18

Specimen 18c

HM001 primer. Same localisation with HMSp2 primer.

AGTCCCCGTTGTTCAGGAAAGCTATAATATCTTTGTTTTATCTCATTCTTTA
CAGAACTCGTCCCTGCCGCTAGAGATCGTTCTACCCCAGTCACCAGACGG
CTTCAACAACACCTGTGTTCCTCGGCTTGAGCCTCCCTCCCGCCTCCCAC
AGCAAGCCCCCCCCCACCCCCCACGTCATGAATTGCGGAAATAGGACCTC
AGTTGCTGGGCGGGATGATTGCACTGGGGGCTGGCCACCTCGCCGGGGG
AGGCTGCCATGTGGCTGCTGCTCTGGTCCCCCCGAAGGTGCTGGGGACT
AAAGAAGCCTAGCTGCCAGGGGCACTGATGCAGATGTGGCGCTCCCGCT
CCTGGGACGTGCCACACATCCCACTACTGTCGACACCACTCTCATTCAGC
CACACCACAG

9.1.17 Lymphoma 19

Specimen 19a

HM001 primer. Same localisation with HMSp2 primer.

AGTCAAATTTGTATCCTTTGCACATGCATTCCAGTACCACACTTGCTAAACT
GGAACTAAAATACCTCACAGTTTACCTTTTCTGTTAGAACATTCTTGGTATT
CCCGGTATAACTTGAGCTGAGCACAAGTGGTTCCCACTATGCGGACTCCC
CTTTGCATGCAGGACCCTGAAGCATCTAAAATTTCCTGATCCCACTACTGT
CGACACCAGTCTCATTCAGCCACAA

Specimen 19b

HmSp2 primer.

GGTGGATGTCATCATGCAGTGGACTCCGGCTGGGAGCTGTCAGTCTCGAG
AAGGTAAAGATTTTGTTTCGTCTCCGATGTAGGGGGGATGACGAGCGCAA
CTGAGGGGTTGGCAGAGATAGATGAATATGAGCCAGCAGGCACAAGAGG
CCGAGTGCTCCTCCTCCTCCCCCTCTTCTTCCTCTTCTTCCTCCTTTCCCT
CTTCCTCTTCCTTTTCCTTTTCTTCATATTTCTCTTTGAATTAATCATTATATC
TTCACATTGCCTATACTGCATATGGTGAAAGACCCCACCTGTAGGTTTGGC
AA

Specimen 19c

HM001 primer.

CCAGGGGGAGAGGTATGAAGACAGGAAGGACTGAATGTTTAACTCATTAA
TTGGAAACTCGTCCTGCCCAGAGGGATCCCCTGAGTGGCCTGGGTCAGCT
GGACATCCGTCACCCTCCATGCCACACATCTGGAGGAAGCTCCAGACTGT
GAACTGGAAGGAGAAGGCCAGCTCCCTTAGTTGTCCTGTGGTTTCCATATA
TGTGCACACCCACACAAACCCGAACACACACATGCACACACACGGGGATG
GGGTGGAGGCAAGTTTTTTTTTTTTAAACAAATTGATTTTTCTTTTTTAAGTC
TTCTCGTGGCCAAATTTTTTTGTAGGGACAGGGGGGGCACACTCCCAATTA
A

Specimen 19d

HmSp2 primer. Same localisation with HM001 primer.

AAGCATGTTCATCATGAGCGTGAAGGAGCGTGCACGACCTGCAAAGGACC
TGCATCCTGCGTGTTAGCCCGGATCTGAGTTCCTGCTCTAACTTCCAAAGA
GGCCACTGTTTGTTTCTCCCTGGGTCTAGCTTATATTTCCGTGTTTCCCTCT
ATAAACCTATCGTTCCATGAACATCCATGAATCGAATCTGTATGCATGGATT
TCACTATGGCCCTCTCTTTCCTGATCTGTATTTCTGATGGTTGACTGATGTT
TGAGTGGTTTTGTGGGGGAGGGTGGGGAAAAAGATTCCATCACGGGTTTT
GTTATCAGACATGGAGCTGCAGAATTTGGGGGTTTCTCTGATGGGTTTGGT
TTGATTTTCCCTTACTATGCTTCATTTCTCCCTTTTTGAACAGGACGATTTTC
TCTATGCCACTGAAAAACCCCTTCTGTAGGTTCGGTTTCTAGGGTCGTGTT
TTCTCCT

Specimen 19e

HM001 primer. Same localisation with HMSp2 primer.

GATCCAGGGTTGGTAAGCCATTGCTCATTAGACACGAATGTTACTGGCCG
GTGCTCAGTGAGACGTGGGACCTTTTATCTCTAAAAGGTTCTGACTTAGTG
GGCTTGCCTTACATGAACAGGACCCTGCGAGAGGCAACTTTCGGTTGGGT
TTGCTCTTCCTCTCCCCCTCCTGTTTTGCCTCGCTCAAGACTTTGAGCTCC
AATTCCCTCGGTCTGTCCGTCCATCTGTTCCTCTCCTTACTGAGCCCGAGG
AGTGTGATTGCCTCGTGTTCTGTGTGGTTGCTTTCACCCCCCCACCTCTCC
CAACCCCCTGGATTCCTGCCCTCGGTGCACACCAATCTCTGGACTGGCAG
GTTCTGTTCTGACTTCCCTGTTTGGACCTCGCTTATTCGAGATTGCCTGTTA
TACCCGCCACACAAACAAGACATCCGGGCTATTATTTTTAAAAGCGGGAGT
GCATGGTTTTGTGTTTGGAGAGACTTCATGACACATTTGGGAATCCAGTAT

CAAACTCTTTGCTTTCTACAAGCCCTGATTGGAAGGTAGGCTGGACAGCAA
TATCCCTCTACCGTAGACACCAGTCTCATTCACACACAA

9.1.18 Lymphoma 20

Specimen 20a

HmSp2 primer. Same localisation with HM001 primer.

GGTAATACTTGACTGGCGGGCAGAGCGGAGTGGGGGAGGGGGTCACCTG
ACCCGGCTGGGGTGCGGATGGGAATCGCTGCTGAGTCACTGGGGACTCC
GGGTTTTTCCCGGCTCAGGCTCCACCTCCGGGCATCCGAGAACCTGAAAG
ACCCCACCTGTAGGTTTGG

Specimen 20b

HMSp2 primer. Same localisation with HM001 primer.

ATGCATAGTTATTTATGCAGTTGATCGTGTTCTGCCTCCTGAGTTCTGGGG
TCAAGGCATGTACCATCACACTCAGCCCTCAACATTTATTTTCTTCATAAAC
AAAAACTGAAGGTATCATCCCAAATAAATAAAGTTCTGAGGGGACAGAATC
TTGGCCCCAAGTGGTTTCATATACTTAGCAAATATCTCAATCAAATAATGTT
TTGAATTTTCCTTGAAACTATAGAAAGGCAACACAAAAAGAGGAAGCAATC
ACTTTGAAAGACCCCACCTGTAGGTTTGGCAA

Specimen 20c

HM001 primer. Same localisation with HMSp2 primer.

ATTTTCCGTCGGGCCCATCACCGTCCTTAGTGTCTTTTCCATCGTATGTTG
TTTAACGCACGGACGTATTTGGTGTCATTTCTTGAAGATAAGTTTTAAATTC
CCTCCCTGGAATCTGTCTCCCTCTCGCCTTCCCTCTGTGCGGTGTTTCACA
GTACAAGGCCCCTTGACTAACAGGAACTGGTAAGATTTTCCCCATCATCAA
GACTCGTGGGTAGAGATGATGCCTGTCTTGTCTCCACCATCCTTTGTACCC
ACCGCCCCTCACTCAGCTCACCGCCCACTCACTCCTCAGTGTGAAAAGCA
ACTCTCCCTTCTAATAAAACGAAATTGTCTCTCTTAAAATTCGTAATCGTCT
AGTTTGTGAACCTACGAGGTCCTTTCAATTCTCGCCCAGCAGATCCCACTA
GTGTCGACACCAGTCTCATTCAGCCACAA

Specimen 20d

HMSp2 primer. Same localisation with HM001 primer.

CCGGTTCTTAGTTATTATGCAATTAGATCTTGAGAGACTCACACAGAGTACT
TTTTTTATGCACCATCTCCTTCATTCCCCGGGTCAATCAACTCCACCTTTAC
CAGTTTGGGGCTTTGGATTCTACCATGTATGTGATTTACAAAATCGGTCTTA
CTCATAATGTAAGGAGGCTTAAAAAAGTTGAACCAAGAGGAGATACTCGTT
CAATATAGACATAATTTGGGACTCAATACTACCCCAGGCCCCAATTTCTTCA
TTCTTGCCATTCCCTACTGAGAGAGATTCAGAAATGGCTCCACAAATCCCT
GTACCTACTACACAACCGTTGGAACACACGGCTCCGTGTCAACCTACGTAA
AAAAAGAATCTTCATGGTATGGTTCAATAACACTACCTCTCTTTTGCAAAA

9.1.19 Lymphoma 22

Specimen 22c

HM001 primer. Same localisation with HM001 primer.

GATCCTGATGTTCTGAAGATAATGAAATCTTTTATTTTATCTCATTACTTGTA
CATTTCCCCCGTGCCGAGAGGGATCCCACAAGTGTGTTTTTTTTTCCATTA
ATCCGTTGTAGTTTTAATTTTGTGTGTGGTATTACTTATGTATGTGTGTGGA
GGCCTGAAGTTAGTTAATTACTTTCAACCATTAAAATTTTGGGGGTGGGAG
GATGGGGCTGGATGGCTGGCTCAGTGATTAAGAGAACTTGTTGCTCCTGC
AAAGGATCCC

9.1.20 Lymphoma 23

Specimen 23a

HM001 primer.

CAGTTTCCAATTCTCTGGAGATAATAGAATCTTTTATTTTATCTCATTACTTG
TACAGCTCGTCCATGCCGAGAGTGATCCCTGAGTGTCCACACCAGCCTCA
TTCAGCCGCACTGAGGGGTGCGGGACAGTGTGGTCTCTCTTATTTGTGGC
TTATGGGGGGGGGGACGAAGTGATTCACTGTCGTTTGAAAAAGACTATGC
AAATCAAAAAAGCTGGTGCCCCAGGCTTCTCCAAATTTAGAACCCAATAAT
GGCGACACCAGGCTCATTCAGCCAC

Specimen 23c

HM001 primer. Same localisation with HMSp2 primer.

CAAAGGGGTCTCTGGGAGAAATAAAATCTTTTATTTTATCTCATTACTTGTA
CAGCTCGTCCATGCCGAGAGTGATCCCACTATTGTCTACTTATTCTGTTCC

TCACATGTCTTGTTCCTGGATCCTGTACCTCTGACCGAGGGGGGGGATTG
GGGCACCGTTTCAAATTCTGGTTTGAAAATATCCAGTGGCCGGAGTTTCAC
TGTCCCAGCGCTTTAAACGGGTTTCTTGAGTGCATAAACACAGAAGCAGAG
AACTGAGTTACTATGTTTACTCTG

9.1.21 Lymphoma 24

Specimen 24a

HM001 primer. Same localisation with HMSp2 primer.

ATTCCTGGCTGCTAGACATAGATTGATCTTTCATCTTATCTTACTTCTTGGA
CAGTTCGTTCATGTATGTGTTGATCGCTTGTGTGTGTGTTGTGTGCATCAT
CAGCACCGTCCCTGACTCACACAACTTAAGTGGAATGAACAGGAAGATCC
CACTAGTGTCGACACCAGTCTCATTCAGCCACAA

Specimen 24b

HM001 primer. Same localisation with HMSp2 primer.

AGGATGGTTGCTTGATAGGGTACAATCTTTTATTTTATCTCATTACTTGTCC
GGCTGTGTCCATGGACTGCAGTGATCCCAGGAGTGTTATCGTCAGTTATC
GACTCTGAAGGCACTTCCTACTTAGTCATCTCATCACAGCAGTCAAGCTTT
CTGCTGTCCTCCAACTAGTAGTTCCAGCCACTAAATGGAGACACGTCTTAA
ATTTATGTATGTGCCCACATGGGCCAGGGTATGTTGGGAGTCCCTGGAGC
GAAAGCTACACAGCCTCTTGTCTATGAACCCCACCTGATACTCCAGAAACC
CTTACCTCATGGTGGGATGATACTGCTCCTATTCCACGTTGTCAACGTCCC
GTCTGAAAGGTTAGAAGAGTAAGAGTCATGAGGGGCAATTAGAACACTTGT
GTTCAGCTTTGGGTCGCCGAGGCTTAAACGACTGCAGTCAGCTAACTAGG
GATGTCGTCAGTTGTCGCATCG

Specimen 24c

HM001 primer.

AATTCCCGGTTTTGCTGGATATAGATAAATCTTTTATCTTCTCTTATTTCTTG
TCCAGATCCTCCCTGAAACTCTCATTTACCCCCAACGTCTTGCTTGGTCAT
CTGTAAAAAGCAGTGCCCTCCTTTCTTTTTGTCCCCACCCCACCGAACTGT
CCTATAGGTGAAGGAGGAAGGCCGGTCATAAAACAGGATGGACAGTTGCT
TTCGGGTGAAACCCACCCAGGGTCCTCAGGCTTGTCGCTGACTGCATTTA
GATTTAACAATCAAGGCCTGTGACCTGGAGGCTCTTTCCAGCTGCTCTCTG

CCATGTTGACATGAGAGAATTTGCTAATTCTGGCCCGGGATTTTCCCTGTG
TGGCTGTTTTTCTTCTTTATCTTCATCAAATGAAGAGCGCTC